

**Some pages of this thesis may have been removed for copyright restrictions.**

If you have discovered material in Aston Research Explorer which is unlawful e.g. breaches copyright, (either yours or that of a third party) or any other law, including but not limited to those relating to patent, trademark, confidentiality, data protection, obscenity, defamation, libel, then please read our [Takedown policy](#) and contact the service immediately ([openaccess@aston.ac.uk](mailto:openaccess@aston.ac.uk))

REINFORCED THERMOPLASTICS

FOR ENGINEERING APPLICATIONS

by

NEIL CHRISTOPHER QUINN

Submitted for the  
Degree of Doctor of Philosophy  
at the  
University of Aston in Birmingham

September 1985

THE UNIVERSITY OF ASTON IN BIRMINGHAM

REINFORCED THERMOPLASTICS FOR

ENGINEERING APPLICATIONS

NEIL CHRISTOPHER QUINN

Submitted for the Degree  
of Doctor of Philosophy

September 1985

SUMMARY

The effect of mechano-chemically bound polypropylene modifiers on the mechanical performance and thermal-oxidative stability of polypropylene composites has been studied. The mechanical performance of unmodified polypropylene containing silane coupled glass and Rockwool (mineral) fibre was poor by comparison with a similar commercially produced glass reinforced composite; this was attributed to poor fibre-matrix adhesion. Mechano-chemical binding with unsaturated additives was obtained in the presence of a free radical initiator (di-cumyl peroxide). This process was inhibited by stabilisers present in commercial grades of polypropylene homopolymer. The binding of these additives was shown to increase the fibre-matrix adhesion of polypropylene composites by chemical bond formation between the chemically bound modifier and the silane coupling agent on the fibre surface, resulting in a dramatic improvement in the mechanical properties, dimensional stability and retention of mechanical performance after immersion in fluids typically found in under-bonnet environments.

A feature unique to some of these modifiers was their ability not only to enhance the mechanical properties of polypropylene composites to levels substantially in excess of currently available commercial materials, but their ability to act as effective thermal-oxidative polypropylene stabilisers. The mode of action was shown to be a chain-breaking mechanism and as a result of the high binding levels achieved during melt processing, these modifiers were able to efficiently stabilise polypropylene in the most severe volatilising and solvent-extracting environments, thus giving much better protection to the polymer than currently available commercially stabilised grades of polypropylene.

KEY WORDS:

POLYPROPYLENE  
MECHANO-CHEMICAL MODIFICATION  
MECHANICAL PERFORMANCE  
THERMAL-OXIDATIVE STABILITY  
UNDER-BONNET COMPONENTS

DECLARATION

The work described herein was carried out at the University of Aston in Birmingham between October 1982 and September 1985. It has been done independently and submitted for no other degree.

*Neil C. Quinn*  
.....

NEIL CHRISTOPHER QUINN

September 1985

## ACKNOWLEDGEMENTS

Firstly I wish to extend my gratitude for the guidance given by my supervisor, Dr.Sahar Al-Malaika, and my associate-advisory supervisor, Professor Gerald Scott.

I am extremely grateful for the help given by the technical staff of the Department of Molecular Sciences (Chemistry), especially Steve Ludlow, Paul Hughes and Dave Hammond.

I am indebted to Lucas Industries for their SERC-CASE award during the first two years of this project and the total financing of my final year.

Special thanks are due to my family for their unceasing support and encouragement during my unexpectedly prolonged stay at University. Alas, all good things must come to an end.

Finally, my sincere appreciation for the typing of this thesis by Mrs. Ludlow. Any final year research student involved in the laborious task of writing-up need look no further.

P.S. Last, but by no means least, many thanks to Mari for spotting so many of my spelling mistakes during the proof-reading.

To Mum, Dad, Andrew and Sally. .

## LIST OF CONTENTS

	Page
Title Page	1
Summary	2
Declaration	3
Acknowledgements	4
Dedication	5
List of Contents	6
List of Figures	15
List of Tables	19
List of Schemes	21
List of Plates	22
CHAPTER ONE INTRODUCTION	23
1.1 Background	24
1.2 Short Fibre Reinforced Thermoplastics	26
1.3 Fibre Reinforced Thermoplastic Composite Production	29
1.3.1 Compounding	29
1.3.2 Injection Moulding	30
1.3.3 Mould Behaviour	31
1.4 Polypropylene	32
1.4.1 Polyolefin Chemical Modification	33
1.5 Size and Coupling Agents	34
1.5.1 Silane Coupling Agents	35
1.6 Adhesion At The Polymer-Fibre Interface Through Coupling Agents	38

	Page	
1.6.1	Chemical Bonding Theory	38
1.6.2	Wetting And Surface Energy Effects	39
1.6.3	Boundary Layer Strengthening	41
1.7	Degradation Of Thermoplastics	42
1.8	Stabilisation Of Thermoplastics	45
1.8.1	Antioxidant Mechanisms	45
1.8.2	Chain Breaking Antioxidants	47
1.8.3	Melt And Thermal Oxidative Stabilisation	48
1.8.4	Conflicting Requirements Of Melt And Thermal Oxidative Stabilisers	51
1.9	Stabiliser Loss From Polymers	51
1.9.1	Prevention Of Stabiliser Loss From Polymers	54
1.10	Aim And Scope	58
CHAPTER TWO EXPERIMENTAL		60
2.1	Materials	61
2.1.1	Polymeric Materials	61
2.1.2	Fibres	61
2.1.2.1	Glass Fibre	61
2.1.2.2	Rockwool Fibre	62
2.1.3	Commercial Antioxidants And Chemicals	68
2.1.4	Synthesised Additives	69
2.1.4.1	N-(-4-Anilinophenyl)maleamic Acid (APMA)	69
2.1.4.2	N-(-4-Anilinophenyl)maleimide (APM)	70
2.1.4.3	N-(-4-Anilinophenyl)succinamic Acid (APSA)	70
2.1.4.4	Maleimide (MAL)	71
2.1.4.5	2N-Allylamino-4,6-dichloro-1,3,5-triazine (ADCT)	73



	Page	
2.1.4.6	2N-Allylamino-4-(N-4-aminodiphenylamine)-6-chloro-1,3,5-triazine (AACT)	74
2.1.4.7	2N-(4-aminodiphenylamine)-4,6-dichloro-1,3,5-triazine (ADDT)	75
2.2	Composite Production	75
2.2.1	Homogenisation Of Additives And Fibres For Polypropylene Composites	75
2.2.2	Injection Moulding	93
2.3	Composite Testing	94
2.3.1	Fibre Length Determination	94
2.3.2	Tensile Property Tests	95
2.3.3	Flexural Property Tests	99
2.3.4	Charpy Impact Strength	100
2.3.5	Dynamic Mechanical Testing	102
2.3.6	Tensile Creep Of Plastics	106
2.3.7	Long Term Durability Tests	107
2.3.8	Tensile Modulus Retention Water Immersion Tests	108
2.3.9	Scanning Electron Microscopy	109
2.4	Melt Processing	109
2.5	Polymer Film Preparation	110
2.6	Melt Stability Of Polypropylene	111
2.6.1	Melt Flow Index	111
2.6.2	Gel Permeation Chromatography	112
2.7	Accelerated Thermal Oxidative Ageing	113
2.7.1	Accelerated Thermal Oxidative Ageing Of Polypropylene Films	113

	Page	
2.7.2	Infra-red Spectroscopy Of Polypropylene Films	113
2.7.3	Accelerated Thermal Oxidative Ageing Of Polypropylene Plaques	115
2.8	Chemical Binding Studies Of Polypropylene Additives	117
2.8.1.1	Continuous Hot Soxhlet Extraction Of Polypropylene Films	117
2.8.1.2	Continuous Hot Soxhlet Extraction Of Polypropylene Granules And Plaques	117
2.8.2	Percentage Binding Calculations For Polypropylene Additives	117
2.8.2.1	Infra-red Spectra	118
2.8.2.2	Ultraviolet Spectra	118
2.8.3	Quantitative Determination Of Bound Additive Concentration In Polypropylene Films	121
2.8.3.1	Ultraviolet Spectra	121
2.8.3.2	Infra-red Spectra: Calibration Graphs	122
2.9	Solution Studies	123
2.9.1	Hydroperoxide Decomposition	123
2.9.2	Oxygen Absorption	125
CHAPTER THREE COMPOSITE PROCESSING OPTIMISATION AND ASSESSMENT OF ROCKWOOL AND GLASS FIBRES IN POLYPROPYLENE		
		132
3.1	Object	133
3.2	Results	137
3.2.1	Optimisation Of The Homogenisation Process Using The Buss Ko-Kneader	137

	Page
3.2.2 Injection Moulding (Edgwick) Optimisation	139
3.2.3 Mechanical Properties Of PP(HWM25) Containing Long(L), Short(S) Rockwool Fibre(RWF) And Glass Fibre(GF)	140
3.2.4 Summary Of The Mechanical Properties Of PP(HWM25) Containing Long Rockwool Fibre(LRWF) And Glass Fibre(GF, Both 30% Loading, A-1100 Coupled) And Commercially Coupled 30% GF Reinforced PP(HW60/GR30)	144
3.2.5 The Effect Of EPDM(0-30% Loading) On The Mechanical Properties Of PP(HWM25)	145
3.2.6 The Effect Of EPDM(10% And 20% Loadings) On Long Rockwool Fibre(LRWF) And Glass Fibre(GF) Filled PP(HWM25)	146
3.3 Discussion	149
3.3.1 Optimisation Of The Homogenisation Process Using The Buss Ko-Kneader	149
3.3.2 Injection Moulding (Edgwick) Optimisation	150
3.3.3 Mechanical Properties Of PP(HWM25) Containing Long(L), Short(S) Rockwool Fibre(RWF) And Glass Fibre(GF)	152
3.3.4 Summary Of The Mechanical Properties Of PP(HWM25) Containing Long Rockwool Fibre (LRWF) And Glass Fibre(GF, Both 30% Loading, A-1100 Coupled) And Commercially Coupled 30% GF Reinforced PP(HW60/GR30)	156
3.3.5 The Effect Of EPDM(0-30% Loading) On The Mechanical Properties Of PP(HWM25)	158

	Page
3.3.6 The Effect Of EPDM(10% And 20% Loadings) On Long Rockwool Fibre(LRWF) And Glass Fibre(GF) Filled PP(HWM25)	159
CHAPTER FOUR MALEIC ANHYDRIDE AND DI-CUMYL PEROXIDE MODIFICATION OF POLYPROPYLENE COMPOSITES	194
4.1 Object	195
4.2 Results	199
4.2.1 The Mechanical Properties Of Chemically Modified PP(HWM25) Composites	199
4.2.2 The Mechanical Properties Of Chemically Modified PP(HF22) Composites	203
4.2.3 The Mechanical Properties Of Succinic Anhydride Modified PP(HF22) Composites	207
4.2.4 Melt Stability Studies Of Maleic Anhydride Mechano-chemically Modified Polypropylene	208
4.2.5 Mechano-chemical Binding Of Maleic Anhydride To Polypropylene	210
4.2.6 Melt Stability And Chemical Binding Studies Of Succinic Anhydride Mechano-chemically Modified Polypropylene	212
4.3 Discussion	213
4.3.1 The Mechanical Properties Of Chemically Modified PP(HWM25) Composites	213
4.3.2 The Mechanical Properties Of Chemically Modified PP(HF22) Composites	215
4.3.3 The Mechanical Properties Of Succinic Anhydride Modified PP(HF22) Composites	216

	Page
4.3.4 Melt Stability Studies Of Maleic Anhydride Mechano-chemically Modified Polypropylene	217
4.3.5 Mechano-chemical Binding Of Maleic Anhydride To Polypropylene	222
4.3.6 Melt Stability And Chemical Binding Studies Of Succinic Anhydride Mechano-chemically Modified Polypropylene	222
CHAPTER FIVE ASSESSMENT OF MORE POLYPROPYLENE MODIFIERS IN THE ENHANCEMENT OF COMPOSITE MECHANICAL PROPERTIES	251
5.1 Object	252
5.2 Results	259
5.2.1 Mechanical Properties Of Mechano-chemically modified PP(HF22) Composites	259
5.2.2 The Effect Of Long-term Fluid Immersion On The Mechanical Properties Of Mechano-chemically Modified PP(HF22) Composites	262
5.2.3 The Effect Of Temperature Upon Charpy Impact Strength Of Mechano-chemically Modified PP(HF22) Composites	265
5.2.4 Dimensional Stability Of Mechano-chemically Modified PP(HF22) Composites	266
5.2.5 Reaction Of Chemical Modifiers With A-1100 Silane Coupling Agent During PP(HF22) Melt Processing	268
5.3 Discussion	269

	Page
5.3.1 Mechanical Properties Of Mechano-chemically Modified PP(HF22) Composites	269
5.3.2 The Effect Of Long-term Fluid Immersion On The Mechanical Properties Of Mechano-chemically Modified PP(HF22) Composites	271
5.3.3 The Effect Of Temperature Upon Charpy Impact Strength Of Mechano-chemically Modified PP(HF22) Composites	274
5.3.4 Dimensional Stability Of Mechano-chemically Modified PP(HF22) Composites	275
5.3.5 Reaction Of Chemical Modifiers With A-1100 Silane Coupling Agent During PP(HF22) Melt Processing	277
CHAPTER SIX THERMAL-OXIDATIVE STABILISATION OF POLYPROPYLENE USING CHEMICALLY BOUND STABILISERS	330
6.1 Object	331
6.2 Results	340
6.2.1 Thermal-oxidative Stability Of Commercially Stabilised PP And PP(HF22) Containing Irganox Compounds	340
6.2.2 Attempted Binding Of ADPA To MA/DCP Modified PP(HF22) And Its Effect Upon Thermal-oxidative Stability	341
6.2.3 Attempted Mechano-chemical Binding Of Stabilisers To PP(HF22) And Its Effect Upon Thermal-oxidative Stability	344

	Page
6.2.4 Thermal-oxidative Stability Of Commercially And Mechano-chemically Modified PP Plaques	348
6.2.5 Cumene Hydroperoxide Decomposition And Oxygen Absorption Studies Of PP Modifiers And Stabilisers	349
6.3 Discussion	351
6.3.1 Thermal-oxidative Stability Of Commercially Stabilised PP And PP(HF22) Containing Irganox Compounds	351
6.3.2 Attempted Binding Of ADPA To MA/DCP Modified PP(HF22) And Its Effect Upon Thermal-oxidative Stability	354
6.3.3 Attempted Mechano-chemical Binding Of Stabilisers To PP(HF22) And Its Effect Upon Thermal-oxidative Stability	358
6.3.4 Thermal-oxidative Stability Of Commercially And Mechano-chemically Modified PP Plaques	365
6.3.5 Cumene Hydroperoxide Decomposition And Oxygen Absorption Studies Of PP Modifiers And Stabilisers	366
 CHAPTER SEVEN CONCLUSIONS AND SUGGESTIONS FOR FURTHER WORK	 409
7.1 Conclusions	410
7.2 Suggestions For Further Work	416
 REFERENCES	 420

LIST OF FIGURES

Figure	Page	Figure	Page
1.1	25	2.23	97
1.2	25	2.24	98
1.3	36	2.25	101
		2.26	105
2.1	82	2.27	116
2.2	82	2.28	119
2.3	83	2.29	120
2.4	83	2.30	128
2.5	84	2.31	128
2.6	84	2.32	129
2.7	85	2.33	129
2.8	85	2.34	130
2.9	86	2.35	130
2.10	86	2.36	131
2.11	87		
2.12	87	3.1	163
2.13	88	3.2	164
2.14	88	3.3	165
2.15	89	3.4	166
2.16	89	3.5	168
2.17	90	3.6	168
2.18	90	3.7	173
2.19	91	3.8	173
2.20	91	3.9	174
2.21	92	3.10	174
2.22	96	3.11	175



Figure	Page	Figure	Page
3.12	175	4.1	226
3.13	176	4.2	226
3.14	176	4.3	227
3.15	177	4.4	228
3.16	178	4.5	228
3.17	178	4.6	229
3.18	178	4.7	229
3.19	178	4.8A and B	230
3.20	180	4.9	231
3.21	180	4.10	232
3.22	181	4.11	233
3.23	181	4.12	233
3.24	184	4.13	234
3.25	184	4.14	234
3.26	185	4.15	236
3.27	185	4.16	236
3.28	186	4.17	237
3.29	186	4.18	237
3.30	187	4.19A and B	238
3.31	187	4.20	239
3.32	188	4.21	240
3.33	188	4.22	241
3.34	189	4.23	241
3.35	189	4.24	242
3.36	190	4.25	242
3.37	190	4.26	243

Figure	Page	Figure	Page
4.27	244	5.18	314
4.28	244	5.19	315
4.29	245	5.20	316
4.30	245	5.21	317
4.31	246	5.22	318
4.32	246	5.23	319
4.33	247	5.24	320
4.34	248	5.25	321
4.35	248	5.26	322
		5.27	323
5.1	291	5.28	324
5.2	291	5.29	325
5.3	292	5.30	326
5.4	292	5.31	328
5.5	293	5.32	328
5.6	293	5.33	329
5.7	294		
5.8A and B	297	6.1	370
5.9A and B	298	6.2	371
5.10A and B	299	6.3A and B	372
5.11A and B	300	6.4	374
5.12A and B	301	6.5	377
5.13	307	6.6A and B	378
5.14	308	6.7A	379
5.15	309	6.7B	380
5.16A and B	312	6.8	382
5.17	313	6.9A and B	383

Figure	Page
6.10	385
6.11A and B	386
6.12	388
6.13A and B	389
6.14	391
6.15A and B	392
6.16	394
6.17A and B	395
6.18	397
6.19	398
6.20	399
6.21	400
6.22	401
6.23	402
6.24	403
6.25	404
6.26	405
6.27	406
6.28	407
6.29	408

LIST OF TABLES

Table	Page	Table	Page
1.1	52	4.1 (I)	224
		4.1 (II)	225
2.1	63	4.2	232
2.2	64	4.3	235
2.3	65	4.4	240
2.4	76	4.5	243
2.5	77	4.6	247
2.6	78		
2.7A	79	5.1A and B	283
2.7B	80	5.2A and B	284
2.8	81	5.3A and B	285
2.9	127	5.4A	286
		5.4B	287
3.1	161	5.5A and B	288
3.2	162	5.6A and B	289
3.3	167	5.7A and B	290
3.4	169	5.8A	295
3.5	170	5.8B	296
3.6	171	5.9	302
3.7	172	5.10	303
3.8	177	5.11	304
3.9	179	5.12	305
3.10	182	5.13	306
3.11	183	5.14	311
		5.15	327

Table	Page
6.1	369
6.2	373
6.3	375
6.4	376
6.5	381
6.6	384
6.7	387
6.8	390
6.9	393
6.10	396
7.1	411

LIST OF SCHEMES

Scheme	Page	Scheme	Page
1.1	37	6.1	333
1.2	43	6.2	334
1.3	44	6.3	335
1.4	46	6.4	336
1.5	50	6.5	337
		6.6	338
3.1	134	6.7	339
3.2	135	6.8	352
3.3	136	6.9A and B	357
		6.10	361
4.1	197	6.11	363
4.2	198	6.12	364
4.3	219		
4.4	220		
5.1	254		
5.2	255		
5.3	256		
5.4	257		
5.5	258		
5.6	280		
5.7	281		
5.8	281		
5.9	282		

LIST OF PLATES

Plate	Page
2.1	66
2.2	66
2.3	67
3.1	191
3.2	191
3.3	192
3.4	192
3.5	193
3.6	193
4.1	249
4.2	249
4.3	250
4.4	250
5.1	310
5.2	310

CHAPTER ONE

INTRODUCTION



## 1.1 Background

Thermoplastics have always found widespread use in commodity, engineering and other specialist applications. The use of commodity plastics is limited by their relatively poor mechanical properties and thermal stability. The incorporation of reinforcing fibres greatly enhances the strength, stiffness and dimensional stability of the thermoplastic. In recent years, there has been rapid growth in glass fibre reinforced thermoplastic replacement of metal components. This is mainly attributable to light weight, ease of high volume manufacture (e.g., injection moulding), low cost and versatility in structural design.

The automotive industry represents the single most important market for reinforced plastics<sup>(1)</sup>. By 1976, the car and truck industry in the U.S.A. was consuming over half of all fibre reinforced thermoplastics. The U.K. currently represents one of the largest growth markets in Europe, although this is because Britain currently lags behind its competitors in the applications of such composites<sup>(2)</sup>.

Components produced for "under bonnet" applications in the automotive industry are also required to have high heat distortion temperatures and durability and stability of the thermoplastic matrix towards heat ageing and aggressive chemical environments during in-service performance. These

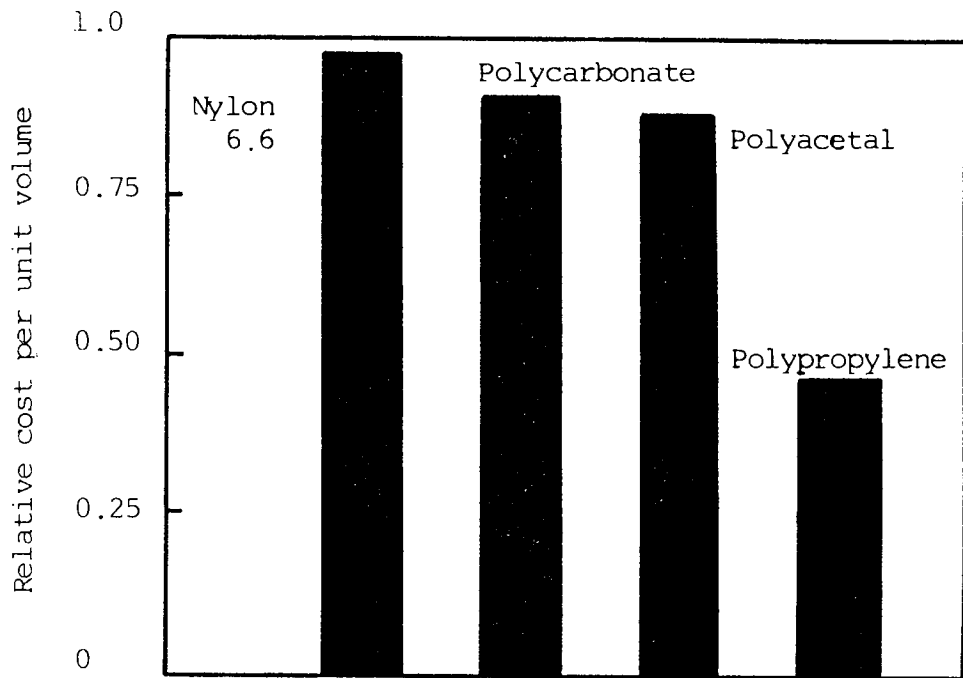


Figure 1.1 Comparison of "relative cost per unit volume" for selected thermoplastics

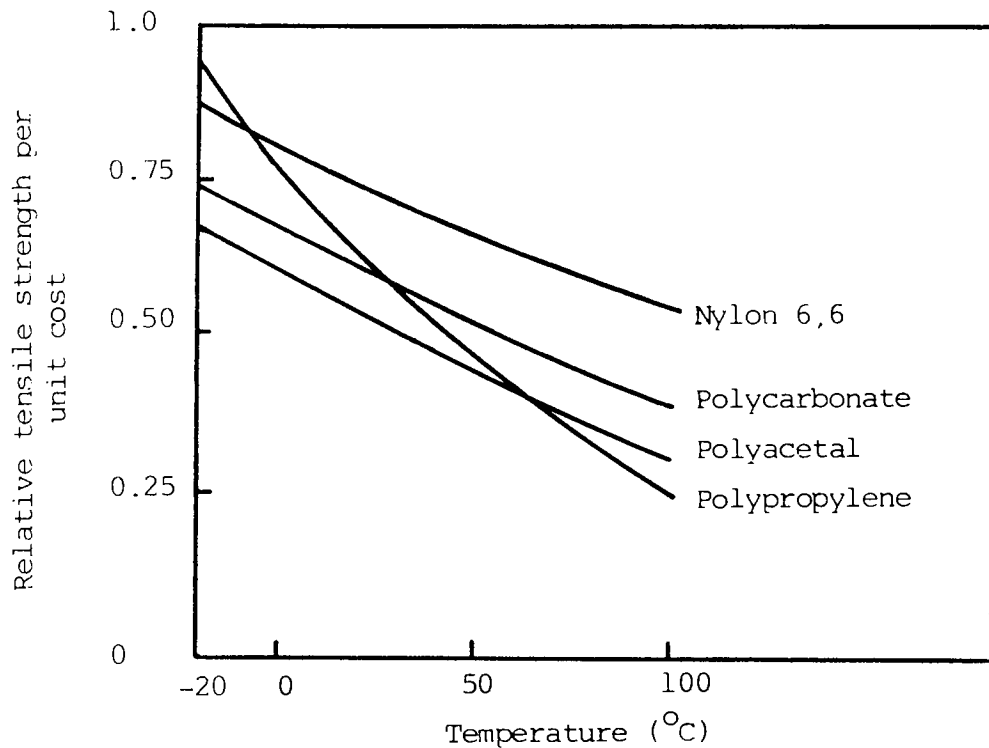


Figure 1.2 Effect of temperature on the "relative tensile strength per unit cost" for selected thermoplastics

requirements are continually increasing due to higher engine operating temperatures used in order to decrease fuel consumption<sup>(3-5)</sup>.

Significant growth in "under bonnet" plastics has been predicted for the mid to late 1980's, by which time there should be 35 kg of plastics replacing metal in U.S. car engines and ancillaries<sup>(6)</sup>.

Any fibre reinforced thermoplastic (F RTP) component that possesses sufficient properties to replace a traditional material should be comparable on price and have significant manufacturer-user advantages. The uncertainty in predicting oil prices is a major factor against the more widespread use of plastics<sup>(7,8)</sup>. The choice of material is governed by economic factors. These are influenced by the "relative cost per unit volume" (Figure 1.1) and "tensile strength per unit cost" (Figure 1.2)<sup>(9)</sup>.

## 1.2 Short Fibre Reinforced Thermoplastics

The simplest theoretical approach to describe the reinforcing effect of high modulus inorganic fibres in thermoplastics is given by the "law of mixtures"<sup>(10,11)</sup>. It assumes composites contain continuous uniaxially aligned fibres with any applied stress being in the same direction. Mechanical properties such as tensile strength may be

estimated by the relative proportions of the two components in the composite<sup>(10)</sup>:

$$\sigma_c = \sigma_f \cdot V_f + \sigma_m \cdot V_m \quad (1)$$

where  $\sigma_c$ ,  $\sigma_f$ ,  $\sigma_m$  = tensile strength of composite, fibre and matrix respectively.

$V_f$ ,  $V_m$  = volume fraction of fibre and matrix respectively.

In practice, to correctly predict the properties of a composite, two additional factors are required for Equation 1.

The first is the addition of a fibre orientation factor ( $\eta$ ) to the  $(\sigma_f V_f)$  term<sup>(10)</sup>. In injection moulded fibre reinforced thermoplastics (FRTPs), the fibres are aligned in all directions. Because fibres only reinforce a composite in the direction in which they lie, the orientation factor is used; its value is between zero and one (if the fibre is in line with the applied stress,  $\eta=1$ . If the fibre is at  $90^\circ$  to the applied stress, there is no reinforcement, thus  $\eta=0$ )<sup>(10,11)</sup>.

The second correction factor involves the effect of having short fibres in an injection moulded composite<sup>(10)</sup>. Fibres improve the strength of a composite by stress transfer from the ductile matrix. The fibre length determines the amount

of stress that may be transferred. The concept of critical length ( $L_c$ ) is important; any fibre shorter than  $L_c$  results in incomplete stress transfer and "fibre pull-out" from the matrix resulting in component failure.  $L_c$  is given by Equation 2<sup>(10)</sup>:

$$L_c = \frac{\sigma_f d}{2\tau} \quad (2)$$

where  $d$  = fibre diameter

$\tau$  = interfacial shear strength

The degree of fibre-matrix bonding is important; the weaker the interfacial shear strength ( $\tau$ ), the longer the fibre required to transfer sufficient stress.

Adding these two correction terms, Equation 1 becomes:

$$\sigma_c = \eta \sigma_f V_f \left(1 - \frac{L_c}{2L}\right) + \sigma_m V_m \quad (3)$$

where  $L_c$  = critical fibre length

$L$  = actual fibre length

$\eta$  = orientation factor

From Equation 3, it is clear that fibre length in a moulded component should exceed  $L_c$  by as much as possible to maximize strength. The tensile strength of moulded composites seldom exceeds 70% of the theoretical value due to non-uniform fibre length ( $L$ ) and the orientation factor ( $\eta$ )<sup>(10-12)</sup>.

## 1.3 Fibre Reinforced Thermoplastic Composite Production

### 1.3.1 Compounding

The compounding stage introduces the fibre to the polymer and produces a feedstock that may be moulded satisfactorily<sup>(13)</sup>. It is a process by which energy is applied to the polymer by internal shear generated by screw rotation within a barrel<sup>(14)</sup>. This mixing action is required to melt the polymer, disperse the filler and homogenise the compound<sup>(13,14)</sup>. The homogenisation process involves large shearing forces resulting in fibre breakage due to bending stresses. Subsequent processing operations (e.g., injection moulding) leads to further fibre length degradation. The main compounding requirements needed for optimum properties in the final product are<sup>(13-17)</sup>:

- I. Low controllable thermal degradation of the base polymer.
- II. Fibres must be wetted out; totally enclosed by the polymer matrix.
- III. Uniform fibre dispersion throughout the matrix.
- IV. Screw speed should be kept to a minimum consistent with good mixing as shear at the flight edge causes substantial fibre breakage.
- V. Fibre breakage may be reduced by setting a high temperature at the feed zone and decreasing it along a

reversed profile towards the die.

It is the excessive fibre breakage caused by high shear rates that is the major disadvantage of compounding<sup>(15)</sup>.

### 1.3.2 Injection Moulding

Fibre length is most important in determining the mechanical properties of a composite together with fibre dispersion, orientation and void content<sup>(18-20)</sup>. From Equation 3, it follows that fibre length should exceed the critical length ( $L_c$ ) by as much as possible, but not too long to interfere with their processability<sup>(21-23)</sup>. It has been shown from fibre length distribution measurements of injection mouldings that fibres are broken down to roughly the same size, independent of their original length<sup>(24)</sup>. There are two major causes of fibre damage during injection moulding<sup>(21,25-28)</sup>.

If the rear zone temperature is low, the temperature profile may excessively reduce fibre length<sup>(21,22)</sup>. Screw retraction times are increased and is accompanied by additional working of the resin by the screw. This may be minimized by using a temperature at the melting point of the polymer causing the outer layers of the granules to soften. Time to melt may be reduced by polymer pre-heating, although care must be taken to avoid thermal oxidative degradation<sup>(21,22)</sup>. To produce a good quality moulding, a homogeneous melt is

required. For an unfilled thermoplastic, this is aided by high screw speed and back pressure. For FRTP's however, these conditions cause excessive fibre damage<sup>(8,22,29,30)</sup>. Increasing screw speed is more detrimental to fibre length than increasing back pressure because fibre damage is more closely related to the peripheral speed of the screw than the amount of internal shear developed in the melt while the screw is working to overcome the imposed hydraulic back pressure<sup>(29,30)</sup>.

### 1.3.3 Mould Behaviour

Feedstock requirements (through compounding, See 1.3.1) and high melt shear during injection moulding (See 1.3.2) ensure only short fibres are present in a finished component. The use of low screw speed and back pressure, wide sprues, runners and gates with large radii of curvature only help to minimize fibre degradation during moulding<sup>(3,12,31,32)</sup>. Uncertainties in design are further complicated by the effect of fibre orientation during the moulding process<sup>(26,29,33)</sup>. The degree of orientation is dependent upon fluid flow behaviour, mould and melt temperature, injection speed and mould geometry<sup>(34-38)</sup>. Because melt flow is pseudoplastic, shear forces are concentrated at the point of contact with the mould surface<sup>(26,29)</sup>. The fibres in the central region of melt flow undergo relatively little shear. This results in two distinct layers of fibre orientation in a simple



mould. At the moulding surface, the fibres are in parallel alignment, and in the core there is very little or no alignment<sup>(34-38)</sup>. Being shear dependent, the degree of alignment increases with injection speed<sup>(26,29)</sup>.

Consequently, stiffness and strength data obtained from injection moulded tensile bars can give a misleading impression of a materials' performance due to the anisotropy caused by irregular fibre alignment if comparisons are made with similar materials not moulded using identical conditions<sup>(26,29,39-42)</sup>.

#### 1.4 Polypropylene

There are significant cost advantages to be gained by enhancing the properties of relatively low performance cheap commodity thermoplastics such as polypropylene. Polypropylene has been commercially available since the early 1960's. The homopolymer is semi-crystalline and non-polar with a melting range of 160-165°C. The basic resins are resistant to a wide range of chemicals including strong acids and bases as well as most organic chemicals. The specific gravity is very low at 0.902. Despite this favourable balance of chemical properties, unfilled polypropylene resins are not generally considered as high performance engineering polymers owing to their low stiffness, strength and heat distortion temperatures. In recent years,

polypropylene has found many new uses as moulders have incorporated fillers and reinforcements for property enhancement and resin extension. On a cost-performance basis, this allows polypropylene to be competitive with engineering polymers such as polycarbonate, nylon and ABS<sup>(43)</sup>.

#### 1.4.1 Polyolefin Chemical Modification

To obtain polypropylene composites with enhanced mechanical properties, it is necessary to increase the interfacial shear strength,  $\tau$ , between the polyolefin matrix and the silane coupling agent on the reinforcing fibre surface. With chemically unreactive covalent polypropylene, this may be achieved by chemically grafted surface modification with groups reactive towards functional groups present in the coupling agent.

Much effort has been spent on the grafting of maleic anhydride (MA) to provide polarity to promote hydrophilicity, adhesion and dyeability, to give functionality for cross-linking, and to promote compatibility with other polymers and fillers<sup>(44,45)</sup>. MA has most commonly been grafted to polyethylene and polypropylene by free radicals in organic solvents<sup>(46-48)</sup>. Mechanochemical with<sup>(49)</sup> or without<sup>(50-54)</sup> peroxide free radical initiation and radiation-initiation techniques<sup>(55)</sup> to a lesser extent have also been attempted. Solvent extraction and infra red spectra have clearly shown

that grafting was achieved. The improved adhesion of such modified polyolefins has been attributed to dispersional and hydrogen bonding forces introduced by the grafted MA residues<sup>(56,57)</sup>. MA grafting to polyethylene has been successfully achieved by degrading the polymer in an extruder at 420°C, followed by heating with 10% MA in an autoclave for 90 minutes at 220°C<sup>(58)</sup>. The product was waxy and gave improved adhesion to polar textiles, metals and plastic films.

Derivatives of MA such as fumarates, maleates and maleimides have also been grafted to polyethylene to change the surface properties and cross-link the polymer<sup>(59-61)</sup>.

Improvements in the mechanical performance of thermoplastic composites has been attained by MA grafting of polyethylene with 40% clay filler<sup>(62)</sup> and in polypropylene-glass fibre blends with dibenzothiazoyl disulphide and bis(maleimides)<sup>(63)</sup>. In both cases, flexural, tensile and impact properties were improved.

### 1.5 Size and Coupling Agents

At the time of forming, reinforcing fibres are given a single treatment of size. This is done from solution and contains a lubricant to prevent damage during handling, a binder necessary for strand integrity, an antistat agent

to prevent the build up of static electricity during handling and a coupling agent to enhance the affinity between the polymer matrix and inorganic fibre<sup>(64)</sup>.

Coupling agents act as molecular bridges at the interface of filler and matrix<sup>(65)</sup>. Coupling gives moulded components with improved physical and mechanical properties due to more efficient stress transfer from the plastic matrix to the reinforcing fibre<sup>(66)</sup>. The degree of coupling affects the critical length ( $L_c$ ) of fibres. The better the coupling, the stronger the interfacial shear strength ( $\tau$ ), the lower the  $L_c$  which is required (See Equation 2). Thus the problem of fibre breakage during moulding may be reduced<sup>(66)</sup>.

Coupling agents are used for a variety of reasons, the most important of which are<sup>(64,66-71)</sup>: improved mechanical properties and dimensional stability, enhanced retention of mechanical properties during exposure to moisture and high temperatures, and improved clarity of composites where the refractive index of filler and clear plastic are similar.

#### 1.5.1 Silane Coupling Agents

These represent the most widely used commercial coupling agents and have the following structure<sup>(67,69,72)</sup>:

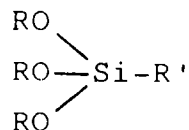


Figure 1.3 Silane coupling agent

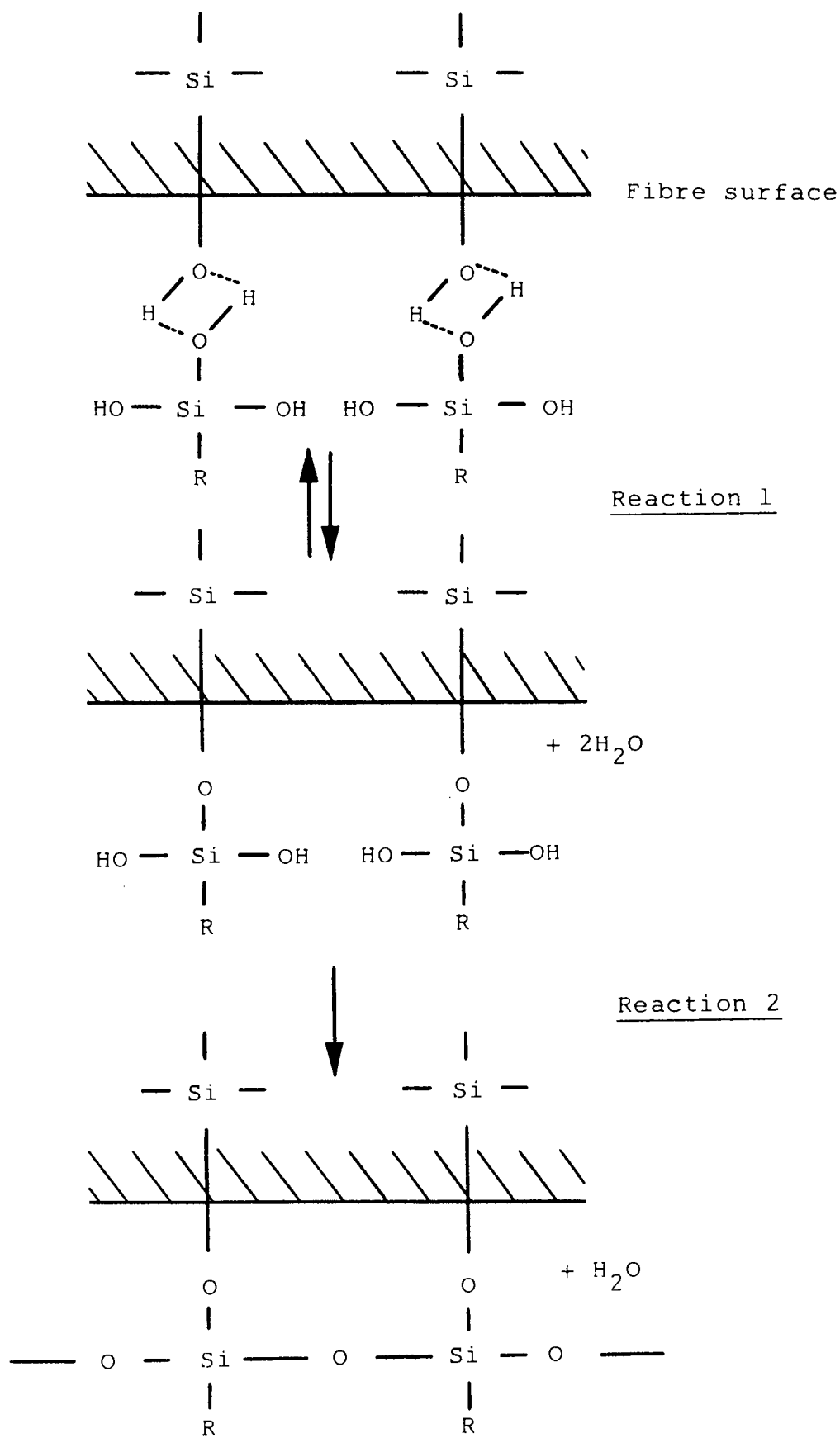
where R' = organo-functional group bonded to Si in a hydrolytically stable manner

OR = alkoxy hydrolyzable group which is converted to silanol on hydrolysis

Prior to silane coupling, hydrolysis of the three alkoxy groups to silanols must be completed in weakly acidified water<sup>(64,67)</sup>. The resultant silanol can then bond to receptive surfaces (hydrated oxides of silica on glass or mineral fibres)<sup>(73,74)</sup>. This filler-silanol condensation reaction is reversible and the dynamic equilibria permits movement at the interface, allowing relief of internal stress within the composite (See Scheme 1.1, reaction 1).

The following drying process can cause condensation through adjacent silanol groups (See Scheme 1.1, reaction 2)<sup>(75-77)</sup>.

Thus a polymer film of siloxane may be formed and held tightly by siloxane linkages. This can be detrimental to the coupling efficiency due to the "burying" of organo-functional groups in the polymeric siloxane film, thus reducing adhesion with the matrix<sup>(73)</sup>.



Scheme 1.1 Silane coupling agent on fibre surface

## 1.6 Adhesion At The Polymer-Fibre Interface Through Coupling Agents

### 1.6.1 Chemical Bonding Theory

This is the oldest and best known theory of how coupling agents enhance the mechanical properties of composites. Attachment of a coupling agent to glass fibre is made by covalent bonding (See 1.5.1). Additionally, a coupling agent may contain an additional functional group which may react with the polymer at the interface, thus creating a continuous chemical linkage between fibre and matrix.

The development of Fourier transform infra red spectroscopy has made possible the observation of chemical reaction in the silane interface region of silane-treated glass fibres in styrene-diluted polyester during cure<sup>(78)</sup>. This chemical bonding mechanism has been shown to enhance the interfacial shear strength ( $\tau$ ). Although thermoplastics do not undergo chemical reaction during moulding, they may be divided into reactive (those containing amide, ester, carboxyl, hydroxyl or halide functional groups) and non-reactive (polyolefins) categories<sup>(79)</sup>. Vinyl silanes on fillers are known to graft to polyethylene during injection moulding<sup>(80)</sup> and are used on particulate fillers in cross-linkable polyethylene for power cable insulation. However, despite vinyl silanes grafting to thermoplastic polyethylene under moulding

conditions, they do not perform as well as non-grafting silanes in polyethylene composites. Azidosilanes react with polyolefins<sup>(68)</sup> during injection moulding. The azide decomposes liberating nitrogen and creates a reactive nitrogen intermediate.

However, chemical bonding is not essential for good fibre-matrix adhesion. There are many organo-functional silanes which are good coupling agents for polyolefins under conditions where no chemical reaction with the polymer can be demonstrated<sup>(80)</sup>.

#### 1.6.2 Wetting And Surface Energy Effects

Zisman<sup>(81)</sup> concluded that the physical adsorption of a resin on a high energy fibre surface would provide adhesive strength in excess of the cohesive strength of organic resins if complete wetting were obtained. To obtain total wetting of a surface, the adhesive (polymer melt) must initially be of low viscosity and have a surface tension  $\gamma_L$  lower than the critical surface tension  $\gamma_c$  of the mineral surface. Surface tension is composed of dispersive  $\gamma^d$  and polar  $\gamma^p$  components which may be determined by contact angle measurements<sup>(82)</sup>.

Although mineral fibres are hydrophilic and possess high critical surface tension  $\gamma_c$ , they adsorb atmospheric moisture and are thus easily covered with a layer of water. Thus poor wetting and spreading of a non-polar material (e.g., polyolefins) would occur on contact with the moist surface of a



polar adherent. The critical surface tension and thus the wettability of glass may be controlled by treatment with silanes<sup>(83,84)</sup>. Coupling through solution compatibility is most successful with glassy polymers like polystyrene, but less effective with crystallizing polymers like polyethylene or polypropylene<sup>(85)</sup>.

Some reactive silanes with amine or methacrylate functional groups perform very well as coupling agents in thermoplastics even though there is no obvious reaction or preferred solubility of the silane and polymer<sup>(83)</sup>. This apparent ambiguity is explained by the formation of interpenetrating polymer networks of siloxanes with thermoplastic resins at the mineral interface. During injection moulding, the siloxane becomes a partial solvent for molten thermoplastic, and after cooling the dissolved thermoplastic phase becomes trapped<sup>(86)</sup>. Kahn<sup>(87)</sup> has supported the likelihood that orientation extends beyond the coupling agent finish into the resin phase. Three main proposals have arisen from this:

#### A. Deformable layer theory

It has been suggested that a flexible deformable phase is required to accommodate stresses at the interface due to differential thermal shrinkage between a resin and filler. The amount of silane on a typical glass finish is insufficient to provide a low modulus layer, but Erickson<sup>(88)</sup>

has proposed that silane-treated surfaces might allow preferential adsorption of one ingredient in a thermosetting resin. Unbalanced cure in the interphase region could provide a flexible resin much thicker than the silane layer.

#### B. Restrained layer theory

This proposes that the resin in the region of the mineral filler should have a modulus between that of the filler and matrix<sup>(89)</sup>. The restrained layer theory suggests that the silane coupling agents function by "tightening up" the polymer structure in the interphase region. It is believed that amino-alkyl silanes do this by forming interpenetrating networks with polyolefins at the interface<sup>(90)</sup>.

#### C. Tough composites from rigid resins

This suggests that maximum toughness is obtained with a deformable layer while maximum chemical resistance is obtained with a restrained layer at the interface. Tough water-resistant composites may be prepared from rigid resins by bonding a thin elastomeric interlayer to the mineral surface through a cross-linkable silane<sup>(91)</sup>.

#### 1.6.3 Boundary Layer Strengthening

Although chemical bonding or surface wetting of fibres are generally proposed as mechanisms of fibre-matrix adhesion,

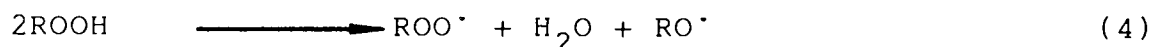
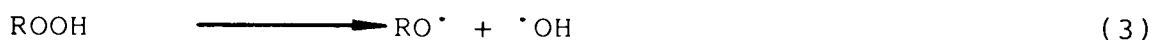
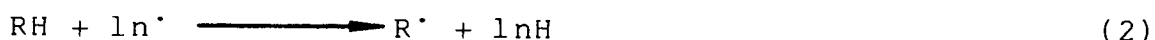
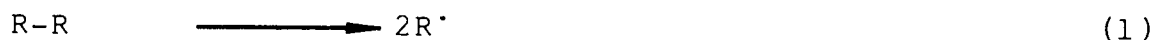
there is evidence that composite failure is often at the boundary of the matrix resin rather than the true interface<sup>(92)</sup>. Thus, to be effective, coupling agents must also strengthen the boundary layer. This is done by establishing a strong interpenetrating network<sup>(92)</sup>. Apart from the solubility of the thermoplastic in the siloxane film, this may also be attributed to, for example talc filler acting as a nucleating agent for polypropylene at the boundary layer, thus increasing the crystallinity and improving the mechanical properties of the polymer<sup>(93)</sup>.

#### 1.7 Degradation Of Thermoplastics

Thermoplastics degrade when subjected to high temperatures in the presence of oxygen during both service and processing. "Under bonnet" components which are expected to perform in aggressive environments at high temperatures are particularly prone to thermal oxidative degradation. Under these conditions, reaction with small amounts of elemental oxygen cause drastic changes in the mechanical properties of polymers by hydroperoxide formation and chain scission<sup>(94,95)</sup>. The oxidative degradation process for polyolefins proceeds via an autocatalytic free radical chain mechanism and was originally explained by Bolland<sup>(96,97)</sup> in the 1940's (See Scheme 1.2).

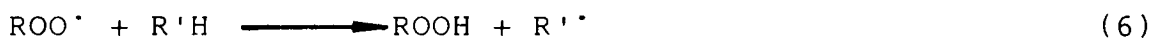
The rate of degradation is affected by the chemical and physical structure of the polymer<sup>(98,99)</sup>, its molecular weight<sup>(100)</sup> and the presence of impurities<sup>(101,102)</sup> such as catalyst residues. Polypropylene is more prone to thermal oxidative degradation than polyethylene due to the presence of tertiary carbon atoms along the polymer chain, making the C-H bond much more labile.

### Initiation

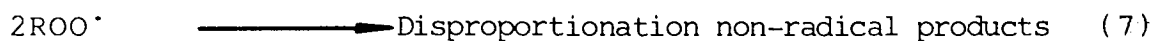


where  $In^{\cdot}$  = free radical initiator

### Propagation

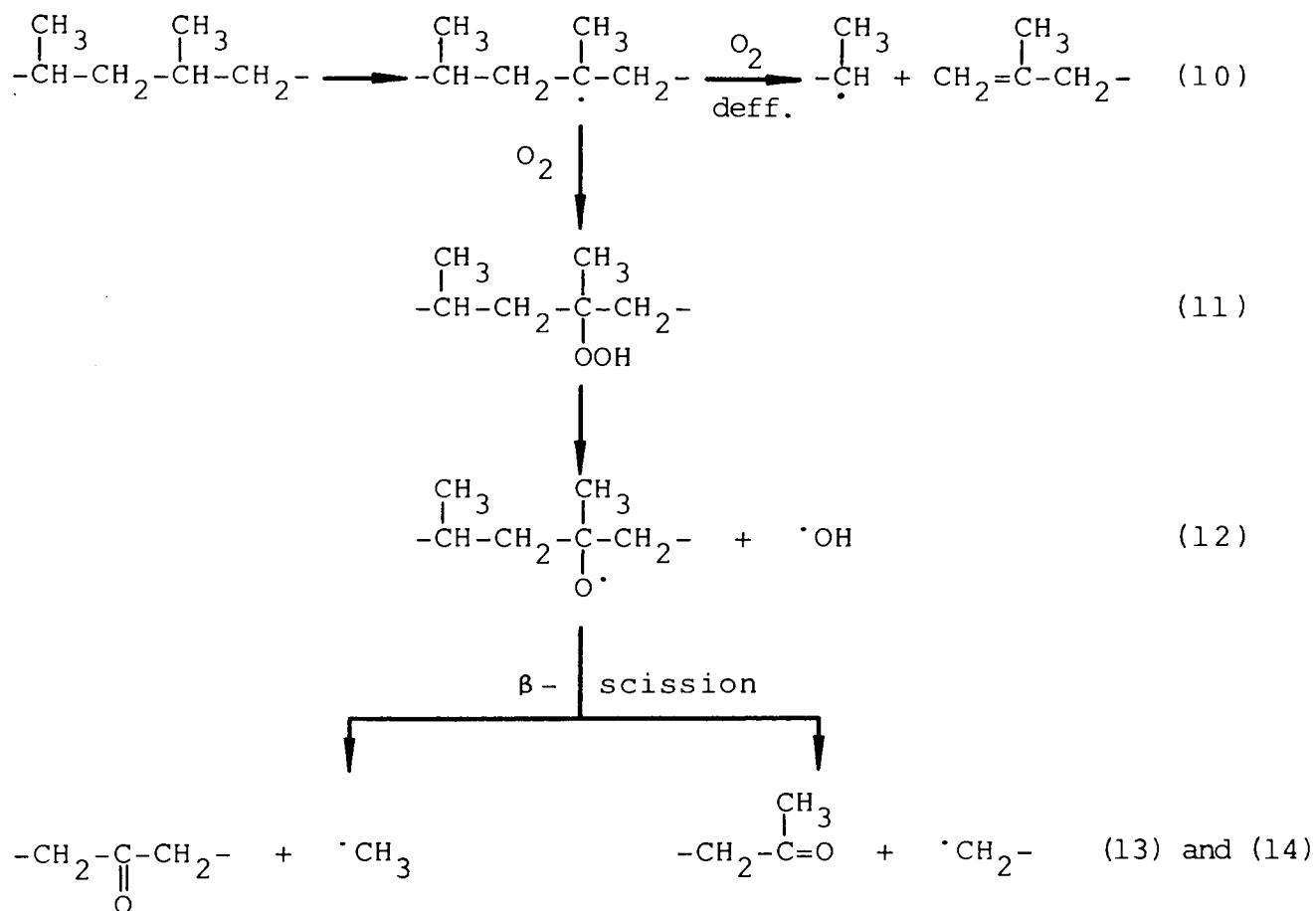


### Termination



Scheme 1.2 Free radical mechanism of polymer degradation

During the processing of polypropylene (e.g., injection moulding) in an oxygen deficient environment, small amounts of hydroperoxide are formed accompanied by a molecular weight decrease due to radical induced depolymerisation<sup>(103)</sup> as shown in Scheme 1.3 (reactions 10 and 11). Evidence from numerous workers<sup>(104-108)</sup> has shown that these polymeric hydroperoxides are responsible for the initial stages of degradation. Once formed in the polymer, cleavage of the O-O bond (especially at elevated temperatures) readily



Scheme 1.3 Polypropylene free radical degradation

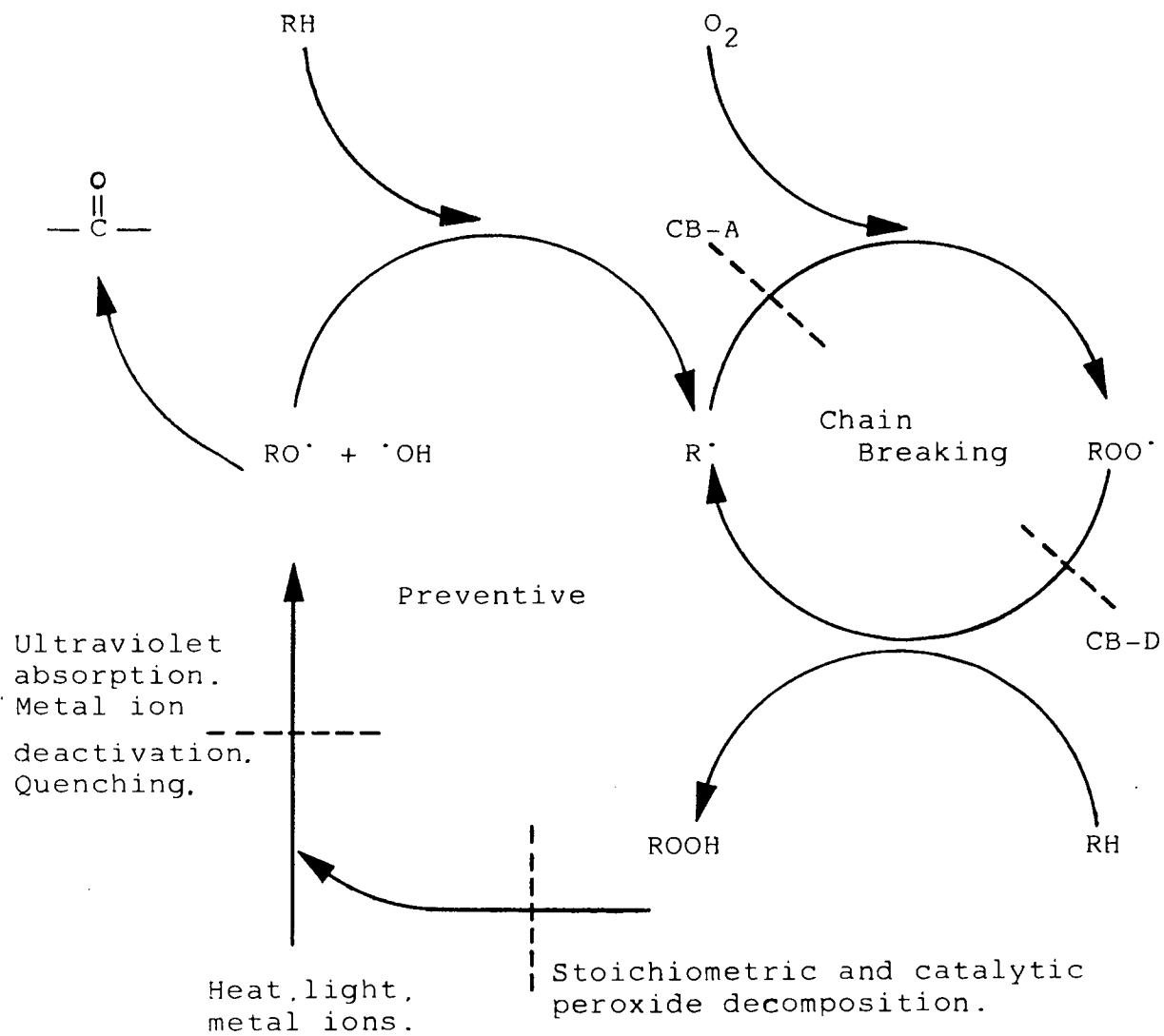
occurs to form reactive alkoxyl radicals (See Scheme 1.3, reaction 12) which can undergo  $\beta$ -scission to give a ketone and a new macro-alkyl free radical<sup>(109-112)</sup> (See Scheme 1.3, reactions 13 and 14), thus decreasing further the molecular weight and creating a new radical which can react with more oxygen to form another hydroperoxide group.

## 1.8 Stabilisation Of Thermoplastics

From 1.7, it follows that polyolefin thermoplastic "under bonnet" components must be protected during melt processing and from in-service thermal-oxidative degradation. Degradation due to ultraviolet radiation does not present a problem because "under bonnet" components operate in darkness.

### 1.8.1 Antioxidant Mechanisms

Polymer degradation proceeds via a free radical process with hydroperoxide formation which by homolysis, gives rise to new radicals that feed the main cycle (See 1.7). The cycle may be broken at two points<sup>(113)</sup>: firstly by chain breaking antioxidants to remove alkyl and alkyl peroxy radicals and secondly by preventive stabilisers that convert radical generating hydroperoxides to non-radical products. Scheme 1.4 shows how and where antioxidants operate in the polymer degradative cycle<sup>(114)</sup>.



Scheme 1.4 Antioxidant mechanisms

### 1.8.2 Chain Breaking Antioxidants

These are usually sterically hindered phenols or amines and were the only class of stabilisers used in this study. They operate by donation of their labile hydrogen in a radical transfer mode. The resultant free radical is delocalised and sterically hindered, thus making further degradation less likely. The degree of antioxidant activity is a function of the ability of the phenol or amine to release a hydrogen atom to alkyl or alkylperoxy radicals. It is important that the antioxidant radical does not contribute further to the degradative process<sup>(115)</sup>. For phenols, the presence of two ortho tert.butyl groups is enough to sterically hinder the phenoxy radical<sup>(115)</sup>. Ease of hydrogen abstraction from phenols and amines is increased by electron releasing groups on the aromatic ring<sup>(116)</sup>.

The chain breaking-donor (CB-D) mechanism is usually observed in hydrocarbons at ambient oxygen pressures because the alkylperoxyl radical is present in highest concentration<sup>(113,117)</sup>. As the oxygen concentration decreases, alkyl termination plays an increasingly important part in uninhibited and inhibited oxidation<sup>(113,118)</sup>. In principle CB-D and chain breaking-acceptor (CB-A) mechanisms may operate together with limited oxygen access<sup>(119)</sup>.

Many commercial systems obtain good long term heat ageing properties by combining a hindered phenol with synergistic



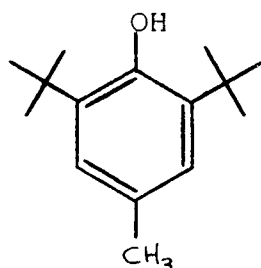
thiodipropionates. The increased stability is due to the eventual formation of sulphur dioxide which catalytically decomposes hydroperoxides to non-radical products<sup>(120,121)</sup>.

### 1.8.3 Melt And Thermal Oxidative Stabilisation

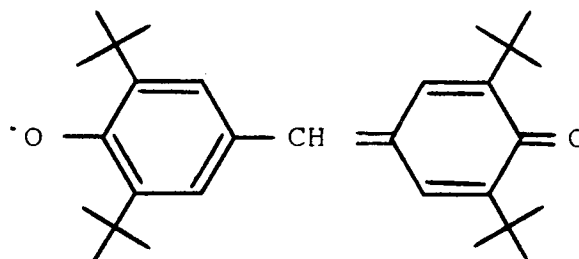
Melt stabilisers are classified according to their interaction with alkyl, alkylperoxy and alkoxy radicals, oxygen and hydroperoxides. Compounds which deactivate alkyl radicals before they react with oxygen are most effective in minimising the reduction of polypropylene molecular weight during melt processing<sup>(122)</sup>. It is important to keep the processing temperature of polypropylene below 270°C otherwise a wide variety of stabilisers become ineffective. This is due to high partial oxygen pressures, alkylperoxy radical formation and subsequent hydroperoxide decomposition taking place so fast that any inhibitor cannot effectively suppress the chain propagation steps<sup>(123)</sup>.

Amongst the best melt stabilisers are those that produce stable free radicals that work in CB-D/CB-A regenerative cycles. BHT(I), a hindered phenol is an effective melt stabiliser acting by a CB-D mechanism, and is rapidly converted to quinonoid oxidation products<sup>(122,124)</sup> which are more effective in melt stabilisation than BHT itself. Galvinoxyl(II) and its phenolic equivalent take part in a CB-D/CB-A cycle by which macro-alkyl and alkylperoxyl

radicals are terminated<sup>(122)</sup>. See Scheme 1.5 for a schematic diagram of the regenerative cycle.



(I) BHT

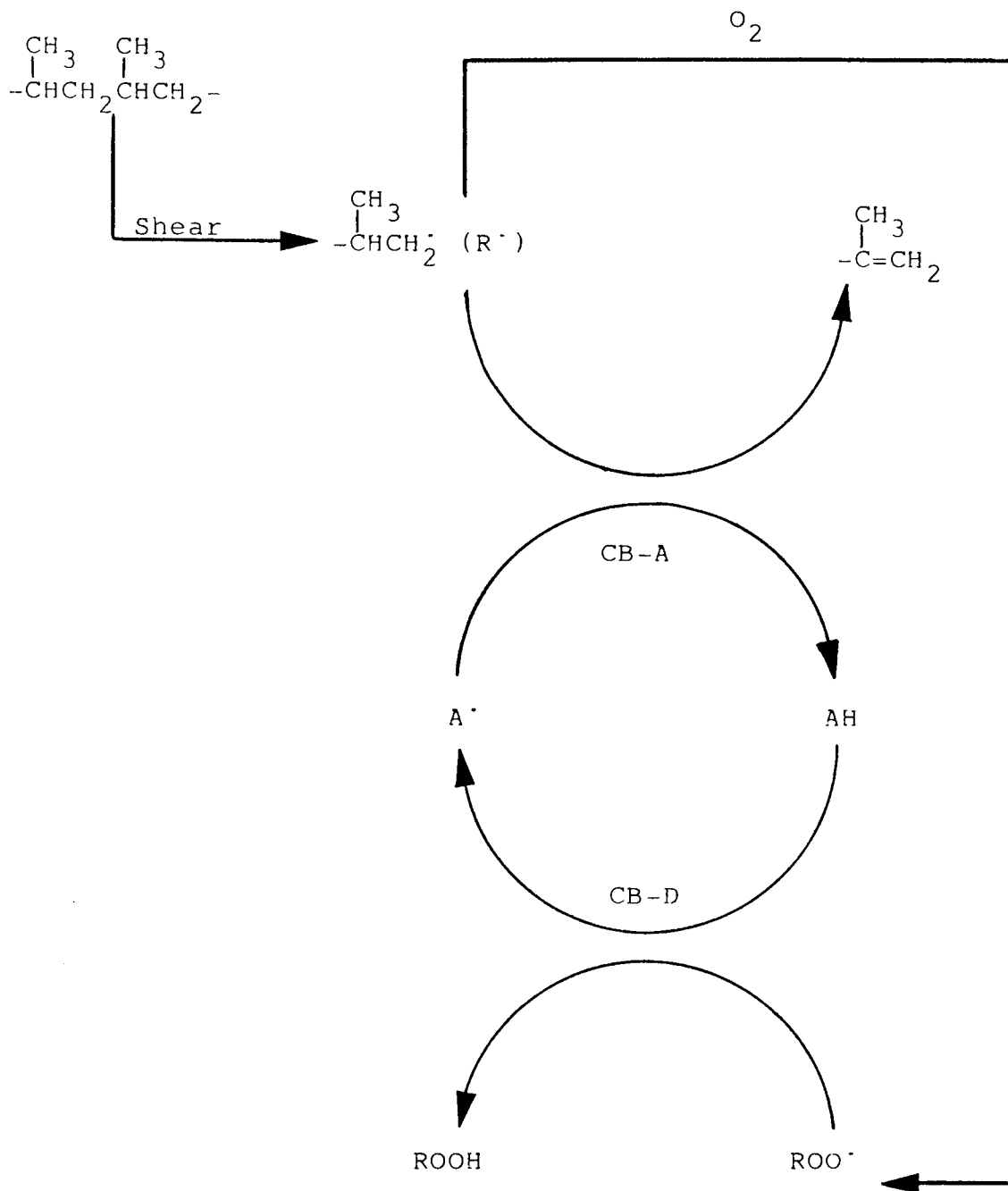


(II) Galvinoxyl

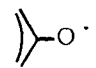
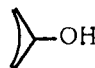
Stable nitroxyl radicals have also been shown to be effective melt stabilisers for polypropylene<sup>(122,125)</sup>. Nitroxyl radicals and their equivalent hydroxylamines constitute an effective CB-D/CB-A redox stabilising system. This is shown in Scheme 1.5.

Work by Lorenz<sup>(126)</sup> on thermal-oxidative stabilisers such as *p*-phenylenediamines has proposed that five or six molecules of oxygen are absorbed per stabilising group (amine) consumed. Work using ESR showed that the regenerative process involving the nitroxyl radical was involved<sup>(126)</sup>.

The ability of an antioxidant to undergo a cyclical regenerative process is advantageous because the number of degradative free radicals terminated per antioxidant molecule is greatly enhanced.



KEY

System	A <sup>·</sup>	AH
Galvinoxyl		
Nitroxyl	$>\text{N}-\text{O} \cdot$	$>\text{N}-\text{OH}$

Scheme 1.5 Catalytic antioxidant mechanism of galvinoxyl and nitroxyl radicals during PP processing

#### 1.8.4 Conflicting Requirements Of Melt And Thermal Oxidative Stabilisers

Any commercial polymer must be able to be processed satisfactorily and possess adequate protection for its in-service environment. Table 1.1<sup>(127)</sup> summarises the properties required for melt and thermal oxidative stabilisers. Many characteristics such as the need for low volatility, melt compatibility and the trapping of alkylperoxy radicals are the same for both types. However, there are some requirements which are different. Melt stabilisers have to be very mobile during processing to terminate as many alkyl free radicals as possible, while thermal oxidative stabilisers need low mobility within the polymer to avoid physical loss during service (See 1.9). Compatibility with solidified polymer is of no importance with melt stabilisers, but good compatibility is desirable for thermal oxidative stabilisers as this reduces the rate of antioxidant loss during service (See 1.9). Melt stabilisers must be active at normal polymer processing temperatures (150-300°C) whereas most thermoplastics are expected to perform at in-service temperatures below 150°C and thus, thermal oxidative stabilisers must be most active in this region.

#### 1.9 Stabiliser Loss From Polymers

One of the main factors contributing to low service lives

Property	Melt stabilisation	Thermal oxidative stabilisation
Mobility.	High	Preferably low
Volatility.	Preferably low	Low
Radical trapping.	-R <sup>•</sup> Yes	Unimportant
	-RO <sub>2</sub> <sup>•</sup> Yes	Yes
RO <sub>2</sub> H decomposer.	Preferably yes	Yes
Oxidation potential.	Low	High
Reaction with O <sub>2</sub> .	Advantageous	Disadvantageous
Polymer-compatibility.	-melt Good	Preferably good
	-solid Unimportant	Must be good
Active range(°C).	High(150-300)	Low(-50-150)

Table 1.1 Conflicting requirements of melt and thermal oxidative stabilisers

of thermoplastics is the physical loss of stabiliser<sup>(128-130)</sup>, especially in hot air and fluid flows found in aggressive "under bonnet" environments. The rate and degree of loss is dependent upon stabiliser compatibility, distribution, volatility and extractability<sup>(131,132)</sup>.

Compatibility represents the totality of effects involved in polymer-additive interaction. It has been shown<sup>(133)</sup> that increasing the alkyl chain length of stabilisers depresses their surface tension, free surface energy and solubility parameters creating a decreased free interfacial surface energy in polypropylene systems. Compatibility is further increased by the substitution of aromatic with aliphatic substituents<sup>(134)</sup>. This is advantageous because the effective area of stabiliser is greater in compatible systems, thus decreasing the probability of non-stabilised sites within the polymer<sup>(134)</sup>. Stabiliser distribution within a semi-crystalline polymer such as polypropylene has been shown by many workers<sup>(135-139)</sup> to be primarily within the amorphous region. This non-uniform distribution is beneficial because it raises stabiliser concentration in the most degradation-sensitive areas.

Volatility loss of stabilisers from polymers has been shown to depend upon temperature<sup>(140-142)</sup>, stabiliser structure and molecular weight<sup>(134,143-147)</sup>, stabiliser concentration and rate of gas flow over the polymer surface<sup>(142)</sup> and to

be inversely proportional to the sample thickness and proportional to its surface area<sup>(134,142)</sup>.

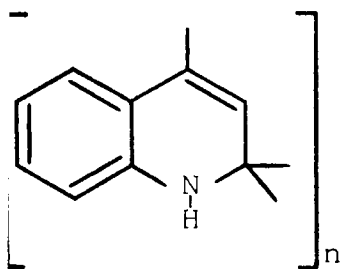
Considerable stabiliser loss may also occur due to extraction (leaching) by liquids, especially at the surface layers which are most sensitive to degradation<sup>(131,132)</sup>. This creates a stabiliser concentration gradient within the polymer.

Weimer and Conner<sup>(148)</sup> have shown that diffusion (the rate of which is influenced by polymer density) then occurs from the bulk to the surface of the polymer, which thus allows for further stabiliser loss from the system.

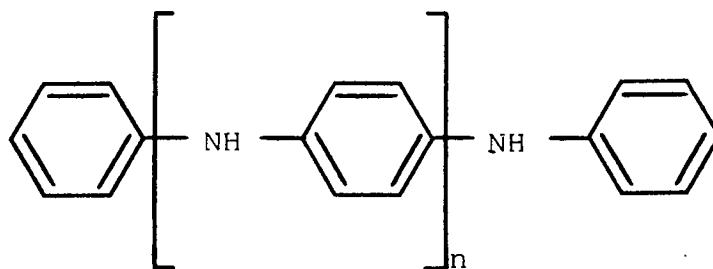
#### 1.9.1 Prevention Of Stabiliser Loss From Polymers

The trend towards the use of polymers in more aggressive environments has led to a search for non-extractable stabilisers. Volatility, migration and leaching may be substantially reduced by using high molecular weight (sometimes polymeric) substantive antioxidants or polymer-bound antioxidants<sup>(149)</sup>.

Effective high molecular weight substantive antioxidants have been used in rubbers<sup>(150)</sup>. Notable amongst these is the use of condensation polymerised 2,4,4-trimethyl-1,2-dihydroquinoline(III). Similarly, Thomas and co-workers at the Royal Aircraft Establishment have used a condensation polymer based on the repeat unit of diaryl- $\rho$ -phenylenediamine (IV)<sup>(151,152)</sup>.

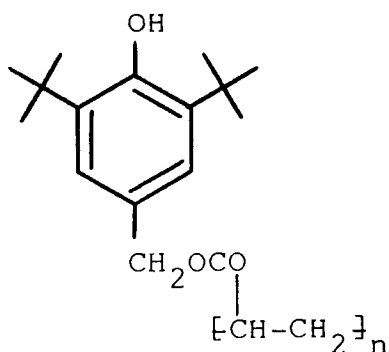


III



IV

Antioxidants possessing a reactive vinyl group like 3,5-di-tert-butyl-4-hydroxybenzylacrylate(V)<sup>(153)</sup> have been polymerised to molecular weights of up to 9.500(Mn).



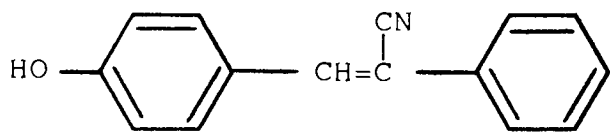
V

Despite substantive antioxidants being much more effective thermal oxidative stabilisers in aggressive environments, chemically bound stabilisers potentially offer the most effective method of protecting a polymer due to improved compatibility, distribution, processability and extractability of such materials.

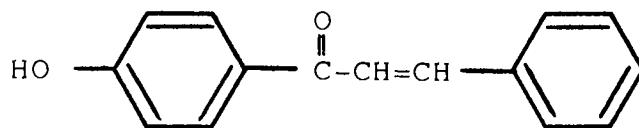
Bound antioxidants may be incorporated into polymers at the various processing stages involved in the manufacture of a final component. For synthetic polymers; the obvious way of introducing antioxidants is via a vinyl group during polymerisation. One of the earliest examples was the incorporation of phenolic groups into rubbers by copolymerisation



of the vinyl monomers (VI and VII) <sup>(154)</sup>.

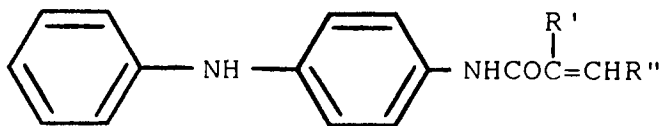


VI

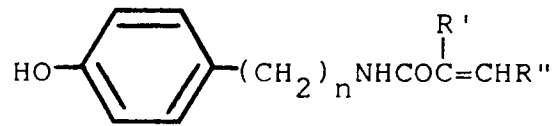


VII

Most of this type of binding has been done by workers at Goodyear to produce commercially modified polymers <sup>(155-158)</sup>. Compounds of the type (VIII and IX) have been successfully used.



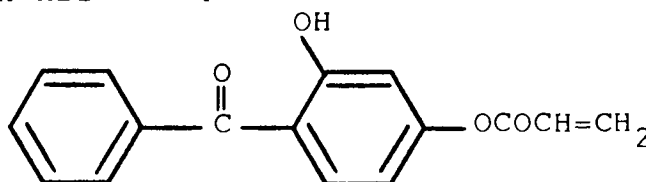
VIII



IX

Horvarth <sup>(158)</sup> successfully used peroxide initiators for vinyl monomers and antioxidants, but serious problems were encountered by other workers <sup>(155)</sup> due to hydrogen abstraction by the peroxides from the phenolic antioxidants.

An example of a polymerisation bound ultraviolet stabiliser used in an engineering polymer is vinyl modified 2-hydroxybenzophenone (X) in ABS <sup>(159)</sup>.

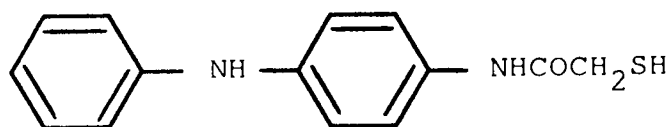


X

The MRPRA <sup>(160,161)</sup> has found that a variety of N-substituted 4-nitroso anilines become chemically bonded during natural

rubber vulcanisation via unsaturation in the carbon backbone. The result is cured rubbers with good thermal oxidative stability in extracting environments<sup>(162,163)</sup>.

Antioxidants have been bound to thermoplastics with some degree of success. Potentially, one of the most cost-effective and commercially useful means of producing polymer-bound stabilisers is by exploiting the production of macro-alkyl free radicals formed during normal mechano-chemical processing. Various workers at the University of Aston in Birmingham have used 4-(1-mercaptoacetylamido)diphenylamine (MADA, XI) in successful mechano-chemical binding using conventional mixing or extrusion techniques with polyethylene<sup>(164)</sup>, polypropylene<sup>(164)</sup>, EPDM<sup>(165)</sup>, NBR<sup>(166)</sup>, SBR<sup>(167)</sup> and natural rubber<sup>(167)</sup>. The degree of MADA binding was shown to be dependent upon processing temperature and time, stabiliser concentration, degree of shear (causing chain scission), and the addition of peroxides to catalyse the free radical binding process. High % binding resulted in good protection of the modified polymers under thermal oxidative attack in extracting environments.



XI MADA

### 1.10 Aim And Scope

The objectives of the research are:

1. To compare the effectiveness of glass fibre (GF) with Rockwool fibre (RWF), a mineral fibre, in the enhancement of polypropylene composite mechanical properties.
2. To improve the mechanical properties of such composites by increasing the interfacial shear strength between the fibre and polymer. This will be attempted by mechano-chemical modification of polypropylene using conventional thermoplastic processing equipment.
3. To develop an efficient stabiliser system to improve the long term performance of reinforced polypropylene under adverse "under bonnet" conditions. To avoid in-service stabiliser loss, polymer-bound antioxidants will be prepared by mechano-chemical binding, again using conventional thermoplastic processing equipment.

At each stage of development, direct comparisons will be made with currently available commercial materials.

These properties are required to obtain a composite of sufficient mechanical properties, chemical resistance and thermal oxidative stability to give a service life of 3,000

hours under stress at temperatures up to 150°C in an "under-bonnet" environment.

Inorganic fibres (e.g., glass and mineral fibres) are normally modified with organic reagents (e.g., silane coupling agents) to make their high surface energies more compatible with low surface energy organic polymers. With chemically inert polymers such as polypropylene, adhesion between the two phases must be further promoted by chemical modification of the polymer; chemical modifiers are chosen such that they have on the one hand a functional group which can chemically graft during processing to the polymer backbone in the presence of free radical initiators, and on the other hand, possess functionality that allows the grafted modifier to react chemically with the organic function (e.g., amino group) present on the silane coupling agent. Formation of a continuous chemical link between the polymer matrix and reinforcing fibre surface increases their interfacial shear strength, resulting in improved composite mechanical properties.

When high temperature thermal-oxidative stability and permanence are required, antioxidants are chosen such that they can be chemically linked to the polymer backbone, in a way similar to that described above. Chain breaking antioxidants (e.g., diarylamines) were chosen and modified in such a way to allow them to graft to the polymer without losing their antioxidant function, and hence offer high stability under the aggressive environments (e.g., hot fluid and air flows) found in "under-bonnet" applications.

CHAPTER TWO

EXPERIMENTAL

## 2.1 Materials

### 2.1.1 Polymeric Materials

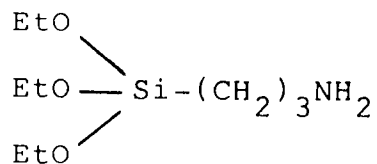
Four different grades of polypropylene, all supplied by Imperial Chemical Industries Ltd., were used in this work. These are described in Table 2.1.

Ethylene propylene diene monomer (EPDM) was used as supplied by Exxon Chemicals Ltd, as Vistalon 6505. This combines high chemical unsaturation with good resistance to heat, weathering and sunlight, and excellent processing behaviour.

### 2.1.2 Fibres

#### 2.1.2.1 Glass Fibre (GF)

The glass fibre used was supplied by Fibre Glass Ltd., as FG CS 1640. This grade uses borosilicate low alkali 'E' type glass and is coupled with A-1100 silane (aminopropyltriethoxysilane, I, Union Carbide). It is commercially used for incorporation into nylons and polyolefins to produce glass reinforced composites. Characteristics of this GF grade are described in Table 2.2. The tough resilient size coating affords advantageous feeding and flow properties during compounding (see Plate 2.3).



I

#### 2.1.2.2 Rockwool Fibre (RWF)

Rockwool fibre, manufactured by Laxa Bruk of Sweden, is a deshotted mineral fibre produced from spun limestone, diabase and coke. It is also referred to as Inorphil fibre. The fibres are immediately surface treated with a layer of 'tenside' to ensure good fibre dispersion. Laxa Bruk are not prepared to disclose the chemical nature of the 'tenside' layer. The fibre is available with A-1100 silane coupling agent. RWF is presently used as a filler for paper and road asphalt and as an asbestos substitute<sup>(168)</sup>. Characteristics of RWF are described in Table 2.3.

Two grades of RWF were used, one short (SRWF) and one long (LRWF) grade, both A-1100 silane coupled over a 'tenside layer'.

##### (a) Short RWF (SRWF)

Weight average length, 0.39mm.

Number average length, 0.27mm.

See Plate 2.1.

ICI Code Name	MFI (g/10min, 230°C, 2.16kg)	Description
Propathene HF22	5.0	Unstabilised powder.
Propathene HWM25	4.5	Highly stabilised injection moulding grade granules.
Propathene GWM22	4.5	Medium stabilised injection moulding grade granules.
Propathene HW60 GR30	-	30% coupled glass reinforced stabilised injection moulding grade granules.

Table 2.1 Polypropylene grades

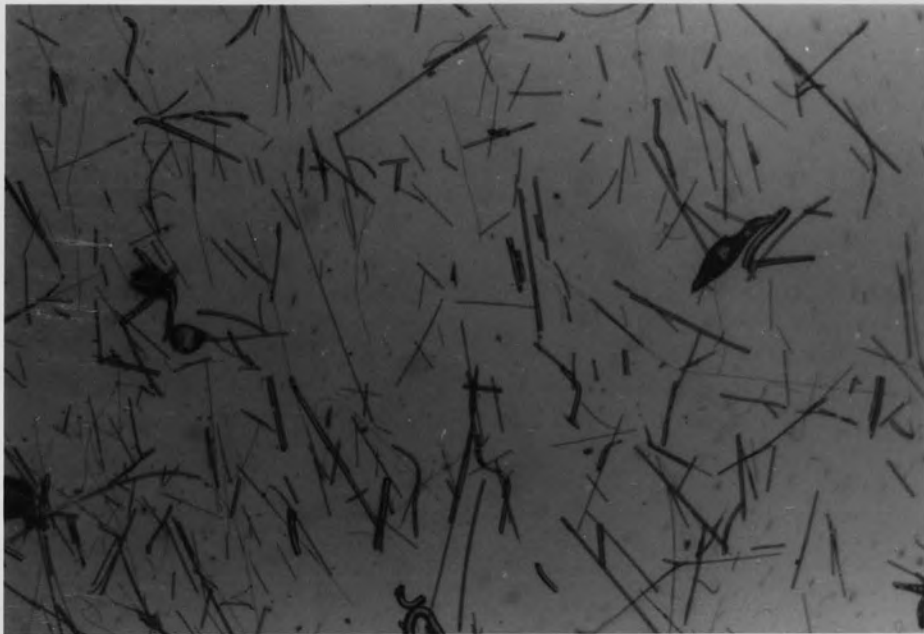


Chemical constitution	B(3.4%), Ca(1.9%), O(61.2%), F(1.4%), Mg(0.6%), Al(7.0%), Si(24.3%)
Fibre diameter	10µm
Fibre length	3mm (weight average) 3mm (number average)
Split strand tex	95tex
Moisture content	0.2%(maximum)
Size content	1.4%±0.2%
Coupling agent	Union Carbide A-1100(aminopropyltriethoxysilane)

Table 2.2 Glass fibre properties and constitution

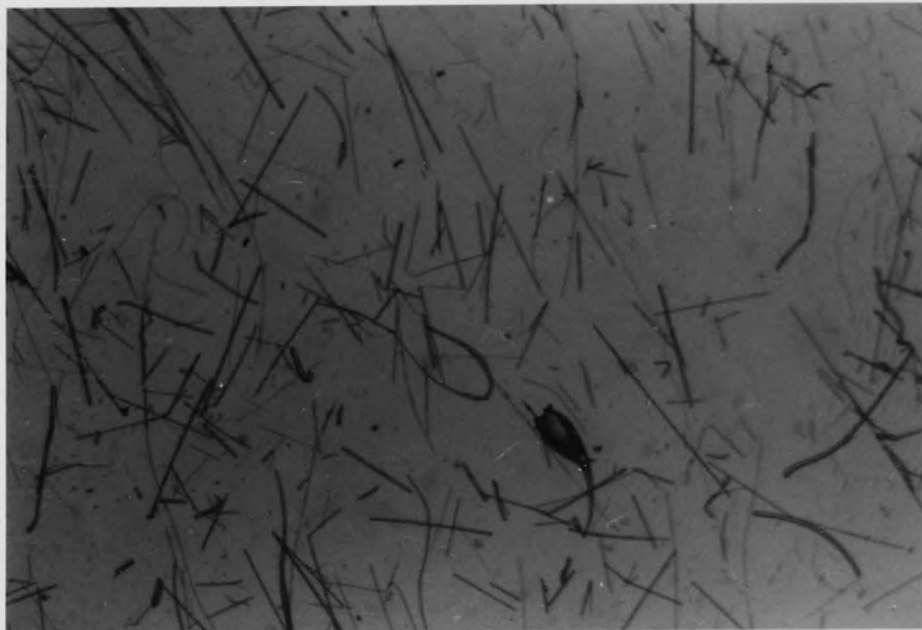
Chemical constitution	SiO(46%), CaO(16%), MgO(12%), Al <sub>2</sub> O <sub>3</sub> (15%), Na <sub>2</sub> O(2.5%), TiO(1.5%), Fe oxides(6.5%), Others(0.5%)
Fibre diameter	4-6µm
Density	2.65g/cm <sup>3</sup>
Thermal stability	>1000°C
Softening point	1200°C
Acid stability	To pH4
Alkaline stability	To pH10
Coupling agent	A-1100 (Union Carbide)

Table 2.3 Rockwool fibre properties and constitution



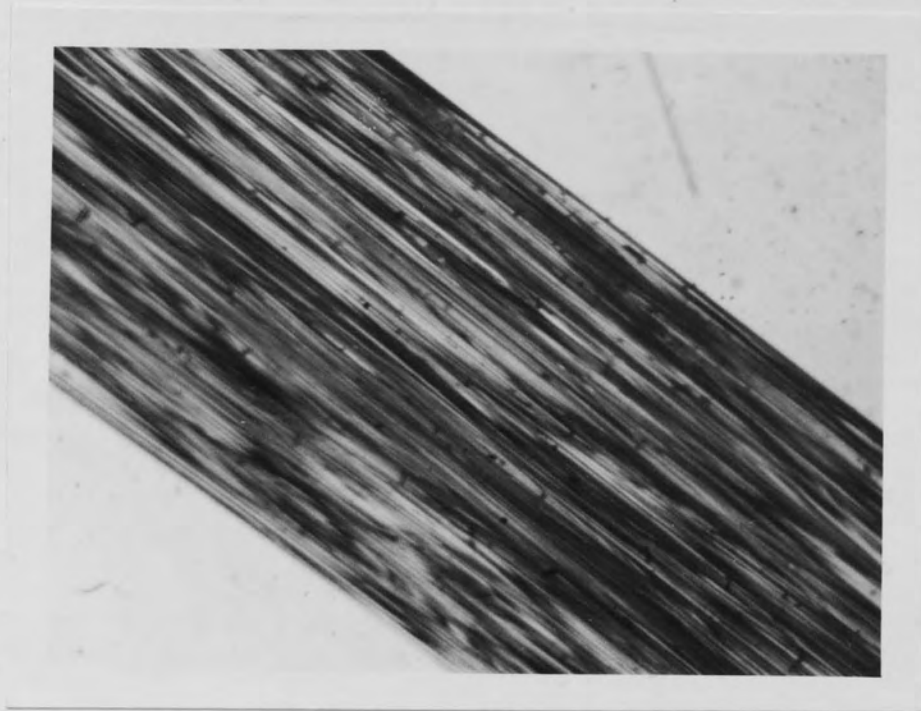
0.5mm

Plate 2.1 Optical micrograph of short Rockwool fibre before processing



0.5mm

Plate 2.2 Optical micrograph of long Rockwool fibre before processing



0.5mm

Plate 2.3 Optical micrograph of glass fibre before processing



(b) Long RWF (LRWF)

Weight average length, 1.10mm

Number average length, 0.64mm

See Plate 2.2

2.1.3 Commercial Antioxidants and Chemicals

Two commercial antioxidants based on sterically hindered phenols were used, Irganox 1076 (I) and Irganox 1010 (II), both supplied by Ciba Geigy (see Table 2.4). Ultraviolet and infra-red spectra are shown in Figures 2.1 and 2.2 with data shown in Table 2.7A. p-Aminodiphenylamine (III, Table 2.4) was supplied by Aldrich Chemical Co. Ltd., with a minimum assay of 98%. See Figures 2.3 and 2.4 and Table 2.7A, for ultraviolet and infra-red spectral characteristics.

Maleic anhydride (IV, Table 2.5) was supplied in briquette form by Aldrich Chemical Co. Ltd., with a purity of 99.5% and was used later for chemical modification of polypropylene. See Table 2.7A and Figures 2.5 and 2.6 for ultraviolet and infra-red spectra.

Cyanuric chloride (V, Table 2.5) supplied by Lancaster Synthesis had a minimum assay of 98% and was used as supplied.

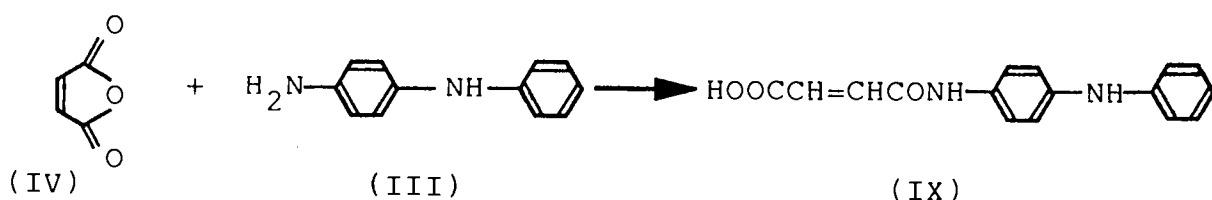
Allylamine (VI, Table 2.5) supplied by Aldrich Chemical Co. Ltd., had a minimum assay of 98% and was used without further purification.

Succinic anhydride (VII, Table 2.5) was used as supplied by BDH with a minimum assay of 99%.

Di-cumyl peroxide (VIII, Table 2.5) was used as supplied by BDH with a minimum assay of 90%.

#### 2.1.4 Synthesised Additives

##### 2.1.4.1 Synthesis Of N-(4-Anilinophenyl)maleamic Acid<sup>(169)</sup> (APMA, IX, Table 2.6)

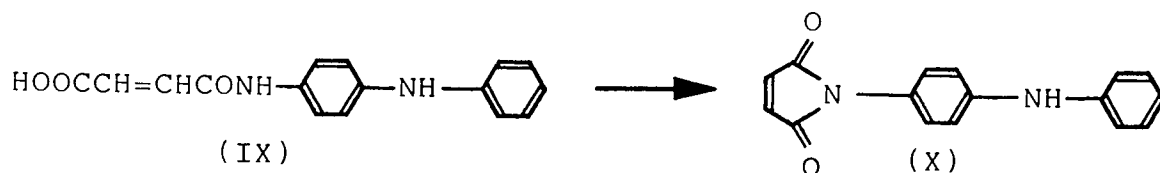


19.6g (0.2 moles) of maleic anhydride (IV) and 36.8g (0.2 moles) of p-aminodiphenylamine (III) were dissolved in 250 ml chloroform. The resultant orange precipitate (IX) was filtered off after 30 minutes, washed with chloroform and dried at room temperature under vacuum to give a yield of 90% with a melting point of 183°C (Lit.184°C<sup>(169)</sup>).

See Table 2.7B and Figures 2.7 and 2.8 for ultraviolet and infra-red data and spectra, and Table 2.8 for elemental analysis.

#### 2.1.4.2 Synthesis Of N-(4-Anilinophenyl)maleimide <sup>(169)</sup>

(APM, X, Table 2.6)

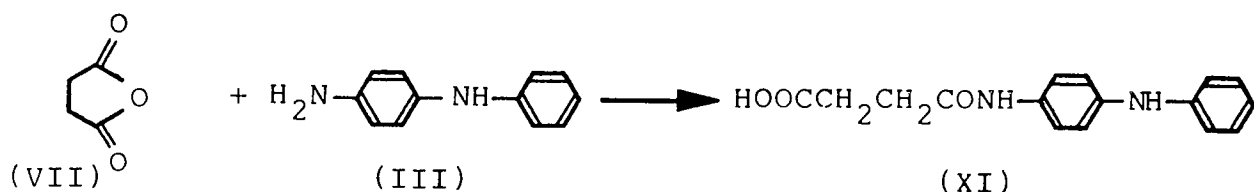


50g (0.177 moles) of N-(4-anilinophenyl)maleamic acid (IX) was dissolved in 200 ml of acetic anhydride at 70°C with 11g (0.14 moles) of sodium acetate. After 10 minutes, the solution was poured into cold water. The resultant scarlet precipitate (X) was filtered off, washed with cold methanol and dried at room temperature under vacuum to give a yield of 70% with a melting point of 165°C (Lit. 160°C<sup>(169)</sup>).

See Table 2.7B and Figures 2.9 and 2.10 for ultraviolet and infra-red data and spectra, and Table 2.8 for elemental analysis.

#### 2.1.4.3 Synthesis Of N-(4-Anilinophenyl)succinamic Acid <sup>(169)</sup>

(APSA, XI, Table 2.6)



10g (0.1 moles) of succinic anhydride (VII) and 18.4g (0.1 moles) of p-aminodiphenylamine (III) were dissolved in 200 ml chloroform. The solution was refluxed for 30

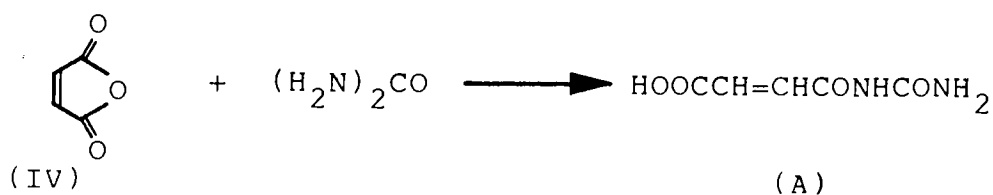
minutes. After cooling to room temperature, the white precipitate (XI) was filtered off, washed with cold chloroform and dried under vacuum to give a yield of 75% with a melting point of 154°C.

See Table 2.7B and Figures 2.11 and 2.12 for ultraviolet and infra-red data and spectra, and Table 2.8 for elemental analysis.

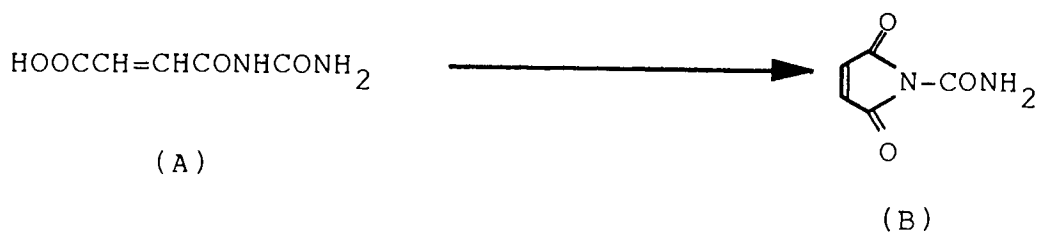
#### 2.1.4.4 Synthesis Of Maleimide<sup>(170)</sup> (MAL, XII, Table 2.6)

The following three stage process was used in the synthesis of maleimide:

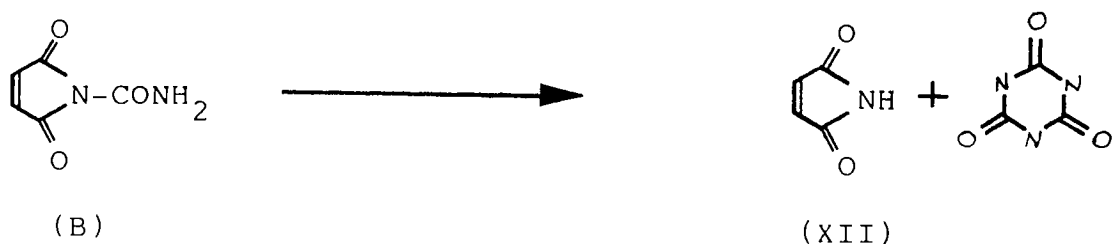
##### Step 1



##### Step 2



##### Step 3





### Step 1 N-Carbamylmaleamic acid (A)

98g (1 mole) of maleic anhydride (IV) and 60g (1 mole) of urea were dissolved in 500 ml glacial acetic acid at 55°C. The solution was left for 12 hours to give a white precipitate of N-carbamylmaleamic acid. This was filtered off and washed with glacial acetic acid and dried at 50°C under vacuum. The yield was 80% and melting point 159°C (Lit. 160°C<sup>(170)</sup>). The product (A) was used for Step 2 without further purification.

### Step 2 N-Carbamylmaleimide (B)

158g (1 mole) of N-carbamylmaleamic acid (A) was dissolved in 500 ml acetic anhydride at 90°C. After 30 minutes, the solution was cooled to room temperature and the white precipitate filtered off and washed with cold acetone. The yield was 70% and melting point 157-158°C (Lit. 157°C<sup>(170)</sup>). The product (B) was used for Step 3 without further purification.

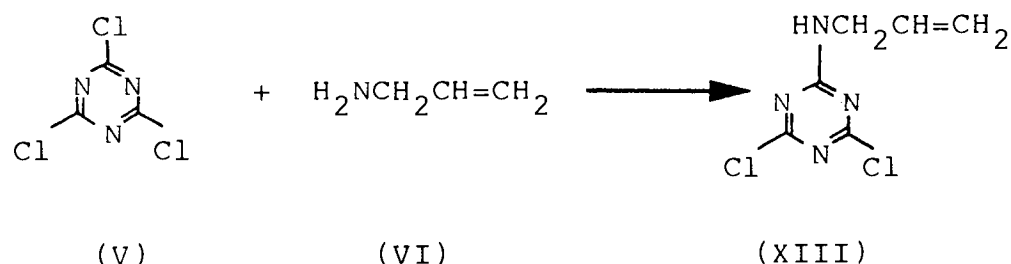
### Step 3 Maleimide (MAL, XII, Table 2.6)

To 300 ml of di-methyl formamide (DMF) at 90-95°C above an oil bath was slowly added 140g (1 mole) of N-carbamylmaleimide (B). During the exothermic period that followed, a maximum temperature of 105°C was recorded, after which 90-95°C was maintained for one hour. After cooling

to room temperature, cyanuric acid was filtered off and DMF removed under vacuum. The product (XII) was purified by distillation under 5mm Hg pressure at 100°C to give crude maleimide which was recrystallised once from ethyl acetate to give a 10% yield and melting point of 92°C (Lit. 94°C<sup>(170)</sup>).

See Table 2.7B and Figures 2.13 and 2.14 for ultraviolet and infra-red data and spectra, and Table 2.8 for elemental analysis.

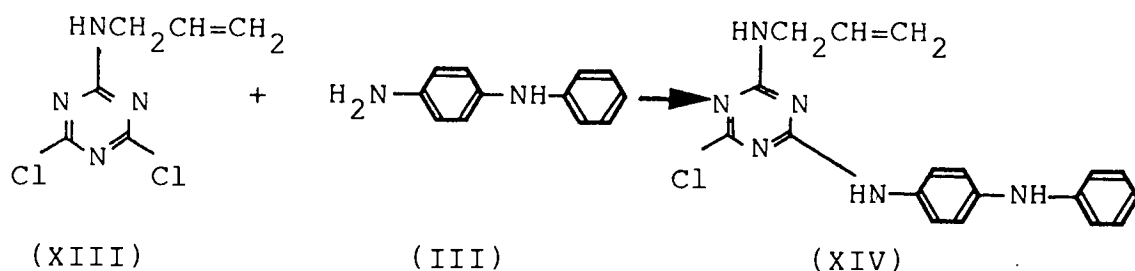
2.1.4.5 Synthesis Of 2N-Allylamino-4,6-dichloro-1,3,5-triazine<sup>(171)</sup> (ADCT, XIII, Table 2.6)



18.4g(0.1 mole) of cyanuric chloride (V) was dissolved in 200 ml of acetone. The solution was cooled over ice-water to 0°C. 11.4g (0.2 moles) of allylamine (VI) was slowly added at a rate whilst stirring to keep the temperature below 5°C. The excess amine was used to neutralise the HCl produced. After 30 minutes, the resultant white precipitate (XIII) was filtered off, washed with cold acetone and vacuum dried. The yield was 85% and melting point 196-198°C.

See Table 2.7B and Figures 2.15 and 2.16 for ultraviolet and infra-red data and spectra, and Table 2.8 for elemental analysis.

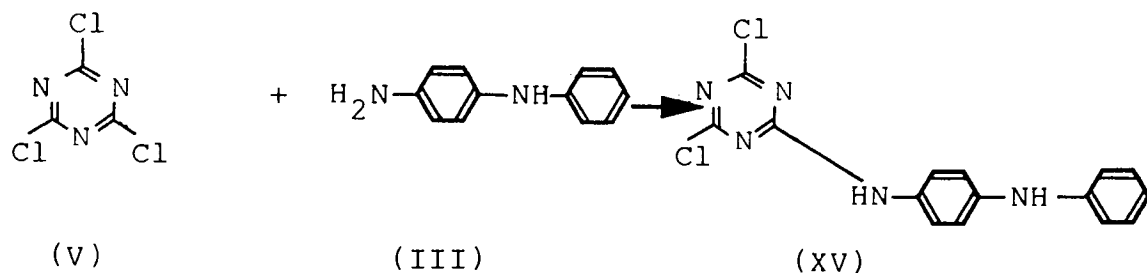
2.1.4.6 Synthesis Of 2N-Allylamino-4-(N-4-aminodiphenylamine)-6-chloro,1,3,5-triazine<sup>(171)</sup> (AACT,XIV, Table 2.6)



20.5g (0.1moles) of 2N-allylamino-4,6-dichloro-1,3,5-triazine (XIII) was dissolved in 200 ml of acetone and heated to 45°C. 18.4g (0.1 moles) of p-aminodiphenylamine (III) in acetone and 0.1 moles of aqueous sodium hydroxide were slowly added. The mixture was refluxed for one hour at 55°C. After cooling to room temperature, the resultant green precipitate (XIV) was filtered off, washed with water, followed by hexane and vacuum dried at 40°C. The yield was 75% and melting point 62-63°C.

See Table 2.7B and Figures 2.17 and 2.18 for ultraviolet and infra-red data and spectra, and Table 2.8 for elemental analysis.

2.1.4.7 Synthesis Of 2N-(4-Aminodiphenylamine)-4,6-dichloro-1,3,5-triazine<sup>(171)</sup> (ADDT, XV, Table 2.6)



18.4g (0.1 moles) of cyanuric chloride (V) was dissolved in 200 ml acetone. After cooling over ice-water to 0°C, 18.4g (0.1 moles) of p-aminodiphenylamine (III) in acetone and 0.1 moles of aqueous sodium hydroxide (at 0°C) were slowly added whilst stirring to keep the temperature below 10°C. After one hour, the resultant green precipitate (XV) was filtered off, washed with water, followed by hexane and vacuum dried. The yield was 80% and melting point 150-152°C.

See Table 2.7B and Figures 2.19 and 2.20 for ultraviolet and infra-red data and spectra, and Table 2.8 for elemental analysis.

## 2.2 Composite Production

### 2.2.1 Homogenisation Of Additives And Fibres For Polypropylene Composites

A laboratory scale Buss Ko-Kneader (Model PR46) was used

No.	Code Name	Structure	M.P. (°C)	Chemical Name	Mol. Wt.
I	Irg.1076		49-54	Octadecyl 3-(3,5 di-tert.butyl-4-hydroxyphenyl)-propionate	531
II	Irg.1010		110-125	Pentaerythryl-tetrakis-[3-(3,5-di-tert.butyl-4-hydroxyphenyl)propionate]	1178
III	ADPA		68-74	p-Aminodiphenylamine	184

Table 2.4 Commercial Antioxidants

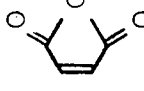
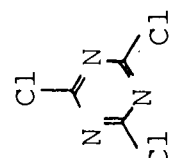

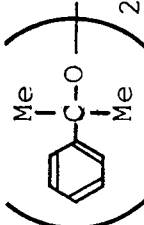
No.	Code Name	Structure	M.P. (°C)	Chemical Name	Mol. Wt.
IV	MA		54-56	Maleic anhydride	98
V	CC		146-148	2,4,6-Trichloro-1,3,5-triazine (cyanuric chloride)	184
VI	AA	$H_2NCH_2CH=CH_2$	53 (b.p.)	Allylamine	57
VII	SA		116-120	Succinic anhydride	100
VIII	DCP		—	Di-cumyl peroxide	270

Table 2.5 Commercial chemicals

No.	Code Name	Structure	M.P. (°C)	Chemical Name	Mol. Wt.
IX	APMA		183	N-(4-Anilinophenyl)maleamic acid	282
X	APM		165	N-(4-Anilinophenyl)maleimide	264
XI	APSA		154	N-(4-Anilinophenyl)-succinamic acid	284
XII	MAL		92	Maleimide	97
XIII	ADCT		196-198	2N-Allylamino-4,6-dichloro-1,3,5-triazine	205
XIV	AACT		62-63	2N-Allylamino-4-(N-4-amino-diphenylamine)-6-chloro-1,3,5-triazine	353
XV	ADDT		150-152	2N-(4-Aminodiphenylamine)-4,6-dichloro-1,3,5-triazine	332

Table 2.6 Synthesised additives

No.	Code Name	Ultraviolet Data			Infra-red Data ( $\text{cm}^{-1}$ )
		Solvent	$\lambda_{\text{nm(max)}}$	log E	
I+II	Irg 1010+1076	HF22 PP film	220	-	1740(m):carbonyl
			275	-	
III	ADPA	95%EtOH	208	4.13	1590(s):aromatic amine
			286	4.30	
IV	MA	MeOH	225	3.40	1782(s),1792(s),1880(m): chemically coupled carbonyl

Table 2.7A Infra-red and ultraviolet data of commercial additives



No.	Code Name	Ultraviolet Data			Infra-red Data ( $\text{cm}^{-1}$ )	
		Solvent	$\lambda_{\text{max}}$ (nm)	log E		
IX	APMA	95%EtOH	216 283 353	4.24 4.23 3.90	1590(m):aromatic amine 1630(w):alkene unsaturation 1700(s):conjugation carbonyl	
X	APM	95%EtOH	208 284 448	3.94 4.00 4.04	1760(s),1780(s),1880(m):coupled carbonyl 1590(s):aromatic amine	
XI	APSA	95%EtOH	208 298	4.06 4.25	1640(s),1690(s),1880(w):carbonyl 1590(s):aromatic amine	
XII	MAL	MeOH	234 275	2.66 2.50	1720(s),1880(w):coupled carbonyl	
XIII	ADCT	MeOH	230 265	2.29 2.35	1795(w):unknown 1635(m):N-H bond 1565(m):aromatic C-N	
XIV	AACT	MeOH	228 313	3.45 3.46	1570(m):aromatic C-N 1602(m):aromatic amine 1630(m):N-H bond (allyl amine)	
XV	ADDT	95%EtOH	211 236 274 324	3.84 3.81 3.93 4.05	1590(s):aromatic amine 3100-3500(m):amine stretch	

Table 2.7B Infra-red and ultraviolet data of synthesised compounds

No.	Code Name	Formula	C%		H%		N%	
			Calc.	Found	Calc.	Found	Calc.	Found
IX	APMA	$C_{16}H_{14}N_2O_3$	68.08	68.96	4.96	4.87	9.93	10.14
X	APM	$C_{16}H_{12}N_2O_2$	72.73	72.16	4.54	4.14	10.60	10.15
XI	APSA	$C_{16}H_{16}N_2O_3$	67.60	68.56	5.64	5.71	9.86	9.52
XII	MAL	$C_4H_3NO_2$	49.48	49.01	3.09	3.42	14.43	14.50
XIII	ADCT	$C_6Cl_2H_6N_4$	35.12	34.76	2.93	2.91	27.32	27.89
XIV	AACT	$C_{18}ClH_{17}N_6$	61.20	62.01	4.82	5.21	23.79	23.75
XV	ADDT	$C_{15}Cl_2H_{11}N_5$	54.21	55.93	3.31	3.35	21.08	22.79

Table 2.8 Elemental analysis of synthesised compounds

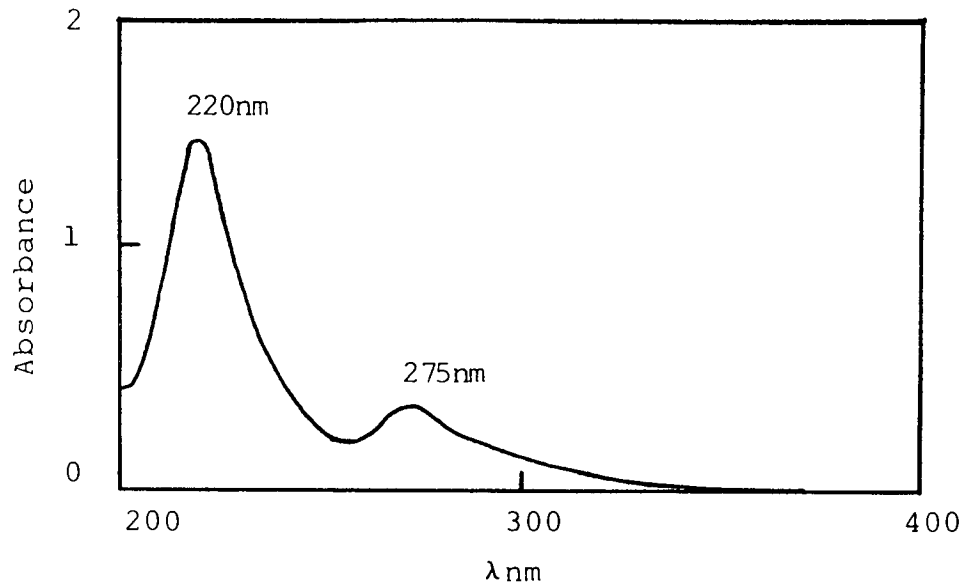


Figure 2.1 Ultraviolet spectrum of Irganox 1010 and 1076(0.5%) in PP(HF22, 200µm film, ref. PP). (Torque rheometer, CM, 8mins, 180°C, 60rpm).

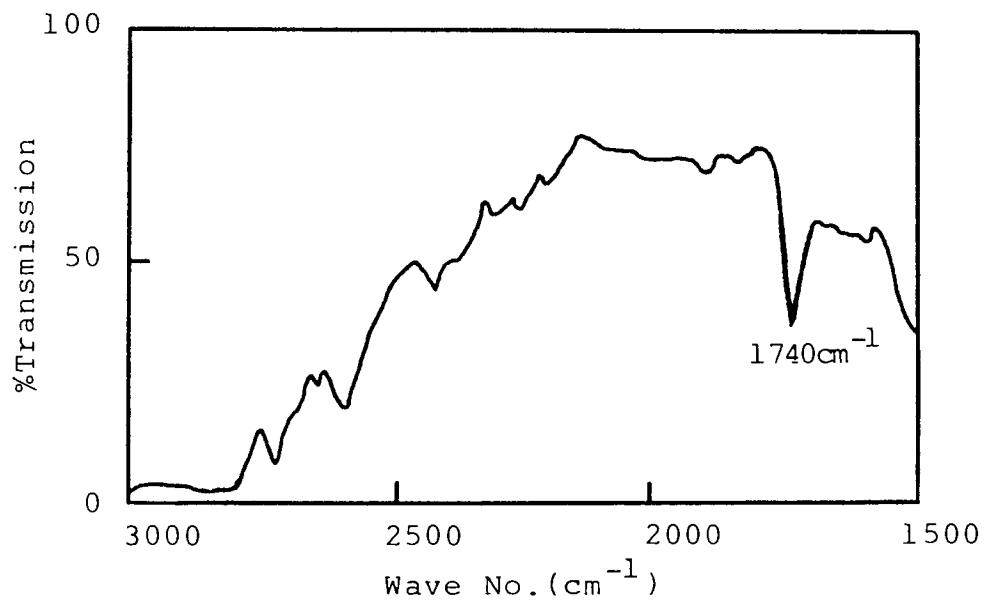


Figure 2.2 Infra-red spectrum of Irganox 1010 and 1076(0.5%) in PP(HF22, 200µm film, ref. air). (Torque rheometer, CM, 8mins, 180°C, 60rpm).

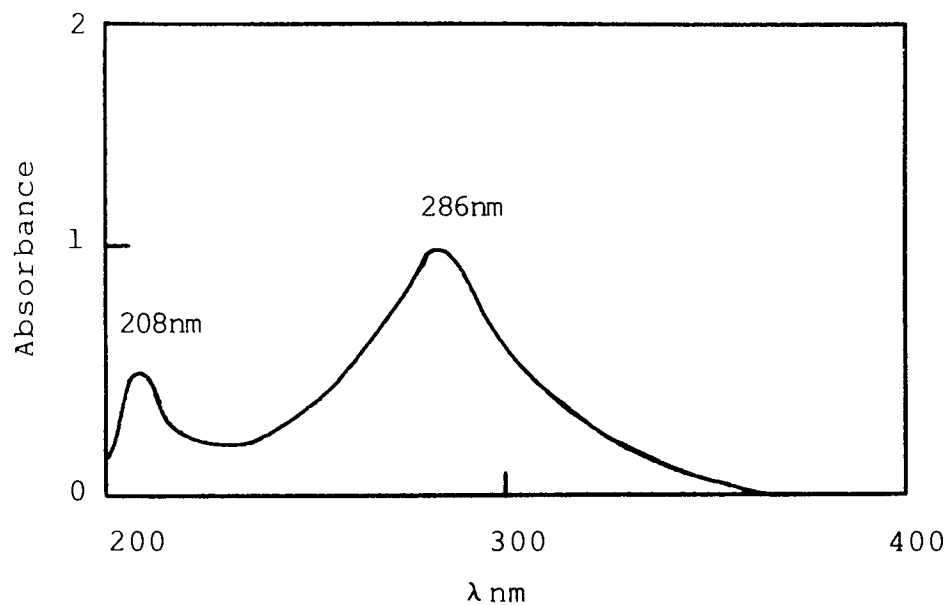


Figure 2.3 Ultraviolet spectrum of ADPA ( $4 \times 10^{-5} \text{ mol dm}^{-3}$ ) in ethanol (ref. ethanol).

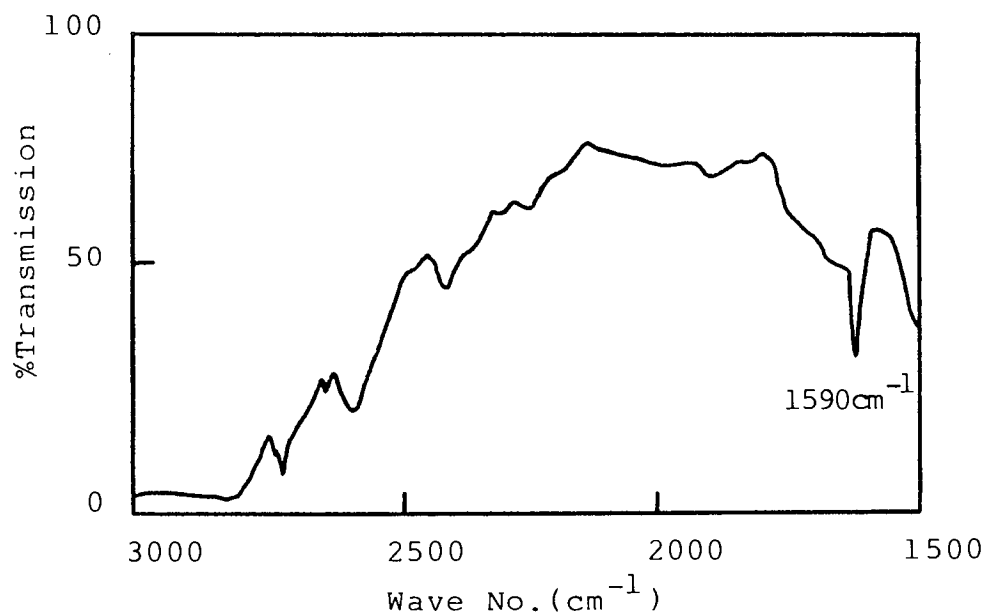


Figure 2.4 Infra-red spectrum of ADPA(1%) in PP(HF22, 200 $\mu\text{m}$  film, ref. air). (Torque rheometer, CM, 8mins, 180 $^{\circ}\text{C}$ , 60rpm).

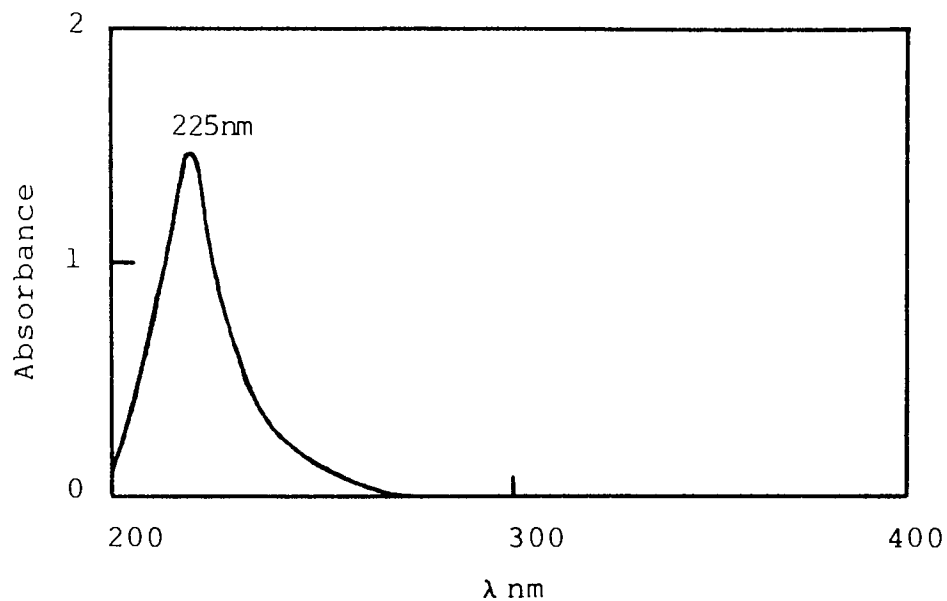


Figure 2.5 Ultraviolet spectrum of maleic anhydride ( $6 \times 10^{-4} \text{ mol dm}^{-3}$ ) in methanol (ref. methanol).

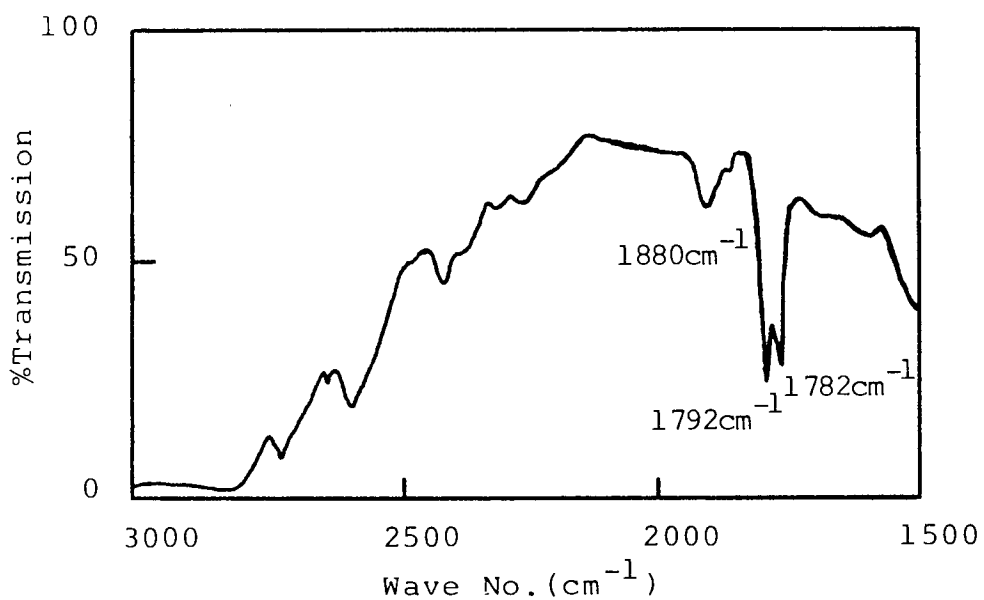


Figure 2.6 Infra-red spectrum of maleic anhydride (1%) in PP (HF22, 200  $\mu\text{m}$  film, ref. air), (Torque rheometer, CM, 8 mins, 180 $^{\circ}$ C, 60 rpm).

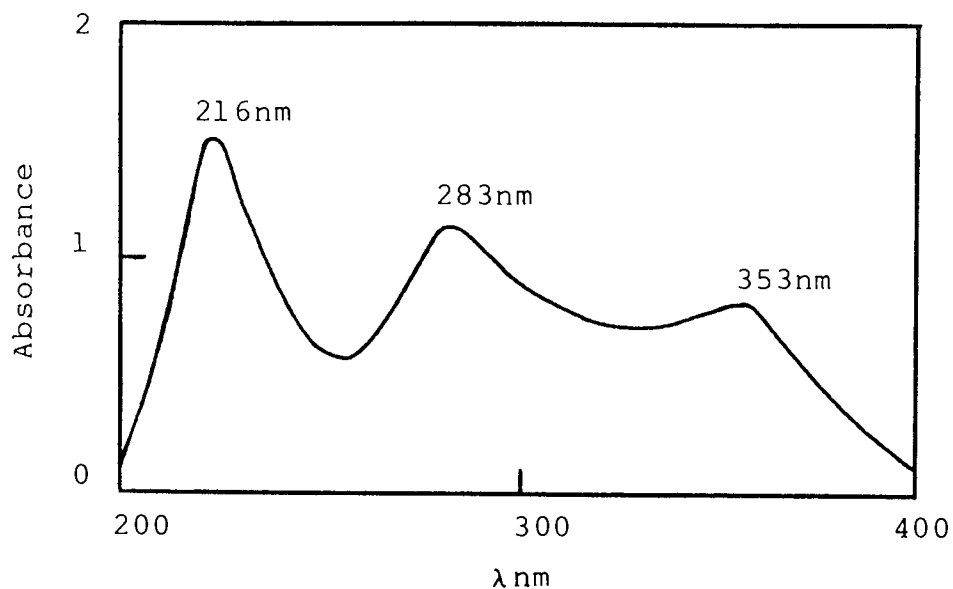


Figure 2.7 Ultraviolet spectrum of APMA ( $4 \times 10^{-5} \text{ mol dm}^{-3}$ ) in ethanol (ref. ethanol).

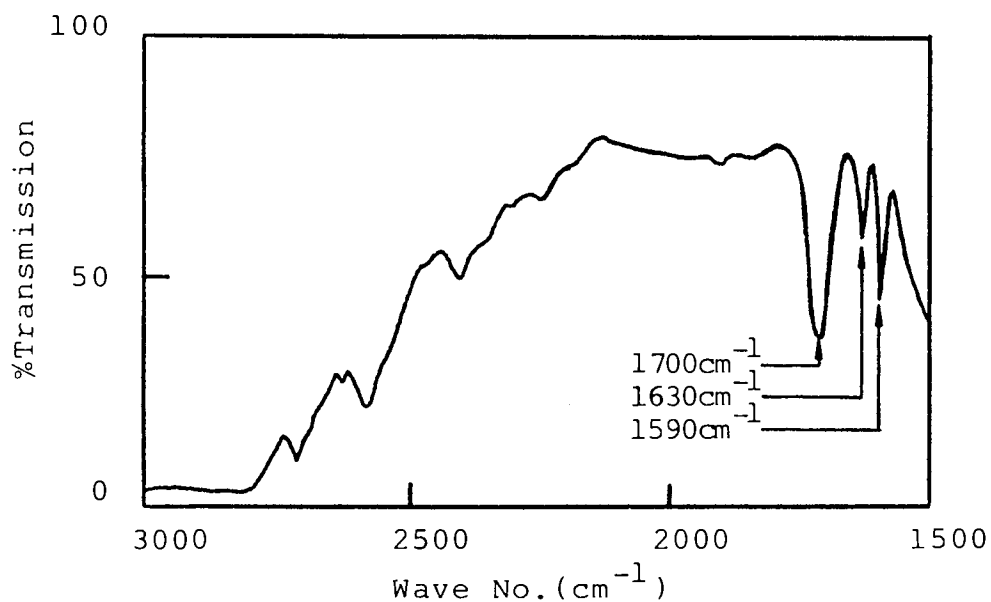


Figure 2.8 Infra-red spectrum of APMA(1%) in PP (HF22, 200 μm film, ref. air). (Torque rheometer, CM, 8 mins, 180°C, 60 rpm).

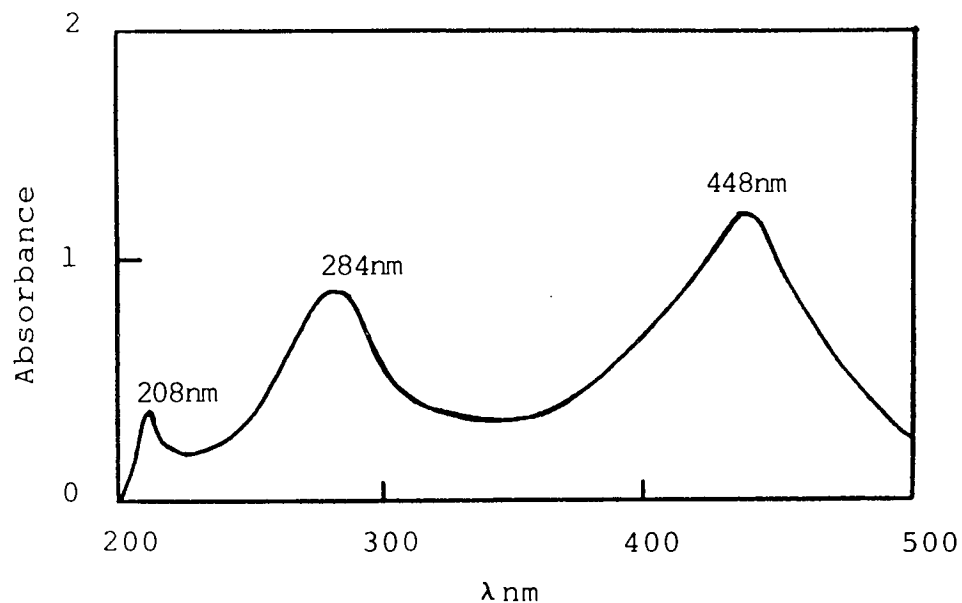


Figure 2.9 Ultraviolet spectrum of APM ( $4 \times 10^{-5} \text{ mol dm}^{-3}$ ) in ethanol (ref. ethanol).

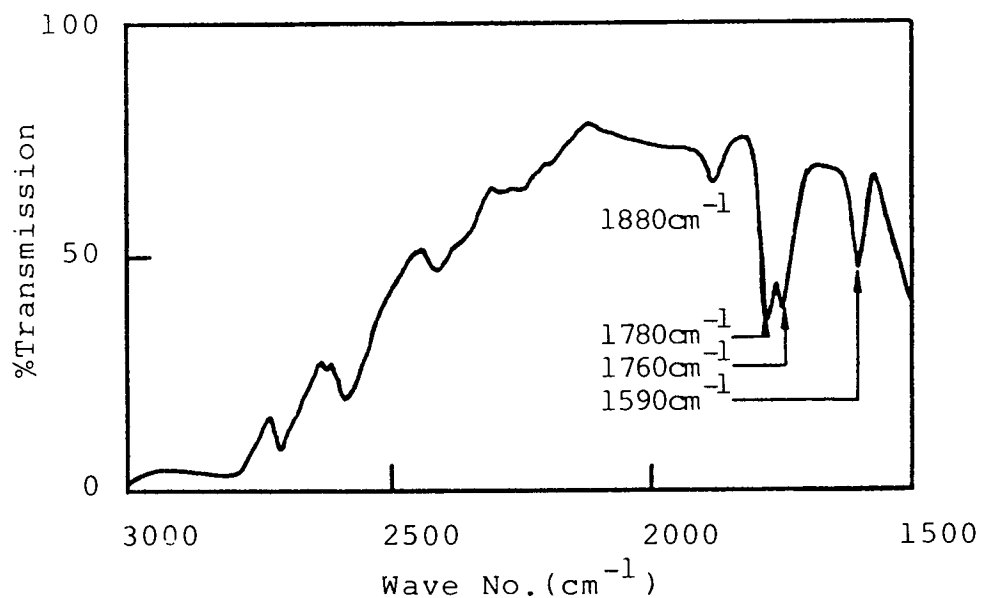


Figure 2.10 Infra-red spectrum of APM(1%) in PP(HF22, 200 μm film, ref. air). (Torque rheometer, CM, 8 mins, 180°C, 60 rpm).

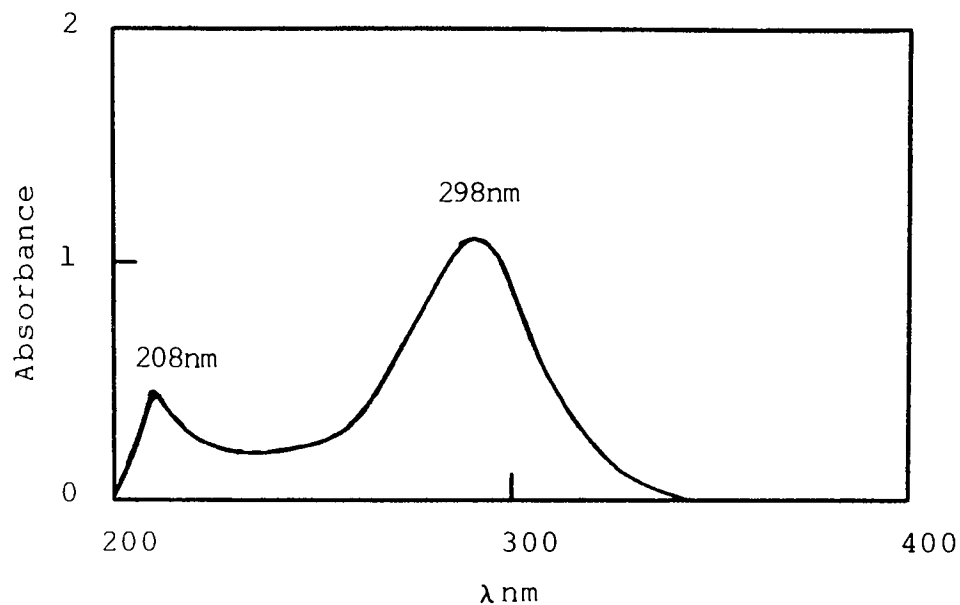


Figure 2.11 Ultraviolet spectrum of APSA ( $4 \times 10^{-5} \text{ mol dm}^{-3}$ ) in ethanol (ref. ethanol)

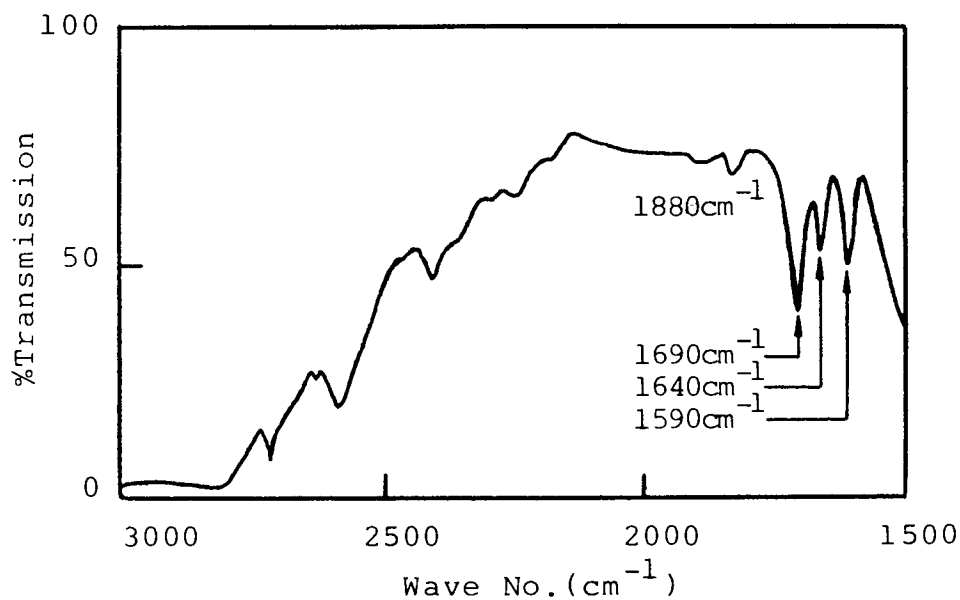


Figure 2.12 Infra-red spectrum of APSA(1%) in PP(HF22, 200 μm film, ref. air). (Torque rheometer, CM, 8 mins, 180 °C, 60 rpm).



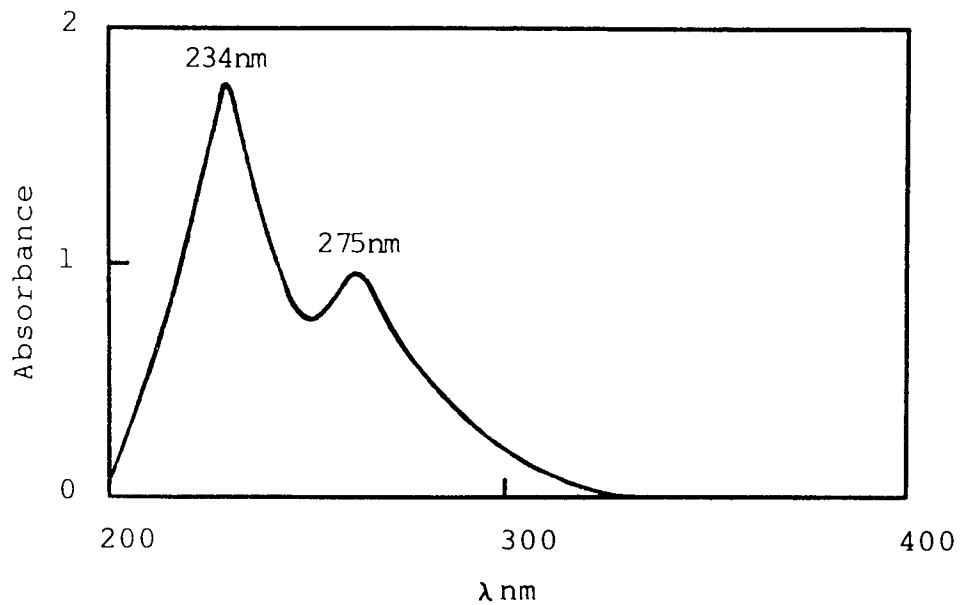


Figure 2.13 Ultraviolet spectrum of maleimide ( $4 \times 10^{-3} \text{ mol dm}^{-3}$ ) in methanol (ref. methanol)

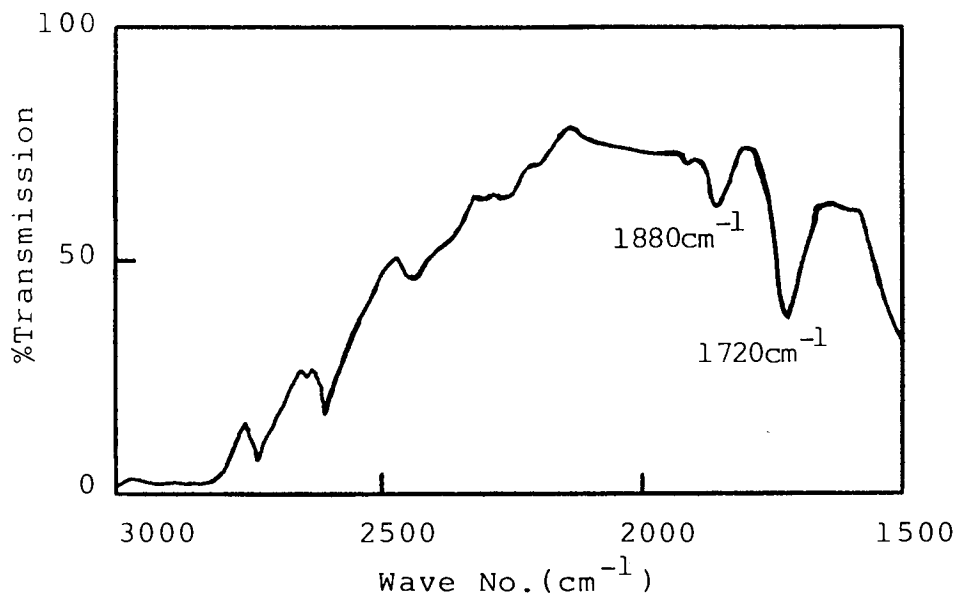


Figure 2.14 Infra-red spectrum of maleimide (1%) in PP (HF22,  $200 \mu\text{m}$  film, ref. air). (Torque rheometer, CM, 8mins,  $180^\circ\text{C}$ , 60rpm).

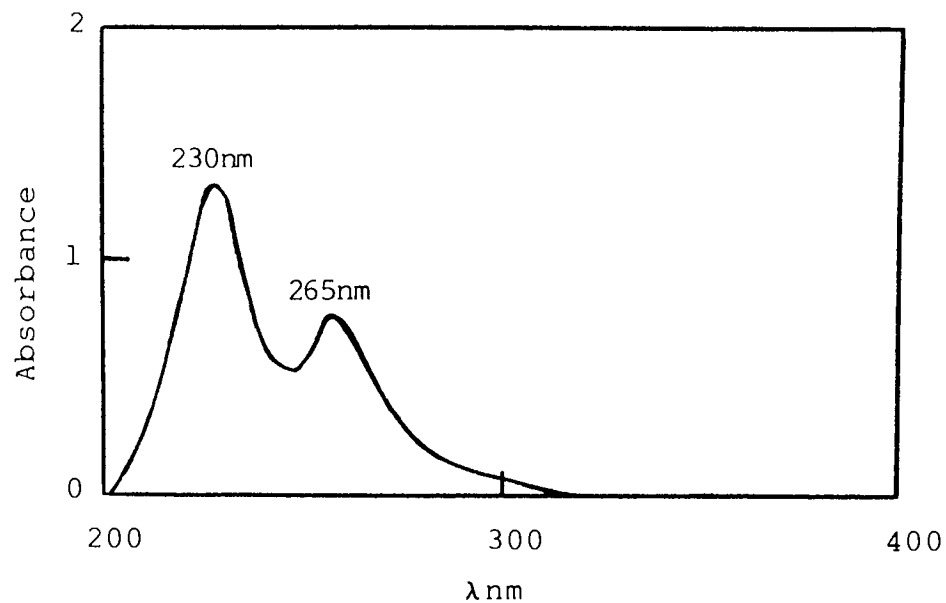


Figure 2.15 Ultraviolet spectrum of ADCT  
 ( $4 \times 10^{-3} \text{ moldm}^{-3}$ ) in methanol  
 (ref.methanol)

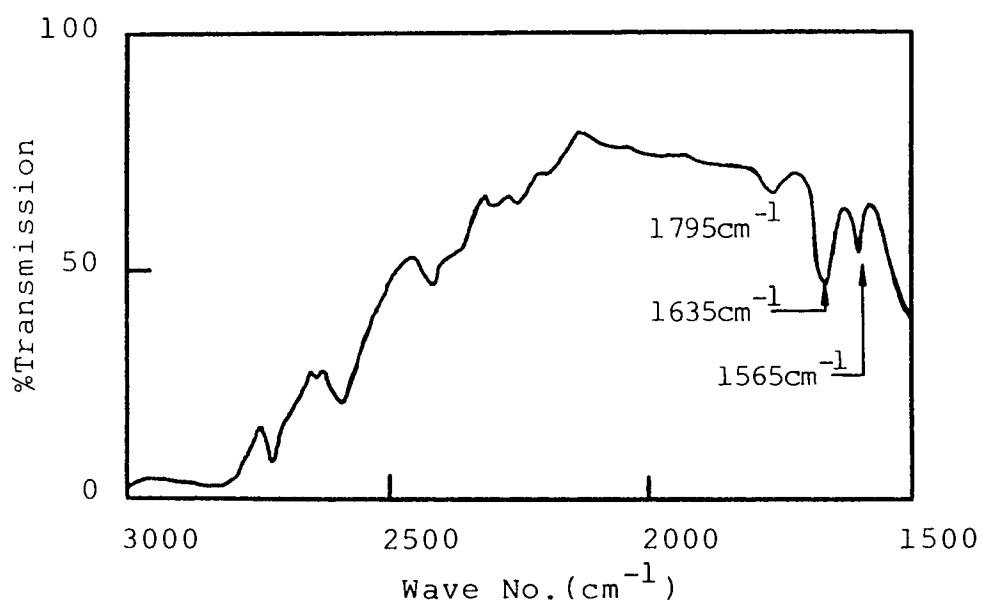


Figure 2.16 Infra-red spectrum of ADCT(1%)  
 in PP(HF22, 200 $\mu\text{m}$  film, ref.air).  
 (Torque rheometer, CM, 8mins, 180 $^{\circ}\text{C}$ ,  
 60rpm).

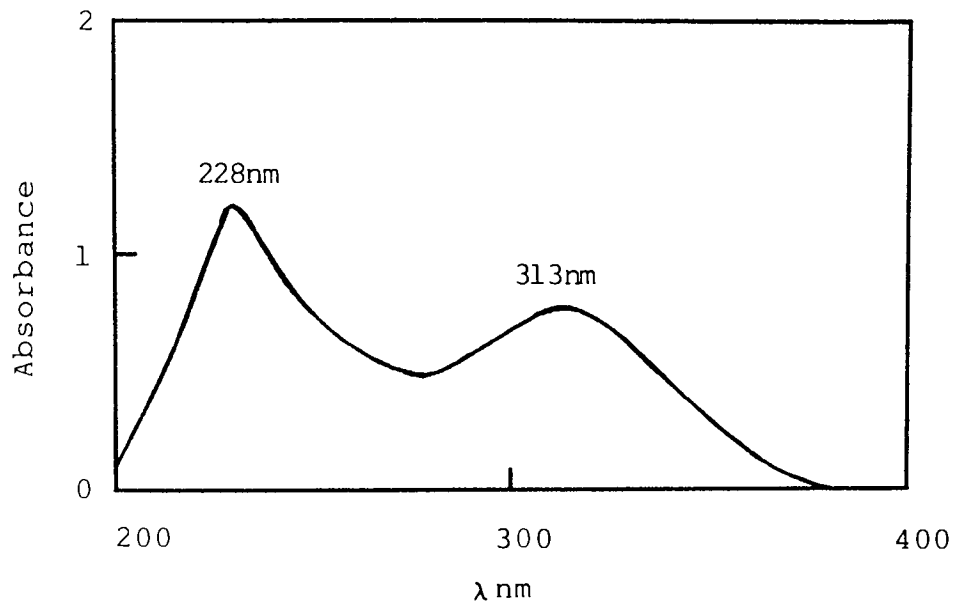


Figure 2.17 Ultraviolet spectrum of AACT ( $4 \times 10^{-4} \text{ mol dm}^{-3}$ ) in methanol (ref. methanol)

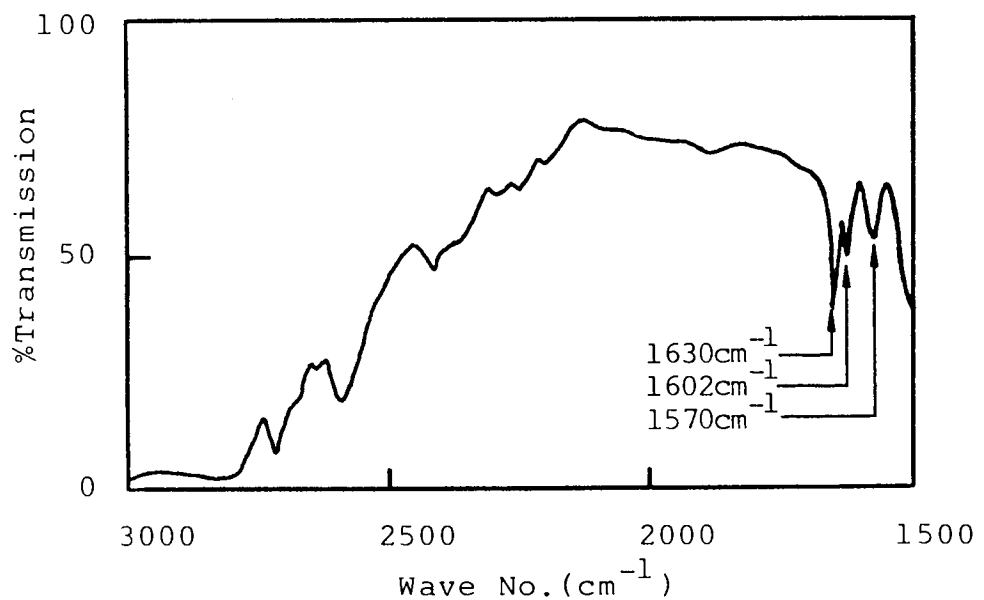


Figure 2.18 Infra-red spectrum of AACT(1%) in PP(HF22, 200  $\mu\text{m}$  film, ref. air). (Torque rheometer, CM, 8 mins,  $180^\circ\text{C}$ , 60rpm).

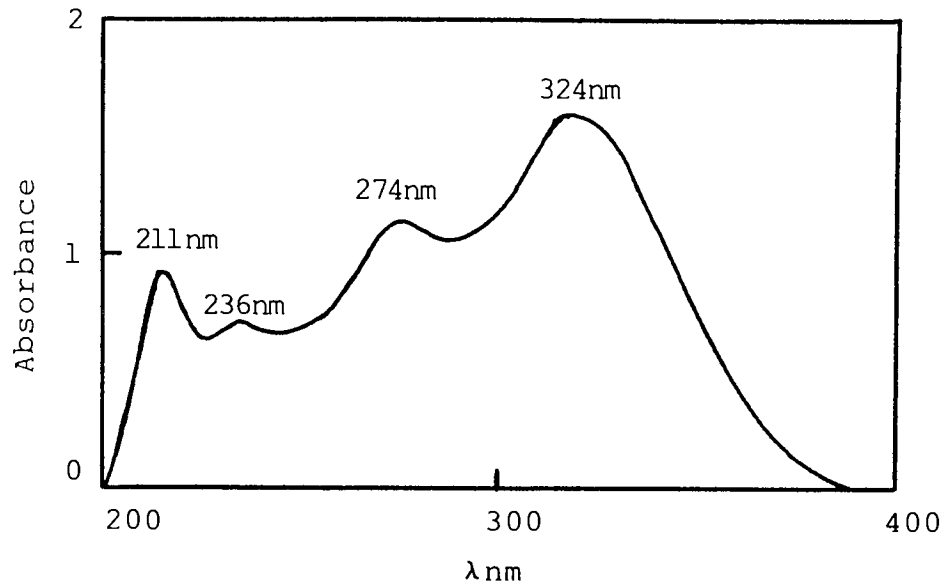


Figure 2.19 Ultraviolet spectrum of ADDT  
 $(4 \times 10^{-5} \text{ mol dm}^{-3})$  in ethanol  
 (ref.ethanol)

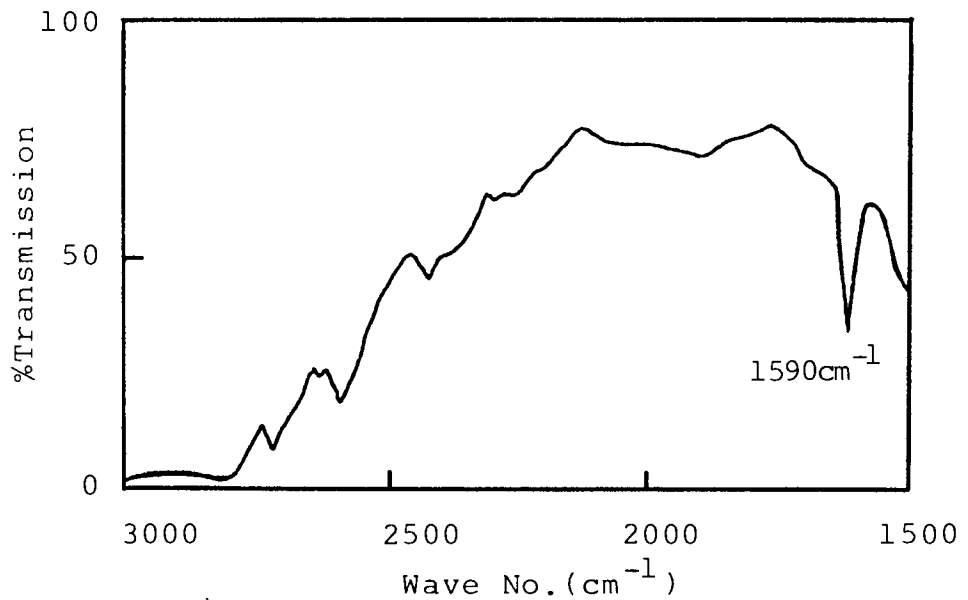


Figure 2.20 Infra-red spectrum of ADDT(1%)  
 in PP(HF22, 200 $\mu$ m film, ref.air).  
 (Torque rheometer, CM, 8mins, 180<sup>o</sup>C,  
 60rpm).

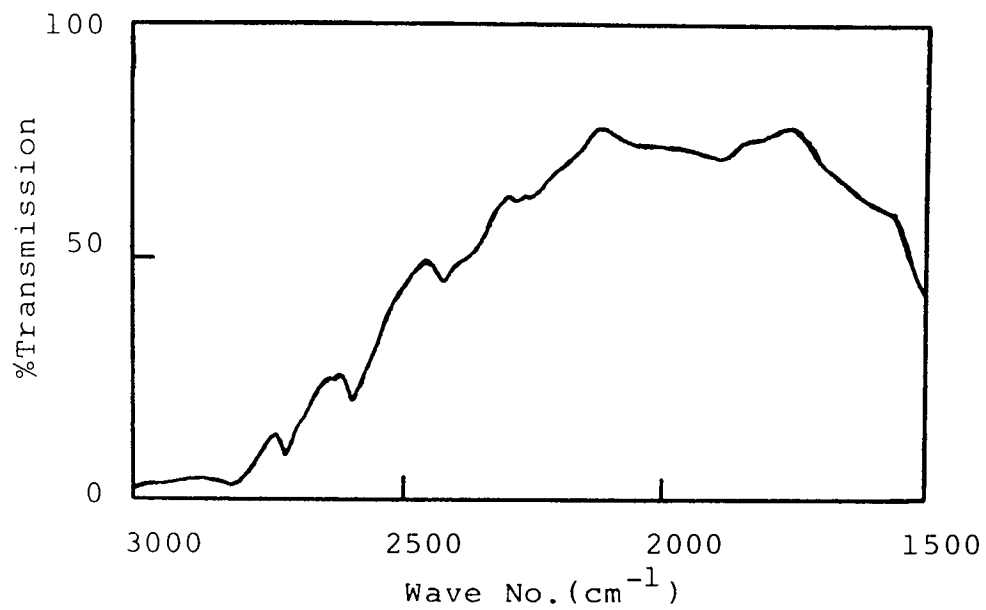


Figure 2.21 Infra-red spectrum of unprocessed PP(HF22, 200 $\mu$ m film, ref. air)

for the homogenisation stages of composite production. A minimum polymer charge of 250 grams is required for its use. The Buss Ko-Kneader (BKK) is a modified screw extruder, the screw rotation being supplemented by a cyclical back and forth motion to ensure high shearing and efficient mixing<sup>(172)</sup>. Temperature is controlled by an oil heater up to a maximum of 230°C. The screw speed is variable in the range 32-48 rpm. Back pressure caused by the die excludes air from the polymer melt. Due to the shearing, there is a positive temperature gradient from the feed zone to the die. Material emerging from the die was either melt granulated or first quenched in cold water and then granulated. The capacity throughput is 2-4kg/hr depending on screw speed and material used.

### 2.2.2 Injection Moulding

All injection moulding of test pieces for impact, flexural, tensile, dynamic modulus and high temperature creep testing and plaques for thermal-oxidative ageing was done with an Edgwick 1214-HY Type S (MkII) machine<sup>(173)</sup>. This is fitted with an electrically heated screw injection unit providing a maximum shot volume of 95 cm<sup>3</sup> with an injection rate of 82 cm<sup>3</sup>/sec and injection stroke of 82.5 cm using a 4.1 cm diameter screw. The total injection force is 15,331 kg. Of this, the injection pressure may

be varied from 0 to 1153 kg/cm<sup>2</sup>. During the moulding cycle the injection force is opposed by the die-locking force of 45,000 kg. Using fully automatic operation, the machine works continuously using power operated dies. Processing variables requiring control are barrel temperature, mould temperature, screw speed, injection pressure and cool time.

## 2.3 Composite Testing

### 2.3.1 Fibre Length Determination

Fibre length is a major factor in determining the degree of reinforcement in a thermoplastic composite. Individual fibre lengths were recorded by photographing the fibres on a glass slide through a Vickers Photoplan optical microscope. To obtain a statistically representative range of fibre lengths, 500 individual fibre lengths were recorded. A photograph of a calibrated grating was taken so that the lengths of the fibres on the photographs could easily be translated to their actual lengths.

To calculate the initial fibre lengths prior to processing, samples were prepared by carefully spreading the fibres over the glass slides. For processed samples, the embedded fibres had to be removed from the polymer matrix.

This was done by placing 2 grams of the composite in a crucible which was then gently heated with a Bunsen burner until all of the polymer was burnt off. After slow cooling to prevent thermal shock, the fibres were slide-mounted for photographing. Examples of unprocessed A-1100 silane coupled, SRWF, LRWF and GF are shown in Plates 2.1 to 2.3 respectively.

The results were used to give histograms of % of Total Count at Each Length Vs. Fibre Length (see Figure 2.22). From these, Number and Weight Average Length were calculated:

$$\text{Number Average Length} = \Sigma NL / \Sigma N$$

$$\text{Weight Average Length} = \Sigma NL^2 / \Sigma NL$$

where N = Number of fibres

L = Fibre length (mm)

### 2.3.2 Tensile Property Tests

Tensile testing used an Instron 1163 tensometer according to the ASTM D638M procedure<sup>(174)</sup>. Five injection moulded dumb-bell test pieces of cross-sectional dimensions  $1.25 \times 10^{-2}$  m by  $0.3125 \times 10^{-2}$  m were used for each determination at room temperature (20°C). At least 40



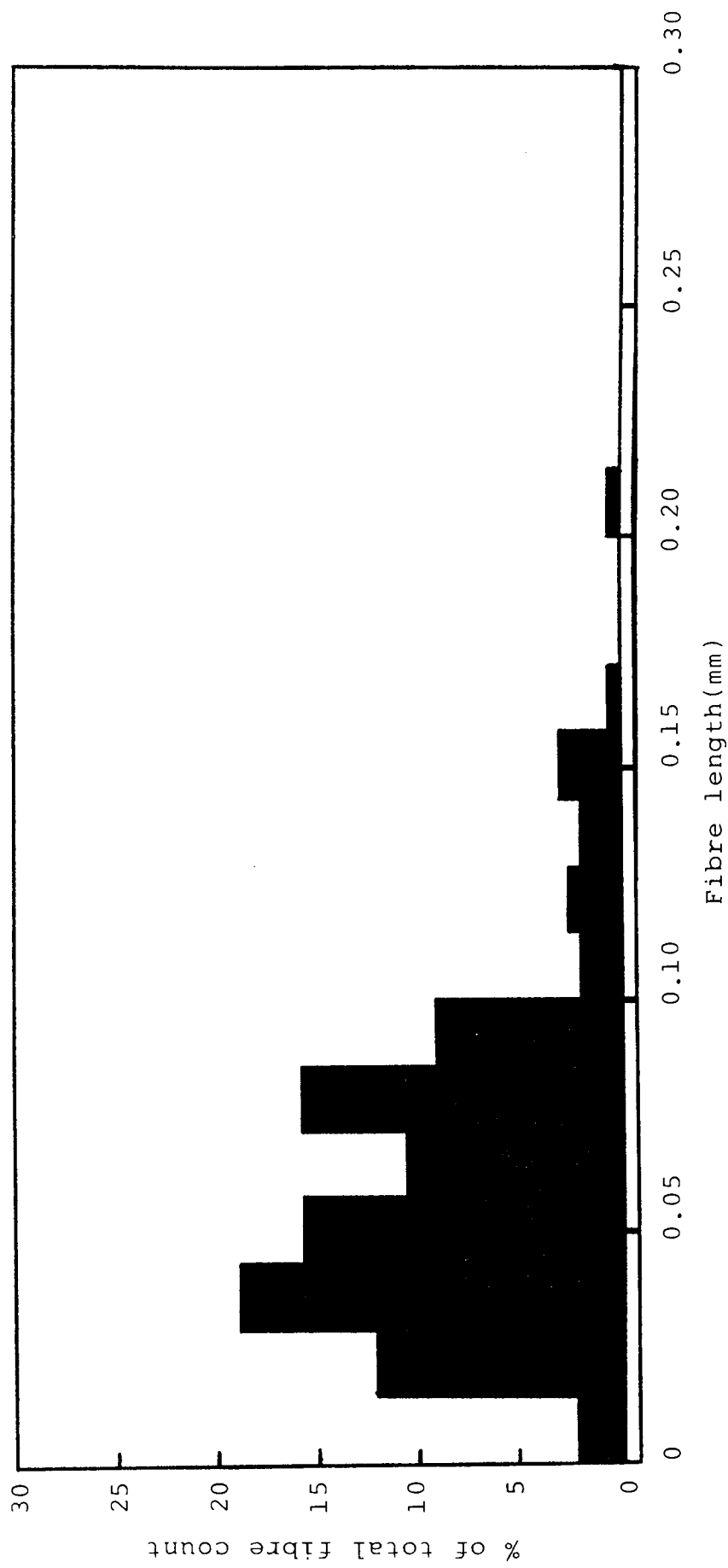


Figure 2.22 Histogram of weight average length distribution of long Rockwool fibres  
 (LRWF, 30% loading) in PP(HWM25) after homogenisation in the Buss Ko-Kneader  
 (185°C, 48rpm)

hours elapsed between moulding and testing. A cross-head speed of  $20 \text{ mmmin}^{-1}$  was chosen such that rigid composite materials and soft rubber modified polymers could be accommodated on an identical test so that direct comparisons could be made between all samples.

The following properties (see Figure 2.23) were recorded:

	<u>UNITS</u>
Yield Strength(YS) = $\frac{\text{Load at Yield(N)}}{\text{Cross Sectional Area (m}^2\text{)}}$	MPa
Tensile Modulus(TM) = $\frac{\text{Stress(Nm}^{-2}\text{)}}{\text{Strain}}$	GPa
Elongation at Yield = $\frac{\text{Extension at Yield(m)}}{\text{Original Length(m)}} \times 100$	%
Elongation at Break = $\frac{\text{Extension at Break(m)}}{\text{Original length(m)}} \times 100$	%

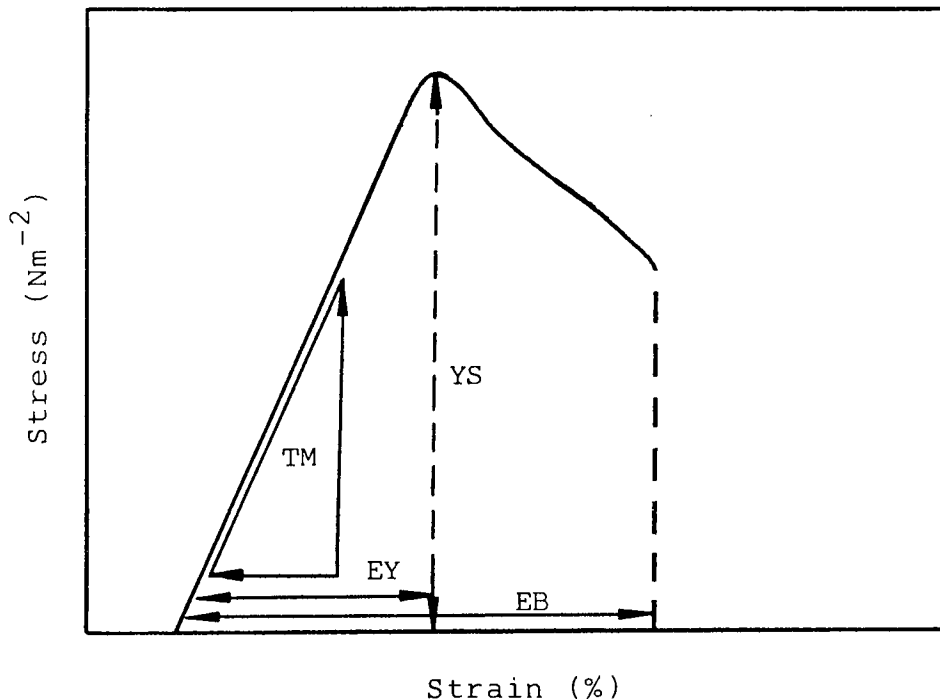


Figure 2.23 Typical polymer stress-strain curve showing tensile modulus(TM), yield strength(YS), elongation at yield(EY) and elongation at break(EB)

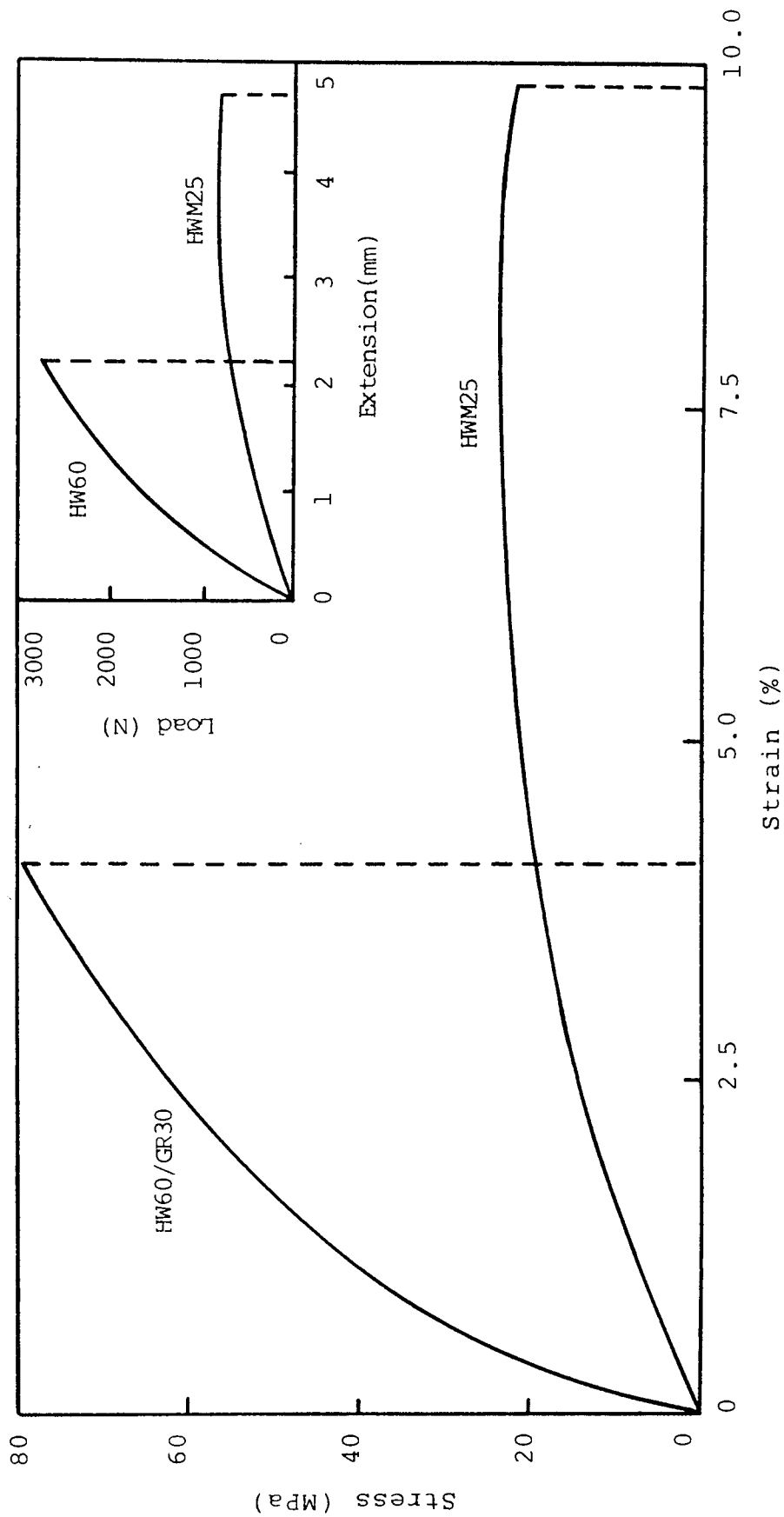


Figure 2.24 Tensile stress-strain curves of commercial grades of PP:HWM25, homopolymer and HW60/GR30, 30% GF coupled. Inset, Load Vs. extension of the same grades

Tensile properties provide useful data for plastics engineering design purposes. However, due to the sensitivity of plastics to strain rate, data obtained by this method cannot be considered valid for applications involving load-time scales widely different from those of this method<sup>(174)</sup>. Standard deviations are shown in the mechanical property tables towards the end of Chapters 3, 4 and 5.

### 2.3.3 Flexural Property Tests

Three point flexural testing was done on an Instron 1163 machine according to the ASTM D790M Method 1 procedure<sup>(175)</sup>. This test is especially useful for quality control and specification purposes. Four injection moulded test pieces were used for each measurement. At least 40 hours elapsed between moulding and testing. Flexural strength and flexural modulus were calculated.

$$\text{Flexural Strength} = 3PL/2bd^2 \quad \text{Units} = \text{MPa}$$

$$\text{Flexural Modulus} = (P/\delta)/(L^3/4bd^3) \quad \text{Units} = \text{GPa}$$

where  $L = \text{Span} (5 \times 10^{-2} \text{m})$

$b = \text{Width} (1.25 \times 10^{-2} \text{m})$

$d = \text{Thickness} (0.3125 \times 10^{-2} \text{m})$

$P = \text{Load (N)}$

$\delta = \text{Deflection (m)}$

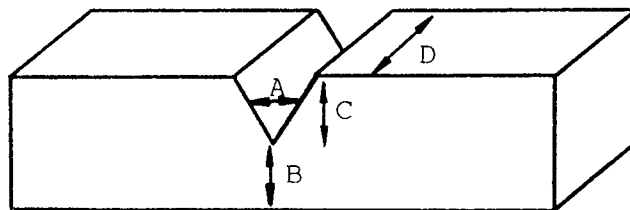
A cross-head speed of  $2\text{mmmin}^{-1}$  was used at room temperature ( $20^{\circ}\text{C}$ ). This was chosen so that rigid composite materials and soft rubber-modified polymers could be accommodated on an identical test so that direct comparisons could be made between all samples. Standard deviations are shown in the mechanical property summary tables towards the end of Chapters 3, 4 and 5.

#### 2.3.4 Charpy Impact Strength

A Hounsfield Plastic Impact Machine was used to calculate the Charpy impact strength of notched samples. Six samples were used for each test. The notched sample is supported at both ends and subjected to impact from a falling pendulum weight on the face opposite the notch.

Impact tests were used only to rank Impact Strength on a comparative basis and cannot be used to satisfactorily predict in-service performance of a component due to the influences of additives, temperature, component geometry, orientation, morphology, surface conditions and impact velocity<sup>(176)</sup>.

Tests were done at temperatures of  $-40$ ,  $-20$ ,  $0$  and  $20^{\circ}\text{C}$ . Those at  $20^{\circ}\text{C}$  were done at room temperature. Samples tested at  $0^{\circ}\text{C}$  were stored in a fridge for one day prior



A = Notch radius ( $2 \times 10^{-4}$  m)

B = Sample thickness ( $4.5 \times 10^{-3}$  m)

C = Notch depth ( $1.5 \times 10^{-3}$  m)

D = Sample width ( $3.125 \times 10^{-3}$  m)

Charpy impact strength units =  $\text{kJm}^{-2} = \frac{\text{Energy to break (J)}}{B \times D}$

Figure 2.25 Notched Charpy impact specimen

to testing. Samples at  $-20^{\circ}\text{C}$  and  $-40^{\circ}\text{C}$  were immersed for 30 minutes in acetone cooled to the appropriate temperature with cardice. Test pieces were taken from the acetone and tested immediately for impact strength. Standard deviations are shown in the mechanical property summary tables towards the end of Chapters 3, 4 and 5.

### 2.3.5 Dynamic Mechanical Testing

#### Theory<sup>(177)</sup>

Polymeric mechanical behaviour may be thought of being composed of a linear elastic component given by Hooke's Law:

$$\sigma = Ee \quad (1)$$

where  $\sigma$  = Stress

$E$  = Young's Modulus

$e$  = Strain

and a time dependent part given by Newton's Law:

$$\eta = de/dt \quad (2)$$

where  $\eta$  = Viscosity

$t$  = Time

When an applied stress is varied sinusoidally according to the equation:

$$\sigma = \sigma_o \sin \omega t \quad (3)$$

where  $\omega$  = angular frequency

the strain varies in a similar manner if the material obeys Hooke's Law:

$$e = e_o \sin \omega t \quad (4)$$

For a polymeric viscoelastic material, the strain lags behind the stress as shown in Equations 5 and 6:

$$e = e_o \sin \omega t \quad (5)$$

$$\sigma = \sigma_o \sin(\omega t + \delta) \quad (6)$$

where  $\delta$  = phase angle; relative angular displacement of stress with strain.

Equation 6 can be expanded to give:

$$\sigma_o = e_o E_1 \sin \omega t + e_o E_2 \cos \omega t \quad (7)$$

It is thus possible to define  $E_1$ , the Storage Modulus which is in phase with the strain and  $E_2$ , the Loss Modulus which is  $\pi/2$  out of phase.

The overall Complex Modulus is given by:

$$E^* = \sqrt{(E_1)^2 + (E_2)^2} \quad (8)$$

$$\text{The Phase Angle is: } \tan \delta = E_2/E_1 \quad (9)$$

#### The Torsional Pendulum

The procedure described by the appropriate ASTM standard was followed for the measurement of  $\tan \delta$  and the three



moduli using a Torsional Pendulum<sup>(178)</sup>. An injection moulded flexural test-piece firmly clamped to an inertia bar was used. The length of each sample was altered to maintain the pendulum oscillating at 1Hz. The weight of the torsion bar is counter-balanced to avoid uniaxial tension or compression in the sample.

The system is oscillated by twisting and releasing the torsion bar. The sinusoidal frequency is dependent upon sample properties and length.

An elastic system oscillates indefinitely. For a polymeric viscoelastic sample, the amplitude decreases with time as shown in Figure 2.26.

The oscillation trace is recorded by scorching a line onto graph paper using an electrical discharge thus avoiding damping from an external source.

The Torsion Pendulum uses shear forces and hence the moduli calculated are the corresponding shear moduli:

$$G^* = \sqrt{(G_1)^2 + (G_2)^2} \quad (10)$$

$G_1$ ,  $G_2$  and  $\tan \delta$  are calculated using the following Equations:

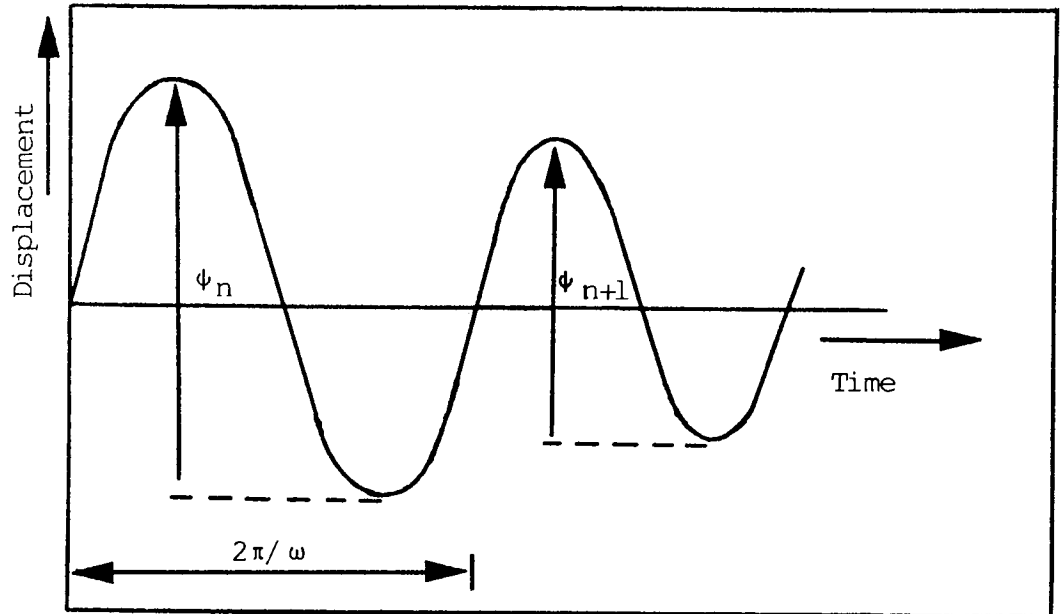


Figure 2.26 Oscillation damping for a viscoelastic material

$$G_1 = 4\pi^2 v^2 IL/g \quad (11)$$

$$G_2 = G_1 \text{Tan } \delta \quad (12)$$

$$\text{Tan } \delta = \Lambda/\pi \quad (13)$$

where  $\Lambda = \text{Log Decrement} = \text{Loge}(\psi_n/\psi_{n+1})$

$\psi_n$  = Amplitude of nth swing

I = Torsional Moment of Inertia

L = Sample Length

v = Frequency of Oscillation

g = Geometrical Shape Factor =  $Cbd^3$

C = Constant dependent on d/b ratio

d = Sample Thickness ( $0.3125 \times 10^{-2}$  m)

b = Sample Width ( $1.25 \times 10^{-2}$  m)

### 2.3.6 Tensile Creep Of Plastics

Injection moulded test pieces from the ASTM tensile test<sup>(174)</sup> were used for the ASTM tensile creep<sup>(179)</sup> investigation (see Section 2.3.2). Strain was measured with a strain gauge transducer over 4.75 cm of the central span of the "dumb-bell" test piece and was recorded continuously for  $1 \times 10^5$  seconds on a calibrated chart recorder. At least two test pieces were used for each sample. To reduce vibration from external sources, the entire apparatus was mounted on a heavy concrete slab. Results were plotted as % Strain Vs. Log time (at each decade up to  $1 \times 10^5$  s) at  $20^\circ\text{C}$ . To obtain isochronous stress-strain curves, samples were tested over a variety of loads, the maximum load depending on the strength of the material.

Using an oven, tensile creep data was obtained for temperatures up to  $150^\circ\text{C}$ . The oven consisted of two halves, which when clamped together totally enclosed the test piece. The oven walls contained electrical heating elements over which an air flow was pumped to maintain even heat distribution over the test piece. Using a thermocouple, the temperature was controlled to within  $\pm 0.5^\circ\text{C}$ . % Strain Vs. Log time graphs were plotted for each sample at temperatures from  $20^\circ\text{C}$  up to  $150^\circ\text{C}$ .

Creep data is necessary to predict the performance of materials under long term loading at different temperatures and to predict dimensional changes that may occur as a result of such loads.

### 2.3.7 Long Term Durability Tests

The resistance of plastic composites to chemical reagents was tested using the American Standards technique<sup>(180)</sup>. The selection of type of test took into account the manner, temperature and duration of contact with chemical reagents present in an "under-bonnet" environment. The specification of such conditions provides a basis for standardisation and serves as a guide to the likely performance of a component. Three test fluids were chosen:

1. 2% Ajax water solution
2. Gunk engine cleaning fluid
3. Lockheed 30L brake fluid

The tests used tensile<sup>(174)</sup> and flexural<sup>(175)</sup> pieces. For each sample, three test pieces were used. All test pieces were fully immersed in the test fluids at 65°C. Care was taken to avoid samples coming into contact with each other or the walls of the vessel.

The Gunk and brake fluid were heated over an oil bath in five litre spherical glass flasks fitted with water cooled

reflux condensers. The 2% Ajax solution was heated in a water bath fitted with a glass roof to reduce excessive water evaporation. Test pieces were removed after periods of three days, one, two, three and four weeks immersion, washed under tap water and then dried with a cloth.

Following a period of at least forty hours, the following results were recorded:

- I. Yield and flexural strength, tensile and flexural modulus. The % retention of the original unimmersed property was then calculated.
- II. Fracture surfaces after tensile testing were observed by scanning electron microscopy (SEM) to help determine the effect of fluid immersion on the fibre-matrix interface (see Section 2.3.9).

#### 2.3.8 Tensile Modulus Retention Water Immersion Tests

This was used as a quick investigation into the effectiveness of adhesion between the reinforcing fibre and polypropylene matrix. The test used three tensile pieces<sup>(174)</sup> which were totally immersed in a water bath at 70°C for 24 hours.

The tensile modulus retention is expressed as a percentage and is calculated from:

$$\text{Tensile modulus retention} = \frac{\text{tensile modulus after 24 hrs water immersion at } 70^{\circ}\text{C}}{\text{original tensile modulus}} \times 100$$

Fracture surfaces after tensile testing were observed by scanning electron microscopy (SEM) to determine the effect of water immersion (24 hours, 70°C) on the fibre-matrix interface (see Section 2.3.9).

### 2.3.9 Scanning Electron Microscopy (SEM)

The fracture surfaces of drawn tensile test pieces (see Section 2.3.2) were investigated by scanning electron microscopy (SEM). Following the fracture of tensile test pieces, surface samples were cut off at a depth of 4mm. These were glued onto clean aluminium discs with Araldite. After thorough drying in a desiccator for one week, samples were gold coated for one minute to produce an electrically conductive surface. The coated samples were then observed under the microscope to study fibre pull-out from the polymer matrix at the fracture surface. Photographs at magnifications of 100 to 1000 were taken.

### 2.4 Melt Processing

The Hampden RAPRA Torque Rheometer<sup>(181)</sup> is an experimental scale internal mixer with a capacity for 36 grams of Polypropylene. The temperature is controlled by an oil jacket

and by using a pneumatic ram, the mixing chamber may be operated open to the atmosphere (open mixer, OM) or closed (closed mixer, CM). This allows polymers and their additives to be processed in the presence or absence of atmospheric oxygen. The torque applied to the variable speed rotor blades may be recorded. Although the torque is related to the viscosity of the polymer melt, it must not be confused with viscosity because it is the result of a very complicated flow system under constantly varying conditions.

The rotor speed is related to the rate of shear in the chamber, but cannot be directly related to the actual shear rate because of the complex geometry of the chamber and its mixing action. Although the RAPRA Torque Rheometer does not provide fundamental viscosity data, it does provide information concerning fusion, cross-linking and degradation of polymeric materials. Immediately after the processing of each sample, the polymer melt was immersed in cold water to quench any further reactions.

## 2.5 Polymer Film Preparation

Polypropylene films (200 $\mu$ m thick) were made by compression moulding 6g of polymer between two steel plates. Cellophane sheet was used to prevent polymer contact with the plates.

Electrically heated platens were maintained at 180°C. Initially, samples were pre-heated for one minute with no pressure. Pressure was gradually increased over thirty seconds until 30 tons on the 12" ram was achieved. This was maintained for one minute before water cooling of the platens to 50°C. The films were removed and stored in a fridge at 0°C.

## 2.6 Melt Stability Of Polypropylene

### 2.6.1 Melt Flow Index (MFI)

The MFI is defined as the weight of polymer extruded through a standard die in ten minutes. The British Standard 2782<sup>(182)</sup> procedure was followed. A temperature of 230°C ( $\pm 0.5^\circ\text{C}$ ) and a 2.16kg weight were used with a die diameter of 0.2095cm(0.0825").

The barrel was charged with 4g polymer in one minute. After excluding trapped air, the material was left to homogenise for four minutes, after which the 2.16kg weight was applied and after another minute, six extruded samples were cut every thirty seconds. The MFI was then calculated from:

$$\text{MFI} = \text{Average Weight Extruded in 30 seconds} \times (600/30)$$



MFI is inversely proportional to the molecular weight of the polymer. Because it is used for comparative purposes, only polypropylene of the same density and chemical nature may be used.

### 2.6.2 Gel Permeation Chromatography

These tests were done on RAPRA torque rheometer melt processed unstabilised PP(HF22) containing maleic anhydride and di-cumyl peroxide at the RAPRA Polymer Supply and Characterisation Centre.

#### GPC operating variables:

I. Columns      1 x 10<sup>6</sup>Å  
                     1 x 10<sup>4</sup>Å  
                     1 x 500Å

II. Flow rate      1ml/min

III. Solvent      1,2 dichlorobenzene stabilised with 2,6-di-tert.-butyl-p-cresol

IV. Temperature      140°C

V. Calibration      Mark-Houwink constants ( $[\eta] = KM^\alpha$ ) used for conversion via Universal Calibration:

a) Polystyrene  $K = 1.38 \times 10^{-4}$ ,  $\alpha = 0.7$

    Polypropylene  $K = 1.03 \times 10^{-4}$ ,  $\alpha = 0.78$

Units of  $K = \text{dl g}^{-1}$

- b) Not corrected for peak broadening effects.
- c) Not corrected for variation of refractive index with molecular weight.

## 2.7 Accelerated Thermal-oxidative Ageing

### 2.7.1 Accelerated Thermal-oxidative Ageing Of Polypropylene Films

The Wallace Air Oven was used to compare the thermal-oxidative stabilities of 200 $\mu$ m thick polypropylene films containing a range of different stabilisers at various concentrations. The oven consists of a cast aluminium block containing seven individual cylindrical cells, each of 7.5cm diameter and 30.5cm long<sup>(183)</sup>. Air (2.5cuft/hr, corresponding to seven complete changes of air per hour<sup>(184)</sup>), pre-heated to 140°C( $\pm$ 1°C) is forced into the bottom of each cell through a calibrated orifice from a common pre-heat chamber. This assures even distribution of air through the seven cells. The air is exhausted through the covers at the top of each cell to eliminate feedback contamination. Test pieces were suspended from specimen racks within the cells. Films were cut to 2x3cm and at least two were used for each test.

### 2.7.2 Infra-red Spectroscopy Of Polypropylene Films

Infra-red spectra of 200 $\mu$ m thick polypropylene films were

taken from 4000 to 200 $\text{cm}^{-1}$  on a Perkin Elmer 599 Spectrophotometer using an air reference. Infra-red spectroscopy is useful for monitoring the increased concentration of degradation products of thermal-oxidation of polypropylene films. The increase in concentration of carbonyl oxidation products such as ketones, aldehydes and carboxylic acids was monitored over a period of time at 1710 $\text{cm}^{-1}$ . Measurement of functional groups was done using the baseline technique<sup>(185)</sup>. A tangential line was drawn between the two adjacent shoulders of an absorption maxima. A perpendicular line was dropped to intersect the peak absorption baseline. The distance between the tangential and baselines was taken as the absorbance which could be read directly off the chart paper.

The absorbance at an absorption maxima is proportional to the concentration of the additive in the polymer film. This may be calculated from the Beer-Lambert Law<sup>(186)</sup>:

$$A = \text{Log}_{10}(I_0/I) = Ecl$$

where A = Absorbance

$I_0$  = Incident infra-red intensity

I = Exit light intensity from sample

c = Molar concentration of additive ( $\text{mol dm}^{-3}$ )

l = Path length (cm)

E = Molar absorptivity ( $\text{mol dm}^{-3} \text{cm}^{-1}$ )

Results from thermal-oxidative ageing of polypropylene films are quoted in terms of carbonyl index. This is defined as the log of the carbonyl absorption at  $1710\text{cm}^{-1}$  divided by the log of a reference absorption at  $2800\text{cm}^{-1}$  which is common to all polypropylene films.

$$\text{Carbonyl Index} = \frac{\log(\text{Carbonyl Absorption at } 1710\text{cm}^{-1})}{\log(\text{Reference Absorption at } 2800\text{cm}^{-1})}$$

The reference peak is used to minimise errors caused by deviations in film thickness between samples. When the carbonyl index was plotted against time of exposure to thermal oxidation, a very slow initial increase was typically observed, after which there was a break in the trend to a very rapid rise. The time to reach this point was called the induction period and represents the useful technological life of the polypropylene film. It is the point when an antioxidant has ceased to be effective in controlling the build up of carbonyl groups within the polymer. Figure 2.27 shows how the carbonyl index induction period was calculated.

### 2.7.3 Accelerated Thermal-oxidative Ageing Of Poly-Propylene Plaques

Injection moulded polypropylene plaques of dimensions  $25 \times 50 \times 1\text{mm}$  were exposed to an air flow of  $2.5\text{cu ft per hr}$  at  $150^{\circ}\text{C}$  in a Wallace air oven until they became crazed.

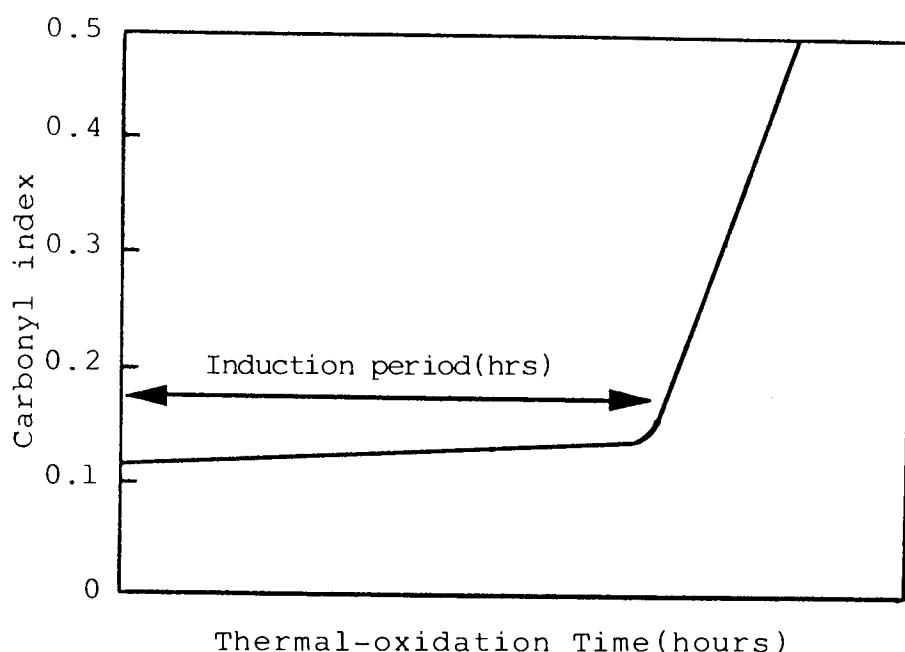


Figure 2.27 Calculation of the induction period from carbonyl index data

Crazing was assessed with the aid of an optical microscope and complete crazing was taken to be when the surface cracks caused the sample to be non-transparent, discoloured and brittle. At least two plaques per sample were used. These were hung individually from specimen racks within the air oven cells.

This test which utilizes 1mm thick plaques is more representative of an "under-bonnet" component in an aggressive environment than the accelerated thermal oxidative ageing of polypropylene films. The results give a more technologically useful comparison of the useful life of different stabilised polypropylene samples.

Infra-red and ultraviolet studies were not used because the samples were too thick.

## 2.8 Chemical Binding Studies Of Polypropylene Additives

### 2.8.1.1 Continuous Hot Soxhlet Extraction Of Polypropylene Films

Extraction of polypropylene films used an electrically heated Soxhlet unit. Samples were mounted on cellulose extraction thimbles. To ensure total extraction of unbound additives, chloroform, acetone and hexane were used as extractive media, each for 24 hours. To avoid atmospheric oxidation, the extraction was done under a stream of nitrogen. After extraction, samples were dried under vacuum for 12 hours at room temperature.

### 2.8.1.2 Continuous Hot Soxhlet Extraction Of Polypropylene Granules And Plaques

The same procedure was used as that of the polymer films. However, one week for each solvent was used (chloroform, acetone and hexane) and the drying time required in the vacuum oven was raised to three days.

### 2.8.2 Percentage Binding Calculations For Polypropylene Additives

This was done using infra-red and ultraviolet spectroscopy.

### 2.8.2.1 Infra-red Spectra

Infra-red spectra were taken of polypropylene films (200 $\mu$ m thick) before and after exhaustive solvent extraction (see Section 2.8.1.1). For each additive a specific wave number corresponding to a strong absorbance was chosen (see Table 2.9). The infra-red absorbance was calculated according to the procedure recorded in Section 2.7.2.

An example is shown in Figure 2.28 using the 1810 $\text{cm}^{-1}$  absorbance band.

The percentage binding was then found using the following equation:

$$\% \text{ Binding} = \frac{A_2 - A_1}{A_3 - A_1} \times 100$$

where  $A_1$  = Absorbance of polypropylene film with no additive.

$A_2$  = Absorbance of polypropylene film with additive after extraction.

$A_3$  = Absorbance of polypropylene film with additive before extraction.

### 2.8.2.2 Ultraviolet Spectra

Ultraviolet spectra were taken of 200 $\mu$ m thick polypropylene

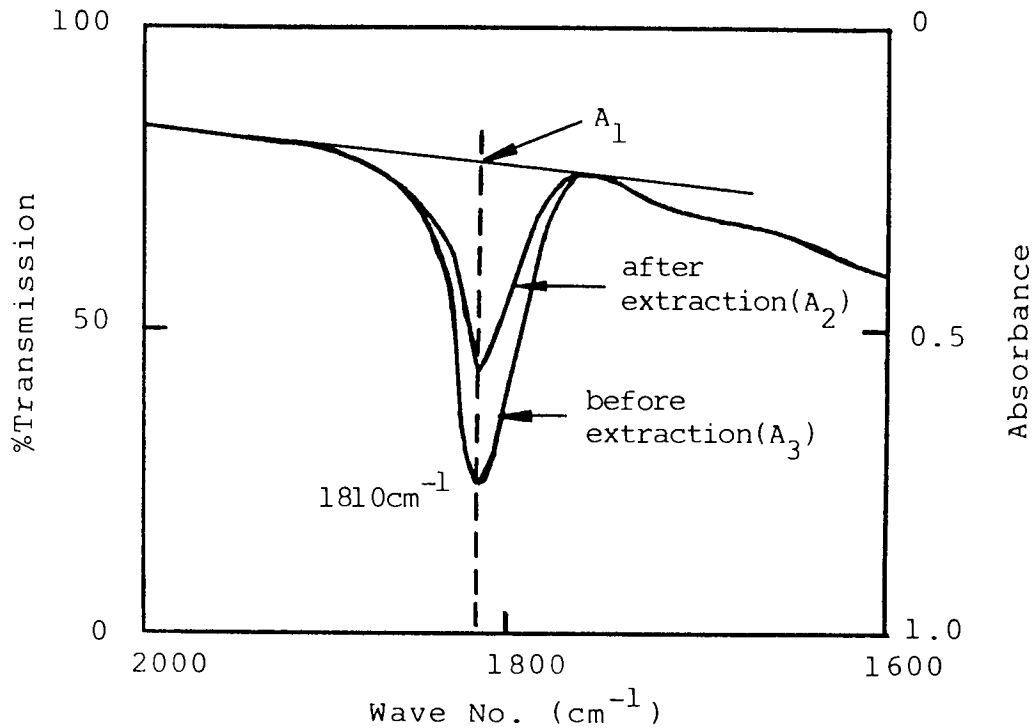


Figure 2.28 Use of an infra-red spectrum for % binding calculations of polypropylene additives

films before and after exhaustive solvent extraction (see Section 2.8.1.1).

For each additive, a wavelength was chosen corresponding to a distinctive  $\lambda_{\max}$  (see Table 2.9). Spectra were taken against a 200 $\mu\text{m}$  reference polypropylene film with no additive using a Unicam SP800 spectrophotometer.

An example is the ultraviolet spectrum using the  $\lambda_{\max}$  at 300nm (Figure 2.29).



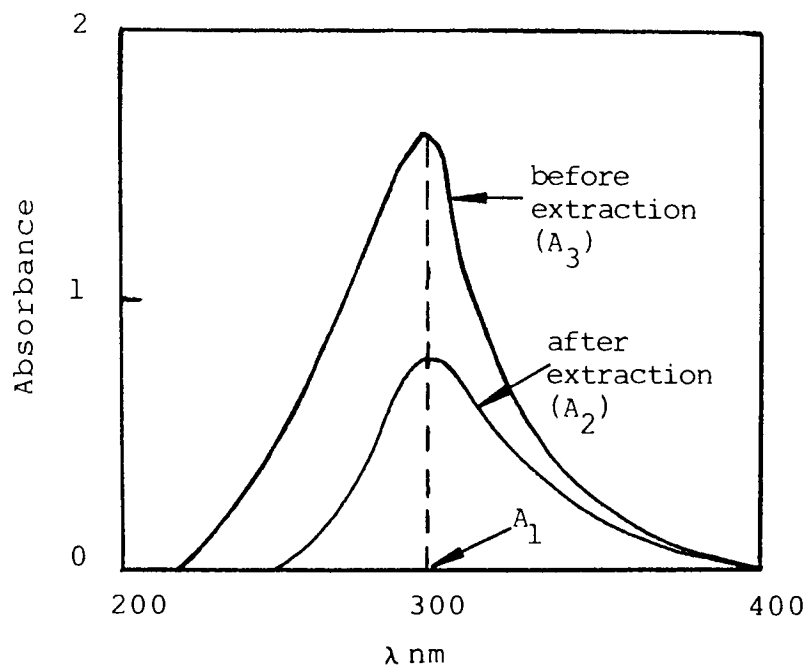


Figure 2.29 Use of an ultraviolet spectrum for % binding calculations of polypropylene additives.

The percentage binding was then found using the same equation used for the infra-red technique (Section 2.8.2.1):

$$\% \text{ Binding} = \frac{A_2}{A_3} \times 100$$

where  $A_2$  = Absorbance of polypropylene film with additive after extraction.

$A_3$  = Absorbance of polypropylene film with additive before extraction.

It is noteworthy that the percentage binding results are calculated on the amount of additive present after melt

processing and thus does not take into account the material lost due to volatilization at the melt temperature.

### 2.8.3 Quantitative Determination Of Bound Additive Concentration In Polypropylene Films

The molar concentration of chemically bound additives in polypropylene films was calculated using ultraviolet and infra-red spectra after exhaustive solvent extraction (see Section 2.8.1.1).

#### 2.8.3.1 Ultraviolet Spectra

Ultraviolet spectra of polypropylene films were taken using the procedure in Section 2.8.2.2.

At a particular  $\lambda_{max}$  chosen (from Table 2.9) for each additive, the absorbance  $A$  was read from the spectrum. Then using the path length  $l$  of the film and the molar extinction coefficient  $E$  (previously calculated from the characterisation of prepared compounds), the molar concentration of the additive was calculated using the Beer-Lambert equation<sup>(186)</sup>:

$$c = \frac{A}{El} = \text{concentration}(\text{mol dm}^{-3})$$

To convert the answer from  $\text{mol dm}^{-3}$  to moles per 100g of

polypropylene, the molar concentration was divided by:

$$1000\text{ml}/90\text{ml (volume of 100g polypropylene)} = \underline{11.11}$$

### 2.8.3.2 Infra-red Spectra: Calibration Graphs

For each additive, a specific wave number was chosen corresponding to a strong absorbance (see Table 2.9). The band was then used to correlate the infra-red absorbance with the additive concentration in a polypropylene film. This was done by measuring the infra-red absorbance at the chosen wave number for additive solutions of known concentration in suitable solvents. Absorbance was calculated according to the procedure given in Section 2.7.2.

A calibration graph was plotted of infra-red absorbance against additive concentration ( $\text{moles dm}^{-3}$ ). To use the calibration graphs to calculate the additive concentration in a polypropylene film from its infra-red spectrum (against an air reference), the absorbance was recorded at the chosen wave number (see Section 2.7.2). The recorded absorbance was then used to read off the molar concentration from the calibration graph. This figure was then multiplied by:

Path length used in calibration curve

Path length (i.e. film width) of PP film

to give the molar concentration ( $\text{dm}^{-3}$ ) in polypropylene.

To obtain the result in moles per 100g polypropylene, the molar concentration was divided by 11.11.

## 2.9 Solution Studies

### 2.9.1 Hydroperoxide Decomposition

#### A. Cumene hydroperoxide (CHP) purification

1. Add 190ml CHP in petroleum ether to 40ml aq. NaOH(conc) at  $0^{\circ}\text{C}$ .
2. Filter off white precipitate and wash with pet. ether.
3. Add acetic acid (glac.) to ppt in separating funnel and separate bottom layer after one hour.
4. Wash bottom layer with  $\text{NaHCO}_3$ (conc) and sparingly with distilled water.
5. Dry with  $\text{MgSO}_4$  and rotary evaporate off remaining pet. ether.
6. Distil (2mm Hg) below  $50^{\circ}\text{C}$  and store in fridge.

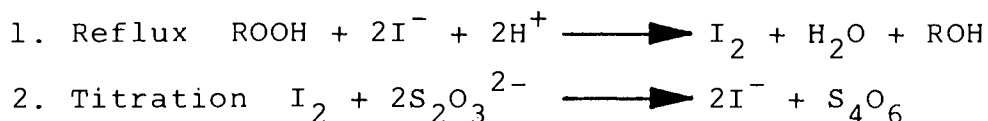
The CHP purity was found to be 97.5% after titration with sodium iodide (see Part C).

## B. Procedure

To a nitrogen purged glass reaction vessel in an oil bath at  $110^{\circ}\text{C}$  was added 10ml distilled chlorobenzene, 5ml of CHP solution and 25ml of chemical modifier/stabiliser additive solution (both in chlorobenzene). In the resultant 40ml solution, the CHP concentration was  $1 \times 10^{-2} \text{ mol dm}^{-3}$ , and the additive concentration varied in the molar ratios [additive]:[CHP] of 1:1, 1:10, 1:50 and 1:100. The remaining concentration of CHP was determined every 6 minutes for the first half hour, every 15 minutes for the next  $1\frac{1}{2}$  hours and then every hour to a combined total of 7 hours.

## C. Hydroperoxide determination

One millilitre was taken from the reaction vessel and transferred to a solution of excess sodium iodide and acetic acid in distilled isopropanol (20ml) and refluxed for ten minutes to liberate iodine after which the solution was titrated against aqueous sodium thiosulphate. From this, the % CHP remaining in the reaction vessel was easily calculated.



## 2.9.2 Oxygen Absorption

### A. Cumene purification

1. Distil at 45°C under vacuum.
2. Wash distillate with aqueous sodium hydroxide to remove cumene hydroperoxide (CHP).
3. Dry with magnesium sulphate.
4. Pass through column packed with activated alumina to remove remaining traces of CHP.
5. Store in fridge.

### B. Procedure

Solutions of azobisisobutyronitrile (AZBN) free radical initiator and the chemical modifier/stabiliser additive to be studied were prepared in purified cumene. The two solutions were mixed prior to oxygen absorption testing (8ml AZBN solution to 2ml additive solution) giving a total of 10ml in which the AZBN concentration was  $1 \times 10^{-2} \text{ mol dm}^{-3}$  and the additive concentration  $5 \times 10^{-4} \text{ mol dm}^{-3}$  giving a molar ratio of 20:1. 5ml of this solution was added by pipette to a magnetically stirred 50ml round-bottomed flask heated at 56°C by an oil bath. This flask, sealed to the atmosphere with vacuum grease was purged with oxygen and connected to an empty identical flask on the opposite side of a pressure transducer.

Oxygen absorption in the first flask creates a pressure drop across the transducer and after calibration, this pressure difference can be interpreted as the number of millilitres of oxygen absorbed by a chart recorder. Data recording commenced ten minutes after addition of the solution to the flask to allow temperature equilibration. Data was taken for up to 20 hours and was plotted as ml(O<sub>2</sub>) absorbed Vs. time(hrs).

Additive	I.R. wave no. ( $\text{cm}^{-1}$ )	U.V. spectra $\lambda_{\text{max}}(\text{nm})$ $\log E$
Maleic anhydride	1792	225    3.40
ADPA	1590	286    4.30
APMA	1590	283    4.23
APM	1780	284    4.00
Maleimide	1720	275    2.50
ADCT	1565	265    2.35
AACT	1630	313    3.46

Table 2.9 Infra-red wave no. ( $\text{cm}^{-1}$ ) and ultraviolet  $\lambda_{\text{max}}(\text{nm})$  and  $\log E$  used for percentage binding and quantitative concentration calculations of polypropylene additives



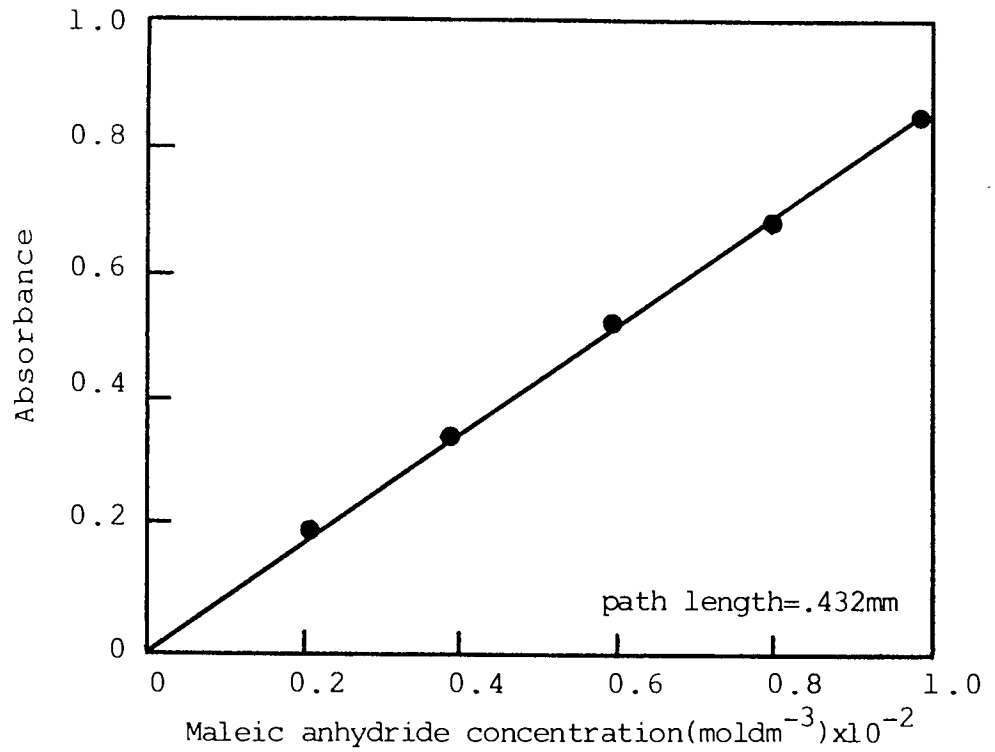


Figure 2.30 Calibration curve of infra-red absorbance ( $1792\text{cm}^{-1}$ ) for maleic anhydride (MA) in chloroform (ref. air)

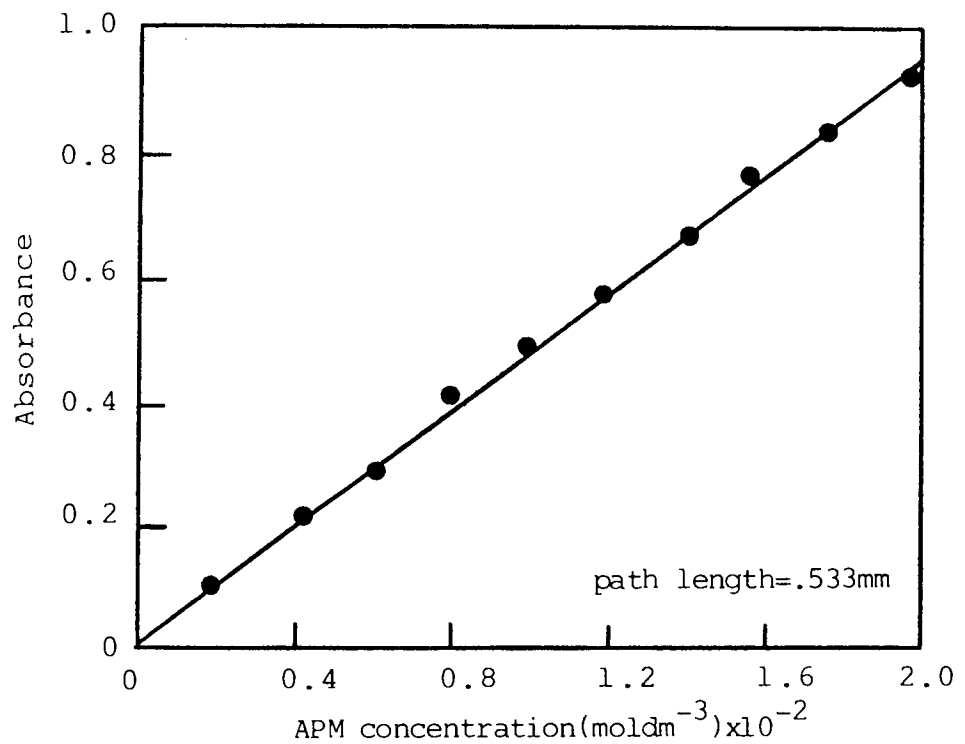


Figure 2.31 Calibration curve of infra-red absorbance ( $1780\text{cm}^{-1}$ ) for APM in chloroform (ref. air)

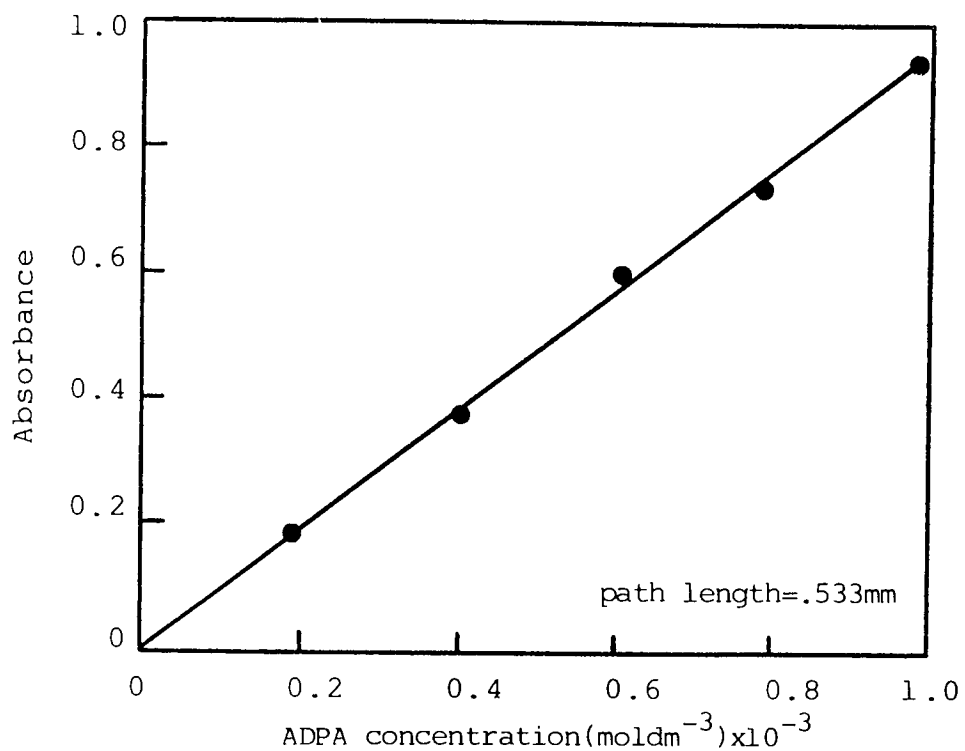


Figure 2.32 Calibration curve of infra-red absorbance( $1590\text{cm}^{-1}$ ) for ADPA in chloroform(ref.air)

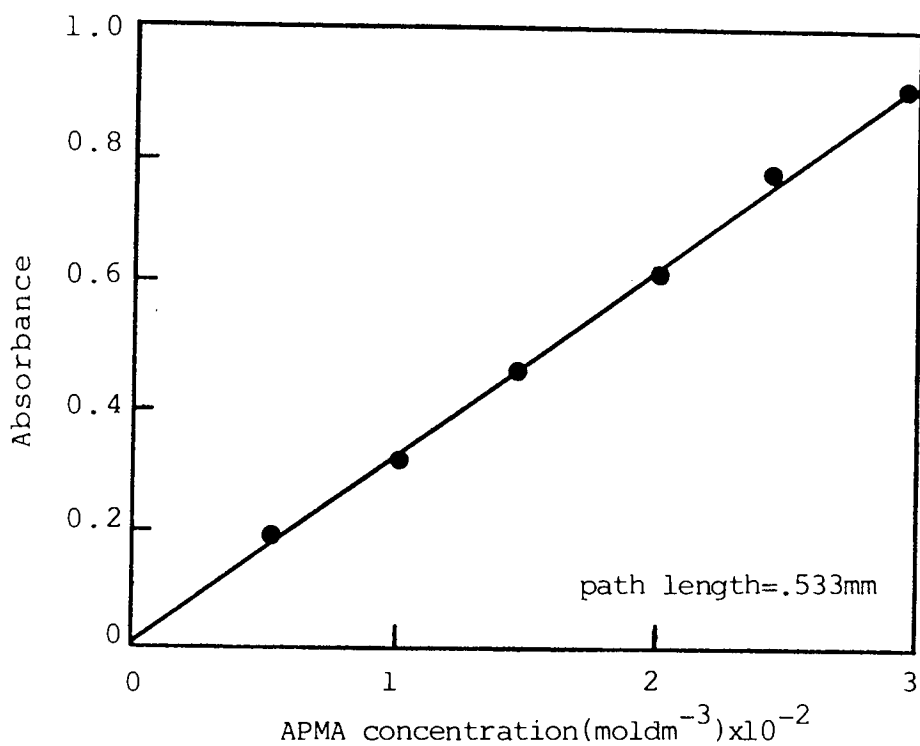


Figure 2.33 Calibration curve of infra-red absorbance( $1590\text{cm}^{-1}$ ) for APMA in chlorobenzene (air.ref)

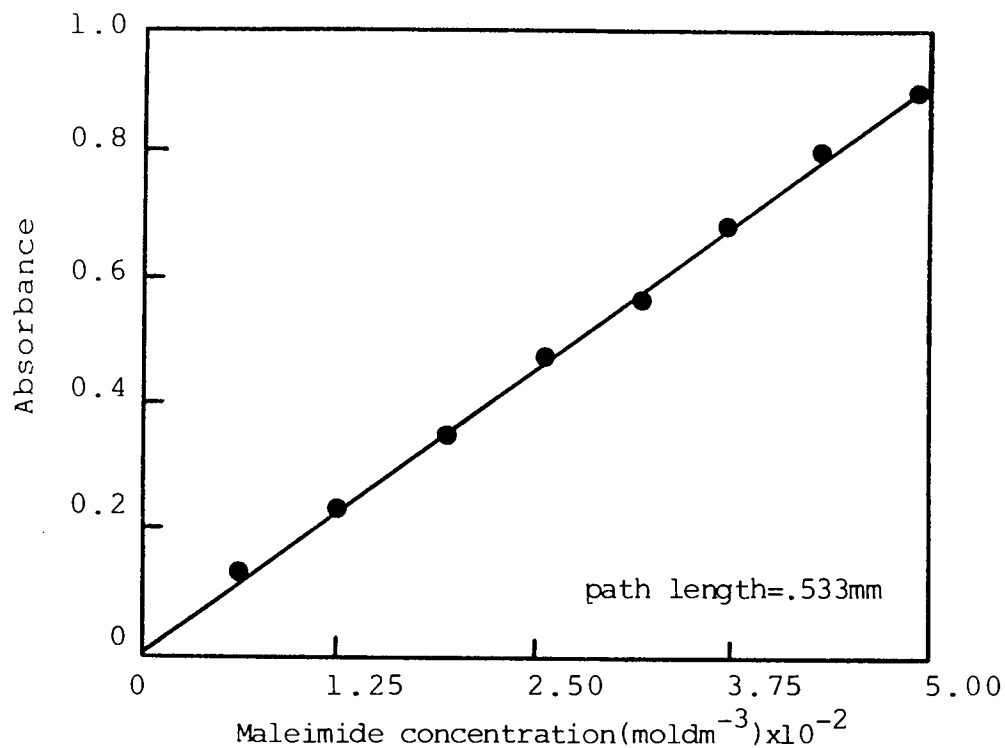


Figure 2.34 Calibration curve of infra-red absorbance( $1720\text{cm}^{-1}$ ) for maleimide in chlorobenzene (ref.air)

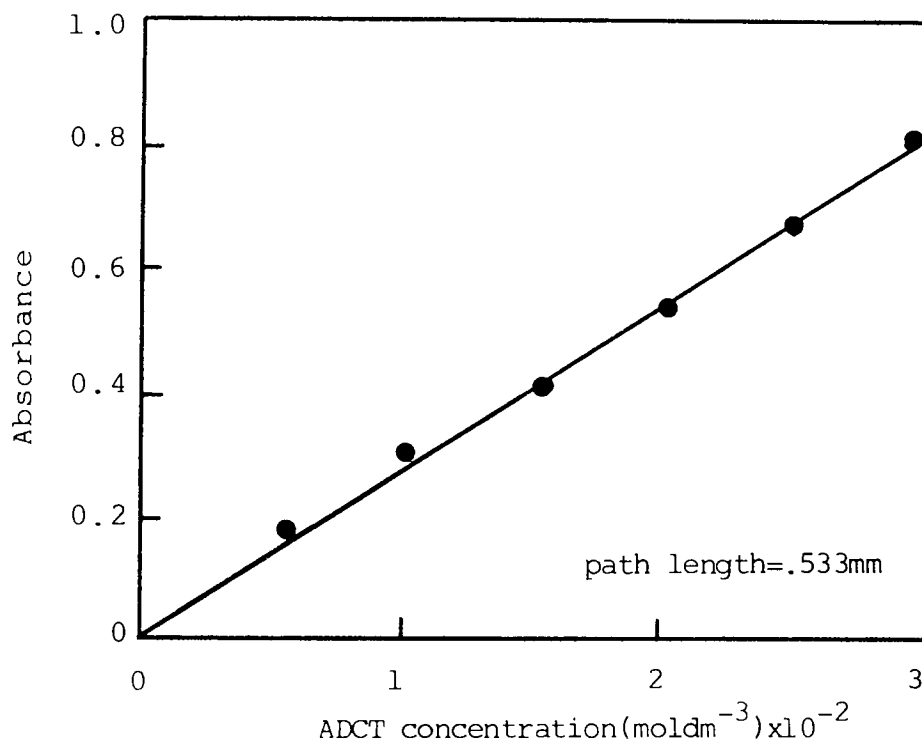


Figure 2.35 Calibration curve of infra-red absorbance( $1565\text{cm}^{-1}$ ) for ADCT in chlorobenzene (ref.air)

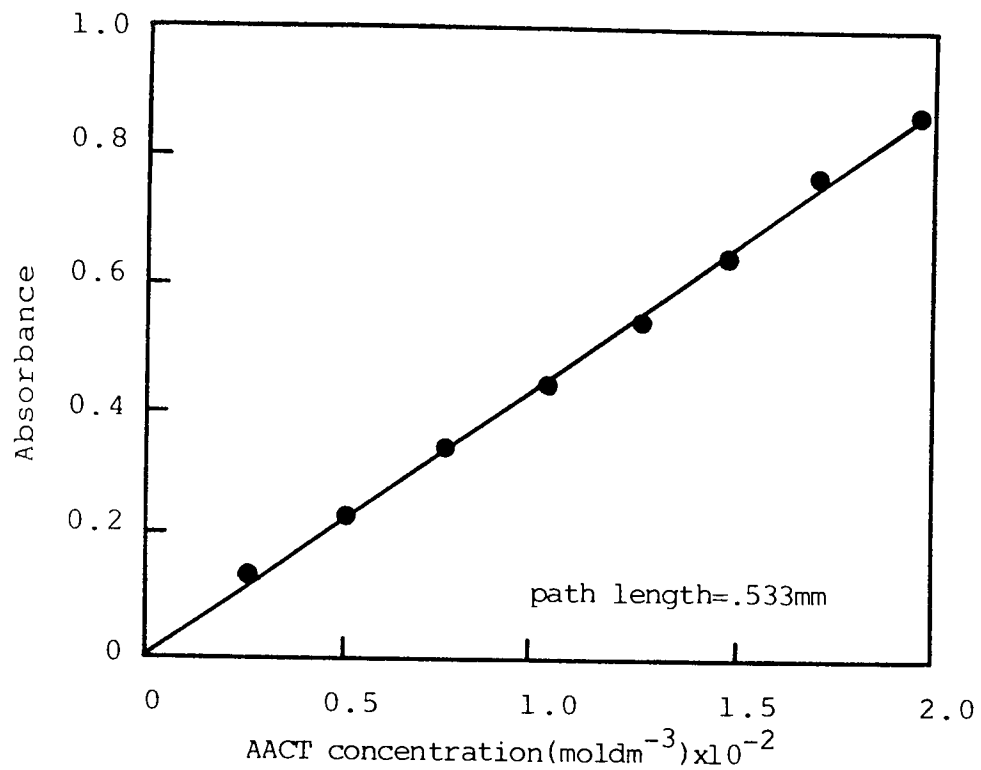


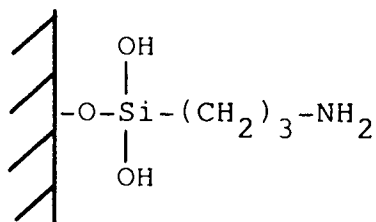
Figure 2.36 Calibration curve of infra-red absorbance( $1630\text{cm}^{-1}$ ) for AACT in chlorobenzene (ref.air)

CHAPTER THREE

COMPOSITE PROCESSING OPTIMISATION  
AND ASSESSMENT OF ROCKWOOL  
AND GLASS FIBRES IN POLYPROPYLENE

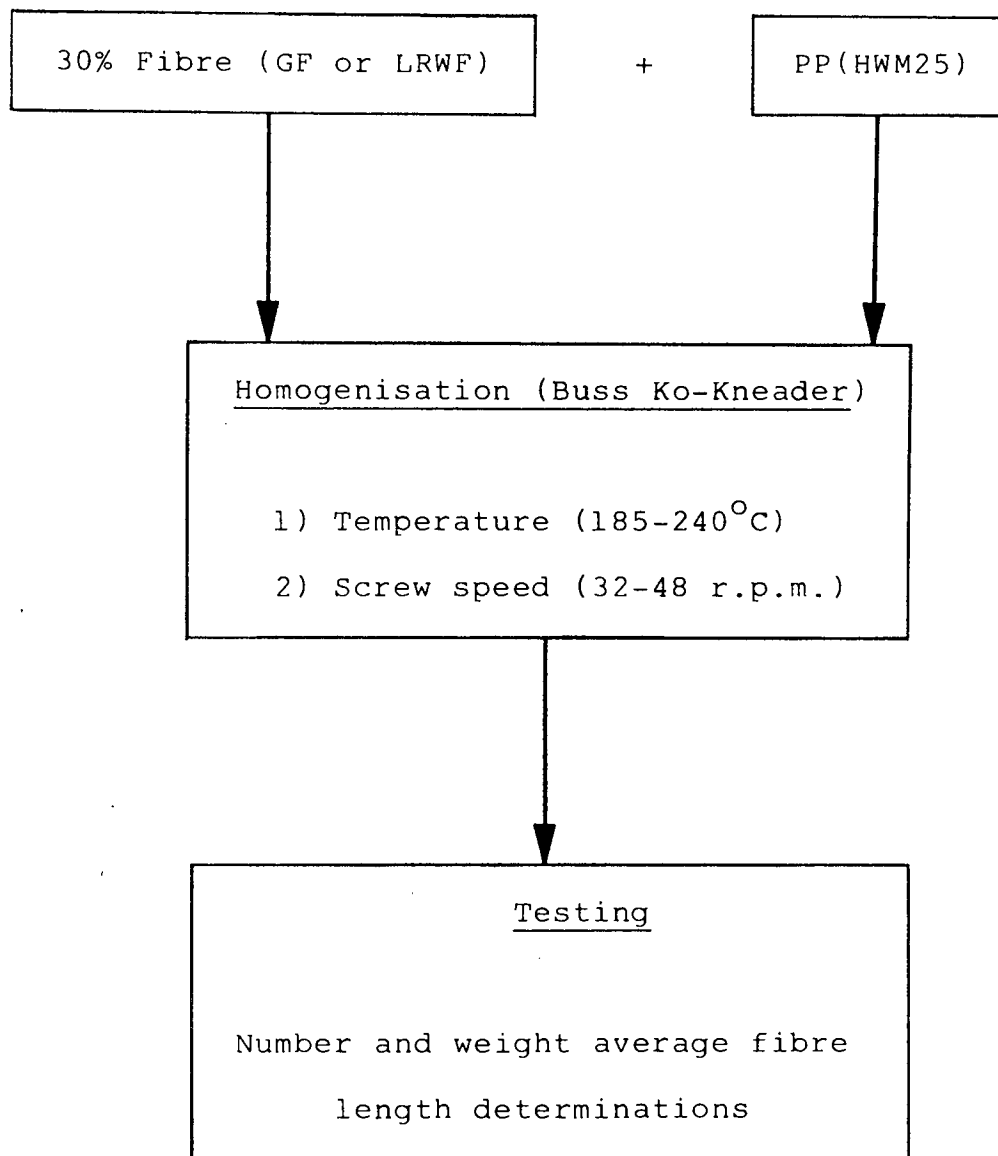
### 3.1 Object

In this chapter the effect of long Rockwool fibre (LRWF), short Rockwool fibre (SRWF) and glass fibre (GF, all treated with A-1100 silane coupling agent I) on the mechanical properties of commercially stabilised

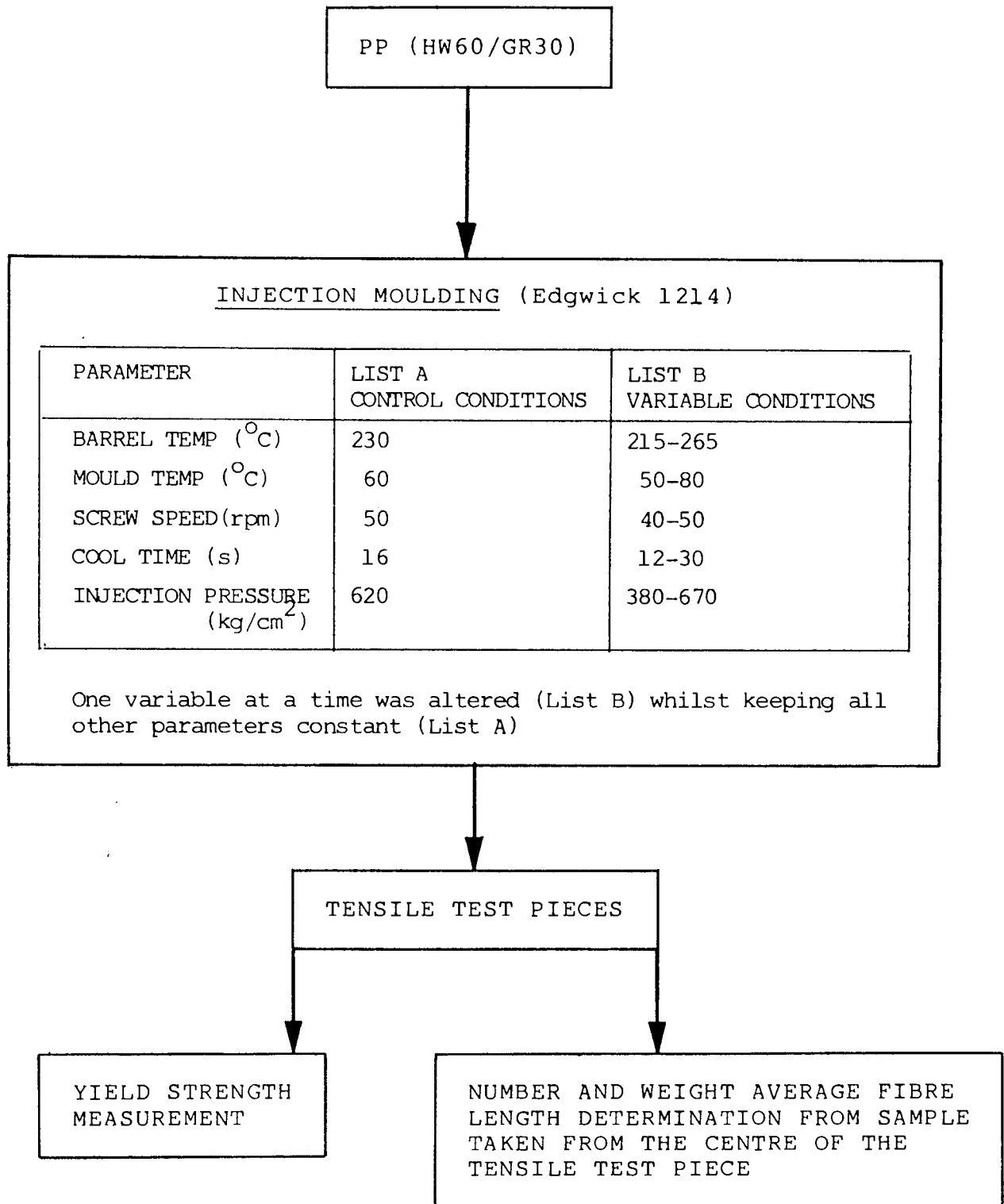


Fibre surface coupled with silane A-1100 (I)

PP(HWM25) are investigated and compared with commercially available 30% coupled glass reinforced PP(HW60/GR30). Levels of fibre used were in the range 0-45% by weight. Prior to this, the homogenisation (Buss Ko Kneader) and injection moulding (Edgwick) stages required for test-piece production were optimised. Both concerned the minimization of fibre breakage during processing which was monitored by measuring the fibre length distribution and the aspect ratios before and after processing. For optimising the homogenisation (Buss Ko-Kneader) stage, LRWF and GF(at 30% loading) were used in PP(HWM25). See Scheme 3.1. Optimisation of the injection moulding process involved a large number of variables and thus only commercially glass reinforced PP (HW60/GR30) was used, see Scheme 3.2. In addition to fibre length

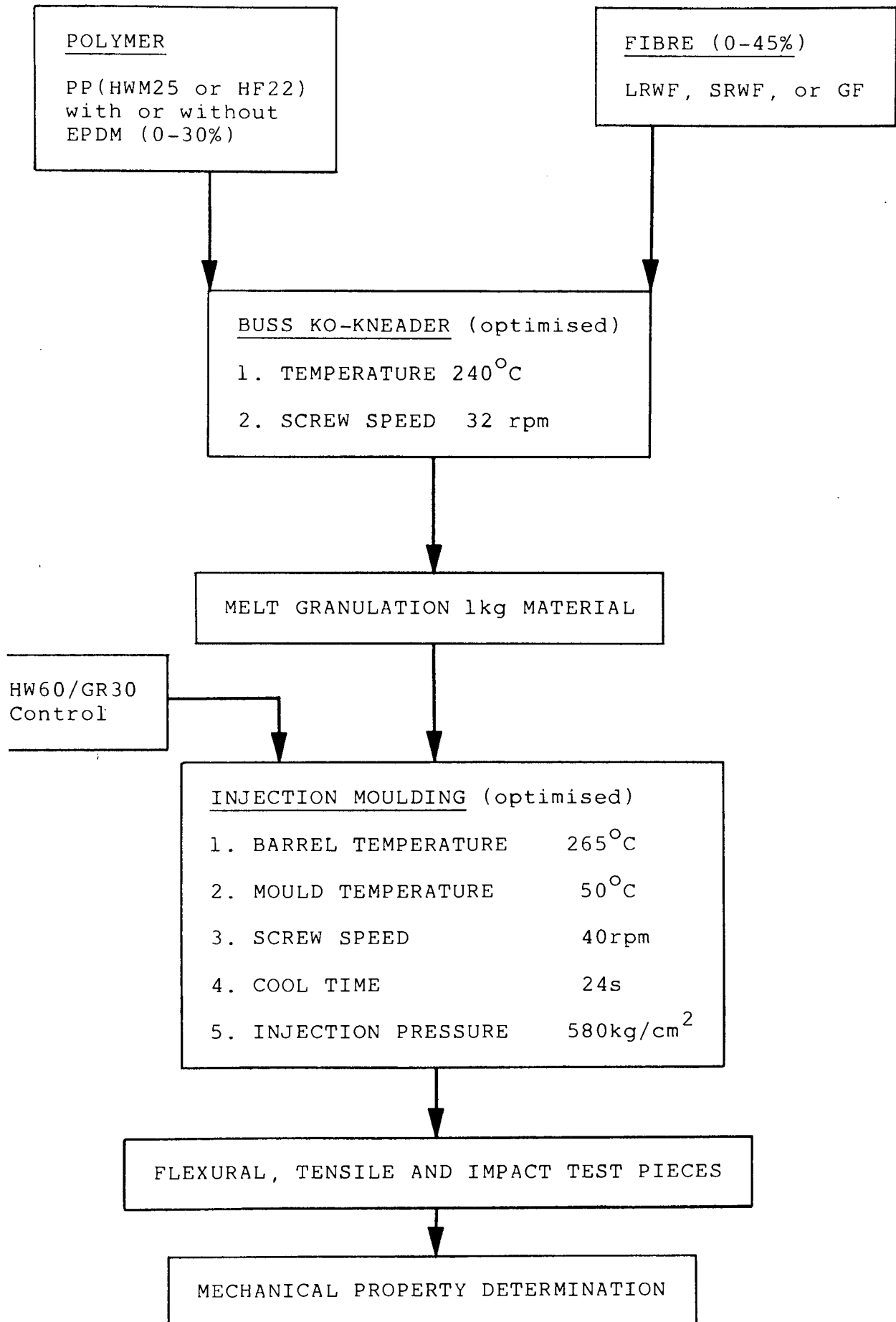


Scheme 3.1 Schematic diagram of the optimisation parameters used for homogenising PP with fibres in a Buss Ko-Kneader



Scheme 3.2 Schematic diagram of the optimisation of injection moulding parameters for reinforced PP





Scheme 3.3 Production of fibre reinforced and rubber modified PP using optimised homogenisation and injection moulding parameters

measurements, yield strength of the moulded tensile test pieces was recorded. The chosen optimum processing parameters were those that gave the greatest fibre length and yield strength. These conditions were then used for the homogenisation and injection moulding of all subsequent composite tensile, flexural and impact test pieces, see Scheme 3.3.

The use of EPDM (0-30% by weight) as an impact modifier has also been investigated in PP(HWM25) with and without LRWF and GF. In any one sample, the total EPDM and fibre weight fraction in PP did not exceed 45%. EPDM modified PP and its composites were homogenised and injection moulded using the same optimised processing conditions shown in Scheme 3.3.

## 3.2 Results

### 3.2.1 Optimisation Of The Homogenisation Process Using The Buss Ko-Kneader

The effect of screw speed and temperature of the Buss Ko-Kneader on fibre lengths, GF and LRWF (both at 30% loading and coupled with silane A-1100) when homogenised with PP(HWM25) are shown in Tables 3.1 and 3.2 respectively. These results are shown graphically in Figures 3.1 and

3.2. It is apparent that increasing the temperature from 185 to 240°C results in a three-fold increase in weight average length of GF and no significant change for LRWF. In contrast to the dominant effect of temperature in determining the final fibre length in homogenised PP (at least in the case of GF), the screw speed has comparatively minor influence with only slight improvements seen in GF fibre length as the screw speed was reduced from 48 to 32rpm. More important than fibre length is the aspect ratio which is the fibre length divided by its diameter. The aspect ratios at different processing temperatures and screw speeds are shown for LRWF and GF in Figure 3.2. Because GF (10µm) is twice the diameter of LRWF (5µm), it follows that GF must be twice as long as LRWF to have the same aspect ratio. After processing at 185°C, LRWF and GF have the same aspect ratio but as the temperature is increased to 240°C, the aspect ratio of GF rises three-fold, while LRWF increases only slightly (see Tables 3.1 and 3.2 and Figure 3.2). As with weight average fibre length, screw speed had very little effect on the aspect ratios. The optimised conditions chosen, and subsequently used in all composite homogenisation, were minimum screw speed of 32rpm and maximum temperature of 240°C. The maximum temperature was limited by the power of the oil heater on the Buss Ko-Kneader. Using these optimised conditions, the weight average length of GF after processing falls from its original 3mm to 0.591mm

(aspect ratio falls from 300 to 59.1), while the corresponding weight average length for LRWF falls from 1.10mm to 0.118mm (aspect ratio falling from 220 to 23.6). Fibres homogenised at the optimum conditions are shown in Plate 3.1 for GF and Plate 3.2 for LRWF after burning off the PP matrix, and are accompanied by fibre length distribution histograms in Figures 3.3 and 3.4 respectively. LRWF before processing is shown in Plate 2.2 and GF in Plate 2.3.

### 3.2.2 Injection Moulding (Edgwick) Optimisation

The effect of different processing parameters on number and weight average fibre length, aspect ratio and yield strength, of 30% coupled glass fibre reinforced PP (HW60/GR30) are shown in Table 3.3. Photographs of glass fibres before and after injection moulding of the composite are given in Plates 3.3 and 3.4 respectively, showing the fibre length degradation due to moulding. Mould temperature and cool-time were found to have no significant influence on fibre length, aspect ratio or yield strength of the moulded tensile test-pieces. The reduction of screw speed from 50 to 40 rpm resulted in an increased aspect ratio from 25.6 to 30.7 and yield strength of 1MPa. It was found that increasing the barrel temperature from 215 to 265°C more than doubled the aspect ratio and increased the yield strength by 5MPa (see Figure 3.5). This direct

relationship between aspect ratio and yield strength at different barrel temperatures is apparently contradicted when the injection pressure is varied; Figure 3.6 shows that raising the injection pressure from 380 to 680 kg/cm<sup>2</sup> nearly halved the aspect ratio while the yield strength remained almost constant. This is probably because the reduced aspect ratio which would normally be associated with reduced yield strength is compensated for by the reduced void content in the moulded composite due to the higher injection pressure. Optimum conditions were chosen as those that gave maximum aspect ratio and yield strength and are listed in Scheme 3.3. The optimised conditions resulted in an increased aspect ratio of 45% and yield strength of 2.3MPa over the control conditions (see Scheme 3.2). The control conditions were used as set processing parameters from which one processing parameter at a time was altered in order to investigate the effect of each parameter on the moulded composite.

### 3.2.3 Mechanical Properties Of PP(HWM25) Containing Long(L), Short(S) Rockwool Fibre(RWF) And Glass Fibre(GF)

The mechanical properties of PP(HWM25) containing LRWF, SRWF and GF (all A-1100 silane coupled, 0-45% loading) were examined and are summarised in Tables 3.5, 3.6 and 3.7 respectively and shown graphically in Figures 3.7-

3.14. Tables 3.5-3.7 also include the mechanical properties of PP(HWM25) homopolymer and commercially coupled glass reinforced PP(HW60/GR30) for comparison purposes. The properties of these two grades are summarised in Table 3.4.

Tan  $\delta$  represents the phase angle lag of  $E_2$  (loss modulus) behind  $E_1$  (storage modulus) of a viscoelastic material on response to an applied stress. Materials exhibiting high hysteresis loss show large values of Tan  $\delta$ . Figure 3.7 shows that increasing the GF content of PP(HWM25) from 0 to 45% causes a gradual reduction in Tan  $\delta$  of 35%. Tan  $\delta$  is independent of LRWF and SRWF loading. At all fibre loadings, Tan  $\delta$  of PP(HWM25) containing GF is always lower than equivalent LRWF or SRWF filled composites with the difference becoming greater at high fibre loadings. These results indicate that the introduction of increased loadings of GF to PP(HWM25) creates a composite of greater stiffness and lower hysteresis loss than the original homopolymer. This behaviour is to be expected because inorganic glass fibres are of higher modulus than PP. The reason for Tan  $\delta$  being independent of fibre loading for LRWF or SRWF filled PP(HWM25) could be due to poor adhesion at the polymer-fibre interface causing hysteresis loss and hence high values of Tan  $\delta$ .

The addition of fibres to PP(HWM25) had similar effects upon Charpy impact strength (notched 0.2mm, Figure 3.8),

flexural modulus (Figure 3.9), flexural strength (Figure 3.10) and tensile modulus (Figure 3.12). For LRWF, SRWF and GF, increasing loadings to 45% in PP(HWM25) results in an improvement in each of these mechanical properties. In each case, the use of GF achieves slightly higher levels than either LRWF or SRWF (both of which record very similar levels). The effect of addition of 45% GF to PP(HWM25) is most clearly seen for flexural modulus (Figure 3.9) which rises 700% and tensile modulus (Figure 3.12) improving by 500% above the level of the homopolymer. For LRWF, SRWF and GF filled PP(HWM25), the flexural strength increases with fibre loading to 35%, above which a plateau is reached. The Charpy impact strength (Figure 3.8) of GF filled PP(HWM25) gradually rises with increased loading to 45% while similar composites containing LRWF or SRWF only show enhanced impact strength when the fibre loading is 20% or higher.

Another factor indicating the poor fibre-matrix adhesion is apparent from the yield strength results (Figure 3.11). The yield strength of PP(HWM25) containing LRWF and SRWF is independent of fibre loading, with only very minor variations observed from the homopolymer yield strength. PP(HWM25) loaded with GF shows a rapid improvement in yield strength in the 20-35% loading range, above which a slight fall is observed and this may be attributed to high fibre loadings together with poor fibre-matrix

adhesion. Further evidence of weak fibre-matrix adhesion is shown in Figure 3.14 which depicts the tensile modulus retention of composites after immersion in water at 70°C for 24 hours. The purpose of this test is to compare the ability of composites to withstand adverse conditions and any reduction in tensile modulus after hot water immersion may be attributed to poor adhesion at the interface of the fibre and matrix (caused by water intrusion at the interface). PP(HWM25) containing up to 20% GF completely retains its tensile modulus after hot water immersion, after which there is a gradual decrease to only 70% modulus retention with 45% GF loading (Figure 3.14). The tensile modulus retention of PP(HWM25) containing LRWF and SRWF appears to be independent of fibre content with the modulus retention in each case being only 80%. The elongation at yield of PP(HWM25) containing LRWF, SRWF and GF (0-45% loading) is shown in Figure 3.13. As expected, elongation at yield decreases with increased fibre loading. This is due to the reduced ductility and diminished ability of the polymer to flow when subjected to an applied stress caused by the introduction of increased loadings of the high modulus fibres.

Visual evidence for the poor fibre-matrix adhesion for PP(HWM25) containing 30% LRWF and 30% GF is given in Plates 3.5 and 3.6 which show the composite tensile



fracture surfaces accompanied by the extremely long fibre pull-out, characteristic of low interfacial adhesion.

3.2.4 Summary Of The Mechanical Properties Of PP(HWM25) Containing Long Rockwool Fibre(LRWF) And Glass Fibre(GF, Both 30% Loading,A-1100 Coupled) And Commercially Coupled 30%GF Reinforced PP(HW60/GR30).

This section directly compares the mechanical properties of PP(HWM25) containing 30% LRWF and 30% GF with a currently available commercially coupled 30% GF reinforced grade of PP (HW60/GR30). The results are shown in Table 3.8 and presented graphically in Figures 3.15-3.19. It is immediately obvious that all of the mechanical properties of HW60/GR30 are considerably greater than PP containing both 30% LRWF and 30% GF. The yield strength (Figure 3.16) and flexural strength (Figure 3.18) of HW60/GR30 are at least double those observed for PP(HWM25) containing 30% LRWF and 30% GF, while the tensile modulus (Figure 3.17) and Charpy impact strength (notched, 0.2mm, Figure 3.15) of the commercially reinforced material are 50% in excess of PP(HWM25) loaded with LRWF and GF. Only the flexural modulus (Figure 3.19) of PP(HWM25) with 30% LRWF and 30% GF approaches the commercial control HW60/GR30. For each property it is seen that although PP(HWM25) containing 30% LRWF compares quite well with its 30% GF equivalent, it consistently under-performs by 20%, except for tensile modulus (Figure 3.17) where the discrepancy is 40%.

### 3.2.5 The Effect Of EPDM (0-30% Loading) On The Mechanical Properties Of PP(HWM25)

EPDM is used for rubber modification of polyolefins and the effect of 0-30% EPDM loadings on the mechanical properties of PP(HWM25) are shown in Table 3.9 and depicted graphically in Figures 3.20-3.23. Increasing the EPDM loading to 30% in PP(HWM25) causes a gradual reduction in yield strength (Figure 3.20) and flexural strength (Figure 3.22) to only 35% of the homopolymer's, while under the same conditions the tensile modulus (Figure 3.21) and flexural modulus (Figure 3.23) are reduced by 50%. These results are to be expected because unvulcanised EPDM rubber is of lower strength and modulus than PP(HWM25) homopolymer. The primary use of EPDM in polyolefins however is to increase their impact strength by decreasing the degree of stress concentration within the polyolefin. This delocalisation of stress throughout the rubber modified polyolefin allows higher impact loads to be accommodated without fracture. This is demonstrated in Figure 3.22 where the addition of 30% EPDM to PP(HWM25) causes a 500% increase in Charpy impact strength (notched, 0.2mm). This high 30% EPDM content makes the PP(HWM25) very ductile, and this results in an elongation at yield being double that of unmodified PP(HWM25) (Figure 3.20). Because rubbers exhibit high degrees of hysteresis (i.e., high damping),

the phase angle lag of the loss modulus behind the storage modulus ( $\tan \delta$ ) is increased by over 50% when PP(HWM25) is modified with 30% EPDM.

### 3.2.6 The Effect Of EPDM (10% and 20% Loadings) On Long Rockwool Fibre (LRWF) And Glass Fibre (GF) Filled PP(HWM25)

Having studied separately the effect of fibres (LRWF, SRWF and GF) and the rubber modifier EPDM on the mechanical properties of PP(HWM25) in 3.2.3 and 3.2.5 respectively, this section describes the use of PP(HWM25) modified with 10% and 20% EPDM and reinforced with up to 35% fibre (LRWF and GF, both A-1100 silane coupled). The maximum combined loading of rubber and fibre in any one PP(HWM25) sample was 45%. Table 3.10 shows the effect of 0-35% fibre (LRWF and GF) with 10% EPDM and Table 3.11, the effect of 0-25% fibre with 20% EPDM on the mechanical properties of PP(HWM25). These results are presented graphically for comparison in Figures 3.24-3.37. The addition of 10% and 20% EPDM to PP(HWM25) containing LRWF and GF (Figures 3.24 and 3.25 respectively) causes the phase angle lag,  $\tan \delta$ , to fall slightly for high loadings of LRWF filled PP(HWM25) and to rise sharply for GF composites. This apparently contradictory behaviour may possibly be explained when one considers the  $\tan \delta$  values of LRWF and GF filled PP(HWM25) without EPDM.

PP(HWM25) containing GF (up to 45% loading) gives low values of  $\tan \delta$  (between 4 and 5) indicating low hysteresis loss and hence reasonable adhesion between fibre and matrix, while LRWF filled PP shows relatively high  $\tan \delta$  levels (between 6 and 7) suggesting poor fibre-matrix adhesion. Incorporation of EPDM into the two systems probably results in coating of the fibres with a thin layer of the elastomer (EPDM) which may cause increased adhesion of LRWF towards PP(HWM25) accompanied by lower hysteresis loss and hence low  $\tan \delta$  while at the same time decreasing adhesion of GF towards PP(HWM25) which increases hysteresis loss and results in the observed higher value of  $\tan \delta$ . Decreased hysteresis loss (i.e., of lower  $\tan \delta$ ) creates a material of increased resilience.

The Charpy impact strength (notched, 0.2mm) of PP(HWM25) containing up to 20% LRWF with 20% EPDM is double the homopolymer's (see Figure 3.26) but EPDM appears to have no significant effect on LRWF loadings above 20%.

Figure 3.27 shows that in the presence of GF there is no significant change in Charpy impact strength with 10% and 20% EPDM except at 25% GF in 20% EPDM modified PP(HWM25) where the impact resistance shows an improvement in excess of 100% over all the other rubber modified PP(HWM25) GF composites. The reason for this sudden improvement is not clear but is probably associated with an optimised

combination of EPDM creating stress dissipation throughout the rubber modified PP(HWM25) in conjunction with the 25% GF.

EPDM modified PP(HWM25) containing LRWF gave similar behaviour with flexural strength (Figure 3.30) and yield strength (Figure 3.32). Below 20% LRWF loadings, both flexural and yield strength are substantially reduced by the EPDM modification of PP(HWM25). Above 20% LRWF loadings, EPDM had no significant effect. The addition of increasing amounts of EPDM (10% and 20%) to PP(HWM25) containing GF, progressively decreases the yield strength (Figure 3.33) and a similar trend is observed for the flexural strength (Figure 3.31).

For both LRWF and GF filled PP(HWM25), the addition of EPDM had very little effect on both flexural modulus (Figures 3.28 and 3.29) and tensile modulus (Figures 3.34 and 3.35). This suggests that the modulus of the rubber modified composites is more dependent upon the loading of high modulus fibre (see Figure 3.29) than any relatively minor reductions in the modulus of the PP(HWM25) matrix due to EPDM modification (see Figure 3.23).

### 3.3 Discussion

#### 3.3.1 Optimisation Of The Homogenisation Process Using The Buss Ko-Kneader

The aim of fibre homogenisation with polymers by melt processing is to obtain a uniform dispersion throughout the matrix. This is easily accomplished using the Buss Ko-Kneader, but as Tables 3.1 and 3.2 and Figures 3.1 and 3.2 show, the high shearing process can cause excessive fibre length degradation which will diminish the mechanical properties of the final injection moulded component. To obtain good fibre dispersion, the Buss Ko-Kneader employs a very high back pressure with screw rotation supplemented by a cyclical back and forth motion, but it is the high-energy input that degrades fibre length. Figures 3.1 and 3.2 show that fibre length degradation may be limited by the use of the correct screw speed and processing temperature. The most probable reason for both LRWF and GF lengths not being significantly increased by reducing the screw speed of the Buss Ko-Kneader from 48 to 32rpm is that the melt shearing is inherently so high (due to the high back pressure) that changes in screw speed only marginally effect the degree of shear in the melt. In contrast, increasing the melt-processing temperature from 185 to 240°C (Figures 3.1 and 3.2) markedly decreases the GF length degradation due to quicker

PP(HWM25) melt formation and its lower viscosity accompanied by reduced back pressure which all contribute to less working of the melt by the screw. The observation that LRWF length is degraded much more than GF (Figures 3.1 and 3.2) is because its diameter at  $5\mu\text{m}$  is only half of that of GF and its woolly texture makes feeding via the hopper extremely difficult. It has been observed that while a strong shear field is required for good fibre dispersion, Erwin<sup>(187)</sup> has recorded that excessive fibre breakage occurs due to the breaking up of bundles due to fibre-fibre interaction. If the bundles are not dispersed, voiding and stress concentration within the final component occurs. The chosen optimum homogenisation conditions were those that gave the lowest shearing of the polymer melt ( $240^{\circ}\text{C}$ , 32rpm, see Scheme 3.3); the much higher aspect ratio (see Tables 3.1 and 3.2) of GF (59.1) over LRWF (23.6) after processing at optimised conditions is expected to result in significant differences between the mechanical properties of their PP(HWM25) composites. (see Section 3.3.3).

### 3.3.2 Injection Moulding (Edgwick) Optimisation

Confirming similar observations from homogenisation optimisation (Section 3.3.1), the melt-processing temperature (injection moulding barrel temperature) had the most influence upon fibre length degradation (Table 3.3 and

Figure 3.5) with a 50°C rise from 215 to 265°C resulting in a doubling of the GF aspect ratio (from the commercial composite, HW60/GR30). This is a well documented observation<sup>(21,188,189)</sup> and is accompanied by an increase in yield strength (Figure 3.5) of the glass reinforced PP(HW60/GR30). Longer fibre length results in higher composite strength because more stress can be transferred to the reinforcing fibre (Chapter One, Section 1.2, Equation 1). The higher temperature also reduces back pressure, allows easier packing of the mould cavity, results in quicker melt formation and hence decreases the degree of shear in the melt. The reduced working of the resin by the screw also results in lower screw retraction times<sup>(21)</sup>. Polyolefin composites such as HW60/GR30 should be moulded at high temperatures (provided thermal degradation of the matrix is avoided) for these reasons. Other advantages are better fibre dispersion and decreased problems associated with weld lines<sup>(189)</sup>. Despite only two screw speeds (40 and 50rpm, Table 3.3) being investigated, the lower one resulted in less fibre length degradation and provided the screw speed is sufficient to provide adequate fibre dispersion<sup>(188)</sup> the minimum screw speed should be used because fibre breakage is related to the peripheral speed of the screw<sup>(21)</sup>. The effect of increasing the injection pressure (Figure 3.6) shows an apparent ambiguity in that while the GF aspect ratio falls, the yield strength of HW60/GR30 rises slightly. However,



whilst the reduced aspect ratio would tend to decrease a composite's strength, this is more than compensated for by the high injection pressure resulting in a moulding of higher quality: better fibre dispersion, mould flow ability, full packing of the mould cavity and reduced voiding<sup>(189)</sup>. Voiding is a major problem associated with injection moulded short fibre reinforced thermoplastics and is easily recognised by a white zone in the core of the moulding<sup>(190)</sup> caused by gases and moisture evolved during the high temperature moulding process as well as crazing to relieve stress during cooling created by differential shrinkage of fibres and matrix. Mould temperature and cool-time (Table 3.3) had no significant effect upon the aspect ratio of GF or yield strength of the HW60/GR30 composite and this is probably due to the small mould cavity not requiring very high temperatures to aid flow (as would be required for long thin sections) or long cool times to avoid excessive voiding in thick sections.

### 3.3.3 Mechanical Properties Of PP(HWM25) Containing Long (L), Short(S) Rockwool Fibre(RWF) And Glass Fibre(GF)

The mechanical properties of unmodified stabilised PP (HWM25) containing 0-45% by weight of A-1100 silane coupled SRWF, LRWF and GF (Tables 3.5-3.7, Figures 3.7-3.14) indicate that GF is the best reinforcing fibre. The

observation that PP(HWM25) containing LRWF and SRWF gave almost identical mechanical performance (Figures 3.7-3.14) despite their initial differences in fibre length prior to processing is not surprising because Richard and Sims<sup>(188)</sup> have reported that there is little advantage in using initially long fibres which are otherwise identical to shorter ones because the homogenisation and injection moulding stages degrade them to the same length.

Increased loading to 45% with SRWF, LRWF and GF of PP(HWM 25) was most effective upon increasing the flexural (Figure 3.9) and tensile (Figure 3.12) moduli because the high modulus fibres dominate the matrix modulus which is low by comparison<sup>(191)</sup>. The "law of mixtures" (Chapter One, Section 1.2, Equation 1) which states that the modulus of a composite is proportional to the relative amounts of fibre and matrix is adhered to and it is reasonable to postulate that because the modulus of a composite is independent of fibre length<sup>(192)</sup>, the higher tensile and flexural moduli observed for GF reinforced PP(HWM25) is due to the higher modulus of the GF itself compared to the mineral fibre grades (LRWF and SRWF).

Both flexural and yield strengths (Figures 3.10 and 3.11) results are more difficult to interpret because they involve a composite failure mechanism. Optimum results with GF reinforced PP(HWM25) were achieved not with the

highest fibre loading (45%) but at 35-40%. This is a common observation<sup>(36,192)</sup> and is attributable to poor adhesion between fibres and matrix, local stresses in the matrix unable to be relieved by local flow processes due to the high fibre loading<sup>(36)</sup> (which also explains the reduced elongation to yield of these composites, Figure 3.13) and increased fibre damage during processing at high loadings due to increased fibre-fibre interaction. In distinct contrast, the yield strengths (Figure 3.11) of LRWF and SRWF filled PP(HWM25) were independent of fibre loading. This may be due to very poor fibre-matrix adhesion<sup>(191)</sup> and fibre stress being greatest in those fibres which are aligned with the test-piece axis causing crack initiation to originate from fracture of the fibre itself<sup>(42)</sup>. The lower aspect ratios of LRWF and SRWF (compared to GF) are a major factor because their shorter length reduces the amount of stress that may be transferred to them from the matrix. In some cases, high fibre loadings ensure higher strength composites because high fibre concentrations tend to increase fibre alignment during moulding<sup>(28)</sup> (which in this case corresponds to the direction of the applied stress during tensile testing). However, less alignment is likely to occur with the two RWF grades because shorter fibres show poorer alignment than longer fibres (such as GF) on moulding<sup>(28)</sup>. Composite failure is often a result of fibre damage with cracks nucleating in the PP matrix at the fibre ends<sup>(11,28)</sup>

causing the reinforced polymer to fail in a brittle manner despite the homopolymer failure being ductile<sup>(28)</sup>; this is supplemented by fibre-induced changes in polymer morphology (such as greater crystallinity) and the notching effect of fibres in which stress concentration is induced in the matrix.

Impact behaviour interpretation is difficult because it is an energy phenomenon dependent upon strain and yield strength at high deformation rates<sup>(36,191)</sup>. Because toughness is influenced by yield strength (Figure 3.11) and elongation (Figure 3.13), it was therefore expected that GF reinforced PP(HWM25) would give better Charpy impact strength than LRWF or SRWF grades (Figure 3.8). Impact strength of PP(HWM25) increased as the loading of all three fibre types was raised, confirming the general belief that composite materials possess higher impact strengths due to fibre pull-out from the matrix; fracture energy is a combination of the work required to debond the fibres from the matrix and the work done against friction in pulling the fibres out of the matrix<sup>(193)</sup>. Fibres shorter than the critical length are pulled out from the matrix rather than breaking during composite crack propagation. Firm evidence of poor fibre-matrix adhesion (Plates 3.5 and 3.6) is shown by the very long pull-out lengths for LRWF and GF from PP(HWM25), together with holes in the matrix from which fibres have been

pulled during fracture; a fibre's critical length is twice the longest pull-out length<sup>(194)</sup>.

PP(HWM25) exhibits very low water absorption compared to other resins<sup>(43)</sup> and thus the loss of tensile modulus (Figure 3.14), especially in composites containing LRWF and SRWF, is attributable to water incursion at the weakly bonded fibre-matrix interface further reducing adhesion and allowing easier slippage between the two phases. The phase angle lag between storage and loss moduli ( $\text{Tan}\delta$ , Figure 3.7) is determined by the properties of the polymer matrix, the reinforcing fibres and the fibre-matrix bonding efficiency. The observation that the addition of GF to PP(HWM25) in increasing amounts reduced  $\text{Tan}\delta$  while similar addition of LRWF and SRWF although increasing the stiffness (Figures 3.9 and 3.12) of PP(HWM25) had no effect upon  $\text{Tan}\delta$  must be attributable to energy absorption (creating decreased resilience) due to friction (caused by slippage) at the fibre-matrix interface.

#### 3.3.4 Summary Of The Mechanical Properties Of PP(HWM25) Containing Long Rockwool Fibre(LRWF) And Glass Fibre(GF,Both 30% Loading,A-1100 Coupled) And Commercially Coupled 30%GF Reinforced PP(HW60/GR30)

Despite careful optimisation of the homogenisation and injection moulding processes (Section 3.3.1 and 3.3.2)

to maintain the lengths of LRWF and GF in PP(HWM25), the mechanical performance of these A-1100 silane coupled 30% loaded composites (Table 3.8, Figures 3.15-3.19) are clearly inferior to the commercially 30%GF reinforced PP(HW60/GR30). This grade is chemically coupled to improve the fibre-matrix interfacial adhesion and this is clearly very successful in improving the mechanical performance (the nature of coupling would not be disclosed by the manufacturer, ICI). 30%GF reinforced PP(HWM25) gave better performance than the equivalent 30%LRWF grade and this is attributable to the higher modulus of the glass fibres, their higher aspect ratio and better adhesion towards the PP(HWM25) matrix. However, despite both LRWF and SRWF being A-1100 silane coupled, their adhesion to PP(HWM25) is still very poor and this is probably because the coupling process has been attempted over the "tenside" layer which is present on the mineral fibre surface to prevent fibre agglomeration (Chapter 2, Section 2.1.2.2). This layer presents a physical barrier to effective coupling with the true fibre surface. The superior mechanical performance of chemically coupled HW60/GR30 manifests itself by providing sites along PP chains where chemical coupling with the coupling agent on the glass fibre surface may occur resulting in higher fibre pull-out energy to give good impact behaviour (Figure 3.15), increased stress transfer (from matrix to fibres) resulting in higher yield and flexural strengths

(Figures 3.16 and 3.18), less movement between the two phases at the interface to give higher tensile and flexural moduli (Figures 3.17 and 3.19) together with a lower critical length requirement for the GF present in this composite (Chapter One, Section 1.2).

It is thus apparent that efficient chemical coupling provides an extremely effective means of enhancing the mechanical performance of covalent PP containing inorganic silane coupled reinforcing fibres. This is attempted using maleic anhydride in Chapter Four and a range of other chemical modifiers in Chapter Five.

### 3.3.5 The Effect Of EPDM(0-30% loading) On The Mechanical Properties Of PP(HWM25)

The addition of EPDM which is amorphous to a semi-crystalline material such as PP(HWM25) is a widespread commercial technique to improve the impact resistance. However, because EPDM is itself of low modulus and strength, the yield and flexural strengths (Figures 3.20 and 3.22) and tensile and flexural moduli (Figures 3.21 and 3.23) of PP(HWM25) are substantially reduced by rubber modification. Through blending of these two materials, the Charpy impact strength of PP(HWM25) has been increased by 500% with 30% EPDM (Figure 3.22) and it has been recorded by Dao<sup>(195)</sup> that the mechanical properties of such blends are

determined by EPDM particle size and dispersion (which is obtained by processing with PP(HWM25) in high shear fields such as the Buss Ko-Kneader). EPDM particles act as craze arrestors, delocalising concentrated stress over the whole component. Toughness, being a function of yield strength and deformational strain, is higher for EPDM/PP (HWM25) blends despite the yield strength (Figure 3.20) being lower; it is the much enhanced deformational ability (Figure 3.20) that is responsible for the substantial improvement in Charpy impact strength.

### 3.3.6 The Effect Of EPDM(10% And 20% Loadings) On Long Rockwool Fibre(LRWF) And Glass Fibre(GF) Filled PP(HWM25)

Reinforcing fibres (LRWF and GF) were homogenised with EPDM modified PP(HWM25) to see if the high impact strength of rubber modified PP(HWM25) could be supplemented by the higher flexural and tensile moduli and strength imparted by the inorganic fibres. The flexural and tensile moduli (Figures 3.28, 3.29 and Figures 3.34, 3.35) of both LRWF and GF filled PP(HWM25) were reduced only slightly by the addition of EPDM (10 and 20%), confirming earlier observations (Section 3.3.3) that the modulus of a composite is more dependent on the fibre's modulus because they are the primary load bearing elements<sup>(191)</sup>. Impact strength (Figure 3.26) of LRWF filled PP(HWM25) was



increased by the addition of EPDM suggesting that energy absorption by fibre pull-out from the matrix<sup>(193,196)</sup> is complemented by impact energy delocalisation due to EPDM<sup>(195)</sup>. The coating of LRWF with EPDM may also contribute because Peiffer<sup>(197)</sup> has suggested that optimum toughness is obtained when there is a uniform rubbery interface located between the reinforcing fibres and matrix. The properties depend on the interlayer thickness and this phenomenon may explain the dramatic improvement in toughness when 20%EPDM is incorporated into PP(HWM25) with 25%GF (Figure 3.27).

Despite higher impact strengths (Figures 3.26 and 3.27) being achieved with EPDM modified PP(HWM25) composites with good retention of flexural and tensile moduli (Figures 3.28, 3.29 and 3.34, 3.35) compared to similar composites without EPDM, the flexural and yield strengths (Figures 3.30, 3.31 and 3.32, 3.33) were very poor by comparison (see Section 3.3.5). For this reason, further work on EPDM modification was not considered because the objectives of this work are to improve upon all the mechanical properties, high temperature dimensional stability and durability of the commercial PP composite, HW60/GR30.

Barrel Temperature						
185°C			205°C			
Screw speed (rpm)	No. Ave length (mm)	Wt. Ave length (mm)	Wt. Ave aspect ratio	No. Ave length (mm)	Wt. Ave length (mm)	Wt. Ave aspect ratio
32	0.143	0.186	18.6	0.168	0.267	26.7
40	0.096	0.155	15.5	0.262	0.337	33.7
48	0.092	0.132	13.2	0.139	0.221	22.1

Barrel Temperature						
225°C			240°C			
Screw speed (rpm)	No. Ave length (mm)	Wt. Ave length (mm)	Wt. Ave aspect ratio	No. Ave length (mm)	Wt. Ave length (mm)	Wt. Ave aspect ratio
32	0.342	0.443	44.3	0.396	0.591	59.1
40	0.301	0.288	28.8	0.409	0.559	55.9
48	0.415	0.567	56.7	0.309	0.448	44.8

Prior to processing, original GF: No. Ave length = 3mm  
 Wt. Ave length = 3mm  
 Fibre diameter = 10µm  
 Wt. Ave aspect ratio = 300

After processing, standard deviation (32rpm, 185°C) = 0.108

Table 3.1 Optimisation of Buss Ko-Kneader parameters (speed, temperature) for the homogenisation of PP (HWM25) with glass fibre (GF, A1100 silane coupled, 30% loading)

Screw speed (rpm)	Barrel Temperature					
	185°C			205°C		
	No. Ave length (mm)	Wt. Ave length (mm)	Wt. Ave aspect ratio	No. Ave length (mm)	Wt. Ave length (mm)	Wt. Ave aspect ratio
32	0.072	0.095	19.0	0.076	0.096	19.2
40	0.068	0.086	17.2	0.065	0.085	17.0
48	0.061	0.081	16.2	0.072	0.091	18.2

Screw speed (rpm)	Barrel Temperature					
	225°C			240°C		
	No. Ave length (mm)	Wt. Ave length (mm)	Wt. Ave aspect ratio	No. Ave length (mm)	Wt. Ave length (mm)	Wt. Ave aspect ratio
32	0.074	0.098	19.6	0.087	0.118	23.6
40	0.073	0.098	19.6	0.079	0.105	21.0
48	0.070	0.090	18.0	0.079	0.100	20.0

Prior to processing, original LRWF: No.ave length = 0.64mm  
 Wt. Ave length = 1.10mm  
 Fibre diameter= 4-6µm

After processing, standard deviation(32rpm,185°C) = 0.136  
 Wt. Ave aspect ratio= 220

Table 3.2 Optimisation of Buss Ko-Kneader parameters (Speed, temperature) for the homogenisation of PP(HWM25) with long Rockwool fibre(LRWF, A-1100 silane coupled, 30% loading)

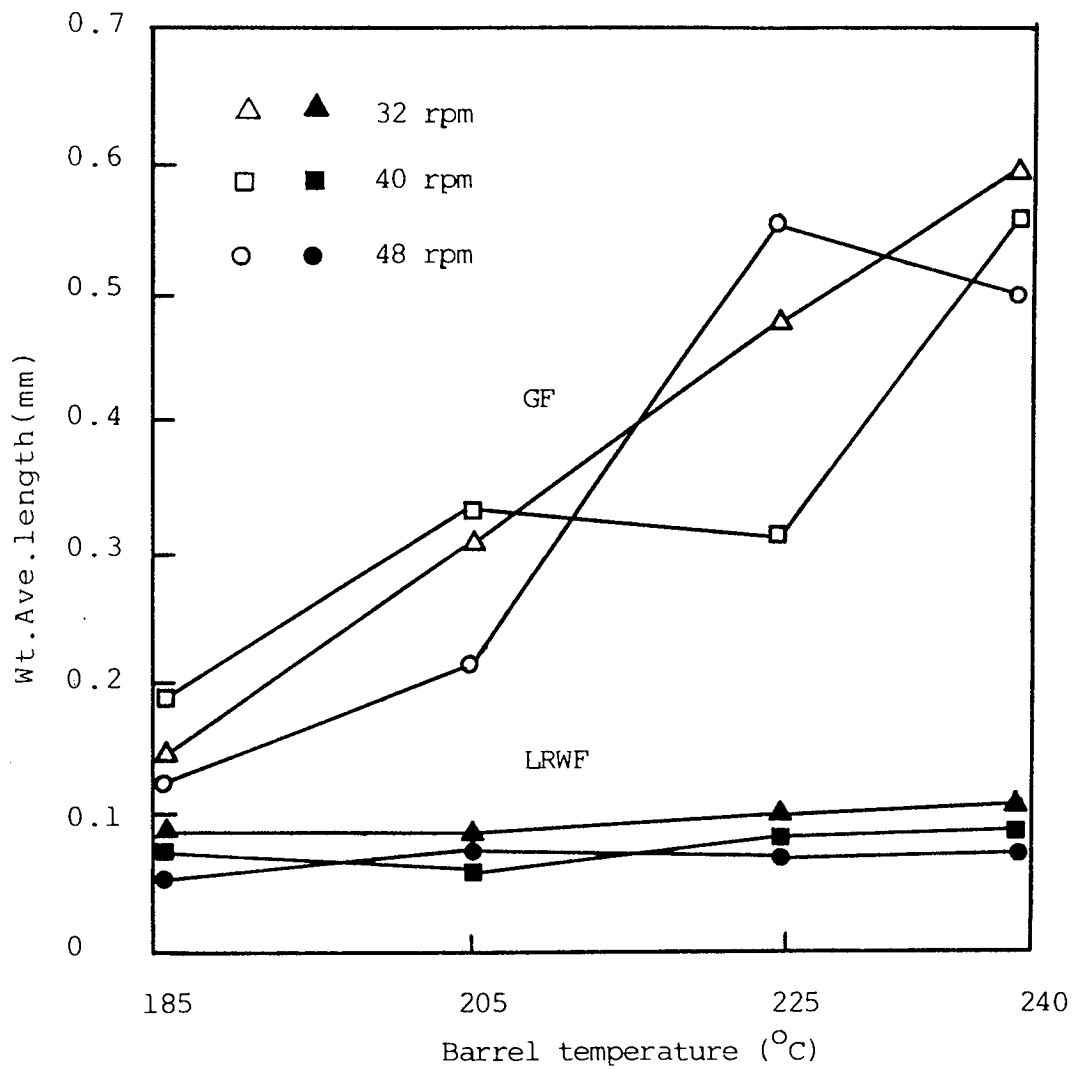


Figure 3.1 Effect of Buss Ko-Kneader parameters (temp, speed) on weight average length of glass fibre (GF) and long Rockwool fibre (LRWF), both 30% loaded A1100 coupled, processed in PP(HWM25)

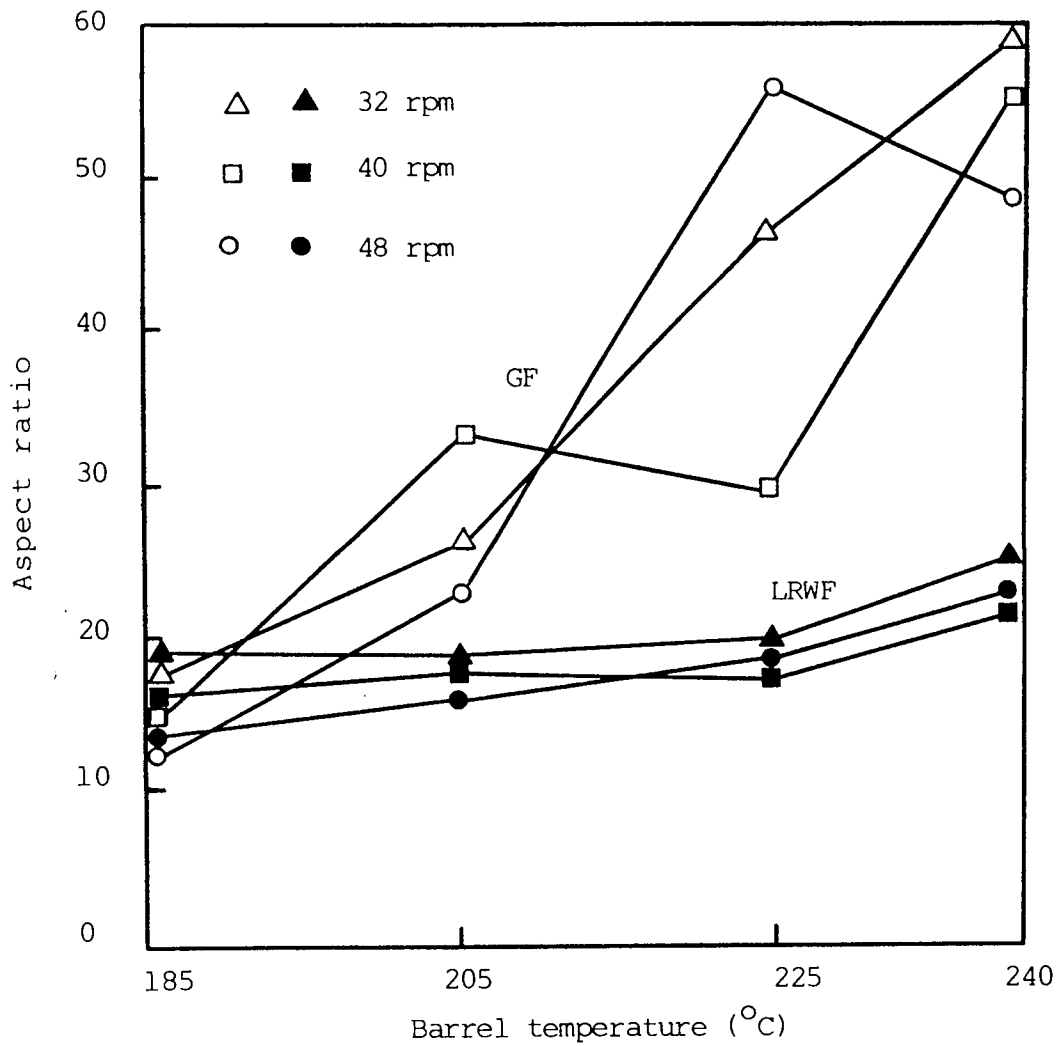


Figure 3.2 Effect of Buss Ko-Kneader parameters (temp, speed) on the aspect ratio of glass fibre (GF) and long Rockwool fibre (LRWF), both 30%, A1100 coupled, processed in PP (HWM25)

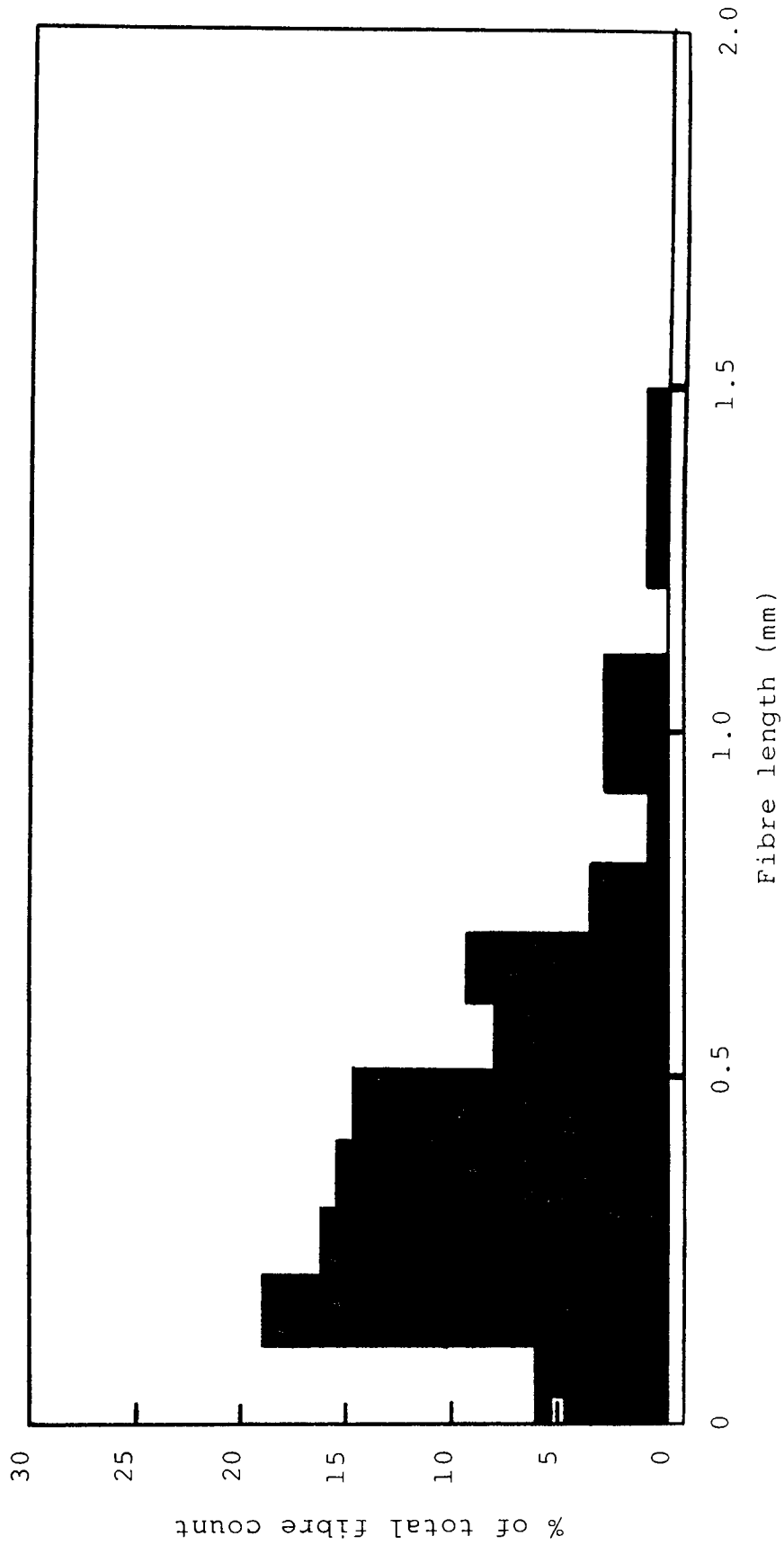


Figure 3.3 Histogram of weight average length distribution of glass fibres (GF, 30% loading) in PP(HWM25) after homogenisation in the Buss Ko-Kneader using optimised conditions (240°C, screw speed 32 rpm)

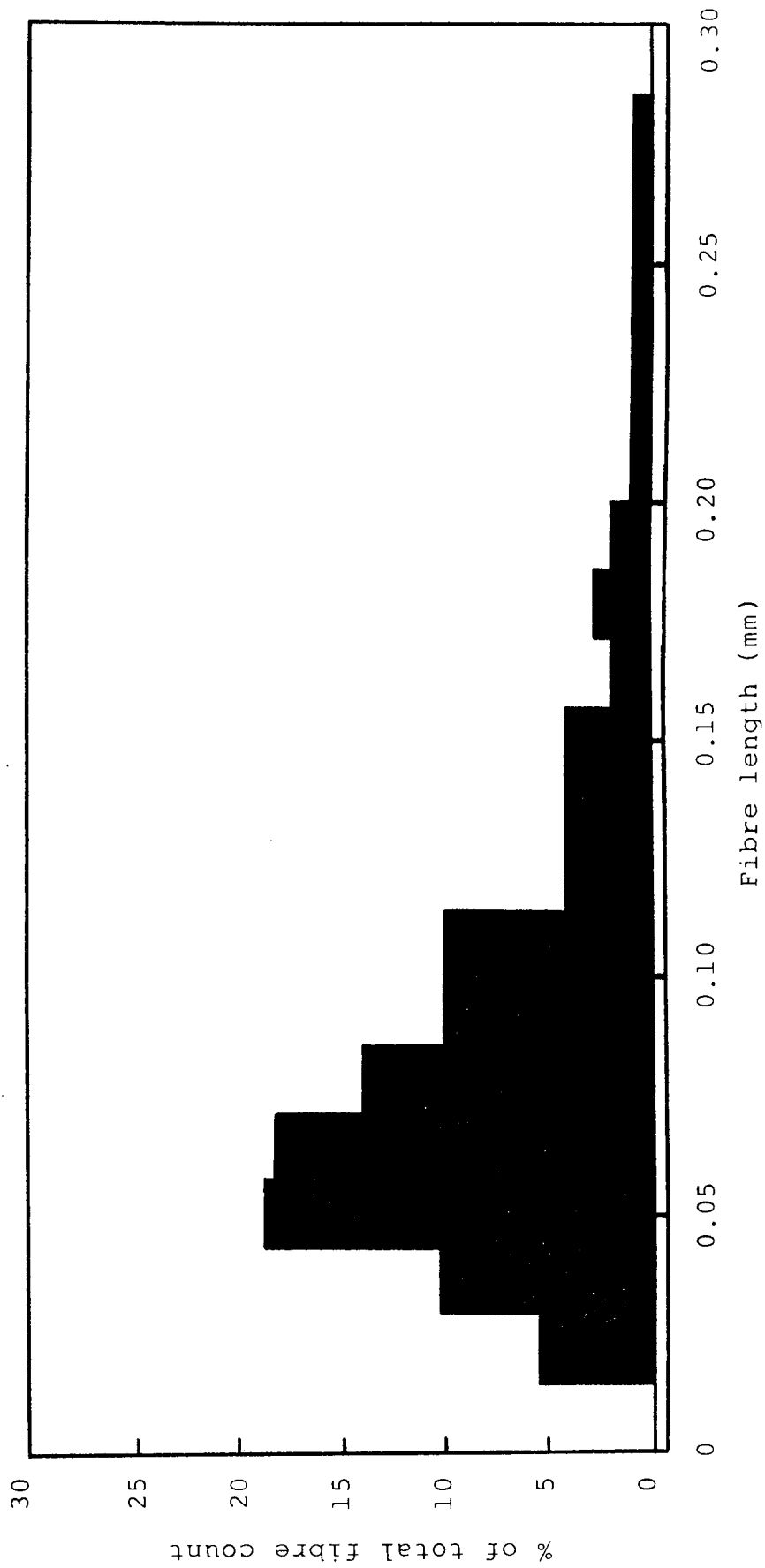


Figure 3.4 Histogram of weight average length distribution of long Rockwool fibres (LRWF, 30% loading) in PP(HWM25) after homogenisation in the Buss Ko-Kneader using optimised conditions(240°C, screw speed 32rpm)

PROCESS CONDITIONS		NO.AVE LENGTH(mm)	WT.AVE LENGTH(mm)	YIELD STRENGTH(MPa)	ASPECT RATIO
BT <sup>a</sup> (°C)	215	0.150	0.291	66.3	21.9
BT	225	0.166	0.243	67.6	24.3
BT	235	0.196	0.303	68.0	30.3
BT	245	0.238	0.336	68.1	33.6
BT	255	0.216	0.394	69.6	39.4
BT	265	0.361	0.436	71.6	43.6
MT <sup>b</sup> (°C)	50	0.241	0.335	72.1	33.5
MT	60	0.206	0.293	72.1	29.3
MT	70	0.172	0.289	72.0	28.9
MT	80	0.228	0.334	71.6	33.4
CT <sup>c</sup> (s)	12	0.176	0.304	70.8	30.4
CT	16	0.188	0.284	69.9	28.4
CT	20	0.216	0.329	70.6	32.9
CT	24	0.183	0.279	69.5	27.9
CT	30	0.199	0.278	69.6	27.8
SS <sup>d</sup> (rpm)	40	0.174	0.307	73.9	30.7
SS	50	0.164	0.256	72.9	25.6
IP <sup>e</sup> (kgcm <sup>2</sup> )	380	0.276	0.406	68.3	40.6
IP	480	0.223	0.325	69.2	32.5
IP	580	0.200	0.312	69.3	31.2
IP	680	0.168	0.213	69.1	21.3
CONTROL CONDITIONS		0.162	0.261	72.2	26.1
OPTIMISED CONDITIONS		0.280	0.376	74.5	37.6

(a) Barrel temperature, (b) Mould temperature, (c) Cool time, (d) Screw speed, (e) Injection pressure

Table 3.3 Optimisation of injection moulding parameters based on fibre length(wt and no.ave.), aspect ratio and yield strength of commercially reinforced(30% GF)polypropylene (HW60/GR30)



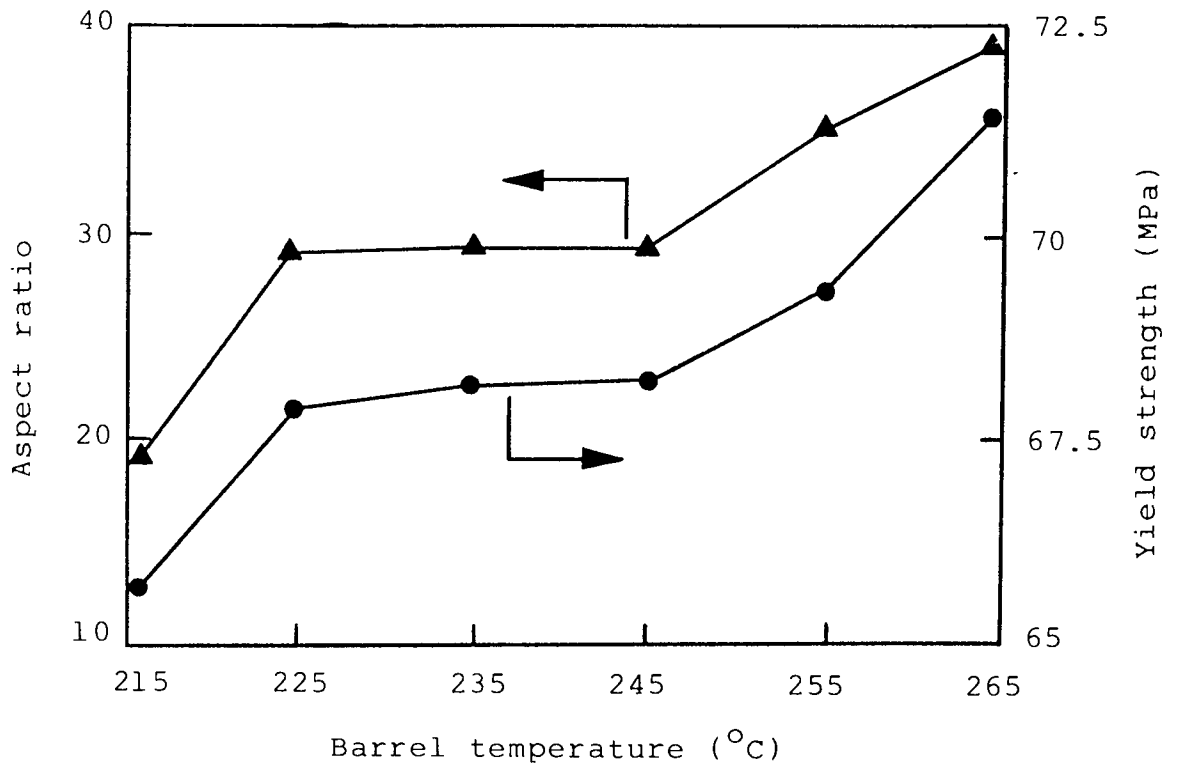


Figure 3.5 Effect of injection moulding (barrel temperature) on the aspect ratio and yield strength of HW60/GR30 (commercial 30% GF coupled PP)

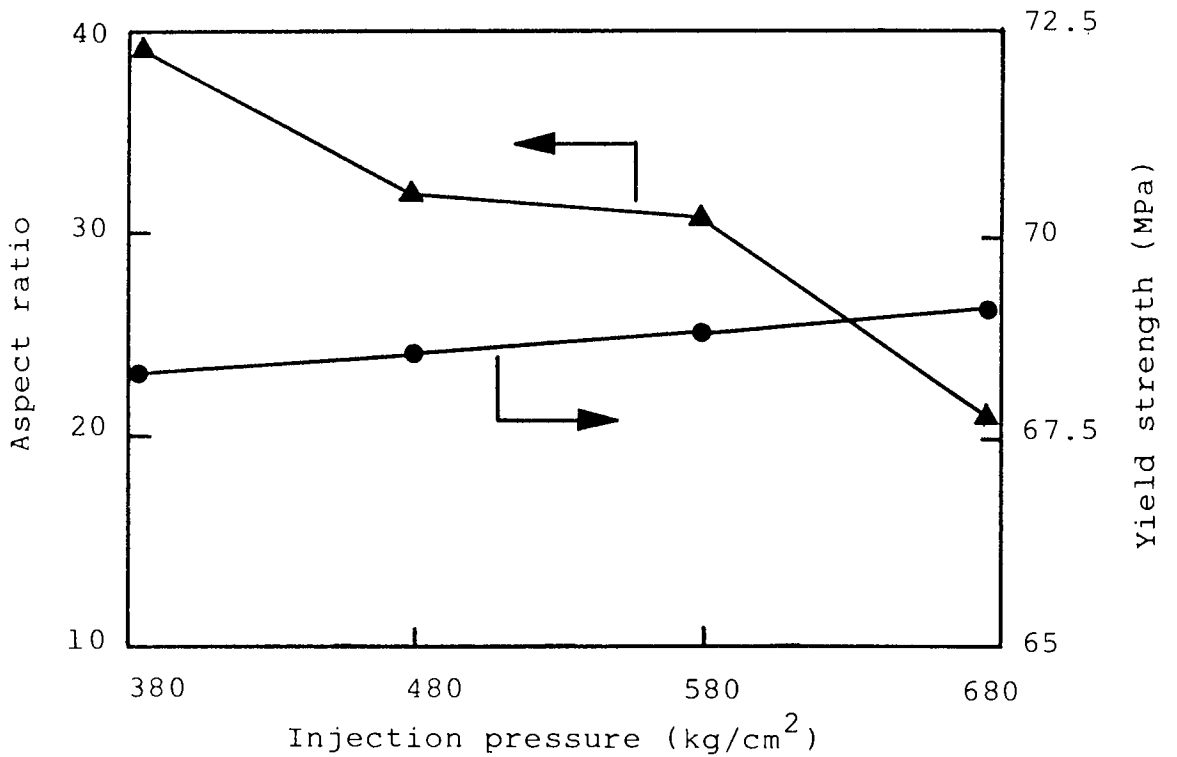


Figure 3.6 Effect of injection moulding (injection pressure) on the aspect ratio and yield strength of HW60/GR30 (commercial 30% GF coupled PP)

GRADE	TAN $\delta \times 10^{-2}$	CHARPY IMPACT STRENGTH kJm <sup>-2</sup>	FLEXURAL MODULUS GPa	FLEXURAL STRENGTH MPa
HWM25	5.8	44	1.30	27
HW60/GR30	3.2	158	6.50	94

GRADE	YIELD STRENGTH MPa	TENSILE MODULUS GPa	ELONGATION AT YIELD %	% TENSILE MODULUS RETENTION AFTER WATER IMMERSION (70°C, 24hrs)
HWM25	29	0.8	10.1	95
HW60/GR30	77	3.0	3.5	100

Table 3.4 Mechanical properties of commercial PP grades:  
HWM25 homopolymer and 30% coupled glass  
reinforced HW60/GR30

% LRWF	TAN $\delta \times 10^{-2}$	CHARPY IMPACT STRENGTH kJm <sup>-2</sup>	FLEXURAL MODULUS GPa	FLEXURAL STRENGTH MPa	YIELD STRENGTH MPa	TENSILE MODULUS GPa	ELONGATION AT YIELD %	% TENSILE MODULUS RETENTION AFTER WATER IMMERSION (70°C, 24 hrs)
0(Control)	5.8	44	1.3	27	29	0.8	10.1	100
5	7.0	38	2.2	30	28	1.3	8.0	77
10	6.9	43	2.4	31	29	1.2	6.5	82
15	6.1	40	2.8	32	29	1.3	6.5	80
20	6.3	44	3.2	33	27	1.3	6.1	83
25	6.3	70	3.6	35	27	1.5	5.8	82
30	6.2	81	5.0	40	27	1.5	5.5	82
35	6.2	78	6.0	41	29	1.9	4.4	76
40	5.9	80	6.8	49	29	2.5	3.7	78
45	5.9	84	8.0	44	29	2.5	3.5	78
HW60/GR30	3.2	158	6.5	94	77	3.0	3.5	100

Table 3.5 Mechanical properties of PP(HWM25) containing long Rockwool fibre (LRWF, A-1100 coupled, 0-45% loading). HW60/GR30 (commercially 30% GF coupled PP) is used as a control

%SRWF	TAN $\delta \times 10^{-2}$	CHAPPY IMPACT STRENGTH $\frac{\text{kJ}}{\text{m}^2}$	FLEXURAL MODULUS GPa	FLEXURAL STRENGTH MPa	YIELD STRENGTH MPa	TENSILE MODULUS GPa	ELONGATION AT YIELD %	% TENSILE MODULUS RETENTION AFTER WATER IMMERSION (70°C, 24 hrs)
0 (control)	5.8	44	1.3	27	29	0.8	10.1	100
5	6.0	42	2.0	31	30	1.2	8.8	83
10	5.2	37	2.2	31	27	1.1	8.0	87
15	6.2	44	2.8	32	27	1.2	7.5	89
20	5.7	52	3.2	33	27	1.3	7.0	87
25	4.9	61	4.4	40	29	1.6	5.5	81
30	5.3	74	5.0	36	27	1.6	5.5	78
35	6.3	79	5.6	39	28	2.0	4.8	75
40	6.1	86	6.4	43	29	2.2	4.4	77
45	5.9	87	6.8	42	29	2.1	3.1	77
HW60/GR30	3.2	158	6.5	94	77	3.0	3.5	100

Table 3.6 Mechanical properties of PP(HWM25) containing short Rockwool fibre (SRWF, A-1100 coupled, 0-45% loading). HW60/GR30 (commercially 30% GF coupled PP) is used as a control.

% GF	TAN $\delta \times 10^{-2}$	CHARPY IMPACT STRENGTH $\text{kJm}^{-2}$	FLEXURAL MODULUS GPa	FLEXURAL STRENGTH MPa	YIELD STRENGTH MPa	TENSILE MODULUS GPa	ELONGATION AT YIELD %	% TENSILE MODULUS RETENTION AFTER WATER IMMERSION (70°C, 24 hrs)
0 (CONTROL)	5.8	44	1.3	27	29	0.8	10.1	100
5	4.8	60	2.6	27	30	1.1	8.0	100
10	4.5	67	2.6	36	30	1.2	7.5	100
15	4.3	83	3.4	34	30	1.4	7.0	100
20	4.5	99	4.0	38	31	1.7	5.7	100
25	4.5	99	5.6	47	32	2.0	4.6	96
30	4.4	105	6.2	48	35	2.2	2.0	94
35	3.9	105	7.7	51	38	2.6	1.8	83
40	4.4	109	8.2	45	36	3.7	1.2	81
45	3.7	110	9.6	49	35	3.6	1.1	70
HW60/GR30	3.2	158	6.5	94	77	3.0	3.5	100

Table 3.7 Mechanical properties of PP(HWM25) containing glass fibre (GF,A-1100 coupled, 0-45% loading).HW60/GR30 (commercially 30% GFcoupled PP) is used as a control

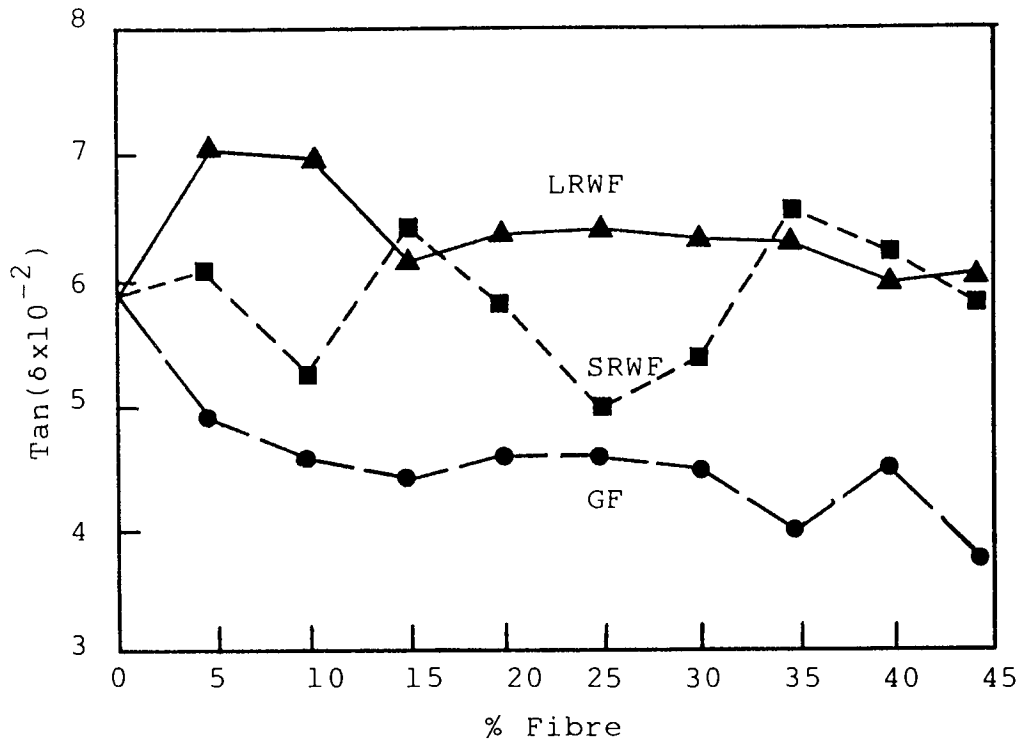


Figure 3.7 Effect of fibre type [short(S) and long(L) Rockwool fibre(RWF) and glass fibre(GF)] on Tan  $\delta$  of PP(HWM25)

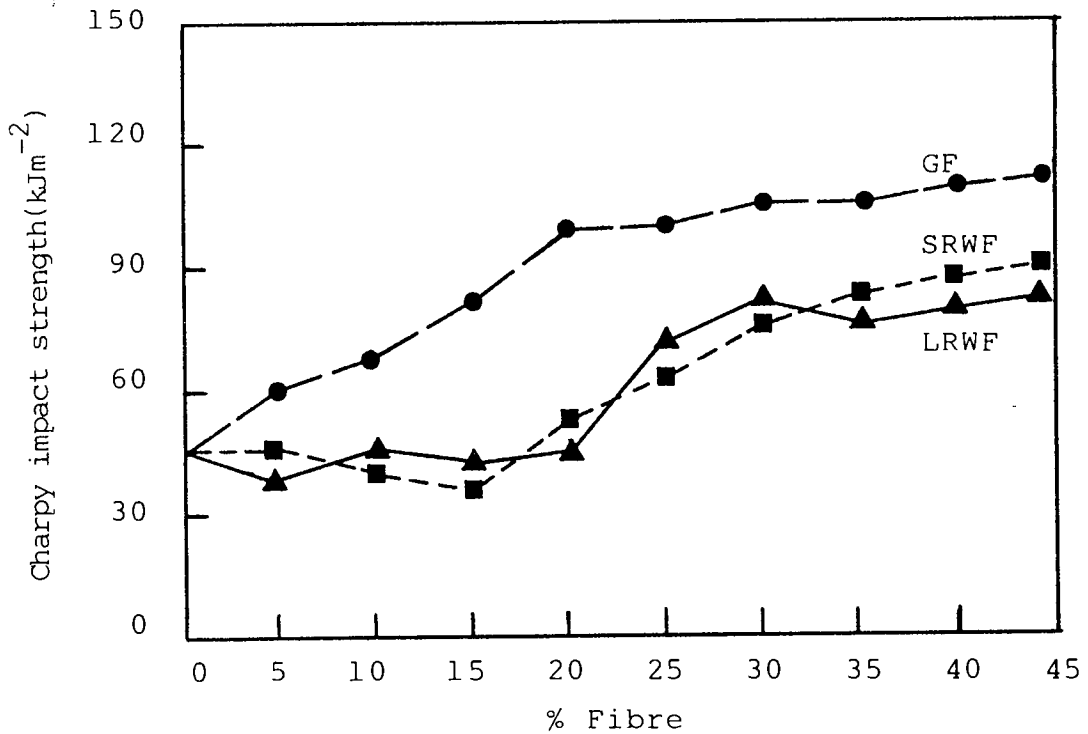


Figure 3.8 Effect of fibre type [short(S) and long(L) Rockwool fibre(RWF) and glass fibre (GF)] on Charpy impact strength (notched, 0.2mm) of PP(HWM25)

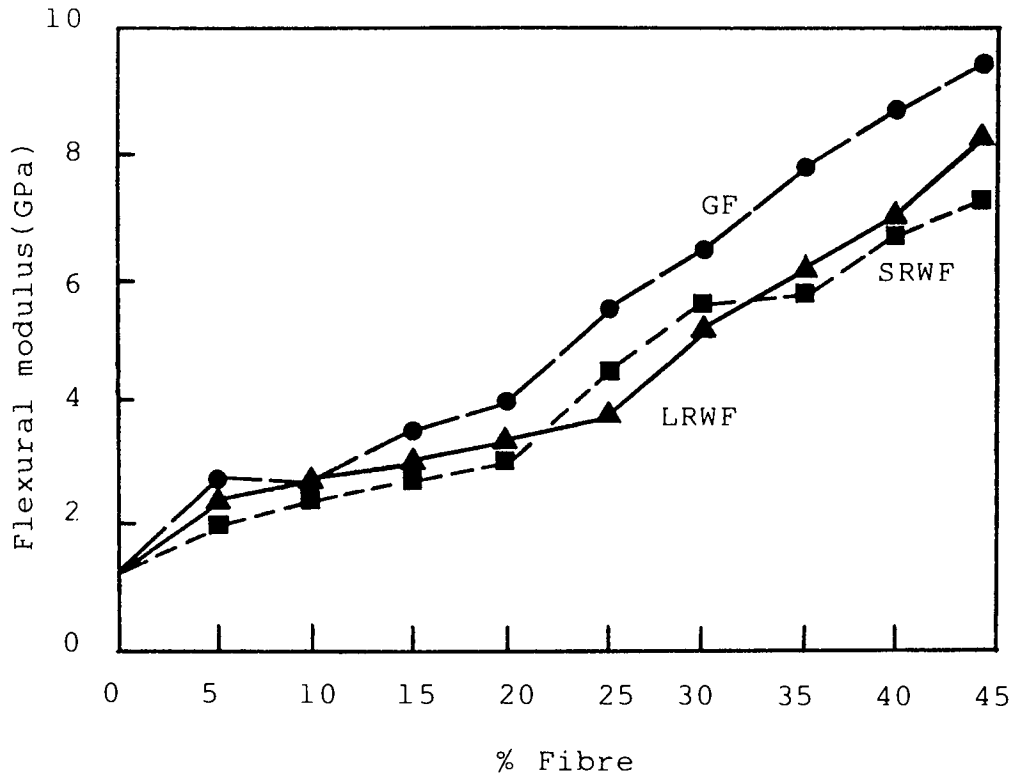


Figure 3.9 Effect of fibre type [short(S) and long(L) Rockwool fibre(RWF) and glass fibre(GF)] on flexural modulus of PP(HWM25)

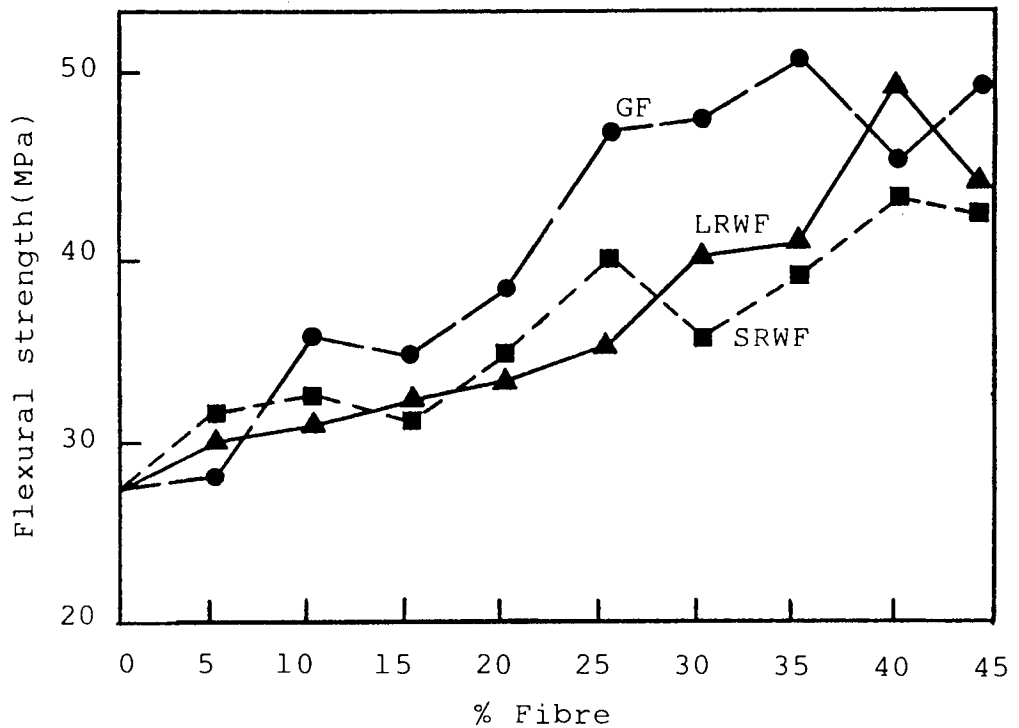


Figure 3.10 Effect of fibre type [short(S) and long(L) Rockwool fibre(RWF) and glass fibre(GF)] on flexural strength of PP(HWM25)

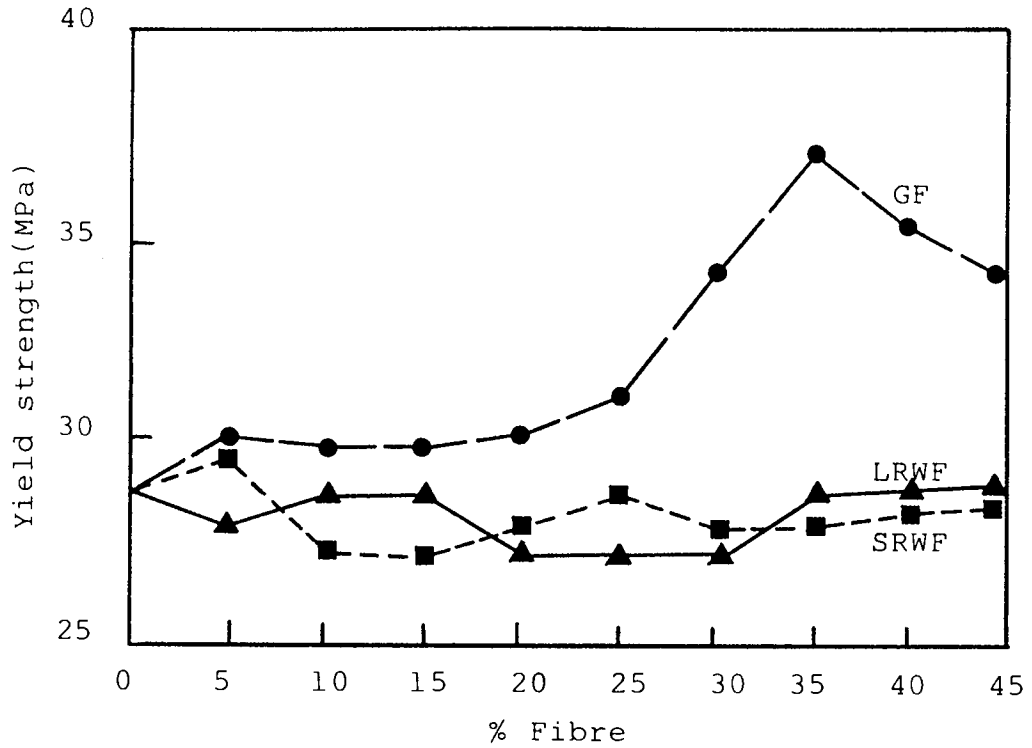


Figure 3.11 Effect of fibre type [short(S) and long(L) Rockwool fibre(RWF) and glass fibre(GF)] on yield strength of PP(HWM25)

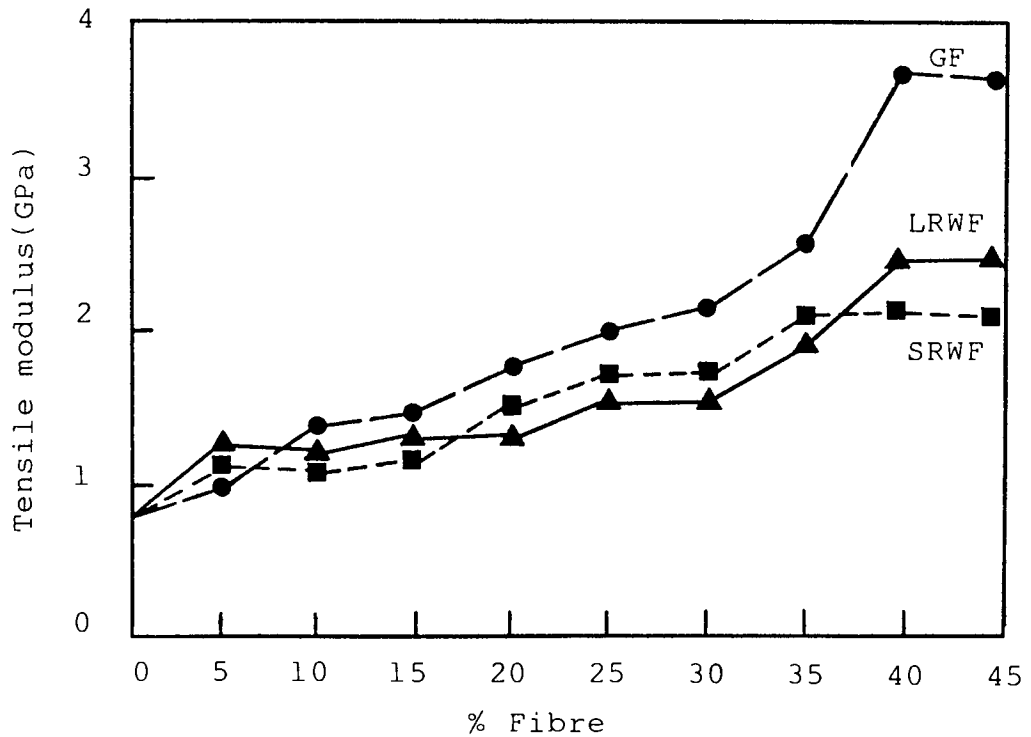


Figure 3.12 Effect of fibre type [short(S) and long(L) Rockwool fibre(RWF) and glass fibre(GF)] on tensile modulus of PP(HWM25)



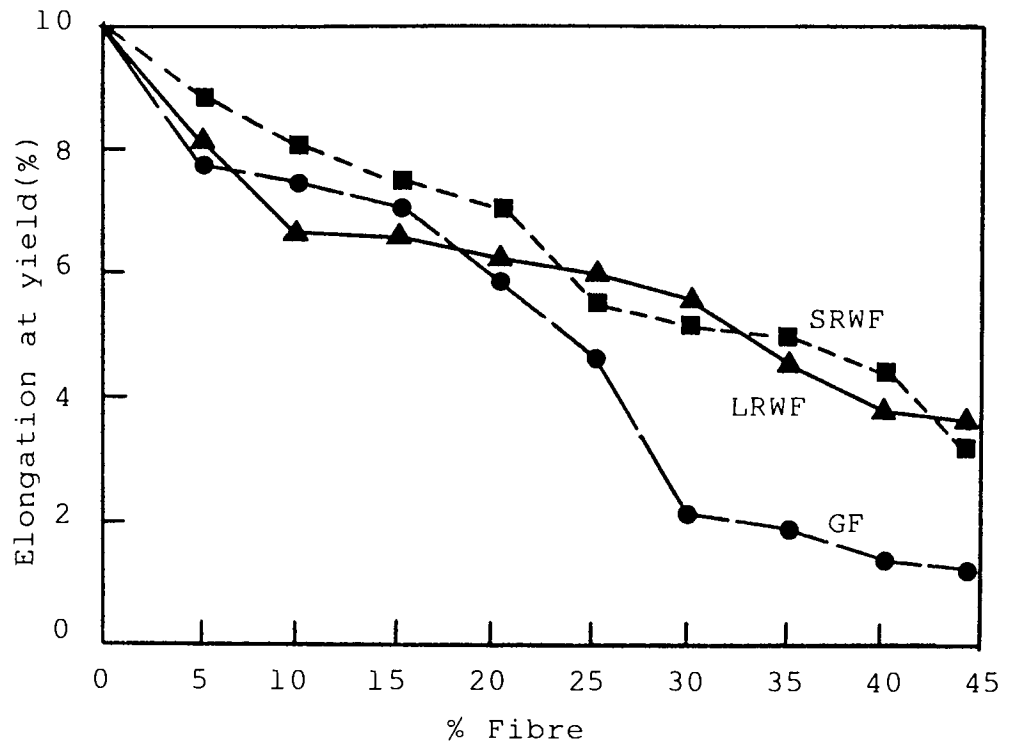


Figure 3.13 Effect of fibre type [short(S) and long(L) Rockwool fibre(RWF) and glass fibre(GF)] on elongation at yield of PP(HWM25)

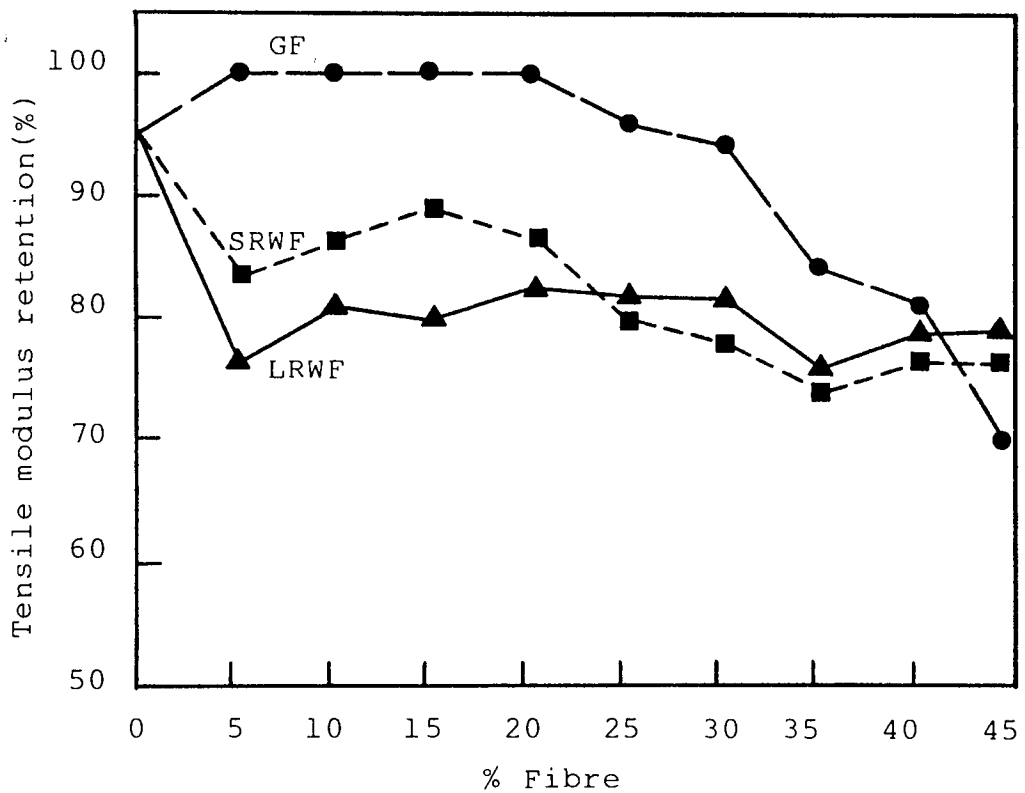


Figure 3.14 Effect of fibre type [short(S) and long(L) Rockwool fibre(RWF) and glass fibre(GF)] on tensile modulus retention (after 24 hrs water immersion at 70°C) of PP(HWM25)

NO.	COMPOSITE	YIELD STRENGTH (MPa)	TENSILE MODULUS (GPa)	FLEXURAL STRENGTH (MPa)	FLEXURAL MODULUS (GPa)	CHARPY IMPACT STRENGTH ( $\text{kJm}^{-2}$ )
1	HW60/GR30	77(1.21)	3.0(0.11)	94(1.10)	6.50(0.08)	158(1.91)
2	30%GF	35(1.29)	2.2(0.10)	48(1.06)	6.20(0.07)	105(1.32)
3	30%LRWF	27(1.36)	1.5(0.13)	40(1.19)	5.0(0.07)	81(1.45)

Table 3.8 Mechanical properties with standard deviations (bracketed) of PP(HWM25) containing long Rockwool fibre(LRWF) and glass fibre(GF, both 30% loading and A-1100 silane coupled).HW60/GR30 is used as a control.

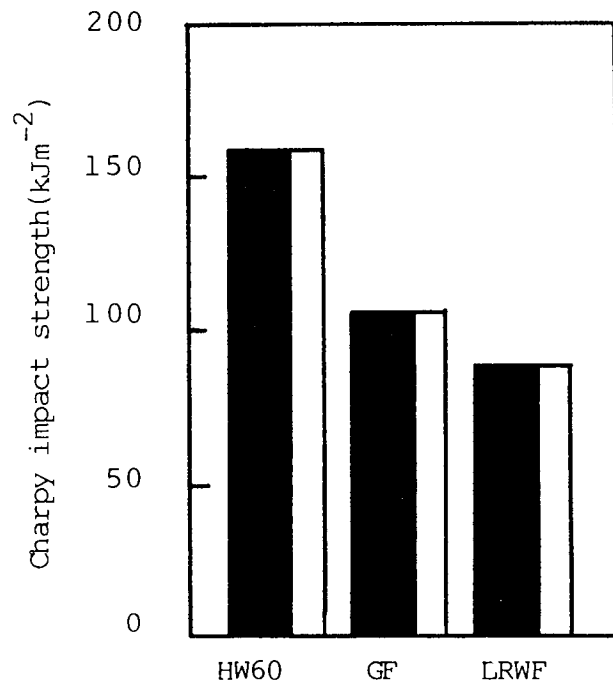


Figure 3.15 Effect of fibre (30% loading) on Charpy impact strength (notch radius 0.2mm) of PP(HWM25). HW60 (commercial 30% GF coupled) is the control

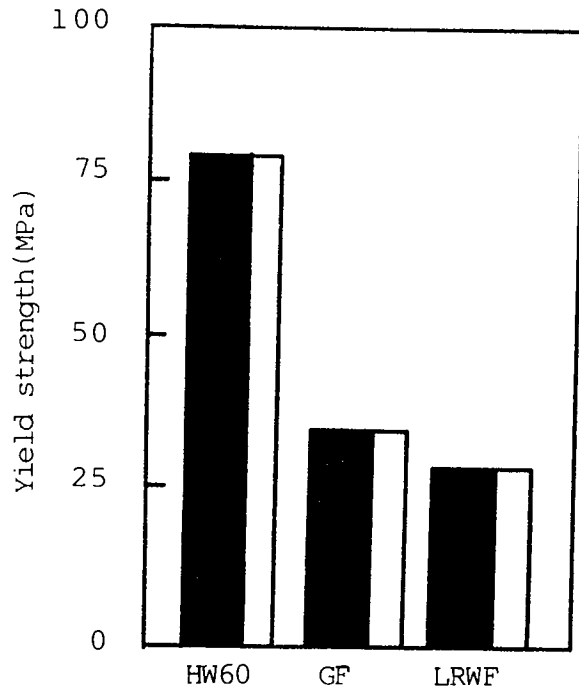


Figure 3.16 Effect of fibre(30% loading) on yield strength of PP (HWM25). HW60 (commercial 30% GF coupled) is the control

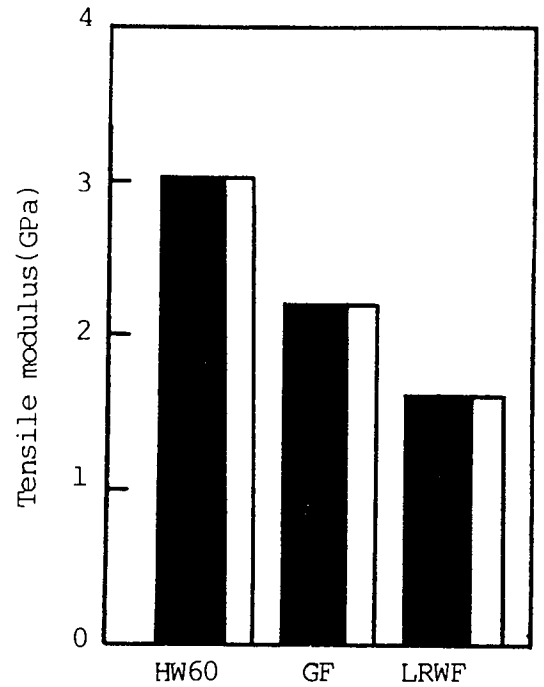


Figure 3.17 Effect of fibre(30% loading) on tensile modulus of PP(HWM25). HW60 (commercial 30% GF coupled) is the control

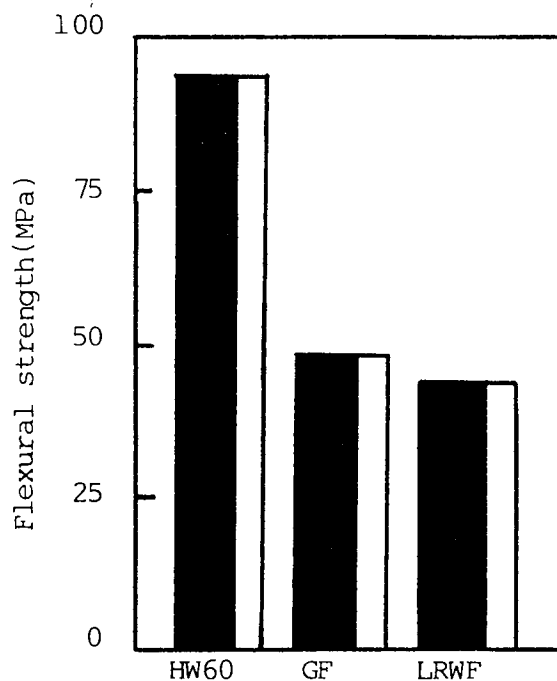


Figure 3.18 Effect of fibre (30% loading) on flexural strength of PP (HWM25). HW60 (commercial 30% GF coupled) is the control.

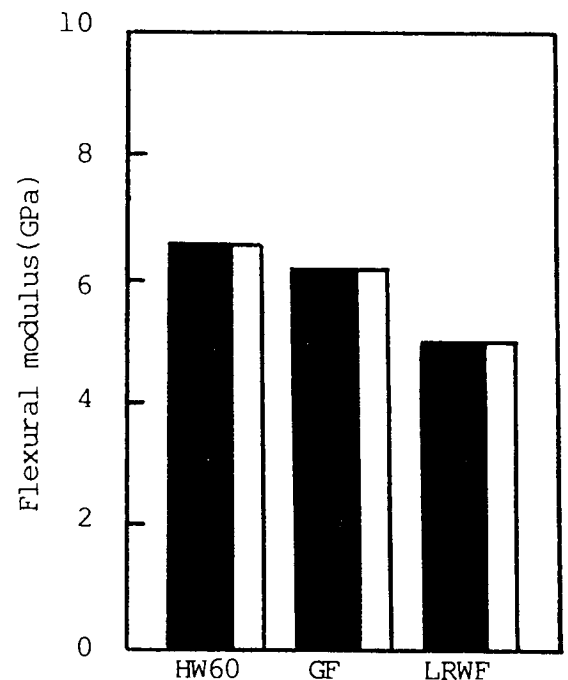


Figure 3.19 Effect of fibre(30% loading) on flexural modulus of PP(HWM25). HW60 (commercial 30% GF coupled) is the control

%EPDM	TAN $\delta \times 10^{-2}$	CHARPY IMPACT STRENGTH $\text{kJm}^{-2}$	FLEXURAL MODULUS GPa	FLEXURAL STRENGTH MPa	YIELD STRENGTH MPa	TENSILE MODULUS GPa	ELONGATION AT YIELD %
0	5.8	44	1.30	27	29	0.7	10.0
5	5.6	54	0.90	27	27	0.7	7.8
10	6.5	69	0.81	26	23	0.7	9.0
15	6.8	86	0.72	20	19	0.7	11.5
20	7.5	98	0.69	17	17	0.5	13.0
25	8.6	136	0.66	14	13	0.4	16.0
30	9.1	197	0.62	11	10	0.3	18.2

Table 3.9 Mechanical properties of EPDM (0-30% loading) modified PP(HWM25)

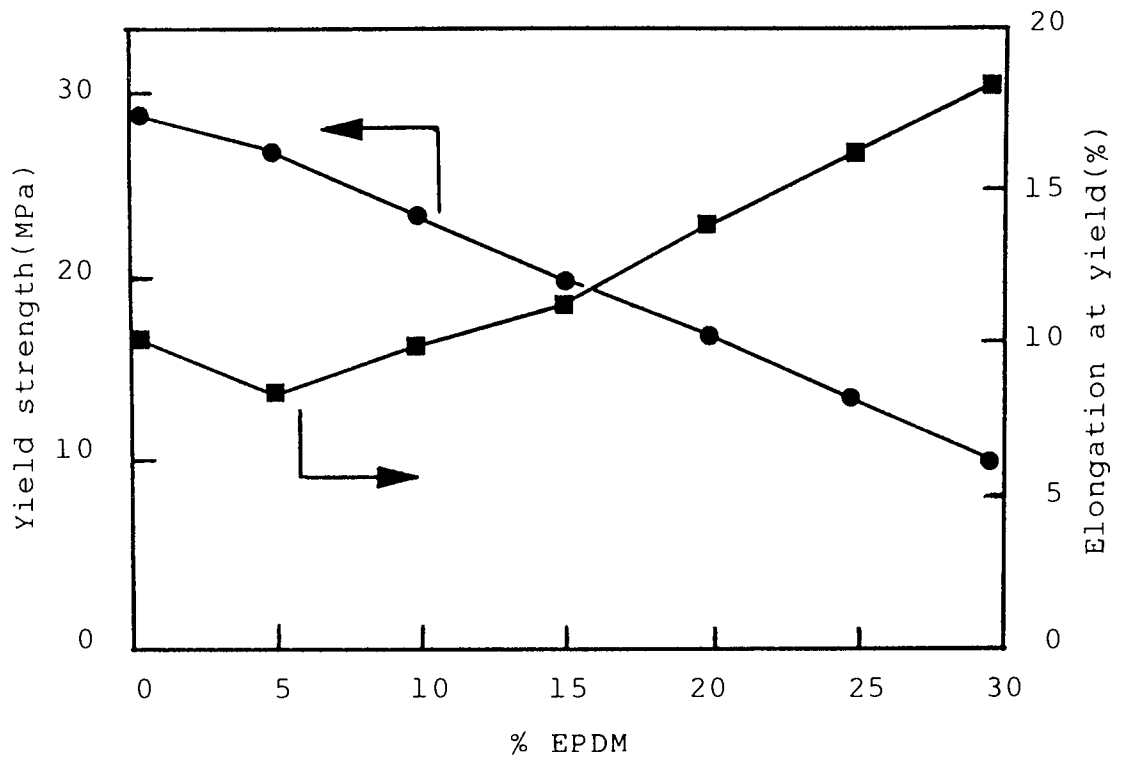


Figure 3.20 Effect of EPDM on the mechanical performance of PP(HWM25)

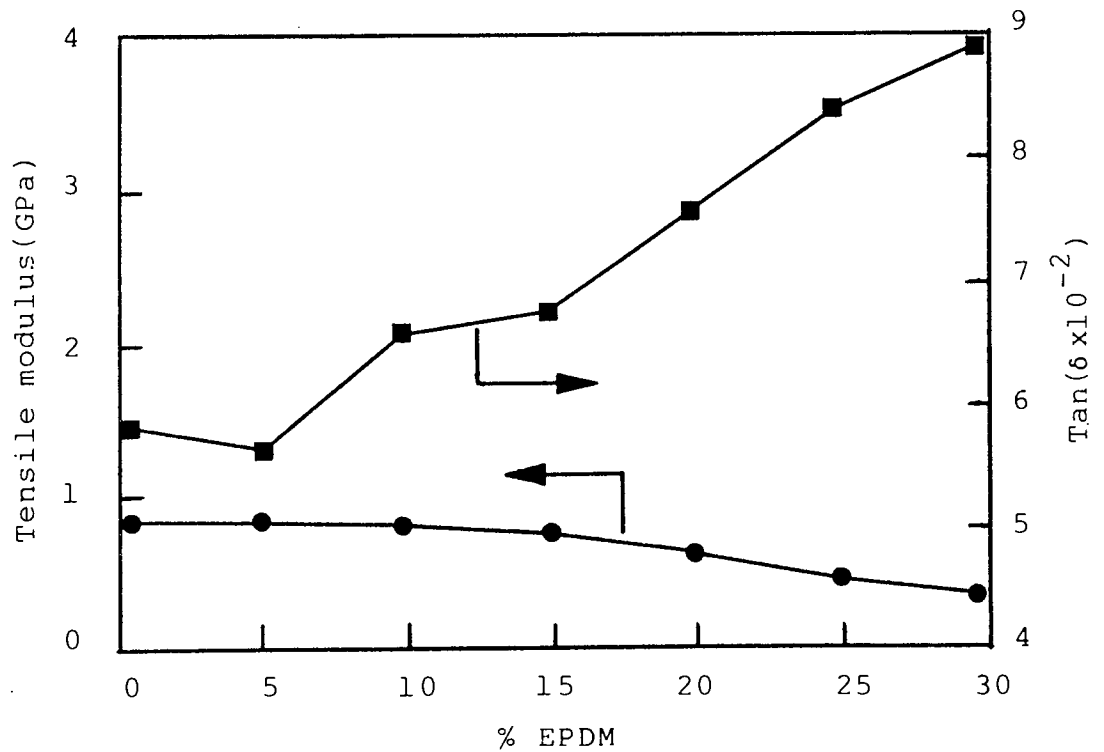


Figure 3.21 Effect of EPDM on the mechanical performance of PP(HWM25)

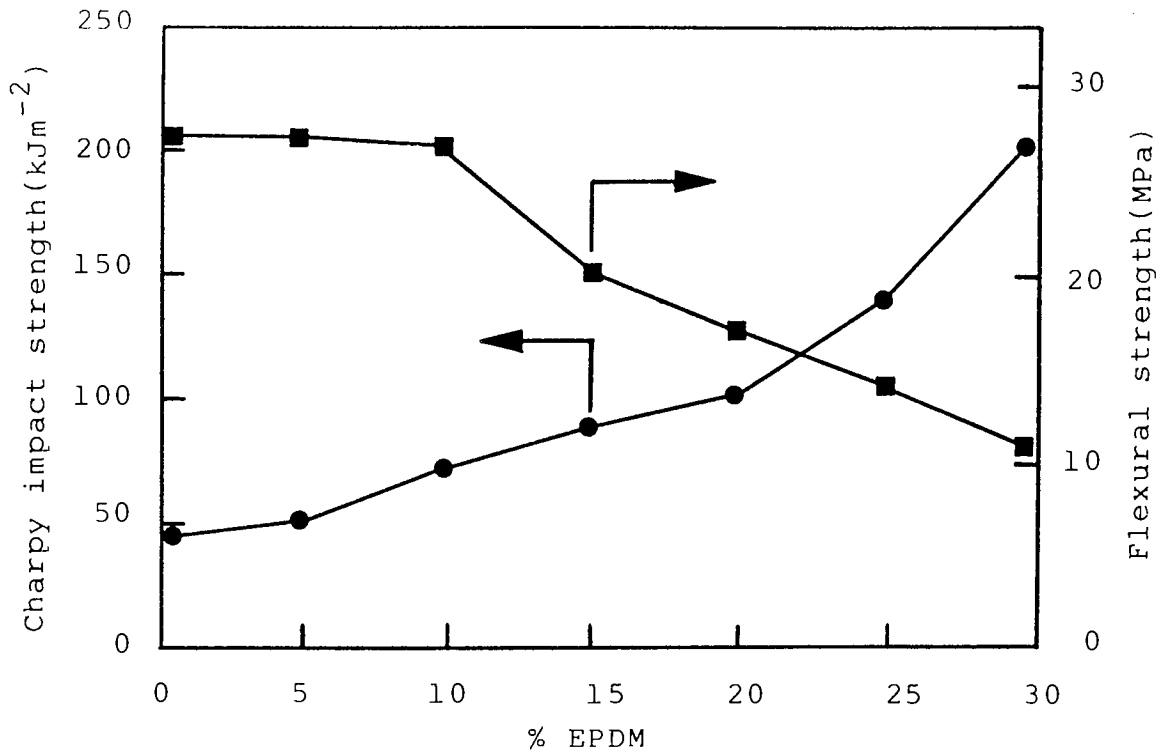


Figure 3.22 Effect of EPDM on the mechanical performance of PP(HWM25)

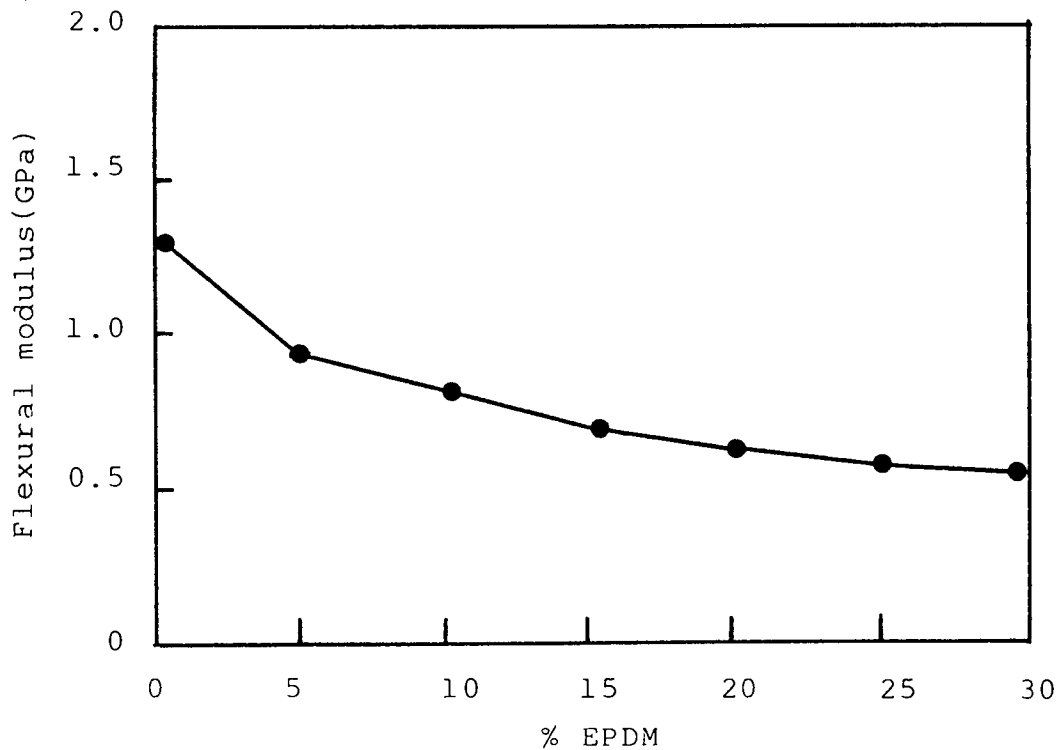


Figure 3.23 Effect of EPDM on the flexural modulus of PP(HWM25)

%FIBRE	%EPDM	TAN $\delta \times 10^{-2}$	CHARPY IMPACT STRENGTH $\text{kJm}^{-2}$	FLEXURAL MODULUS GPa	FLEXURAL STRENGTH MPa	YIELD STRENGTH MPa	TENSILE MODULUS GPa	ELONGATION AT YIELD %
0	10	6.5	69	0.8	26	27	0.7	9.0
5LRWF	10	6.7	54	1.6	25	23	1.0	8.0
10LRWF	10	7.2	58	2.0	25	23	1.1	7.0
15LRWF	10	6.5	59	2.4	28	22	1.1	6.5
20LRWF	10	6.4	59	2.8	30	24	1.5	5.0
25LRWF	10	6.0	74	4.0	41	25	1.7	5.0
30LRWF	10	5.7	89	5.0	40	32	1.7	2.5
35LRWF	10	4.5	84	5.3	43	32	2.0	2.0
5GF	10	6.0	62	1.8	31	25	1.0	8.0
10GF	10	5.9	71	3.0	35	24	1.3	7.5
15GF	10	4.6	90	3.6	37	26	1.4	5.5
20GF	10	4.7	104	4.0	37	26	1.7	4.5
25GF	10	5.1	118	5.2	39	26	2.1	3.0
30GF	10	5.3	124	5.2	38	26	2.2	3.5
35GF	10	4.9	127	5.2	37	25	1.9	3.0

Table 3.10 Mechanical properties of EPDM (10% loading) modified PP(HWM25) containing long Rockwool fibre (LRWF) and glass fibre (GF, both A-1100 coupled, 0-35% loading)

%FIBRE	%EPDM	TANδx10 <sup>-2</sup>	CHARPY IMPACT STRENGTH <sup>-2</sup> kJ/m	FLEXURAL MODULUS GPa	FLEXURAL STRENGTH MPa	YIELD STRENGTH MPa	TENSILE MODULUS GPa	ELONGATION AT YIELD %
0	20	7.5	98	0.7	17	17	0.5	13.0
5LRWF	20	7.5	78	1.6	23	20	0.9	7.3
10LRWF	20	6.4	75	1.8	24	22	0.9	6.1
15LRWF	20	7.2	67	2.0	25	22	1.1	5.5
20LRWF	20	4.7	78	3.0	33	24	1.2	3.5
25LRWF	20	5.6	67	3.2	35	28	1.3	2.8
5GF	20	6.3	59	1.6	21	21	0.9	7.5
10GF	20	6.6	88	2.4	21	21	1.1	7.9
15GF	20	7.3	85	2.8	22	22	1.3	6.5
20GF	20	6.9	109	3.0	22	22	1.6	6.1
25GF	20	5.9	232	3.8	20	20	1.7	4.8

Table 3.11 Mechanical properties of EPDM (20% loading) modified PP (HWM25) containing long Rockwool fibre (LRWF) and glass fibre (GF, both A-1100 coupled, 0-25% loading)



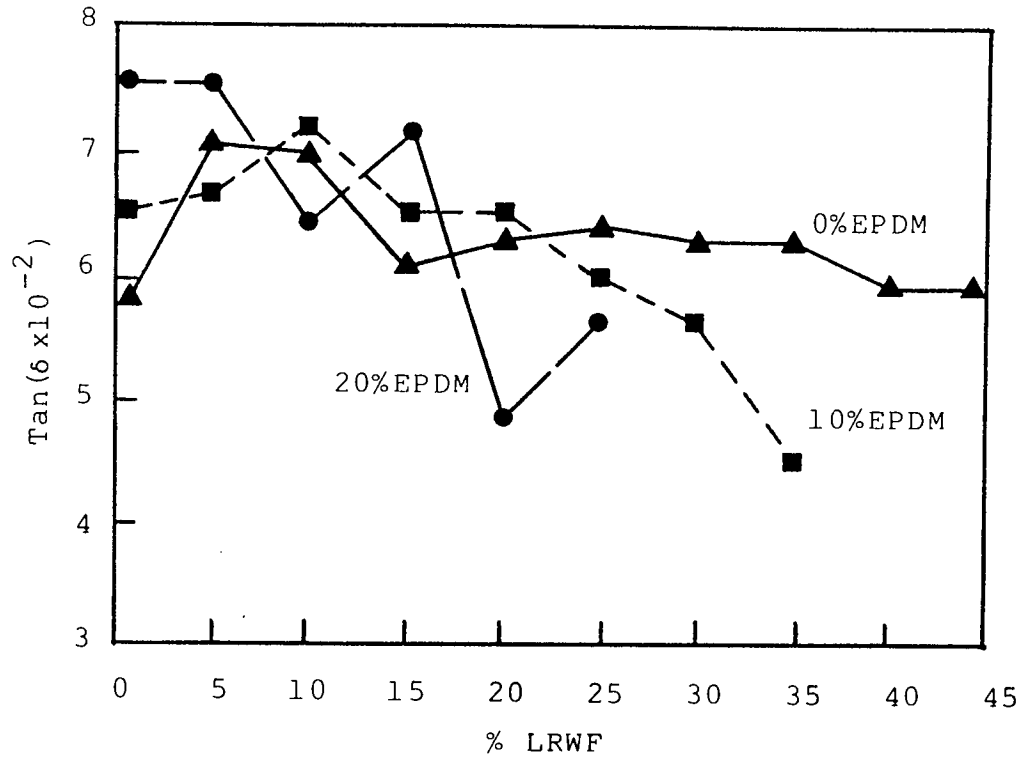


Figure 3.24 Effect of EPDM(10,20%) on Tan  $\delta$  of long Rockwool fibre(LRWF) filled PP(HWM25)

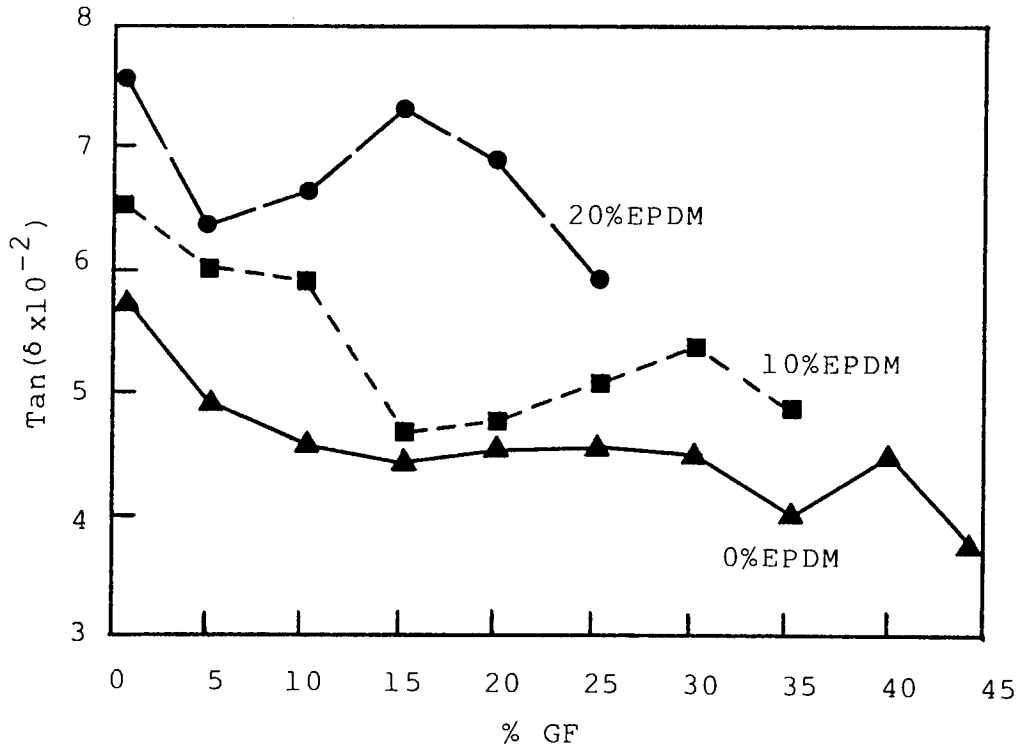


Figure 3.25 Effect of EPDM(10,20%) on Tan  $\delta$  of glass fibre (GF) filled PP(HWM25)

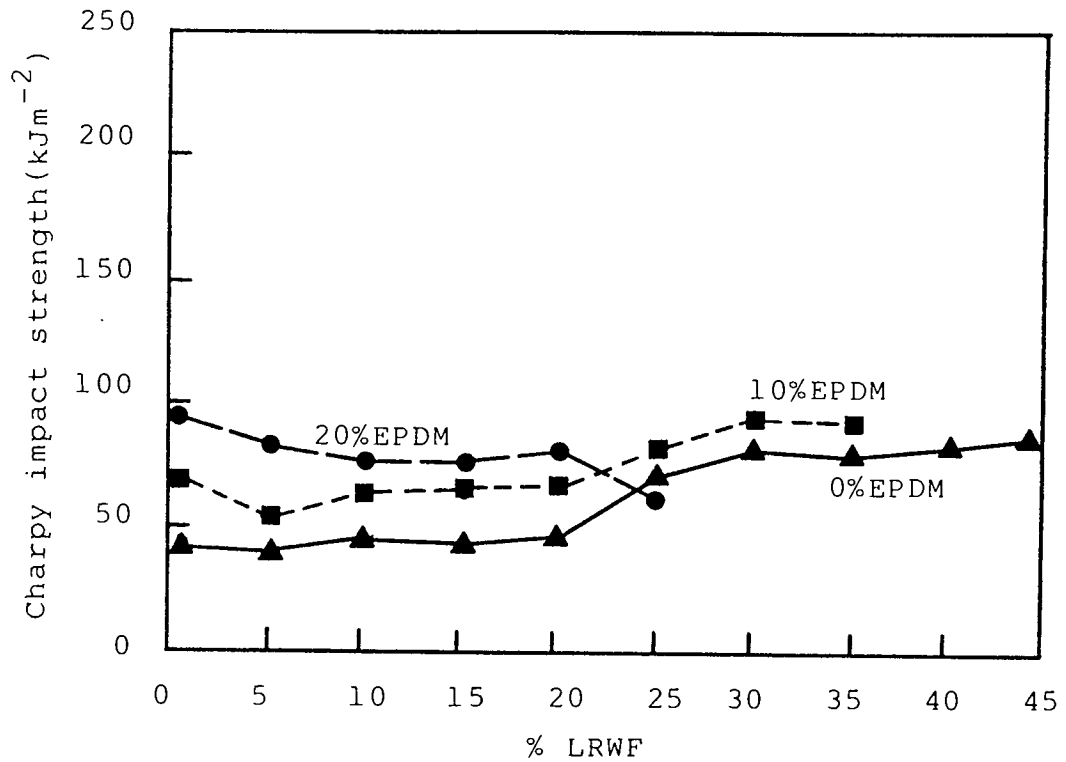


Figure 3.26 Effect of EPDM (10,20%) on Charpy impact strength (notched 0.2mm) of long Rockwool fibre(LRWF) filled PP(HWM25)

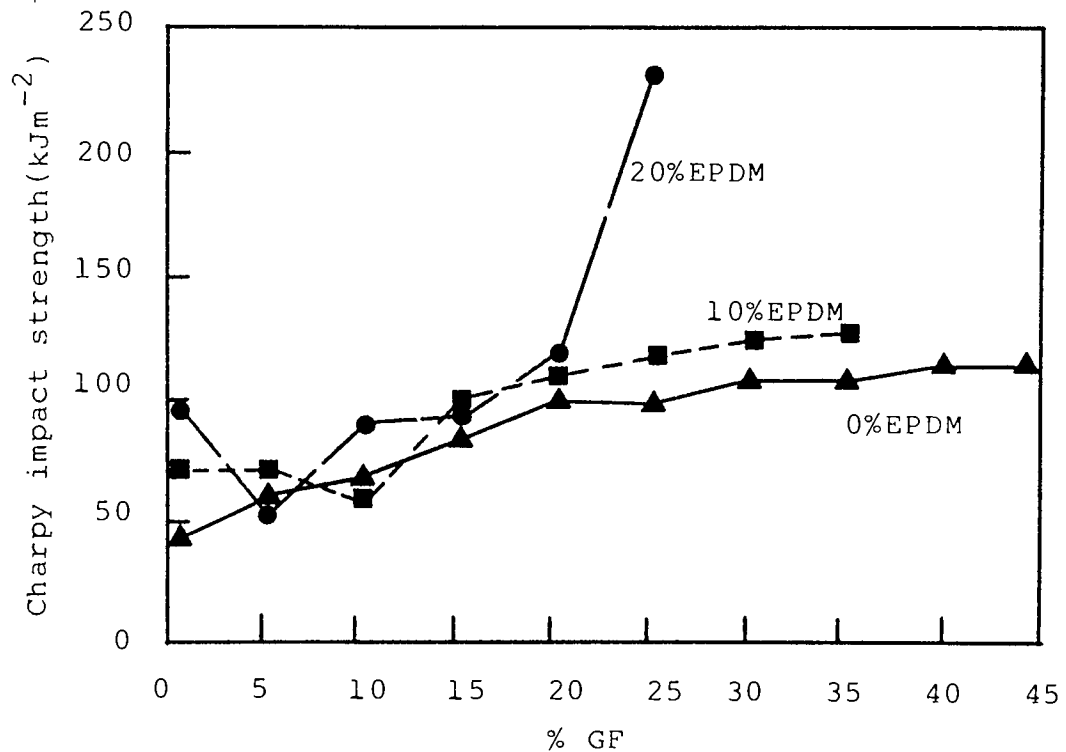


Figure 3.27 Effect of EPDM (10,20%) on Charpy impact strength (notched 0.2mm) of glass fibre (GF) filled PP(HWM25)

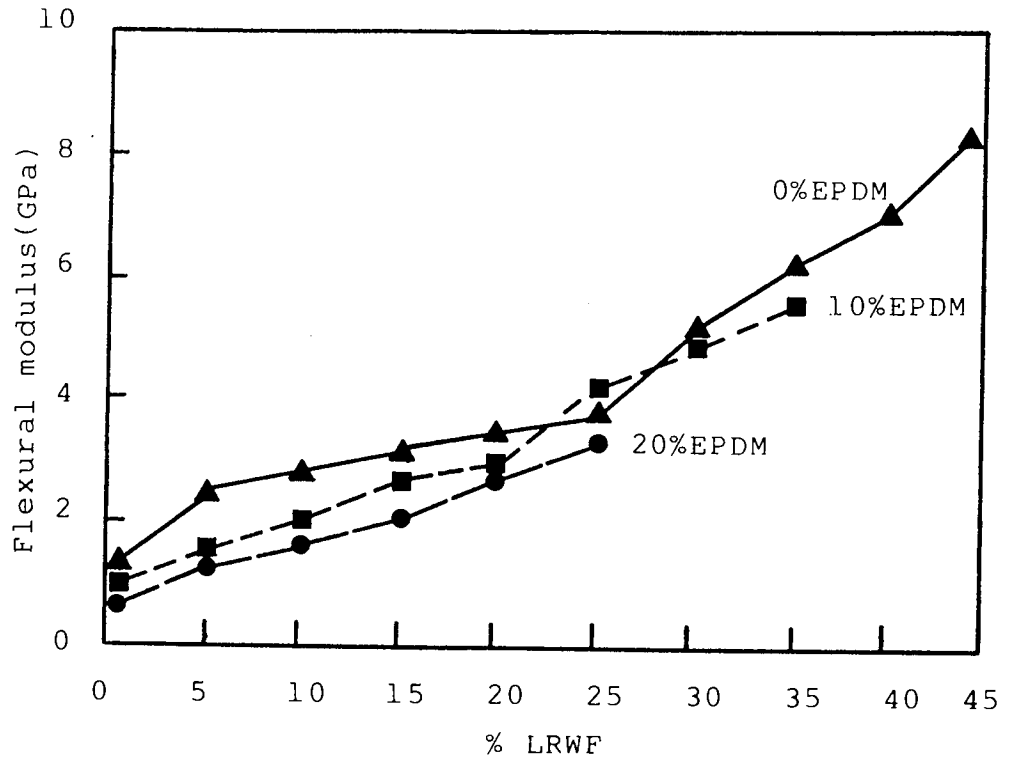


Figure 3.28 Effect of EPDM (10,20%) on flexural modulus of long Rockwool fibre(LRWF) filled PP(HWM25)

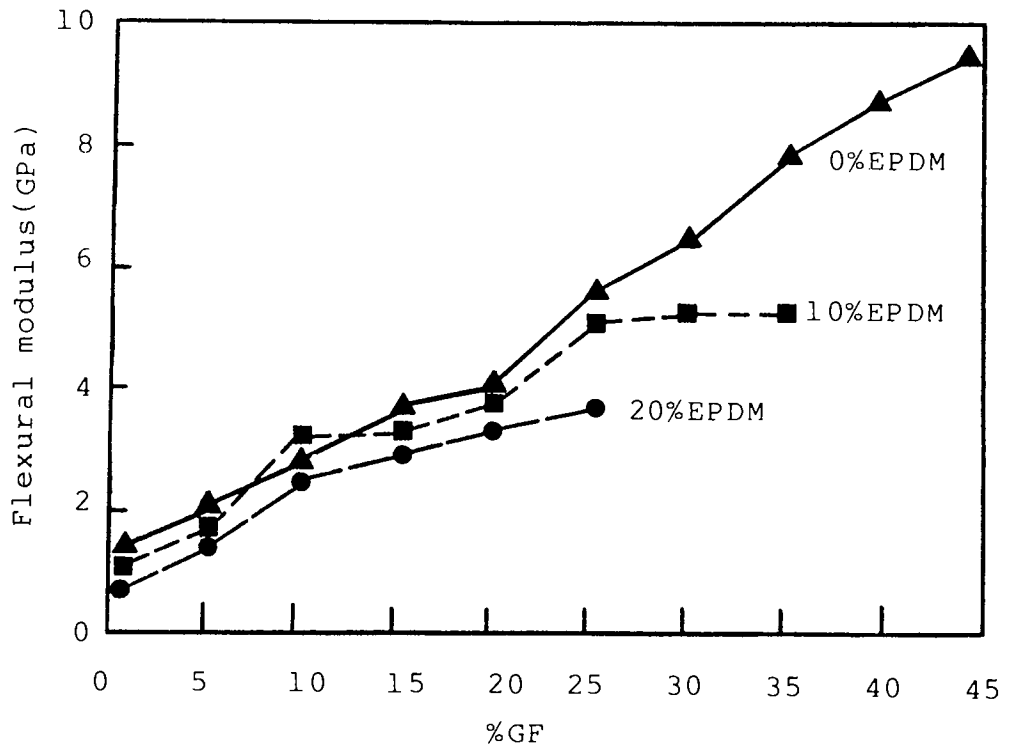


Figure 3.29 Effect of EPDM (10,20%) on flexural modulus of glass fibre (GF) filled PP(HWM25)

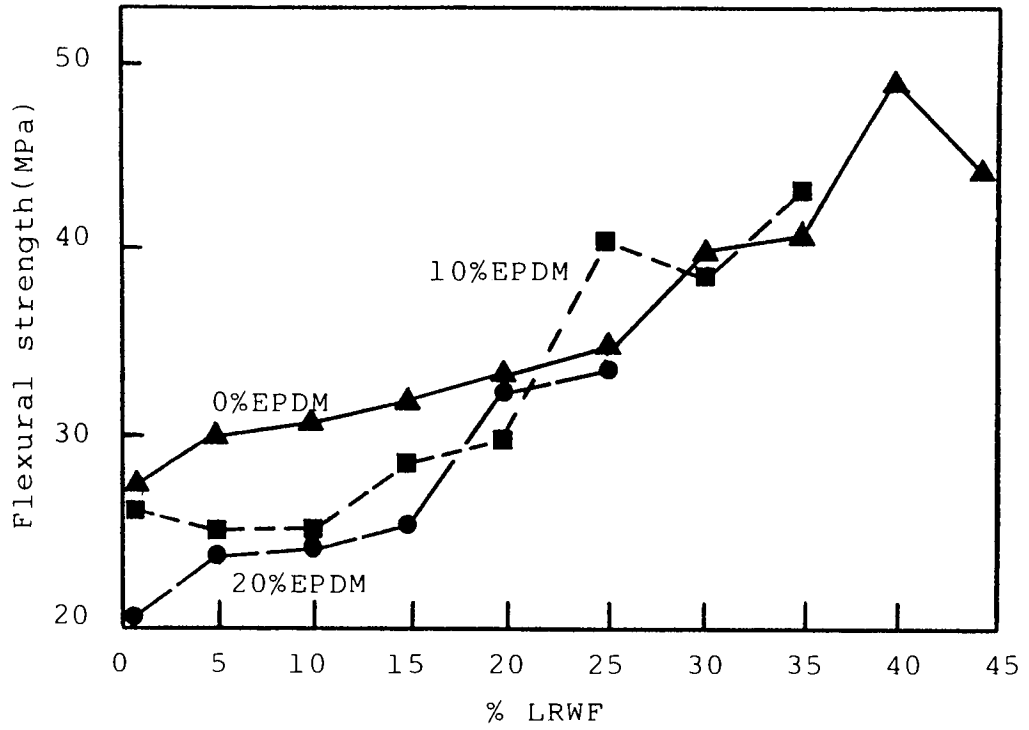


Figure 3.30 Effect of EPDM (10,20%) on flexural strength of long Rockwool fibre(LRWF) filled PP(HWM25)

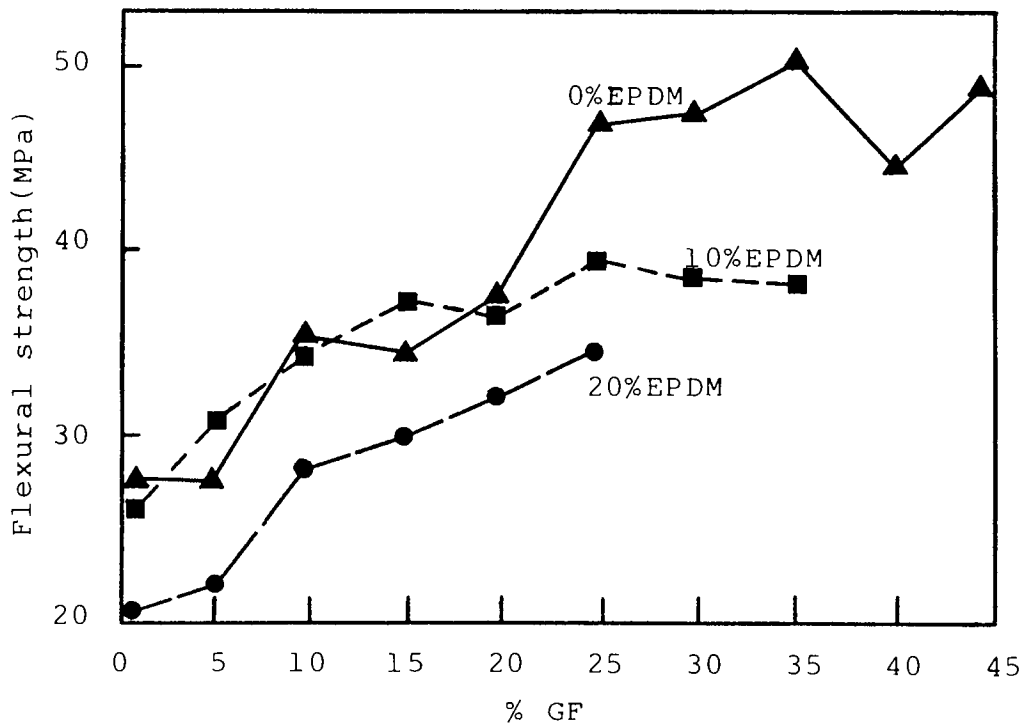


Figure 3.31 Effect of EPDM (10,20%) on flexural strength of glass fibre (GF) filled PP(HWM25)

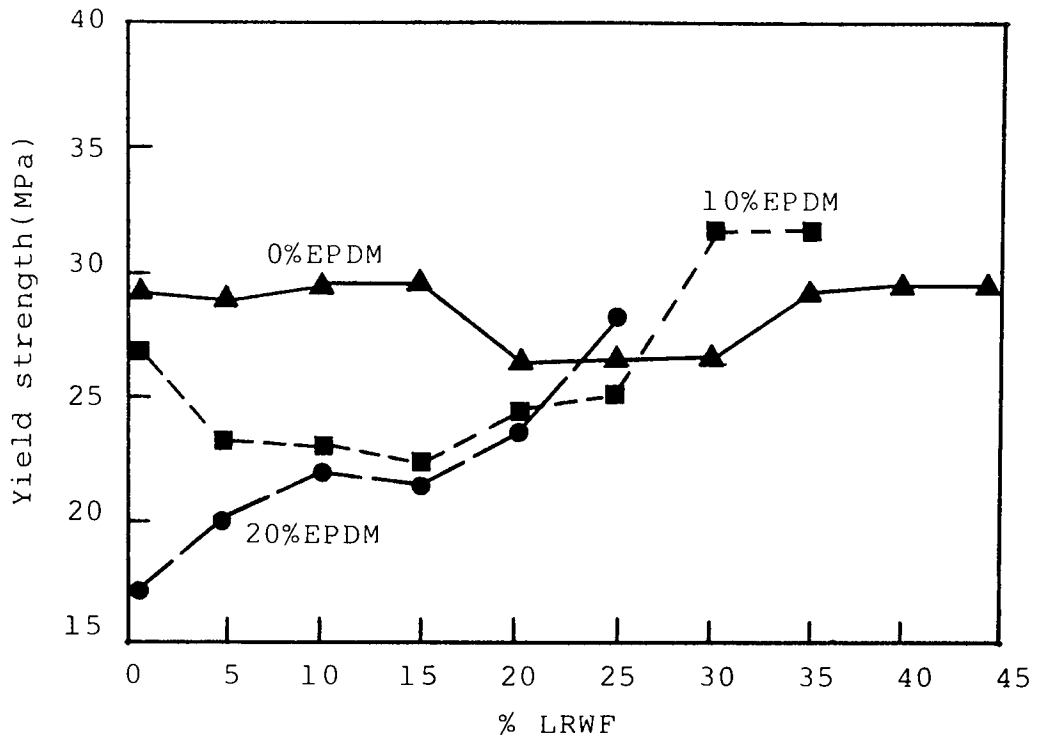


Figure 3.32 Effect of EPDM (10,20%) on yield strength of long Rockwool fibre(LRWF) filled PP(HWM25)

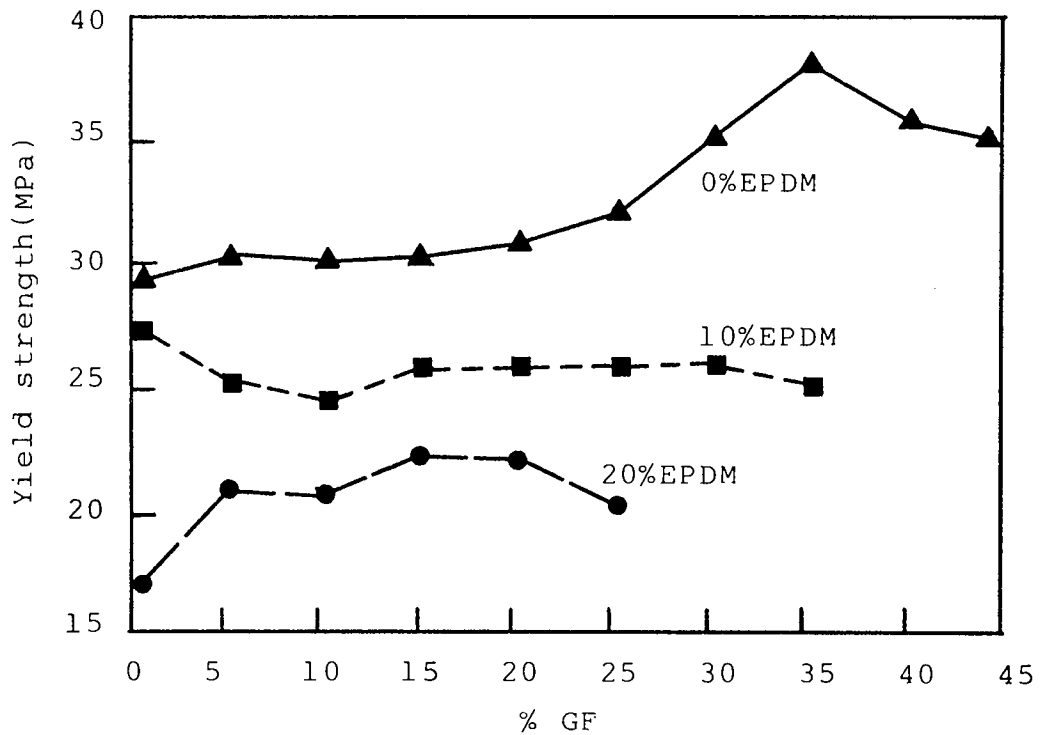


Figure 3.33 Effect of EPDM (10,20%) on yield strength of glass fibre (GF) filled PP(HWM25)

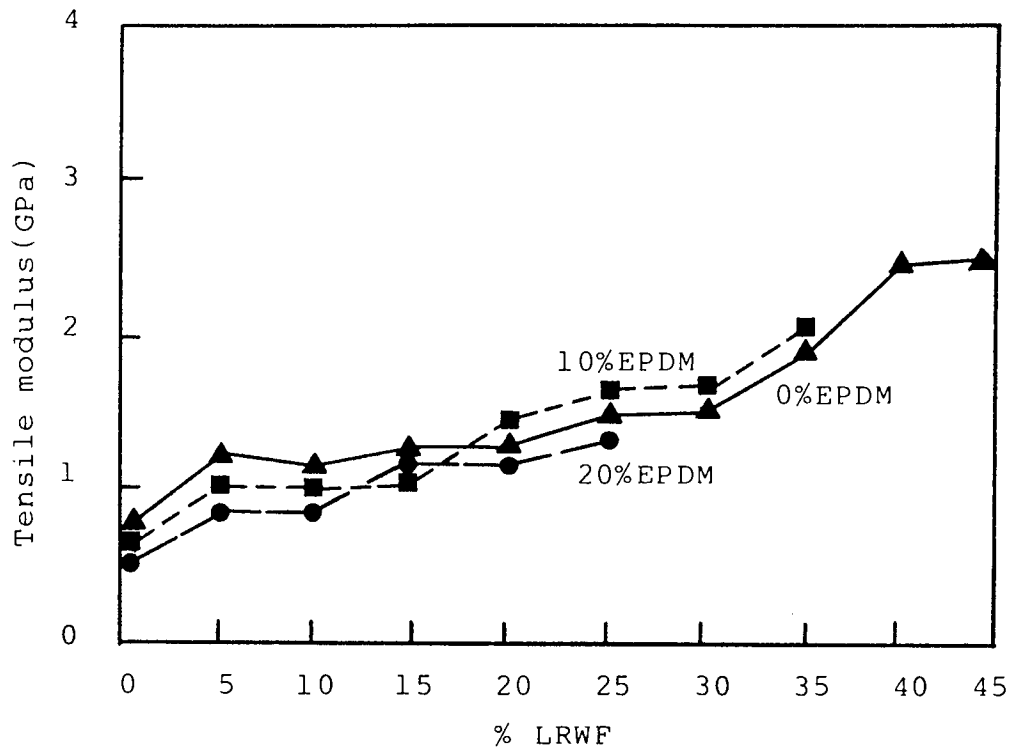


Figure 3.34 Effect of EPDM(10,20%) on tensile modulus of long Rockwool fibre(LRWF) filled PP(HWM25)

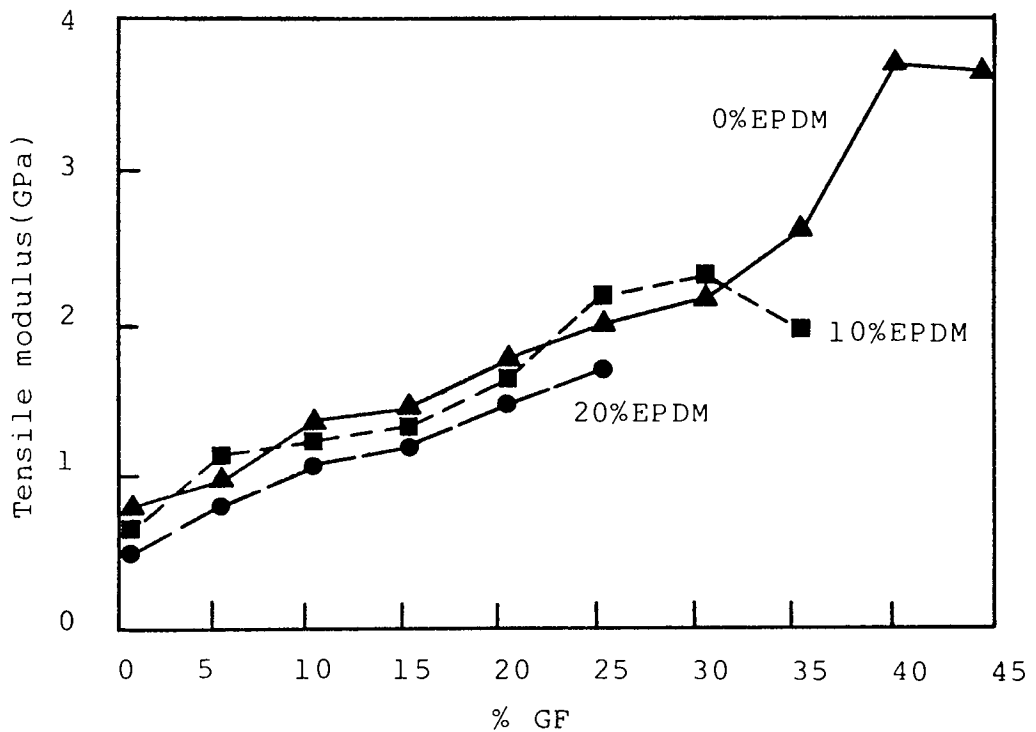


Figure 3.35 Effect of EPDM(10,20%) on tensile modulus of glass fibre (GF) filled PP(HWM25)

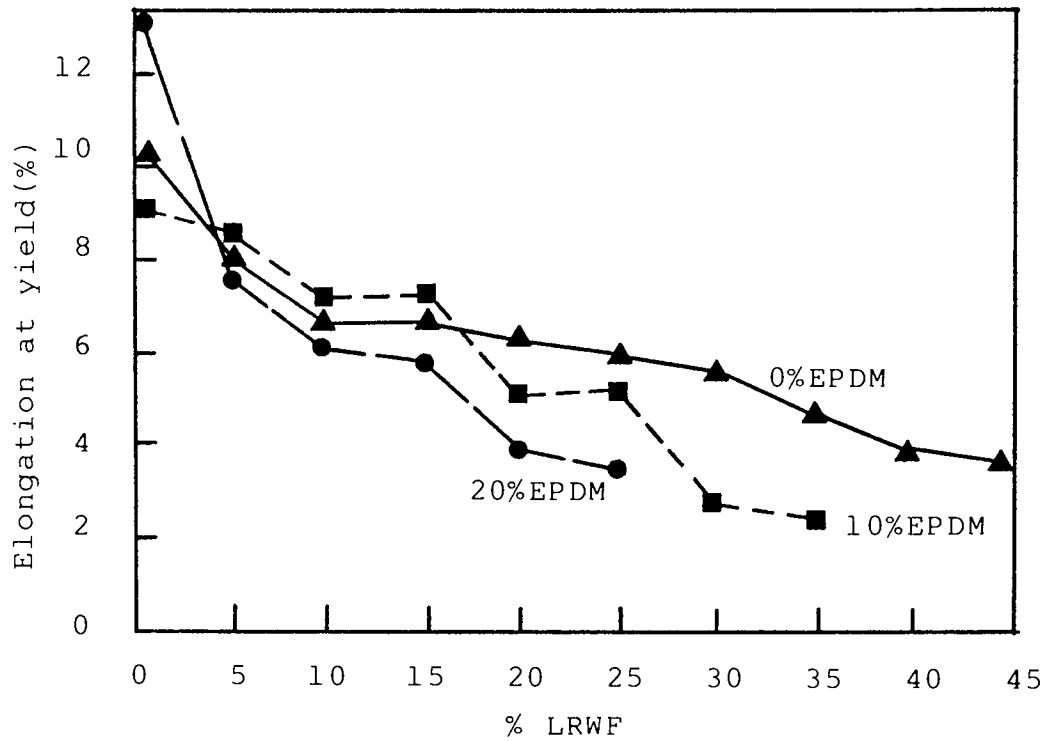


Figure 3.36 Effect of EPDM(10,20%) on elongation at yield of long Rockwool fibre(LRWF)filled PP(HWM25)

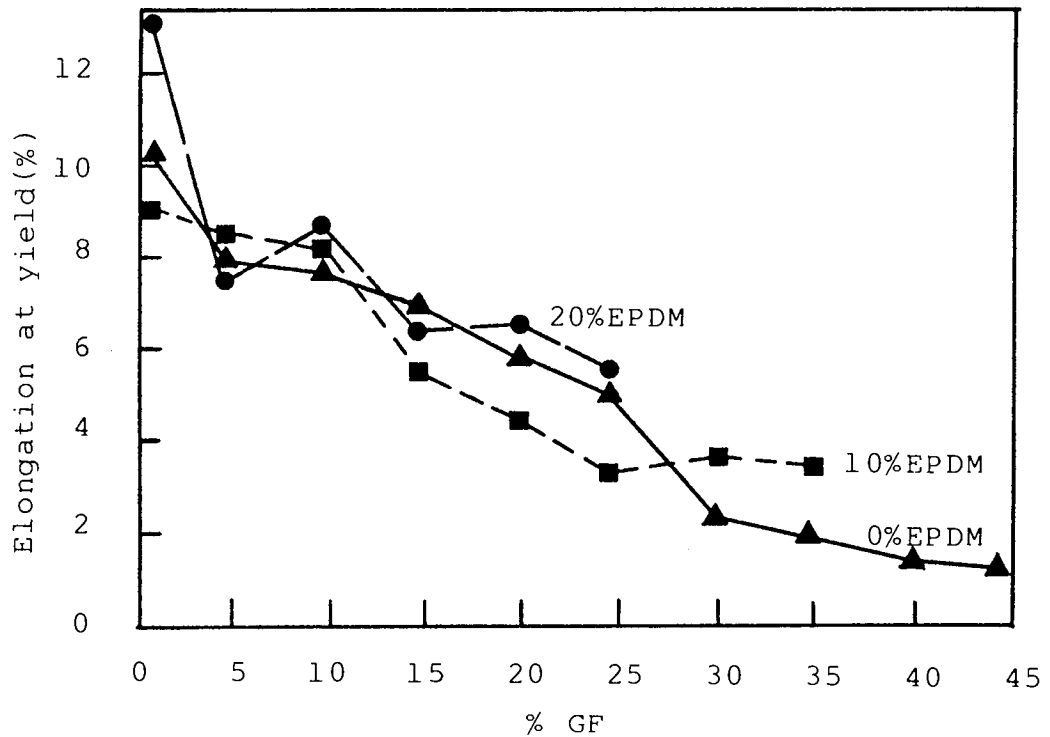
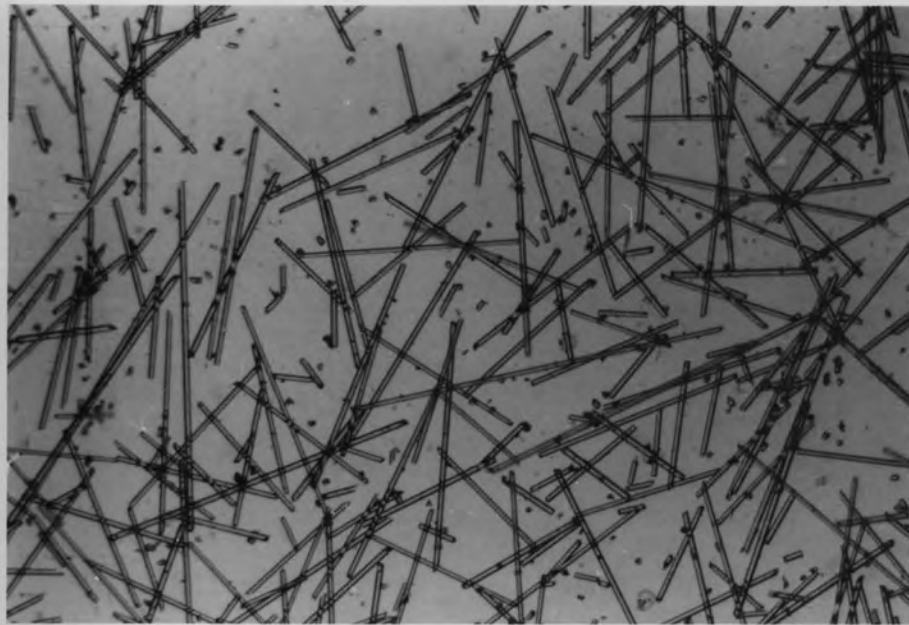


Figure 3.37 Effect of EPDM(10,20%) on elongation at yield of glass fibre (GF) filled PP(HWM25)



0.5mm

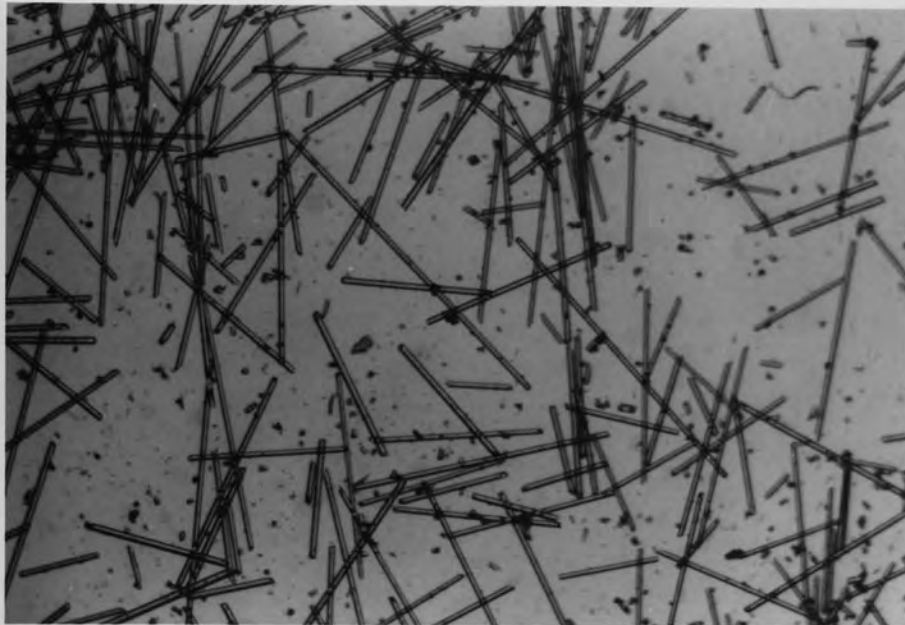
Plate 3.1 Optical micrograph of glass fibre after homogenisation with PP(HWM25), Buss Ko-Kneader, 32rpm, 240°C



0.5mm

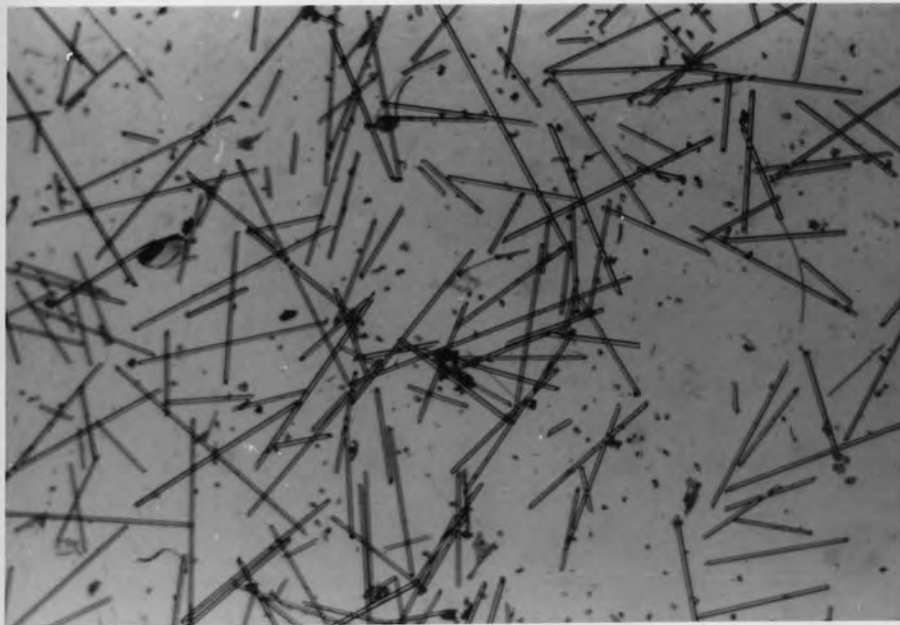
Plate 3.2 Optical micrograph of long Rockwool fibre after homogenisation with PP(HWM25), Buss Ko-Kneader, 32rpm, 240°C





0.5mm

Plate 3.3 Optical micrograph of glass fibres from  
PP(HW60/GR30) before processing



0.5mm

Plate 3.4 Optical micrograph of glass fibres from  
PP(HW60/GR30) after injection moulding  
(Edgwick, 265°C, 40rpm, 580kg/cm<sup>2</sup>)

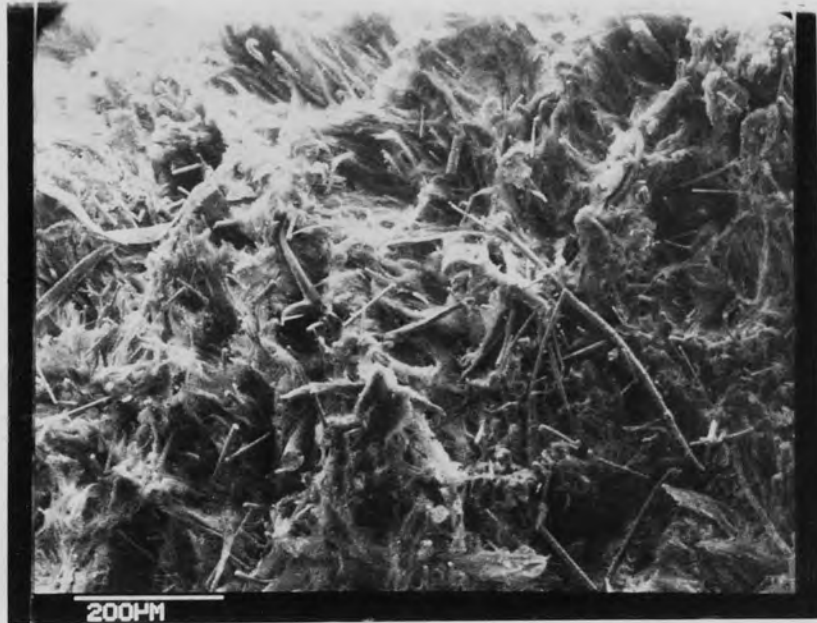


Plate 3.5 Scanning electron micrograph of the tensile fracture surface of PP(HWM25) containing 30% long Rockwool fibre (A-1100 silane coupled)



Plate 3.6 Scanning electron micrograph of the tensile fracture surface of PP(HWM25) containing 30% glass fibre (A-1100 silane coupled)

CHAPTER FOUR

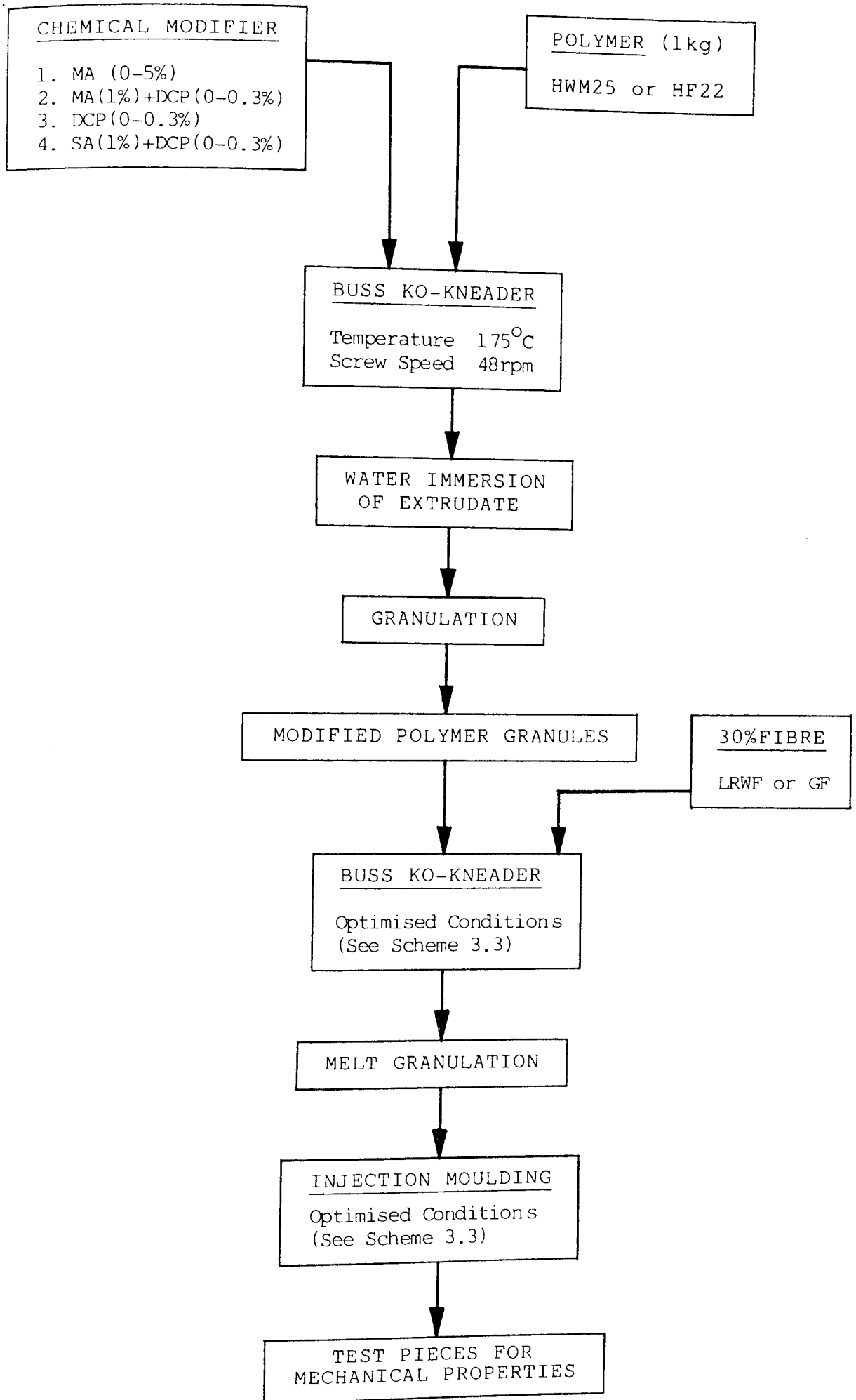
MALEIC ANHYDRIDE AND DI-CUMYL PEROXIDE  
MODIFICATION  
OF POLYPROPYLENE COMPOSITES

#### 4.1 Object

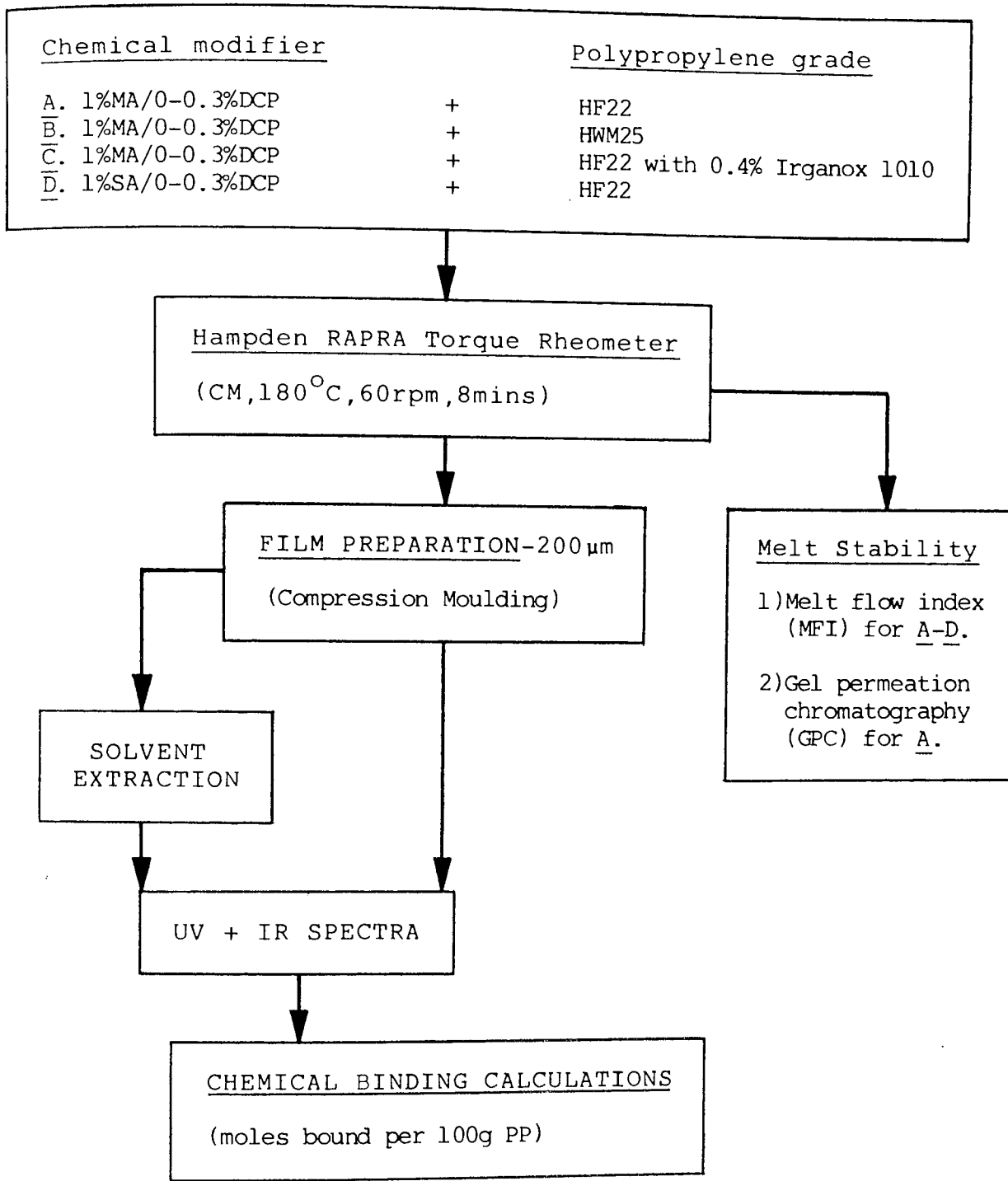
In this chapter the chemical binding of reactive anhydride groups onto polypropylene (PP) is attempted to obtain enhanced mechanical properties of PP containing long Rockwool fibre (LRWF) and glass fibre (GF), both A-1100 silane coupled. The mechano-chemical modification was done in the polymer melt utilising shear-generated free radicals produced in the Buss Ko-Kneader (see Scheme 4.1). Processing conditions were chosen for maximum shear (high screw speed, 48 rpm) and minimum volatilization of additives (low temperature, 175°C). Maleic anhydride (MA) was used with and without di-cumyl peroxide (DCP), a free radical initiator. Two grades of PP (unstabilised HF22 and stabilised HWM25) were used to determine the effect on chemical modification of melt and thermal-oxidative stabilisers present in HWM25. On completion of processing in the Buss Ko-Kneader, the modified PP melt was quenched in water to prevent further reaction and granulated. The mechanical properties of chemically modified PP (HF22 and HWM25) containing LRWF and GF were investigated and compared to unmodified PP composites (see Chapter 3) and commercially 30% GF coupled PP (HW60/GR30). These composites were produced using the previously optimised homogenisation (Buss Ko-Kneader) and injection moulding (Edgwick) procedures (see Scheme 3.3).

To show that MA chemical binding occurs by a free radical mechanism and is responsible for the enhancement of PP composite mechanical properties, experiments listed in Scheme 4.2 were done. These involve the melt processing (in the Hampden RAPRA torque rheometer) of PP with MA and DCP using unstabilised PP(HF22), commercially stabilised PP(HWM25) and PP(HF22) with 0.4% Irganox 1010 in order to investigate the importance of DCP and the effect of stabilisers on the MA mechano-chemical binding. The melt stability after processing was investigated by melt flow index (MFI) and gel permeation chromatography (GPC) for weight average molecular weight ( $\bar{M}_w$ ). The amount of chemically bound MA was recorded using infra-red and ultraviolet spectra taken before and after extraction of 200  $\mu\text{m}$  PP films. The necessity of the anhydride to possess carbon-carbon unsaturation (i.e., MA) in order to chemically bind to PP was investigated by using succinic anhydride (SA), the saturated equivalent of MA. SA was melt processed with DCP in PP (HF22) using the Hampden RAPRA torque rheometer. Chemical binding of SA was recorded together with the melt stability of the modified PP using MFI.

Finally, the role of carbon-carbon unsaturation in anhydride binding to PP and its subsequent importance in enhancing the mechanical properties of PP composites was investigated by producing (see Scheme 4.1) SA/DCP modified



Scheme 4.1 Production and testing of chemically modified polypropylene composites 197.



Scheme 4.2 Chemical binding and melt stability studies of modified PP

PP(HF22) containing GF (30% loading, A-1100 silane coupled).

## 4.2 Results

### 4.2.1 The Mechanical Properties Of Chemically Modified PP (HWM25) Composites

This section describes the effect of maleic anhydride (MA) and di-cumyl peroxide (DCP) mechano-chemical modification on the mechanical properties of commercially stabilised PP (HWM25) with or without long Rockwool fibre (LRWF) and glass fibre (GF), both 30% loaded and A-1100 silane coupled.

PP(HWM25) was initially modified with either MA(0-5%), DCP(0-0.3%) or a combination of 1% MA and DCP(0-0.3%) according to the procedure given in Scheme 4.1. The mechanical properties of this modified PP (HWM25) without reinforcing fibres are listed in Table 4.1 (Part I) and it is clear that for most of them, MA and DCP modification of PP(HWM25) has no significant effect as shown in Figure 4.1, which depicts the small changes (10%) in yield strength. Only the flexural modulus (Table 4.1) and Charpy impact strength (Figure 4.2) give major improvements (30% and 100% respectively) when PP (HWM25) is modified with MA/DCP.



Table 4.1 (Parts I and II) also shows the effect of MA (0- 5%) and DCP(0-0.3%) separately on the mechanical properties of PP(HWM25) containing 30%LRWF and 30%GF, one representative of which, yield strength, is shown graphically in Figure 4.3 and clearly indicates that the addition of DCP to PP(HWM25) containing 30%GF has no effect on yield strength, but that similarly modified composites containing 30%LRWF give an increase of 70% when only 0.05%DCP is used. Incorporation of MA into PP(HWM25) containing 30%LRWF and 30%GF results in yield strength enhancement of 25% and 35% respectively. The other mechanical properties of these modified composites give similar trends.

The range of mechanical properties of DCP(0-0.3%) modified PP(HWM25) with or without MA(1%) and containing 30% LRWF and 30%GF are shown graphically in Figures 4.4-4.9 from tabulated results recorded in Table 4.1 (Parts I and II). The highest value for each mechanical property is obtained using a combination of 1%MA with 0.2%DCP in the mechano-chemical modification of PP(HWM25) containing 30%GF; for example, the yield strength of such PP composites modified with 1%MA alone gives 44MPa (see Figure 4.4) and the addition of 0.1%DCP improves this by 50% (68MPa), while 0.2%DCP results in a 75% enhancement (80MPa). Higher concentrations of peroxide (0.3%) with 1%MA gave a 65% improvement. The use of DCP modification alone of PP (HWM25) containing 30%GF showed no change from the

equivalent unmodified composite. However, the mechanical properties of mechano-chemically modified PP(HWM25) containing 30%LRWF exhibit different behaviour; the best results were obtained with DCP modification alone (Figures 4.4-4.9). While in each case the magnitude of mechanical property is consistently below that of the best MA/DCP modified PP(HWM25) containing 30%GF, the use of 0.2%DCP in PP(HWM25) containing 30%LRWF gives increases in yield strength (100%, Figure 4.4), tensile modulus (20%, Figure 4.5), flexural strength (75%, Figure 4.6) and flexural modulus (20%, Figure 4.7). Only the Charpy impact strength (Figure 4.9) of such composites was unaffected by mechano-chemical modification. PP(HWM25) containing 30%LRWF and modified with a combination of 1%MA/DCP(0-0.3%) consistently underperformed DCP-only modified samples, usually by 10-20%, the exception being Charpy impact strength (Figure 4.9) where the use of 1%MA with DCP resulted in a minor improvement.

Figures 4.8A and B show the effect of water immersion for 24 hours at 70°C on the tensile modulus of DCP modified PP(HWM25) with or without 1%MA using 30%LRWF and 30%GF. This test which is used to compare the stability of the fibre-matrix adhesion towards moisture showed that PP(HWM25) modified with DCP alone or 1%MA/DCP and containing 30%LRWF retained 95% of its tensile modulus after hot water immersion (Figure 4.8A). This compares to the

equivalent unmodified composite retaining only 85% of its original tensile modulus. Good results were also obtained with 1%MA/DCP modified PP(HWM25) containing 30%GF (Figure 4.8B, 95% retention) while the DCP-only modified material gave a modulus retention of 90%, both representing a useful improvement over unmodified samples.

Table 4.2 summarises the mechanical properties of unmodified PP(HWM25) containing 30%LRWF and 30%GF and compares them with the best modified composites: 0.2%DCP modified PP(HWM25) containing 30%LRWF and 1%MA/0.2%DCP modified PP(HWM25) containing 30%GF. To assess the progress towards achieving mechanical properties in excess of currently available commercial materials, HW60/GR30 (30% coupled GF reinforced PP) is also listed. The results are shown graphically in Figures 4.10-4.14. The use of 1%MA/0.2%DCP and 0.2%DCP in PP(HWM25) containing 30%GF and 30%LRWF respectively improves their yield strength (Figure 4.11) by 100% and flexural strength (Figure 4.13) by over 75% over the same system used without the MA and/or DCP. It is also clear that 1%MA/0.2%DCP modification of PP(HWM25) containing 30%GF results in similar mechanical performance (e.g., flexural and tensile modulus and flexural, yield and Charpy impact strengths, see Figures 4.10-4.14) to those observed for the commercial control HW60/GR30. In spite of the substantial improvements in mechanical properties shown in Figures 4.11-4.14

(with the exception of Charpy impact strength, Figure 4.10) of DCP modified PP(HWM25) containing 30%LRWF, they are still 30% below the levels given by the commercial control (HW60/GR30) except the flexural modulus (Figure 4.14) which was found to be equal to the commercial composite.

#### 4.2.2 The Mechanical Properties Of Chemically Modified PP(HF22) Composites

The mechano-chemical modification using MA and DCP of stabilised PP(HWM25) containing 30%LRWF and 30%GF resulted in substantial improvements in mechanical properties (see Table 4.2, Figures 4.10-4.14). Composites reinforced with 30%GF achieved parity with the commercial control HW60/GR30, while those containing 30%LRWF gave comparable mechanical performance but in most cases up to 30% below that of the commercial material.

Further enhancement of the mechanical properties of 30% fibre reinforced PP is next attempted using unstabilised PP(HF22) because the thermal-oxidative and thermal stabilisers present in PP(HWM25) are thought to inhibit free radical mechano-chemical modification during melt processing; the use of unstabilised PP(HF22) allows MA and DCP to be used without such inhibition. The mechanical properties of PP(HF22) modified with DCP(0-0.3%) and 1%MA/DCP(0-0.3%) containing 30%LRWF and 30%GF are shown in

Table 4.3 together with the commercial control HW60/GR30. These results are plotted in Figures 4.15-4.20 and it is clear from these results that although the mechano-chemical modification of PP(HF22) using MA and DCP and containing 30%LRWF and 30%GF gives the same trends as similar modification of PP(HWM25), Figures 4.4-4.9, the effects here are more pronounced indicating that the absence of stabilisers within PP(HF22) decreases free radical inhibition within the polymer during melt processing. As with PP(HWM25), the best results were achieved with 1%MA/0.2%DCP modification of PP(HF22) containing 30%GF. The use of 0.1-0.3%DCP with 1%MA increases the yield strength (Figure 4.15) of 30%GF reinforced PP(HF22) by 110% (the equivalent using HWM25 is only 75%, Figure 4.4) to a level which is 30% in excess of the commercial HW60/GR30. For each mechanical property, the use of 0.1%DCP with 1%MA created a rapid improvement, with higher concentrations of DCP(0.2-0.3%) achieving only minor further rises. The most striking result was seen in the 300% improvement in Charpy impact strength (Figure 4.20) due to modification of PP(HF22) containing 30%GF with 1%MA/0.2%DCP. GF reinforced PP(HF22) modified with only DCP gave no change from unmodified samples (Figures 4.15-4.20), mirroring the behaviour of similarly modified PP(HWM25, Figures 4.4-4.9).

The use of DCP modification alone for PP(HF22) containing 30%LRWF gave the best results with this type of reinforcement (as was observed with stabilised PP(HWM25)). With the exception of Charpy impact strength (Figure 4.20) which remained unaltered, improvements of up to 100% (compared to only 50-75% for similarly modified HWM25) were obtained with the use of 0.3%DCP in PP(HF22) containing 30%LRWF (Figures 4.15-4.20). The flexural modulus however, was only improved upon by 10% (Figure 4.18). As with PP(HWM25), the use of 1%MA with DCP in the modification of PP(HF22) containing 30%LRWF did result in the improvement of mechanical properties, but these were not to the same level achieved by the use of DCP alone, indicating that MA inhibits in some way the free radicals in the polymer melt during processing created by DCP and mechano-chemical shearing.

Very good results were obtained for tensile modulus retention after 24 hours water immersion at 70°C (Figures 4.19A and B). This test gives a good guide to the strength and stability with respect to moisture of the adhesion between the matrix and fibre. PP(HF22) modified with 1%MA/0.2%DCP gave 100% retention for LRWF and GF reinforced composites. 100% retention was also achieved with DCP modification of PP(HF22) containing 30%LRWF, while similar treatment of PP(HF22) containing 30%GF resulted in no change of tensile modulus retention at 90%.

The best values achieved for modified PP(HWM25) composites (Figures 4.8A and B) were in the range 90-95%, thus indicating another advantage of using unstabilised PP(HF22) for mechano-chemical modification.

Table 4.4 compares the mechanical properties of optimised modified PP(HF22) materials (1%MA/0.2%DCP/30%GF and 0.3%DCP/30%LRWF) with previously optimised modified and unmodified PP(HWM25) composites. The mechanical properties of the commercially produced 30%GF reinforced PP(HW60/GR30) are included in order to ascertain the effectiveness of mechano-chemical modification of fibre-filled PP(HWM25 and HF22) in achieving PP composites with superior mechanical properties. These results are depicted graphically in Figures 4.21-4.25 for easy comparison. Immediately obvious is the progressive enhancement of mechanical properties from using unmodified stabilised PP(HWM25) through to modified PP(HWM25) and finally modified unstabilised PP(HF22) containing both 30%LRWF and 30%GF. In general terms, unmodified composites are very inferior to the commercial material (HW60/GR30) with yield and flexural strength (Figures 4.22 and 4.24) being only half of the commercial composite's. The introduction of chemical modifiers to PP(HWM25, 1%MA/0.2%DCP with 30%GF and 0.2%DCP with 30%LRWF) results in significant improvements in mechanical properties with GF reinforced modified PP(HWM25) reaching parity with HW60/GR30 and modified

PP(HWM25) containing 30%LRWF in most cases approaching those of the commercial material. The change in PP grade from stabilised HWM25 to unstabilised HF22 results in a further major improvement in the mechanical properties of composites containing LRWF and GF which indicates that the stabilisers present in HWM25 inhibit the mechano-chemical modification process. Optimum modification was obtained with 1%MA/0.2%DCP/30%GF and 0.3%DCP/30%LRWF for PP(HF22). This resulted in the mechanical properties of modified PP(HF22) containing 30%GF being in general 30% in excess of HW60/GR30 (the exception being Charpy impact strength, Figure 4.21, where the excess is 100%). The mechanical properties of 0.3%DCP modified PP(HF22) containing 30%LRWF were equal to those of HW60/GR30 with the exception of Charpy impact strength (Figure 4.21) where only half the level of the commercial control was attained. Indeed it is noteworthy that the Charpy impact strength was the only mechanical property of PP(HWM25 and HF22) containing 30%LRWF that was not improved by mechano-chemical modification.

#### 4.2.3 The Mechanical Properties Of Succinic Anhydride Modified PP(HF22) Composites

The mechanical properties of PP(HF22) modified with succinic anhydride (1%SA) and DCP(0-0.3%) and containing 30%GF are shown in Table 4.5. The procedure for mechano-



chemical modification was the same as used for MA/DCP (see Scheme 4.1). From Table 4.5, it is clear that using SA/DCP modification for GF reinforced PP(HF22) has no effect on the mechanical properties. Figure 4.26 compares the effectiveness of 1%SA with 1%MA when used in the modification with DCP(0-0.3%) of PP(HF22) containing 30%GF in terms of yield strength. As described in Section 4.2.2, the addition of just 0.1%DCP to 1%MA modified samples increases the yield strength of PP(HF22) containing 30%GF by over 100%, but modification using 1%SA with DCP in PP(HF22) also containing 30%GF results in no change in yield strength and this provides evidence for the necessity of an effective PP modifier to possess carbon-carbon double bond unsaturation in order that interaction with free radicals in the polymer melt may occur.

#### 4.2.4 Melt Stability Studies Of Maleic Anhydride Mechano-chemically Modified Polypropylene

This section has been designed to decipher why mechano-chemical modification of PP(HWM25 and HF22) using MA/DCP and containing A-1100 silane coupled reinforcing fibres causes improvements in their mechanical properties. The melt stability of stabilised PP(HWM25 and HF22 with 0.4% Irganox 1010) and unstabilised PP(HF22) modified with DCP, MA and MA/DCP were investigated by MFI (Figures 4.27-4.29). The addition of only 0.1% DCP causes a rapid increase in

MFI to levels in excess of 45g/10mins (readings above this level could not be measured due to the low melt viscosity) and because MFI is inversely proportional to molecular weight, it is apparent that drastic polymer degradation is occurring. The addition of 0.5%MA causes a small rise in MFI (Figures 4.27-4.29), but incorporation of higher concentrations (1-5%) results in a gentle decrease indicating that cross-linking is occurring. The MFI of PP(HWM25) processed with 1%MA/DCP(0-0.3%) rises with increasing DCP content (Figure 4.27), but the increase is significantly less than samples using DCP alone, suggesting that the 1%MA present stabilises the melt by taking up the free radicals produced by shear generated mechano-chemical degradation of the polymer and thermal decomposition of DCP. PP(HWM25) is a highly stabilised injection moulding grade known to contain thermal and thermal-oxidative stabilisers of which one, as determined by infra-red and ultraviolet spectrophotometry is a hindered phenolic. PP(HF22) is unstabilised and because of this the two grades exhibit different melt stability behaviour when processed with MA, DCP and MA/DCP (Figures 4.27-4.29). Both are catastrophically degraded by only 0.1%DCP while addition of MA results in a slight degree of cross-linking, but when processed with 1%MA/DCP(0-0.3%), the free radical inhibition by stabilisers within PP(HWM25) is evident by the depression of MFI (Figure 4.27) compared to the unstabilised PP(HF22)(Figure 4.29), processed under identical

conditions. Confirmation that stabilisers within PP(HWM25) were responsible for this free radical inhibition came from using PP(HF22) modification with MA, DCP and MA/DCP in the presence of 0.4% Irganox 1010, a hindered phenolic stabiliser; melt stability tests (MFI, Figure 4.28) showed identical behaviour to commercially stabilised PP(HWM25).

Gel permeation chromatography (GPC) was used to investigate the weight average molecular weight ( $\bar{M}_w$ ) of unstabilised PP(HF22) modified with MA, DCP and MA/DCP (Figure 4.30) to supplement MFI determination of identical samples (Figure 4.29). Because MFI is inversely proportional to molecular weight, the graphs of  $\bar{M}_w$  and MFI (Figures 4.29 and 4.30) are mirror images of each other. Indeed, Figure 4.30 confirms that the molecular weight of PP(HF22) falls as its MFI rises (Figure 4.29) with low concentrations of MA (up to 1%) and then increases (cross-links) with higher amounts (1-5%). Surprisingly, MA/DCP and DCP modified PP(HF22) give similar  $\bar{M}_w$  behaviour on melt processing (Figure 4.30) and only at high levels of DCP(0.2-0.3%) is the molecular weight of DCP-only modified PP(HF22) lower than that modified with 1%MA/DCP(0.2-0.3%), providing further evidence that MA inhibits the free radical degradative process.

#### 4.2.5 Mechano-chemical Binding Of Maleic Anhydride To Polypropylene

This section describes investigations into the chemical

binding of MA to stabilised PP(HWM25) and unstabilised PP(HF22, with and without 0.4% Irganox 1010 stabiliser) resulting from melt processing in the RAPRA torque rheometer. The effect of DCP(0-0.3%) on the degree of binding is investigated and together with melt stability (MFI and GPC, Section 4.2.4) studies, these results will help in understanding why the mechano-chemical modification of stabilised PP(HWM25) composites results in significant improvements in mechanical properties and why similar modification of unstabilised PP(HF22) composites gives superior properties resulting in better performance than HW60/GR30, the commercially available composite. Chemical binding studies of MA were done using infra-red spectrophotometry of PP(HF22) films (200 $\mu$ m) at 1792 $\text{cm}^{-1}$  before and after exhaustive Soxhlet extraction (Figures 4.31 and 4.32). It is clear from Figure 4.32 that when PP(HF22) is processed with 1%MA only, all MA present in the system is completely removed by extraction resulting in no detectable chemical binding. Figure 4.31 shows that the addition of 0.2%DCP to 1%MA modification of PP(HF22) allows only 50% of the MA to be removed after Soxhlet extraction. A more detailed investigation of this behaviour is presented in Table 4.6 and Figure 4.33 and this shows the degree of binding when 1%MA was processed with DCP(0-0.3%) using stabilised PP(HWM25 and HF22 with 0.4% Irganox 1010) and unstabilised PP(HF22). With all PP grades, no MA binding was achieved when processed without DCP, and optimum binding was obtained using 0.2 - 0.3% DCP (Figure 4.33).

However, it is clear that DCP catalysed chemical binding of MA processed in the presence of free radical inhibiting stabilisers found in PP(HWM25 and HF22/Irgl010) results in binding levels 50% below those obtained with unstabilised PP(HF22). Of great significance is that the binding levels of MA (Figure 4.33) and their dependence upon DCP concentration and the absence of stabilisers within the polymer correlates exactly with the trends in mechanical properties of GF reinforced modified PP (Figures 4.4-4.25); that optimum properties are found with 1%MA/0.2%DCP corresponding to high MA binding (Figure 4.33) and that unstabilised modified PP(HF22) achieves the best mechanical performance by not possessing stabilisers that inhibit the free radical MA binding process.

#### 4.2.6 Melt Stability And Chemical Binding Studies Of Succinic Anhydride Mechano-chemically Modified Polypropylene

The melt stability of PP(HF22) processed with SA, DCP and SA/DCP in the RAPRA torque rheometer was studied by MFI using the same concentrations and conditions as similar studies using MA (Section 4.2.4). The use of up to 5%SA causes a slight increase in MFI (Figure 4.34) and shows none of the cross-linking associated with MA (Figure 4.29). The addition of DCP(0-0.3%) and 1%SA/DCP(0-0.3%) both gave rapid increases in MFI indicating a high degree of polymer

degradation (Figure 4.34) and thus SA did not show any of the inhibiting behaviour observed when 1%MA was processed with DCP(0-0.3%, Figure 4.29). These results together with evidence that SA does not chemically bind to PP(HF22) in the presence of DCP (Figure 4.35) and that SA/DCP modification of PP(HF22) composites has no effect on their mechanical properties (Figure 4.26, Table 4.5) indicates the importance of a PP chemical modifier possessing alkene unsaturation in order to achieve chemical binding with subsequent increases in the mechanical properties of fibre reinforced modified PP composites.

### 4.3 Discussion

#### 4.3.1 The Mechanical Properties Of Chemically Modified PP(HWM25) Composites

From Table 4.1 (Parts I and II) and Figures 4.1-4.9, it is apparent that the use of 1%MA alone in the mechano-chemical modification of commercially stabilised PP(HWM25) is insufficient to enhance the mechanical properties of composites containing A-1100 silane coupled GF and LRWF; the vast improvement (Figures 4.4-4.9) in performance on using 0.2%DCP during melt processing mechano-chemical modification (with 1%MA for 30%GF and with or without 1%MA for 30%LRWF respectively) of PP(HWM25) shows that PP melt modification occurs by a free radical mechanism and that

the concentration of macro-alkyl free radicals generated by shearing alone is insufficient to feed this system. It is clear that PP(HWM25) must be catalytically degraded using the thermal decomposition of DCP to enhance the free radical concentration within the polymer melt during processing. The use of 1%MA/0.2%DCP modification to enhance the mechanical properties of PP(HWM25) containing 30%GF (Figures 4.4-4.9) illustrates that the peroxide catalyst must allow the anhydride to bond the polymer to the reinforcing fibre (via the A-1100 silane coupling agent); the use of DCP or MA alone do not exhibit this behaviour. It was thus surprising that similarly coupled LRWF achieved optimum performance with 0.2%DCP only modified PP(HWM25); this grade of mineral fibre is coated with a layer of tenside (the nature of which will not be disclosed by the manufacturer, Laxabruk AB, Sweden) to prevent fibre agglomeration during processing and handling. This step is unavoidable as it is an integral stage of the manufacturing process, and it is thus concluded that proper silane coupling cannot occur because the fibres are protected by an effective barrier layer of tenside preventing direct contact with the mineral surface. The observation (Figures 4.4-4.9) that 0.2%DCP alone is effective in enhancing the mechanical performance of PP(HWM25) containing 30%LRWF suggests that the tenside coating may contain chemically unsaturated groups which bond to the polymer by macro-alkyl free radical addition during melt processing.

#### 4.3.2 The Mechanical Properties Of Chemically Modified PP(HF22) Composites

The reason for the substantial improvements in mechanical performance of 1%MA/0.2%DCP (and 0.3%DCP) modified unstabilised PP(HF22) containing 30%GF and 30%LRWF respectively (Figures 4.15-4.20) over the similarly modified and reinforced stabilised PP(HWM25) shown in Figures 4.4-4.9 is due solely to the absence of free radical inhibiting stabilisers during melt processing of PP(HF22). These stabilisers (hindered phenols) are present in PP(HWM25) to stabilise the melt<sup>(115,118,122)</sup> against free radical (shear generated and thermally induced peroxide decomposition) degradation (Chapter One, Scheme 1.4) and thus inhibit the effectiveness of DCP catalysed PP modification with or without MA which in turn reduces the scope for enhancement of modified stabilised PP(HWM25) composite mechanical performance compared to that containing unstabilised PP(HF22).

The short fibre pull-out lengths (SEM Plates 4.2 and 4.4) in the tensile fracture surfaces of mechano-chemically modified unstabilised PP(HF22) GF and LRWF composites present additional evidence for effective bonding resulting in increased interfacial adhesion at the polymer-fibre interface (compared to long fibre pull-out with unmodified composites, Plates 3.5 and 3.6). Efficient



bonding between the two phases allows a greater degree of stress transfer to the fibre<sup>(10)</sup> which explains the excellent mechanical properties exhibited by these materials and also reduces the critical length of reinforcing fibres<sup>(10)</sup> (Chapter One, Section 1.2, Equation 2) which means that fibre length degradation due to homogenisation and injection moulding is less critical with modified as opposed to unmodified PP composites. Similar SEM Plates 4.1 and 4.3 showing modified stabilised PP(HWM25) GF and LRWF composites exhibit longer fibre pull-out lengths than those using modified unstabilised PP(HF22, Plates 4.2 and 4.4) which provides further evidence for the inhibition of mechano-chemical modification by PP melt stabilisers reducing the scope for improvement of interfacial adhesion and consequently the mechanical properties of modified PP composites.

#### 4.3.3 The Mechanical Properties Of Succinic Anhydride Modified PP(HF22) Composites

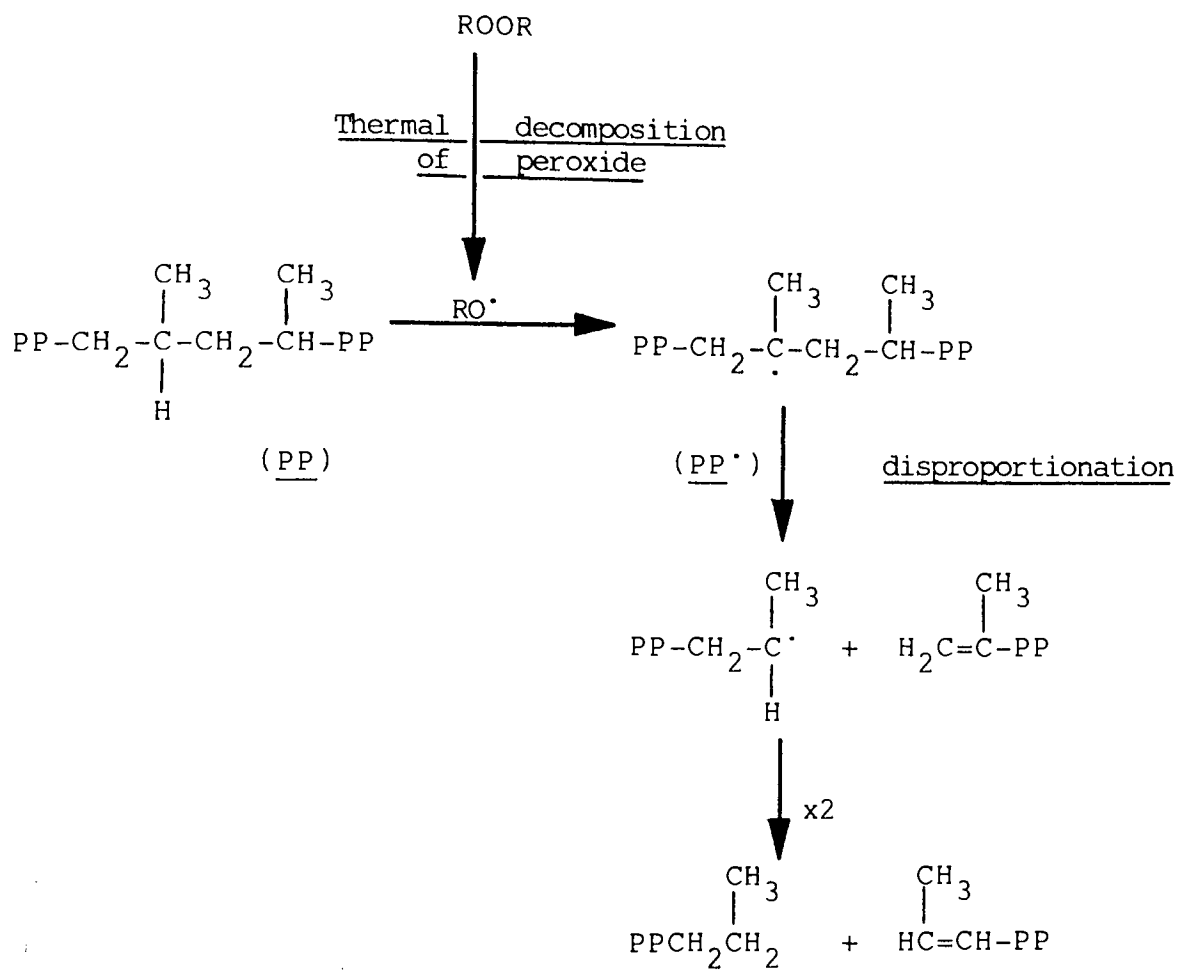
The total failure of SA modification with and without DCP of PP(HF22) to improve the mechanical performance of GF reinforced composites (Table 4.5 and Figure 4.26) clearly illustrates the requirement for a PP mechano-chemical modifier to possess chemical unsaturation so that it may utilise the macro-alkyl free radicals within the polymer melt (originating from mechano-chemical shear and thermally

induced decomposition of DCP) without which bonding between PP(HF22) and A-1100 silane coupled GF cannot occur.

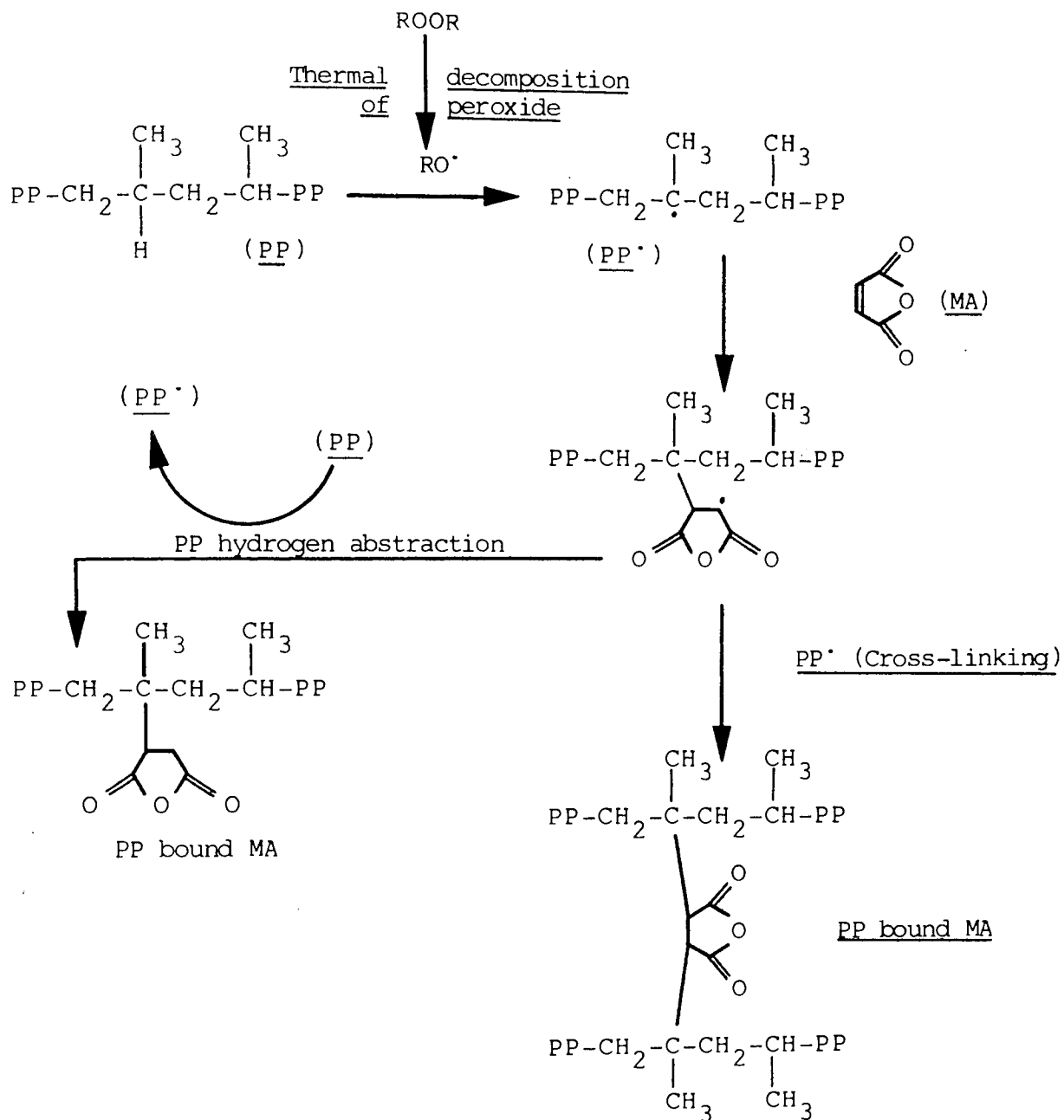
#### 4.3.4 Melt Stability Studies Of Maleic Anhydride Mechano-Chemically Modified Polypropylene

The rapid increases in MFI on DCP addition to stabilised PP(HWM25 and HF22/Irgl010) shown in Figures 4.27-4.28 accompanied by decreased  $\bar{M}_w$  (Figure 4.30) is due to DCP thermal decomposition; the half-life of DCP at the melt processing temperature ( $180^\circ\text{C}$ ) is two minutes<sup>(198)</sup> and therefore the eight minutes of melt processing provides ample time for the peroxide to thermally dissociate to provide highly reactive alkoxyl free radicals in the PP melt. It should be noted however, that this DCP half-life was calculated in solution and that melt shearing of the polymer can drastically alter this figure. These alkoxyl free radicals attack PP, mainly at the labile hydrogen of the tertiary carbon atom in the main chain to generate macro-alkyl free radicals (Scheme 4.3) which disproportionate in the absence of MA<sup>(199,200)</sup> quickly reducing the PP molecular weight. The rate of disproportionation is proportional to the initial DCP concentration and melt processing temperature<sup>(200)</sup>. Stabilised PP(HWM25 and HF22/Irgl010 in Figures 4.27 and 4.28) show slightly better melt stability than unstabilised PP(HF22, Figure 4.29) when processed with DCP (with and without MA)

and this is attributable to the chain-breaking free radical trapping ability of hindered phenolic stabilisers (Chapter One, Scheme 1.4) which are traditionally incorporated into commercially stabilised PP<sup>(201)</sup>. Phenolic antioxidants such as Irgl010 are particularly effective due to their low volatility and high mobility within the sheared polymer melt<sup>(127,201)</sup> (Table 1.1) and the kinetic termination of these free radicals is not limited by diffusion as it is in the solid phase<sup>(201)</sup>. Melt processing of stabilised PP(HWM25 and HF22/Irgl010) and unstabilised PP(HF22) with DCP in the presence of MA (Figures 4.27-4.29) results in greatly enhanced PP melt stability. The mechanisms contributing to this are shown in Scheme 4.4<sup>(199,202-204)</sup>. In the presence of MA, macro-alkyl free radicals (produced by hydrogen abstraction by alkoxyl radicals originating from thermal dissociation of DCP<sup>(199,202,203)</sup>) do not undergo disproportionation<sup>(199,200)</sup> but add preferentially to the anhydride resulting in radical transfer to the MA entity<sup>(199,202,203)</sup>. The transferred radical may terminate either by abstracting a hydrogen from an adjacent PP chain (thus creating another macro-alkyl free radical which in turn may add to another MA molecule, thus creating a cycling of radicals) or alternatively the grafted MA radical may terminate with a macro-alkyl PP free radical resulting in a cross-linked structure via the MA entity (Scheme 4.4). The former mechanism has a negligible effect on molecular weight of



Scheme 4.3 Peroxide catalysed degradation of polypropylene



Scheme 4.4 Peroxide catalysed mechano-chemical modification of polypropylene using maleic anhydride

melt processed PP, while the cross-linking mechanism will contribute to increased molecular weight. Thus the final molecular weight and melt stability of MA/DCP modified PP is determined by the relative ratios of disproportionation caused by DCP and MA grafting terminating with or without cross-linking (Schemes 4.3 and 4.4).

The addition of MA alone to stabilised PP(HWM25 and HF22/Irgl010) and unstabilised PP(HF22) causes a slight degree of cross-linking during melt processing (Figures 4.27-4.30). The free radicals in this system are created by mechano-chemical shearing and small amounts of oxygen present in the melt resulting in hydroperoxide formation<sup>(104-108)</sup>; the absence of additional DCP means that the concentration of free radicals within the melt is low. Because the macro-alkyl free radicals react preferentially with MA<sup>(199,200)</sup> (Scheme 4.4), in the absence of DCP the degree of disproportionation is very low and thus even small amounts of cross-linking occurring via grafted MA groups show up as increases in  $\bar{M}_w$  (Figure 4.30) or decreases in MFI (Figures 4.27-4.29). Further evidence (Figures 4.27-4.30) that this is happening is shown by the fact that the higher the concentration of MA (to 5%) in the PP melt, the better the melt stability because the higher anhydride concentration makes the addition reaction of a macro-alkyl PP free radical more likely and its disproportionation less probable.

#### 4.3.5 Mechano-chemical Binding Of Maleic Anhydride To Polypropylene

The chemical binding studies of MA to stabilised PP(HWM25 and HF22/Irgl010) in Table 4.6 and Figure 4.33, show clearly that the presence of hindered phenols inhibits the DCP catalysed free radical mechano-chemical process (see Section 4.3.4) by acting in a chain-breaking mode<sup>(115,116,201)</sup> (Chapter One, Scheme 1.4) and that the use of unstabilised PP(HF22) allows double the chemically bound concentration of MA to PP. The use of DCP is essential as a free radical catalyst to provide a sufficient macro-alkyl PP free radical concentration to allow binding of MA (Scheme 4.4). Figures 4.32 and 4.33 show that no chemical binding of MA could be detected by infra-red spectrophotometry when melt processed in PP(stabilised and unstabilised) in the absence of DCP, although evidence from melt stability studies (Section 4.3.4) which show cross-linking via anhydride molecules suggests that binding under these conditions does occur, albeit at a very low concentration not detectable in the infra-red.

#### 4.3.6 Melt Stability And Chemical Binding Studies Of Succinic Anhydride Mechano-chemically Modified Polypropylene

The fundamental requirement of a PP mechano-chemical modifier to possess chemical unsaturation in order that

chemical binding may occur during melt processing in the presence of a free radical catalyst (DCP) is proved by the use of SA (Figure 4.34). SA being saturated and thus unreactive towards macro-alkyl PP free radicals confers no melt stability upon PP(HF22) containing DCP (Figure 4.34) unlike MA (Figure 4.29); the same degree of catastrophic degradation occurs with SA/DCP as with DCP alone indicating that in the absence of a free radical acceptor, the macro-alkyl PP free radicals disproportionate (Scheme 4.3). When SA is melt processed in unstabilised PP(HF22) in the absence of DCP (Figure 4.34), the degradation (as opposed to cross-linking for MA, Figure 4.29) is due to the inability of SA to react with the low concentration of macro-alkyl free radicals originating from mechanochemical shearing and the presence of small amounts of oxygen causing hydroperoxide formation<sup>(104-108)</sup>; thus disproportionation of the macro-alkyl PP free radicals occurs<sup>(199,200)</sup> (Scheme 4.3). Because SA is excluded from free radical reactions due to its saturation, it is not therefore surprising to find that SA does not chemically bind to PP(HF22) even in the presence of DCP (Figure 4.35) and because of this, SA is totally ineffective in enhancing the mechanical properties of PP(HF22) composites (Figure 4.26).



%MA	%DCP	%LRWF	%GF	Charpy Impact Strength $\text{kJm}^{-2}$	Flexural Modulus GPa	Flexural Strength MPa	Yield Strength MPa	Tensile Modulus GPa	%Tensile modulus retention after water immersion ( $70^{\circ}\text{C}$ , 24hrs)
-	-	-	-	44	1.30	27	29	0.7	100
0.5	-	-	-	74	1.41	33	30	0.7	100
1.0	-	-	-	60	1.45	33	30	0.7	100
2.0	-	-	-	92	1.62	33	30	0.7	100
5.0	-	-	-	55	1.73	34	33	0.7	100
-	0.05	-	-	46	1.69	34	32	0.7	100
-	0.1	-	-	40	1.71	34	32	0.7	100
-	0.2	-	-	35	1.70	35	31	0.7	100
-	0.3	-	-	38	1.71	35	31	0.7	100
1.0	0.05	-	-	83	1.70	31	30	0.7	100
1.0	0.1	-	-	70	1.68	32	31	0.7	100
1.0	0.2	-	-	46	1.70	35	32	0.7	100
1.0	0.3	-	-	50	1.70	34	32	0.7	100
0.5	-	30	-	85	5.30	55	37	1.8	92
1.0	-	30	-	81	5.92	50	38	1.7	98
2.0	-	30	-	66	5.60	49	36	1.5	96
5.0	-	30	-	83	5.58	49	38	1.6	100
0.5	-	-	30	97	5.50	48	44	1.9	100
1.0	-	-	30	97	5.92	48	44	2.1	85

Table 4.1 (Part I) Mechanical properties of maleic anhydride(MA) and di-cumyl peroxide (DCP) modified stabilised PP(HWM25) with and without long Rockwool fibre(LRWF) and glass fibre(GF), both A-1100 coupled,30% loading. HW60/GR30 (commercially 30%GF coupled PP) is used as a control.

%MA	%DCP	%LRWF	%GF	Charpy Impact Strength $\text{kJm}^{-2}$	Flexural Modulus GPa	Flexural Strength MPa	Yield Strength MPa	Tensile Modulus GPa	%Tensile modulus retention after water immersion ( $70^{\circ}\text{C}, 24\text{hrs}$ )
2.0	-	-	30	111	6.62	48	46	2.0	88
5.0	-	-	30	113	7.68	55	48	2.0	80
1.0	0.05	30	-	64	5.23	53	43	1.6	97
1.0	0.1	30	-	81	5.68	58	49	1.8	97
1.0	0.2	30	-	76	5.28	57	47	1.7	100
1.0	0.3	30	-	75	5.54	64	48	1.8	96
1.0	0.05	-	30	87	5.95	62	57	1.8	94
1.0	0.1	-	30	95	6.41	76	68	2.5	97
1.0	0.2	-	30	155	6.68	92	80	2.7	96
1.0	0.3	-	30	145	6.43	88	75	2.5	95
-	0.05	30	-	78	6.29	62	50	1.7	94
-	0.1	30	-	80	6.10	66	54	1.7	98
-	0.2	30	-	80	5.90	69	54	1.8	96
-	0.3	30	-	69	5.95	61	52	2.0	94
-	0.05	-	30	83	6.22	44	34	1.9	96
-	0.1	-	30	86	6.23	43	33	2.1	90
-	0.2	-	30	82	6.23	43	35	2.1	92
-	0.3	-	30	78	6.34	42	34	2.2	93
HW60/GR30				158	6.50	94	77	3.0	100

Table 4.1 (Part II) Mechanical properties of maleic anhydride(MA) and di-cumyl peroxide

(DCP) modified stabilised PP(HWM25) containing long Rockwool fibre

(LRWF) and glass fibre(GF) both A-1100 coupled, 30% loading. HW60/GR30

(commercially 30%GF coupled PP) is used as a control.

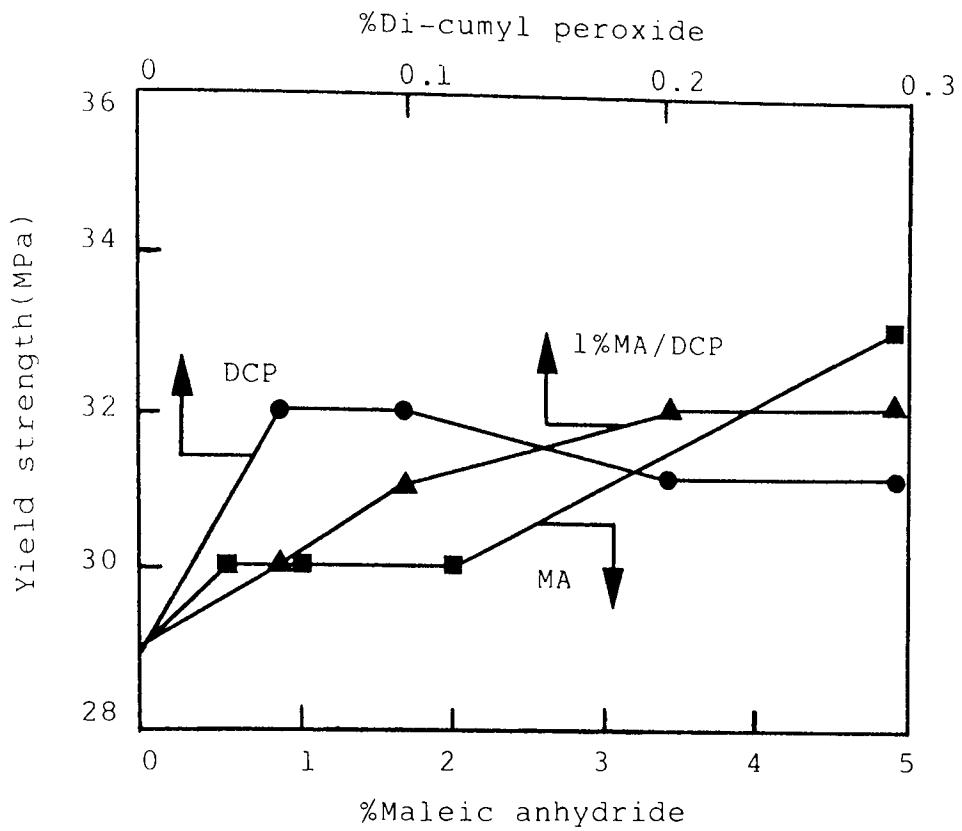


Figure 4.1 Effect of maleic anhydride(MA) and di-cumyl peroxide(DCP) on the yield strength of PP(HWM25). See Table 4.1.

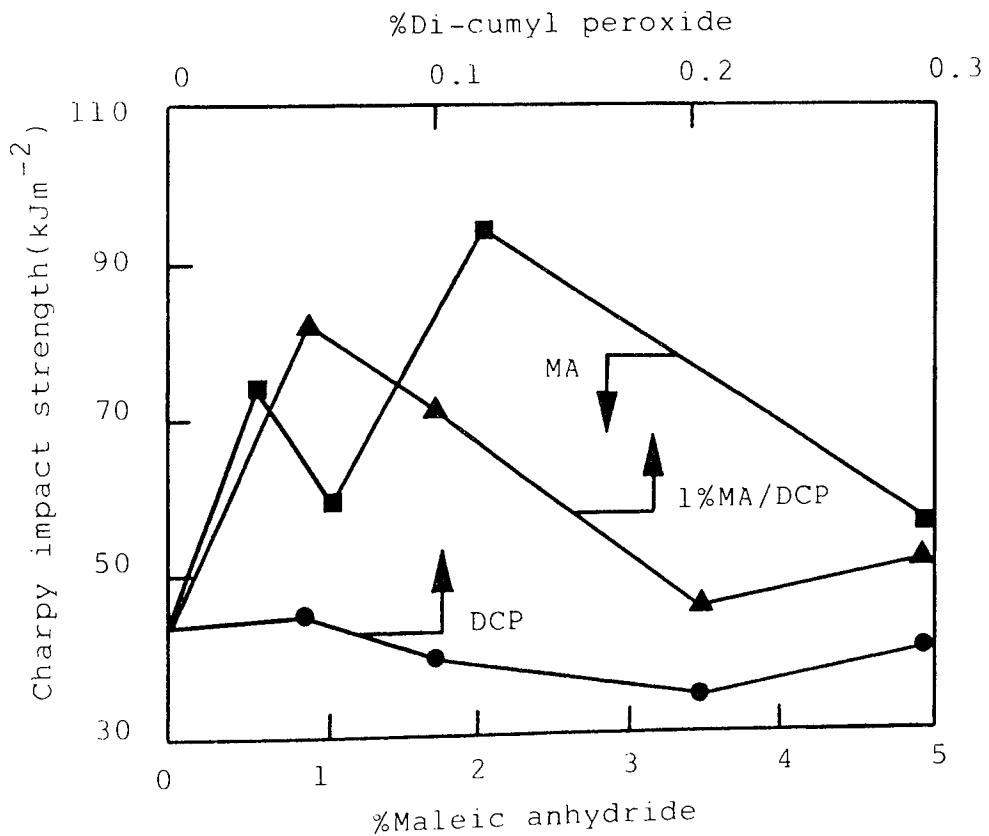


Figure 4.2 Effect of maleic anhydride(MA) and di-cumyl peroxide(DCP) on the Charpy impact strength (notched, 0.2mm) of PP(HWM25). See Table 4.1.

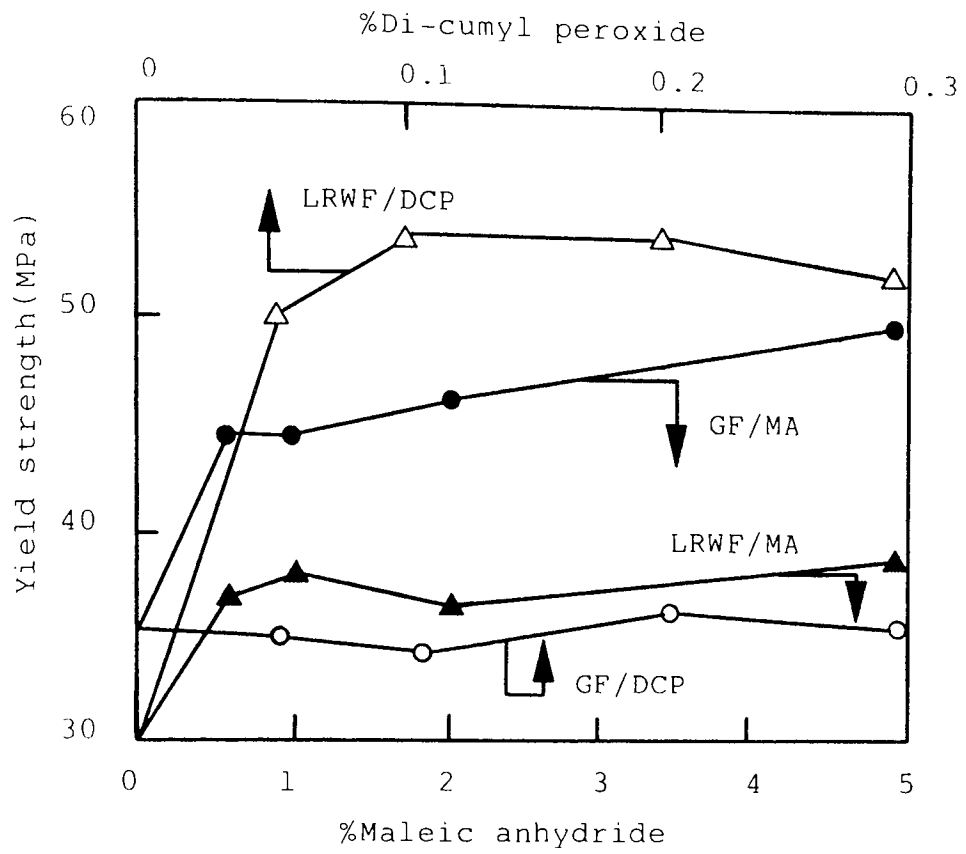


Figure 4.3 Effect of maleic anhydride(MA) and di-cumyl peroxide(DCP) on the yield strength of PP(HWM25) containing 30% glass fibre(GF) and 30% long Rockwool fibre(LRWF). See Table 4.1.

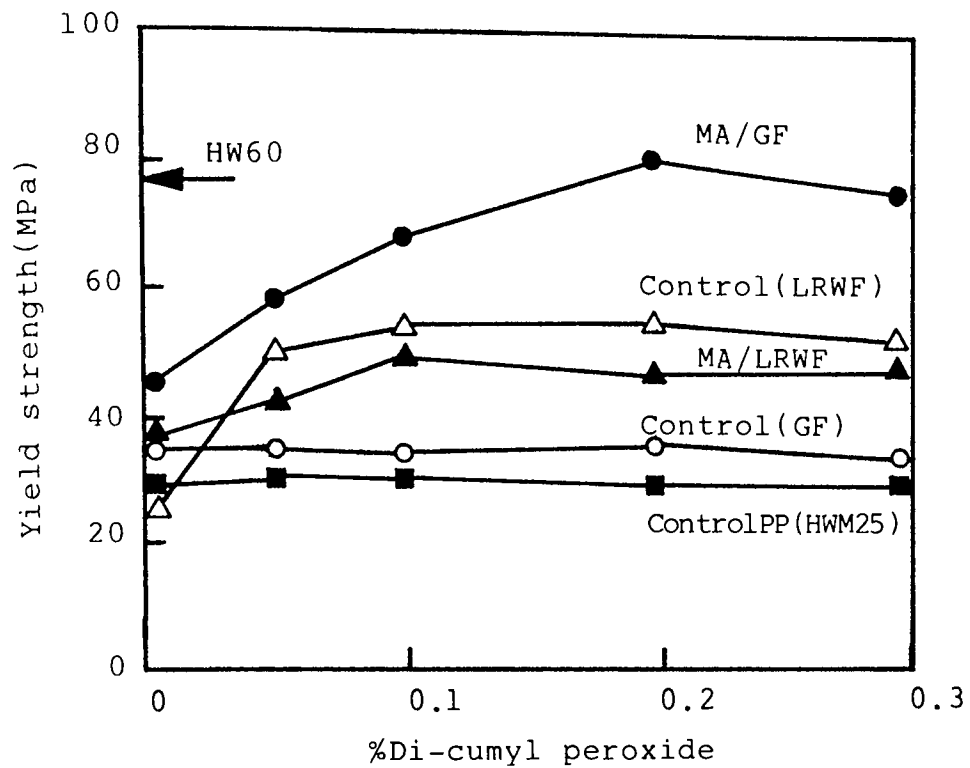


Figure 4.4 Effect of 1% maleic anhydride(MA) on the yield strength of di-cumyl peroxide modified PP(HWM25) containing 30% glass fibre(GF) and 30% long Rockwool fibre(LRWF). PP controls are shown without MA and with or without 30% fibre. See Table 4.1.

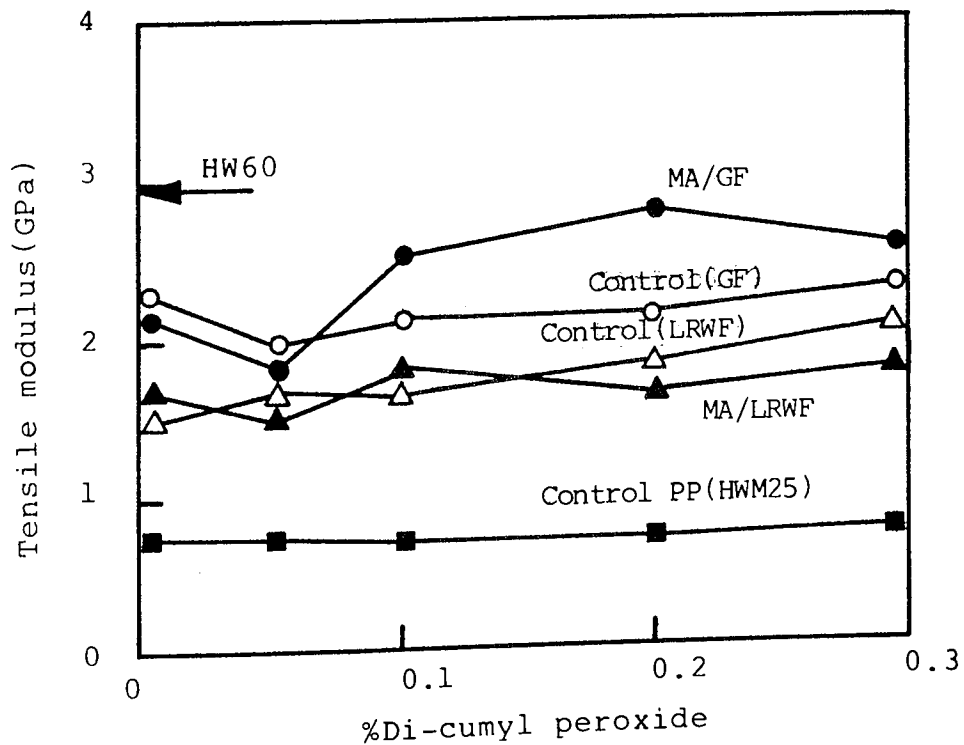


Figure 4.5 Effect of 1% maleic anhydride(MA) on the tensile modulus of di-cumyl peroxide modified PP(HWM25) containing 30% glass fibre(GF) and 30% long Rockwool fibre(LRWF). PP controls are shown without MA and with or without 30% fibre. See Table 4.1.

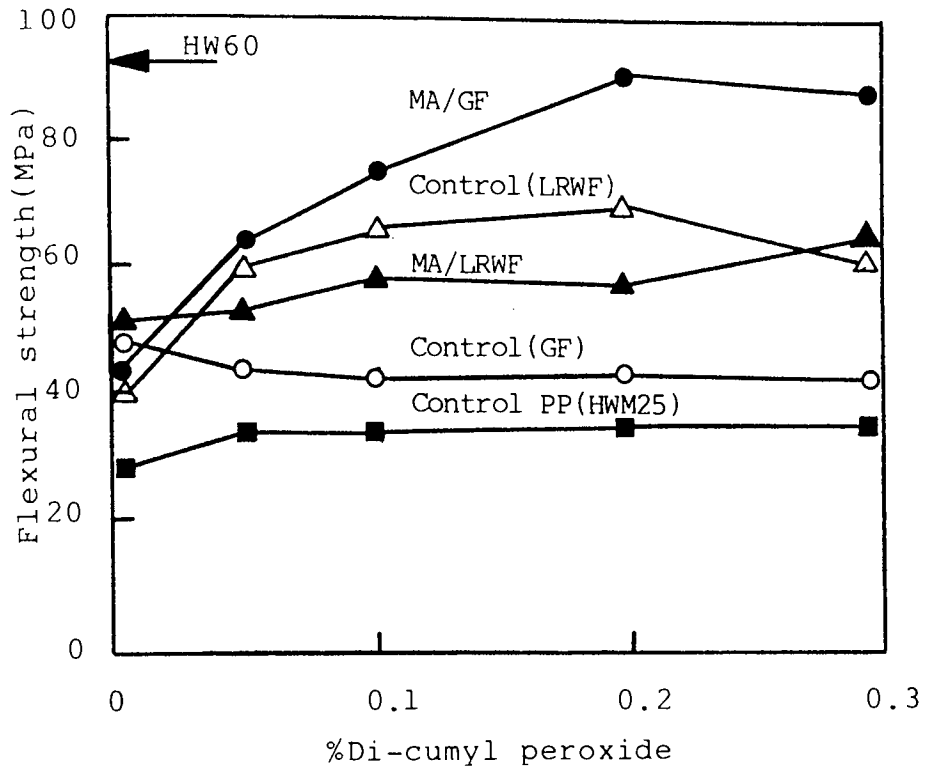


Figure 4.6 Effect of 1% maleic anhydride on the flexural strength of di-cumyl peroxide modified PP(HWM25) containing 30% glass fibre (GF) and 30% long Rockwool fibre (LRWF). PP controls are shown without MA and with or without 30% fibre. See Table 4.1.

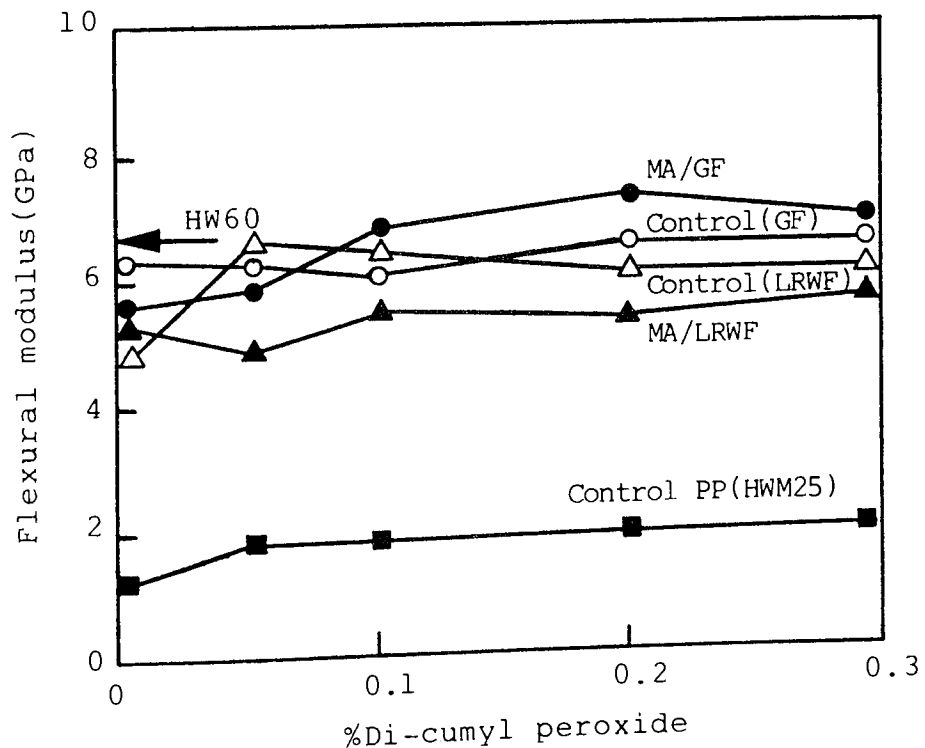


Figure 4.7 Effect of 1% maleic anhydride on the flexural modulus of di-cumyl peroxide modified PP(HWM25) containing 30% glass fibre (GF) and 30% long Rockwool fibre (LRWF). PP controls are shown without MA and with or without 30% fibre. See Table 4.1.

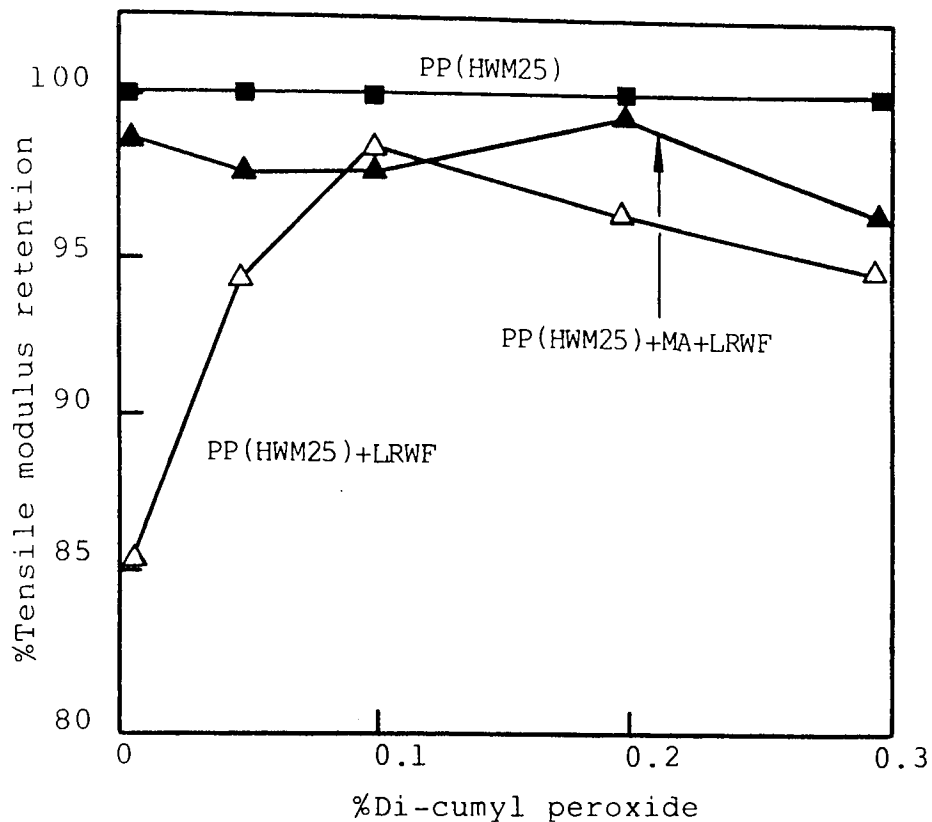


Figure 4.8A Effect of 1% maleic anhydride(MA) on the Tensile modulus retention(after 24hrs water immersion at 70°C)of di-cumyl peroxide modified PP(HWM25) containing 30% long Rockwool fibre(LRWF). PP controls containing no MA or fibre and that without MA but with 30%LRWF are also shown. See Table 4.1.

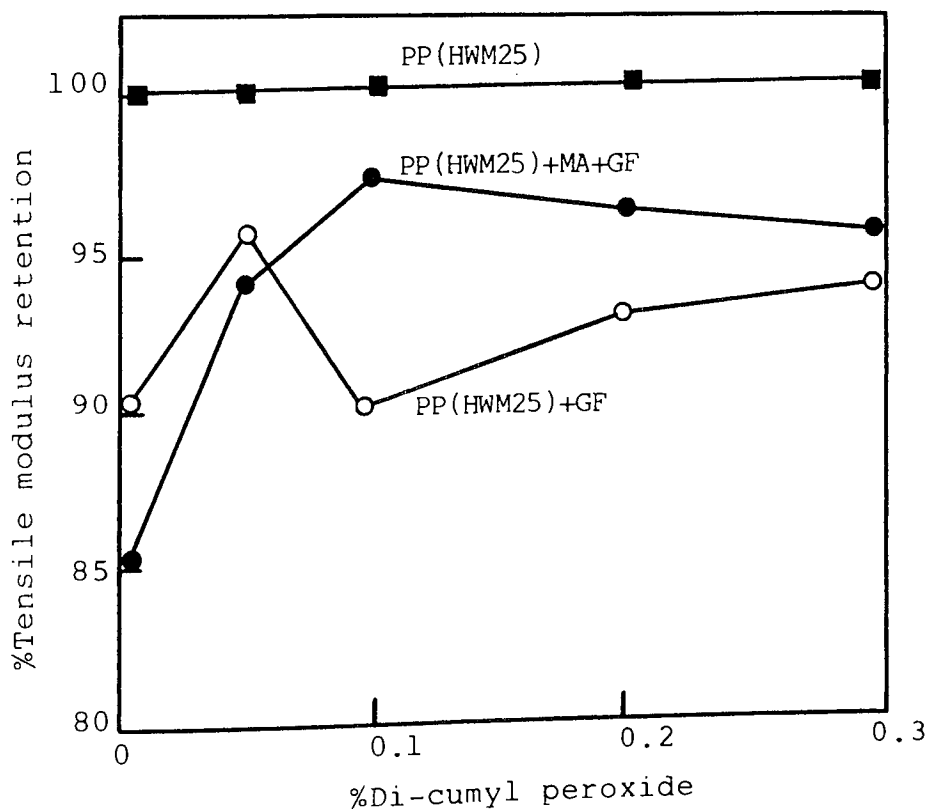


Figure 4.8B Effect of 1% maleic anhydride(MA) on the Tensile modulus retention(after 24hrs water immersion at 70°C)of DCP modified PP(HWM25) containing 30% GF. PP controls containing no MA and no fibre and that without MA but with 30%GF are also shown.

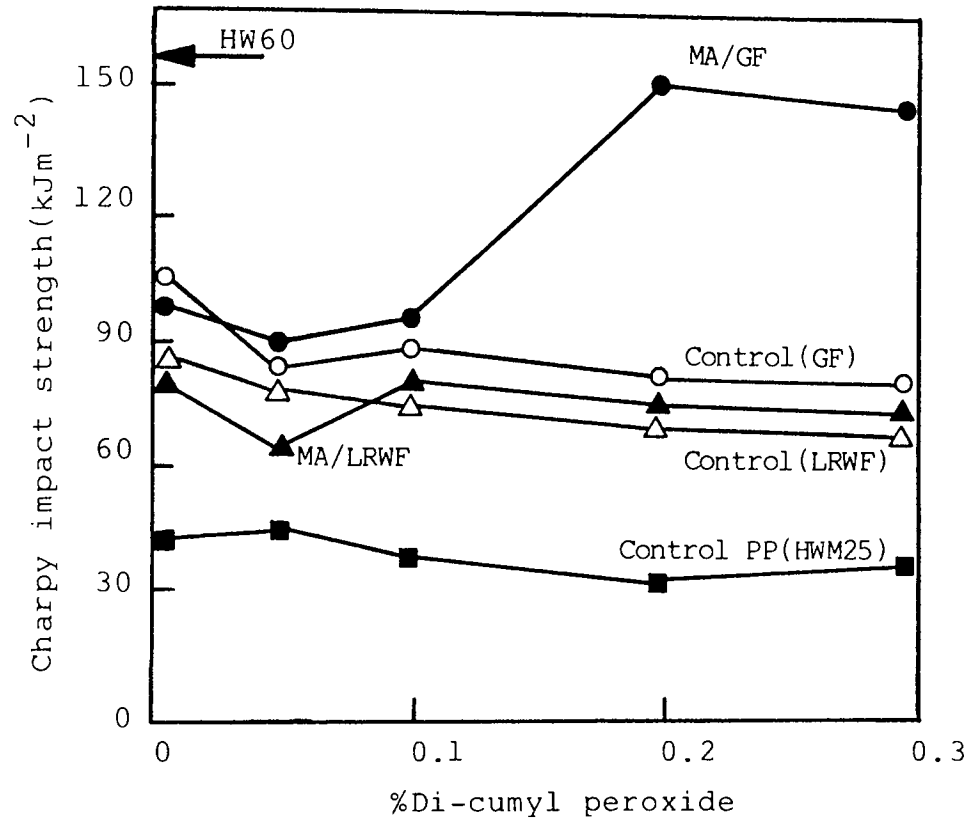


Figure 4.9 Effect of 1% maleic anhydride (MA) on the Charpy impact strength (notched, 0.2mm radius) of di-cumyl peroxide modified PP (HWM25) containing 30% glass fibre (GF) and 30% long Rockwool fibre (LRWF). PP controls are shown without MA and with or without 30% fibre. See Table 4.1.



No.	Composite	Yield strength MPa	Tensile modulus GPa	Flexural strength MPa	Flexural modulus GPa	Charpy impact strength $\text{kJm}^{-2}$
1	HW60/GR30	77 (1.21)	3.0 (0.11)	94 (1.10)	6.50 (0.08)	158 (1.91)
2	30%GF/HWM25	35 (1.29)	2.2 (0.10)	48 (1.06)	6.20 (0.07)	105 (1.32)
3	30%LRWF/HWM25	27 (1.36)	1.5 (0.13)	40 (1.19)	5.00 (0.07)	81 (1.45)
4	1%MA/0.2%DCP 30%GF/HWM25	80 (0.91)	2.7 (0.14)	92 (1.21)	6.68 (0.06)	155 (1.32)
5	0.2%DCP 30%LRWF/HWM25	54 (0.95)	1.8 (0.11)	69 (1.18)	5.90 (0.08)	80 (1.41)

Table 4.2 Mechanical properties with standard deviations (bracketed) of unmodified and modified PP(HWM25) containing 30% fibre to optimum conditions shown. HW60(30%GF commercially coupled PP) is used as a control.

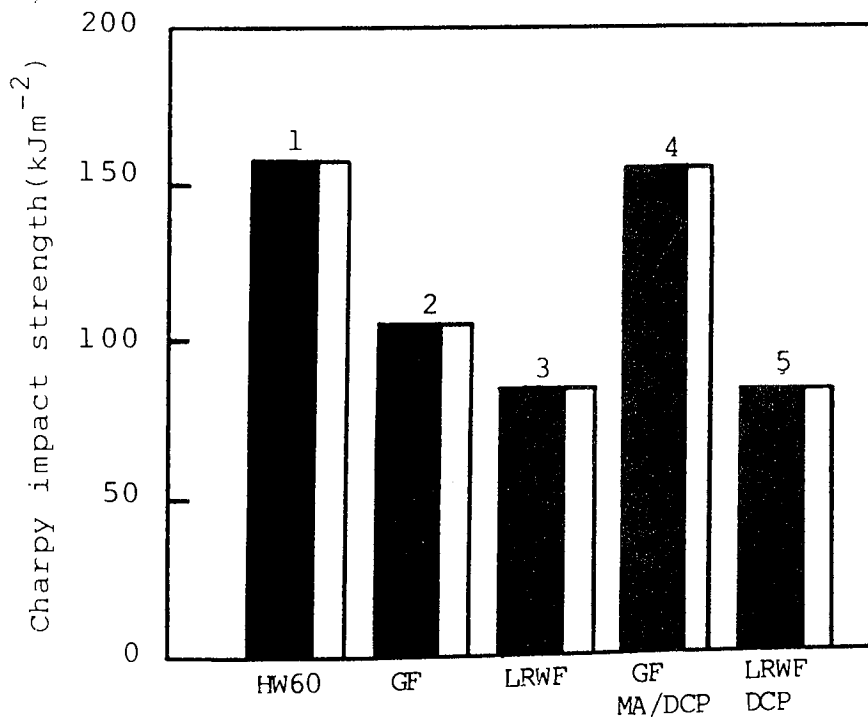


Figure 4.10 Charpy impact strength (notched, 0.2mm radius) of unmodified and modified PP(HWM25) containing 30% fibre. Optimum modification obtained with 1%MA and 0.2%DCP in presence of 30%GF and with only 0.2%DCP (no MA) with 30%LRWF. HW60(30%GF commercially coupled PP) is control. See Table 4.2.

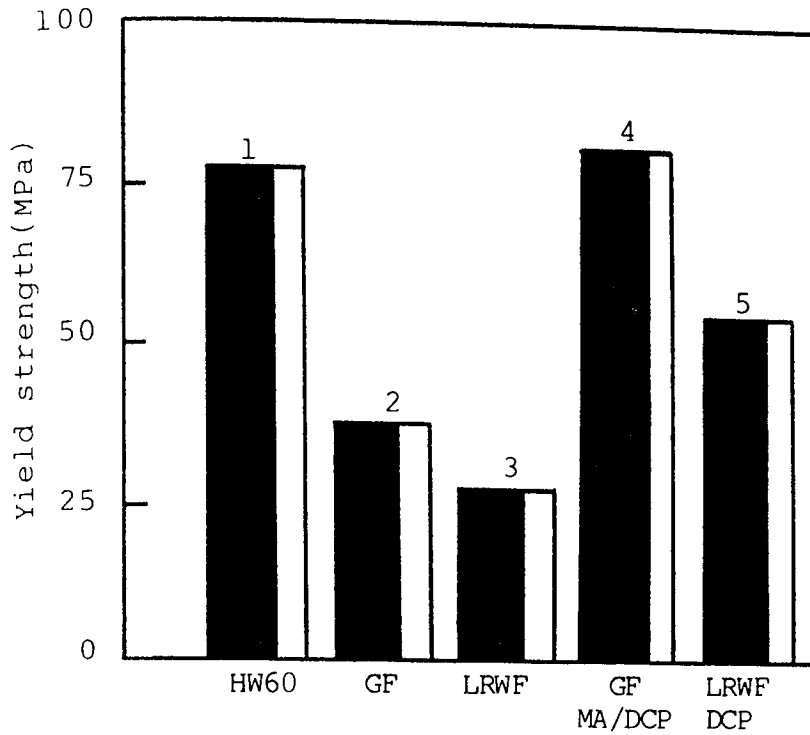


Figure 4.11 Yield strength of unmodified and modified PP (HWM25) containing 30% fibre. Optimum modification obtained with 1%MA and 0.2%DCP in presence of 30%GF and with only 0.2%DCP (no MA) with 30%LRWF. HW60 (30%GF commercially coupled PP) is control. See Table 4.2.

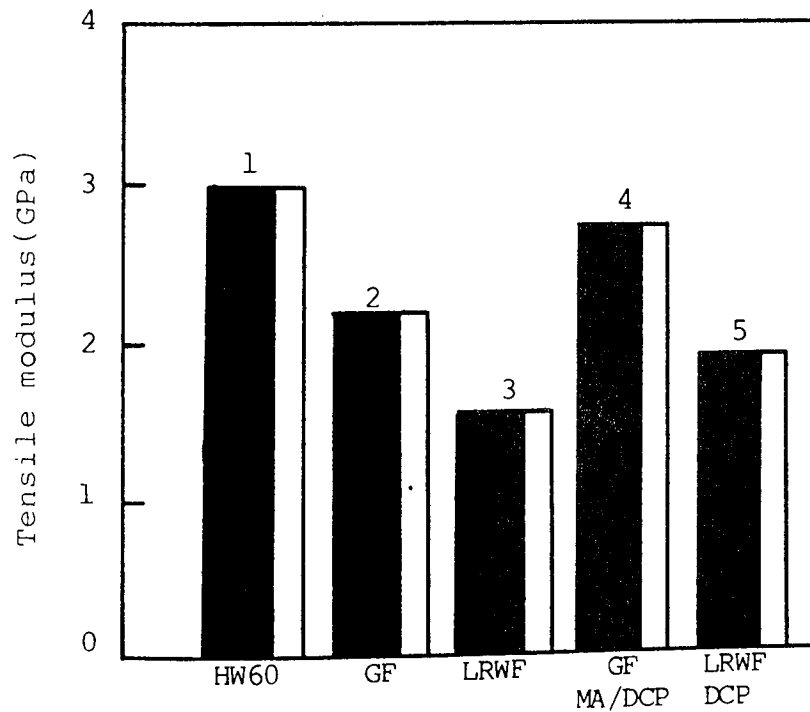


Figure 4.12 Tensile modulus of unmodified and modified PP (HWM25) containing 30% fibre. Optimum modification obtained with 1%MA and 0.2%DCP in presence of 30%GF and with only 0.2%DCP (no MA) with 30%LRWF. HW60 (30%GF commercially coupled PP) is control. See Table 4.2.

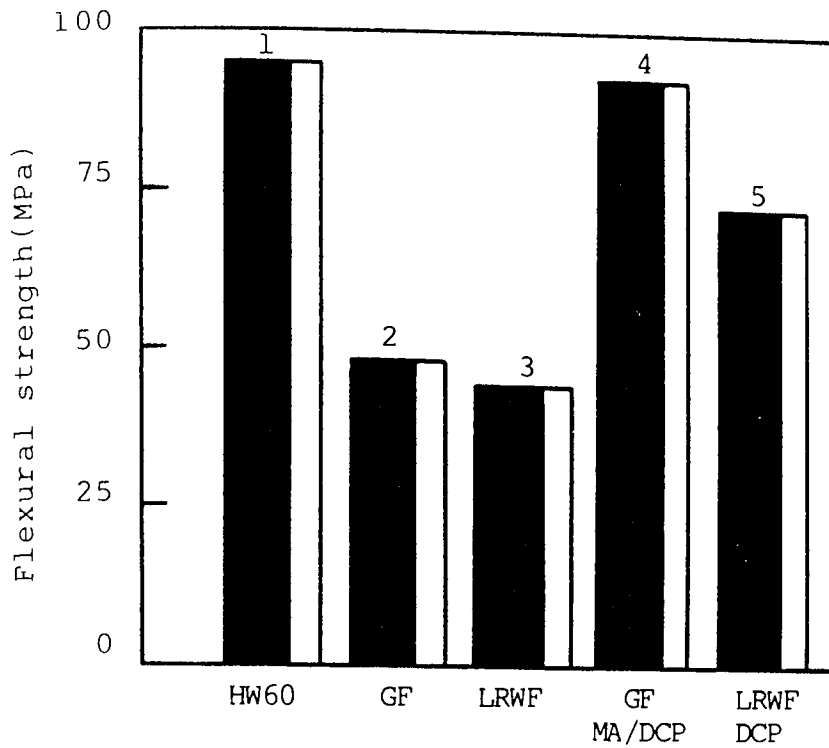


Figure 4.13 Flexural strength of unmodified and modified PP (HWM25) containing 30% fibre. Optimum modification obtained with 1% MA and 0.2% DCP in presence of 30% GF and with only 0.2% DCP (no MA) with 30% LRWF. HW60 (30% GF commercially coupled PP) is control. See Table 4.2.

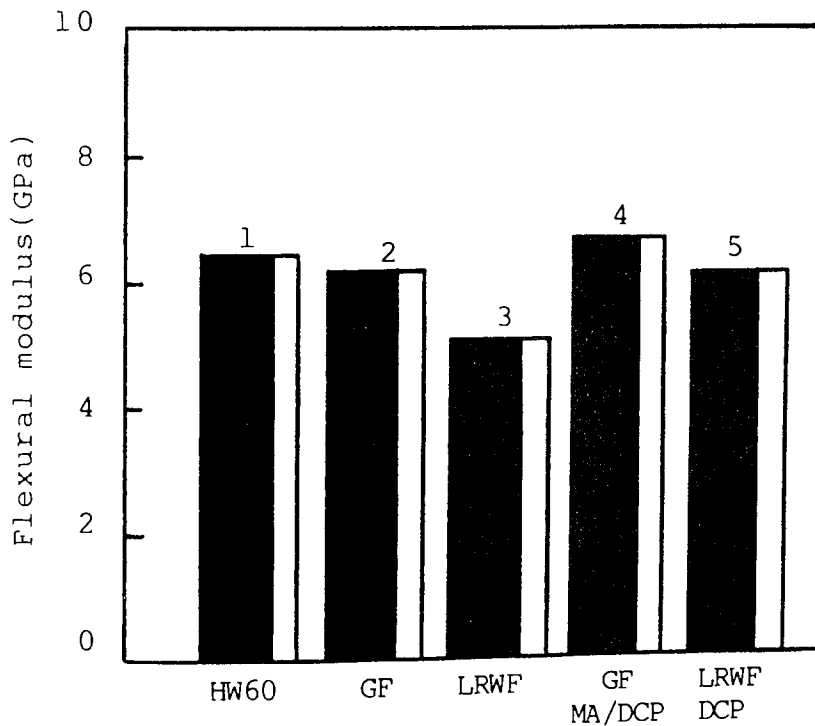


Figure 4.14 Flexural modulus of unmodified and modified PP (HWM25) containing 30% fibre. Optimum modification obtained with 1% MA and 0.2% DCP in presence of 30% GF and with only 0.2% DCP (no MA) with 30% LRWF. HW60 (30% GF commercially coupled PP) is control. See Table 4.2.

%MA	%DCP	%LRWF	%GF	Charpy Impact Strength $\text{kJm}^{-2}$	Flexural Modulus GPa	Flexural Strength MPa	Yield Strength MPa	Tensile Modulus GPa	%Tensile modulus retention after water immersion (70°C, 24hrs)
-	-	-	-	45	1.30	27	29	0.7	100
-	0	30	-	80	5.00	42	32	1.5	85
-	0.1	30	-	67	5.37	58	43	3.2	100
-	0.2	30	-	83	5.50	78	59	3.1	100
-	0.3	30	-	94	5.52	82	60	3.2	100
1	0	30	-	82	5.00	50	38	1.7	99
1	0.1	30	-	80	5.13	52	39	2.0	100
1	0.2	30	-	81	5.21	60	50	2.2	100
1	0.3	30	-	87	5.27	62	54	2.2	100
-	0	-	30	110	6.20	45	39	2.3	90
-	0.1	-	30	112	6.19	46	41	2.2	91
-	0.2	-	30	114	6.23	48	42	2.3	92
-	0.3	-	30	118	6.20	50	41	2.2	91
1	0	-	30	108	6.21	50	44	2.2	90
1	0.1	-	30	280	8.10	125	100	4.2	100
1	0.2	-	30	316	8.32	126	101	4.3	100
1	0.3	-	30	280	8.30	125	100	4.0	100
HW60/GR30				158	6.50	94	77	3.0	100

Table 4.3 Mechanical properties of maleic anhydride(MA) and di-cumyl peroxide(DCP) modified unstabilised PP(HF22) containing long Rockwool fibre(LRWF) and glass fibre(GF), both A-1100 coupled, 30% loading. HW60/GR30 (commercially 30%GF coupled PP) is used as a control.

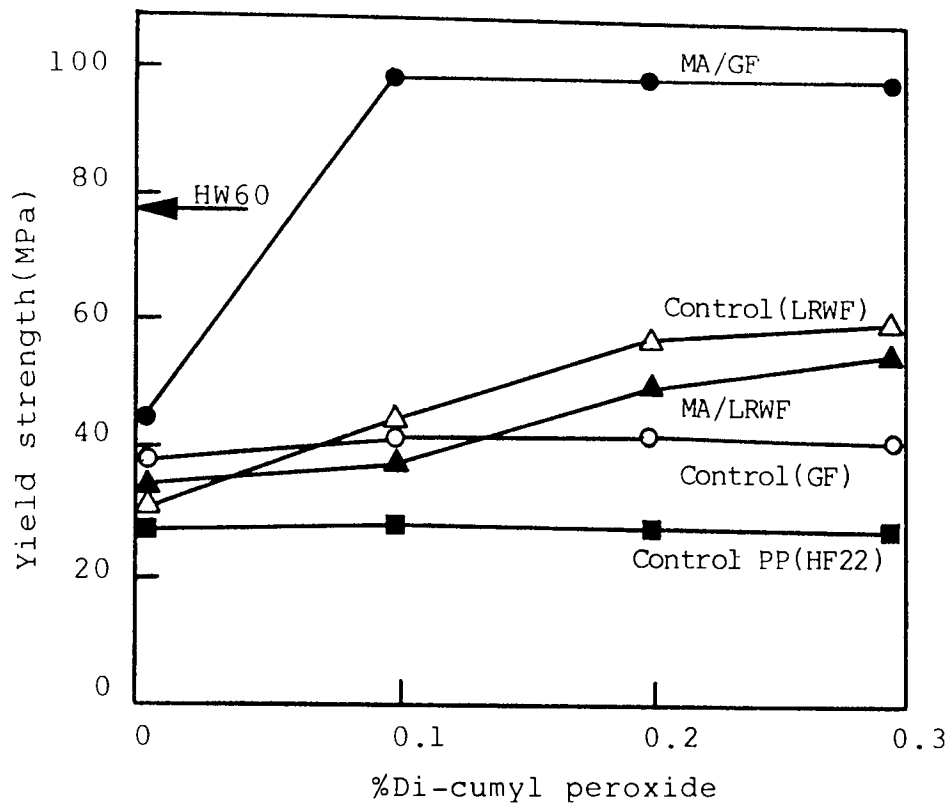


Figure 4.15 Effect of 1% maleic anhydride(MA) on yield strength of di-cumyl peroxide modified PP(HF22) containing 30% glass fibre(GF) and 30% long Rockwool fibre(LRWF).PP controls are shown without MA and with or without 30% fibre. See Table 4.3.

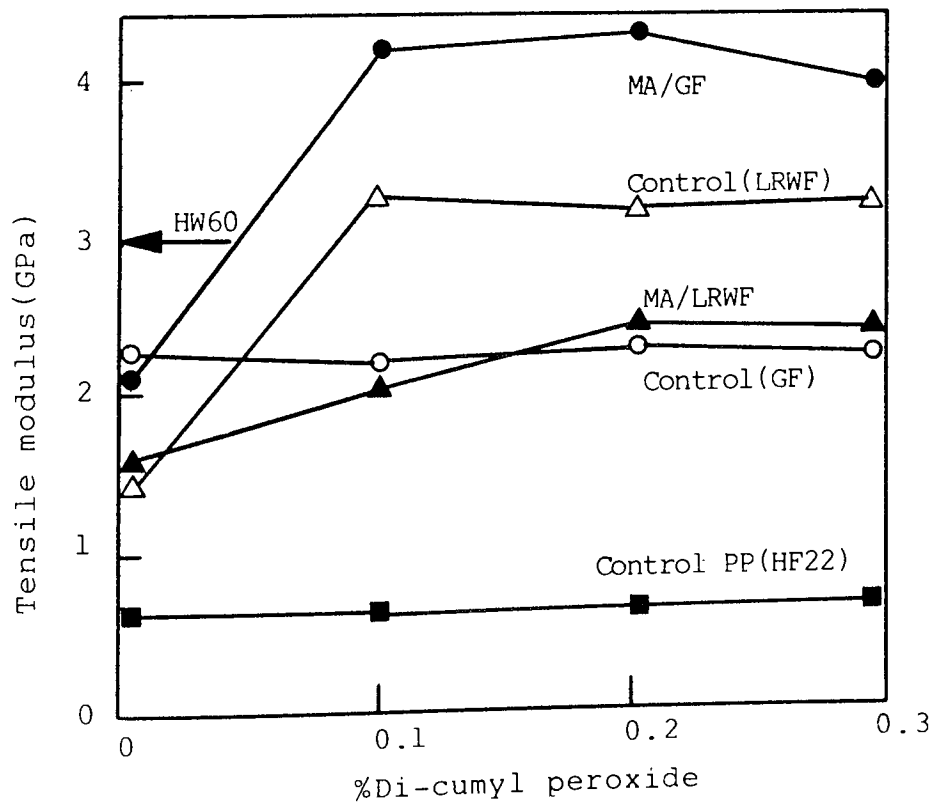


Figure 4.16 Effect of 1% maleic anhydride(MA) on tensile modulus of di-cumyl peroxide modified PP(HF22) containing 30% glass fibre(GF) and 30% long Rockwool fibre(LRWF).PP controls are shown without MA and with or without 30% fibre. See Table 4.3.

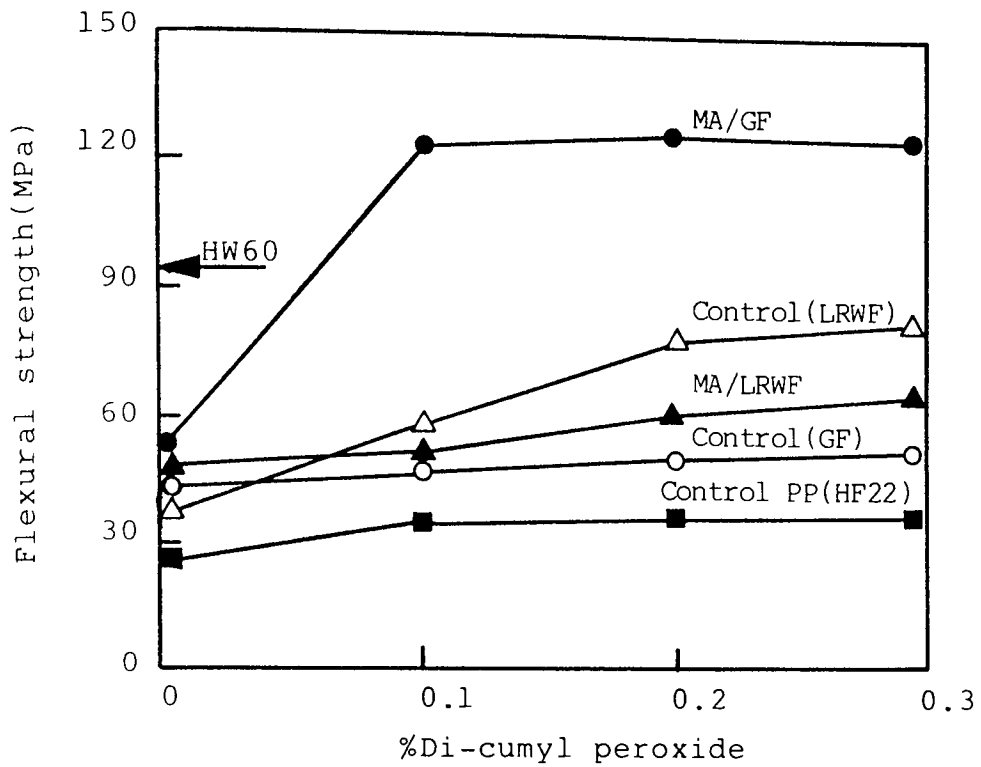


Figure 4.17 Effect of 1% maleic anhydride(MA) on flexural strength of di-cumyl peroxide modified PP(HF22) containing 30% glass fibre(GF) and 30% long Rockwool fibre(LRWF).PP controls are shown without MA and with or without 30% fibre. See Table 4.3.

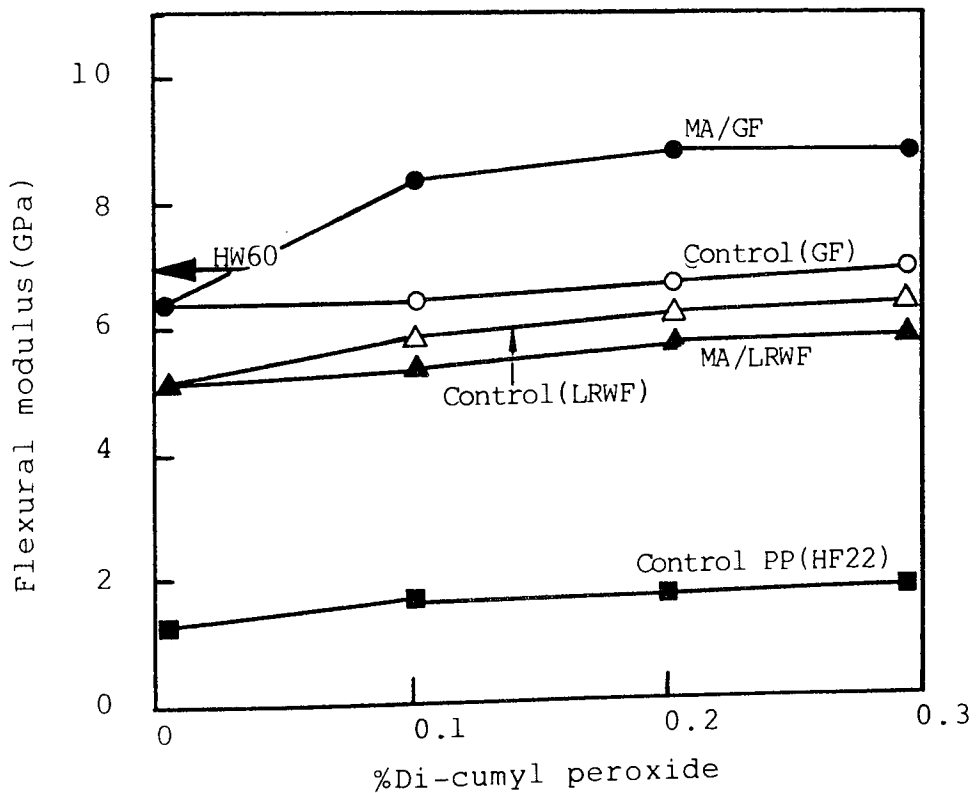


Figure 4.18 Effect of 1% maleic anhydride(MA) on flexural modulus of di-cumyl peroxide modified PP(HF22) containing 30% glass fibre(GF) and 30% long Rockwool fibre(LRWF).PP controls are shown without MA and with or without 30% fibre. See Table 4.3.

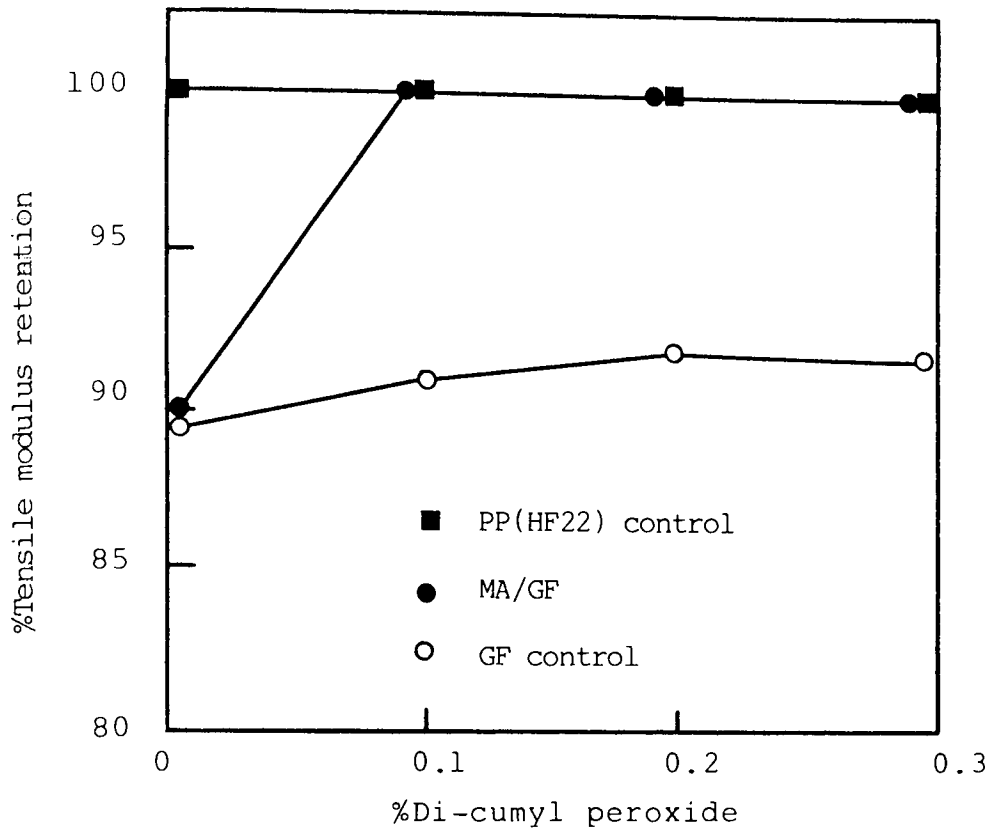


Figure 4.19A Effect of 1% maleic anhydride(MA) on %Tensile modulus retention(after 24hrs water immersion at 70°C)of di-cumyl peroxide modified PP(HF22) containing 30%glass fibre(GF).PP controls are shown without MA and with or without 30%GF.PP containing LRWF is shown in Figure 4.19B. See Table 4.3

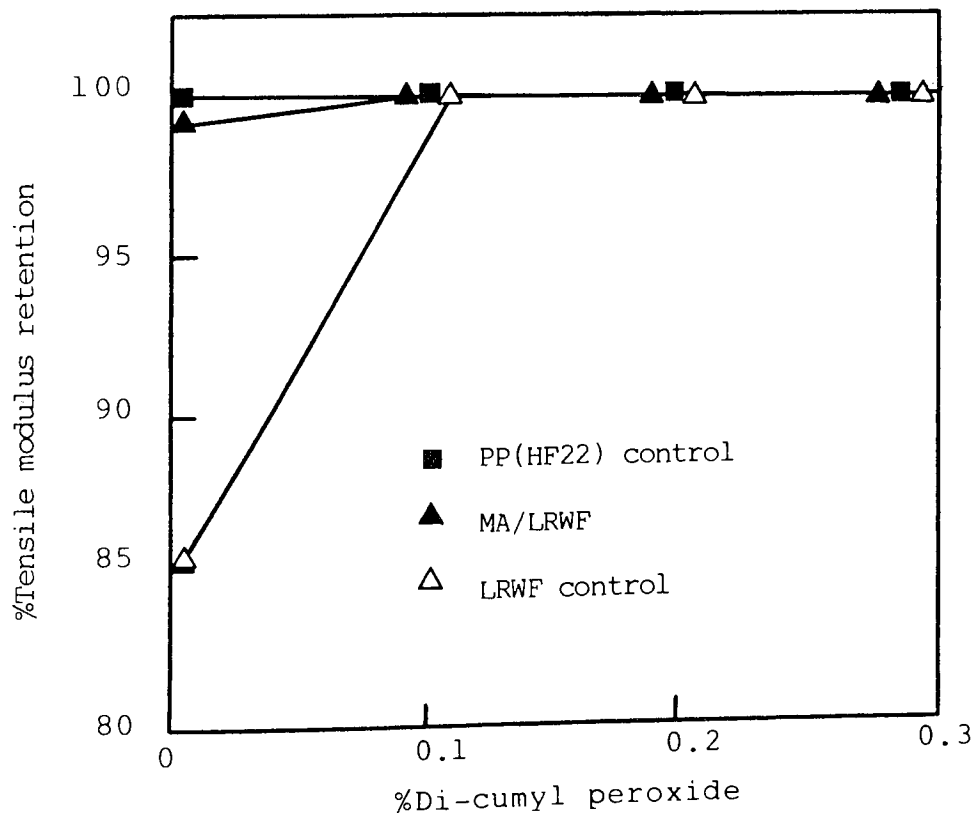


Figure 4.19B Effect of 1% MA on %Tensile modulus retention (after 24hrs water immersion at 70°C)of DCP modified PP(HF22) containing 30%LRWF.PP controls are shown without MA and with or without 30%LRWF. PP containing GF is shown in Fig.4.19A. See Table 4.3.

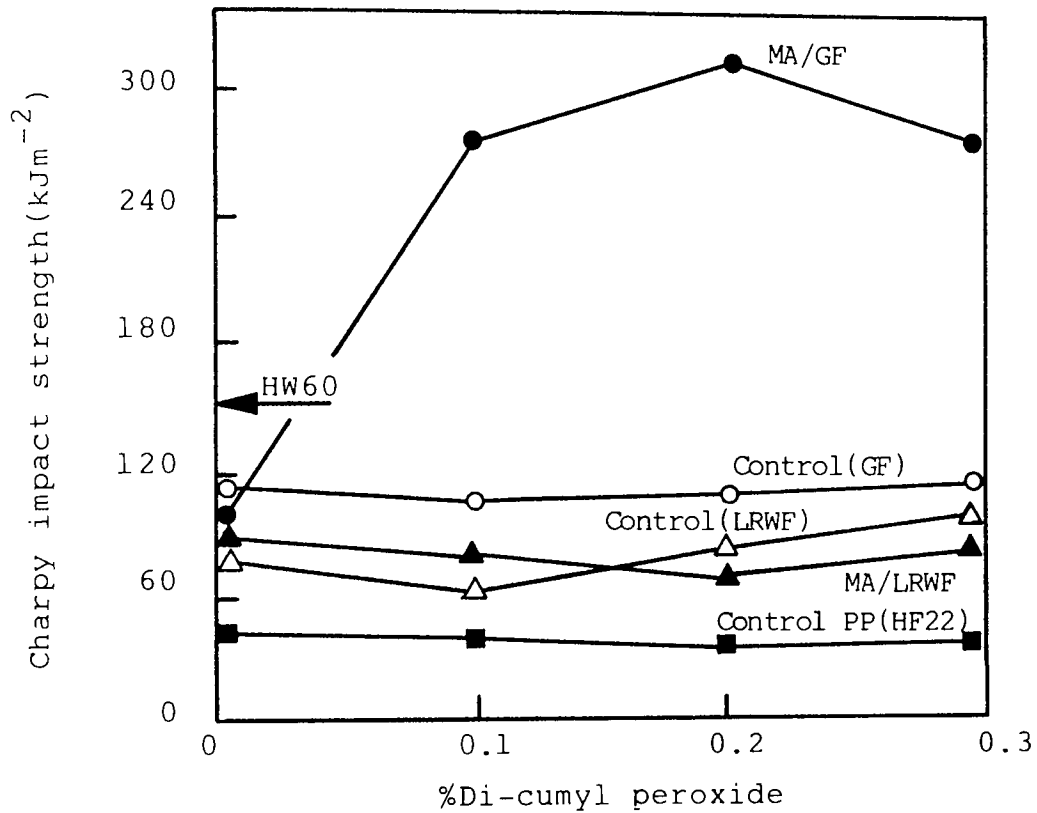


Figure 4.20 Effect of 1% maleic anhydride(MA) on the Charpy impact strength (notched, 0.2mm radius) of di-cumyl peroxide modified PP(HF22) containing 30% glass fibre(GF) and 30% long Rockwool fibre(LRWF). PP controls are shown without MA and with or without 30% fibre. See Table 4.3.



No.	Composite	Yield strength MPa	Tensile modulus GPa	Flexural strength MPa	Flexural modulus GPa	Charpy impact strength $\text{kJm}^{-2}$
1	HW60/GR30	77 (1.21)	3.0 (0.11)	94 (1.10)	6.50 (0.08)	158 (1.91)
2	30%GF/HWM25	35 (1.29)	2.2 (0.10)	48 (1.06)	6.20 (0.07)	105 (1.32)
3	30%LRWF/HWM25	27 (1.36)	1.5 (0.14)	40 (1.19)	5.00 (0.07)	81 (1.45)
4	1%MA/0.2%DCP 30%GF/HWM25	80 (0.91)	2.7 (0.14)	92 (1.21)	6.68 (0.06)	155 (1.32)
5	0.2%DCP 30%LRWF/HWM25	54 (0.95)	1.8 (0.11)	69 (1.18)	5.90 (0.08)	80 (1.41)
6	1%MA/0.2%DCP 30%GF/HF22	101 (1.01)	4.3 (0.12)	126 (1.11)	8.32 (0.06)	316 (1.51)
7	0.3%DCP 30%LRWF/HF22	60 (0.91)	3.2 (0.13)	82 (1.07)	5.52 (0.06)	94 (1.45)

Table 4.4 Mechanical properties with standard deviations (bracketed) of unmodified PP(HWM25) and modified PP(HWM25 and HF22) containing 30% fibre. Optimum modification with GF was obtained with 1% maleic anhydride(MA) and 0.2% di-cumyl peroxide(DCP) and for LRWF with 0.2-0.3%DCP (no MA) only. HW60(30% GF commercially coupled PP) is the control.

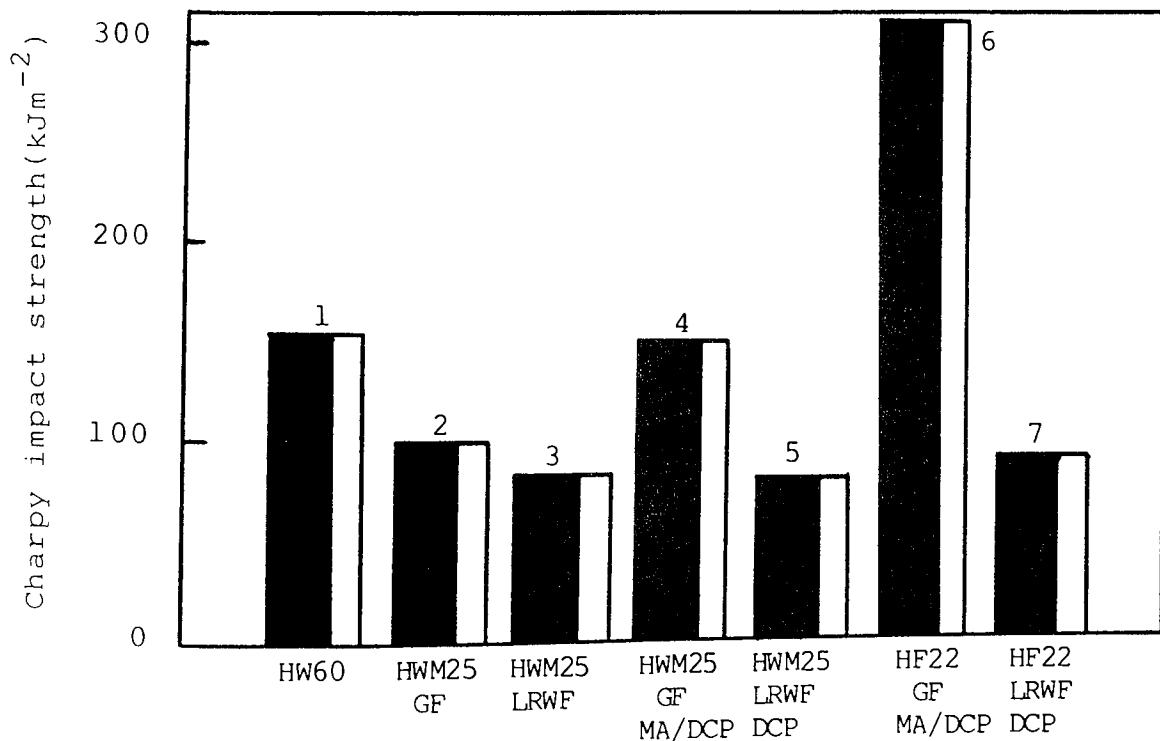


Figure 4.21 Charpy impact strength(notched, 0.2mm radius) of unmodified PP(HWM25) and modified PP(HWM25 and HF22) containing 30% fibre. Optimum modification obtained with 1%MA and 0.2 or 0.3%DCP. HW60 (commercially coupled 30%GF) is the control. See Table 4.4.

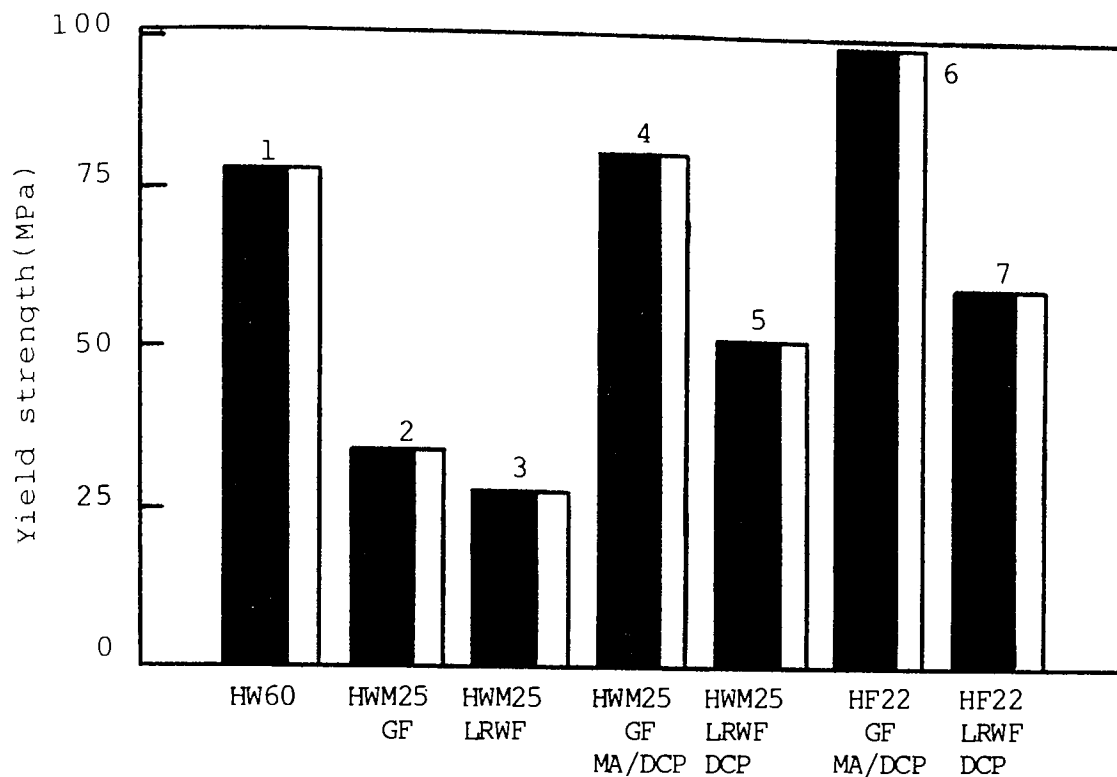


Figure 4.22 Yield strength of unmodified PP(HWM25) and modified PP(HWM25 and HF22) containing 30% fibre. Optimum modification obtained with 1% maleic anhydride(MA) and 0.2 or 0.3% di-cumyl peroxide (DCP). HW60 (commercially coupled 30%GF) is the control. See Table 4.4.

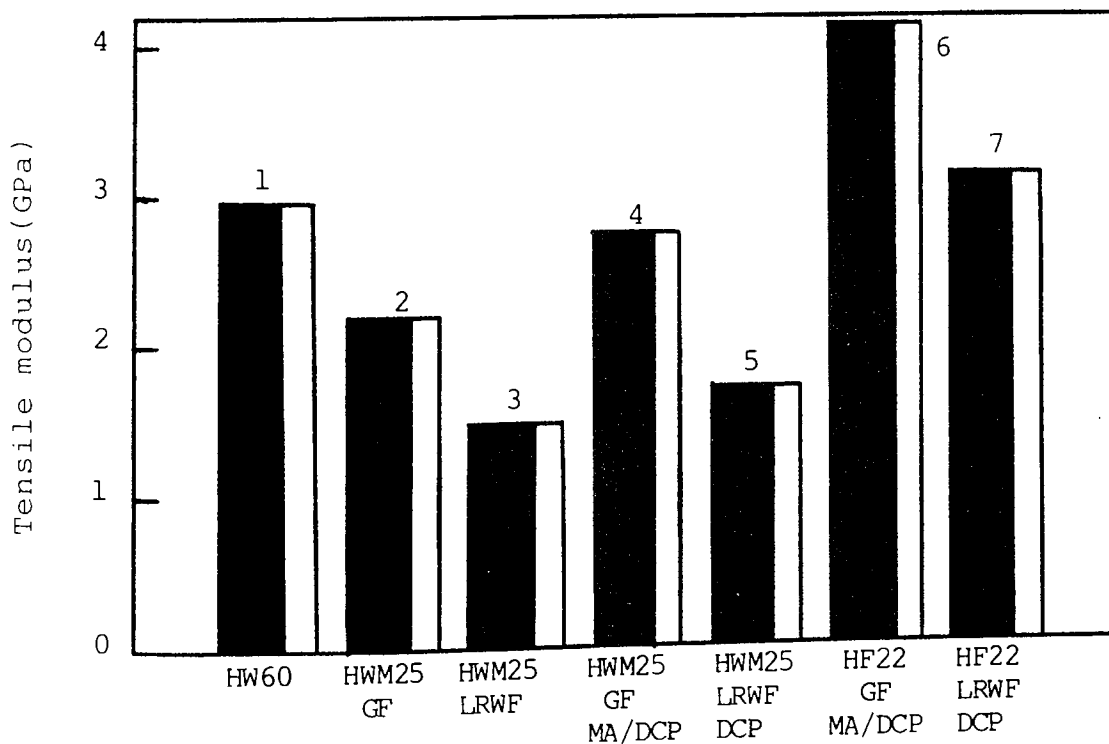


Figure 4.23 Tensile modulus of unmodified PP(HWM25) and modified PP(HWM25 and HF22) containing 30% fibre. Optimum modification obtained with 1% MA and 0.2 or 0.3% DCP. HW60 (commercially coupled 30%GF) is the control. See Table 4.4.

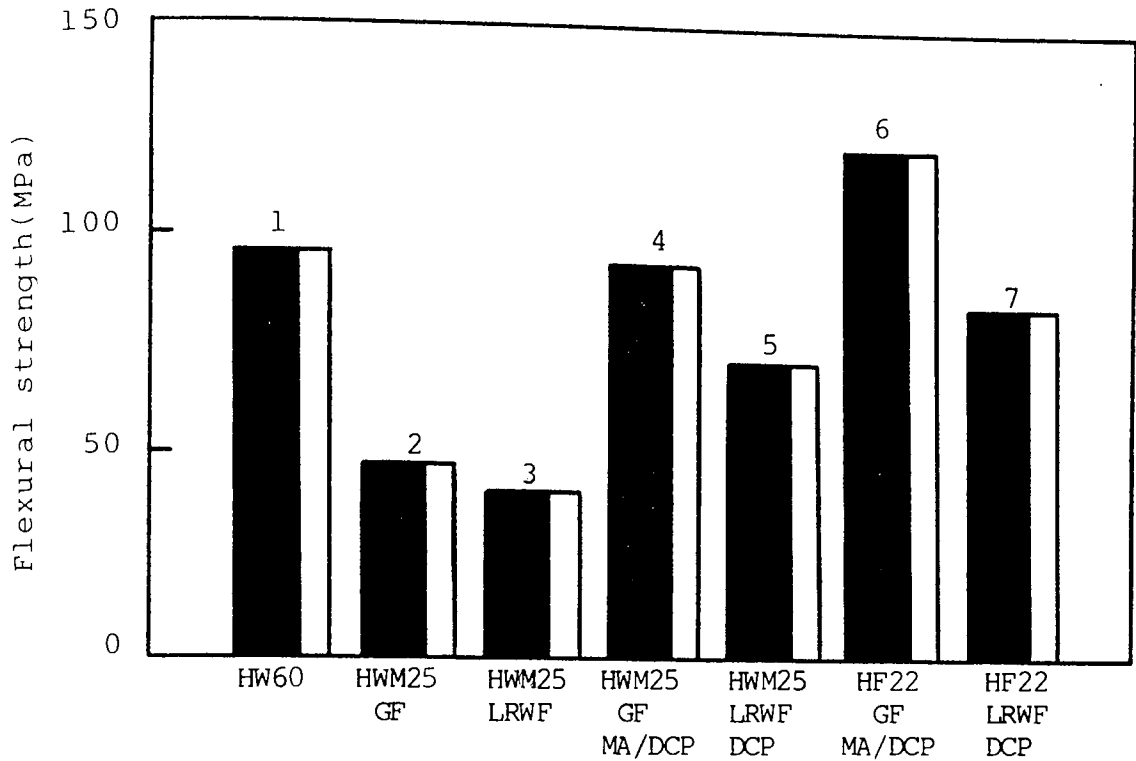


Figure 4.24 Flexural strength of unmodified PP(HWM25) and modified PP(HWM25 and HF22) containing 30% fibre. Optimum modification obtained with 1% maleic anhydride(MA) and 0.2 or 0.3% di-cumyl peroxide (DCP). HW60 (commercially coupled 30%GF) is the control. See Table 4.4.

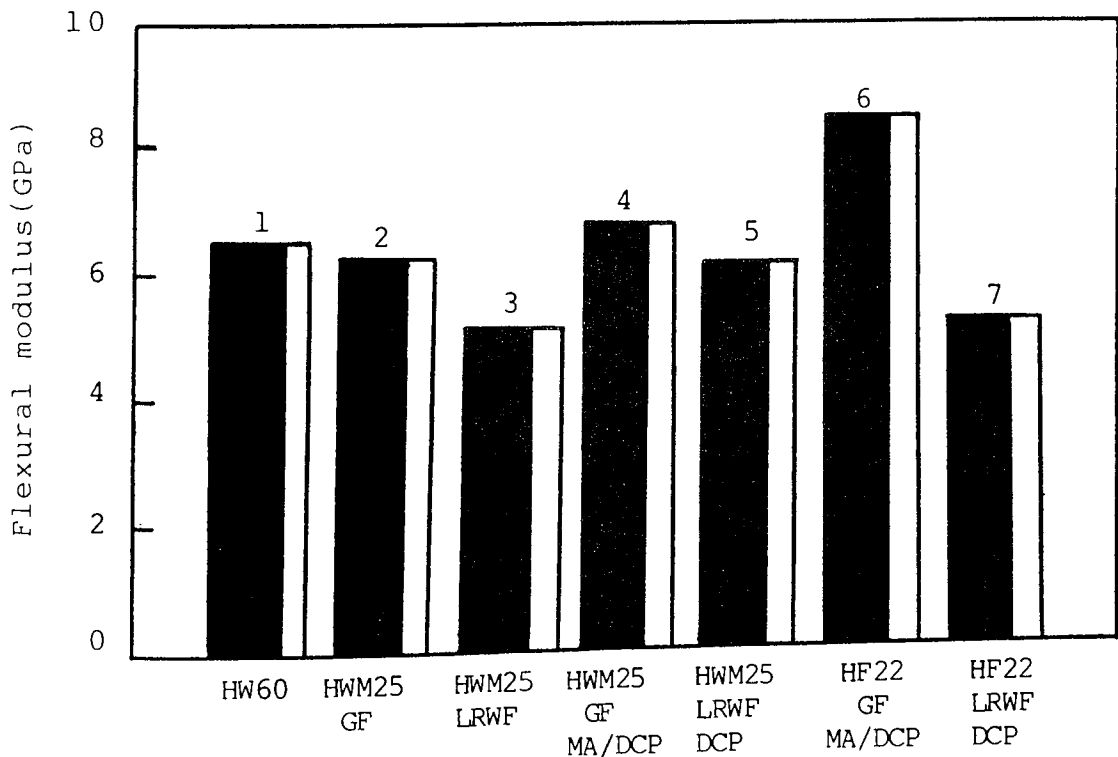


Figure 4.25 Flexural modulus of unmodified PP(HWM25) and modified PP(HWM25 and HF22) containing 30% fibre. Optimum modification obtained with 1% MA and 0.2 or 0.3% DCP. HW60 (commercially coupled 30%GF) is the control. See Table 4.4.

%DCP	Charpy impact strength $\text{kJm}^{-2}$	Flexural modulus GPa	Flexural strength MPa	Yield strength MPa	Tensile modulus GPa
0	110	6.20	45	39	2.3
0.1	113	6.20	45	42	2.2
0.2	115	6.25	47	41	2.2
0.3	115	6.23	50	41	2.3

Table 4.5 Effect of 1% succinic anhydride (SA) on the mechanical properties of di-cumyl peroxide(DCP) modified PP(HF22) containing 30% glass fibre(GF)

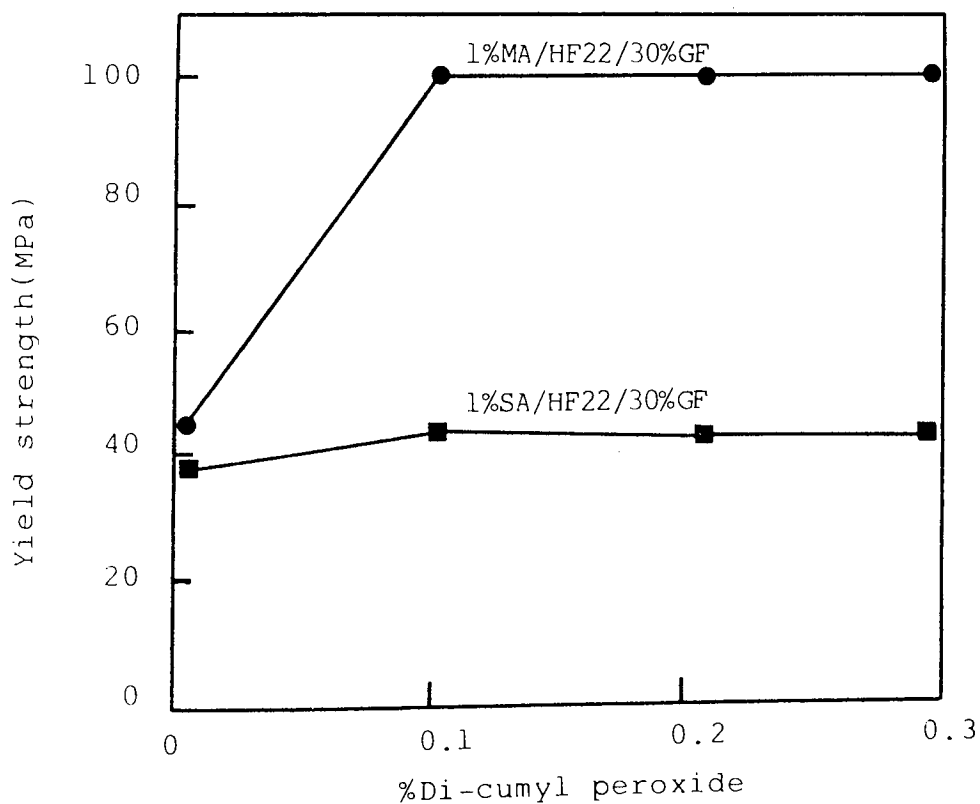


Figure 4.26 Effect of 1% succinic anhydride(SA) and 1%MA on the yield strength of DCP modified PP(HF22) containing 30%GF.

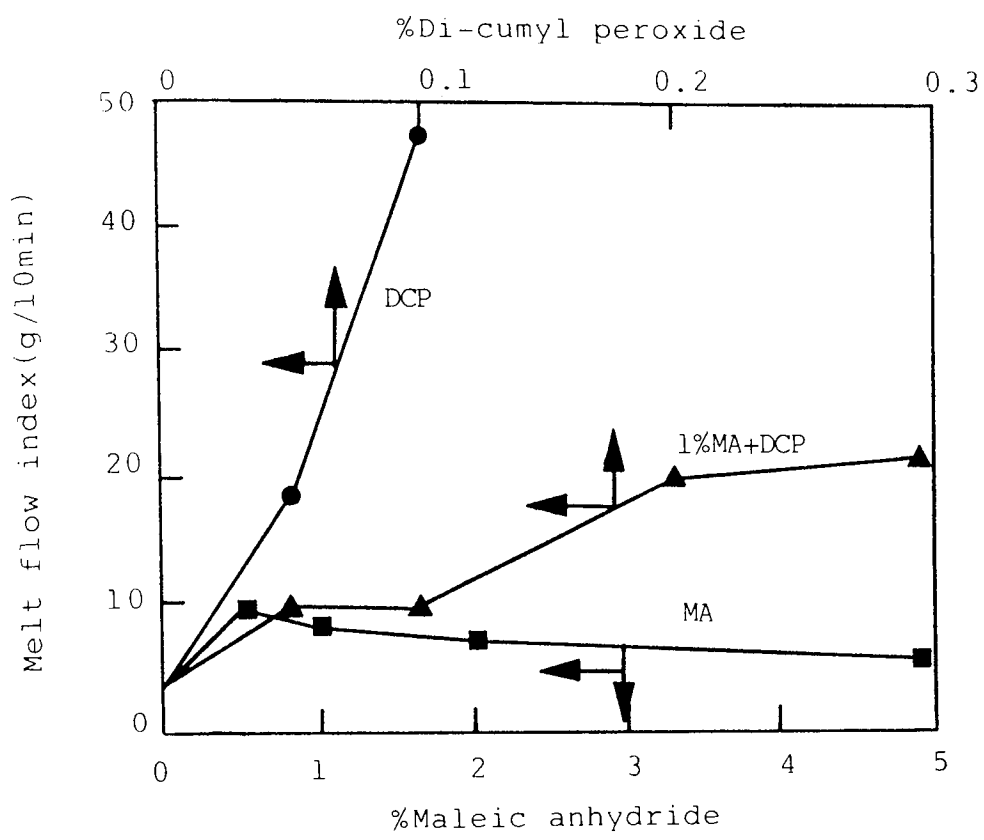


Figure 4.27 Effect of maleic anhydride(MA) and di-cumyl peroxide(DCP) on the melt stability of PP(HWM25) after processing in the Hampden RAPRA torque rheometer(180°C,60rpm,8mins,CM).

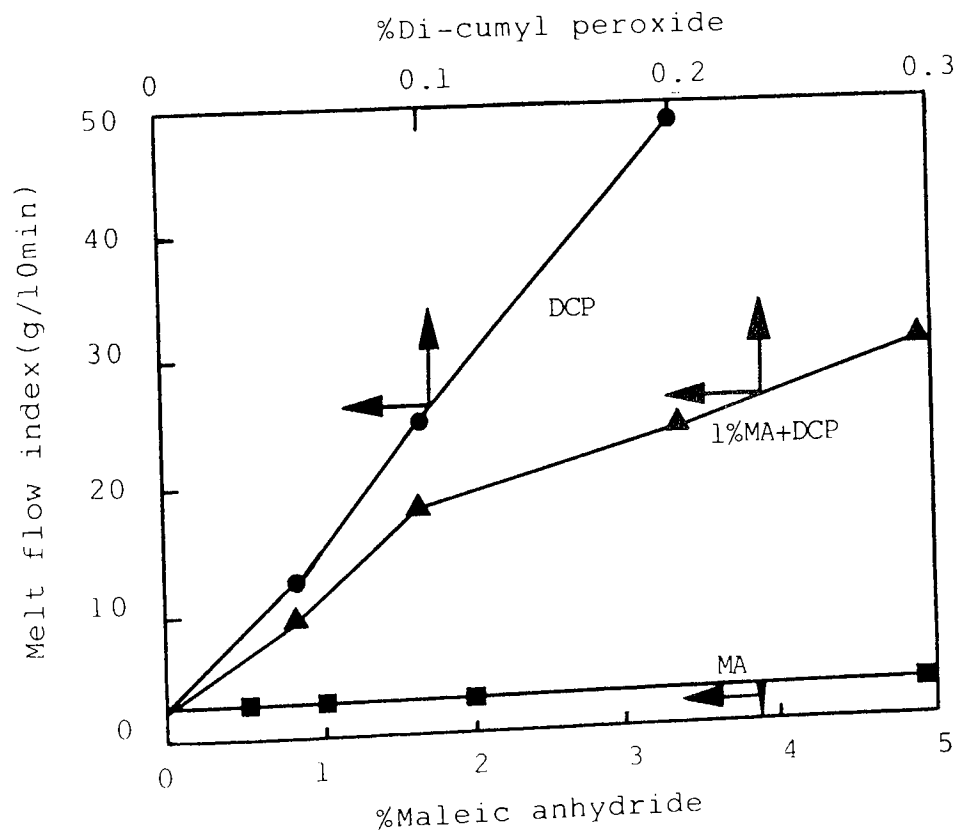


Figure 4.28 Effect of MA and DCP on the melt stability of PP(HF22) with 0.4%Irganox1010 after processing in the Hampden RAPRA torque rheometer(180°C, 60rpm,8mins,CM). 244.

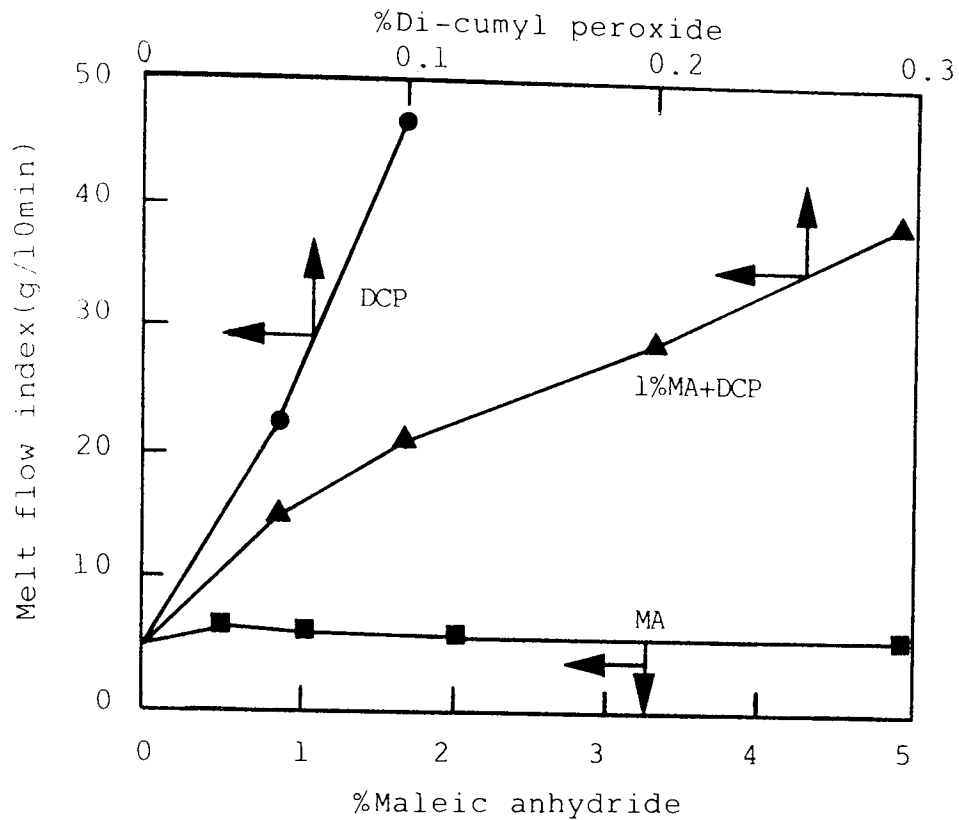


Figure 4.29 Effect of maleic anhydride(MA) and di-cumyl peroxide(DCP)on the melt stability of PP(HF22) after processing in the Hampden RAPRA torque rheometer (180°C,60rpm,8mins,CM).

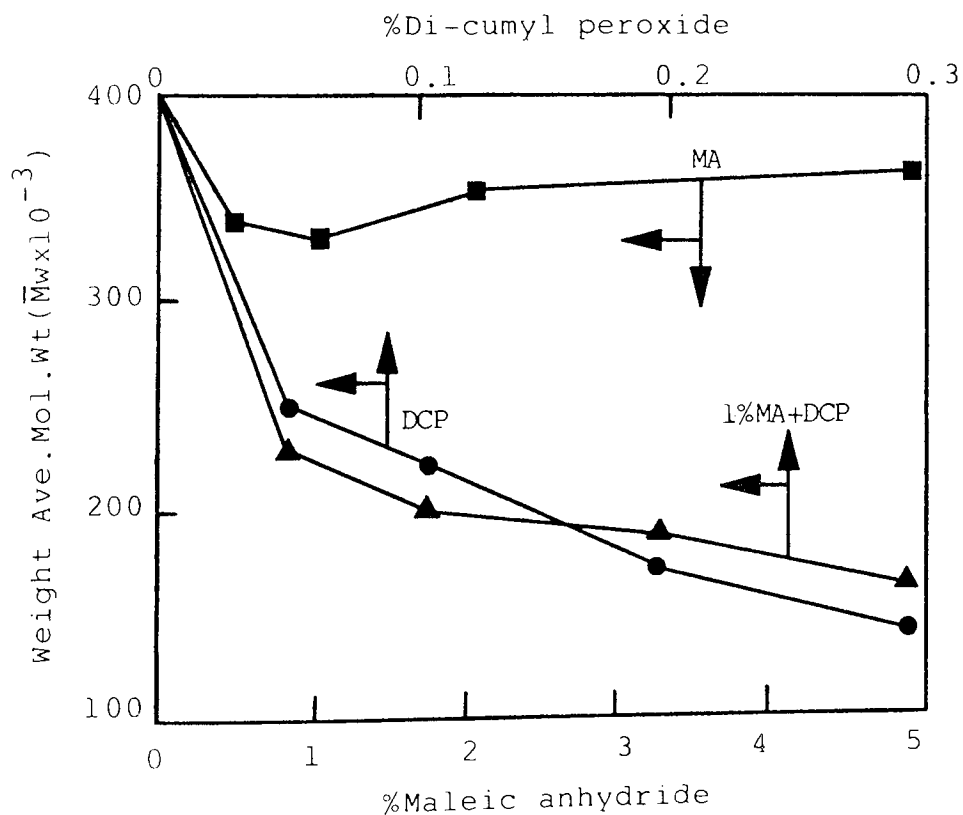


Figure 4.30 Effect of MA and DCP on weight average molecular weight of PP(HF22) after processing in the Hampden RAPRA torque rheometer(180°C,60rpm,8mins,CM).

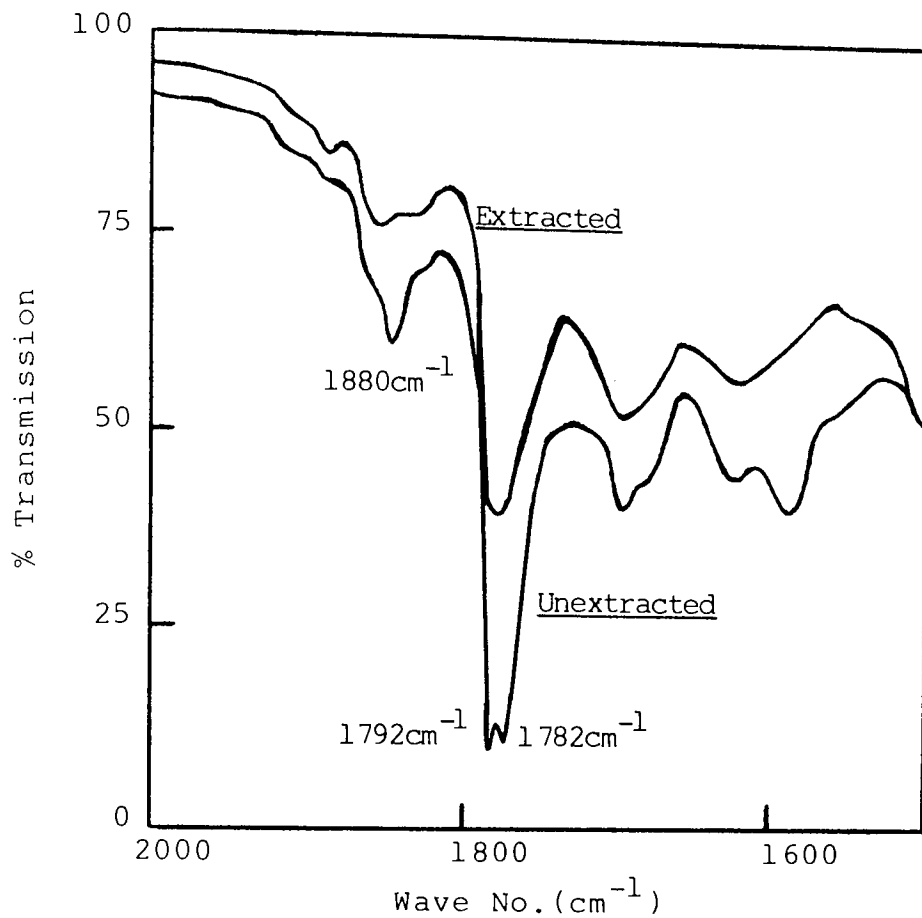


Figure 4.31 Infra-red spectra of PP film(HF22,200 $\mu$ m) processed with 1%MA and 0.2%DCP in the Hampden RAPRA torque rheometer(180 $^{\circ}$ C,60rpm,8mins,CM) before and after Soxhlet extraction (chloroform, acetone,hexane;each 24hrs).

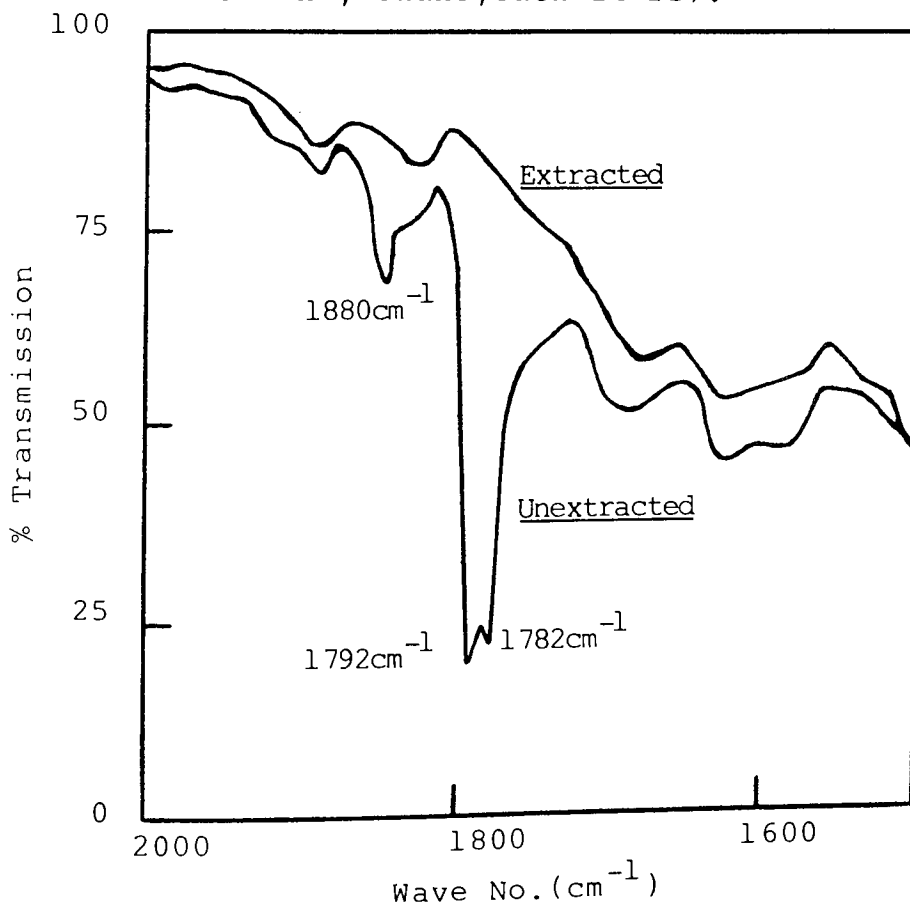


Figure 4.32 Infra-red spectra of PP film(HF22,200 $\mu$ m) processed with 1%MA in the Hampden RAPRA torque rheometer(180 $^{\circ}$ C,60rpm,8mins,CM) before and after Soxhlet extraction (chloroform, acetone,hexane; each 24hrs).

DCP (%)	Bound MA (moles $\times 10^{-4}$ /100g PP)		
	PP(HF22)	PP(HF22)+0.4% Irg 1010	PP(HWM25)
0.00	0.0(0)	0.0(0)	0.0(0)
0.05	1.6(34)	0.7(12)	0.6(10)
0.10	1.8(38)	0.8(15)	0.7(12)
0.20	3.0(55)	1.1(20)	1.2(22)
0.30	2.8(51)	1.3(23)	1.2(22)

Table 4.6 Effect of stabilisers on the di-cumyl peroxide (DCP) catalysed mechano-chemical binding of maleic anhydride(1%MA) to PP(HF22,with and without 0.4% Irganox1010) and commercially stabilised PP(HWM25). Torque rheometer processing conditions (CM,180°C,60rpm,8mins). Numbers in brackets are % binding of MA (based on amount of MA present after melt processing).

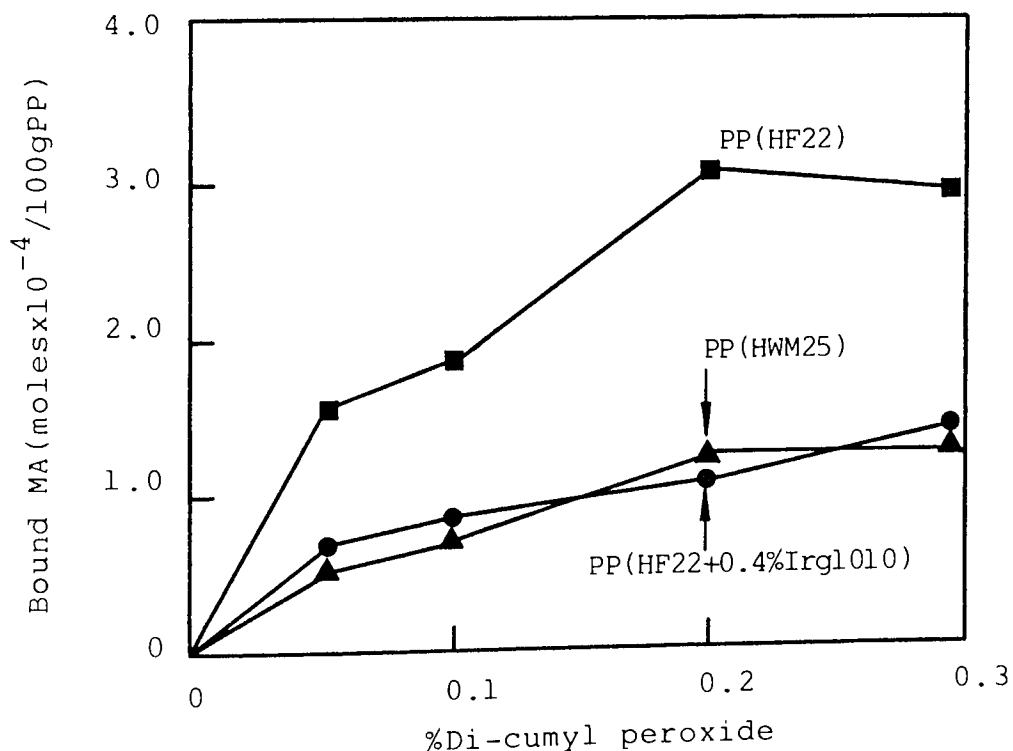


Figure 4.33 Effect of stabilisers on the DCP catalysed mechano-chemical binding of 1%MA to PP(HF22,with and without 0.4%Irganox1010)and commercially stabilised PP(HWM25). Torque rheometer processing conditions (CM,180°C,60rpm,8mins). See Table 4.6.



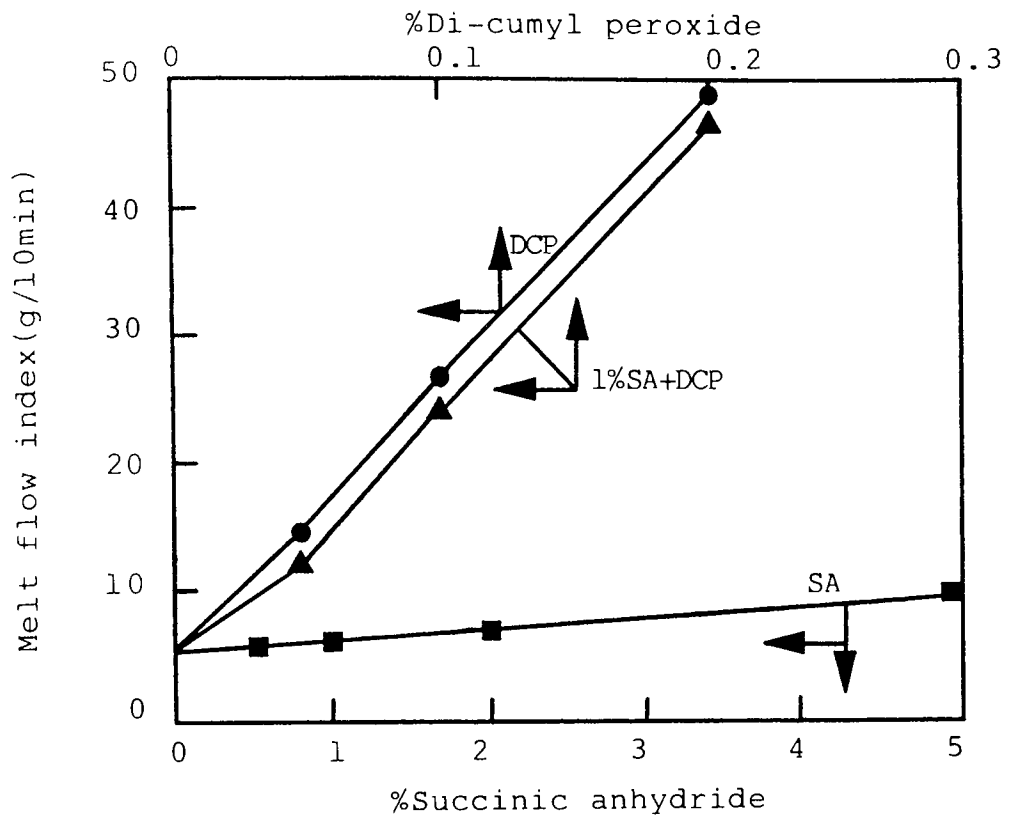


Figure 4.34 Effect of succinic anhydride(SA) and di-cumyl peroxide(DCP) on the melt stability of PP(HF22) after processing in the Hampden RAPRA torque rheometer (180°C,60rpm,8mins,CM).

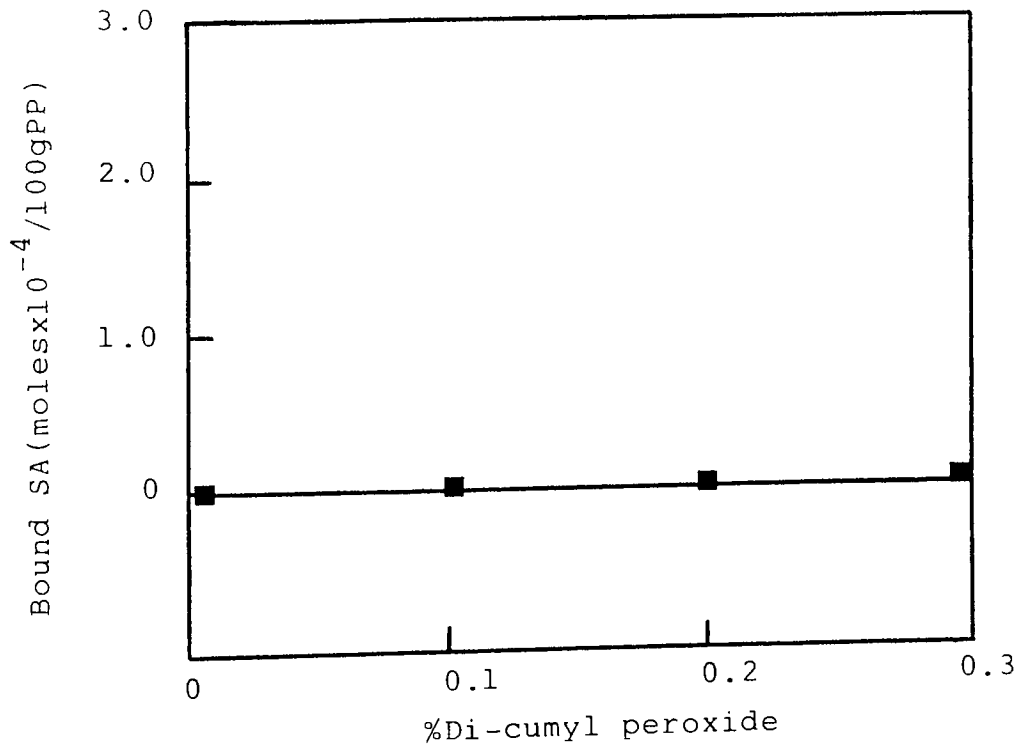


Figure 4.35 Effect of DCP modification of PP(HF22) on the chemical binding of 1%SA after processing in the Hampden RAPRA torque rheometer(180°C,60rpm,8mins,CM).



Plate 4.1 Scanning electron micrograph of the tensile fracture surface of 1%MA/0.2%DCP modified stabilised PP(HWM25) containing 30% glass fibre (A-1100 silane coupled)

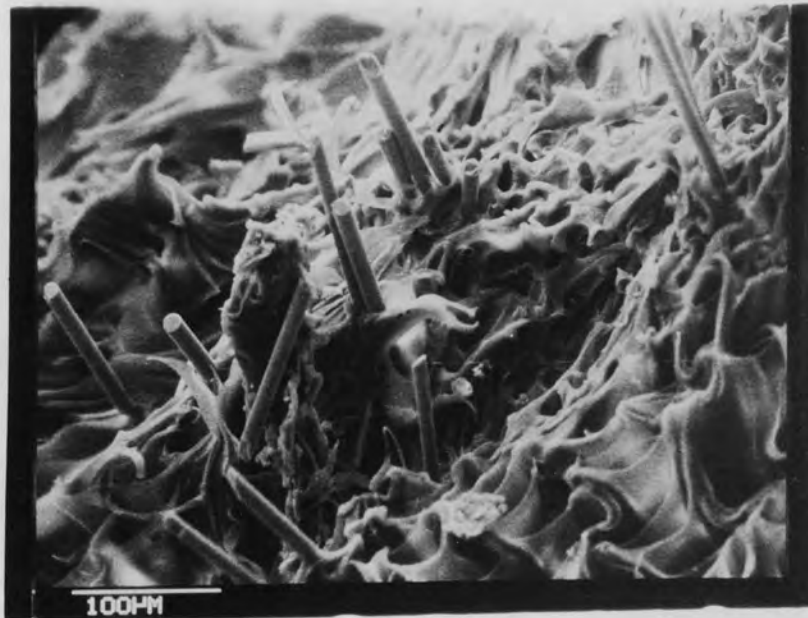


Plate 4.2 Scanning electron micrograph of the tensile fracture surface of 1%MA/0.2%DCP modified unstabilised PP(HF22) containing 30% glass fibre (A-1100 silane coupled)

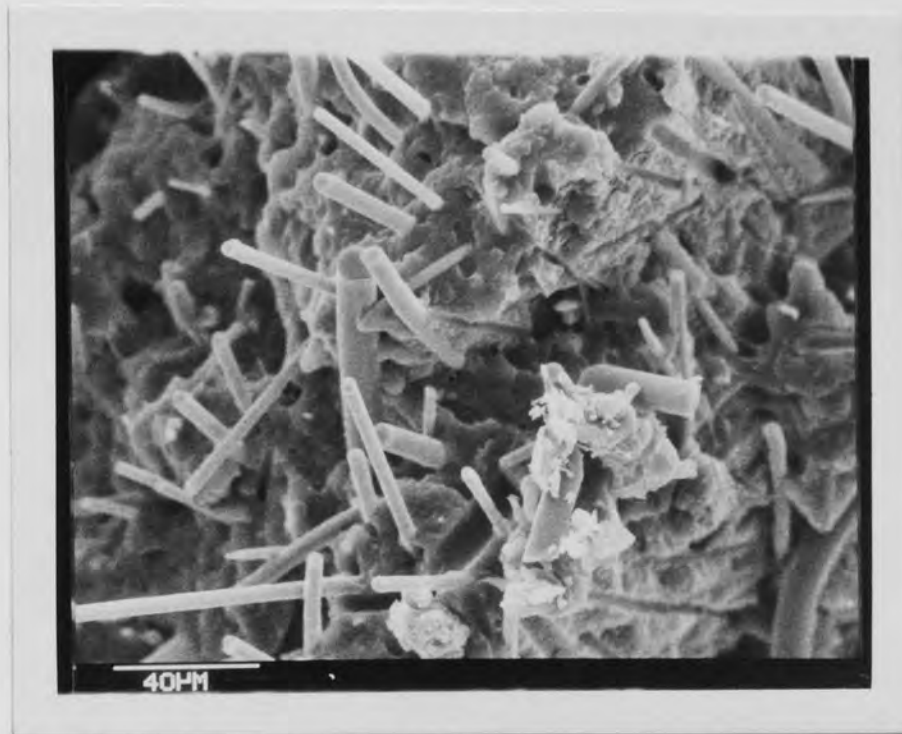


Plate 4.3 Scanning electron micrograph of the tensile fracture surface of 0.2%DCP modified stabilised PP(HWM25) containing 30% long Rockwool fibre (A-1100 silane coupled)

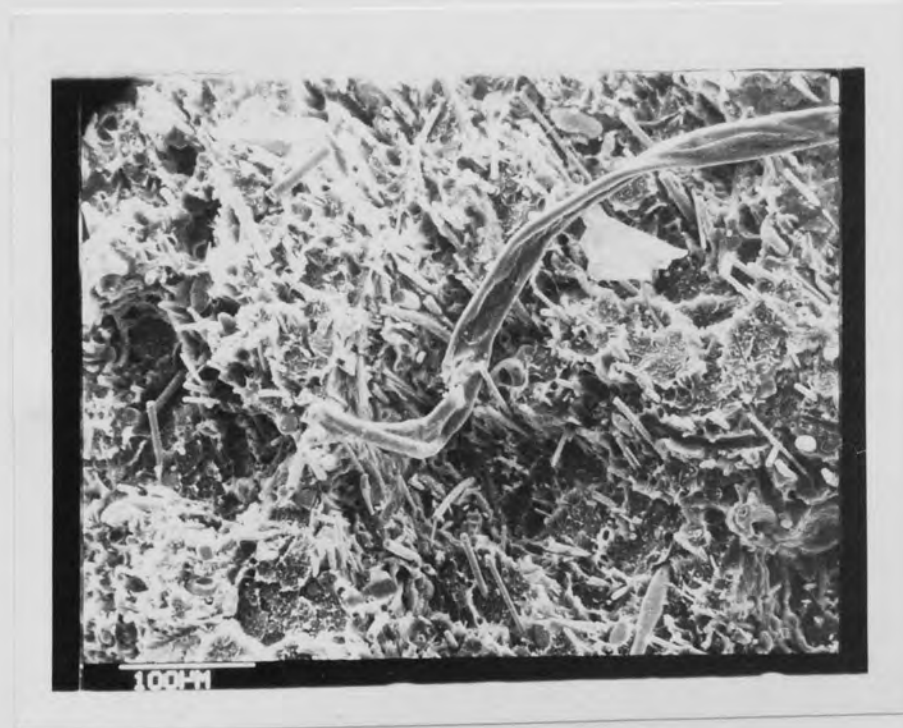


Plate 4.4 Scanning electron micrograph of the tensile fracture surface of 0.3%DCP modified unstabilised PP(HF22) containing 30% long Rockwool fibre (A-1100 silane coupled)

CHAPTER FIVE

ASSESSMENT OF MORE POLYPROPYLENE  
MODIFIERS IN THE ENHANCEMENT  
OF COMPOSITE MECHANICAL PROPERTIES

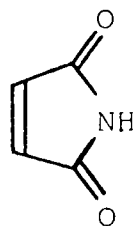
## 5.1 Object

This chapter describes the use of a variety of chemical modifiers (listed in Scheme 5.1) in enhancing the mechanical properties of unstabilised PP(HF22) containing A-1100 silane coupled glass fibre (GF) and long Rockwool fibre (LRWF). Each modifier was melt-processed (Buss Ko-Kneader) with and without di-cumyl peroxide (DCP), a free radical initiator (Scheme 5.2). Melt stability (melt flow index) and chemical binding of additives (monitored by infra-red and ultraviolet spectrophotometry) of the modified polymer were examined. Modified PP(HF22) was subsequently homogenised (Buss Ko-Kneader) and injection moulded (Edgwick) using previously optimised processing conditions (Chapter Three, Scheme 3.3) into test pieces to investigate the full range of mechanical properties, Charpy impact strength (notched, 0.2mm) from 20°C down to -40°C, tensile creep and long-term durability in a variety of fluids typically found in an "under-bonnet" environment (see Scheme 5.3). Scanning electron microscopy (SEM) was used to compare tensile fracture surfaces of modified PP(HF22) composites before and after fluid immersion to observe changes at the polymer-fibre interface.

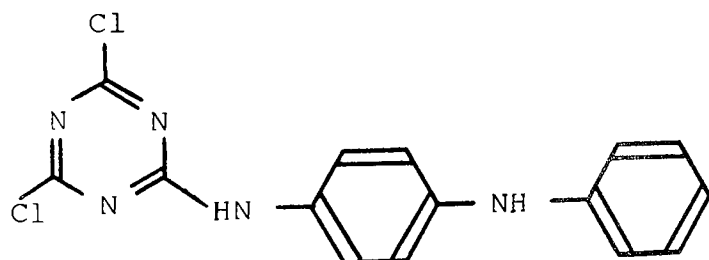
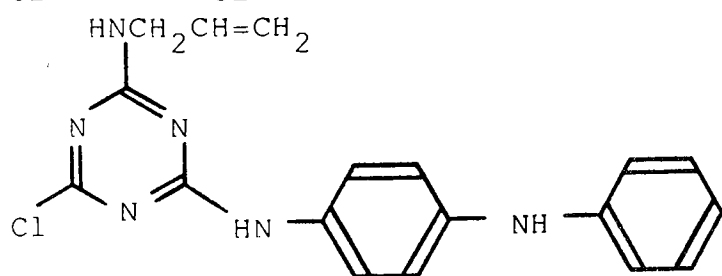
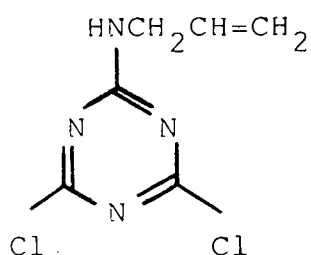
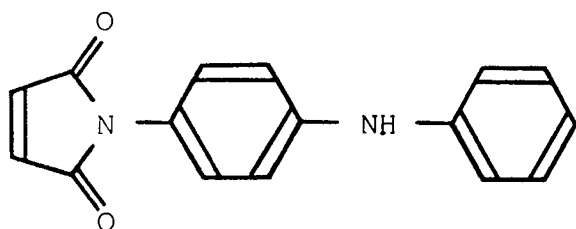
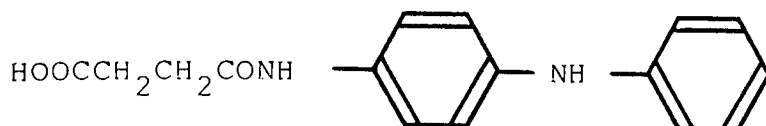
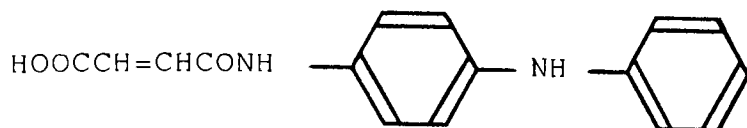
Direct comparisons of PP(HF22) composites containing these modifiers with MA/DCP modified PP(HF22) composites (Chapter Four, Section 4.2.2) and HW60/GR30 (commercially 30% GF coupled PP) are made.

The effect of additional coupling agent (A-1100 silane) on melt processing with the best mechano-chemical modifiers in PP(HF22) was studied (Scheme 5.4) to see if this would result in any further improvement in the mechanical performance of 30% glass fibre reinforced composites.

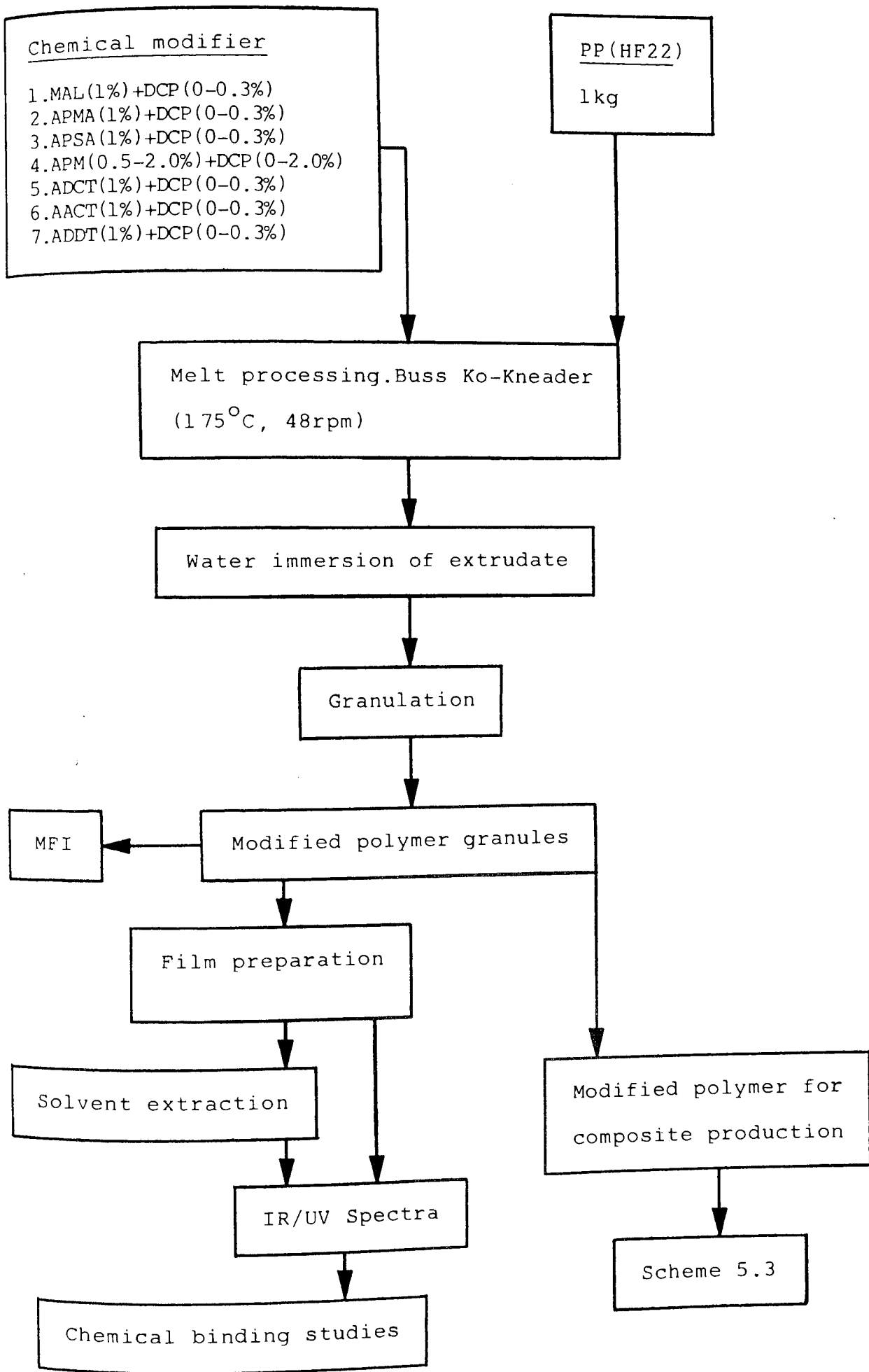
The chemical reaction during melt processing of mechano-chemically modified PP(HF22) and A-1100 silane coupling agent was studied by infra-red and ultraviolet spectrophotometry (Scheme 5.5). This was supplemented by infra-red studies of the melt processing reaction of MA/DCP modified PP(HF22) with A-1100 silane coupling agent on the glass fibre surface.



MAL

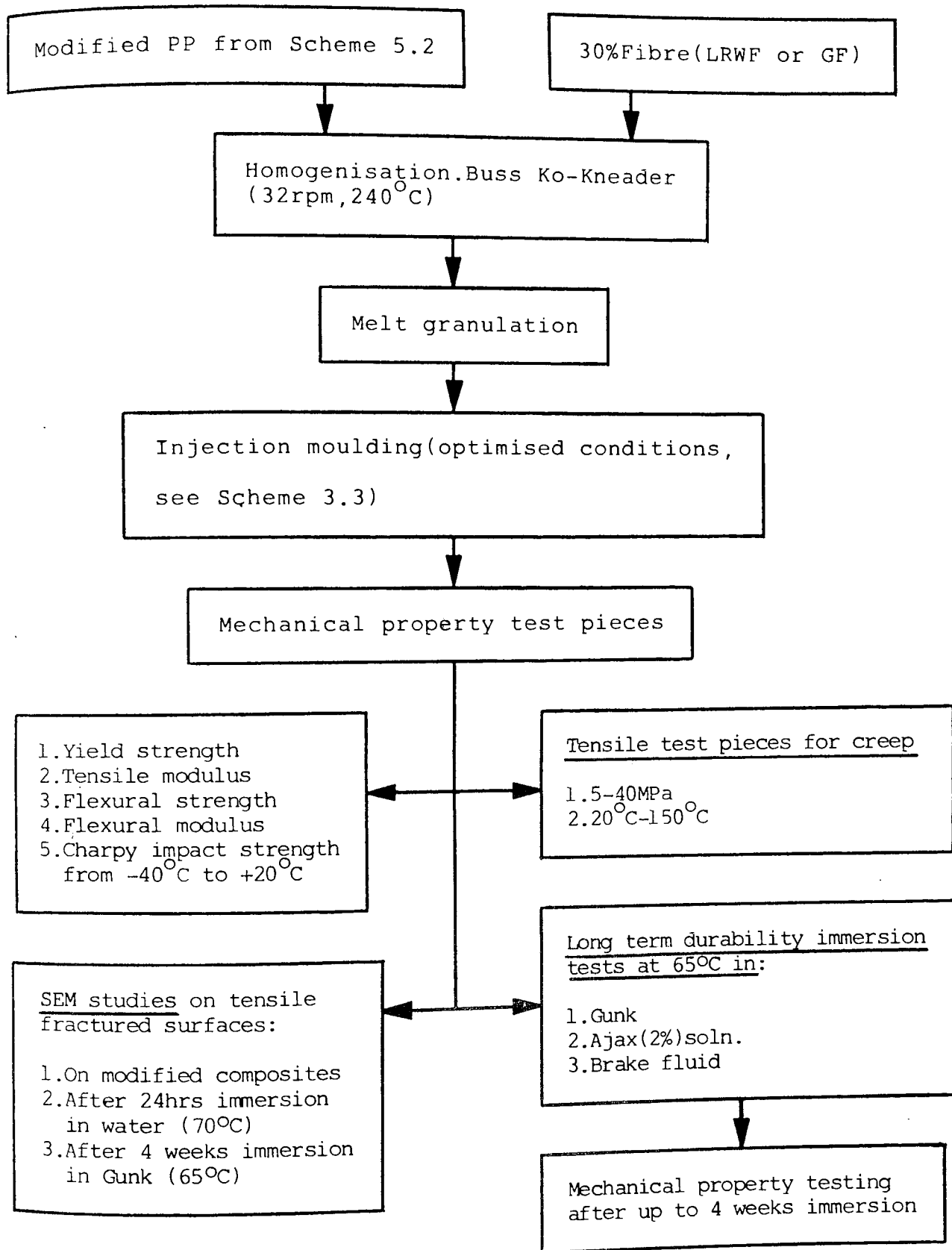


Scheme 5.1 Chemical formulae and abbreviations of chemical modifiers used in Chapter Five.

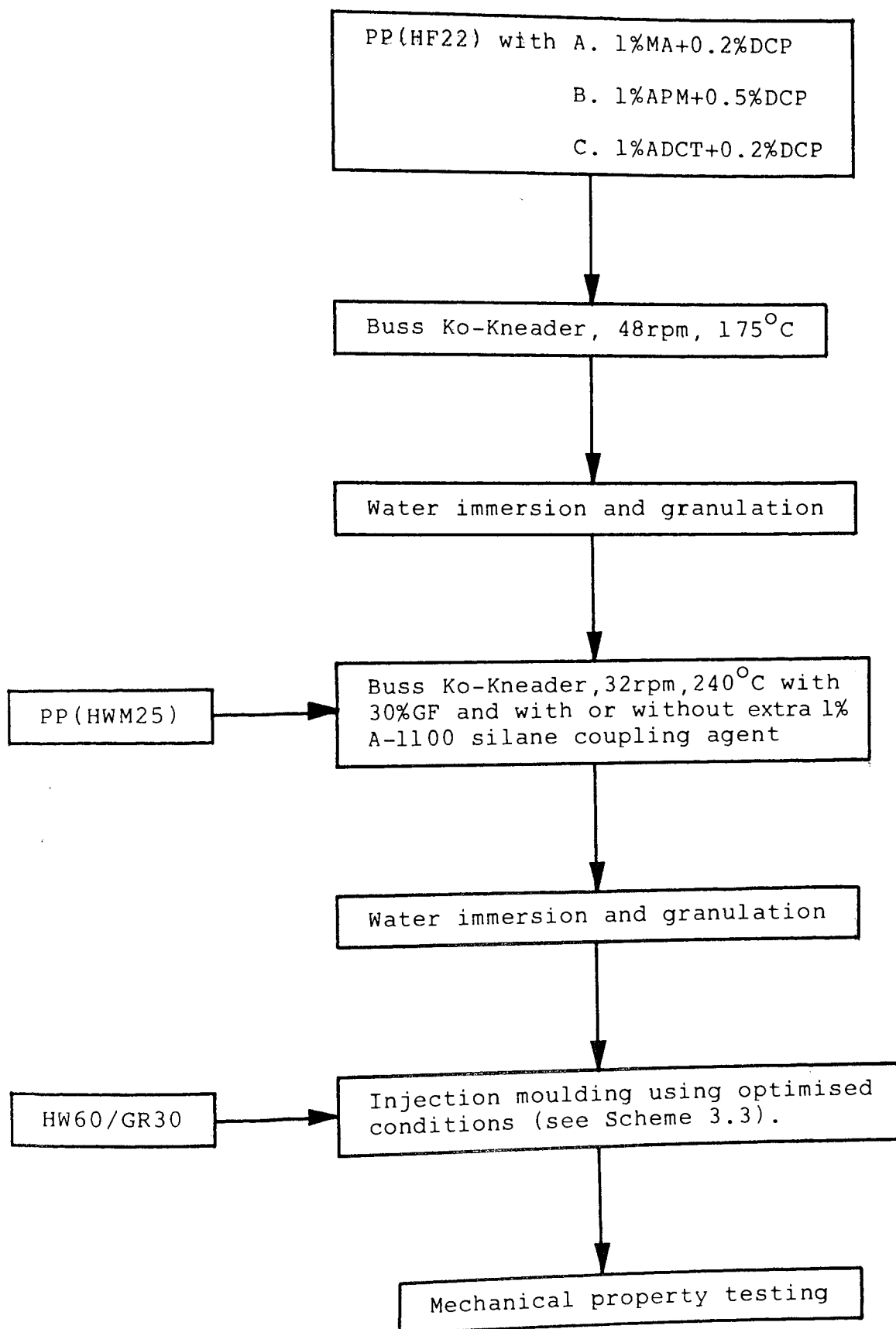


Scheme 5.2 Chemical modification of PP(HF22)

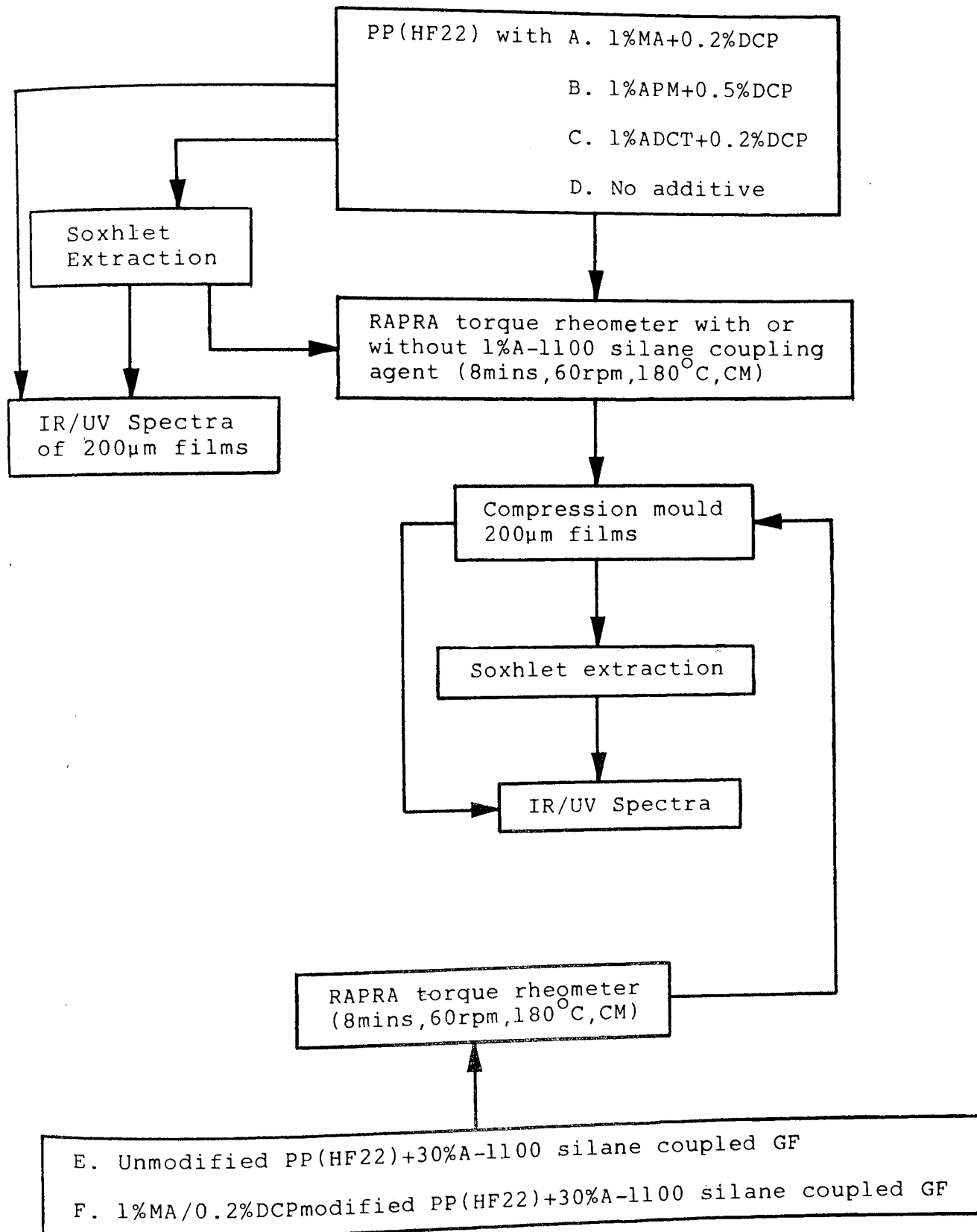




Scheme 5.3 Chemically modified PP(HF22) composite production and testing



Scheme 5.4 Production of mechano-chemically modified PP(HF22) silane coupled glass fibre composites containing an additional 1%A-1100 silane coupling agent



Scheme 5.5 Study of the reaction during PP(HF22) melt processing of mechano-chemical modifiers with A-1100 silane coupling agent

## 5.2 Results

### 5.2.1 Mechanical Properties Of Mechano-chemically Modified PP(HF22) Composites

The % binding of chemical modifiers (listed in Scheme 5.1) to unstabilised PP(HF22) together with their effect on melt stability and the mechanical properties of composites containing LRWF and GF (both 30% loading and A-1100 silane coupled) are shown in Tables 5.1-5.7. Figures 5.1-5.7 depict the relationship between chemical modifier binding and yield strength of the modified PP(HF22) composites. All modifiers containing alkene unsaturation become chemically bound to PP(HF22) during melt processing in the presence of the free radical catalyst DCP and this resulted in substantial yield strength enhancement of modified PP(HF22) containing GF (Figures 5.1-5.7). Optimum modifier binding and resultant mechanical performance of modified PP(HF22) composites containing 1% modifier was obtained with 0.2-0.3% DCP (which confirms similar observations with 1%MA/DCP modified PP(HF22) containing GF, Chapter Four, Section 4.2.5). All modifiers used in PP(HF22) were found to stabilise the melt in the presence of DCP (Tables 5.1-5.7) with the exception of APSA and ADDT, both of which lack alkene unsaturation resulting in zero binding and consequently the failure to improve the mechanical properties

of GF reinforced PP(HF22, Figures 5.3 and 5.7 respectively). Confirming earlier investigations on MA/DCP modified PP(HF22) it is clear from Tables and Figures 5.1-5.7 that unsaturated chemical modifiers with DCP in PP(HF22) containing 30%GF result in superior improvement in mechanical performance to those containing 30%LRWF. However, the mechanical properties of modified PP(HF22) containing 30% LRWF was better than with 30%GF only when the saturated modifiers APSA and ADDT (both 1% concentration, Tables and Figures 5.3 and 5.7 respectively) were used; these additives do not offer any melt stability or chemical binding within the polymer.

Particularly disappointing was the use of AACT with DCP in the modification of PP(HF22) containing 30%GF (see Scheme 5.1). This compound was designed and synthesised to contain a PP binding group (allylic amine), an amino-silane reactive group (chlorine) and a stabiliser group (diphenylamine). Poor chemical binding figures were achieved (Table 5.6A and B, Figure 5.6) with consequent poor mechanical properties which may in part be attributed to the diphenylamine group stabilising the melt and inhibiting free radical binding. However, despite this, other modifiers containing diphenylamine stabilising groups such as APMA (Figure 5.2) and APM (Figure 5.4) gave good binding and good mechanical properties with DCP in 30%GF reinforced PP(HF22).

The mechanical properties of optimised chemically modified PP(HF22)/GF and LRWF composites are shown in Tables 5.8A and B respectively and in Figures 5.8-5.12. HW60/GR30 (commercially 30%GF coupled PP) and the previously optimised (Chapter Four, Section 4.2.2) 1%MA/0.2%DCP/PP(HF22)/30%GF and 0.3%DCP/PP(HF22)/30%LRWF are included for comparison purposes. From Figures 5.8B-5.12B it is apparent that the type of modifier used in PP(HF22) containing 30%LRWF makes very little difference to the mechanical properties; it is the use of DCP rather than the chemical modifier that is responsible for any enhancement of mechanical performance. This is similar to the behaviour of MA/DCP modified PP(HF22) containing LRWF studied in Chapter Four, Section 4.2.2. With GF reinforced PP(HF22), chemical modifiers do have a significant effect upon the composite's mechanical performance (Figures 5.8A-5.12A). Despite the fact that none of the modifiers described in this Chapter (see Scheme 5.1) achieved the performance of 1%MA/0.2%DCP/PP(HF22)/30%GF (Chapter Four, Section 4.2.2), three of these modifying systems (1%APMA/0.2%DCP, 1%APM/0.5%DCP and 1%ADCT/0.2%DCP in PP(HF22) containing 30%GF) gave better results than the commercial composite (HW60/GR30, Table 5.8A, Figures 5.8A-5.12A). A similar system, but containing 1%MAL with 0.3%DCP gave properties on a par with HW60/GR30. All of these systems gave high degrees of chemical binding; APSA, AACT and ADDT systems which gave little or no binding gave poor enhancement of mechanical properties of GF reinforced PP(HF22, Figures 5.8A-5.12A).

5.2.2 The Effect Of Long-term Fluid Immersion On The  
Mechanical Properties Of Mechano-chemically Modified  
PP(HF22) Composites

This section describes the behaviour of a selected range of the best modified PP(HF22) composites (listed in Table 5.9) with respect to yield strength, tensile modulus and flexural strength and modulus (Tables 5.10-5.13 respectively) after four weeks immersion at 65°C in Gunk engine cleaning fluid, Brake fluid and 2% aqueous Ajax solution. Comparisons are made with the commercial control (HW60/GR30, 30%GF reinforced coupled PP) and unmodified PP(HWM25) containing 30%GF.

Because the trends in deterioration of each mechanical property were similar, only the effect of such immersion on yield strength of composites for each fluid is shown graphically (Figures 5.13-5.15). Figure 5.13 shows the yield strength performance of modified PP(HF22) composites after Brake fluid immersion. All modified materials described in Table 5.9 show yield strength retention in excess of 95% including the commercial control, HW60/GR30, with the exception of two composites modified with APMA and APM (both of which contain diphenylamine antioxidant groups) which show only 61% and 73-74% yield strength retention respectively. The unmodified control (PP(HWM25)/30%GF) gave yield strength retention of 80% to give 27MPa after 4 weeks Brake fluid immersion compared to 91MPa for 1%MA/0.2%DCP modified PP(HF22) also containing 30%GF. The use of 2%

aqueous Ajax solution (Figure 5.14) causes slightly more yield strength deterioration than Brake fluid (Figure 5.13), although the control, HW60/GR30, together with MA and ADCT modified PP(HF22) containing 30%GF still retain at least 95% of their original value. Again, composites using modifiers containing amino-antioxidants (APMA and APM) gave the worst performance, although the yield strength retention after four weeks Ajax immersion at 65°C of APM modified composites containing 30%GF was still a respectable 74% (Figure 5.14). By comparison, the unmodified PP(HWM25) containing 30%GF gave 83% yield strength retention, but because its original yield strength was so low, the large differential between modified and unmodified composites remained after Ajax immersion. It was Gunk engine cleaning fluid (Figure 5.15) that caused drastic yield strength deterioration of all samples, although there were large differences in the degree of retention. PP(HWM25) containing 30%GF retained just over half of its original value, but again because its original yield strength was only one-third of some of the modified composites, its yield strength after immersion was comparatively very low. As with Brake fluid and Ajax, APMA and APM modifiers with the diphenylamine group fared poorly after four weeks Gunk immersion (Figure 5.15) with yield strength retention as low as 35%. Outstanding performances were achieved by MA and ADCT in PP(HF22) containing DCP and 30%GF (Figure 5.15) with yield strength retention in excess of 60% which results in the



yield strength after four weeks Gunk immersion at 65°C being 60% in excess of the 30%GF commercially coupled PP (HW60/GR30). Good results were also achieved with MAL/DCP/PP(HF22)/30%GF and DCP/PP(HF22)/30%LRWF (Figure 5.15).

Despite the trends in drastic mechanical performance deterioration caused by four weeks Gunk immersion at 65°C being similar for each mechanical property (Tables 5.10-5.13), the reduction of flexural modulus (Table 5.13) of the unmodified PP(HWM25)/GF control was particularly severe (falling from 6.20GPa to only 0.87GPa, 14% Retention). This result in particular illustrates the necessity for PP to be chemically modified for use with GF because these gave (Table 5.9) flexural modulus retention under identical conditions of at least 50%.

APM was used at 1% and 0.5% concentrations (with 0.5% and 0.25%DCP respectively) in PP(HF22) containing 30%GF (Table 5.9). The results (Tables 5.10-5.13, Figures 5.13-5.15) show that the composite using 1%APM was initially 5-10% superior in terms of mechanical performance and this status was maintained after four weeks immersion in the three test fluids.

1%MA/0.2%DCP modified PP(HF22) containing 30%GF was tested by four weeks immersion (Ajax, Brake fluid and Gunk at 65°C) with and without the inclusion of 0.4% Irganox 1010. This

is a thermal-oxidative stabiliser and was included to investigate its effect upon the modified composites' mechanical performance before and after fluid immersion. From Tables 5.10-5.13, it is apparent that the inclusion of 0.4% Irganox 1010 reduces the mechanical properties of 1%MA/0.2%DCP modified PP(HF22) containing 30%GF by 10-20%. The use of this stabiliser did not alter the % Retention of mechanical property (Tables 5.10-5.13) after four weeks immersion, and thus the original 10-20% differential was maintained.

### 5.2.3 The Effect Of Temperature Upon Charpy Impact Strength Of Mechano-chemically Modified PP(HF22) Composites

The effect of temperature reduction from 20°C to -40°C on the Charpy impact strength (notched, 0.2mm) of modified PP (HF22) composites together with PP(HWM25) homopolymer and HW60/GR30 (30%GF coupled PP) commercial controls is shown in Table 5.14 and Figures 5.16A and B. Particularly noticeable from Figure 5.16A is the sharp decline in impact strength of MA/DCP modified PP(HF22) containing 30%GF on temperature reduction from 20°C to 0°C. Further temperature reduction, however, caused only minor falls in impact strength. Most composites gave between 50 and 80% impact strength retention (Figure 5.16B) on temperature reduction from 20°C to -40°C, but PP(HF22) composites modified with MAL and ADCT and both containing DCP and 30%GF actually

achieved higher impact strength at  $-40^{\circ}\text{C}$  than at  $20^{\circ}\text{C}$ . Figure 5.16A shows that PP(HF22) containing 30%GF and modified with MA and ADCT (both with DCP) give impact strengths comfortably in excess of the commercial control (HW60/GR30) at  $-40^{\circ}\text{C}$  while modification with MAL and APM results in parity with the commercial material. DCP modified PP(HF22) containing 30%LRWF gave consistently poor performance (Figure 5.16A).

#### 5.2.4 Dimensional Stability Of Mechano-chemically Modified PP(HF22) Composites

The dimensional stability of chemically modified PP(HF22) composites subjected to a variety of stresses and temperatures is shown in Figures 5.20-5.30. The effect of fibre loading on the tensile creep of unmodified PP(HWM25) containing LRWF and GF (both A-1100 silane coupled) is shown in Figures 5.17 and 5.18 and for both, increasing fibre loading to 40% substantially reduces strain at  $20^{\circ}\text{C}$  and 20MPa. The dimensional stability of PP(HWM25) homopolymer is seen to be very poor (Figures 5.17 and 5.18) and PP(HWM25) containing GF gives substantially better performance than LRWF. Figure 5.19 compares the isochronous creep behaviour of unmodified PP(HWM25) containing LRWF and GF (both 30% loading and A-1100 silane coupled) with HW60/GR30 (commercially 30%GF coupled PP) and it is apparent that the commercial material exhibits far superior performance.

Although the use of GF in PP(HWM25) gave better behaviour than LRWF (Figure 5.19), both were so poor that a maximum stress of only 25MPa could be accommodated.

The effect of stress (10-40MPa at 20°C) on a range of mechano-chemically modified PP(HF22)/30% fibre reinforced composites together with the commercial control (HW60/GR30) is shown in Figures 5.20-5.25 with the resultant isochronous curves given in Figure 5.26. The chemically modified composites show superior isochronous creep behaviour (Figure 5.26) to the unmodified PP(HWM25) composites (Figure 5.19) and this may be attributed to the increased interfacial shear strength resulting from mechano-chemical modification. The isochronous creep characteristics of modified PP(HF22) composites in Figure 5.26 shows that the order of their dimensional stability is the same as the order of their mechanical property performance (Figures 5.8-5.12) with MA and ADCT modified PP(HF22) containing DCP and 30%GF giving the best performance (both substantially better than the commercial HW60/GR30) followed by APM and MAL, with only DCP modified PP(HF22) containing 30%LRWF showing just slightly inferior behaviour to the commercial GF reinforced PP composite (HW60/GR30).

The effect of temperature on the dimensional stability of modified PP(HF22) composites and the commercial material (HW60/GR30) is shown in Figures 5.27-5.30. At 50°C with a

stress of 30MPa (Figure 5.27), the best results are given by MA and ADCT modified PP(HF22) with DCP and 30%GF and show less than 50% of the strain given by the commercial control (HW60/GR30). DCP modified PP(HF22) containing 30%LRWF gave similar behaviour to the commercial composite. The same trends are observed at 100°C (Figure 5.28) with a stress of 10MPa, except that this time, DCP modified PP(HF22) containing 30%LRWF gives slightly less strain than HW60/GR30 after longer time periods. The maximum possible temperature for creep testing of DCP modified PP(HF22) containing 30%LRWF was 135°C with a stress of 5MPa (Figure 5.29) where it gave slightly superior performance to HW60/GR30. PP(HF22) modified with MA/DCP and containing 30%GF again gave superior performance and this is exemplified in Figure 5.30, which shows the effect of 5MPa at 150°C on the dimensional stability of modified PP(HF22) GF composites. Again, composites using MA and ADCT modifiers (with DCP) gave the best behaviour and showed considerably less strain than the commercial HW60/GR30. Good performances were also exhibited by APM and MAL (both with DCP).

#### 5.2.5 Reaction Of Chemical Modifiers With A-1100 Silane Coupling Agent During PP(HF22) Melt Processing

Table 5.15 shows that the addition of 1%A-1100 silane coupling agent during homogenisation (Buss Ko-Kneader) to 30%GF reinforced PP composites had no effect upon the mechanical properties of unmodified stabilised PP(HWM25)/30%GF, but

resulted in a general improvement of about 10% for composites containing modified (MA, APM and ADCT) unstabilised PP(HF22). This is highlighted in Figure 5.31 which shows the increase in yield strength of such composites and compares them with the commercial material (HW60/GR30).

Figure 5.33 shows the effect of 1%A-1100 silane coupling agent upon the infra-red spectrum of MA/DCP modified PP(HF22). Figures 5.33A and B present the infra-red absorbance of PP(HF22) itself and PP(HF22) containing 1%A-1100 silane. The MA coupled carbonyl absorptions at 1880 and 1792/1782 $\text{cm}^{-1}$  (discussed in Chapter Four, Section 4.3.5) of MA/DCP modified PP(HF22) are shown in Figure 5.33C. When this material was melt processed with 1%A-1100 silane coupling agent (Figure 5.33D), the 1880 and 1792/1782 $\text{cm}^{-1}$  bands disappeared and were replaced by bands at 1710 $\text{cm}^{-1}$  (strong) and 1640 $\text{cm}^{-1}$  (weak). A similar spectrum was obtained (Figure 5.32) when similarly modified PP(HF22) was melt processed with A-1100 silane coupled glass fibre.

### 5.3 Discussion

#### 5.3.1 Mechanical Properties Of Mechano-chemically Modified PP(HF22) Composites

The effect of chemical modifiers studied in this Chapter (Scheme 5.1) on enhancing the mechanical performance of PP(HF22)/30%GF/DCP composites is similar to that observed

when MA was used (Chapter Four, Sections 4.3.2 and 4.3.5). The extent of mechanical performance enhancement by these unsaturated modifiers (in the presence of DCP) depends on their percentage binding, which in turn (Figures 5.1-5.7) determines the number of polymer-bound reactive sites available for reaction with silane (A-1100) coupling agent on glass fibres (Section 5.3.5). The presence of an unsaturated centre in the modifiers was essential for binding to take place. Saturated modifiers, APSA and ADDT (Figures 5.3 and 5.7), gave no binding even in the presence of DCP and consequently were incapable of improving the mechanical performance of GF reinforced PP(HF22) composites. 30%LRWF/PP(HF22) composites modified with DCP (Figures 5.3 and 5.7) gave superior mechanical performance when compared to similar composites containing GF instead of the mineral fibre. In Chapter Four (Section 4.3.1), it was shown that the mechanical performance of LRWF composites was best improved by using DCP alone, the mineral fibre's tensile surface layer probably containing unsaturated groups where macro-alkyl free radical addition occurs during melt processing; APSA and ADDT (Tables 5.3 and 5.7) have no effect upon this free radical process whereas unsaturated modifiers (APMA and ADCT, Tables 5.2 and 5.5) stabilise the melt. In the case of APM (Figure 5.4), although it offered the best binding (97%), it did not give the best mechanical performance in modified PP(HF22) containing 30%GF (Figures 5.1-5.7). This is probably because the maleimide ring through which chemical binding has occurred during PP(HF22) melt

processing (Chapter Six, Section 6.3.3), becomes sterically hindered by its bulky diaryl-amino thermal-oxidative stabilising group, thus reducing the chance of reaction between the maleimide ring and the amino silane (A-1100) coupling agent on the GF surface (infra-red spectrophotometric evidence for this phenomenon was difficult to interpret, see Section 5.3.5). There are two reasons for the higher binding and better mechanical performance of PP(HF22)/30%GF composites modified with ADCT (Figure 5.5) in the presence of DCP compared to AACT (Figure 5.6, Scheme 5.1). Firstly, in the case of AACT, the diaryl-amino group partially stabilises the polymer during melt processing (stabilisation mechanisms are discussed in Chapter Six, Section 6.3.3), thus inhibiting the mechano-chemical binding process. Secondly, there is a possibility that this group reacts with the chloro group (6-position on the cyanuric ring) during melt processing, resulting in N-C bond formation with liberation of HCl (see Scheme 5.9). Loss of this chlorine reduces the capacity of this modifier when bound to PP(HF22) to react with A-1100 amino silane on the GF surface. ADCT possesses two chloro groups (4 and 6-positions) resulting in sterically less hindered access to the amino GF coupling agent.

### 5.3.2 The Effect Of Long-term Fluid Immersion On The Mechanical Properties Of Mechano-chemically Modified PP(HF22) Composites

Polypropylene resins give high resistance to chemical attack<sup>(205)</sup>. The resistance of its composites to Brake



fluid and 2% aqueous Ajax solution at 65°C (Figures 5.13 and 5.14) was generally good, confirming similar literature reports<sup>(205)</sup>; reductions in mechanical performance may be attributed to fluid diffusibility into the polymer<sup>(206)</sup> and along the polymer-fibre interface. Oliver<sup>(207)</sup> states that effective polymer-fibre bonding increases a composite's resistance to chemical attack in aggressive environments, a view supported by the observation that unmodified PP(HWM25)/30%GF gave very much inferior performance when compared with mechano-chemically modified PP(HF22) composites (Figures 5.13 and 5.14). Gunk engine cleaning fluid (whose function is to disperse oil and grease, and contains detergent and solvents for hydrocarbons) was the only test-fluid to severely reduce the mechanical performance of both unmodified and modified composites (Figure 5.15). The swelling of Gunk observed into all samples indicates rapid diffusion of Gunk constituents with PP(HF22), the rate of which is accelerated by the presence of voids formed during injection moulding. The decrease in mechanical performance is accompanied by a change in fracture behaviour of such chemically modified composites (Plates 5.1-5.2). For ADCT/DCP modified PP(HF22) containing 30%GF which gave good retention of mechanical performance after Gunk immersion, the major change in tensile fracture behaviour (Plates 5.1-5.2) was not increased fibre pull-out lengths from the matrix (due to good interfacial adhesion, caused by chemical modification) but the increased ductility and yielding behaviour of the polymer matrix, a consequence of plasticisation caused by

the swelling of Gunk into PP(HF22). Because MA and ADCT modified PP(HF22) composites gave the best polymer-fibre adhesion (based on mechanical performance data, Figure 5.15), their deterioration during Gunk immersion was limited by the decreased ability of Gunk constituents to intrude at the interface. The reduction in performance was thus limited to swelling (diffusion) of Gunk constituents into the matrix itself<sup>(208)</sup>.

APM and APMA modification resulted in good polymer-fibre adhesion (resulting in good mechanical performance, Section 5.3.1) but these have demonstrated poor retention of tensile and flexural properties (Figures 5.13-5.15) on fluid immersion. This may be due to the fact that they both possess a sterically bulky diaryl-amino group present at the interface (a result of free radical binding to the polymer and reaction with the A-1100 silane coupling agent on the GF surface) allowing easier diffusion (their physical size separating the fibre and polymer) of test-fluid molecules (from Brake fluid, Ajax solution and Gunk, Figures 5.13-5.15) between the polymer and fibre, thus reducing interfacial adhesion leading to deterioration of mechanical performance (Scheme 5.8).

The use of MA/DCP modified PP(HF22) containing 30%GF with and without 0.4%Irganox 1010 (Table 5.9), showed that the hindered phenolic stabiliser suppressed the mechanical performance because the free radical binding mechanism of

MA was inhibited (Chapter Four, Section 4.3.4-5 and Chapter Six, Section 6.3.1 and Scheme 6.8). This in turn reduces the number of sites where the bound MA groups may react during melt processing with A-1100 silane coupled GF (see Chapter Four, Section 4.3.5 and Chapter Five, Section 5.3.5).

### 5.3.3 The Effect Of Temperature Upon Charpy Impact Strength Of Mechano-chemically Modified PP(HF22) Composites

Satisfactory impact performance necessitates avoidance of low energy brittle fracture; the tendency to change from tough to brittle fracture is enhanced by decreasing the temperature and introducing stress concentrations (notches). Orientation resulting from injection moulding increases the tendency to crack parallel to the direction of orientation. The complexity of PP's impact behaviour in the  $-40^{\circ}\text{C}$  to  $20^{\circ}\text{C}$  range has meant that it is not currently possible to develop formulae for the rational design of plastic components<sup>(209)</sup>. Indeed, Plueddemann<sup>(210)</sup> has reported that Charpy impact strength enhancement in the  $-40^{\circ}\text{C}$  to  $20^{\circ}\text{C}$  range is not a reliable guide to good coupling at the polymer-fibre interface because it could indicate efficient adhesion or release properties on fracture. Samples with poor interfacial polymer-fibre adhesion (unmodified PP(HF22) containing GF and LRWF, Chapter Three, Section 3.3.3) gave poor Charpy impact strength throughout the test temperature range (Figure 5.16A and B) due to low resistance to release of fibres from the matrix. The use

of temperatures as low as  $-40^{\circ}\text{C}$  (Figure 5.16A and B) had little effect upon the Charpy impact strength of modified PP(HF22) composites because the failure mechanism is initiated by the high degree of stress concentration induced by the 0.2mm radius notch. The explanation for the fall in impact strength of 1%MA/0.2%DCP modified PP(HF22) containing 30%GF on temperature reduction from  $20^{\circ}\text{C}$  to  $0^{\circ}\text{C}$  is less clear, but in the  $-40^{\circ}\text{C}$  to  $20^{\circ}\text{C}$  range, the superior impact performance of MA and ADCT modified PP(HF22)/30%GF (when compared to the commercial composite, HW60/GR30, Figure 5.16A and B) must be attributable to good polymer-fibre adhesion.

#### 5.3.4 Dimensional Stability Of Mechano-chemically Modified PP(HF22) Composites

Numerous tensile creep curves were constructed because the strain of a plastic (homopolymer and composite) depends upon the magnitude and duration of an applied stress; the prolonged duration of creep testing dictates the use of semi-logarithmic plots (Figures 5.17-5.30). Increased fibre content (10-40%) in PP(HWM25) substantially reduced strain (Figures 5.17-5.19), a consequence of their increased tensile modulus (Chapter Three, Section 3.3.3). The superior performance of PP(HWM25) loaded with GF (Figure 5.18) rather than LRWF (Figure 5.17) is due to the high tensile modulus imparted by GF. Figures 5.20-5.26 show the importance of good interfacial adhesion (by mechano-chemical

modification of the polymer) in reducing tensile strain during prolonged loading and the ability to accept higher stresses (40MPa, Figures 5.20-5.26, compared to only 25MPa for unmodified materials, Figures 5.17-5.19); this is because these materials possess high tensile moduli and yield strength (Section 5.2.1).

It is well documented<sup>(211-214)</sup> that the tensile modulus of PP falls with increased temperature and thus strain increases with a given loading. One of the reasons why 0.3%DCP modified PP(HF22) containing 30%LRWF (Figure 5.29) could be tested at a maximum temperature of only 135°C compared with 150°C for other modified composites containing 30%GF (Figure 5.30) is that the mineral fibre's tensile layer is thought to be responsible for the prevention of A-1100 silane coupling (Chapter Three, Section 3.3.3), resulting in poor adhesion to the polymer matrix. Probably a more significant factor is that the PP(HF22) matrix has been substantially degraded by 0.3%DCP modification (Chapter Four, Section 4.3.4) prior to homogenisation and injection moulding with 30%LRWF; its very high melt flow index allows much easier deformation, especially at high temperatures (to 135°C). These creep curves underline the accepted phenomenon that PP exhibits non-linear viscoelasticity for any deformation of practical importance<sup>(215)</sup>.

### 5.3.5 Reaction Of Chemical Modifiers With A-1100 Silane Coupling Agent During PP(HF22) Melt Processing

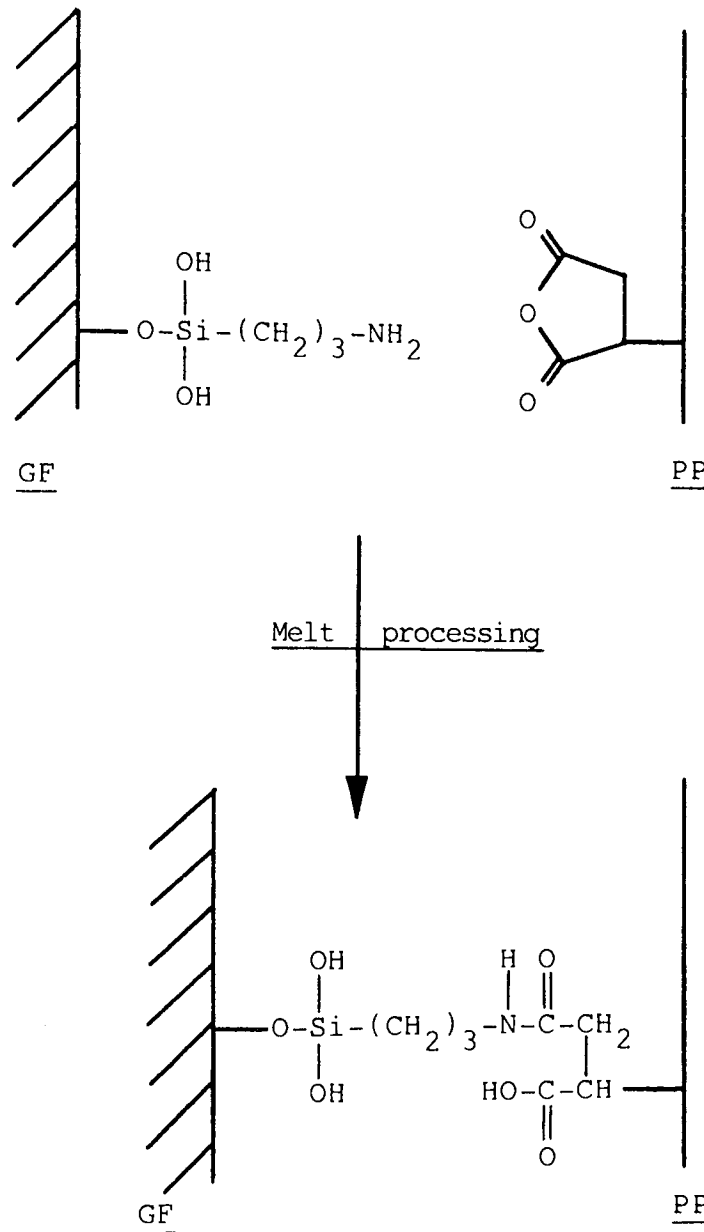
An additional 1%A-1100 silane coupling agent (Table 5.15 and Figure 5.31) had no influence on the mechanical performance of unmodified PP(HWM25) containing 30%GF. This confirms (Chapter Three, Section 3.3.3) that the adhesion between these two composite constituents is poor; it is known<sup>(216)</sup> that semi-crystalline polymers are generally incompatible with non-reactive organofunctional silanes. Similar addition to chemically modified PP(HF22) composites (Table 5.15 and Figure 5.31) resulted in a 10% increase in mechanical performance, indicating that the silane aids fibre-matrix adhesion by reaction in the melt with mechanochemically bound PP(HF22) modifiers (Schemes 5.6-5.8). The same silane must also couple to the GF surface, suggesting that free sites are available for coupling on the GF or that chemical mobility of coupling agents during processing (homogenisation and injection moulding) allows silane exchange<sup>(217)</sup>.

Figure 5.33 demonstrates that melt processing of MA/DCP modified PP(HF22) with 1%A-1100 amino silane causes anhydride ring opening to give a polymer-bound unextractable silane coupling agent (via an amide bond, infra-red band  $1710\text{cm}^{-1}$ , Figure 5.33D).

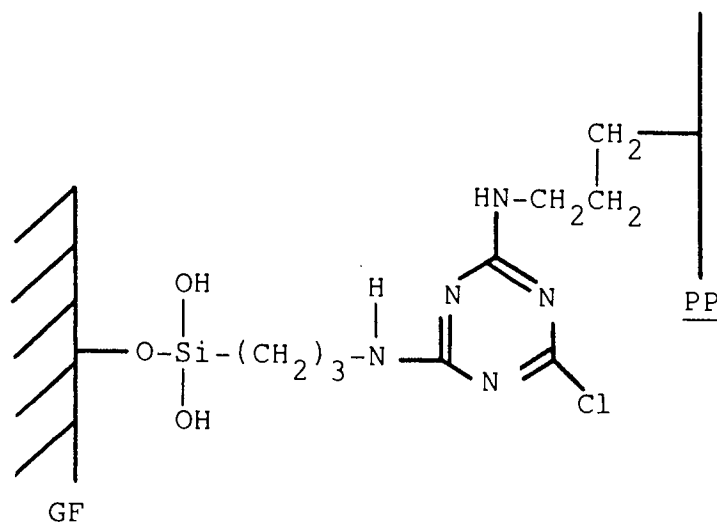
Infra-red spectrophotometry is an effective means of studying the changes occurring in coupling agents on fibre surfaces; absorption intensities are inherently weak but may be enhanced by increasing the geometrical path length by making multiple reflections of incident radiation at various angles<sup>(218,219)</sup> (attenuated total-reflectance, ATR). However, conventional transmission infra-red spectrophotometry of 200 $\mu$ m MA/DCP modified PP(HF22) films containing A-1100 silane coupled GF (30% loading) was adequate for observation of chemical bond formation between the coupling agent and PP(HF22)-bound MA, as seen by the appearance of the 1710 $\text{cm}^{-1}$  amide band (Figure 5.32) during melt processing. This condensation reaction (Scheme 5.6) is responsible for the enhancement of the mechanical performance of MA/DCP modified PP(HF22)/silane coupled GF composites. The degree of enhancement is proportional to the number of such chemical bonds formed and is thus dependent upon the bound MA concentration within the polymer (which is determined by the DCP free radical initiator concentration used during melt processing, Chapter Four, Section 4.3.5). Similar spectrophotometric studies on ADCT and APM modified PP(HF22) with A-1100 silane coupling agent proved inconclusive; the formation of new chemical bonds during melt processing could not be detected. However, it is likely that new bond formation does occur: ADCT (Scheme 5.7) bound to PP(HF22) via its allylic group reacting with the amino coupling agent with one of the chloro groups (4 or 6-positions on the cyanuric ring), and APM (Scheme 5.8) by opening the maleimide ring (where it has

bound to the polymer) on condensation with the amino silane, a mechanism similar to that of MA (Scheme 5.6).

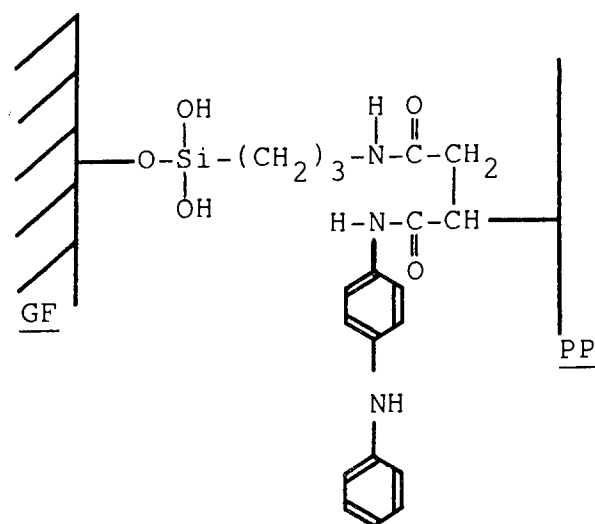




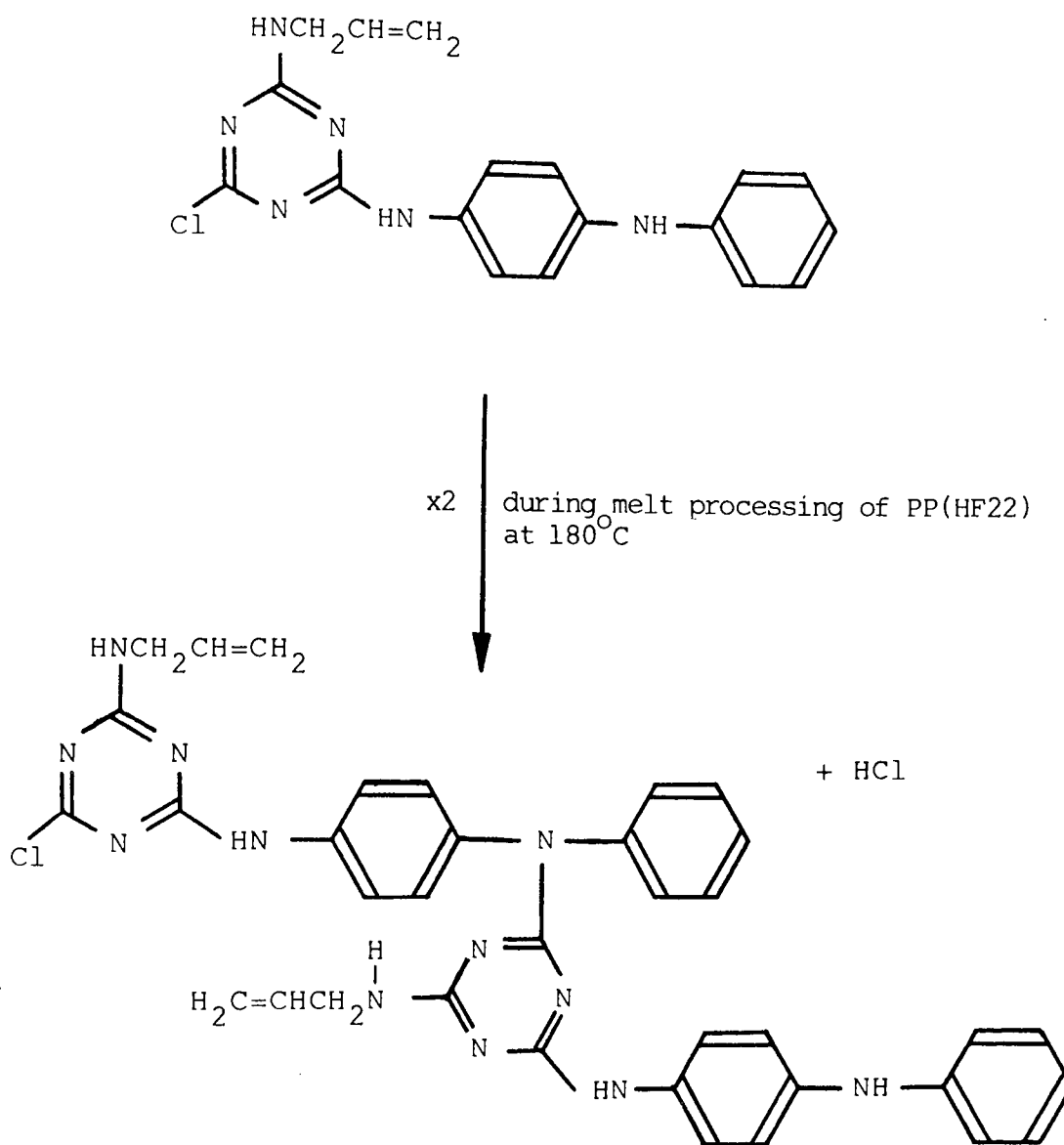
Scheme 5.6 Proposed bonding between glass fibre A-1100 silane coupling agent and chemically bound MA(PP)



Scheme 5.7 Proposed bonding between glass fibre A-1100 silane coupling agent and chemically bound ADCT(PP)



Scheme 5.8 Proposed bonding between glass fibre A-1100 silane coupling agent and chemically bound APM(PP)



Scheme 5.9 Proposed reaction between the 6-chloro and diaryl amino groups of AACT during the melt processing of PP(HF22) at 180°C

%MAL	%DCP	MFI	%Binding of modifier to PP	Yield Strength (MPa)	Tensile Modulus (GPa)	Flexural Strength (MPa)	Flexural Modulus (GPa)	Charpy Impact Strength ( $\text{kJm}^{-2}$ )
1.0	0.0	3.53	30	54	3.25	67	5.86	75
1.0	0.1	8.98	75	65	3.25	79	6.37	89
1.0	0.2	25.20	80	65	3.25	82	5.75	101
1.0	0.3	40.00	83	72	3.26	80	5.22	122

Table 5.1A Mechanical properties of MAL/DCP modified PP(HF22) containing glass fibre (30% loading and A-1100 silane coupled)

%MAL	%DCP	MFI	%Binding of modifier to PP	Yield Strength (MPa)	Tensile Modulus (GPa)	Flexural Strength (MPa)	Flexural Modulus (GPa)	Charpy Impact Strength ( $\text{kJm}^{-2}$ )
1.0	0.0	3.53	30	39	3.16	55	5.41	59
1.0	0.1	8.98	75	47	3.11	59	5.36	61
1.0	0.2	25.20	80	52	3.09	63	5.47	73
1.0	0.3	40.00	83	55	3.13	71	5.55	84

Table 5.1B Mechanical properties of MAL/DCP modified PP(HF22) containing long Rockwool fibre (30% loading and A-1100 silane coupled)

%APMA	%DCP	MFI	%Binding of modifier to PP	Yield Strength (MPa)	Tensile Modulus (GPa)	Flexural Strength (MPa)	Flexural Modulus (GPa)	Charpy Impact Strength ( $\text{kJm}^{-2}$ )
1.0	0.0	3.12	15	41	3.37	47	6.15	90
1.0	0.1	9.8	31	71	3.49	91	6.83	115
1.0	0.2	22.1	50	85	3.90	108	7.46	152
1.0	0.3	39.6	52	81	3.72	101	7.17	149

Table 5.2A Mechanical properties of APMA/DCP modified PP(HF22) containing glass fibre (30% loading and A-1100 silane coupled)

%APMA	%DCP	MFI	%Binding of modifier to PP	Yield Strength (MPa)	Tensile Modulus (GPa)	Flexural Strength (MPa)	Flexural Modulus (GPa)	Charpy Impact Strength ( $\text{kJm}^{-2}$ )
1.0	0.0	3.12	15	39	2.89	39	5.76	62
1.0	0.1	9.8	31	46	2.92	51	5.84	69
1.0	0.2	22.1	50	48	2.91	56	5.89	71
1.0	0.3	39.6	52	50	2.94	59	5.91	75

Table 5.2B Mechanical properties of APMA/DCP modified PP(HF22) containing long Rockwool fibre (30% loading and A-1100 silane coupled)

%APSA	%DCP	MFI	%Binding of modifier to PP	Yield Strength (MPa)	Tensile Modulus (GPa)	Flexural Strength (MPa)	Flexural Modulus (GPa)	Charpy Impact Strength ( $\text{kJm}^{-2}$ )
1.0	0.0	4.95	0.0	40	3.00	43	5.89	73
1.0	0.1	17.5	0.0	39	2.97	42	5.75	75
1.0	0.2	*	0.0	39	2.95	42	5.84	76
1.0	0.3	*	0.0	38	2.98	43	5.82	74

\* Too high to be measured

Table 5.3A Mechanical properties of APSA/DCP modified PP(HF22) containing glass fibre (30% loading and A-1100 silane coupled)

%APSA	%DCP	MFI	%Binding of modifier to PP	Yield Strength (MPa)	Tensile Modulus (GPa)	Flexural Strength (MPa)	Flexural Modulus (GPa)	Charpy Impact Strength ( $\text{kJm}^{-2}$ )
1.0	0.0	4.95	0.0	31	2.81	38	5.81	65
1.0	0.1	17.5	0.0	40	2.94	47	5.68	68
1.0	0.2	*	0.0	51	2.93	54	5.71	71
1.0	0.3	*	0.0	55	2.96	61	5.73	79

\* Too high to be measured

Table 5.3B Mechanical properties of APSA/DCP modified PP(HF22) containing long Rockwool fibre (30% loading and A-1100 silane coupled)

%APM	%DCP	MFI	%Binding of modifier to PP	Yield Strength (MPa)	Tensile Modulus (GPa)	Flexural Strength (MPa)	Flexural Modulus (GPa)	Charpy Impact Strength ( $\text{kJm}^{-2}$ )
0.5	0.0	2.12	75	80	3.60	95	6.48	118
0.5	0.25	3.15	90	78	4.00	96	7.91	139
0.5	0.50	3.22	95	77	4.00	100	8.28	139
1.0	0.0	2.08	70	80	3.59	93.5	6.58	117
1.0	0.5	2.54	89	84	3.95	103	7.70	168
1.0	1.0	3.01	94	73	3.65	96	7.90	206
2.0	0.0	2.09	61	79	3.56	90	6.50	121
2.0	1.0	2.69	77	77	3.87	96	7.20	163
2.0	2.0	3.28	81	65	3.45	90	6.31	136

Table 5.4A Mechanical properties of APM/DCP modified PP(HF22) containing glass fibre (30% loading and A-1100 silane coupled)

%APM	%DCP	MFI	%Binding of modifier to PP	Yield Strength (MPa)	Tensile Modulus (GPa)	Flexural Strength (MPa)	Flexural Modulus (GPa)	Charpy Impact Strength ( $\text{kJm}^{-2}$ )
0.5	0.0	2.12	75	38	3.16	56	5.59	65
0.5	0.25	3.15	90	57	3.20	73	5.76	76
0.5	0.50	3.22	95	56	3.21	74	5.74	83
1.0	0.0	2.08	70	39	3.19	57	5.54	66
1.0	0.5	2.54	89	59	3.21	77	5.59	79
1.0	1.0	3.01	94	60	3.18	79	5.61	89
2.0	0.0	2.09	61	38	3.20	59	5.49	66
2.0	1.0	2.69	77	52	3.18	69	5.38	72
2.0	2.0	3.28	81	51	3.16	58	5.39	75

Table 5.4B Mechanical properties of APM/DCP modified PP(HF22) containing long Rockwool fibre (30% loading and A-1100 silane coupled)



%ADCT	%DCP	MFI	%Binding of modifier to PP	Yield Strength (MPa)	Tensile Modulus (GPa)	Flexural Strength (MPa)	Flexural Modulus (GPa)	Charpy Impact Strength ( $\text{kJm}^{-2}$ )
1.0	0.0	5.4	7	42	3.45	51.5	6.60	88
1.0	0.1	18.7	47	77	3.56	97	7.07	123
1.0	0.2	31.3	68	87	3.85	115	7.67	181
1.0	0.3	56.0	72	83	3.79	108	7.43	173

Table 5.5A Mechanical properties of ADCT/DCP modified PP(HF22) containing glass fibre (30% loading and A-1100 silane coupled)

%ADCT	%DCP	MFI	%Binding of modifier to PP	Yield Strength (MPa)	Tensile Modulus (GPa)	Flexural Strength (MPa)	Flexural Modulus (GPa)	Charpy Impact Strength ( $\text{kJm}^{-2}$ )
1.0	0.0	5.4	7	35	3.25	51.5	5.84	70
1.0	0.1	18.7	47	49	3.24	72	5.91	78
1.0	0.2	31.3	68	58	3.25	81	5.95	84
1.0	0.3	56.0	72	64	3.29	84	6.02	87

Table 5.5B Mechanical properties of ADCT/DCP modified PP(HF22) containing long Rockwool fibre (30% loading and A-1100 silane coupled)

%AACT	%DCP	MFI	%Binding of modifier to PP	Yield Strength (MPa)	Tensile Modulus (GPa)	Flexural Strength (MPa)	Flexural Modulus (GPa)	Charpy Impact Strength ( $\text{kJm}^{-2}$ )
1.0	0.0	3.9	6	40	3.34	48	6.00	97
1.0	0.1	21.9	15	42	3.35	50	6.49	101
1.0	0.2	30.9	25	42	3.30	53	6.95	108
1.0	0.3	41.0	27	41	3.29	54	6.79	105

Table 5.6A Mechanical properties of AACT/DCP modified PP(HF22) containing glass fibre (30% loading and A-1100 silane coupled)

%AACT	%DCP	MFI	%Binding of modifier to PP	Yield Strength (MPa)	Tensile Modulus (GPa)	Flexural Strength (MPa)	Flexural Modulus (GPa)	Charpy Impact Strength ( $\text{kJm}^{-2}$ )
1.0	0.0	3.9	6	38	2.90	52	5.47	56
1.0	0.1	21.9	15	39	2.91	55	5.61	65
1.0	0.2	30.9	25	42	2.90	59	5.78	69
1.0	0.3	41.0	27	40	2.90	58	5.85	71

Table 5.6B Mechanical properties of AACT/DCP modified PP(HF22) containing long Rockwool fibre (30% loading and A-1100 silane coupled)

%ADDT	%DCP	MFI	%Binding of modifier to PP	Yield Strength (MPa)	Tensile Modulus (GPa)	Flexural Strength (MPa)	Flexural Modulus (GPa)	Charpy Impact Strength ( $\text{kJm}^{-2}$ )
1.0	0.0	5.02	0.0	40	2.97	41	5.85	72
1.0	0.1	18.36	0.0	39	2.99	41	5.89	73
1.0	0.2	*	0.0	38	2.97	41	5.85	75
1.0	0.3	*	0.0	39	2.97	40	5.84	74

\* Too high to be measured

Table 5.7A Mechanical properties of ADDT/DCP modified PP(HF22) containing glass fibre (30% loading and A-1100 silane coupled)

%ADDT	%DCP	MFI	%Binding of modifier to PP	Yield Strength (MPa)	Tensile Modulus (GPa)	Flexural Strength (MPa)	Flexural Modulus (GPa)	Charpy Impact Strength ( $\text{kJm}^{-2}$ )
1.0	0.0	5.02	0.0	33	2.87	37	5.85	67
1.0	0.1	18.36	0.0	39	2.95	49	5.69	68
1.0	0.2	*	0.0	51	2.94	55	5.75	73
1.0	0.3	*	0.0	53	2.98	60	5.92	80

\* Too high to be measured

Table 5.7B Mechanical properties of ADDT/DCP modified PP(HF22) containing long Rockwool fibre (30% loading and A-1100 silane coupled)

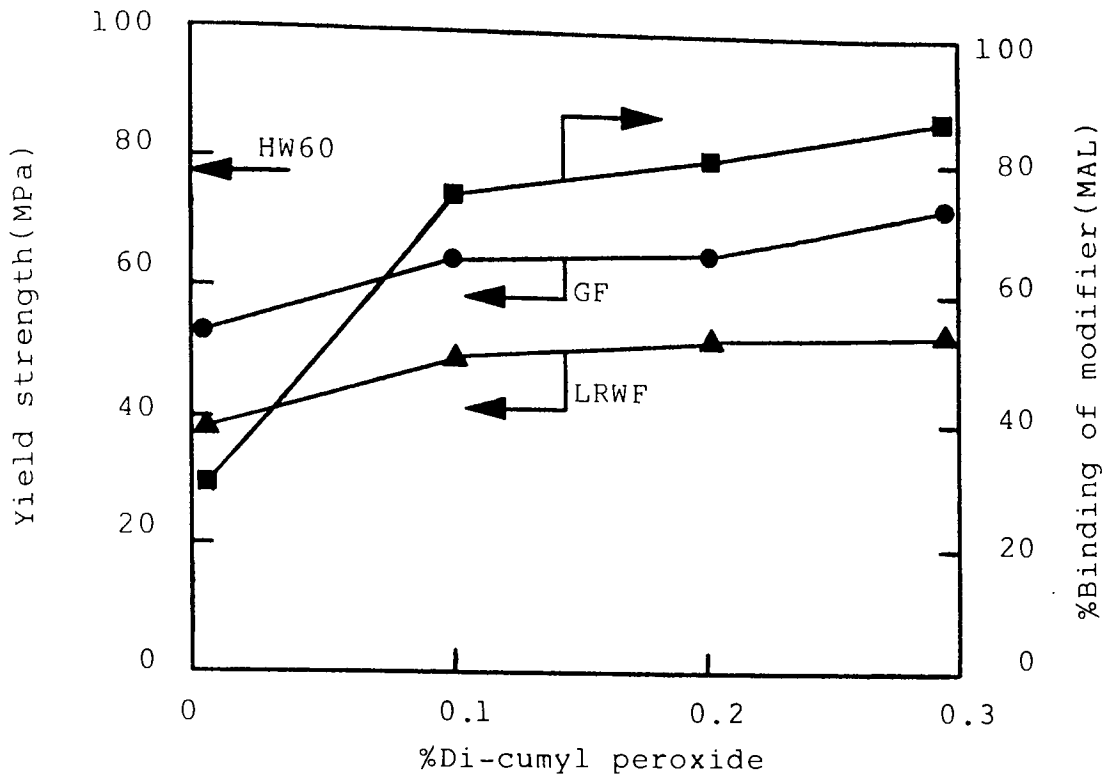


Figure 5.1 Effect of di-cumyl peroxide on the %Binding of 1% MAL in PP(HF22). The yield strength of this modified PP(HF22) containing 30% glass fibre (GF) and 30% long Rockwool fibre (LRWF) is shown. HW60 (commercially 30% GF coupled PP) is the control.

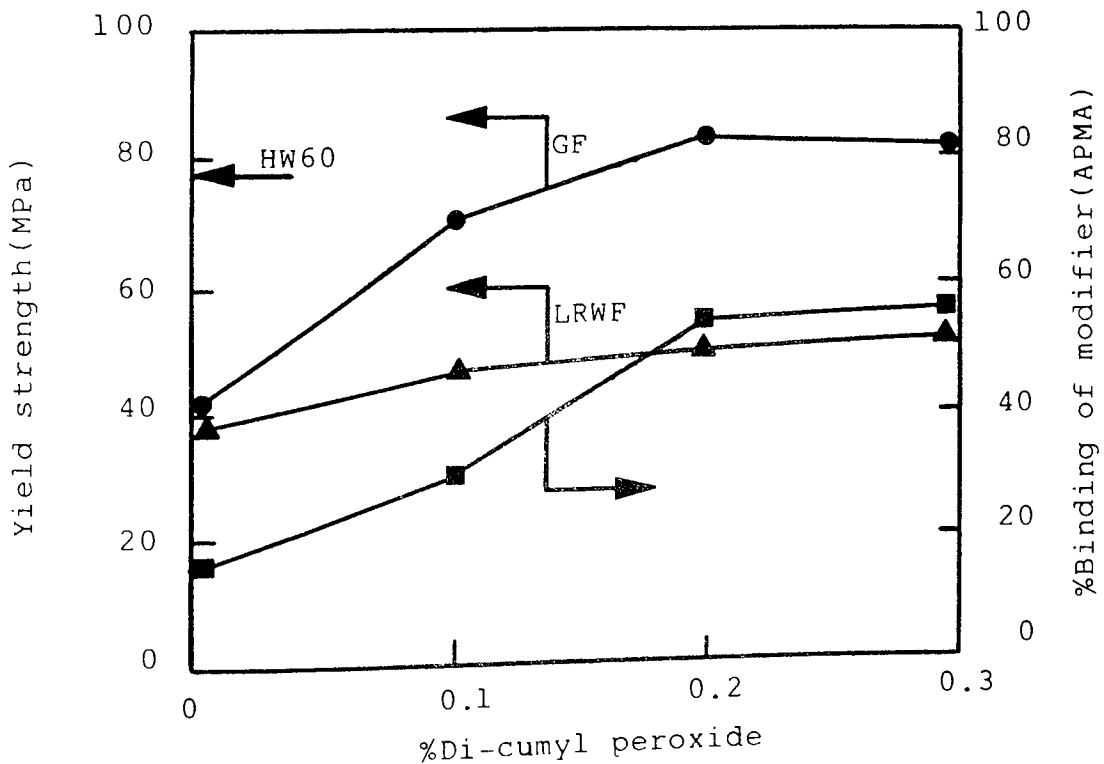


Figure 5.2 Effect of DCP on %Binding of 1% APMA in PP (HF22). Yield strength of this modified PP(HF22) containing 30% GF and 30% LRWF is shown. HW60 (commercially 30% GF coupled PP) is the control.

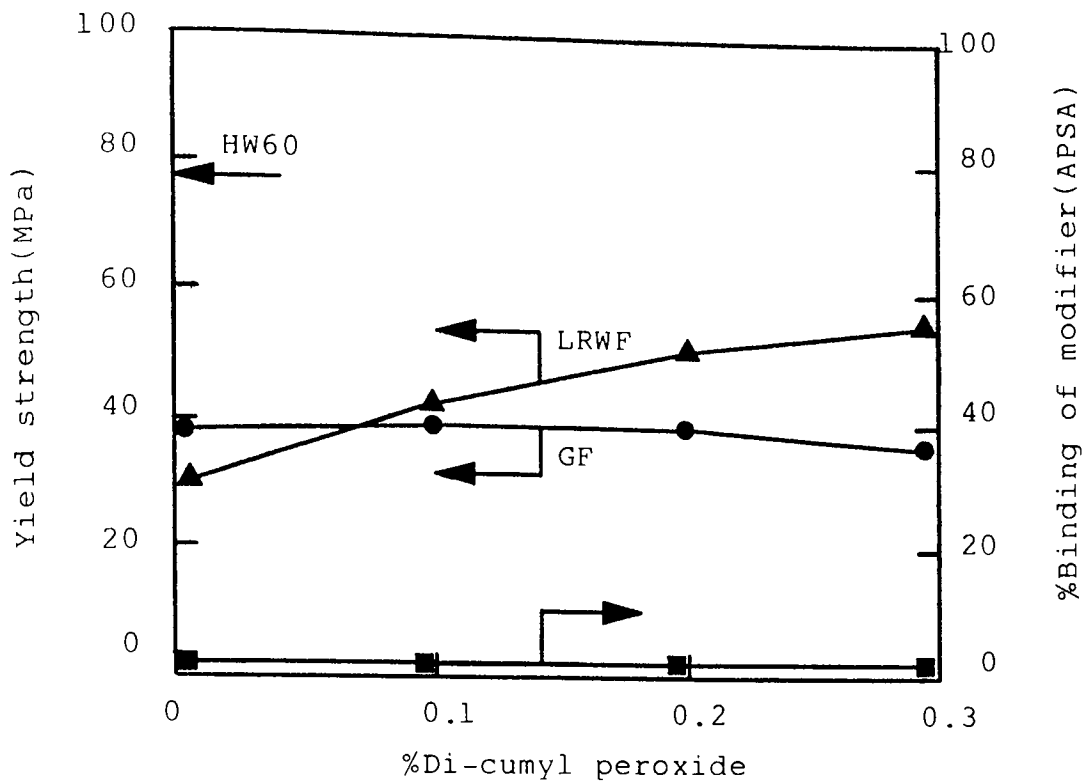


Figure 5.3 Effect of di-cumyl peroxide on the %Binding of 1%APSA in PP(HF22).The yield strength of this modified PP(HF22) containing 30%glass fibre(GF) and 30%long Rockwool fibre(LRWF) is shown.HW60 (commercially 30%GF coupled PP) is the control.

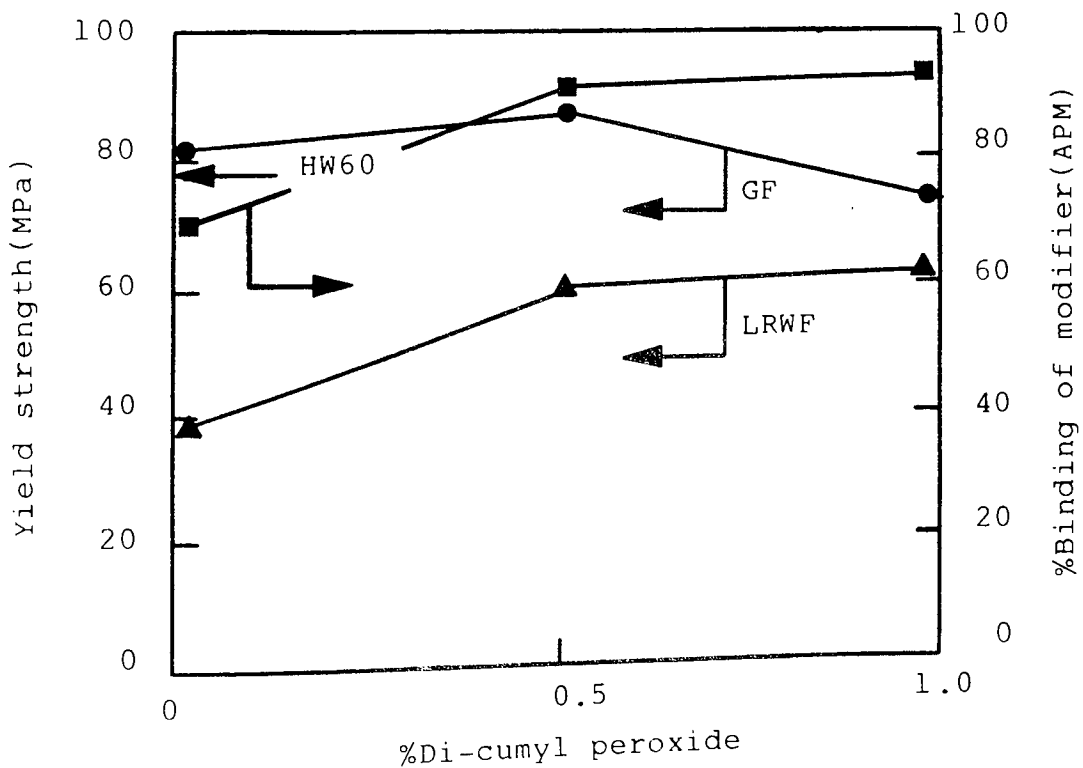


Figure 5.4 Effect of DCP on %Binding of 1%APM in PP (HF22).Yield strength of this modified PP (HF22) containing 30%GF and 30%LRWF is shown. HW60 (commercially 30%GF coupled PP)is control.

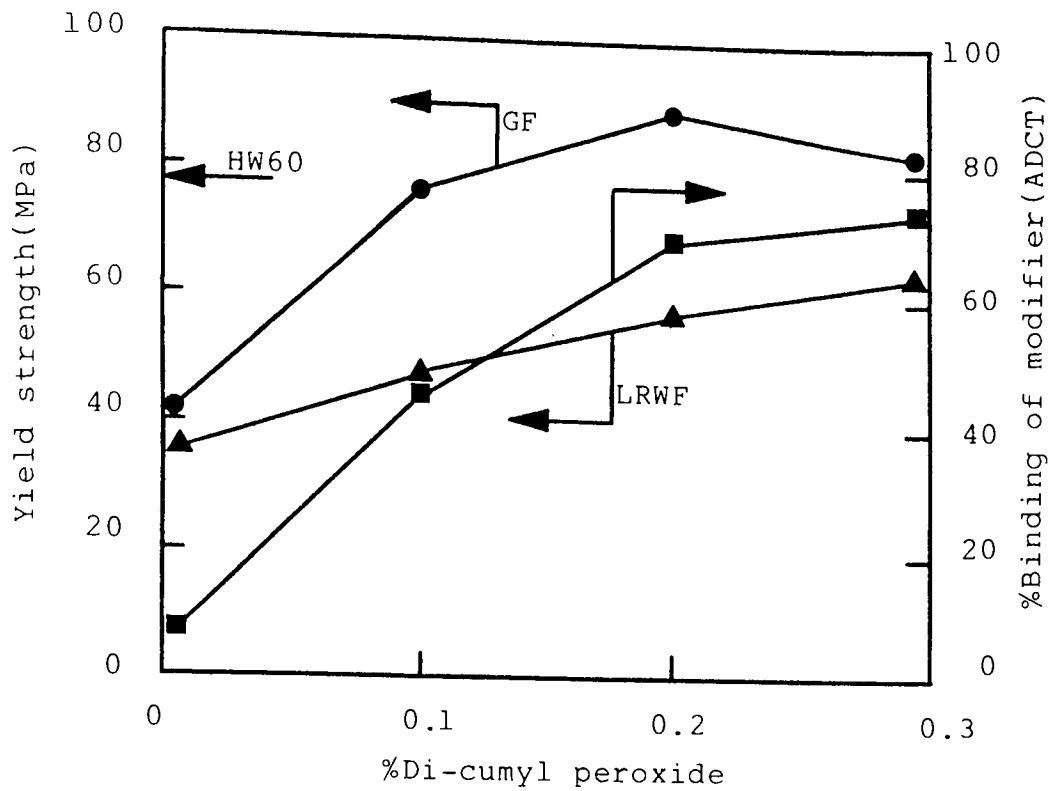


Figure 5.5 Effect of di-cumyl peroxide on the %Binding of 1%ADCT in PP(HF22).The yield strength of this modified PP(HF22) containing 30%glass fibre(GF) and 30%long Rockwool fibre(LRWF) is shown.HW60 (commercially 30%GF coupled PP) is the control.

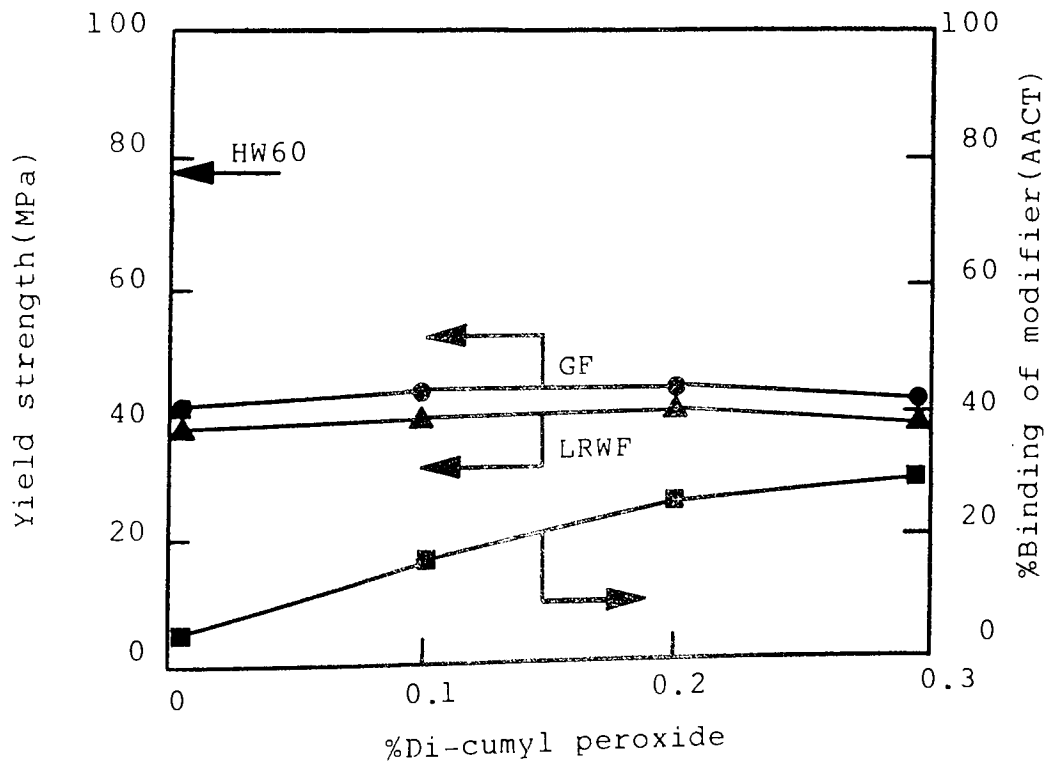


Figure 5.6 Effect of DCP on %Binding of 1%AACT in PP (HF22).Yield strength of this modified PP (HF22) containing 30%GF and 30%LRWF is shown. HW60 (commercially 30%GF coupled PP) is control.

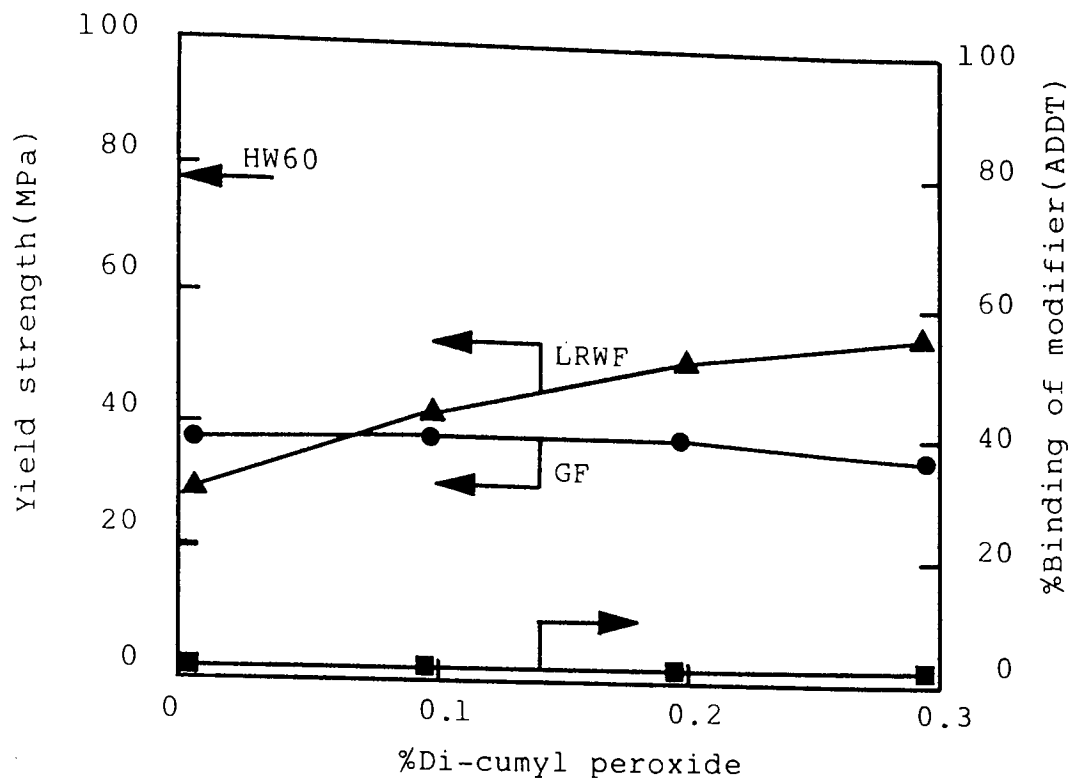


Figure 5.7 Effect of di-cumyl peroxide on the %Binding of 1%ADDT in PP(HF22).The yield strength of this modified PP(HF22) containing 30%glass fibre(GF) and 30% long Rockwool fibre(LRWF) is shown.HW60 (commercially 30%GF coupled PP) is the control.

No.	Composite	Yield Strength MPa	Tensile Modulus GPa	Flexural Strength MPa	Flexural Modulus GPa	Charpy Impact Strength kJm <sup>-2</sup>
1	HW60/GR30	77 (1.21)	3.0 (0.11)	94 (1.10)	6.50 (0.08)	158 (1.91)
2	1%MA/0.2%DCP	101 (1.01)	4.3 (0.12)	126 (1.11)	8.32 (0.06)	316 (1.51)
3	1%MAL/0.3%DCP	72 (1.01)	3.26 (0.13)	80 (1.10)	5.22 (0.07)	122 (2.37)
4	1%APMA/0.2%DCP	85 (1.11)	3.90 (0.09)	108 (1.01)	7.46 (0.06)	152 (2.21)
5	1%APSA/0.2%DCP	39 (0.99)	2.95 (0.10)	42 (1.01)	5.84 (0.06)	76 (2.31)
6	1%APM/0.5%DCP	84 (1.02)	3.95 (0.12)	103 (1.07)	7.70 (0.09)	168 (2.11)
7	1%ADCT/0.2%DCP	87 (1.07)	3.85 (0.14)	115 (1.05)	7.67 (0.08)	181 (1.98)
8	1%AACT/0.2%DCP	42 (1.10)	3.30 (0.12)	53 (1.05)	6.95 (0.07)	108 (1.91)
9	1%ADDT/0.2%DCP	38 (1.03)	2.97 (0.10)	41 (1.09)	5.85 (0.07)	75 (2.11)
10	HF22/30%GF	39 (1.30)	2.3 (0.12)	45 (1.10)	6.20 (0.08)	110 (1.41)

Table 5.8A Comparison of the optimised mechanical properties of chemically modified PP(HF22) containing glass fibre (30% loading and A-1100 silane coupled). HW60/GR30 (commercially 30%GF coupled PP) and PP(HF22)/30%GF are controls. Figures in brackets are standard deviations.



No.	Composite	Yield Strength MPa	Tensile Modulus GPa	Flexural Strength MPa	Flexural Modulus GPa	Charpy Impact Strength kJm <sup>-2</sup>
1	HW60/GR30	77 (1.21)	3.0 (0.11)	94 (1.10)	6.50 (0.08)	158 (1.91)
2	0.3%DCP	60 (0.91)	3.2 (0.13)	82 (1.07)	5.52 (0.06)	94 (1.45)
3	1%MAL/0.3%DCP	55 (1.05)	3.13 (0.15)	71 (1.01)	5.55 (0.07)	84 (2.00)
4	1%APMA/0.3%DCP	50 (1.08)	2.94 (0.10)	59 (1.17)	5.91 (0.07)	75 (1.92)
5	1%APSA/0.3%DCP	55 (1.16)	2.96 (0.16)	61 (1.11)	5.73 (0.07)	79 (1.93)
6	0.5%APM/0.5%DCP	56 (1.01)	3.21 (0.09)	74 (1.13)	5.74 (0.06)	83 (2.11)
7	1%ADCT/0.3%DCP	64 (1.20)	3.29 (0.08)	84 (1.20)	6.02 (0.08)	87 (2.08)
8	1%AACT/0.3%DCP	40 (1.15)	2.90 (0.10)	58 (1.06)	5.85 (0.07)	71 (2.05)
9	1%ADDT/0.3%DCP	53 (1.16)	2.98 (0.11)	60 (1.14)	5.92 (0.06)	80 (2.12)
10	HF22/30%LRWF	32 (1.35)	1.5 (0.11)	42 (1.27)	5.00 (0.08)	80 (1.47)

Table 5.8B Comparison of the optimised mechanical properties of chemically modified PP(HF22) containing long Rockwool fibre (30% loading and A-1100 silane coupled). HW60 (commercially 30%GF coupled PP) and PP(HF22)/30%LRWF are controls. Figures in brackets are standard deviations.

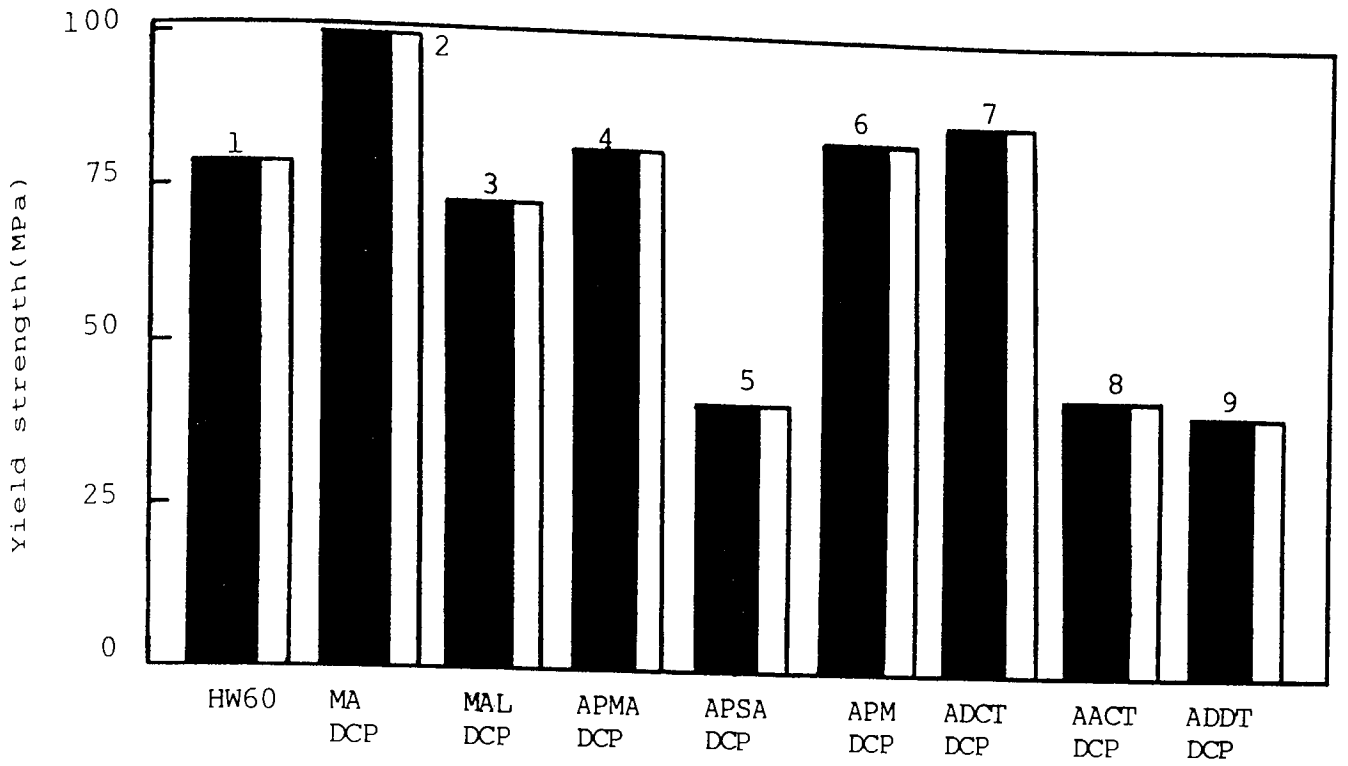


Figure 5.8A

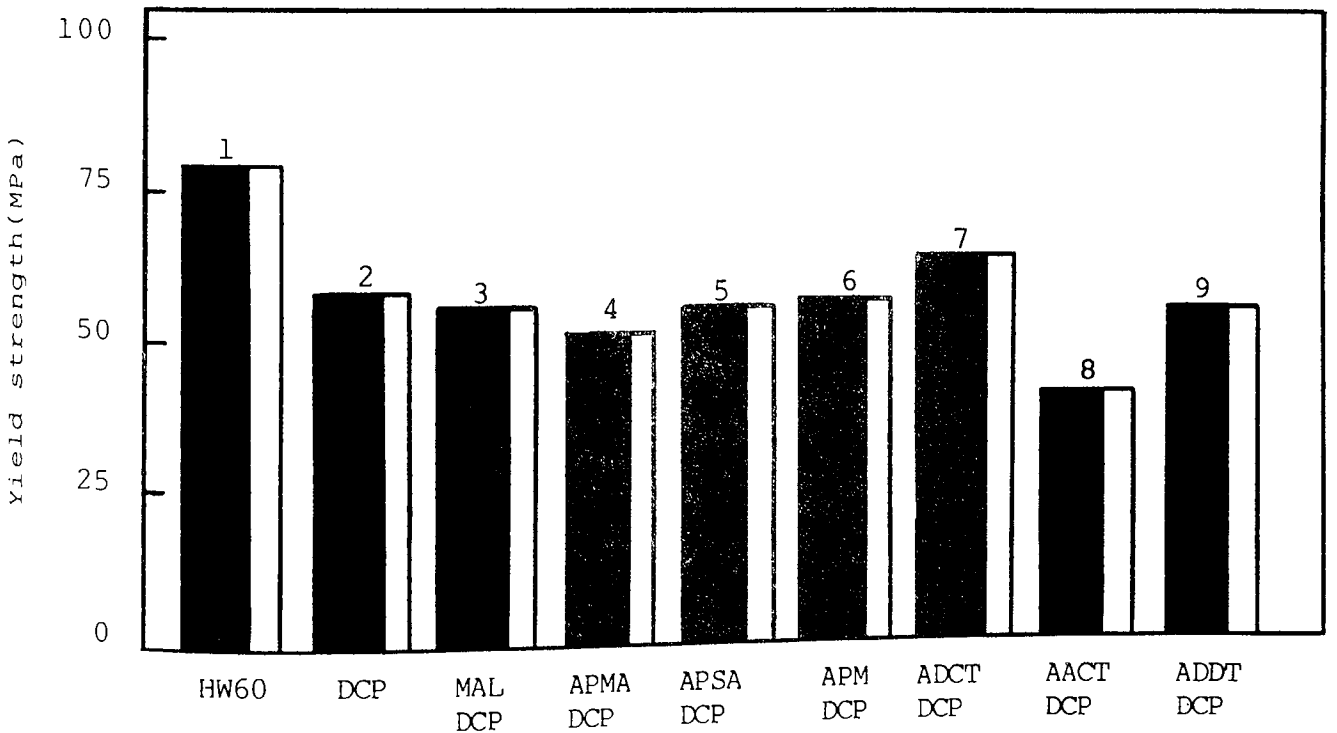


Figure 5.8B

Figure 5.8 Yield strength of chemically modified PP(HF22) containing 30%GF(A) and 30%LRWF(B), both A-1100 silane coupled. HW60 (commercially 30%GF coupled PP) is control. See Table 5.8A and B for details.

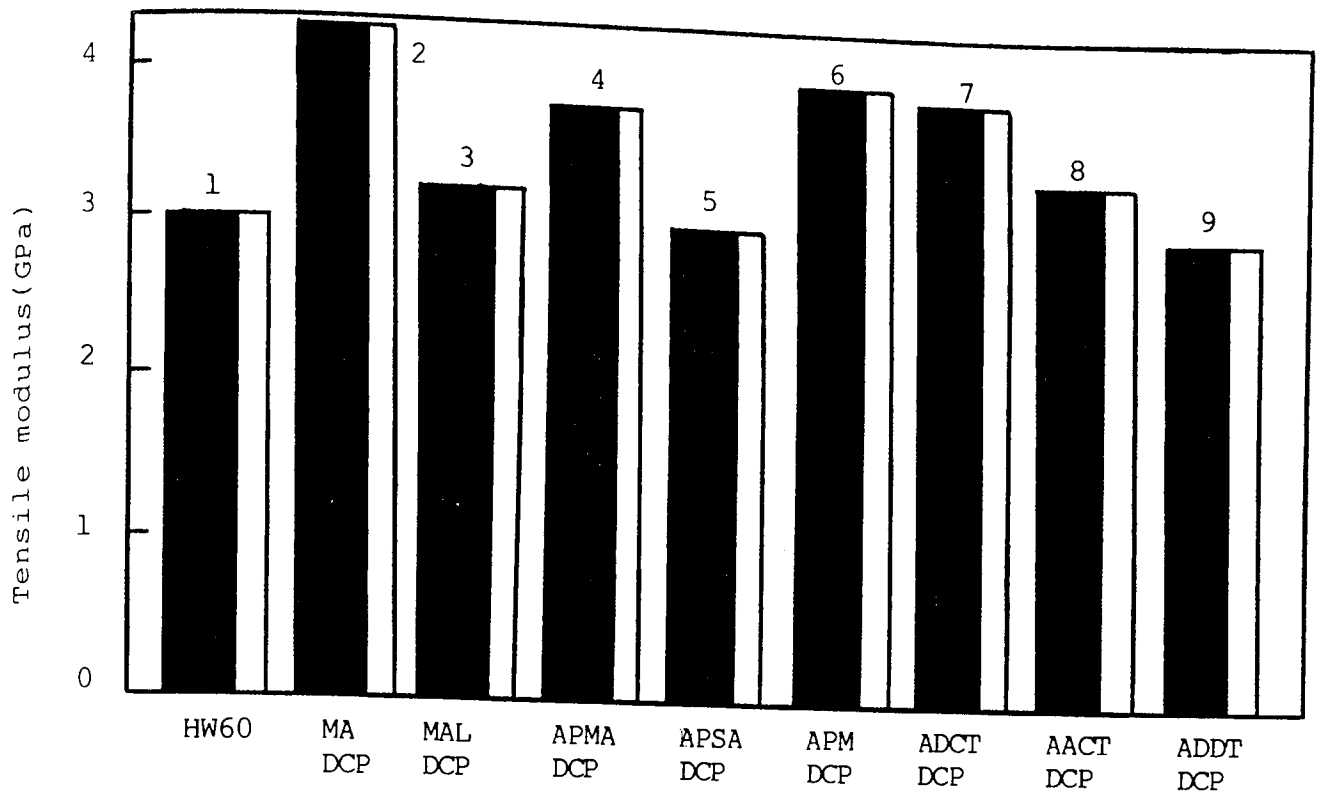


Figure 5.9A

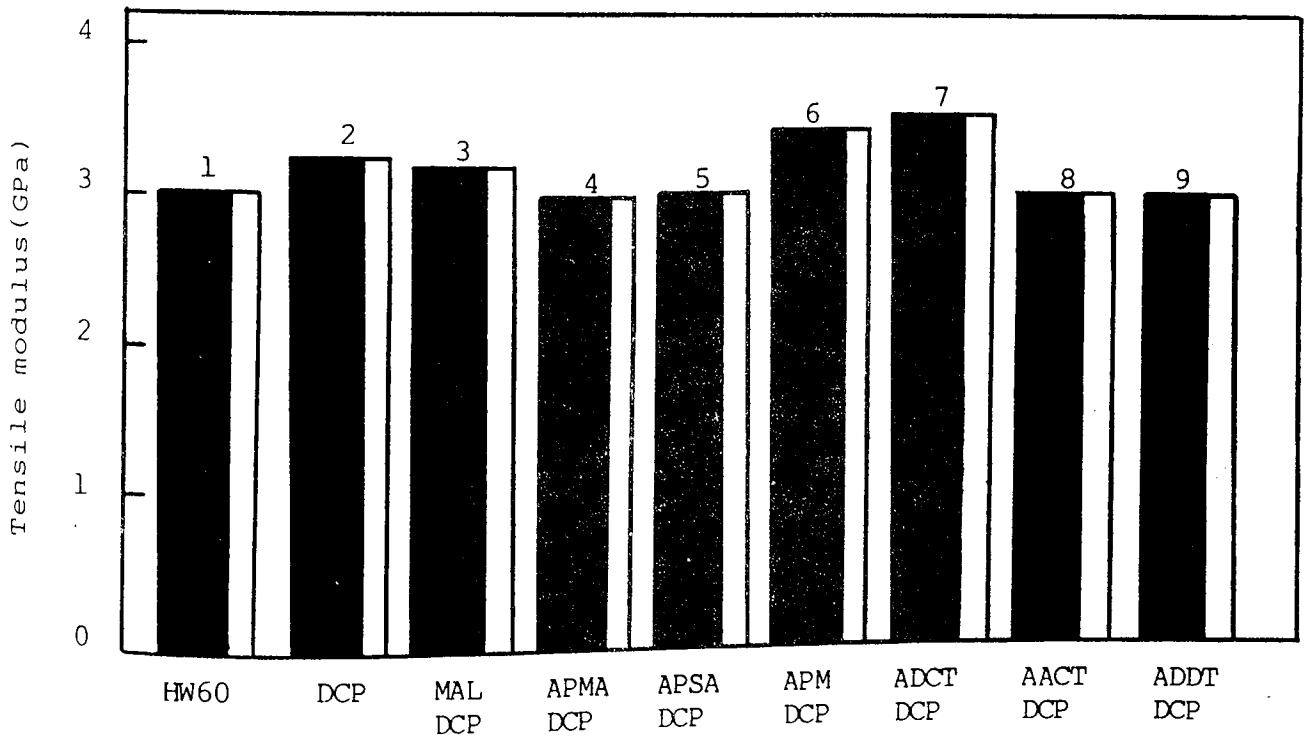


Figure 5.9B

Figure 5.9 Tensile modulus of chemically modified PP(HF22) containing 30%GF(A) and 30%LRWF(B), both A-1100 silane coupled. HW60 (commercially 30%GF coupled PP) is the control. See Table 5.8A and B for details.

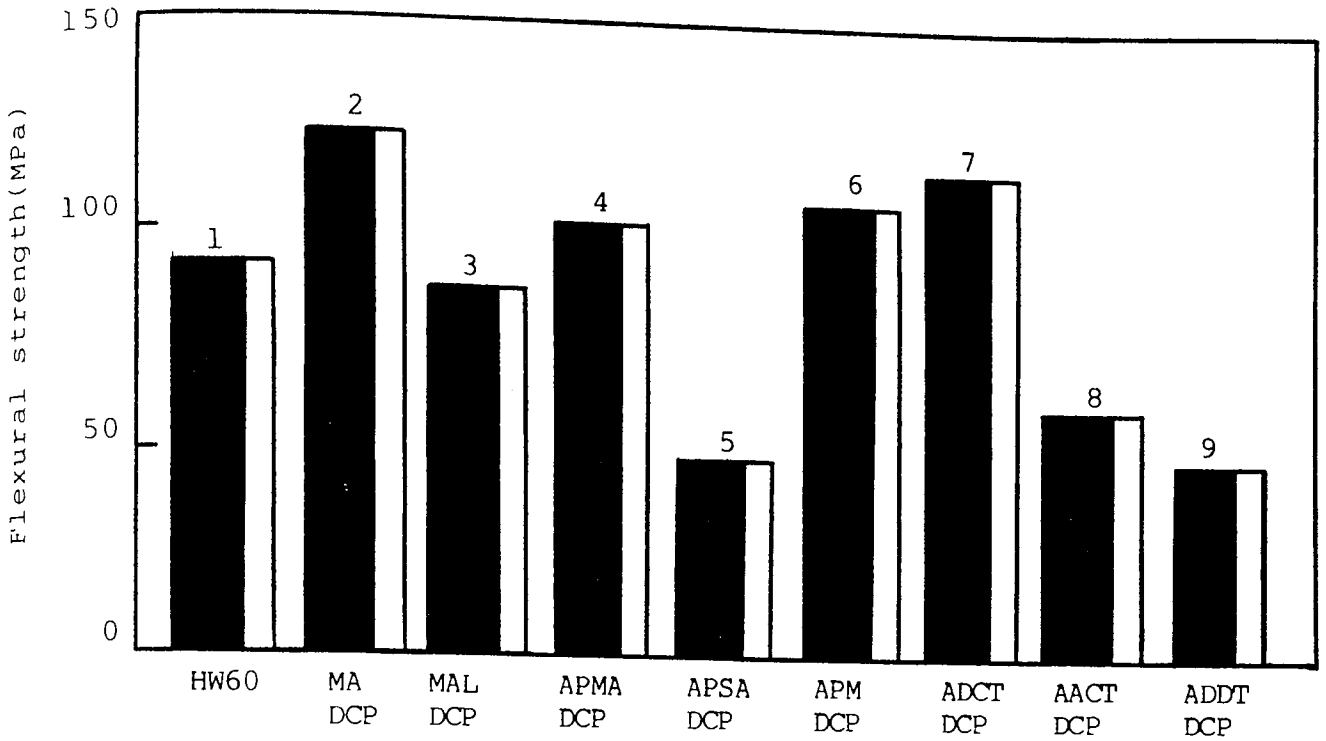


Figure 5.10A

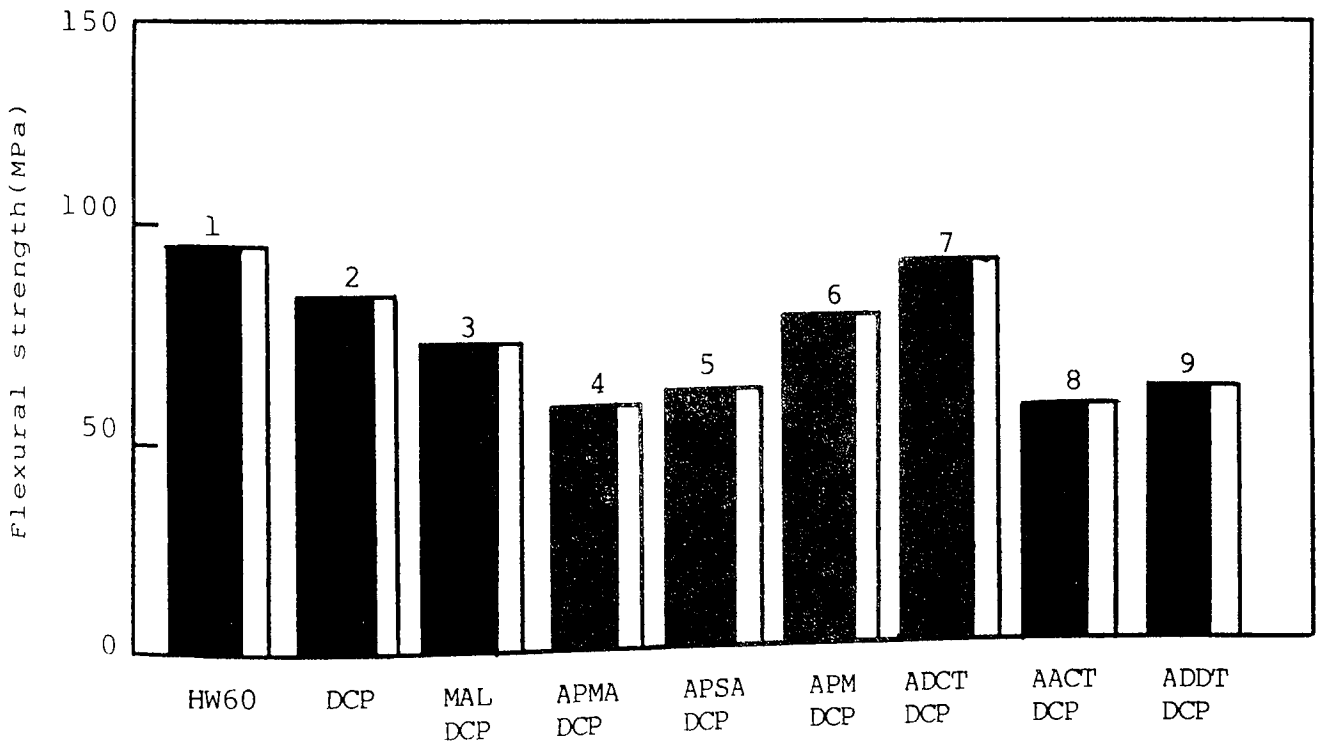


Figure 5.10B

Figure 5.10 Flexural strength of chemically modified PP(HF22) containing 30%GF(A) and 30%LRWF(B), both A-1100 silane coupled. HW60 (commercially 30%GF coupled PP) is the control. See Table 5.8A and B for details.

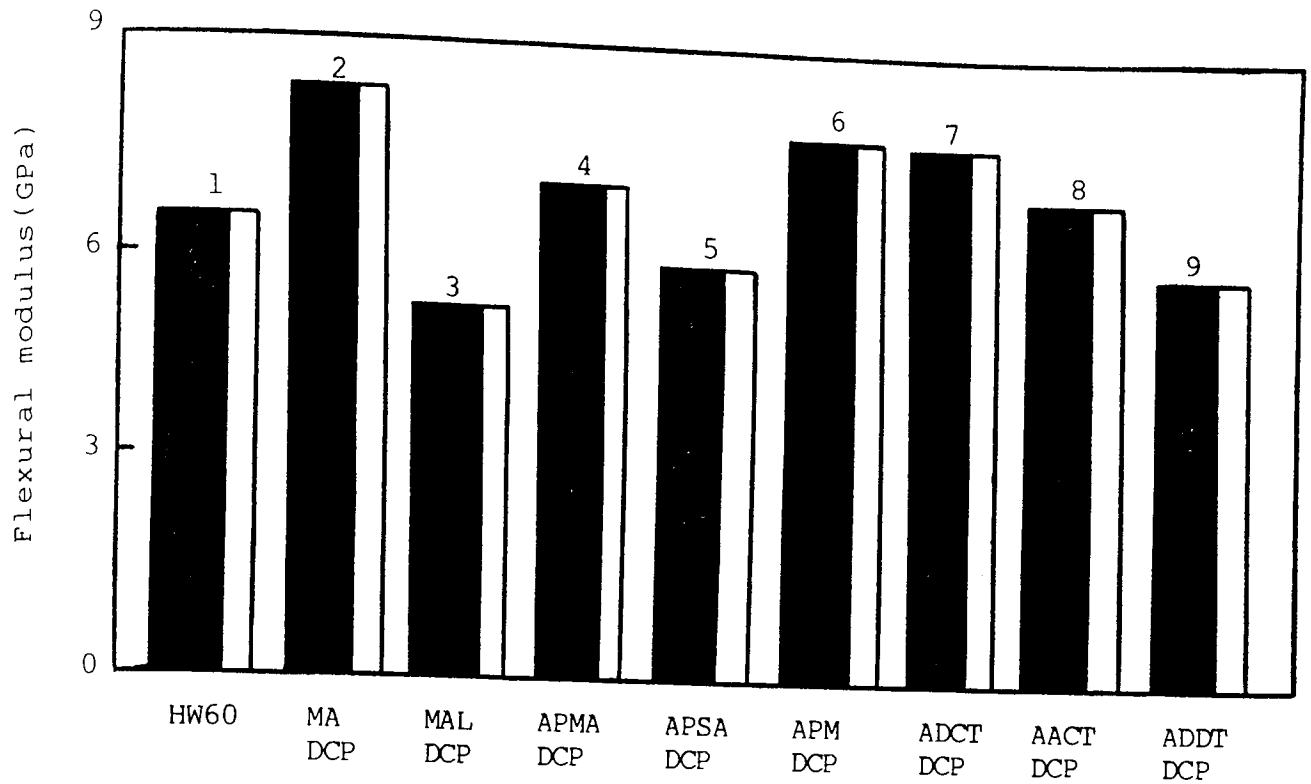


Figure 5.11A

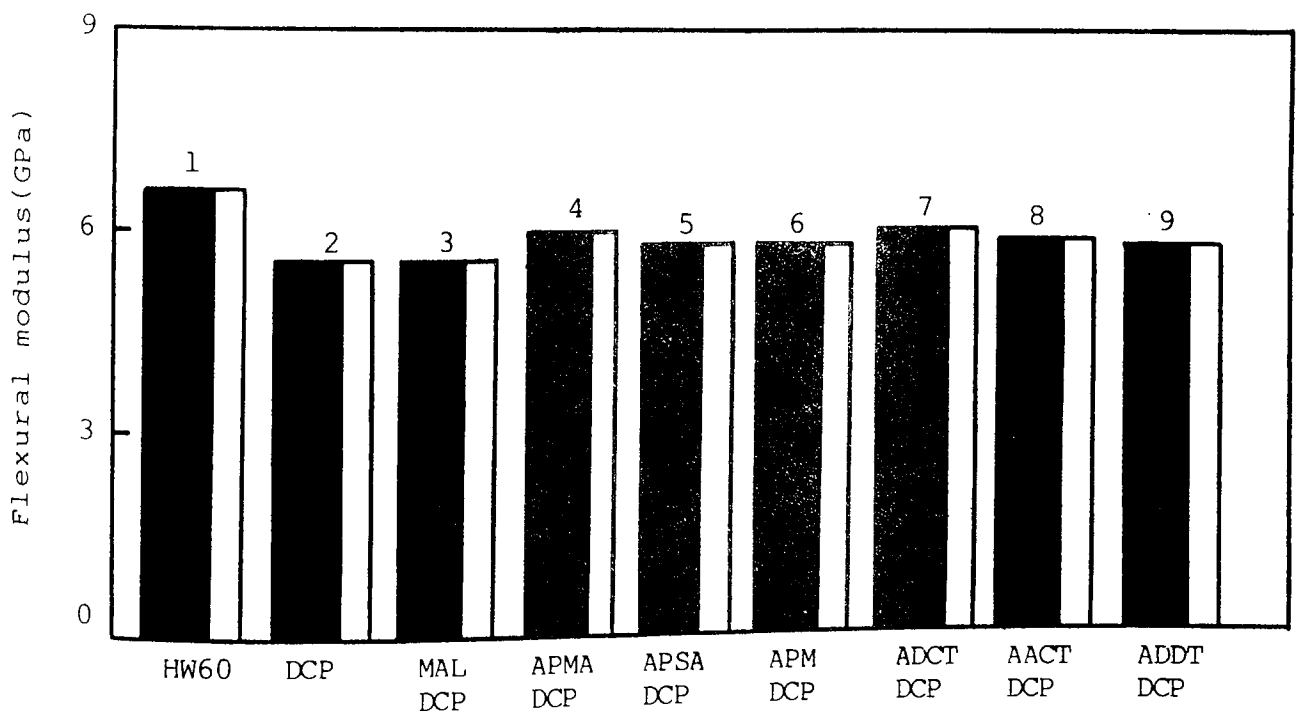


Figure 5.11B

Figure 5.11 Flexural modulus of chemically modified PP(HF22) containing 30%GF(A) and 30%LRWF(B), both A-1100 silane coupled. HW60 (commercially 30%GF coupled PP) is the control. See Table 5.8A and B for details.

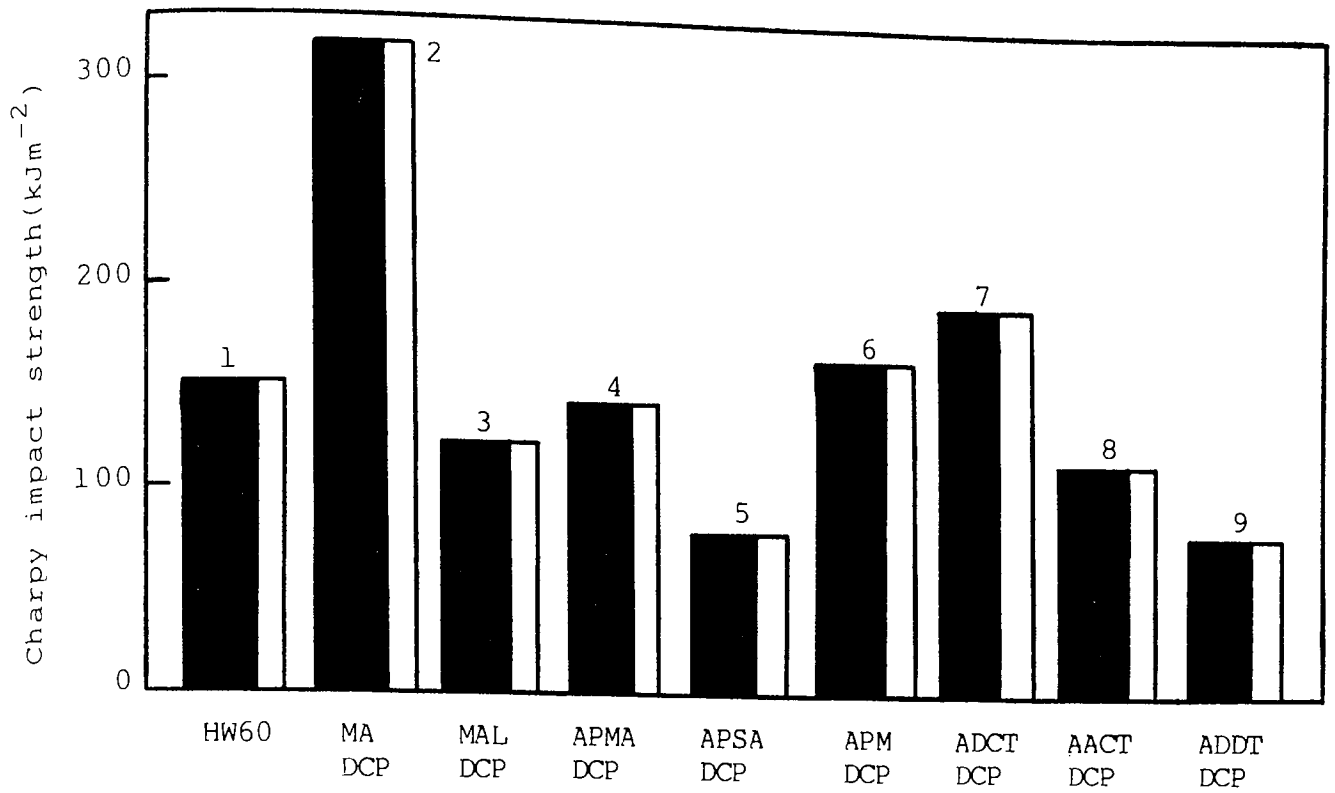


Figure 5.12A

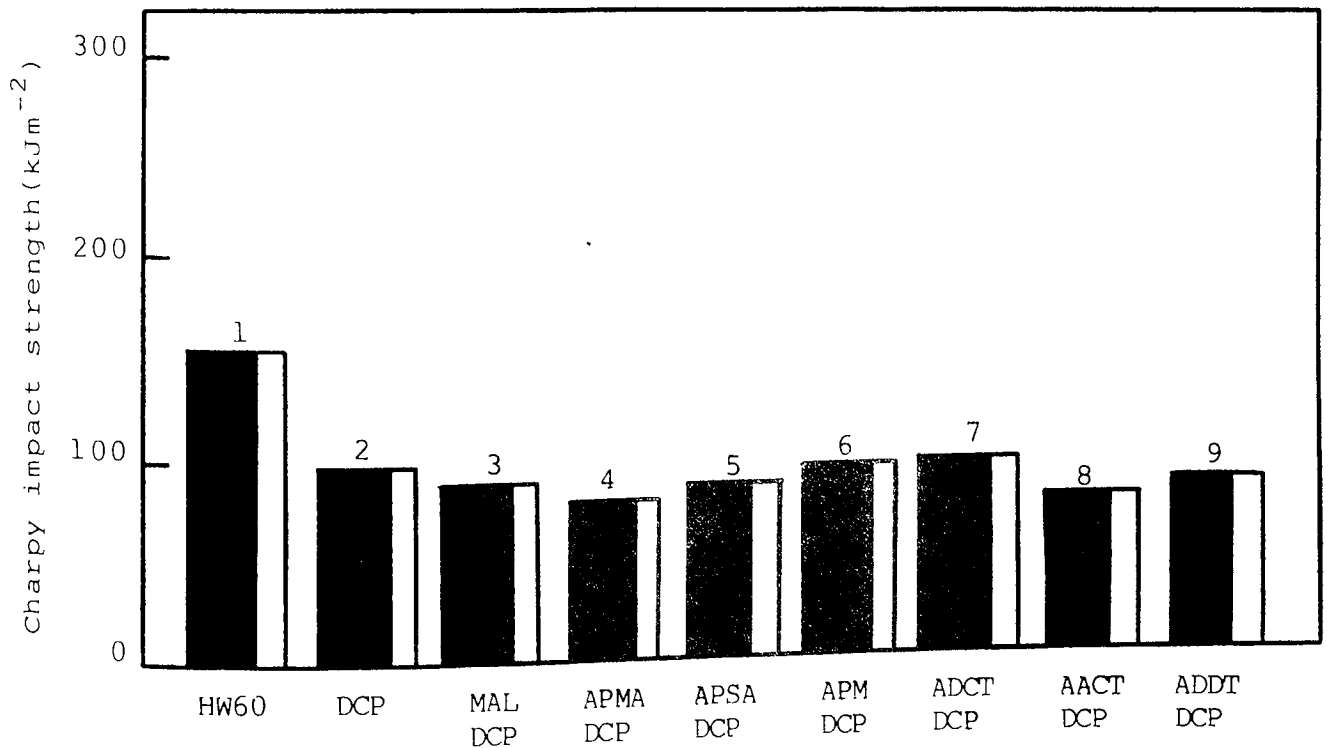


Figure 5.12B

Figure 5.12 Charpy impact strength (notched, 0.2mm) of chemically modified PP (HF22) containing 30%GF(A) and 30%LRWF(B), both A-1100 silane coupled. HW60 (commercially 30%GF coupled PP) is control. See Table 5.8A and B for details.

Sample No.	Polypropylene	Chemical Modifiers	Added Fibre (30%)	Added Stabiliser
1	HWM25	-	GF	-
2	HW60/GR30	-	-	-
3	HF22	1%MA/0.2%DCP	GF	0.4% Irganox1010
4	HF22	1%MA/0.2%DCP	GF	-
5	HF22	0.3%DCP	LRWF	-
6	HF22	1%MAL/0.3%DCP	GF	-
7	HF22	1%APMA/0.2%DCP	GF	-
8	HF22	0.5%APM/0.25%DCP	GF	-
9	HF22	1%APM/0.5%DCP	GF	-
10	HF22	1%ADCT/0.2%DCP	GF	-

Table 5.9 Type of chemical modification of PP(HF22) and fibre used for long term durability testing in Gunk, Brake fluid and Ajax. HW60(30%GF coupled PP) and PP(HWM25)/30% GF are controls.

Sample No.	Yield Strength(MPa)			%Retention of Yield Strength After 4 Weeks			
	Initial	After 4 Weeks in:			Ajax	Brake Fluid	Gunk
		Ajax	Brake Fluid	Gunk			
1	34	28	27	18	83	80	54
2	77	73	76	38	95	98	48
3	83	82	83	55	99	100	66
4	93	91	91	55	98	98	59
5	58	51	58	36	88	100	62
6	72	64	71	38	89	99	53
7	85	63	52	27	74	61	32
8	78	61	57	27	78	73	35
9	84	72	62	30	86	74	36
10	89	88	85	55	99	95	62

Table 5.10 Effect of immersion in Gunk, Brake fluid and Ajax for 4 weeks at 65°C on the yield strength of chemically modified PP(HF22) containing 30% fibre (GF and LRWF). See Table 5.9 for sample compositions.



Sample No.	Tensile Modulus (GPa)			%Retention of Tensile Modulus After 4 Weeks			
	Initial	After 4 Weeks in:		Ajax	Brake Fluid	Gunk	
		Ajax	Brake Fluid	Gunk	Ajax	Brake Fluid	Gunk
1	2.20	1.91	1.76	0.59	87	80	27
2	3.00	2.75	2.64	1.17	92	88	39
3	3.87	3.75	3.73	2.07	97	97	54
4	4.06	3.86	3.76	2.21	95	93	55
5	3.35	3.01	2.92	1.32	89	87	40
6	3.26	3.12	2.45	1.61	96	75	49
7	3.90	3.50	3.65	1.89	90	94	49
8	4.00	3.62	3.73	2.09	91	93	52
9	3.95	3.90	3.59	2.02	98	91	51
10	3.86	3.71	3.71	2.12	96	96	55

Table 5.11 Effect of immersion in Gunk, Brake fluid and Ajax for 4 weeks at 65°C on the tensile modulus of chemically modified PP(HF22) containing 30% fibre (GF and LRWF). See Table 5.9 for sample compositions.

Sample No.	Flexural Strength(MPa)			%Retention of Flexural Strength After 4 Weeks			
	Initial	After 4 Weeks in:			Ajax	Brake Fluid	Gunk
		Ajax	Brake Fluid	Gunk			
1	50	42.5	46.5	26	85	93	52
2	94	84	89	55	89	95	58
3	106	95	101	71	90	95	67
4	125	108	118	80	86	95	64
5	85	70	80	58	82	94	68
6	80	66	75	51	83	94	64
7	108	68	61	48	63	56	44
8	96	68	67	43	71	70	45
9	103	75	66	46	73	64	45
10	115	106	110	76	92	96	66

Table 5.12 Effect of immersion in Gunk, Brake fluid and Ajax for 4 weeks at 65°C on the flexural strength of chemically modified PP(HF22) containing 30% fibre (GF and LRWF). See Table 5.9 for sample compositions.

Sample No.	Flexural Modulus(GPa)			%Retention of Flexural Modulus After 4 Weeks			
	Initial	After 4 Weeks in:			Ajax	Brake Fluid	Gunk
		Ajax	Brake Fluid	Gunk			
1	6.20	5.76	4.89	0.87	93	79	14
2	6.50	6.37	5.98	3.90	98	92	60
3	7.07	6.88	6.40	4.33	97	90	61
4	8.20	7.55	7.30	4.91	92	89	60
5	5.55	5.50	5.04	2.71	99	91	49
6	5.22	5.03	4.67	2.73	96	89	52
7	7.46	7.21	6.12	4.80	97	82	64
8	7.89	7.27	6.55	4.02	92	83	51
9	7.70	7.60	6.94	4.23	98	86	55
10	7.69	7.53	6.84	4.84	98	89	63

Table 5.13 Effect of immersion in Gunk, Brake fluid and Ajax for 4 weeks at 65°C on the flexural modulus of chemically modified PP(HF22) containing 30% fibre (GF and LRWF). See Table 5.9 for sample compositions.

Figure 5.13 Yield strength of chemically modified PP(HF22) containing 30% glass fibre(GF) and 30% long Rockwool fibre(LRWF) before(A) and after(B) 4 weeks immersion in Brake fluid(65°C).%Retention of yield strength after 4 weeks immersion is shown in the upper scale.HW60(30%GF coupled PP) and PP(HWM25)/30%GF are controls.See Table 5.10 for details.

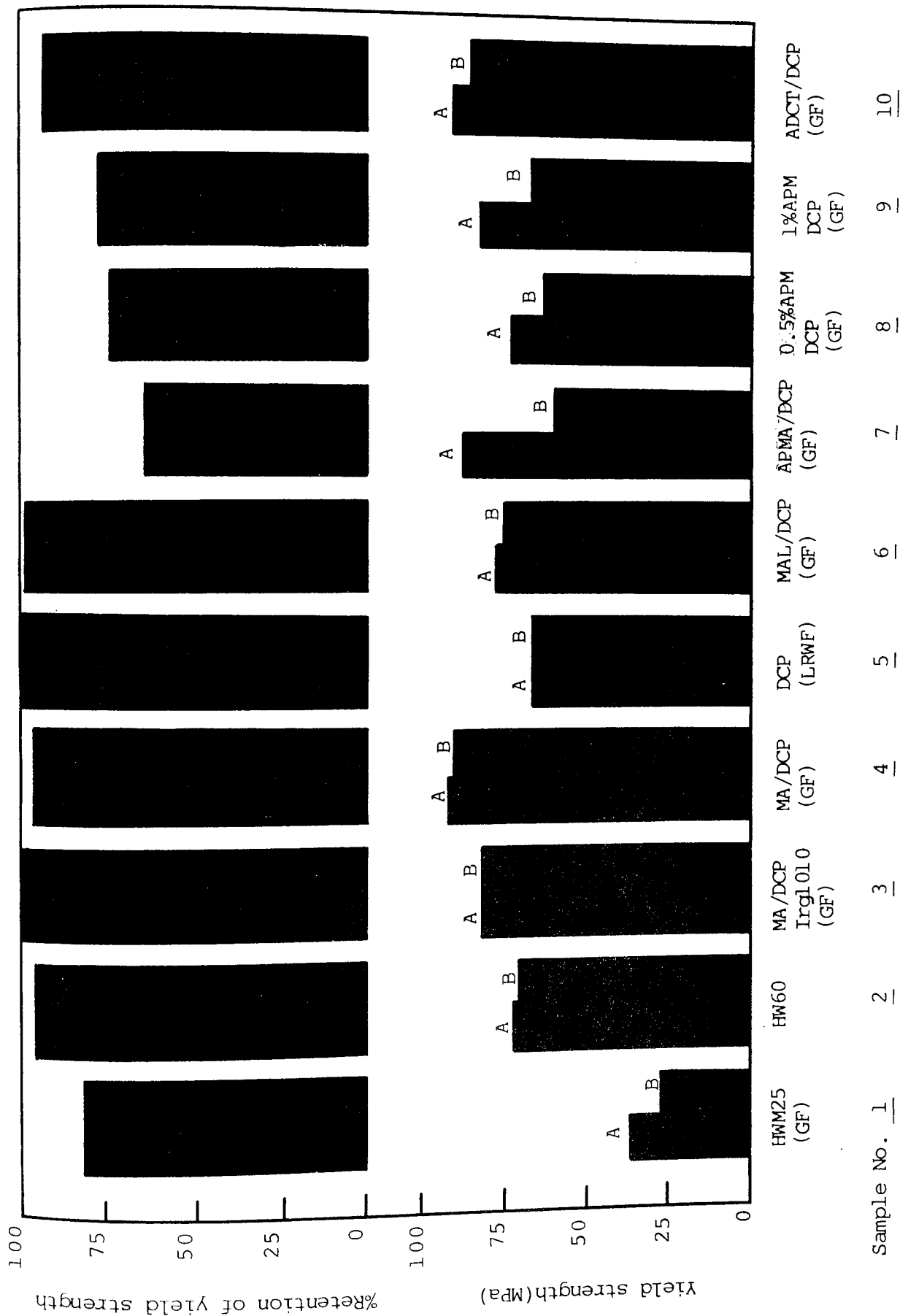


Figure 5.14 Yield strength of chemically modified PP(HF22) containing 30% glass fibre(GF) and 30% long Rockwool fibre(LRWF) before (A) and after (B) 4 weeks immersion in 2% aqueous Ajax solution (65°C).%Retention of yield strength after 4 weeks immersion is shown in the upper scale.HW60(30%GF coupled PP) and PP(HWM25)/30%GF are controls.See Table 5.10 for details.

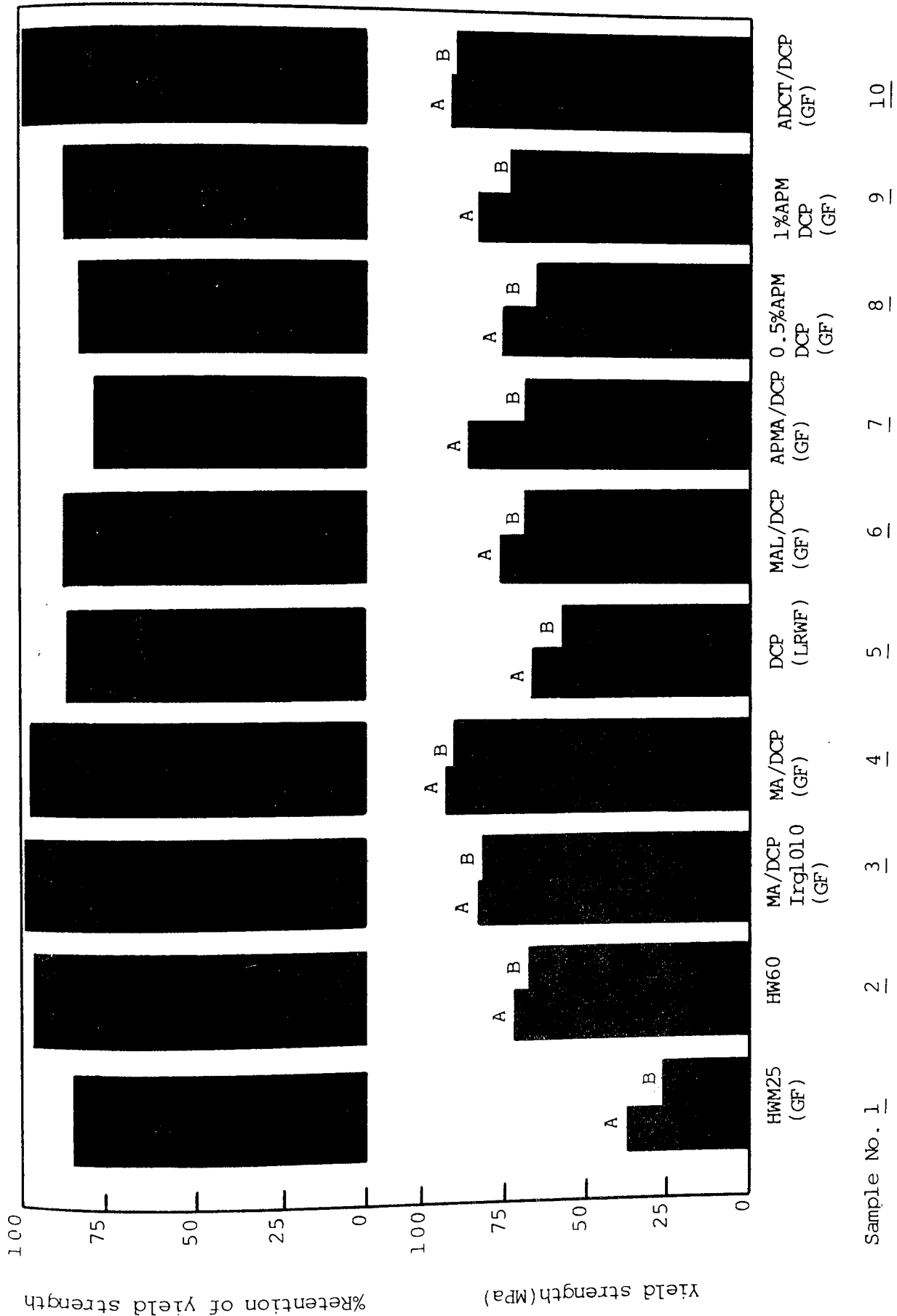
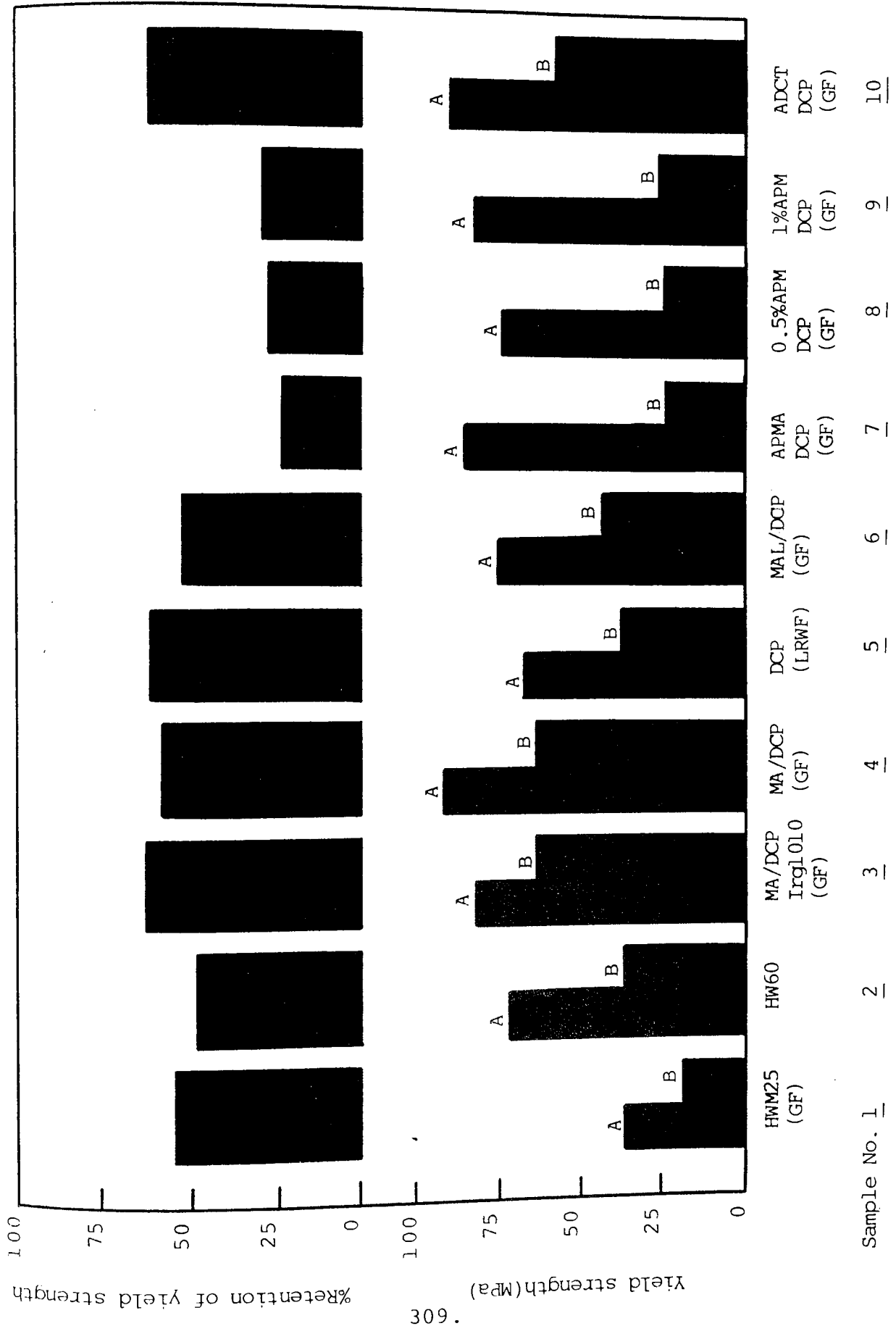


Figure 5.15 Yield strength of chemically modified PP(HF22) containing 30% glass fibre(GF) and 30% long Rockwool fibre(LRWF)before(A) and after(B) 4 weeks immersion in Gunk engine cleaning fluid(65°C). %Retention of yield strength after 4 weeks immersion is shown in the upper scale.HW60(30%GF coupled PP)and PP(HWM25)/30%GF are controls. See Table 5.10 for details.



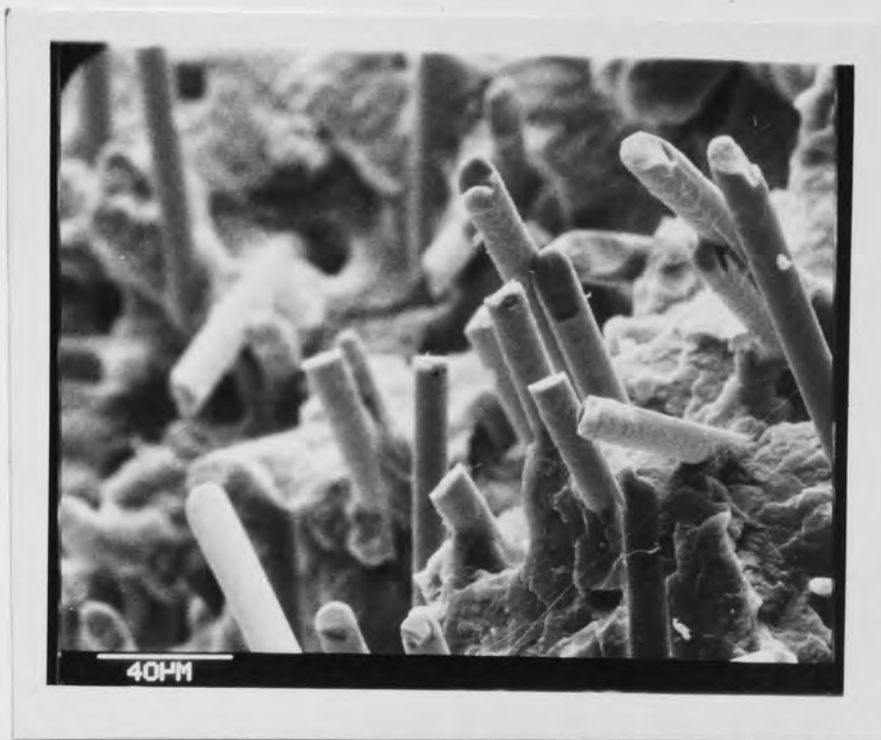


Plate 5.1 Scanning electron micrograph of the tensile fracture surface of 1%ADCT/0.2%DCP modified unstabilised PP(HF22) containing 30% glass fibre (A-1100 silane coupled)



Plate 5.2 Scanning electron micrograph of the tensile fracture surface of 1%ADCT/0.2%DCP modified unstabilised PP(HF22) containing 30% glass fibre (A-1100 silane coupled) after 4 weeks Gunk immersion (65°C) 310.

Sample No.	Polymer	Chemical Modifier	Added Fibre (30%)	Charpy Impact Strength ( $\text{kJm}^{-2}$ ) at:		
				-40°C	-20°C	0°C +20°C
1C	HWM25	-	-	31	33	34 44
2C	HW60/GR30	-	-	145	155	177 158
3	HF22	-	GF	110	113	114 105
4	HF22	-	LRWF	52	56	72 81
5	HF22	1%MA/0.2%DCP	GF	182	184	196 316
6	HF22	0.3%DCP	LRWF	70	69	72 94
7	HF22	1%MAL/0.3%DCP	GF	142	137	142 122
8	HF22	1%APMA/0.2%DCP	GF	112	115	118 152
9	HF22	1%APM/0.5%DCP	GF	135	148	160 168
10	HF22	1%ADCT/0.2%DCP	GF	201	207	223 181

Table 5.14 Effect of temperature on the Charpy impact strength (notched, 0.2mm) of chemically modified PP(HF22) containing glass fibre(GF) and long Rockwool fibre(LRWF, both 30% loading and A-1100 silane coupled). HW60/GR30 (30%GF coupled PP) and PP(HWM25) are commercial controls.



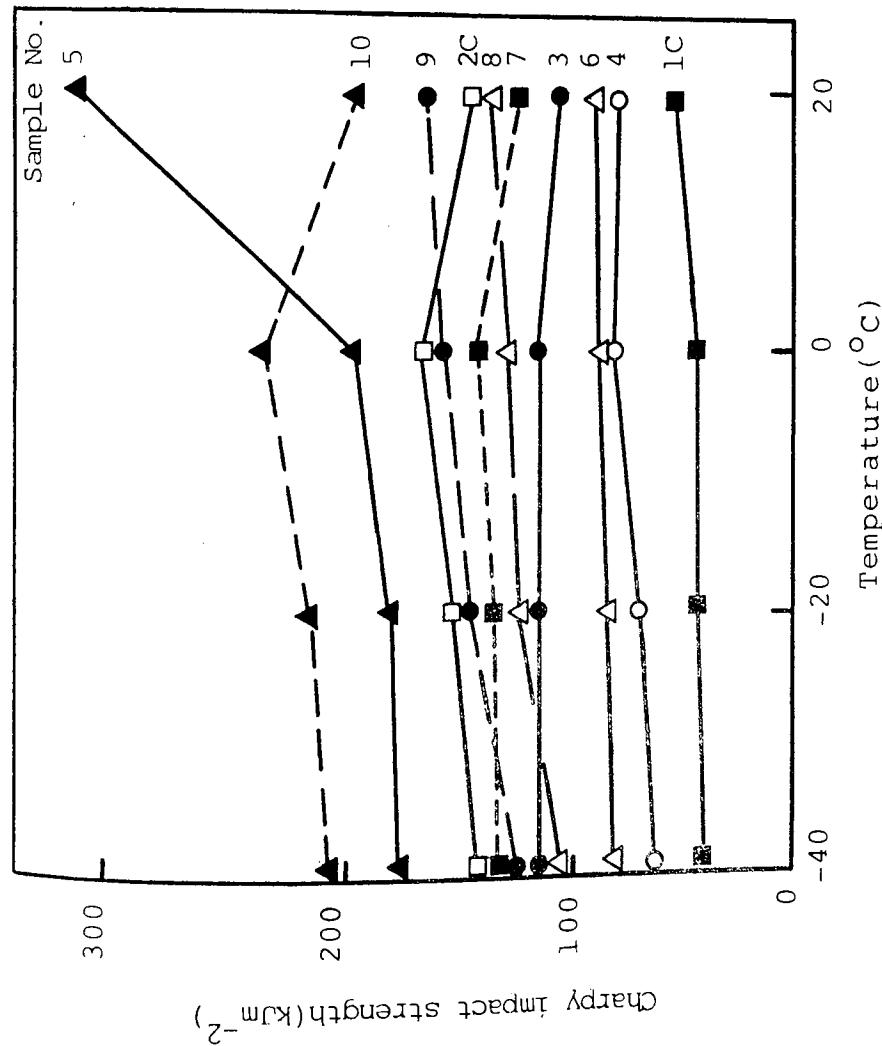


Figure 5.16A Effect of temperature on Charpy impact strength (notched, 0.2mm) of chemically modified PP (HF22) containing fibres (30%). HW60(2C, 30%GF coupled PP) and PP(1C, HWM25) are commercial controls. See Table 5.14 for details.

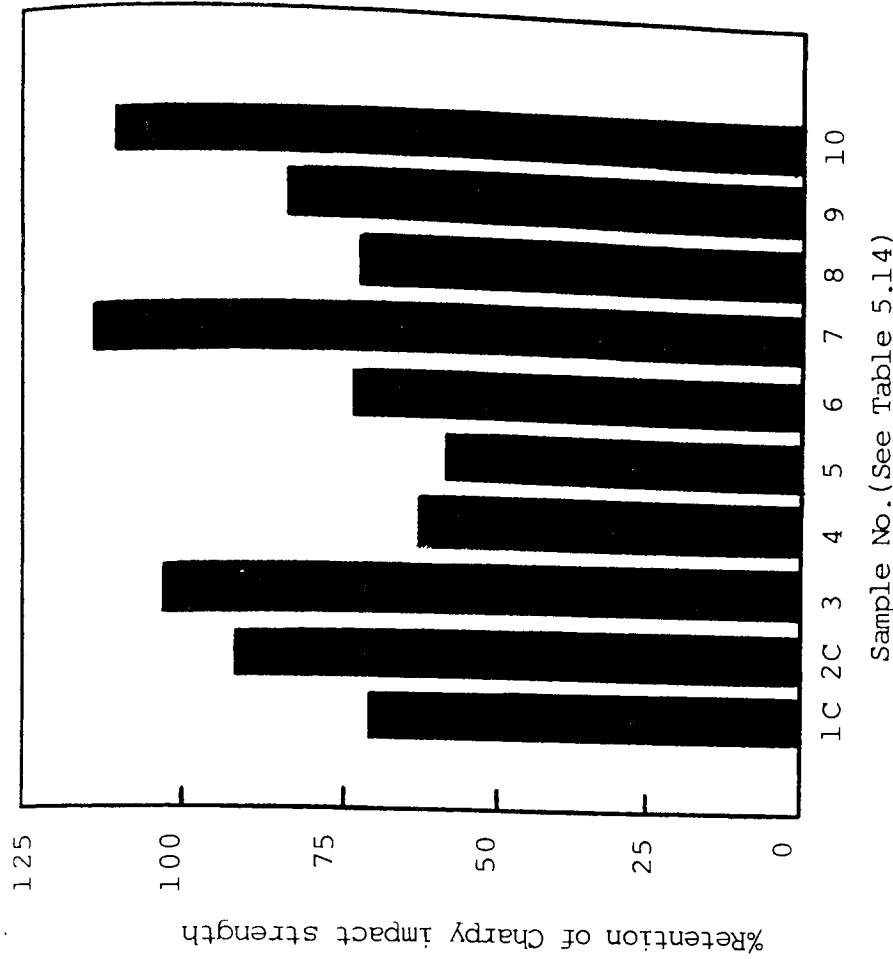


Figure 5.16B %Retention of Charpy impact strength (notched, 0.2mm) on temperature reduction from 20°C to -40°C of chemically modified PP(HF22) containing fibres(30%). HW60(2C, 30%GF coupled PP) and PP(1C, HWM25) are commercial controls. See Table 5.14 for details.

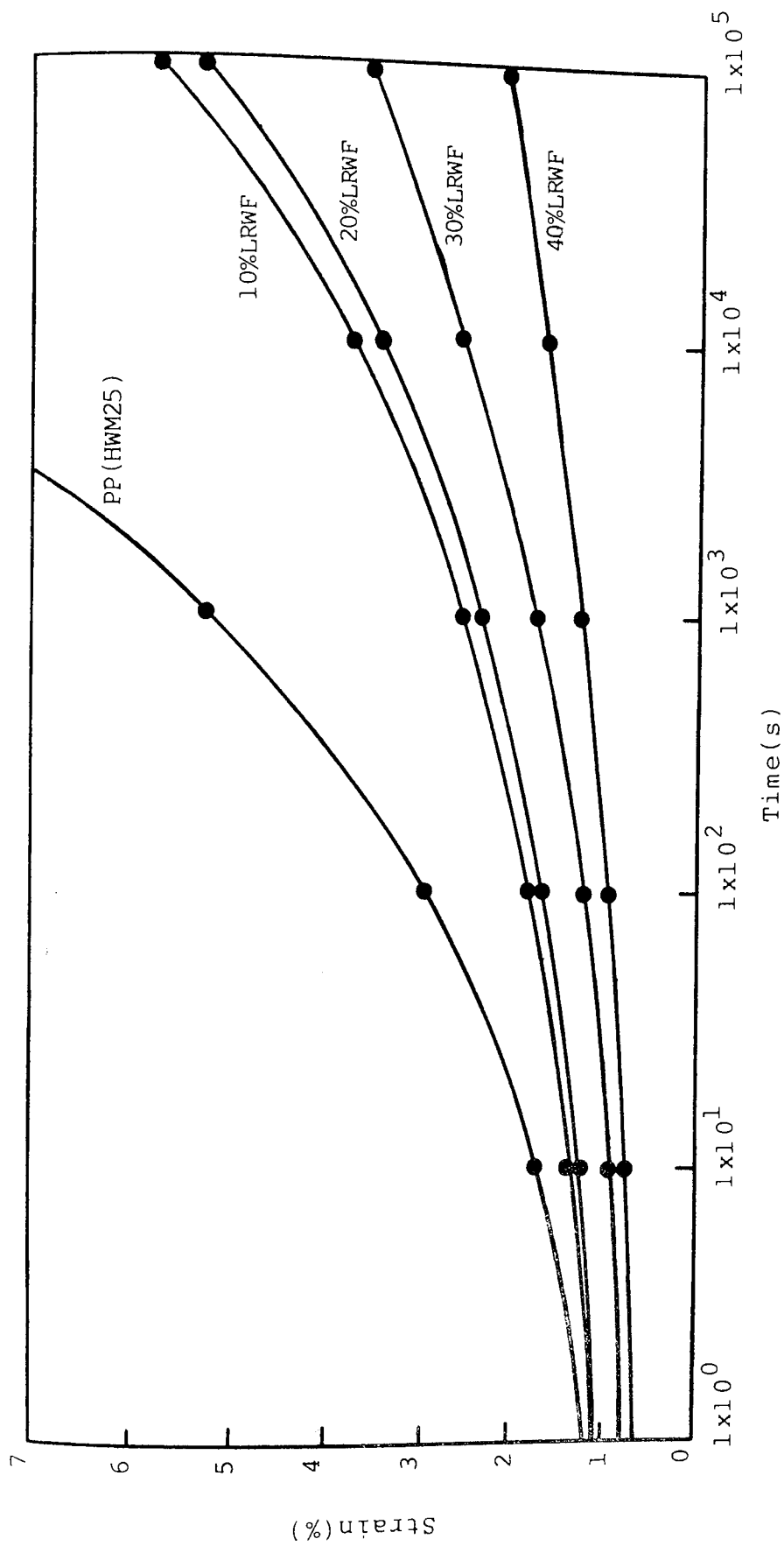


Figure 5.17 Effect of long Rockwool fibre (LRWF, A-1100 silane coupled) loading on the tensile creep (stress 20MPa, temperature 20°C) of PP(HWM25)

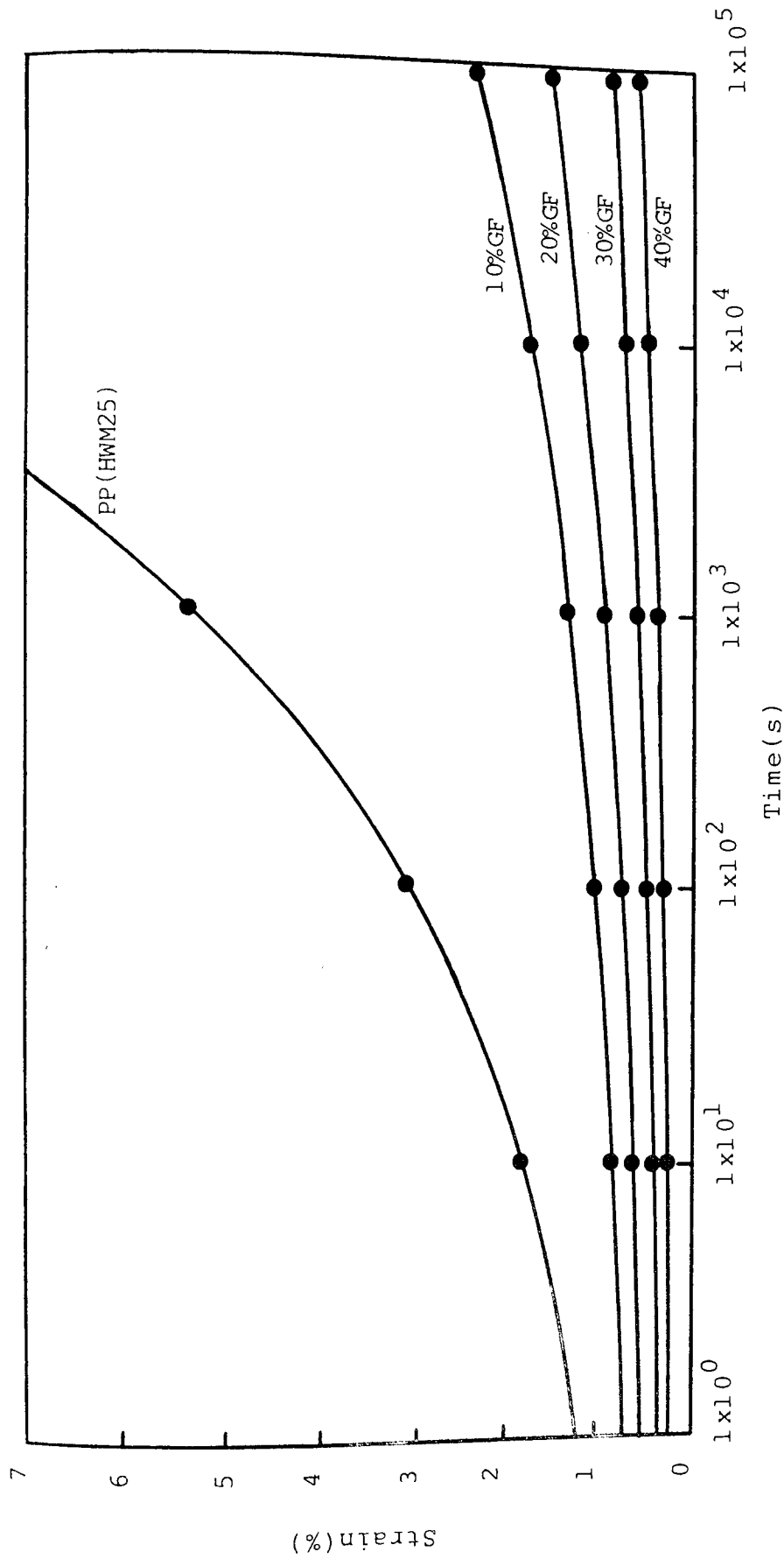


Figure 5.18 Effect of glass fibre (GF,A-1100 silane coupled) loading on the tensile creep (stress 20MPa,temperature 20°C) of PP(HWM25)

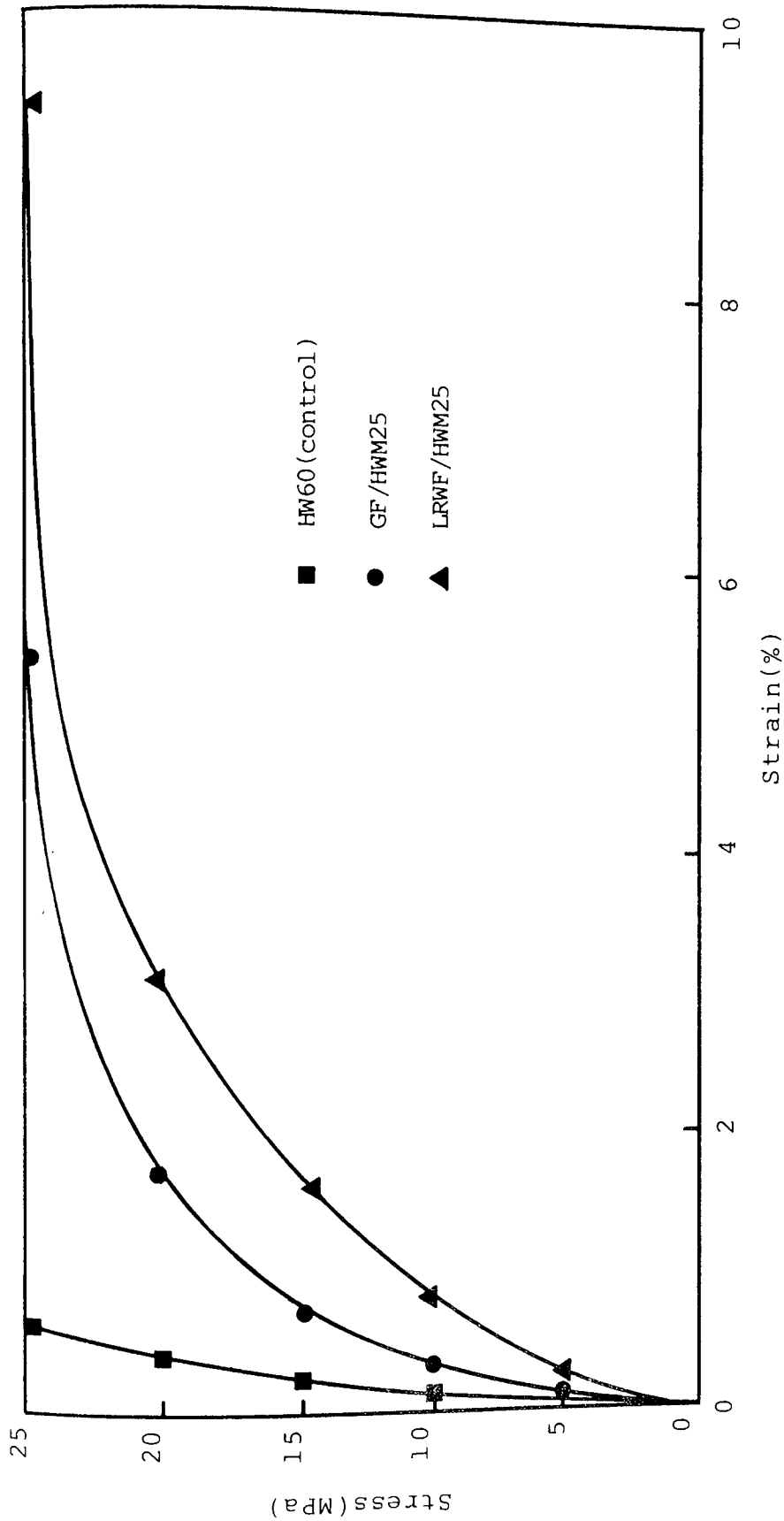


Figure 5.19 Isochronous creep curves ( $20^{\circ}\text{C}, 1 \times 10^5 \text{s}$ ) of PP(HWM25) containing long Rockwool fibre(LRWF) and glass fibre (GF, both 30% loading and A-1100 silane coupled). HW60 (commercially 30%GF coupled PP) is the control.

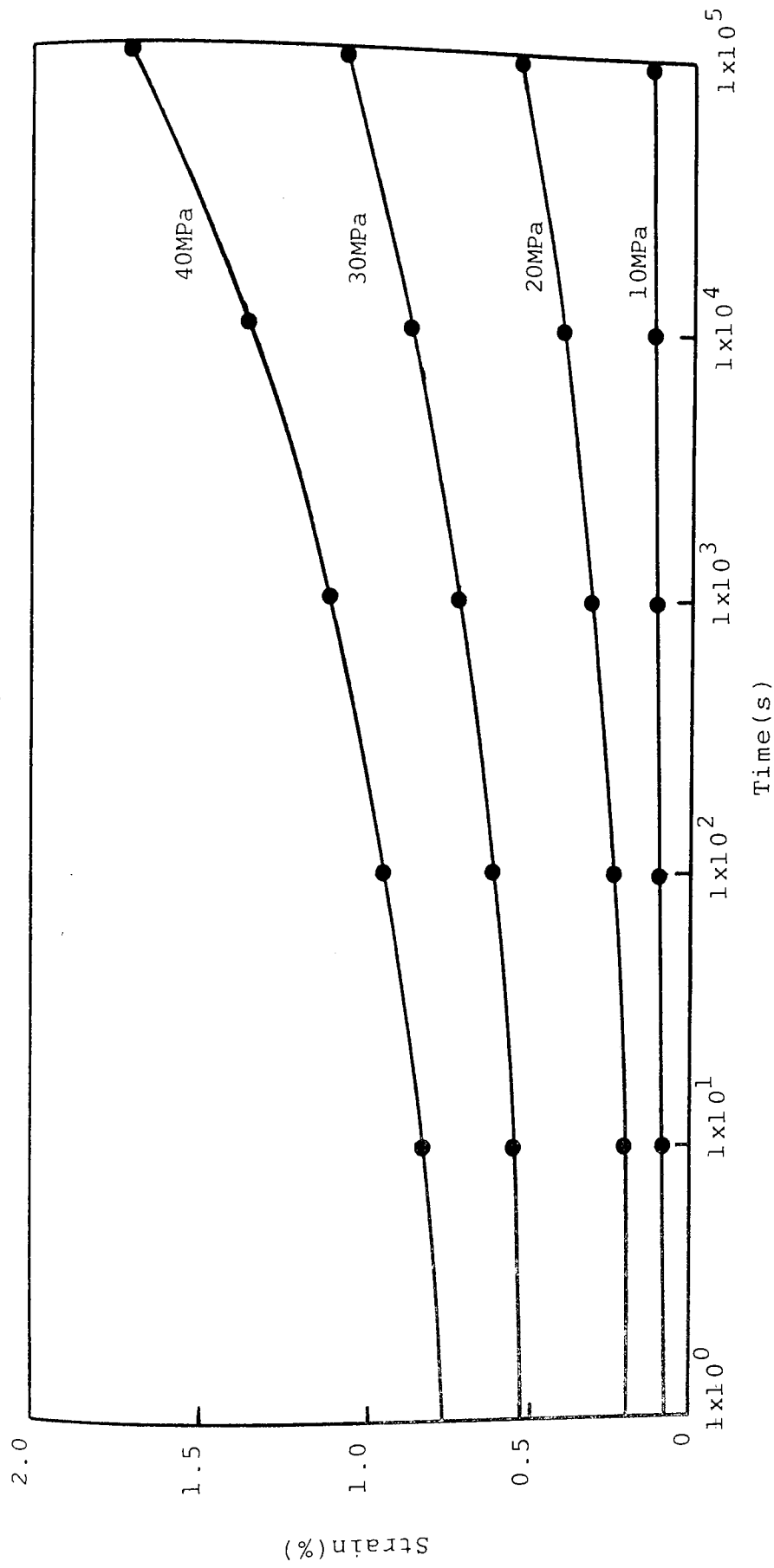


Figure 5.20 Effect of stress on the tensile creep (temperature 20°C) of HW60/GR30  
(commercially 30%GF coupled PP)

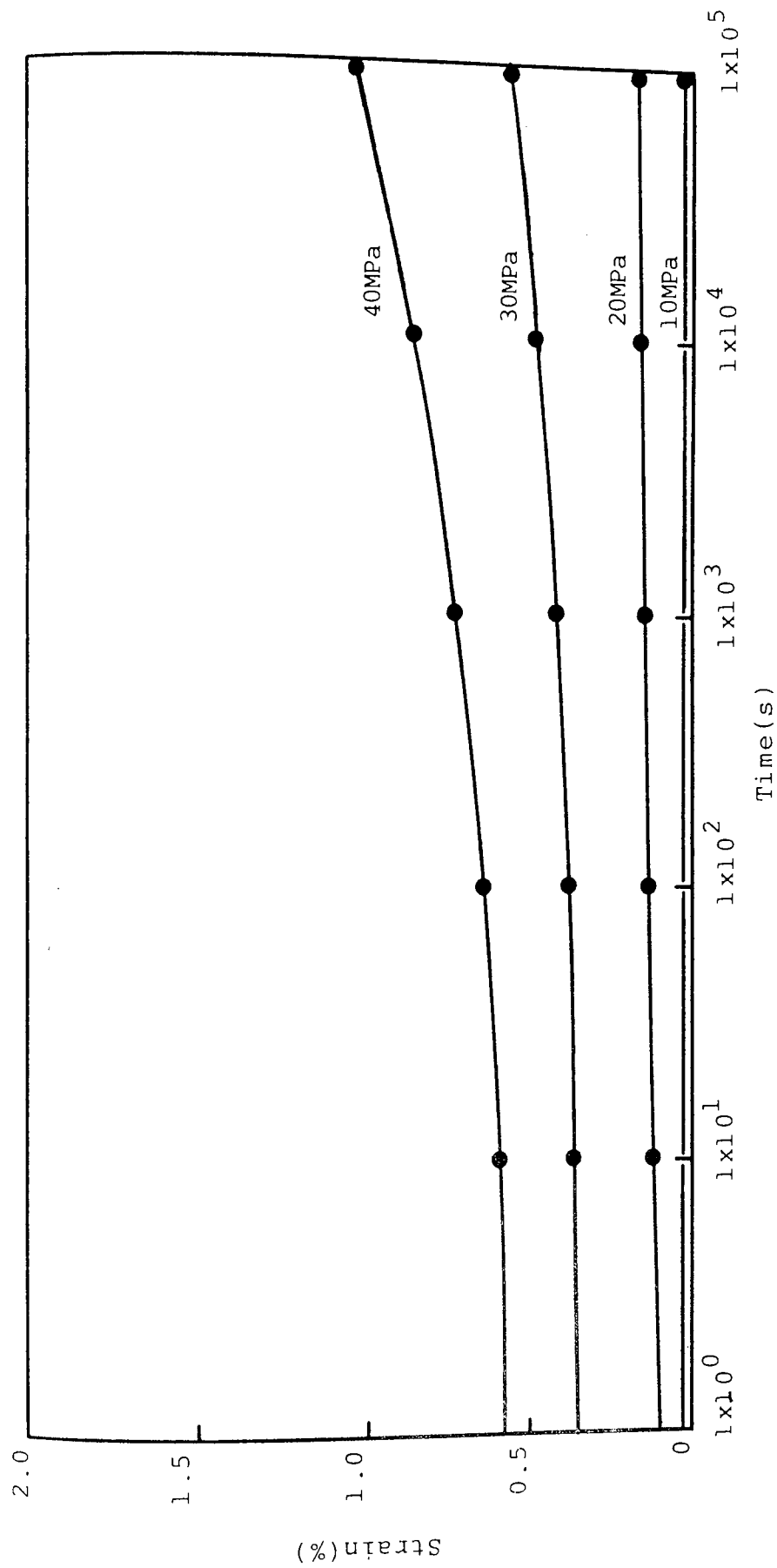


Figure 5.21 Effect of stress on the tensile creep (temperature 20°C) of 1%MA/0.2%DCP modified PP(HF22) containing glass fibre (30% loading and A-1100 silane coupled).

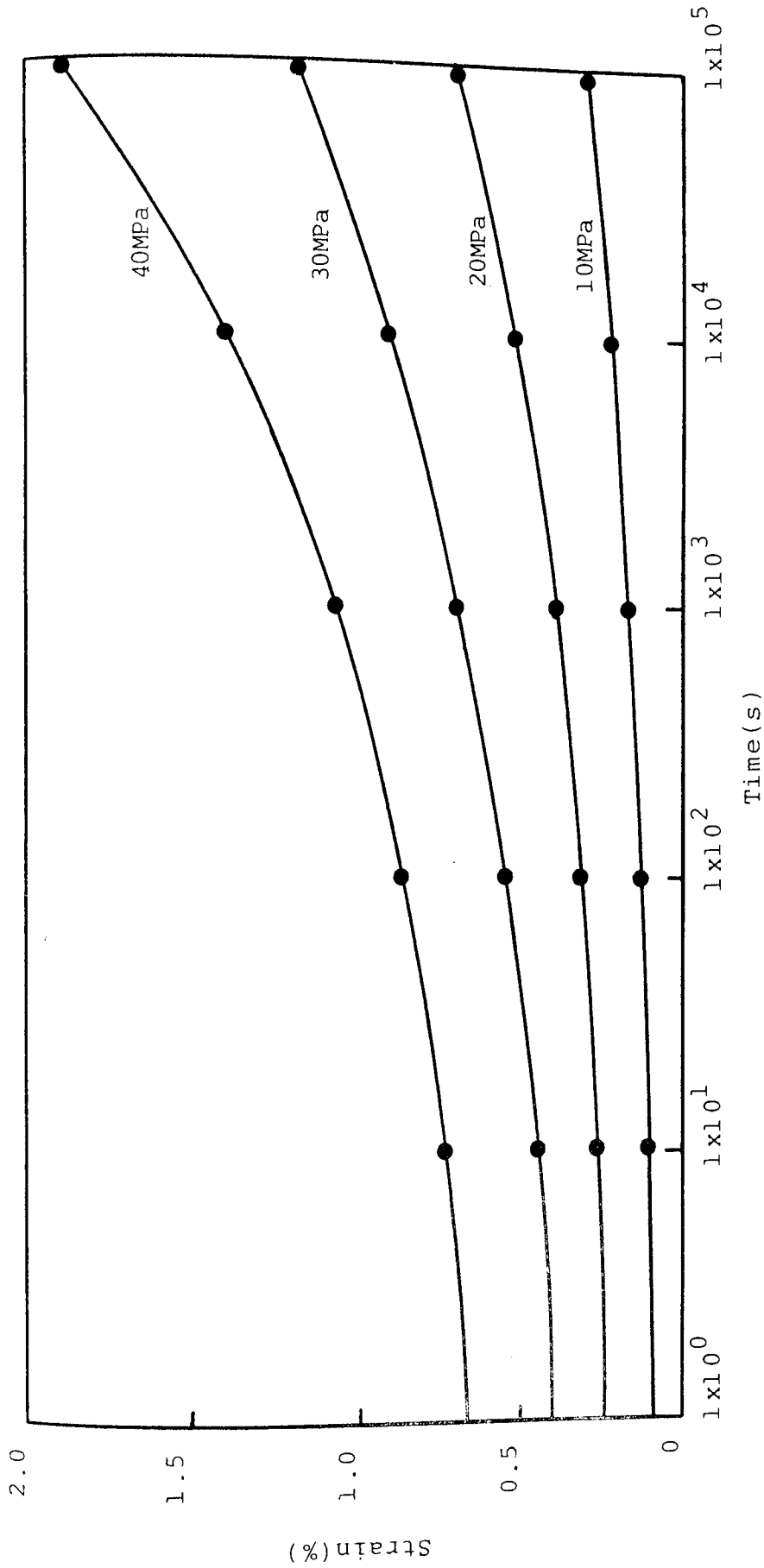


Figure 5.22 Effect of stress on the tensile creep (temperature 20°C) of 0.3%DCP modified PP(HF22) containing long Rockwool fibre (30% loading and A-1100 silane coupled).

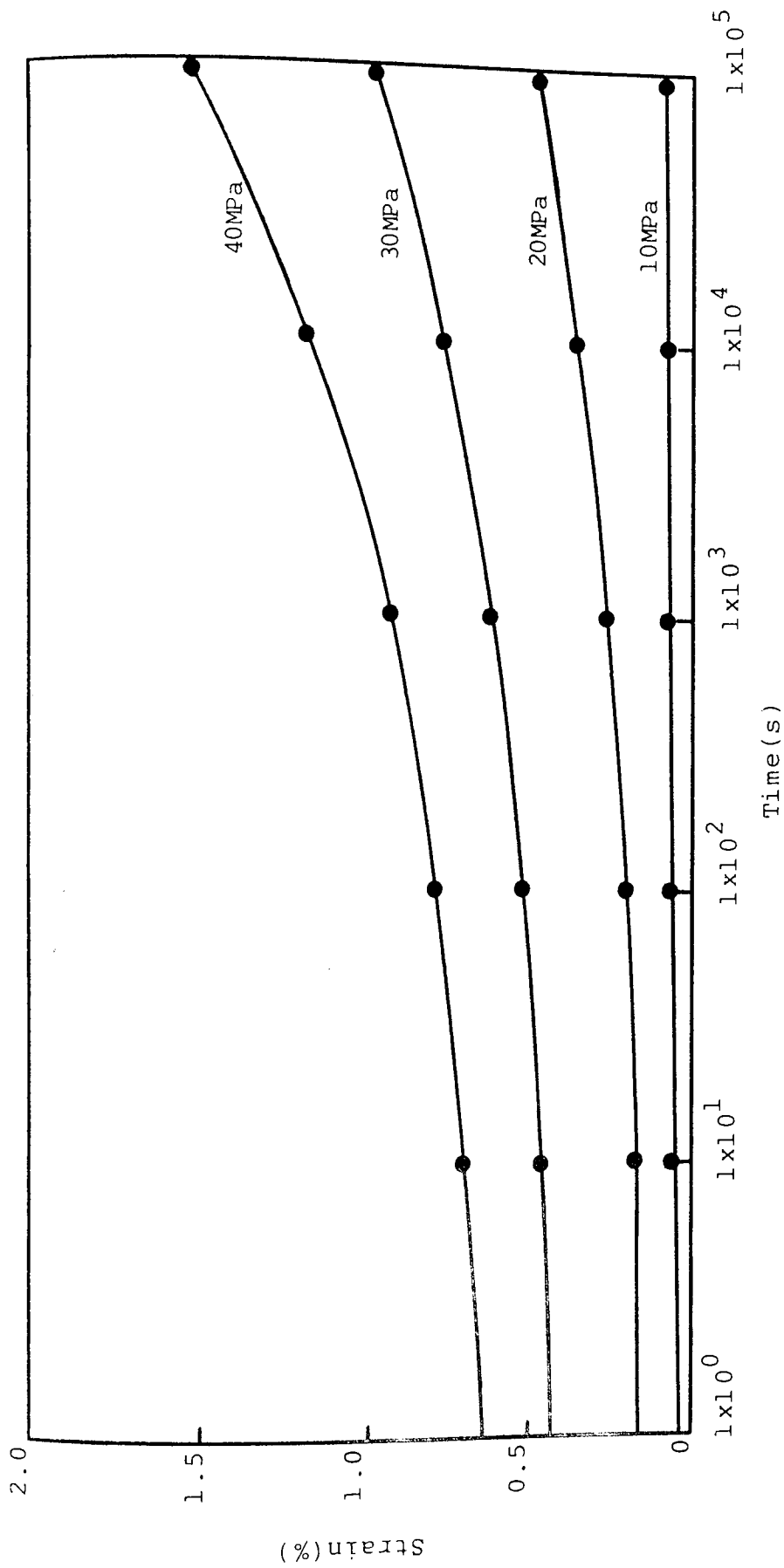


Figure 5.23 Effect of stress on the tensile creep (temperature  $20^{\circ}\text{C}$ ) of 1%MAL/0.3%DCP modified PP(HF22) containing glass fibre (30% loading and A-1100 silane coupled).



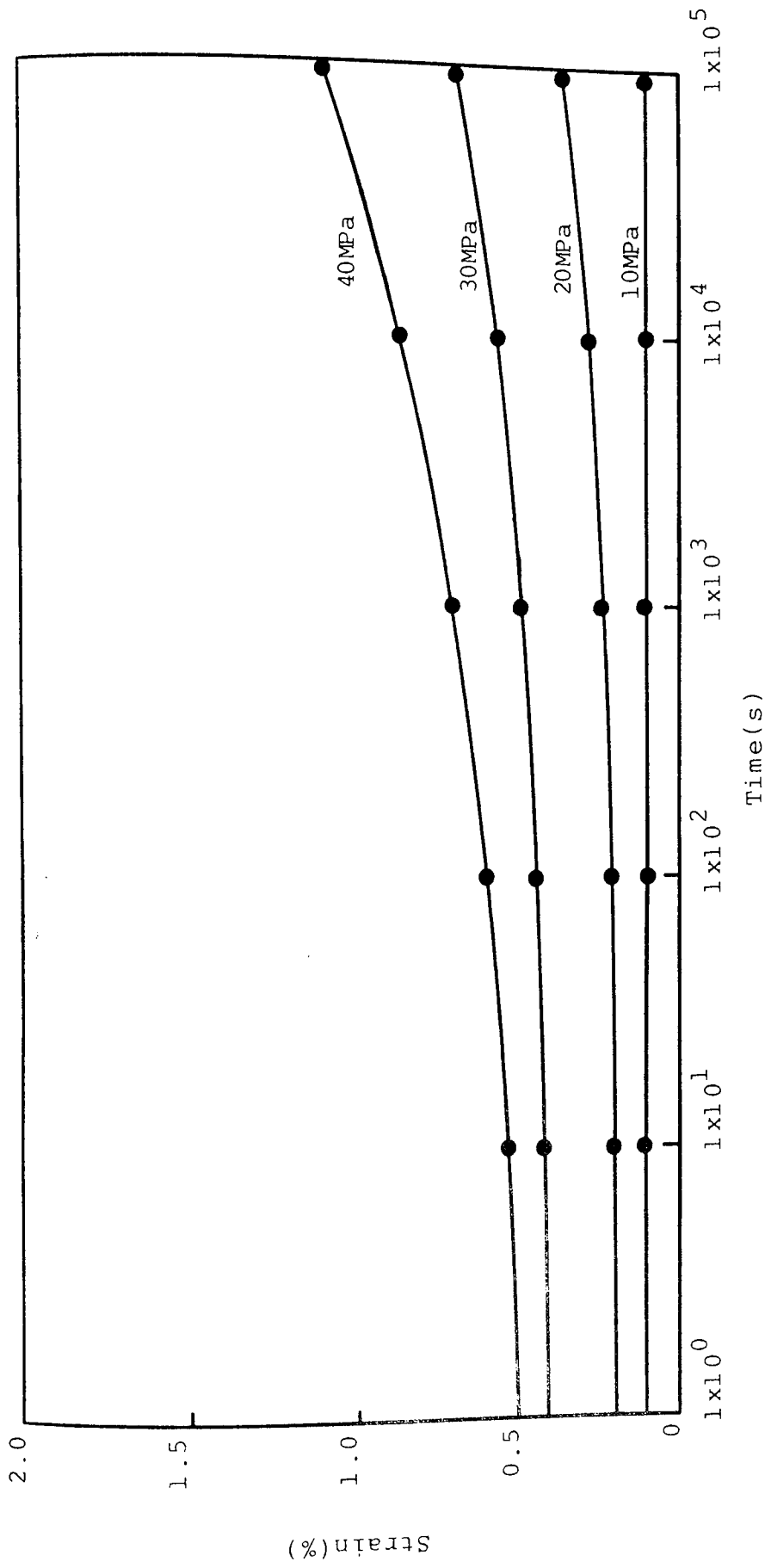


Figure 5.24 Effect of stress on the tensile creep (temperature 20°C) of 1%APM/0.5%DCP modified PP(HF22) containing glass fibre (30% loading and A-1100 silane coupled).

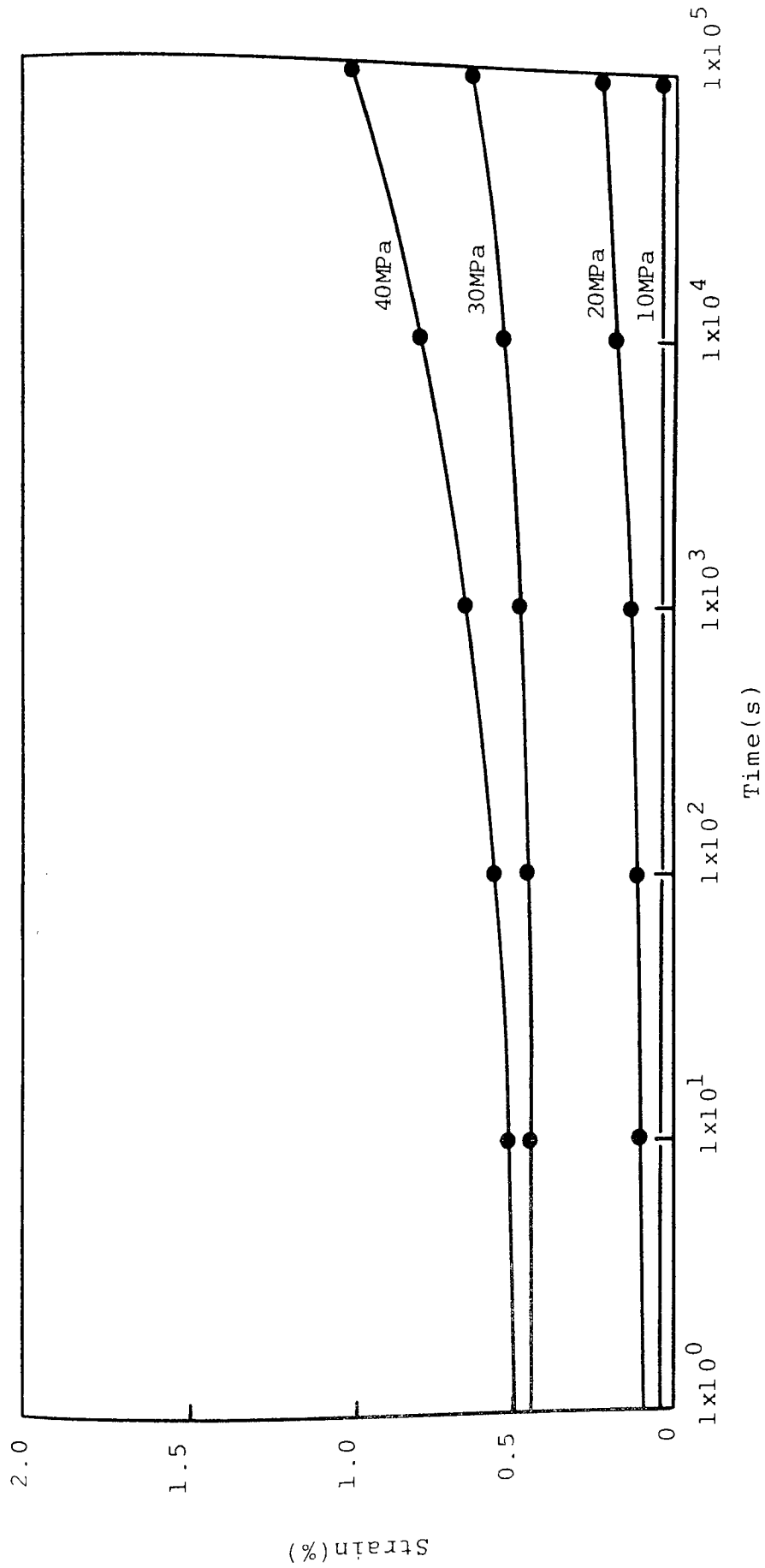


Figure 5.25 Effect of stress on the tensile creep (temperature 20°C) of 1%ADCT/0.2%DCP modified PP(HF22) containing glass fibre (30% loading and A-1100 silane coupled).

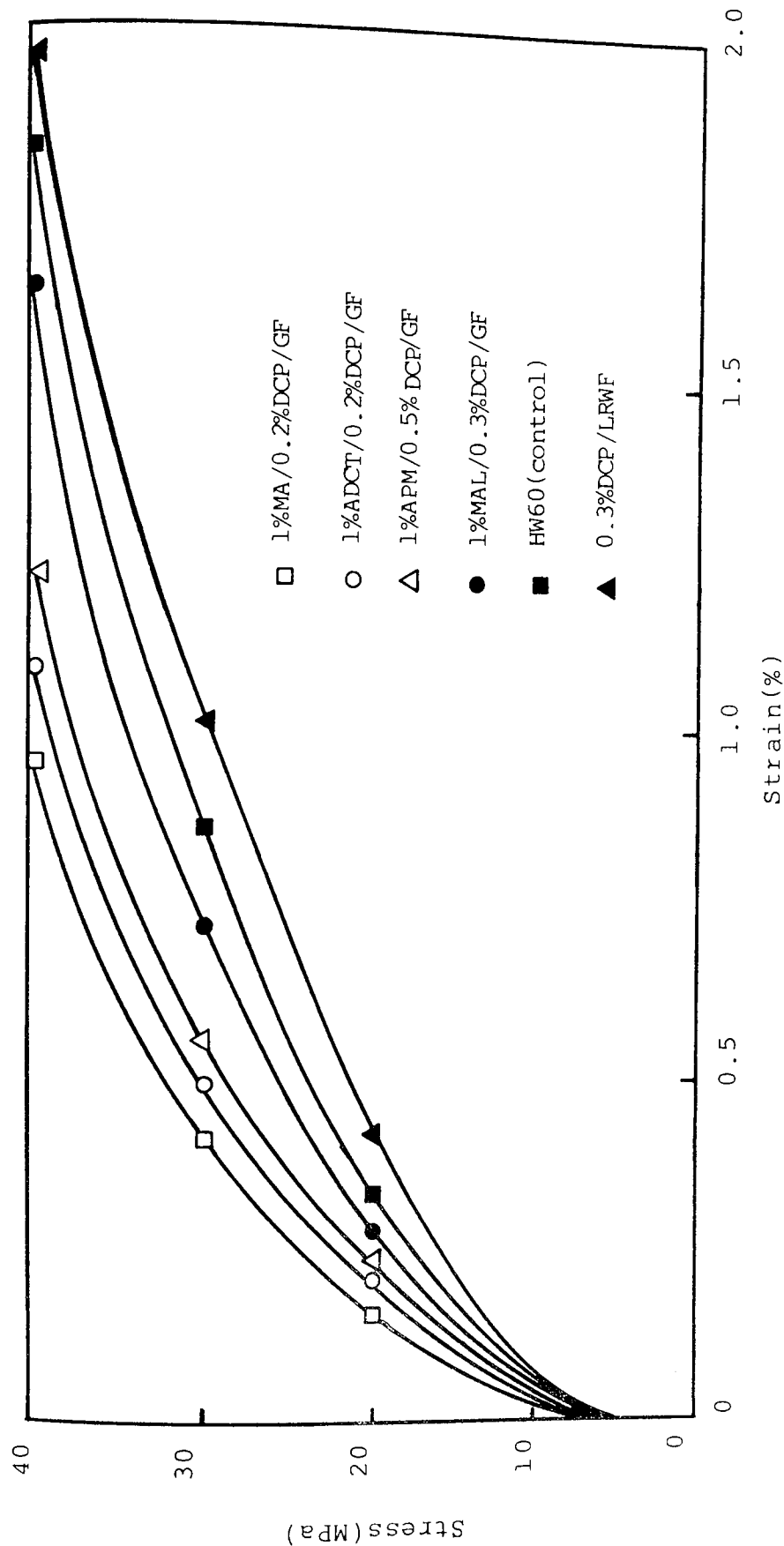


Figure 5.26 Isochronous creep curves ( $20^{\circ}\text{C}, 1 \times 10^5 \text{s}$ ) of chemically modified PP(HF22) containing long Rockwool fibre (LRWF) and glass fibre (GF, both 30% loading and A-1100 silane coupled). HW60 (commercially 30%GF coupled PP) is the control.

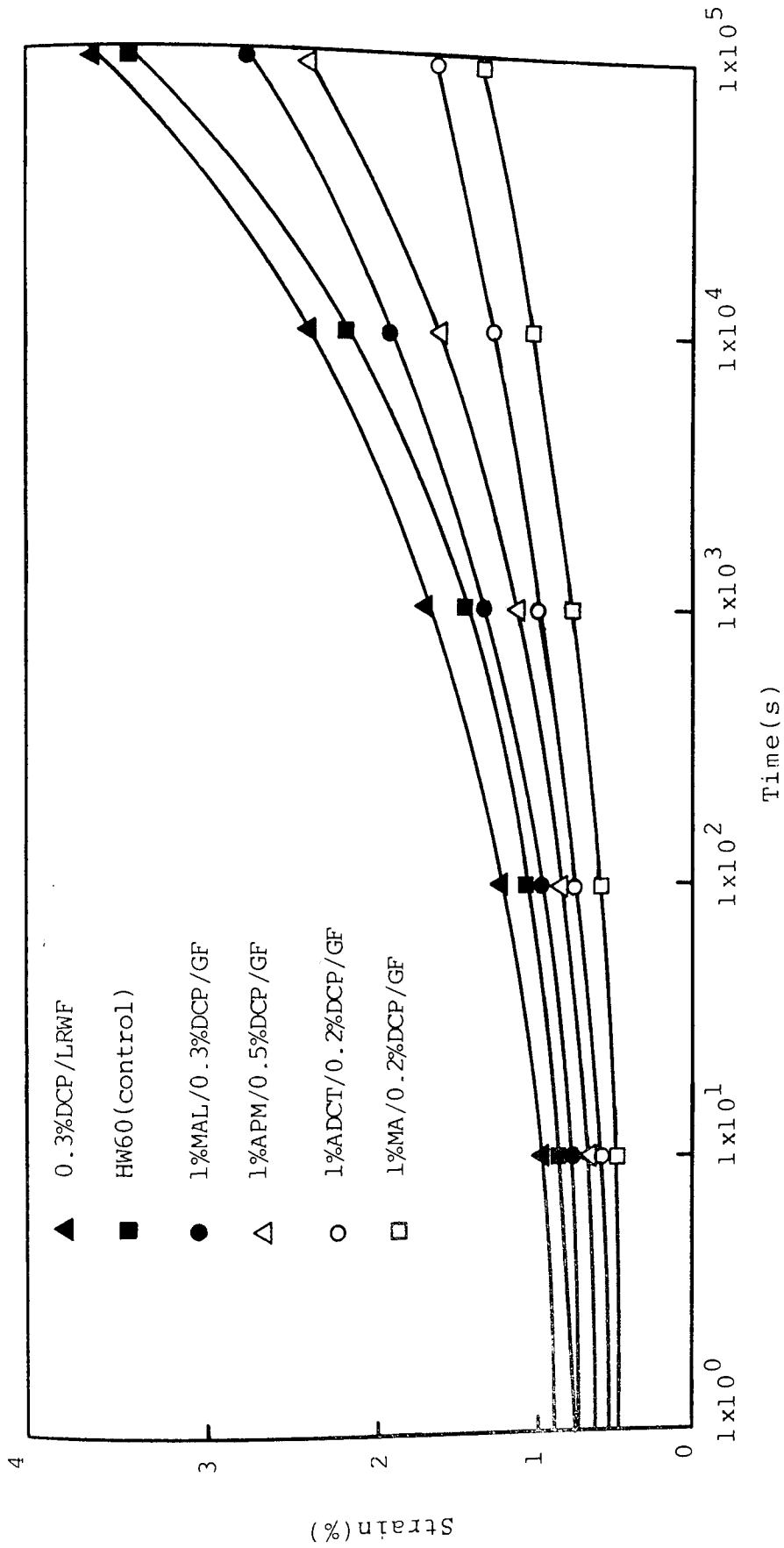


Figure 5.27 Tensile creep (stress 30MPa, temperature 50°C) of chemically modified PP(HF22) containing long Rockwool fibre(LRWF) and glass fibre (GF), both 30% loading and A-1100 silane coupled). HW60 (commercially 30%GF coupled PP) is the control.

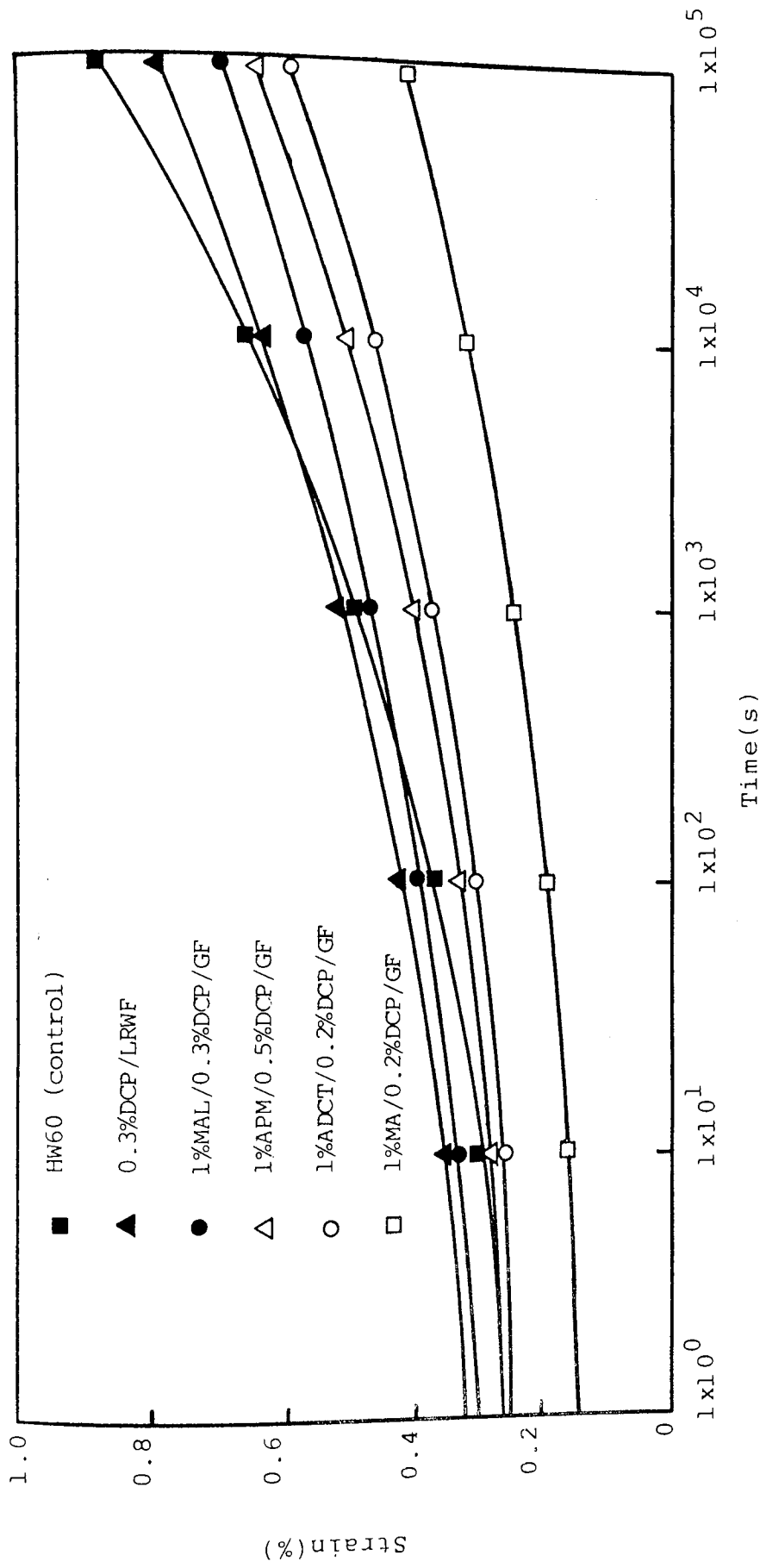


Figure 5.28 Tensile creep (stress 10MPa, temperature 100°C) of chemically modified PP (HF22) containing long Rockwool fibre (LRWF) and glass fibre (GF, both 30% loading and A-1100 silane coupled). HW60 (commercially 30%GF coupled PP) is the control.

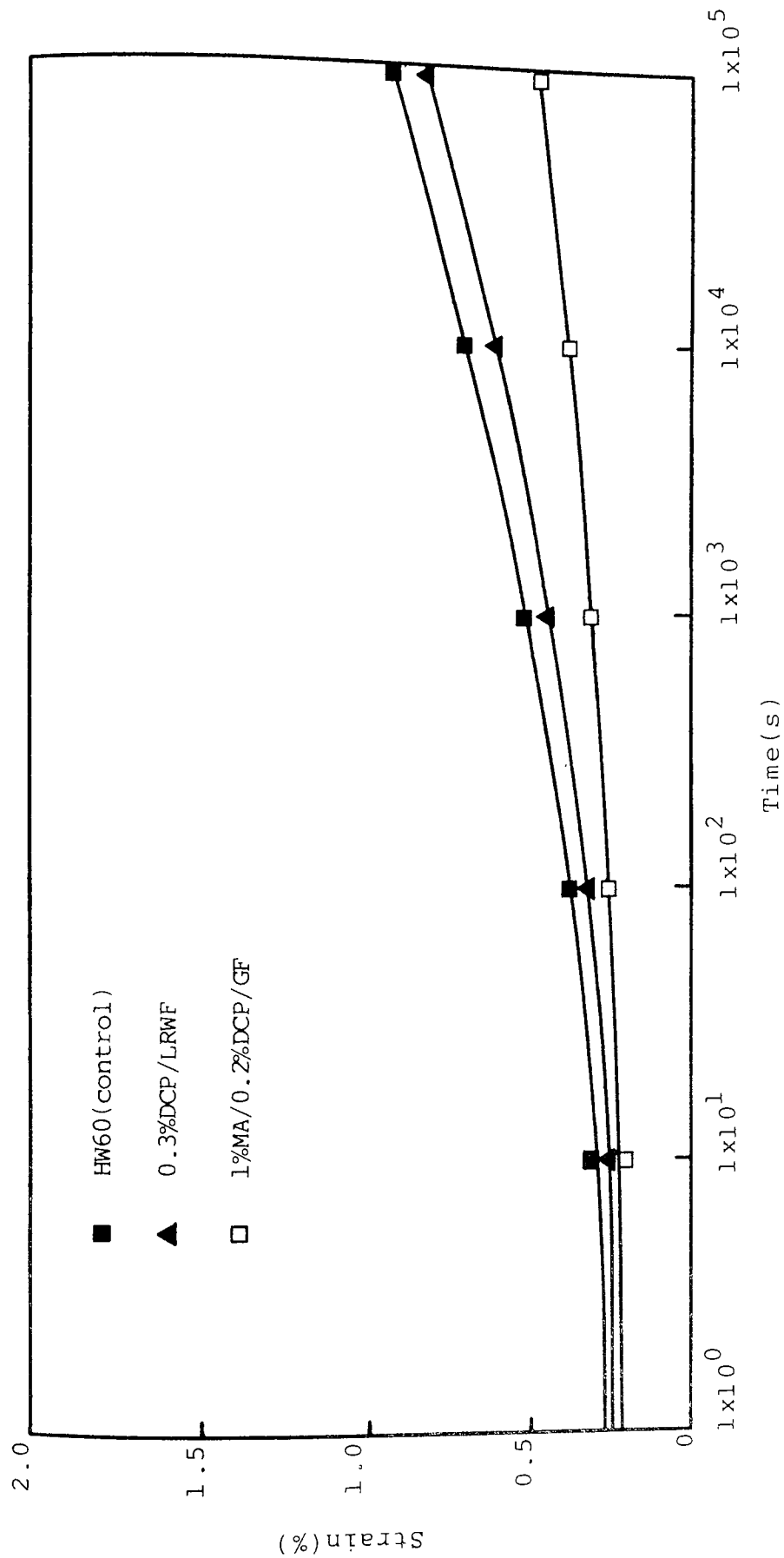


Figure 5.29 Tensile creep (stress 5MPa, temperature 135°C) of chemically modified PP(HF22)

containing long Rockwool fibre (LRWF) and glass fibre (GF, both 30% loading

and A-1100 silane coupled). HW60 (commercially 30%GF coupled PP) is the control.

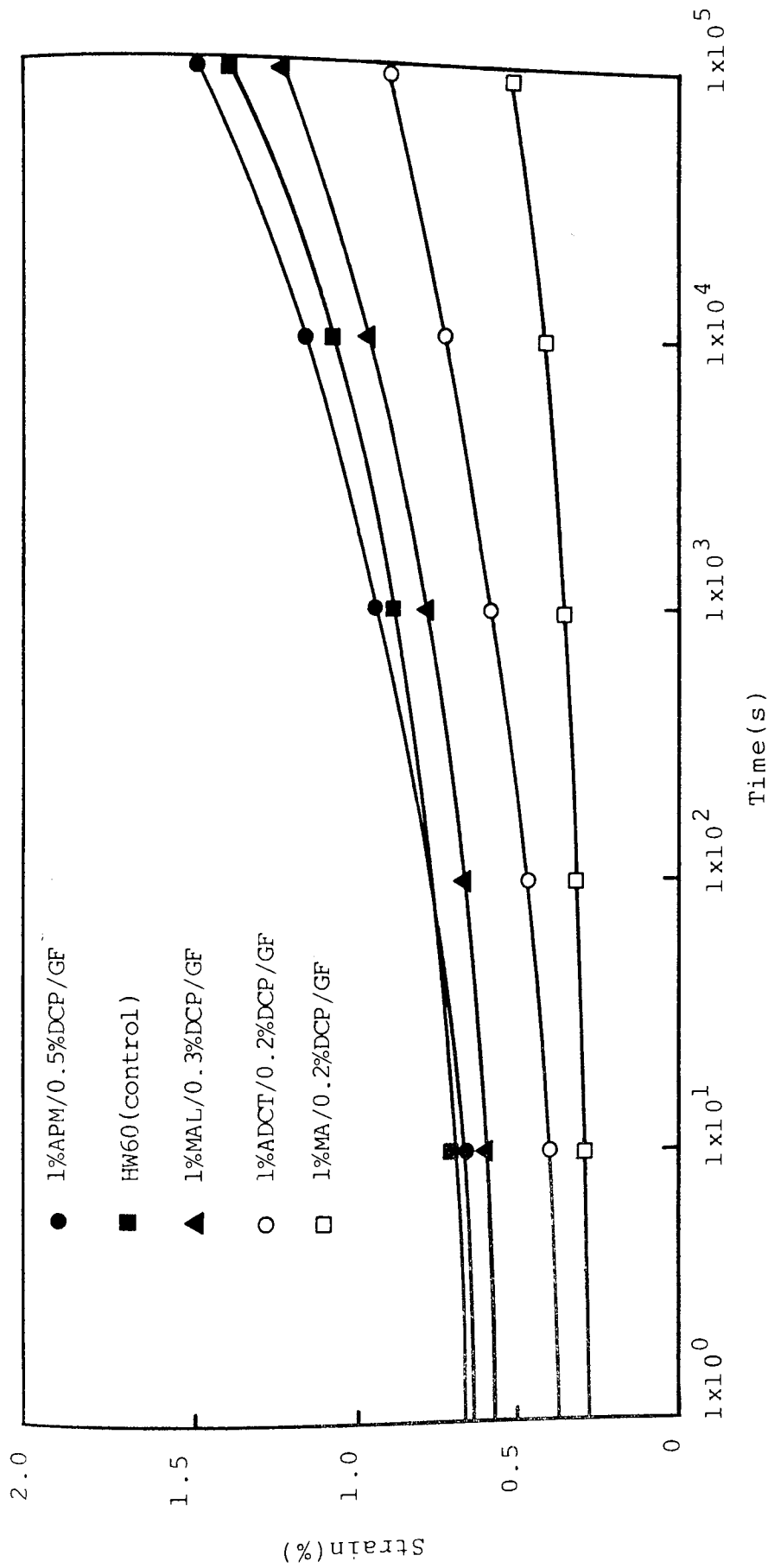


Figure 5.30 Tensile creep (stress 5MPa, temperature 150°C) of chemically modified PP(HF22) containing glass fibre (GF, 30% loading and A-1100 silane coupled). HW60 (commercially 30%GF coupled PP) is the control.

No.	Composite	Homogenised with 1% A-1100 silane?	Yield Strength MPa	Tensile Modulus GPa	Flexural Strength MPa	Flexural Modulus GPa	Charpy Impact Strength $\text{kJm}^{-2}$
1	HW60/GR30 (control)	No	77	3.0	94	6.50	158
2A	Unmodified PP(HWM25)	No	35	2.2	48	6.20	105
2B	(control)	Yes	36	2.2	49	6.20	107
3A	1%MA	No	101	4.3	126	8.32	316
3B	+0.2%DCP	Yes	115	4.51	139	8.56	331
4A	1%APM	No	84	3.95	103	7.70	168
4B	+0.5%DCP	Yes	98	4.39	115	8.32	189
5A	1%ADCT	No	87	3.85	115	7.67	181
5B	+0.2%DCP	Yes	103	4.35	128	8.43	205

Table 5.15 Mechanical properties of chemically modified unstabilised PP(HF22) containing

GF(A-1100 silane coupled, 30% loading) with or without additional 1%A-1100 (homogenised in Buss Ko-Kneader). HW60/GR30 (commercially 30%GF coupled PP) and unmodified PP(HWM25)/GF are used as controls.



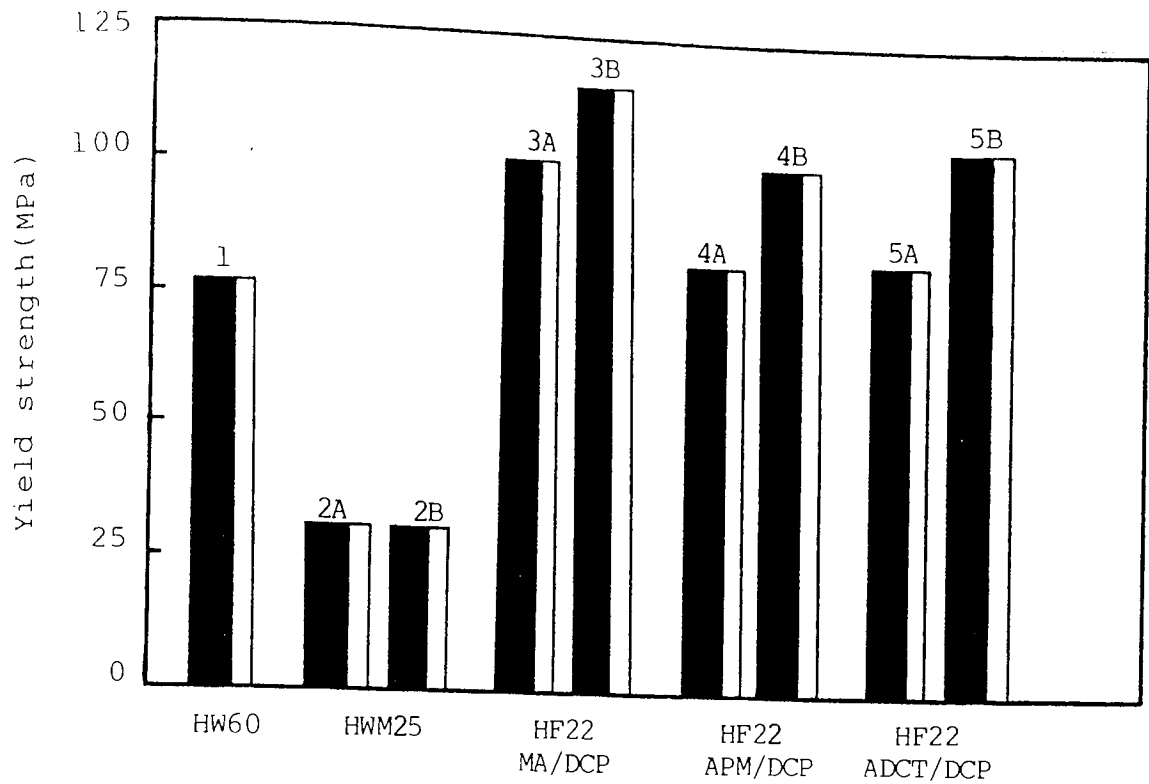


Figure 5.31 Yield strength of chemically modified PP(HF22) containing 30% glass fibre (A-1100 silane coupled) without (A) and with (B) an additional 1% A-1100 silane. HW60/GR30 and PP(HWM25)/GF are controls. See Table 5.15.

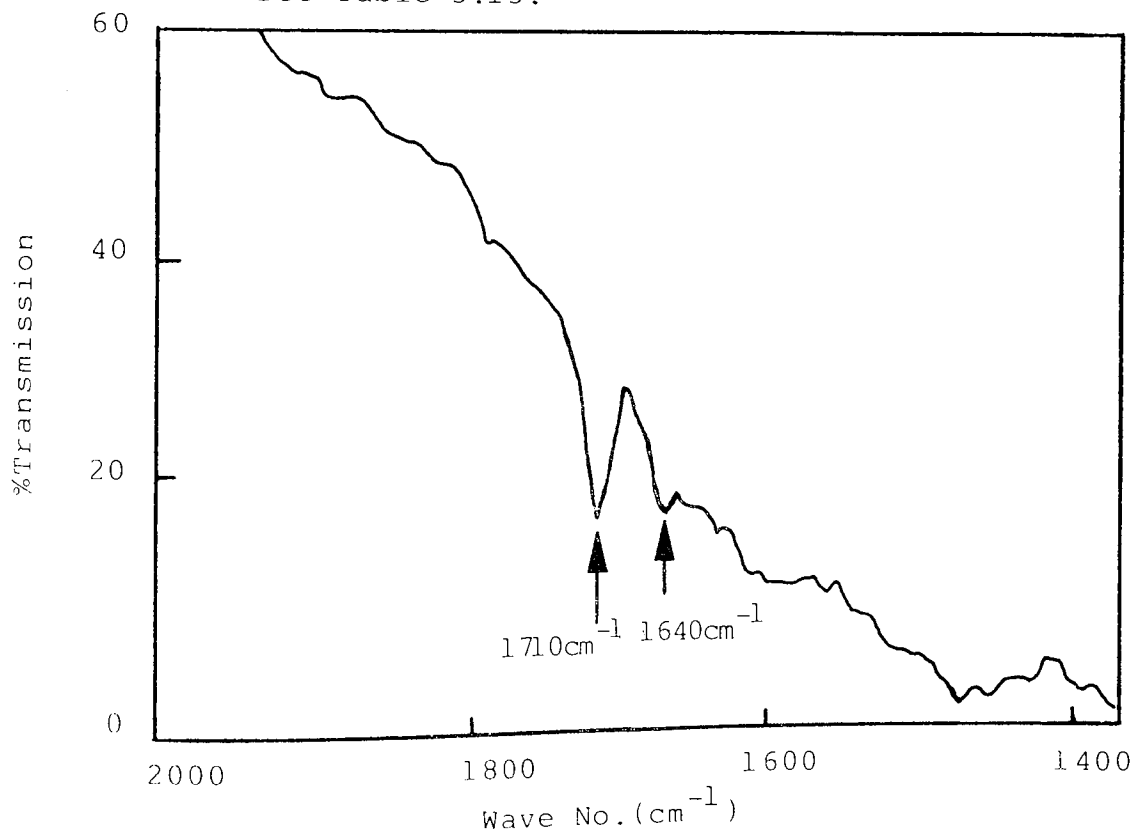


Figure 5.32 Infra-red spectrum of 1% MA/0.2% DCP modified PP(HF22) containing 30% glass fibre (A-1100 silane coupled)

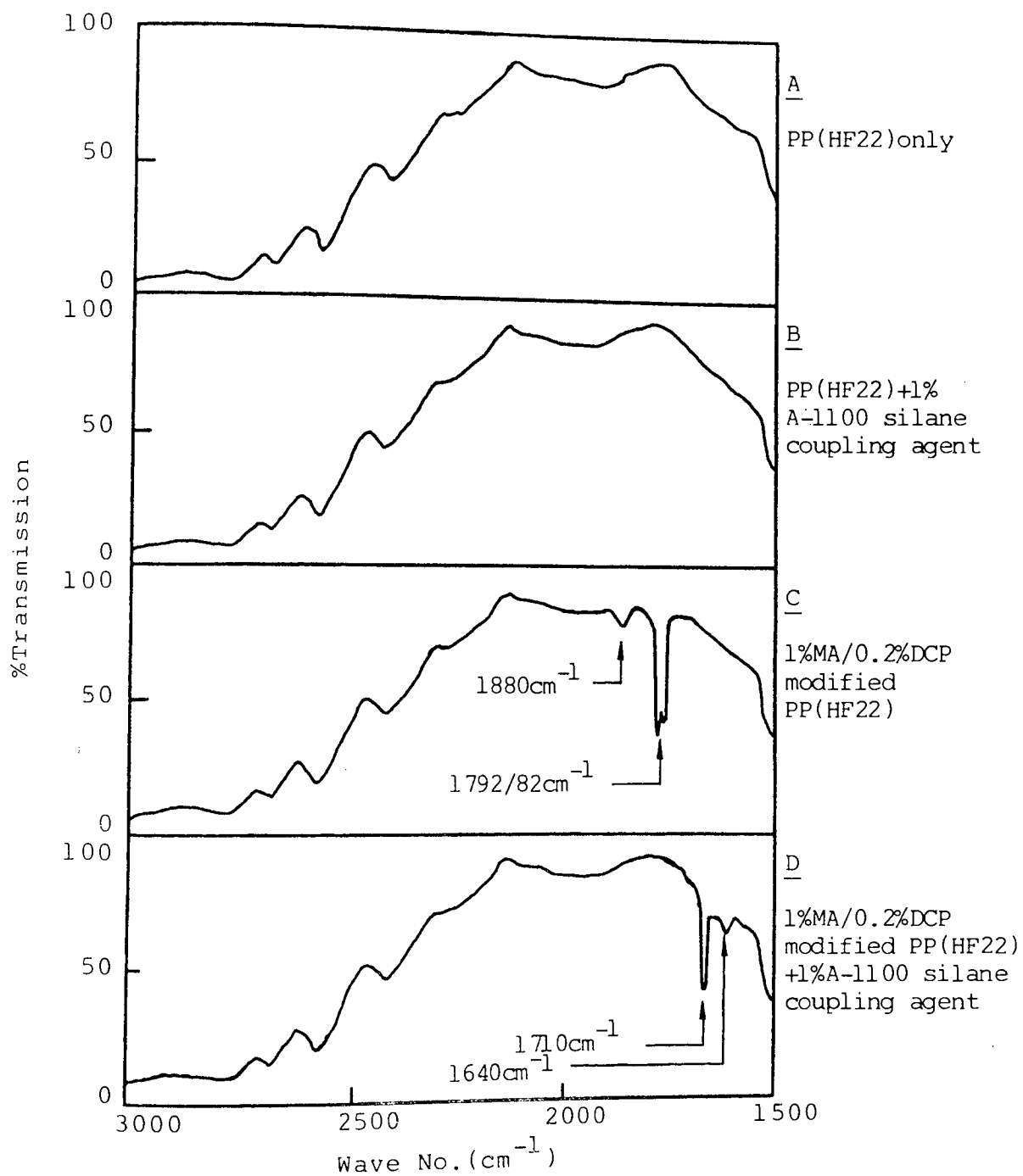


Figure 5.33 Infra-red spectra showing the effect of the addition of 1%A-1100 silane coupling agent to maleic anhydride(MA)/di-cumyl peroxide(DCP) modified PP(HF22) after melt processing.

CHAPTER SIX

THERMAL-OXIDATIVE STABILISATION OF  
POLYPROPYLENE  
USING CHEMICALLY BOUND STABILISERS

## 6.1 Object

In this chapter, the chemical binding of a variety of chemical modifying antioxidants (listed in Scheme 6.1) to unstabilised PP(HF22) is attempted in order to obtain enhanced thermal-oxidative stability, especially in hot, highly extracting environments. To assess the performance of such PP-bound antioxidants, direct comparisons are made with commercial PP(HWM25 and GWM22, highly and medium stabilised grades) and with PP(HF22) containing commercial stabilisers (Irganox 1076 and 1010). Scheme 6.2 shows the procedure followed for producing the commercial controls. All thermal-oxidative ageing was done using compression moulded 200  $\mu\text{m}$  PP films (before and after Soxhlet extraction) in a Wallace air oven at 140°C. Infra-red spectra were taken at intervals to monitor the carbonyl absorption at 1710  $\text{cm}^{-1}$  in order to obtain the carbonyl index induction period.

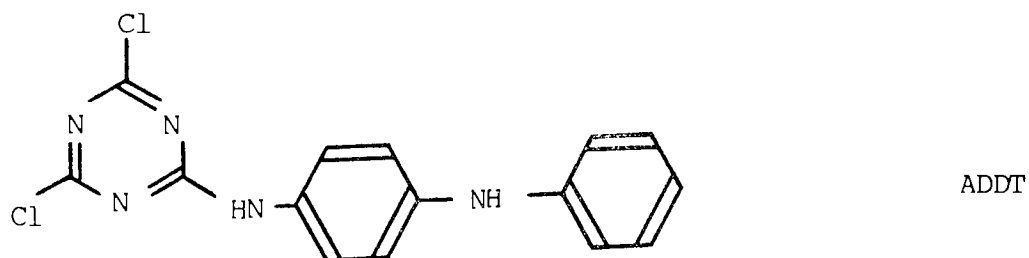
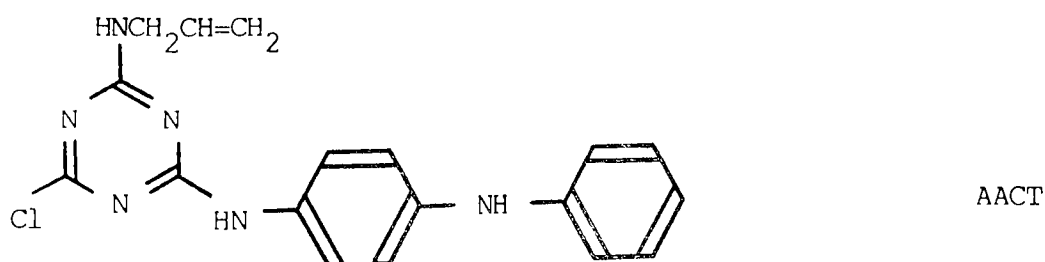
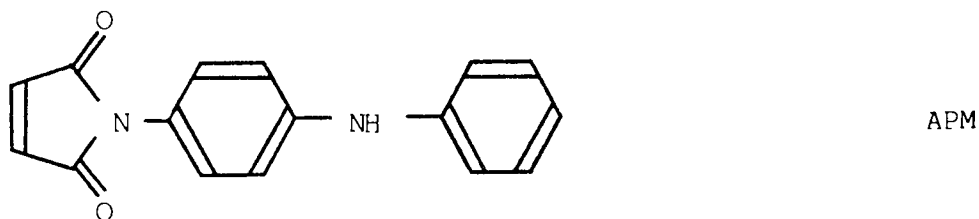
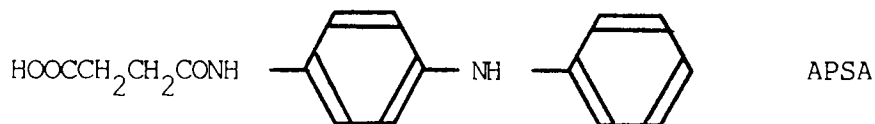
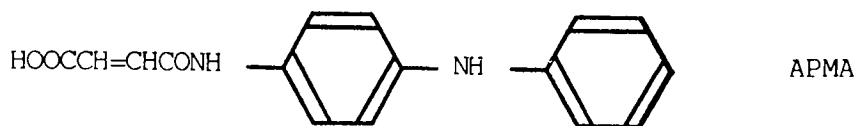
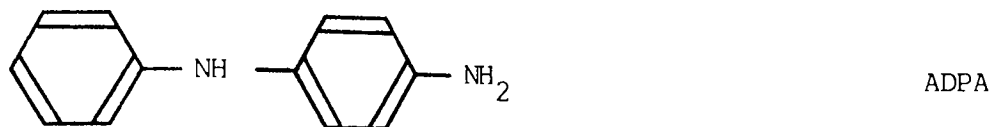
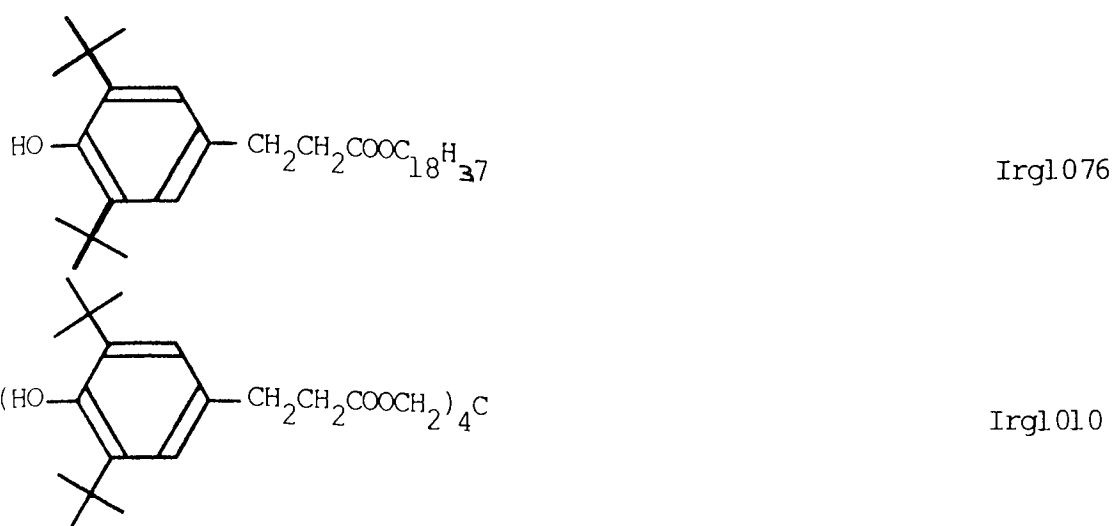
Two approaches to the problem of obtaining mechano-chemically bound stabilisers in PP(HF22) were attempted. The first was done by initially modifying PP(HF22) with maleic anhydride (MA) and di-cumyl peroxide (DCP) in the Buss Ko-Kneader (Scheme 6.3). This modified PP(HF22) was used in extracted (by Soxhlet to remove chemically unbound MA and DCP residues) and unextracted forms for melt processing with ADPA in the RAPRA torque rheometer (Scheme 6.4). The objective is to obtain chemically bound ADPA using its primary

amine group via chemically bound anhydride groups of MA modified PP(HF22).

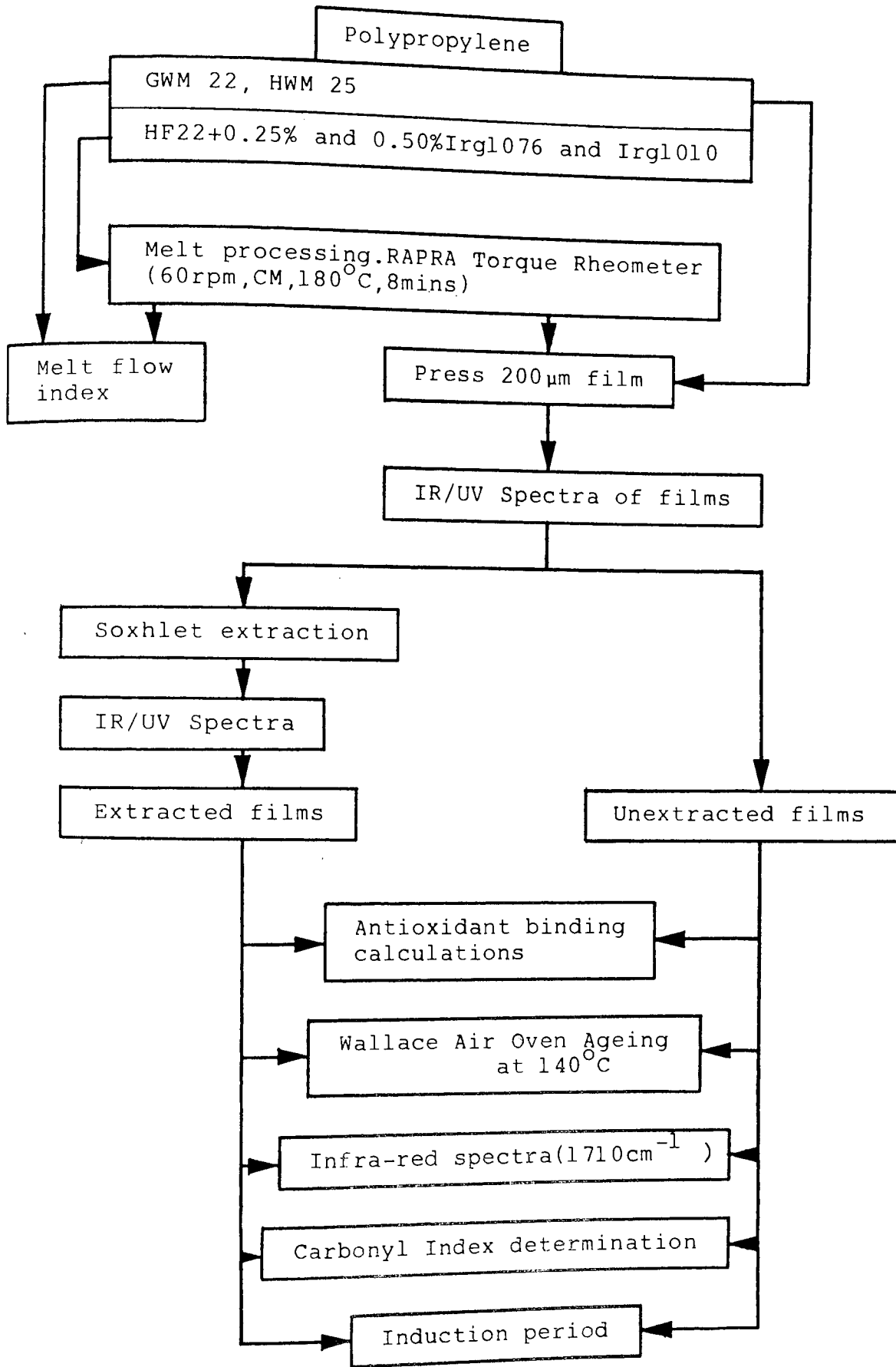
The second technique represents a more direct approach to obtaining chemically bound PP stabilisers and utilises DCP free radical catalysed binding of unsaturated stabilisers (Scheme 6.1) during PP(HF22) melt processing (RAPRA torque rheometer, Scheme 6.5). Melt flow index (MFI) studies were conducted to investigate melt stability of processed samples. For all such stabilised PP(HF22), chemical binding was assessed by infra-red and ultraviolet spectrophotometry and thermal-oxidative ageing assessed in a Wallace air oven at 140°C using 200µm PP(HF22) films before and after Soxhlet extraction.

In order to obtain thermal-oxidative stability data more representative of what an "under-bonnet" component would expect to experience during service, 1mm thick injection moulded PP plaques were subjected to Wallace air oven ageing at 150°C (Scheme 6.6). A wide variety of commercially and mechano-chemically stabilised PP grades were used (before and after Soxhlet extraction) with and without long Rockwool fibre (LRWF) and glass fibre (GF), both 30% loading and A-1100 silane coupled.

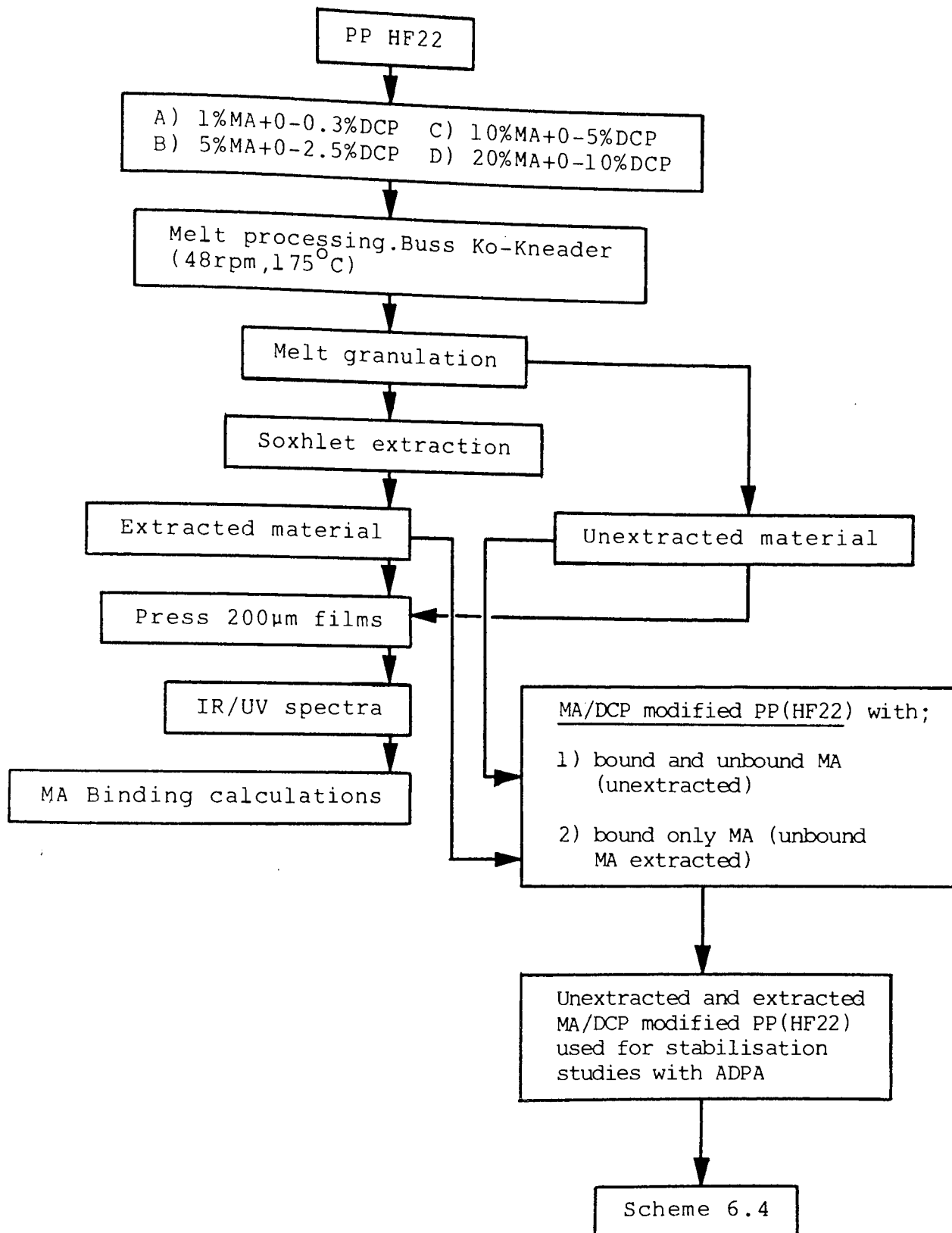
Hydro-peroxide decomposition and oxygen absorption solution behaviour of the additives listed in Scheme 6.1 were examined according to the procedure in Scheme 6.7 to discover



Scheme 6.1 Chemical formulae and abbreviations of stabilisers  
 used in Chapter Six

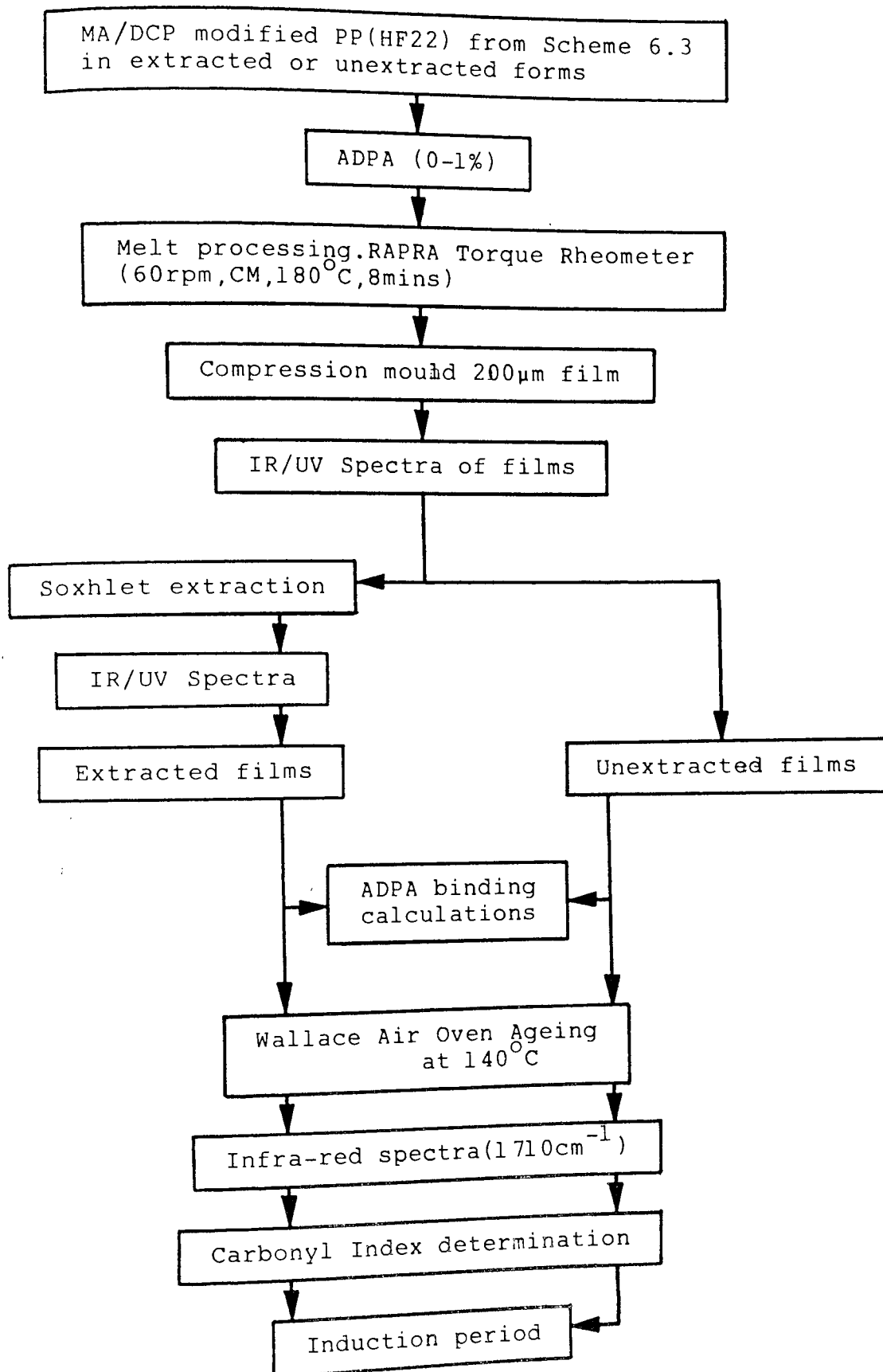


Scheme 6.2 Production of commercially stabilised PP films for thermal-oxidative ageing

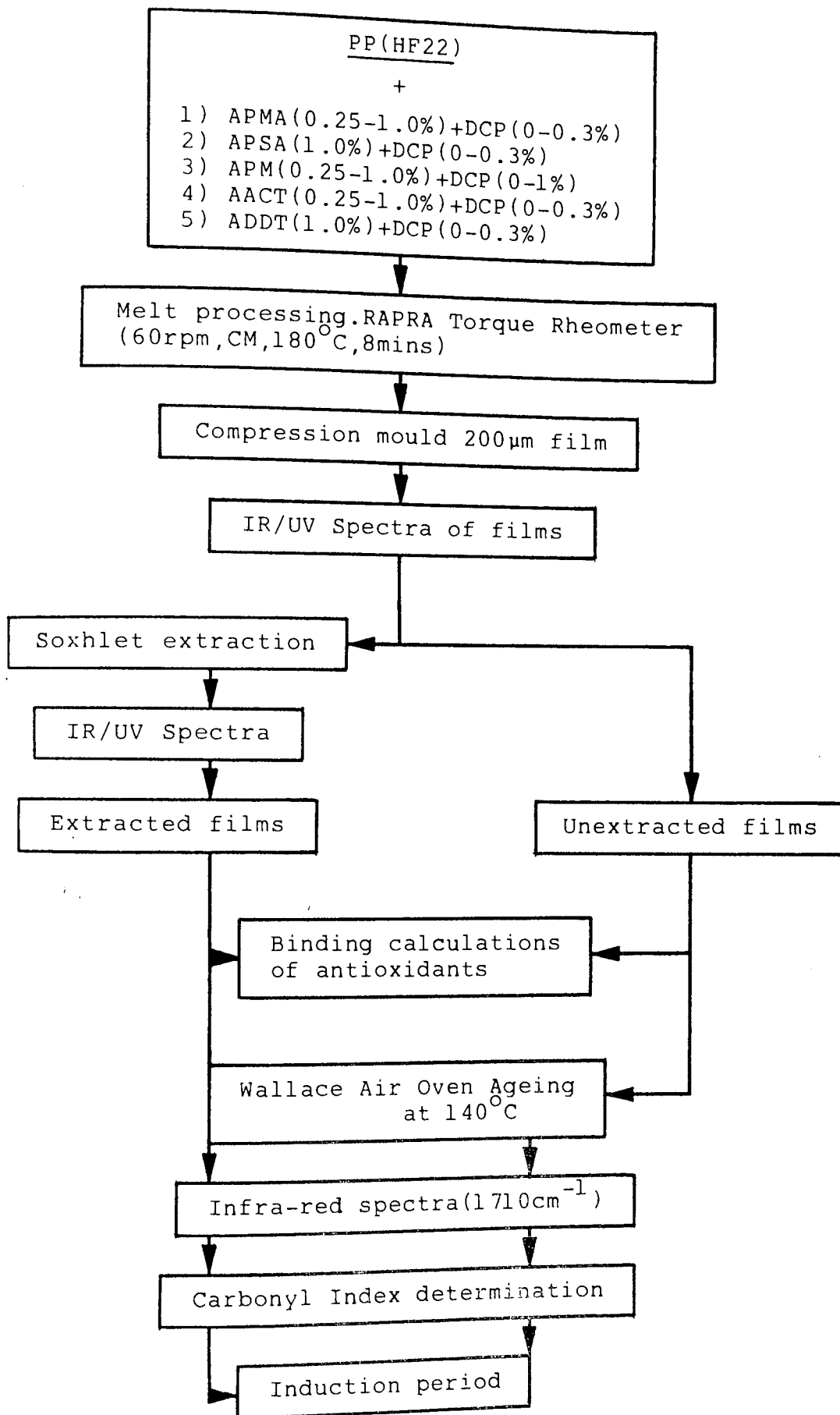


Scheme 6.3 Production of optimum binding of maleic anhydride(MA) using di-cumyl peroxide(DCP) for the chemical binding of ADPA (Scheme 6.4)

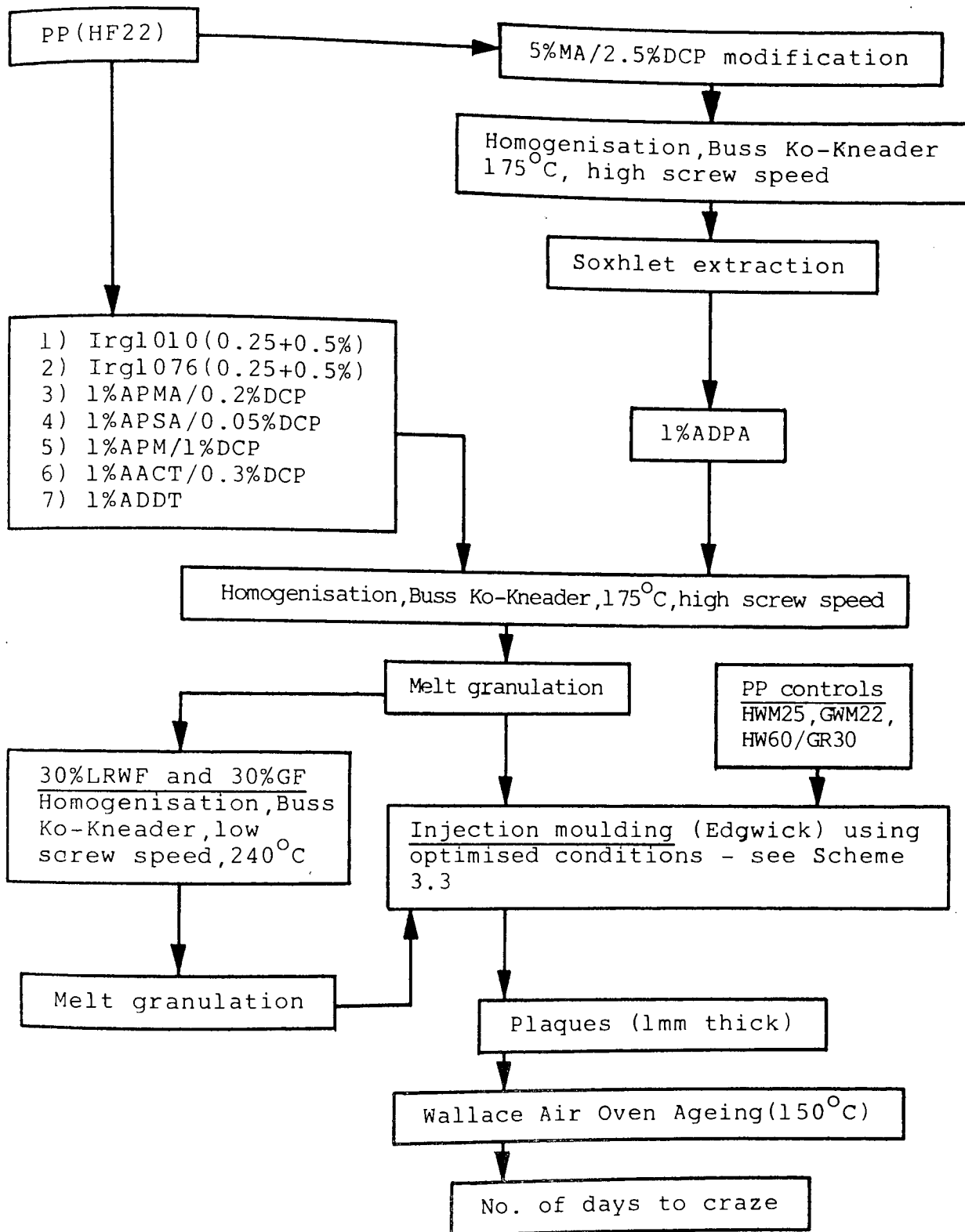




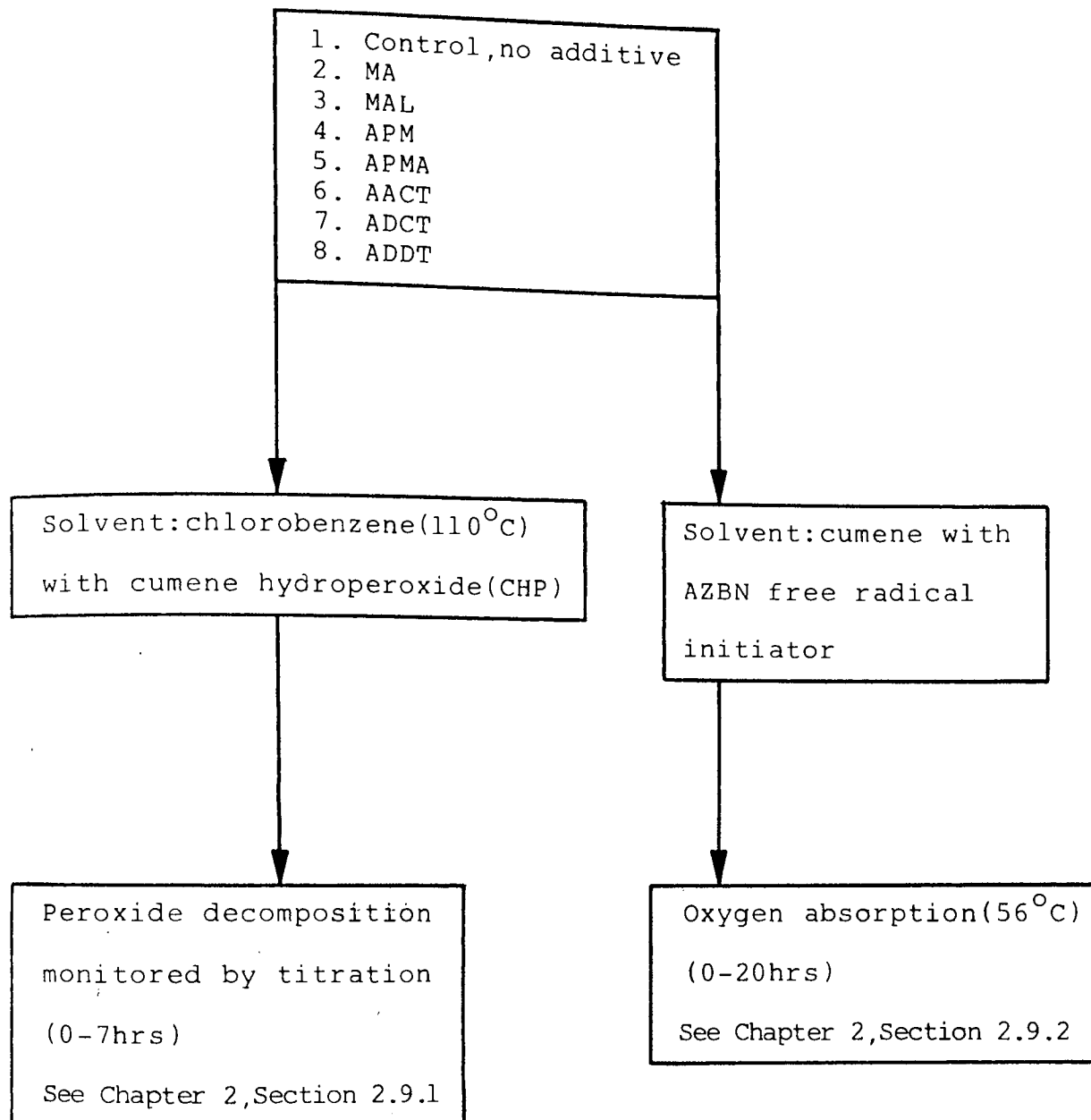
Scheme 6.4 Production of MA/DCP modified PP(HF22) containing chemically bound ADPA for thermal-oxidative ageing



Scheme 6.5 Production of mechano-chemically modified stabilised PP films for thermal-oxidative ageing



Scheme 6.6 Production of modified PP(HF22) plaques containing chemically bound stabilisers, some with reinforcing fibres added. Commercially stabilised PP controls are included.



Scheme 6.7 Hydro-peroxide decomposition and oxygen absorption solution studies on PP modifiers/ stabilisers

the additive stabilisation mechanisms (hydro-peroxide decomposing or chain-breaking free radical).

## 6.2 Results

### 6.2.1 Thermal-oxidative Stability Of Commercially Stabilised PP And PP(HF22) Containing Irganox Compounds

Melt stability, antioxidant binding and thermal-oxidative stability in the Wallace air oven at 140°C of commercially stabilised PP(HWM25 and GWM22) and unstabilised PP(HF22) with and without Irganox 1076 and 1010 are shown in Table 6.1 after processing (see Scheme 6.2). From the low MFI results, it is clear that these antioxidants are good melt stabilisers. The induction periods of these stabilised 200µm PP films are very good (Figure 6.2) with the best results obtained from PP(HWM25) at 1350 hours and PP(HF22) containing 0.5%Irganox 1010 at 1700 hours. Unstabilised PP(HF22) gave an expected poor result of only 5 hours (Figure 6.2) and this rapid increase in carbonyl absorption at  $1710\text{cm}^{-1}$ , a result of uncontrolled degradation due to the absence of thermal-oxidative stabilisers is shown in Figure 6.1. Results of similar ageing experiments on the same stabilised PP grades but after Soxhlet solvent extraction gave an induction period of only 5 hours, irrespective of original stabiliser type and concentration. This phenomenon is explained by data obtained from ultraviolet and infra-red spectra of Figures 6.3A and B which show that

Soxhlet extraction removes all traces of Irganox stabiliser from PP(HF22). Thus with all antioxidant removed from these PP grades (0% binding, Table 6.1), these films were unable to resist the thermal-oxidative Wallace air oven ageing.

#### 6.2.2 Attempted Binding Of ADPA To MA/DCP Modified PP(HF22) And Its Effect Upon Thermal-oxidative Stability

Initially, ADPA binding to 1%MA/0.2%DCP modified PP(HF22) by melt processing was attempted (Schemes 6.3 and 6.4). 1%MA/0.2%DCP was chosen because this system gave optimum mechanical properties in mechano-chemically modified PP (HF22) containing 30% glass fibre (Chapter Four, Section 4.2.5). It is shown in Table 6.2 and Figure 6.4 that 1%MA/0.2%DCP modification alone of PP(HF22) has no effect upon the thermal-oxidative stability of PP(HF22) on Wallace air oven ageing at 140°C. PP(HF22) modification using 1%MA/0.2%DCP gave  $3 \times 10^{-4}$  moles MA bound per 100g PP(HF22) or 50% binding based on the amount of MA present in the polymer after processing (Table 6.3) and it was found that after the addition of 1%ADPA by melt processing (Table 6.2), 5% of the 1%ADPA had become chemically bound to the modified PP(HF22). However, it was found that ADPA binding was doubled (to 10%) by Soxhlet extraction of the MA/DCP modified PP(HF22) prior to ADPA melt processing (Table 6.2). This ensured that any reaction of ADPA with MA during melt processing was with bound MA, thus rendering the ADPA unextractable. Despite the achievement of 10% ADPA binding

to extracted 1%MA/0.2%DCP modified PP(HF22), the induction periods of 200 $\mu$ m PP films before and after Soxhlet extraction were only 45 and 15 hours respectively (Figure 6.4) and thus could not be considered as a serious challenger to commercial grades such as PP(HWM25) which gave an induction period before extraction of 1350 hours (Figure 6.2).

To improve the thermal-oxidative stability of modified PP(HF22) containing ADPA, it was thought necessary to increase the amount of chemically bound MA in the system. Using the Buss Ko-Kneader (Table 6.3) and a wide range of MA/DCP combinations (the maximum amount of MA used, 20%, being limited by excessive fume evolution and poor mixing), optimum binding was obtained with 5%MA/2.5%DCP which gave  $22 \times 10^{-4}$  moles MA bound per 100g PP(HF22) and this grade was used for the next series of experiments for ADPA (0.1-1%) melt processing (Table 6.4). The best system was found to be Soxhlet extracted (to remove unbound MA) 5%MA/2.5%DCP modified PP(HF22) with 1%ADPA which resulted in 70%ADPA binding to the polymer. This material gave an induction period of 300 hours before extraction and 150 hours afterwards (Figure 6.5). This should be seen in context when 1%ADPA was melt processed with unextracted (containing bound and unbound MA) 5%MA/2.5%DCP modified PP(HF22) which gave only 30% binding (Table 6.4) and unextracted and extracted induction periods of 200 hours and 110 hours respectively (Figure 6.5).

An insight to the mechanisms involved in the chemical binding of ADPA to MA/DCP modified PP(HF22) via bound MA may be seen starting with the ultraviolet and infra-red spectra in Figures 6.6A and B respectively, which show results of 200 $\mu$ m unmodified PP(HF22) films containing 1%ADPA before and after Soxhlet extraction and clearly indicate that all of this stabiliser is removed (0%binding, Table 6.2). This explains the poor induction periods on Wallace air oven ageing at 140 $^{\circ}$ C. Figures 6.7A and B show the infra-red and ultraviolet spectra at the various stages of production of MA/DCP modified PP(HF22) containing 1%ADPA. The first spectra of each Figure (6.7A and B) show PP(HF22) alone and the second PP(HF22) containing 1%ADPA showing the characteristic aromatic amino absorption at 1590 $\text{cm}^{-1}$  in the infra-red, and 208nm and 286nm in the ultraviolet. Looking at the third spectra in Figures 6.7A and B, the distinctive spectra of MA/DCP modified PP(HF22) are shown with the strong characteristic 1792/1782 $\text{cm}^{-1}$  carbonyl absorption in the infra-red and the 225nm peak in the ultraviolet. When this modified polymer is melt processed with 1%ADPA, the infra-red and ultraviolet spectra (fourth spectra of Figures 6.7A and B) change dramatically; the MA absorptions at 1792/1782 $\text{cm}^{-1}$  disappear and are replaced by strong 1700/1690 $\text{cm}^{-1}$  and 1640 $\text{cm}^{-1}$  absorptions, characteristic of carboxylic acid and amide formation. The 1590 $\text{cm}^{-1}$  aromatic amine absorption remains. The ultraviolet spectrum (Figure 6.7B) shows the disappearance of MA (225nm) and the formation of peaks at 216, 283 and 353nm which corresponds exactly to the ultra-



violet spectrum of APMA (Chapter Two, Figure 2.7). On extraction of 5%MA/2.5%DCP modified PP(HF22) containing 1%ADPA (fifth infra-red spectrum, Figure 6.7A), the  $1700\text{cm}^{-1}$  absorption disappeared, while those of  $1690\text{cm}^{-1}$  and  $1590\text{cm}^{-1}$  were reduced to 30% of their original value, corresponding to the % binding of ADPA recorded for this system (Table 6.4). The ultraviolet spectrum of the same material (Figure 6.7B) shows the disappearance of the strong peaks at 216, 283 and 353nm and the appearance of weaker ones at 208 and 298nm, which corresponds to the ultraviolet spectrum of APMA (Chapter Two, Figure 2.11).

Despite significant progress made in achieving chemically bound ADPA to MA/DCP modified PP(HF22), the thermal-oxidative stability (Tables 6.2 and 6.4) of these materials was still not sufficient to be considered as a potential replacement for commercial systems such as PP(HWM25 and GWM22, Table 6.1 and Figure 6.2). The requirement for solvent extraction to remove unbound MA in the modified PP(HF22) before melt processing with ADPA in order to achieve significant bound stabiliser concentration was thought to be uneconomic.

### 6.2.3 Attempted Mechano-chemical Binding Of Stabilisers To PP(HF22) And Its Effect Upon Thermal-oxidative Stability

The results of PP(HF22) stabilisation using a variety of

free radical initiated chemically bound antioxidants listed in Scheme 6.1 are shown in Tables 6.5-6.9. APMA (Table 6.5) gave up to 70% binding on melt processing with DCP and this is shown graphically in the ultraviolet and infra-red spectra of 200 $\mu$ m PP(HF22) films containing APMA and DCP before and after Soxhlet extraction to remove unbound stabiliser (Figures 6.9A and B). The thermal-oxidative stability (Figure 6.8) of PP(HF22) containing 1%APMA and 0.2%DCP showed the highest induction period of 370 hours which was reduced to only 100 hours after Soxhlet extraction. The importance of an antioxidant to possess alkenic unsaturation for free radical binding during melt processing is demonstrated by the use of APSA as a stabiliser (Table 6.6). Lacking the alkenic unsaturation of APMA (see Scheme 6.1), APSA did not chemically bind to PP(HF22) as shown by the complete removal of this stabiliser on Soxhlet extraction in the ultraviolet and infra-red spectra of Figures 6.11A and B. Very poor thermal-oxidative stability of PP(HF22) was obtained with 1%APSA (Figure 6.10), giving an induction period of 30 hours which was reduced to only 5 hours after extraction.

Excellent thermal-oxidative stability of mechano-chemically modified PP(HF22) containing 1%APM and 1%DCP was obtained (Table 6.7 and Figure 6.12). The ultraviolet and infra-red spectra of this material (Figures 6.13A and B) before and after extraction show that melt processing resulted in an extraordinarily high binding figure of 97% (see also Table

6.7). A unique feature of 1%APM/1%DCP modified PP(HF22) was that its thermal-oxidative stability was greater after Soxhlet extraction (i.e., with unbound APM removed) as clearly seen in Figure 6.12 which shows the excellent induction periods of 2100 hours before extraction and 2500 hours afterwards.

The thermal-oxidative stability of PP(HF22) modified with the cyanuric chloride derivatives, AACT and ADDT gave poor results (Tables 6.8 and 6.9 respectively). Despite AACT containing an allylic amino group, maximum binding of only 27% was achieved when melt processed with 0.3%DCP (Table 6.8 and Figures 6.15A and B) and this resulted in induction periods of 30 hours before extraction and only 10 hours afterwards (Figure 6.14). As expected, ADDT, which does not possess allylic unsaturation, did not exhibit chemical binding to PP(HF22, Table 6.9) as seen by its complete removal on extraction from PP(HF22) films in the ultraviolet and infra-red spectra of Figures 6.17A and B and consequently gave very poor induction periods of 25 hours before extraction and 5 hours afterwards (Figure 6.16).

Table 6.10 compares the binding of stabilisers and induction periods (Figure 6.18) before and after extraction of commercially stabilised PP(HWM25 and GWM22) and PP(HF22) with and without Irganox 1076 and 1010 phenolic stabilisers with the optimised chemically bound antioxidant systems using PP(HF22). From Figure 6.18 it is clear that the commercial

grades give excellent thermal-oxidative stability, but because these stabilisers are not chemically bound, PP stabilised in this way deteriorates rapidly after Soxhlet solvent extraction. Significant increases in the thermal-oxidative stability of Soxhlet extracted PP(HF22) were achieved by initially modifying PP(HF22) using 5%MA/2.5%DCP followed by melt processing with 1%ADPA to obtain ADPA binding via polymer-bound MA (Figure 6.18). Good progress was also obtained with the mechano-chemical modification of PP(HF22) with APMA using DCP, but the carbonyl index induction periods of these two modified PP(HF22) grades before extraction (Figure 6.18) proved no match for the commercially stabilised PP grades. Both AACT and ADDT contributed very little to the thermal-oxidative stability of PP(HF22). However, extremely high binding (97%, Table 6.10) of 1%APM/1%DCP modified PP(HF22) contributed to the excellent thermal-oxidative stability (Figure 6.18); induction periods of 2100 hours and 2500 hours before and after extraction respectively, which compares extremely favourably to the commercially stabilised PP(HWM25) which gave 1350 hours (unextracted) and 5 hours (extracted).

The carbonyl indices during Wallace air oven ageing at 140°C of commercially and mechano-chemically stabilised PP(HF22) are shown in Figures 6.19-6.23. Each shows the induction period characteristic of each PP grade prior to the rapid increase in the rate of polymer degradation as shown by the rising carbonyl absorption at  $1710\text{cm}^{-1}$ . It was noted that

there is considerable variation in the initial carbonyl indices of commercially stabilised PP(Figure 6.19) and mechano-chemically modified PP(HF22) in Figures 6.20-6.23 and this is attributable to some additives (such as APMA, APSA and APM) themselves possessing carbonyl groups and thus absorbing in the  $1710\text{cm}^{-1}$  region of the infra-red. However, because the induction period is the time to rapid carbonyl concentration increase, the induction period calculation is not affected.

#### 6.2.4 Thermal-oxidative Stability Of Commercially And Mechano-chemically Modified PP Plaques

To obtain thermal-oxidative data on larger PP samples more representative of "under-bonnet" components, injection moulded 1mm PP plaques were aged in a Wallace air oven at  $150^{\circ}\text{C}$ . Because the plaques are too thick for infra-red spectroscopy, the carbonyl index could not be monitored but instead, the time to craze formation (i.e., appearance of surface cracks and onset of brittleness) was monitored. The thermal-oxidative stability of commercially stabilised PP plaques (HWM25 and GWM22) and PP(HF22) with and without Irganox stabilisers is shown in Figure 6.24 before and after Soxhlet extraction. Confirming earlier observations of similarly stabilised PP films (Figure 6.18), very good thermal-oxidative stability was obtained for unextracted samples (e.g., HWM25 took 60 days to craze), but after Soxhlet extraction, these PP grades lasted only  $1\frac{1}{2}$  days.

This large fall is attributable to the complete removal by solvent of stabilisers. Figure 6.25 shows the behaviour of mechano-chemically modified PP(HF22) plaques using the same ageing conditions and indicates that the use of 1%APM with 1%DCP in PP(HF22) mechano-chemical modification is the only chemically bound stabiliser to give good thermal-oxidative stability to 1mm plaques (65 days to craze before extraction and 75 days afterwards), confirming earlier trends observed with similarly modified PP(HF22) films (Figure 6.18). The effect of glass fibre and long Rockwool fibre (both 30% loading and A-1100 silane coupled) on the thermal-oxidative stability of commercially and mechano-chemically stabilised 1mm PP plaques is shown in Figures 6.26 and 6.27 respectively. The general observation is made that for both types of fibre, there is a reduction in time of 20% before crazing occurs compared with similarly stabilised homopolymer plaques (Figures 6.24 and 6.25).

#### 6.2.5 Cumene Hydroperoxide Decomposition And Oxygen Absorption Studies Of PP Modifiers And Stabilisers

Results of the cumene hydroperoxide decomposition behaviour by the modifiers/stabilisers listed in Scheme 6.7 are not shown graphically because all were found not to possess any decomposing activity, even after 7 hours at 110°C in chlorobenzene. Similarly, no decomposition was observed with the control which contained no additive.

However, all additives (Scheme 6.7) had some effect upon oxygen absorption in cumene containing AZBN (a free radical initiator) at 56°C. Figure 6.28 shows the oxygen absorption during the first 3 hours to highlight the initial stages, and Figure 6.29 shows the same samples over a period of 20 hours. Figures 6.28 and 6.29 show that the additive-free control started to absorb oxygen immediately and that 30mls were absorbed in only 8 hours. The addition of AACT and ADCT gave similar behaviour, although it was observed that ADCT tended to increase the rate of oxygen absorption (especially obvious during the latter stages of oxygen absorption, Figure 6.29). Other additives which did not show an induction period were the modifiers MA and MAL; both gave an appreciable reduction in the rate of oxygen absorption compared to the control (Figures 6.28 and 6.29) with MA being the most retardant. Three additives, APMA, APM and ADDT, showed what was initially an extremely low rate of oxygen absorption (or induction period), followed by a faster rate of absorption (Figure 6.29) similar to that of the control, with the exception of APM, which showed an absorption rate much lower than the control.

## 6.3 Discussion

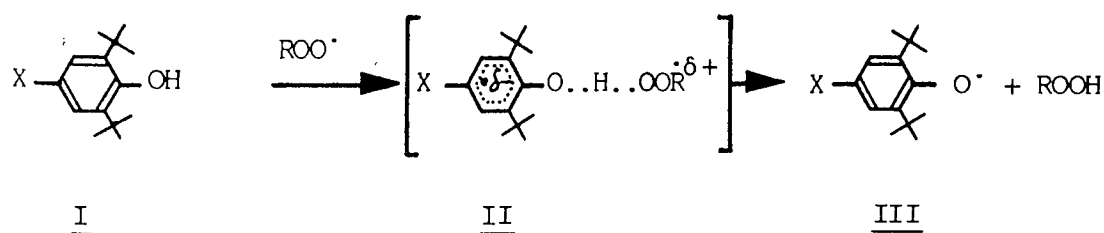
### 6.3.1 Thermal-oxidative Stability Of Commercially Stabilised PP And PP(HF22) Containing Irganox Compounds

The accelerated thermal-oxidative Wallace air oven test at 140°C is a compromise on the requirements to obtain realistic data about the comparative behaviour of different stabilisers in PP films in a reasonable time-span. Oxidation of such films is initially slow, the latter stages being auto-accelerative after an induction period (as monitored by carbonyl index, Figures 6.19-6.23) is reached, leaving the polymer discoloured and brittle<sup>(220)</sup>. For unstabilised PP(HF22), the induction period is small (Table 6.1), but compared to stabilised samples, is rather ill-defined (Figure 6.1). The stability conferred upon a polymer by an anti-oxidant depends not only on its inherent stabilising activity but also its permanence within the sample. Billingham<sup>(220)</sup> has shown that for a 10µm PP film, stabiliser loss is predominantly due to volatilisation; while loss in a 100µm film is volatility and diffusion controlled. The induction periods of 200µm PP films used in this chapter are thus a function of the inherent stabilising activity of the additive and the rate of loss controlled by diffusion and volatilisation during ageing.

Table 6.1 and Figure 6.2 show the effectiveness of Irganox 1010 and 1076 stabilisers in PP(HF22) during Wallace air



oven ageing. These stabilisers are often used in industry (their presence in commercial PP grades, GWM22 and HWM25, was confirmed by infra-red and ultraviolet studies of their films) and are particularly effective for two reasons. Their high chain-breaking antioxidant behaviour (Chapter One, Scheme 1.4) by phenolic hydrogen donation to deactivate degradative radicals (alkyl, alkoxy, alkylperoxy) in PP is a result of the two adjacent (ortho position) t-butyl groups which sterically hinder and stabilise the phenoxyl radical produced thus preventing further propagation of the degradative process. The substituents on the aromatic ring reduce the activation energy required for the formation of the transition state (II, Scheme 6.8) which involves electron transfer to the peroxy radical and electron delocalisation in the aromatic ring<sup>(113)</sup>.



Scheme 6.8 Mechanism of stabilising action of a hindered phenol with an alkylperoxy radical

The main function of the substituent in the para position (Irganox compounds, Scheme 6.1) is to increase compatibility<sup>(221)</sup>, while the increased molecular weight results in reduced rates of physical loss from the polymer<sup>(149,220,221)</sup>. Thus the high inherent antioxidant behaviour of both Irganox

1076 and 1010 coupled with their low loss-rate from polymers at high temperatures explains the excellent induction periods when these materials are incorporated into PP(HF22); see Figure 6.2.

Chain breaking Irganox stabilisers act stoichiometrically<sup>(124)</sup>; their effectiveness is thus limited by their concentration within the polymer which is dependent upon their solubility parameters<sup>(222)</sup> and cost. The concentration dependence is clearly shown (Figure 6.2) by the increase in length of induction periods of PP(HF22) when stabilised with 0.5% Irganox (1076 and 1010) compared with using only 0.25%. PP(HWM25) shows higher thermal-oxidative stability than PP(GWM22), Figure 6.2, because of the former's higher stabiliser concentration (Chapter Two, Table 2.1). Irganox 1010 was found to give superior induction periods to Irganox 1076 (Figure 6.2) and this is attributable to the lower volatility<sup>(222,223)</sup> of Irganox 1010 (mol. wt. 1178) compared with Irganox 1076 (mol. wt. 531) in addition to the fact that Irganox 1010 contains four hindered phenolic groups.

Despite the excellent thermal-oxidative stability of PP(HF22) containing Irganox compounds (Figure 6.2) under severe conditions (Wallace air oven, 140°C, constant air flow), complete removal of these additives was easily achieved by Soxhlet extraction (as shown in Figure 6.3A and B) rendering the polymer unable to resist thermal-oxidative ageing and resulting in very short induction periods (Table 6.1, Figure

6.2). Under-bonnet components must withstand severe operating conditions; high temperatures and constant or intermittent contact with extracting fluids<sup>(149)</sup> (Chapter Five, Section 5.2.2), conditions in which substantive stabilisers of the Irganox type are lost from the polymer<sup>(146,224)</sup>.

### 6.3.2 Attempted Binding Of ADPA To MA/DCP Modified PP(HF22) And Its Effect Upon Thermal-oxidative Stability

To render a stabiliser permanent within a polymer, a chemical bond between the two is required. This was initially attempted by introducing chemically bound reactive maleic anhydride groups (in the presence of di-cumyl peroxide during melt processing, Chapter Four, Section 4.2.5) to the polymer to create reactive sites where chemical binding might occur during subsequent melt-processing with ADPA (Scheme 6.3). This concept has been suggested (but not attempted) for natural rubber<sup>(225)</sup>, and successfully achieved using the reaction between chemically bound epoxide groups in rubbers with  $\beta$ -naphthylamine during melt processing<sup>(224,226)</sup>.

Incorporation of 1%ADPA to unmodified PP(HF22) has very little effect upon the polymers' thermal-oxidative stability (Table 6.2, Figure 6.4); the short induction period (25 hours) must be due to the rapid volatilisation of the low molecular weight ADPA (184) from the PP(HF22) film. Figure 6.6A and B shows that ADPA was completely removed from the

polymer by Soxhlet extraction, rendering the polymer with no protection against oxidation. Despite the achievement of ADPA chemical binding to modified PP(HF22), Table 6.2, induction periods of such samples (Figure 6.4) were still very low and this is attributable to the low concentration of bound MA ( $3 \times 10^{-4}$  mol/100gPP(HF22)) within the polymer providing an insufficient number of reactive sites to achieve an adequate chemically bound ADPA stabiliser concentration.

The bound MA concentration was increased seven-fold to  $22 \times 10^{-4}$  mol/100gPP(HF22) by melt processing with 5%MA/2.5%DCP (Table 6.3) and after extraction to remove unbound MA, a similar increase in the binding of ADPA (to 70%) was achieved (Table 6.4). This high level of binding, rendering the majority of stabiliser permanent within the polymer explains the increase in induction period for this material to 300 hours (Figure 6.5), compared with only 25 hours for unmodified PP(HF22) containing 1%ADPA.

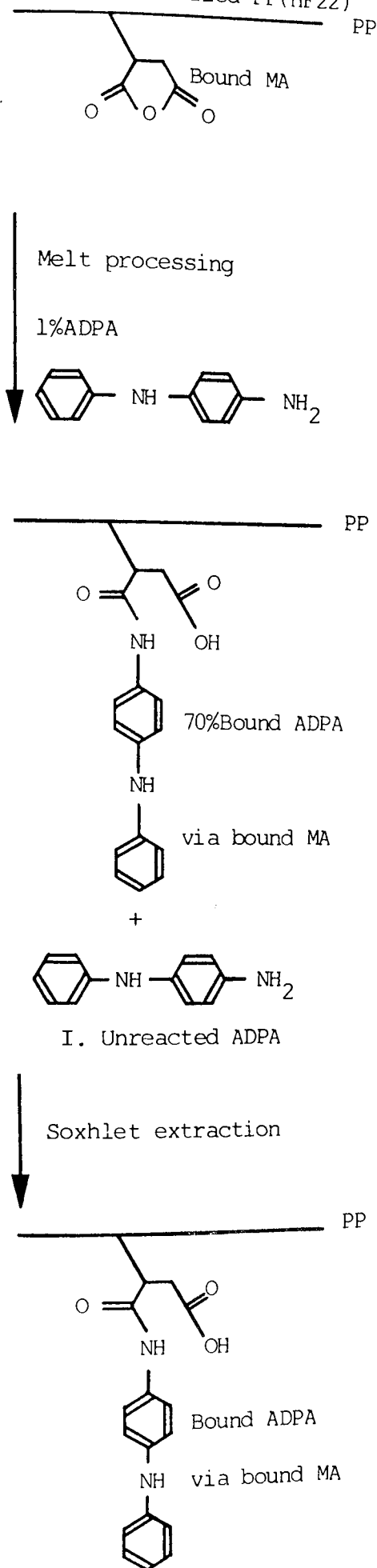
From the infra-red and ultraviolet spectrophotometric studies of Figures 6.6A and B - 6.7A and B, the mechanism of ADPA binding to MA modified PP(HF22) may be postulated (Scheme 6.9A and B).

Scheme 6.9A shows the ADPA binding mechanism to MA modified PP(HF22) which has been Soxhlet extracted to remove unbound MA. With its sterically unhindered primary amino group,

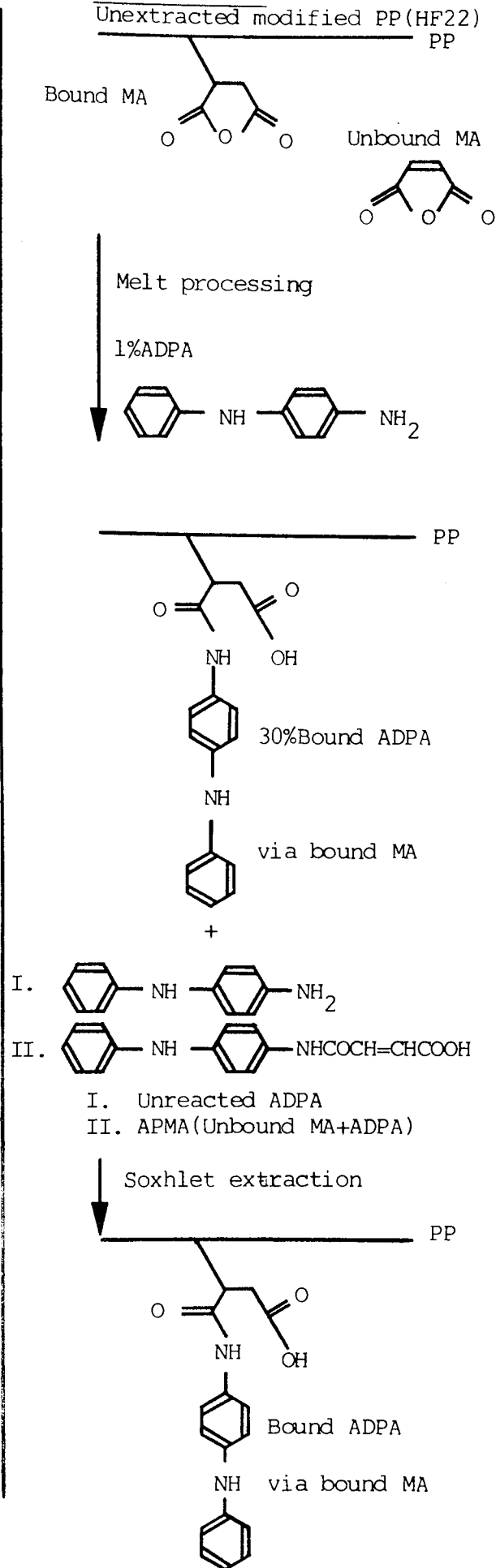
ADPA readily reacts with the bound anhydride during melt processing at 180°C by a simple condensation reaction (to give 70% ADPA binding, Table 6.4), involving anhydride ring opening, carboxylic acid formation and an amide bond linking the bound modifying group to the diaryl-amino stabiliser. This is accompanied by the appearance of infra-red absorptions at 1690 and 1640cm<sup>-1</sup> (Figure 6.7A.5) and ultraviolet λ<sub>max</sub> at 208 and 298nm (Figure 6.7B.5), both characteristic of 4-anilinophenylsuccinamic acid (APSA), the product of reaction in solution between succinic anhydride (SA, the saturated equivalent of MA) and ADPA (Chapter Two, Section 2.1.4, Figures 2.11 and 2.12). Scheme 6.9A also shows that ADPA which did not participate in the reaction with MA modified PP(HF22) remained in the polymer unaltered, which was confirmed by infra-red and ultraviolet studies on the Soxhlet extracted material.

Similarly modified PP(HF22) containing bound and unbound MA (i.e., not Soxhlet extracted) gave ADPA binding of only 30% (Table 6.4) which contributed to inferior thermal-oxidative stability of PP(HF22), Figure 6.5. This phenomenon is explained in Scheme 6.9B from evidence collected in Figure 6.7A and B. The infra-red spectrum of MA (bound and unbound) in PP(HF22), Figure 6.7A.3, shows the characteristic coupled carbonyl absorptions (1880, 1792/1782cm<sup>-1</sup>) which disappear during melt processing with 1%ADPA (Figure 6.7A.4) to be replaced by strong bands at 1700/1690 and 1640cm<sup>-1</sup> which are attributable to two different reaction

Scheme 6.9A  
Extracted modified PP(HF22)



Scheme 6.9B  
Unextracted modified PP(HF22)



Scheme 6.9A and B Chemical binding of ADPA to MA modified  
PP(HF22)

products (Scheme 6.9B). The first is the ring-opening condensation reaction between ADPA and unbound MA to form 4-anilinophenylmaleamic acid (APMA); this is confirmed by the ultraviolet spectrum (Figure 6.7B.4) which shows the presence of APMA ( $\lambda_{\max}$ , 216, 283 and 353nm, Chapter Two, Figure 2.7). The second reaction is between ADPA and PP(HF22)-bound MA to give the anilinophenylsuccinamic acid derivative described earlier in this section. Its presence in the polymer however, is masked by the infra-red and ultraviolet absorptions of APMA (Figures 6.7A.4 and 6.7B.4). Extraction of APMA and any unreacted ADPA reveals the presence of the bound succinamic acid species (Scheme 6.9B, Figures 6.7A.5 and 6.7B.5). This extraction results in a 70% reduction in infra-red intensity at  $1590\text{cm}^{-1}$  (diaryl-amino absorption) which corresponds to the binding of ADPA (30%) recorded (Table 6.4). This figure was confirmed by infra-red and ultraviolet studies of the extracted material.

### 6.3.3 Attempted Mechano-chemical Binding Of Stabilisers To PP(HF22) And Its Effect Upon Thermal-oxidative Stability

To further improve the thermal-oxidative stability of PP(HF22) in highly volatilising and extracting environments, stabilisers (listed in Scheme 6.1) containing vinyl unsaturation were bound to PP(HF22) using a free radical catalyst (DCP) in one melt processing stage (compared with two required for the binding of ADPA to MA modified PP(HF22)),

Section 6.3.2). A unique feature of these stabilisers is that some have been successful as chemical modifiers, enhancing the mechanical performance of 30%GF reinforced PP(HF22) composites (Chapter Five, Scheme 5.1, Section 5.2.1). All of the stabilisers listed in Scheme 6.1 are derived from ADPA (Chapter Two, Section 2.1.4) and consequently the thermal-oxidative stabilities of PP(HF22) containing these additives are comparable on the basis of antioxidant structural features concerning the modifying group para to the diphenylamine stabiliser, and the permanence (%chemical binding) of the additive within the polymer.

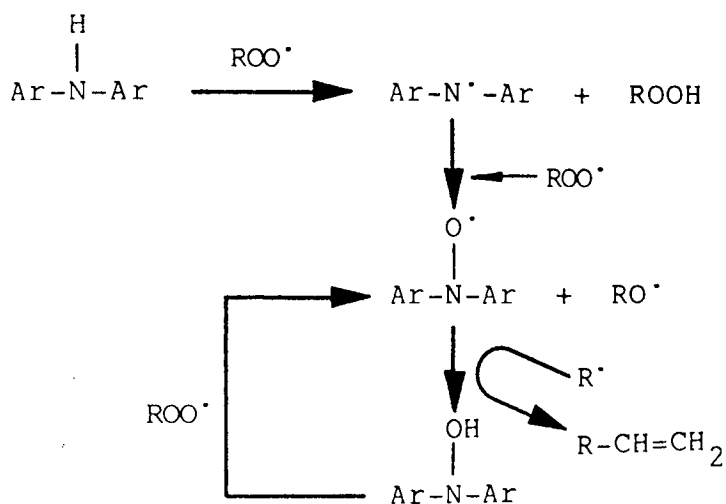
The degree of binding is dependent upon the concentration of DCP used (as described in Chapter Five, Section 5.2.1), and this determines the amount of stabiliser loss either by volatilisation during Wallace air oven ageing at 140°C or by solvent extraction by Soxhlet. APSA (Table 6.6) and ADDT (Table 6.9) which both lack vinylic unsaturation, did not chemically bind to PP(HF22) and consequently showed very poor melt and thermal-oxidative stability (Figures 6.10 and 6.16).

The use of 1%APM/1%DCP conferred outstanding thermal-oxidative stability to 200µm PP(HF22) films with respect to Wallace air oven ageing at 140°C before or after Soxhlet solvent extraction (Table 6.7). Giving 70% binding to PP(HF22) by melt processing even in the absence of DCP, the



very high reactivity of APM was accentuated using 1%DCP to give 97% binding, which is attributable to the effect of the diaryl-amino group attached to the maleimide ring; the ultraviolet spectrum of APM (Chapter Two, Figure 2.9) shows that there is electronic interaction between the maleimide and phenyl rings since electronic maxima appear at much longer wavelengths than the ultraviolet spectra of maleimide itself (Chapter Two, Figure 2.13) or the additional ADPA group (Chapter Two, Figure 2.3). Indeed, Tawney<sup>(227)</sup> has noted that the electron releasing effect of the aromatic ring is transmitted to the maleimide ring and the resultant enhanced electron density in the maleimide ring leads to its greater reactivity. Although Tawney<sup>(227)</sup> used bis-maleimides as rubber curing agents, the same principle applies, with chemical binding to the polymer being the objective. Despite 70%APM binding being achieved in the absence of DCP, poor thermal-oxidative stability was observed in PP(HF22) (induction period of only 50 hours, Figure 6.12). Melt processing with 1%DCP increased the binding to 97% and the induction period to 2100 hours (Figure 6.12). This increase in chemical binding (from 70 to 97%) when 1%DCP is used is not sufficient to explain the large increase in thermal-oxidative stability; APM stabilises in a free radical trapping mode<sup>(224,225)</sup> and Table 6.7 shows that despite the very high levels of DCP used (up to 1%), very good PP(HF22) melt stability is observed. Whilst a proportion of free radicals in the PP(HF22) melt (stemming from thermal decomposition of DCP and mechano-chemical

shear) are utilised by APM for free radical binding to the polymer (in a similar way to MA, Chapter Four, Section 4.2.5), the remainder are exploited by the diaryl-amino group conferring excellent thermal-oxidative stability to PP(HF22). It is suggested<sup>(124)</sup> that the maleimide ring confers auto-synergism to the diaryl-amine, and it is known<sup>(124,228)</sup> that such diaryl amines react with alkylperoxyl radicals (present in the PP(HF22) melt at high concentration due to the presence of 1%DCP) as shown in Scheme 6.10<sup>(229,230)</sup>.



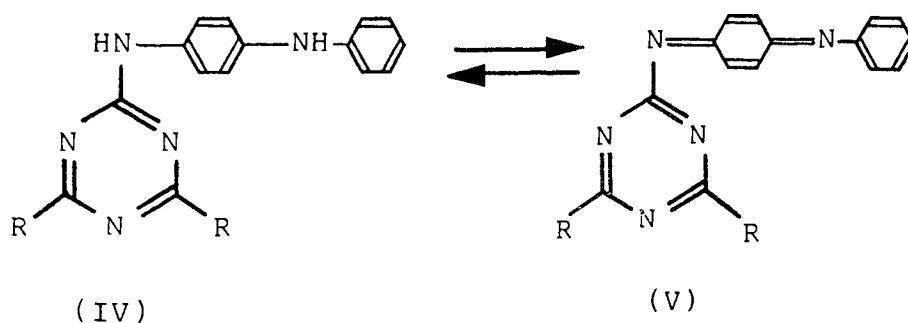
Scheme 6.10 Cyclical reaction mechanism of alkylperoxyl and alkyl radicals with nitroxyl radicals originating from diaryl-amino adducts

This results in hydrogen abstraction from the diaryl-amine and is the rate determining step of the chain breaking mechanism<sup>(124)</sup>, but because this breaks only one kinetic chain, this alone is not sufficient to explain the extraordinarily high stability of PP(HF22) containing APM.

Scheme 6.10 shows that the resultant amino radical reacts with another alkylperoxyl radical producing a nitroxyl and alkoxy radical. The chances of the amino radical abstracting hydrogen from PP(HF22) to reform the amine and create a macro-alkyl free radical are low<sup>(124)</sup> due to the steric hinderance of the diaryl group. After oxidation of the amine to the nitroxyl, the stabiliser enters a catalytic cycle (Scheme 6.10) involving alternate scavenging of alkyl and alkylperoxyl radicals<sup>(231)</sup>; alkyl radicals are utilised by the nitroxyl to give olefin and hydroxylamine which in turn reduces an alkylperoxyl radical with simultaneous nitroxyl regeneration<sup>(229-231)</sup>. The total number of alkylperoxyl radicals deactivated per stabilising molecule coincides with the number of interrupted degradative chains and is known as the stoichiometric coefficient; possessing a high coefficient explains why the thermal-oxidative stability of 1%APM/1%DCP modified PP(HF22) is so good. The increase in the thermal-oxidative stability of 1%APM/1%DCP modified PP(HF22) after extraction (Figure 6.12) may be due to the fact that 97% of the APM present is chemically bound to the polymer (Table 6.7) and thus, extraction removes only the remaining 3%. Moreover, DCP residues are also removed and this must be responsible for the increase in thermal-oxidative stability (the induction period increases from 2100 to 2500 hours).

The cyanuric chloride derivatives, AACT and ADDT (Tables 6.8 and 6.9 respectively) despite being less volatile than

ADPA gave poor thermal-oxidative stability in PP(HF22), Figure 6.18, and this is due in part to poor chemical binding (ADDT lacking allylic unsaturation gave no binding) of these additives which also resulted in poor melt stability. Poor binding of AACT is possibly due to the presence of diarylamine which acts stoichiometrically as a hydrogen donor toward alkoxy and alkylperoxy radicals formed by thermal decomposition of DCP. However, because the melt stability was poor (Table 6.8), it is probable that this reaction was not of great importance. It is most likely that during the melt processing of AACT or ADDT with PP(HF22), the chlorines on the cyanuric ring react with the diaryl amine to produce a dimer and liberate hydrogen chloride, thus depriving the modifier of its stabilising activity. It has been suggested<sup>(232)</sup> that the hydrogen donating capacity of cyanuric chloride-ADPA derivatives such as AACT and ADDT may be further reduced by oxidation to (V) shown in Scheme 6.11.

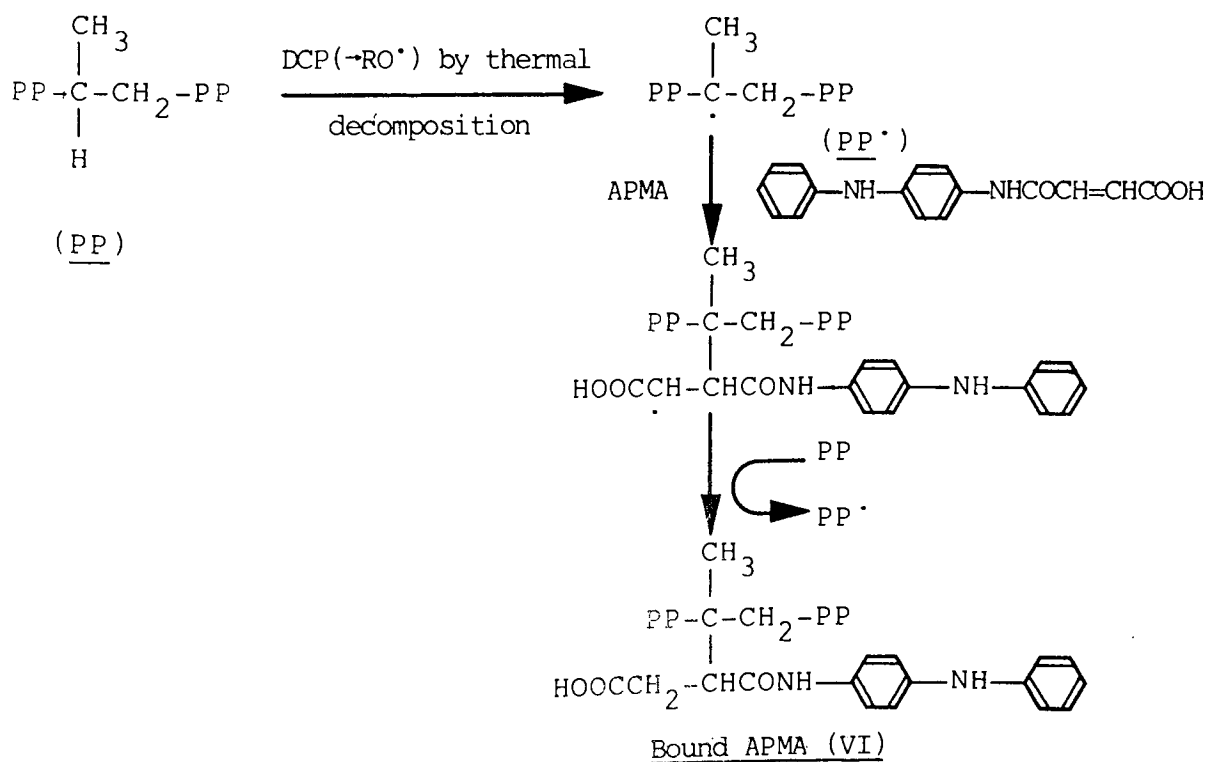


Scheme 6.11 Oxidation of cyanuric chloride-ADPA derivatives

Formation of (V) diminishes the effectiveness of the stabiliser by reducing its hydrogen-donating capacity, and it is for this reason that despite cyanuric chloride derivatives

having been used by workers with varying degrees of success in stabilising polymers<sup>(232,233)</sup>, cyanuric chloride-ADPA derivatives have been shown<sup>(232)</sup> to be poor stabilisers with low reactivity towards alkoxyl and alkylperoxyl radicals.

APMA chemically binds to PP(HF22) in the presence of DCP in appreciable quantities (Table 6.5), but due to the lack of a maleimide ring, its binding, melt and thermal-oxidative stability are inferior to that of PP(HF22) containing APM (Tables 6.5 and 6.7, Figures 6.8, 6.12 and 6.18). However, infra-red and ultraviolet spectrophotometric studies of APMA binding to PP(HF22) produced interesting results which are described in Scheme 6.12 (Figure 6.9A and B).



Scheme 6.12 Chemical binding of APMA to PP(HF22)

The infra-red and ultraviolet spectra (Figure 6.9A and B) of the chemically bound unextractable material (i.e., after Soxhlet extraction of unbound APMA and DCP residues) display different absorption characteristics to the starting material (APMA), indicating that its vinyl unsaturation is lost during free radical addition to PP(HF22), resulting in a chemically bound stabiliser (VI, Scheme 6.12). Both the infra-red and ultraviolet spectra of the bound adduct (VI) are identical to the spectra of APSA (Chapter Two, Figures 2.11 and 2.12), indicating that the free radical binding mechanism has occurred across the vinylic unsaturation resulting in a chemically bound saturated species almost identical to APSA.

#### 6.3.4 Thermal-oxidative Stability Of Commercially And Mechano-chemically Modified PP Plaques

Thermal-oxidative ageing tests were conducted upon 1mm thick stabilised PP(HF22) plaques with and without reinforcing fibres (Figures 6.24-6.27); despite air-oven ageing of films being a conveniently quick method for stabiliser comparison (Section 6.3.1), it is volatility that is primarily responsible for antioxidant loss and low induction periods. In larger components (1mm or greater), stabiliser loss by diffusion becomes more important<sup>(220)</sup> and this contributes to a longer lifetime of the polymer. For this reason, plaques were aged at 150°C (compared with 140°C for films) so that crazing occurs within a reasonable time.

Irganox stabilisers (present in PP(HF22) and HWM25 and GWM22) are of high molecular weight and gave excellent thermal-oxidative stability to plaques (Figure 6.24) because of their low diffusability. Unbound stabilisers of much lower molecular weight (ADPA, APSA and ADDT) gave poor stability to PP(HF22) due to rapid diffusion to the plaque's surface where volatilisation occurs (Figure 6.25). The excellent stability imparted to PP(HF22) plaques by 1%APM/1%DCP (Figure 6.25) is attributable to the very high binding level (97%, Table 6.7) rendering the stabiliser unable to diffuse, volatilise or be solvent extracted from the polymer. The general 20% reduction in the time for samples to craze when fibres (30%) were moulded with the polymer (Figures 6.26 and 6.27) is probably due to the fibres introducing imperfections at the surface and voids in the interior of the plaque, which present areas for easier initiation and propagation of thermal-oxidative attack of the polymer. The fact that stabilisers such as APMA and APM have also been shown to react with silane coupling agents on the surface of glass fibres (Chapter Five, Section 5.2.5) to enhance the mechanical properties of composites, may also affect their ability to stabilise the polymer matrix.

#### 6.3.5 Cumene Hydroperoxide Decomposition And Oxygen Absorption Studies Of PP Modifiers And Stabilisers

It is well-documented<sup>(97,234)</sup> that hydrocarbon autoxidation occurs by a free radical process, the main chain carrying

species being peroxy radicals<sup>(235)</sup>; the result of thermal decomposition of hydroperoxides. Two types of antioxidant act to suppress this behaviour (Chapter One, Scheme 1.4); chain-breaking which act by alkyl and alkylperoxy radical removal, and hydroperoxide decomposers which are removed in a non-radical manner.

Because all modifiers/stabilisers tested were shown to have no peroxide decomposing ability at all, these additives act solely via a chain-breaking mode.

The additive-free control (Figures 6.28 and 6.29) undergoes autoxidation by a free radical mechanism<sup>(97,235)</sup>. With the exception of ADCT, inhibition of oxidation starts from the beginning indicating that it is the stabilisers themselves being involved in removal of free radicals and not their decomposition products. The chain-breaking activity of the additives is attributable to two factors (Figures 6.28 and 6.29); firstly the behaviour of unsaturated modifiers such as MA and MAL which are able to utilise free radicals as they have been shown to do during their mechano-chemical binding to PP(HF22) on melt processing in the presence of DCP (MA, Chapter Four, Section 4.2.5 and MAL, Chapter Five, Section 5.2.1). For both additives (Figures 6.28 and 6.29), this is evident by their oxygen absorption suppression compared with the additive-free control. This characteristic also contributes to the oxygen absorption behaviour of APMA and APM; these PP(HF22) modifiers/stabilisers, in addition



to the presence of carbon-carbon unsaturation (through which chemical binding to the polymer occurs) possess a diarylamino group. This group, present to stabilise PP(HF22) against free radical degradation (Section 6.2.3), is responsible for the oxygen absorption induction periods (APMA, 3.5 hours and APM, 9 hours, Figure 6.29). It is significant that APM, which gave the longest oxygen absorption induction period (Figure 6.29), was the best melt and thermal-oxidative stabiliser in PP(HF22), (Section 6.2.3). The significantly reduced rate of oxygen absorption of cumene containing APM after the induction period of 9 hours, is probably due to free radical uptake by its maleimide ring (Figure 6.29), a process in which during the melt processing of PP(HF22) in the presence of 1%DCP leads to 97% binding, the highest of any modifier/stabiliser tested (Section 6.2.3). The suppression of oxygen absorption by ADDT (Figures 6.28 and 6.29) was in apparent contradiction to the poor melt and thermal-oxidative behaviour conferred upon PP(HF22) (Section 6.2.3). This is probably because during oxygen absorption at 56°C, ADDT's diarylamino group can participate in the free radical chain-breaking process; at the melt processing temperature of PP(HF22), 180°C, reaction of chlorine on the cyanuric ring with the diarylamino group can occur<sup>(171)</sup> (Section 6.2.3), thus diminishing ADDT's free radical stabilising ability.

Sample No.	Polymer (PP)	Added Stabiliser (%)	Concentration of added stabiliser (molx10 <sup>-3</sup> /100gPP)	MFI (g/10min)	%Binding of stabiliser to PP	Carbonyl Index Induction Period of 200µm PP films (hours)	
						Unextracted	Extracted
1	HF22	-	-	5.0	-	5	5
2	GWM22	-	-	4.5	0	1100	5
3	HWM25	-	-	4.5	0	1350	5
4	HF22	Irganox1076(0.25%)	0.47	3.21	0	1100	5
5	HF22	Irganox1076(0.5%)	0.94	3.07	0	1450	5
6	HF22	Irganox1010(0.25%)	0.21	2.94	0	1200	5
7	HF22	Irganox1010(0.5%)	0.42	2.10	0	1700	5

Table 6.1 Melt flow index(MFI), %Binding of stabilisers and carbonyl index induction periods

(Wallace air oven,140°C before and after extraction of 200µm PP films)of commercially stabilised PP(HWM25 and GWM22) and unstabilised PP(HF22) with and without Irganox stabilisers (processed in RAPRA torque rheometer,180°C,60rpm,8mins,CM).

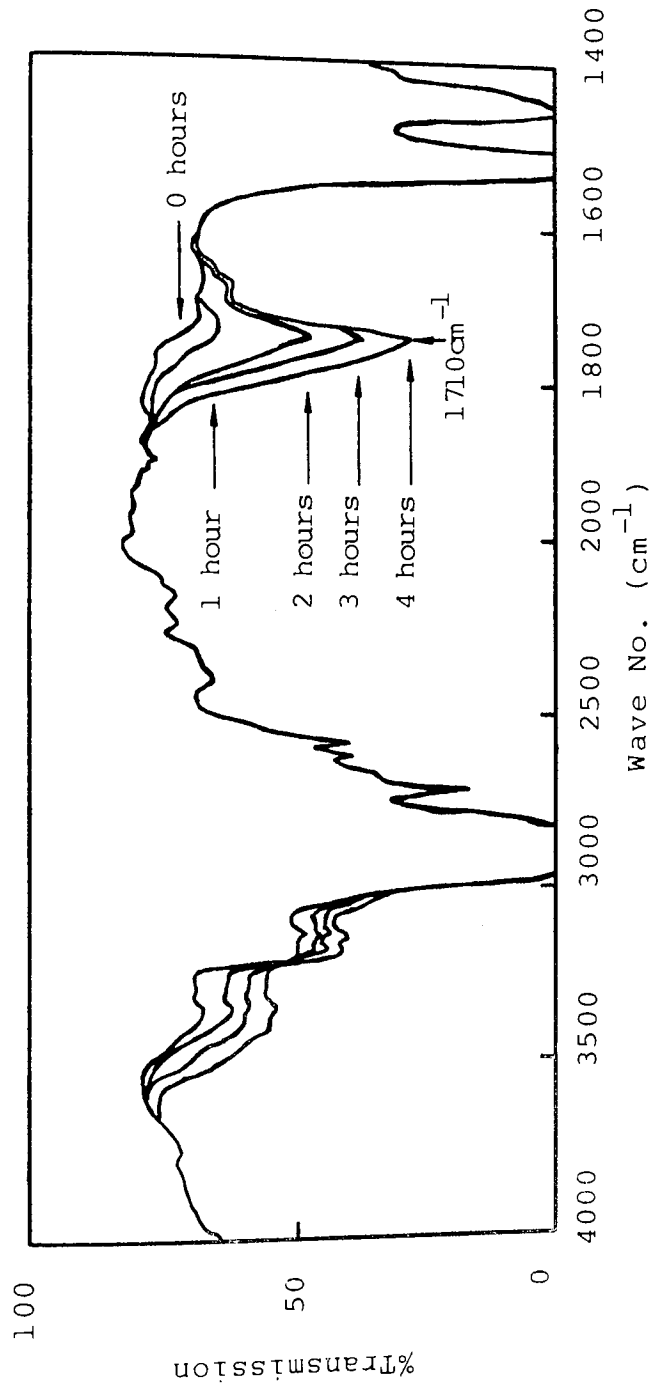


Figure 6.1 Infra-red spectrum of 200µm PP(HF22) film showing the increase in carbonyl absorption ( $1710\text{cm}^{-1}$ ) during Wallace air oven ageing at  $140^{\circ}\text{C}$ .

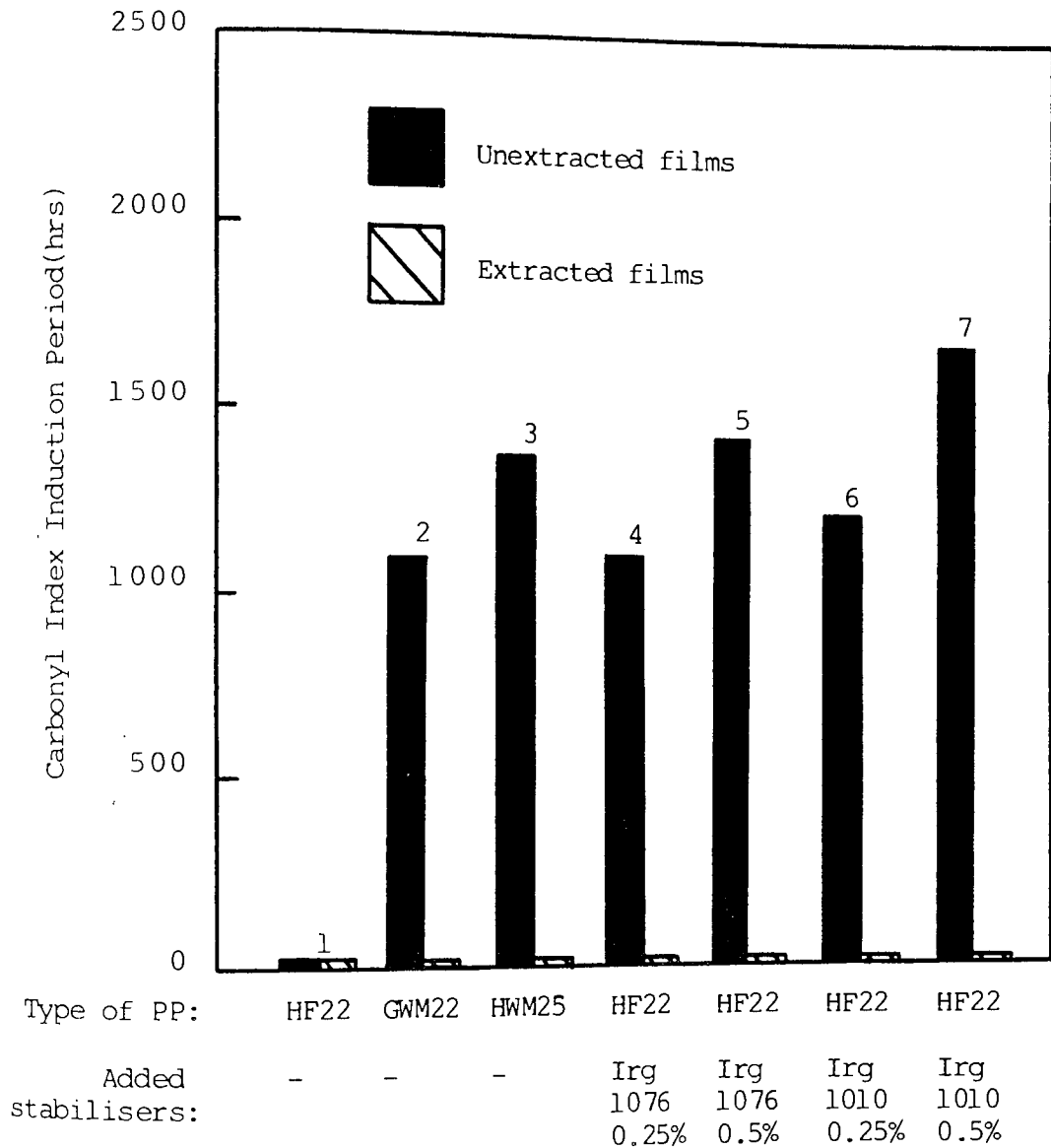


Figure 6.2 Carbonyl index induction periods (Wallace air oven, 140°C before and after extraction of 200µm PP films) of commercially stabilised PP(HWM25 and GWM22) and unstabilised PP(HF22) with and without Irganox stabilisers(processed in RAPRA torque rheometer, 180°C,60rpm,8mins,CM). See Table 6.1.

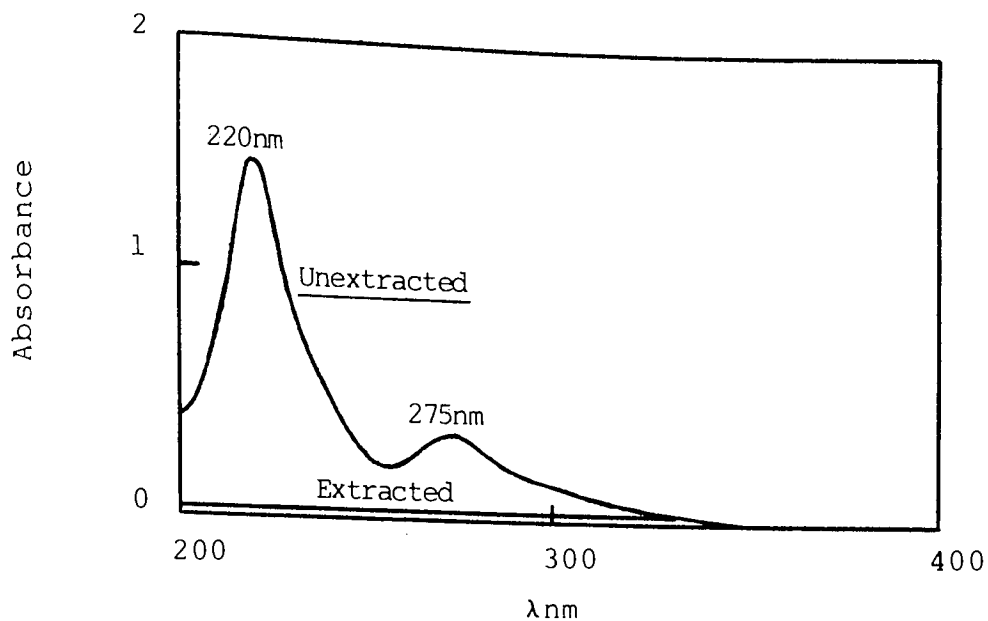


Figure 6.3A Ultraviolet spectrum before and after extraction of 200 $\mu$ m PP(HF22) film containing 0.25%Irganox1010 processed in the RAPRA torque rheometer(180 $^{\circ}$ C,60rpm,8mins,CM). See Table 6.1.

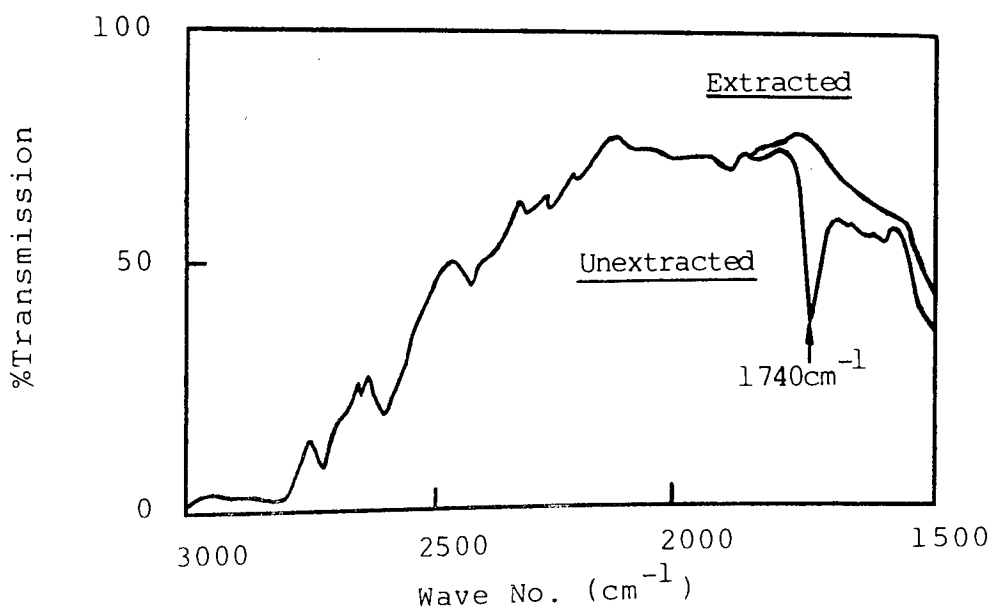


Figure 6.3B Infra-red spectrum before and after extraction of 200 $\mu$ m PP(HF22) film containing 0.25%Irganox1010 processed in RAPRA torque rheometer (180 $^{\circ}$ C,60rpm,8mins,CM).See Table 6.1.

Sample No.	Modified PP (HF22)		ADPA (%)	Concentration of ADPA $3$ (molx10 <sup>-3</sup> /100gPP)	%Binding of ADPA to modified PP	Carbonyl Index Induction Period of 200 $\mu$ m PP films (hours)	
	Modifier for PP (HF22)	Extracted to remove unbound modifier residues before addition of antioxidant (ADPA)				Unextracted	Extracted
1	Unmodified PP (HF22) control	-	-	-	-	5	5
2	1%MA/0.2%DCP	No (Unex)	-	-	-	5	5
3	Unmodified PP (HF22)	-	1.0	5.45	0	25	5
4	1%MA	No (Unex)	1.0	5.45	0	35	5
5	0.2%DCP	No (Unex)	1.0	5.45	0	25	5
6	1%MA/0.2%DCP	No (Unex)	1.0	5.45	5	40	5
7	1%MA/0.2%DCP	Yes (Ex)	1.0	5.45	10	45	15

Table 6.2 Melt flow index (MFI), %Binding of stabiliser (ADPA) and carbonyl index induction periods (Wallace air oven, 140°C before and after extraction of 200 $\mu$ m PP films) of unmodified and 1%MA and 0.2%DCP modified PP (HF22) containing 1%ADPA

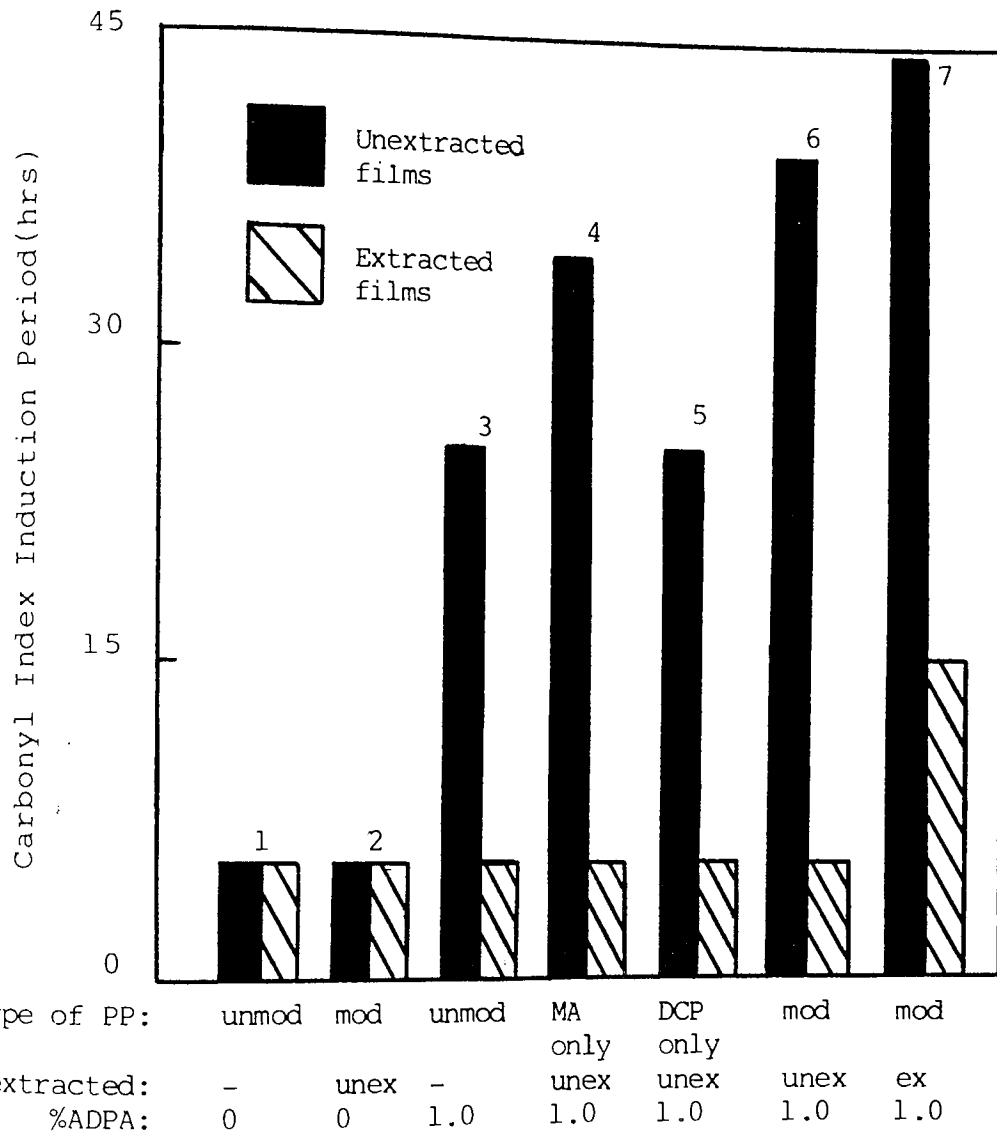


Figure 6.4 Carbonyl index induction periods (Wallace air oven, 140°C before and after extraction of 200µm PP films) of unmodified and 1% maleic anhydride (MA) and 0.2% di-cumyl peroxide (DCP) modified PP (HF22) containing 1% ADPA processed in the RAPRA torque rheometer (180°C, 60rpm, 8mins, CM). See Table 6.2.

%MA	%DCP	MFI(g/10min)	Bound MA(molesx10 <sup>-4</sup> /100gPP)
1	0	4.95	0
1	0.05	15.1	1.6
1	0.1	22.3	1.8
1	0.2	28.7	3.0
1	0.3	39.9	2.8
5	0	7.32	0
5	0.5	8.11	4.0
5	1.0	11.32	4.5
5	1.5	13.31	18.0
5	2.0	14.83	19.5
5	2.5	21.79	22.0
10	0	6.64	0
10	1.0	7.51	5.0
10	2.0	7.98	6.0
10	3.0	13.35	14.0
10	4.0	18.14	13.5
10	5.0	24.37	19.6
20	0	6.79	0
20	2.0	7.32	7.0
20	3.0	7.56	8.0
20	4.0	34.40	20.0
20	5.0	40.93	21.0
20	10.0	51.27	21.0

Table 6.3 Optimisation of maleic anhydride(MA) binding to PP(HF22) with di-cumyl peroxide(DCP) processed in the Buss Ko-Kneader (see Scheme 6.3)



Sample No.	Modified PP (HF22)		ADPA (%)	Concentration of ADPA <sup>-3</sup> /100gPP (molX10 <sup>-3</sup> )	%Binding of ADPA to modified PP	Carbonyl Index Induction Period of 200µm PP films (hours)	
	Modifier for PP (HF22)	Extracted to remove unbound modifier residues before addition of antioxidant (ADPA)				Unextracted	Extracted
1	Unmodified PP (HF22) control	-	-	-	-	5	5
2	Unmodified PP (HF22)	-	1.0	5.45	0	25	5
3	5%MA/2.5%DCP	Yes(Ex)	0.1	0.545	80	40	5
4	5%MA/2.5%DCP	Yes(Ex)	0.2	1.09	80	40	25
5	5%MA/2.5%DCP	Yes(Ex)	0.3	1.64	75	150	25
6	5%MA/2.5%DCP	Yes(Ex)	0.5	2.72	70	300	50
7	5%MA/2.5%DCP	Yes(Ex)	1.0	5.45	70	300	150
8	5%MA/2.5%DCP	No(Unex)	1.0	5.45	30	200	110

Table 6.4 Melt flow index(MFI), %Binding of stabiliser(ADPA) and carbonyl index induction periods (Wallace air oven, 140°C before and after extraction of 200µm PP films) of unmodified and 5%maleic anhydride(MA) and 2.5%di-cumyl peroxide(DCP) modified PP(HF22) containing ADPA(0.1-1%)

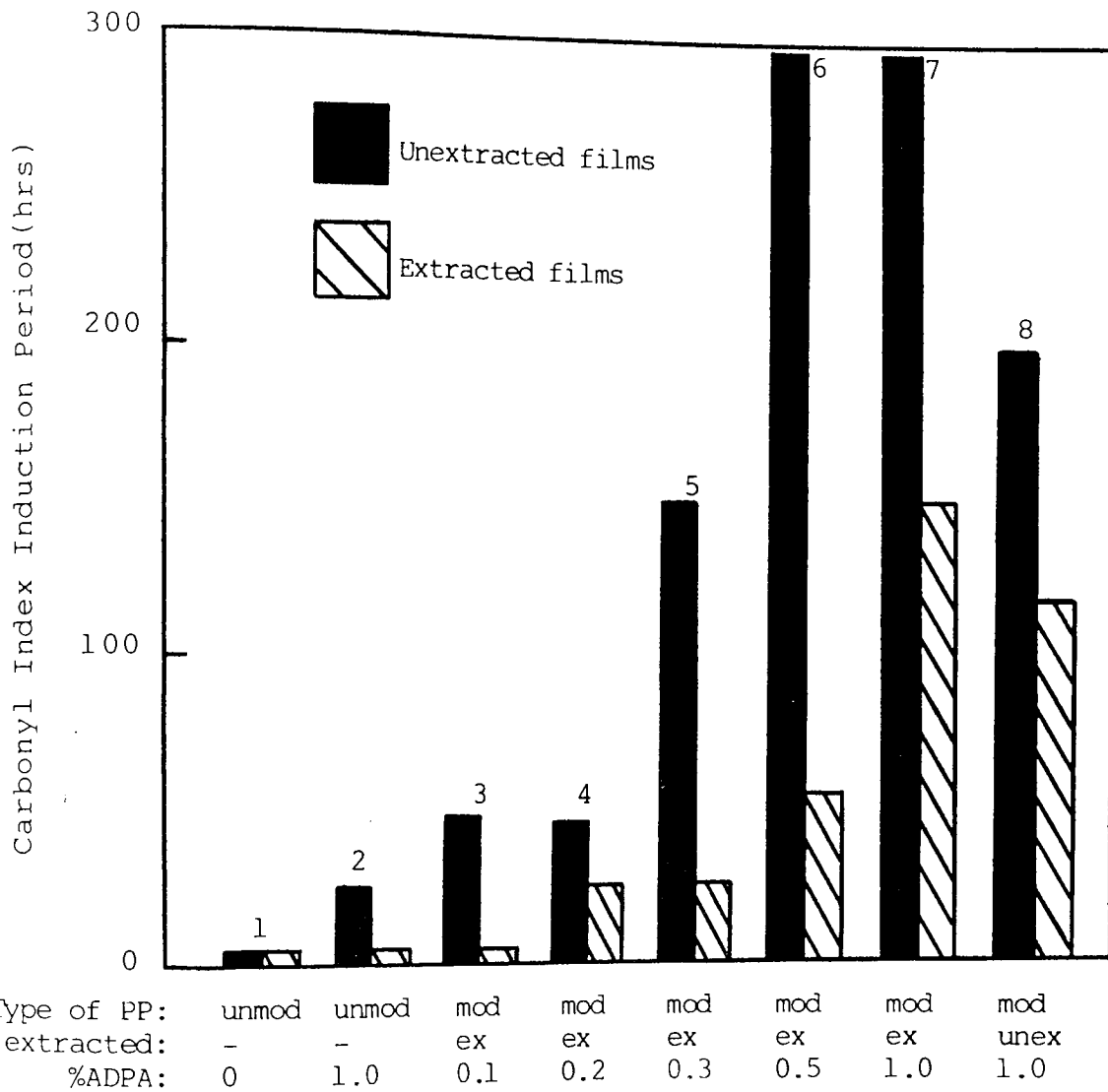


Figure 6.5 Carbonyl index induction periods(Wallace air oven, 140°C before and after extraction of 200µm PP films)of unmodified and 5%maleic anhydride(MA) and 2.5%di-cumyl peroxide(DCP) modified PP(HF22) containing up to 1%ADPA processed in the RAPRA torque rheometer(180°C,60rpm,8mins,CM).See Table 6.4.

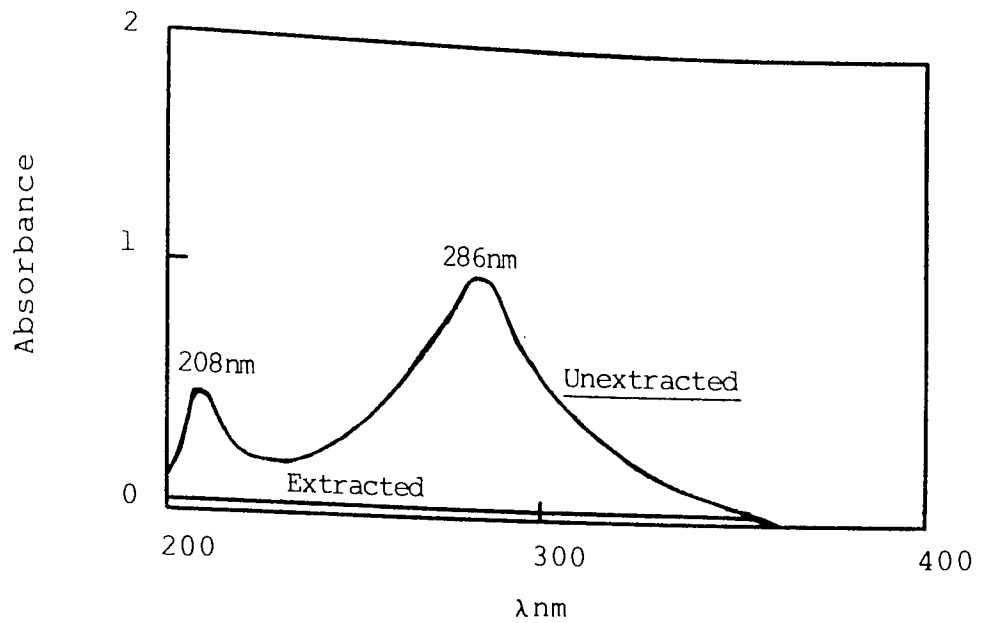


Figure 6.6A Ultraviolet spectrum before and after extraction of a 200μm PP(HF22) film containing 1%ADPA processed in the RAPRA torque rheometer(180°C,60rpm,8mins,CM).See Table 6.2.

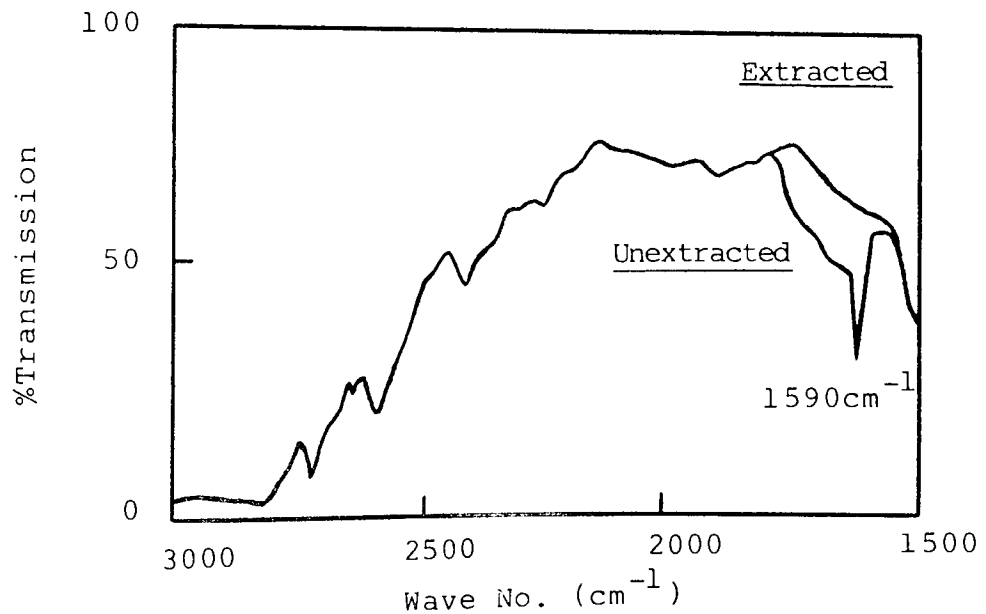


Figure 6.6B Infra-red spectrum before and after extraction of a 200μm PP(HF22) film containing 1%ADPA processed in the RAPRA torque rheometer(180°C,60rpm,8mins,CM).See Table 6.2.

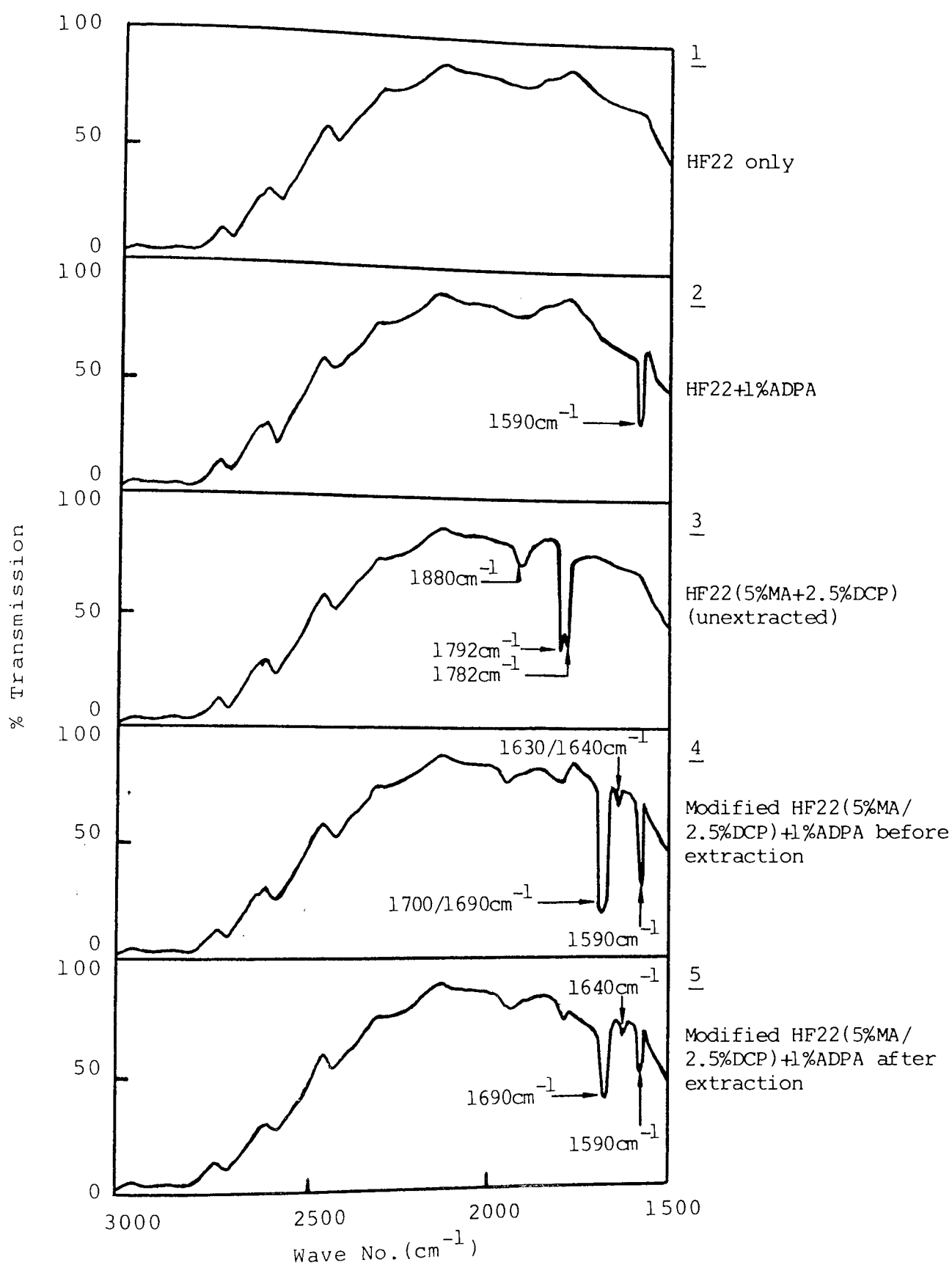


Figure 6.7A Infra-red spectra of 200  $\mu\text{m}$  PP(HF22) films showing the effectiveness of 5%maleic anhydride(MA)/2.5% di-cumyl peroxide(DCP) modification of PP(HF22) on the chemical binding of 1%ADPA processed in the RAPRA torque rheometer( $180^{\circ}\text{C}$ , 60rpm, 8mins, CM). See Table 6.4.

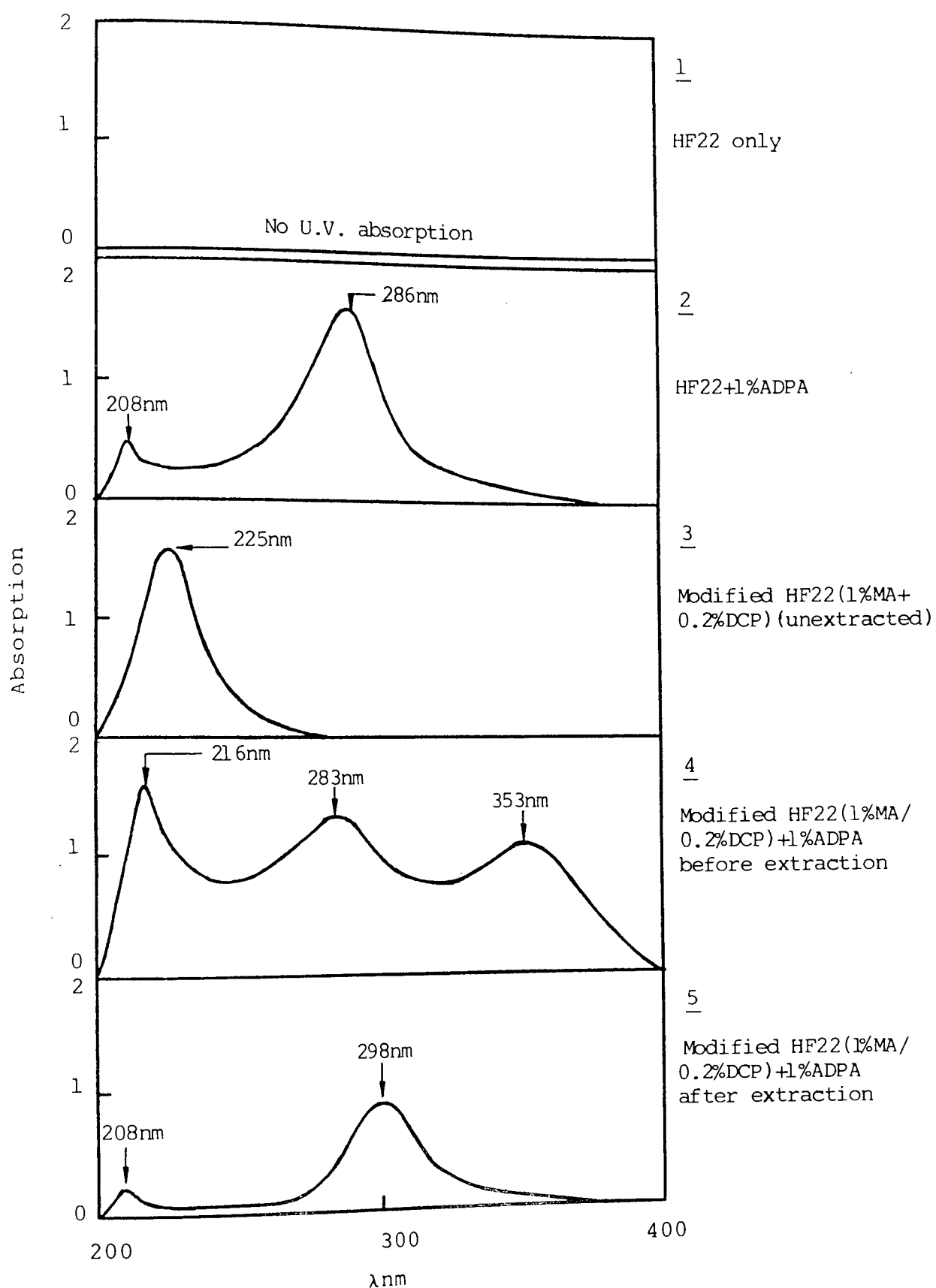


Figure 6.7B Ultraviolet spectra of 200 $\mu$ m PP(HF22) films showing the effectiveness of 1%maleic anhydride (MA)/0.2%di-cumyl peroxide(DCP) modification of PP(HF22) on the chemical binding of 1%ADPA processed in the RAPRA torque rheometer(180 $^{\circ}$ C, 60rpm,8mins,CM). See Table 6.2.

Sample No.	APMA (%)	Di-cumyl peroxide (%)	Concentration of APMA (molx10 <sup>-3</sup> /100gPP)	MFI (g/10min)	%Binding of APMA in PP	Carbonyl Index Induction Period of 200µm PP films(hours)	
						Unextracted	Extracted
1	0.25	0	0.89	2.04	44	25	5
2	0.25	0.05	0.89	8.96	51	25	5
3	0.25	0.10	0.89	19.04	54	50	30
4	0.375	0	1.33	2.01	42	25	5
5	0.375	0.07	1.33	18.46	55	75	30
6	0.375	0.14	1.33	39.26	61	75	30
7	0.50	0	1.77	2.04	31	25	5
8	0.50	0.1	1.77	30.93	65	100	30
9	0.50	0.2	1.77	43.21	70	100	30
10	1.0	0	3.55	3.12	15	25	5
11	1.0	0.1	3.55	9.80	31	250	80
12	1.0	0.2	3.55	22.10	50	370	100
13	1.0	0.3	3.55	39.60	52	350	100

Table 6.5 Melt flow index(MFI), %Binding of stabiliser(APMA) and carbonyl index induction periods(Wallace air oven, 140°C before and after extraction of 200µmPP films)of APMA modified PP(HF22) with and without DCP processed in RAPRA torque rheometer.

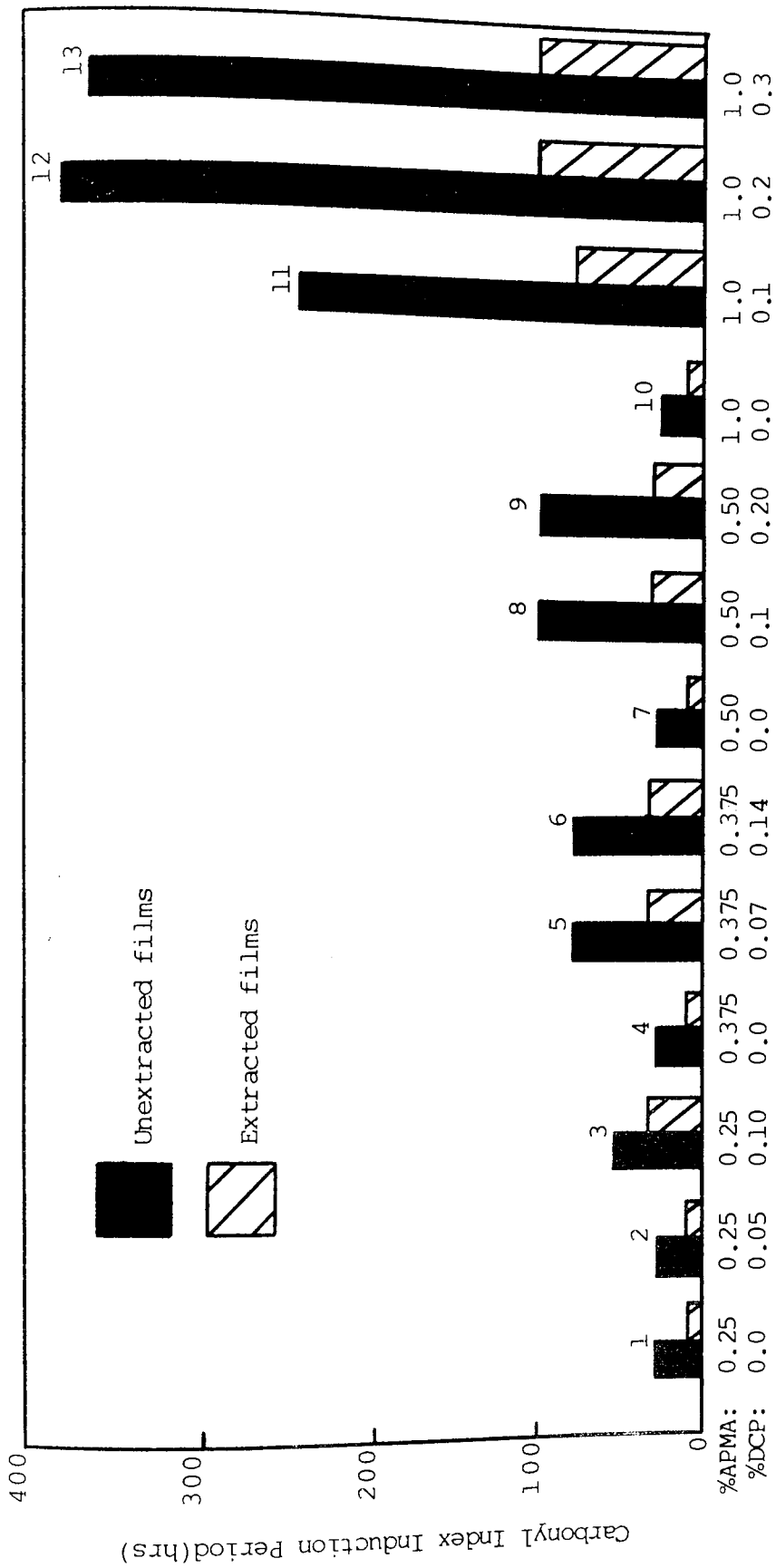


Figure 6.8 Carbonyl index induction periods(Wallace air oven,140°C before and after extraction of 200µm PP films) of APMA modified PP(HF22) with and without di-cumyl peroxide(DCP) processed in the RAPRA torque rheometer(180°C,60rpm,8mins,CM).See Table 6.5.

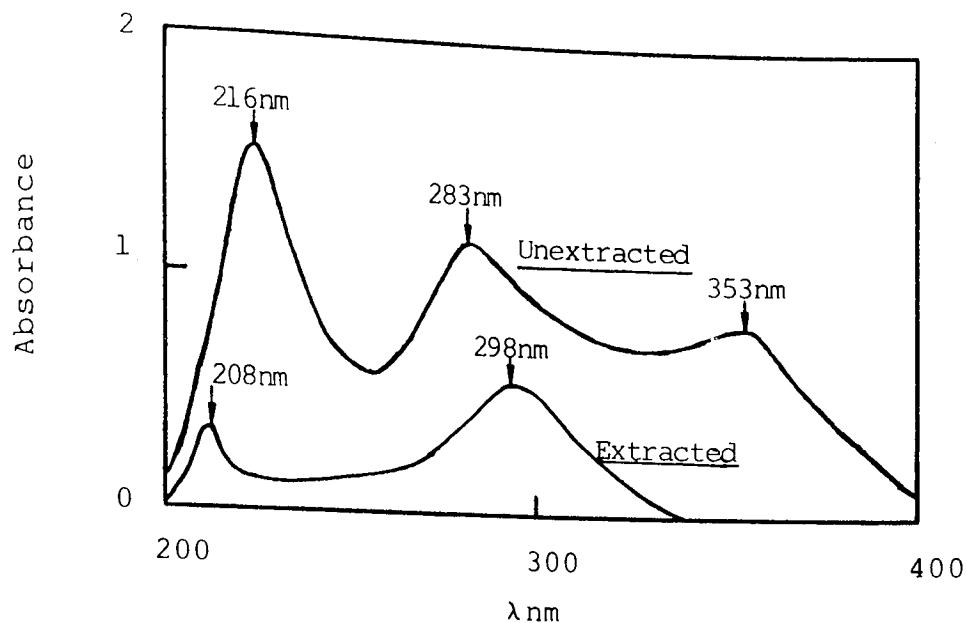


Figure 6.9A Ultraviolet spectrum before and after extraction of a 200 $\mu$ m PP(HF22) film containing 1%APMA and 0.2% di-cumyl peroxide(DCP) processed in the RAPRA torque rheometer(180 $^{\circ}$ C,60rpm,8mins,CM). See Table 6.5.

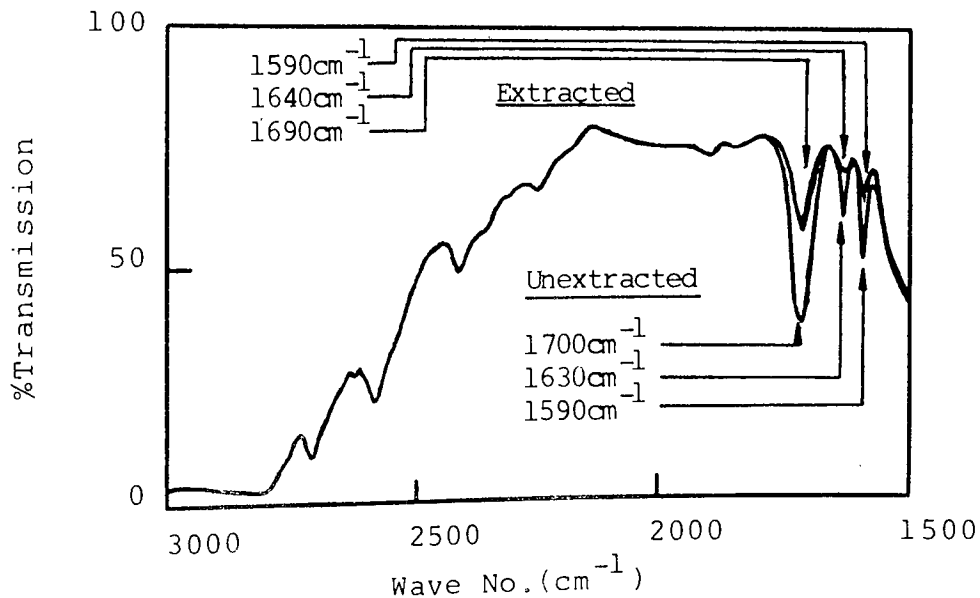


Figure 6.9B Infra-red spectrum before and after extraction of a 200 $\mu$ m PP(HF22) film containing 1%APMA and 0.2%di-cumyl peroxide(DCP) processed in the RAPRA torque rheometer(180 $^{\circ}$ C,60rpm,8mins,CM). See Table 6.5.



Sample No.	APSA (%)	Di-cumyl peroxide (%)	Concentration of APSA (molx10 <sup>-3</sup> /100gPP)	MFI (g/10min)	%Binding of APSA in PP	Carbonyl Index Induction Period of 200µm PP films(hours)	
						Unextracted	Extracted
1	1.0	0	3.52	4.95	0	25	5
2	1.0	0.05	3.52	8.33	0	30	5
3	1.0	0.10	3.52	17.50	0	30	5
4	1.0	0.20	3.52	*	0	30	5
5	1.0	0.30	3.52	*	0	30	5

\*Too high to be measured

Table 6.6 Melt flow index(MFI), %Binding of stabiliser(APSA) and carbonyl index induction periods (Wallace air oven,140°C before and after extraction of 200µm PP films) of APSA modified PP(HF22) with and without di-cumyl peroxide(DCP) processed in the RAPRA torque rheometer (180°C,60rpm,8mins,CM).

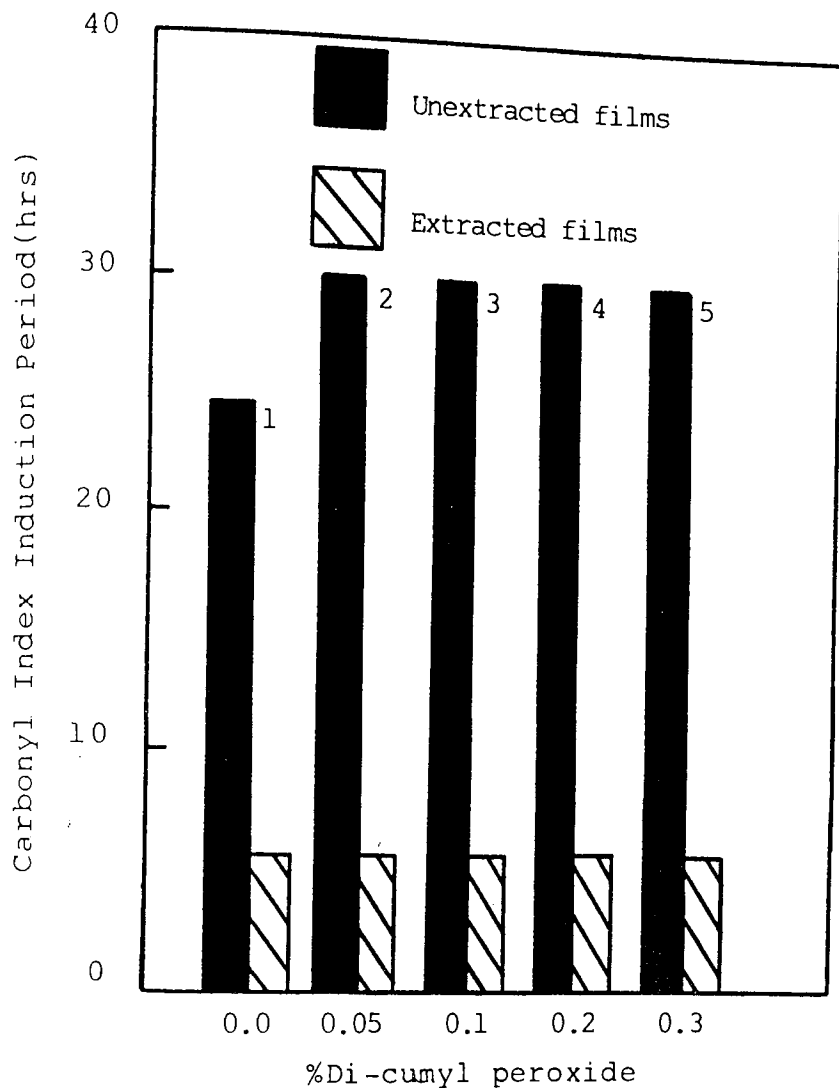


Figure 6.10 Carbonyl index induction periods (Wallace air oven,  $140^{\circ}\text{C}$  before and after extraction of  $200\mu\text{m}$  PP films) of 1%APSA modified PP (HF22) with and without di-cumyl peroxide (DCP) processed in the RAPRA torque rheometer ( $180^{\circ}\text{C}$ , 60rpm, 8mins, CM). See Table 6.6.

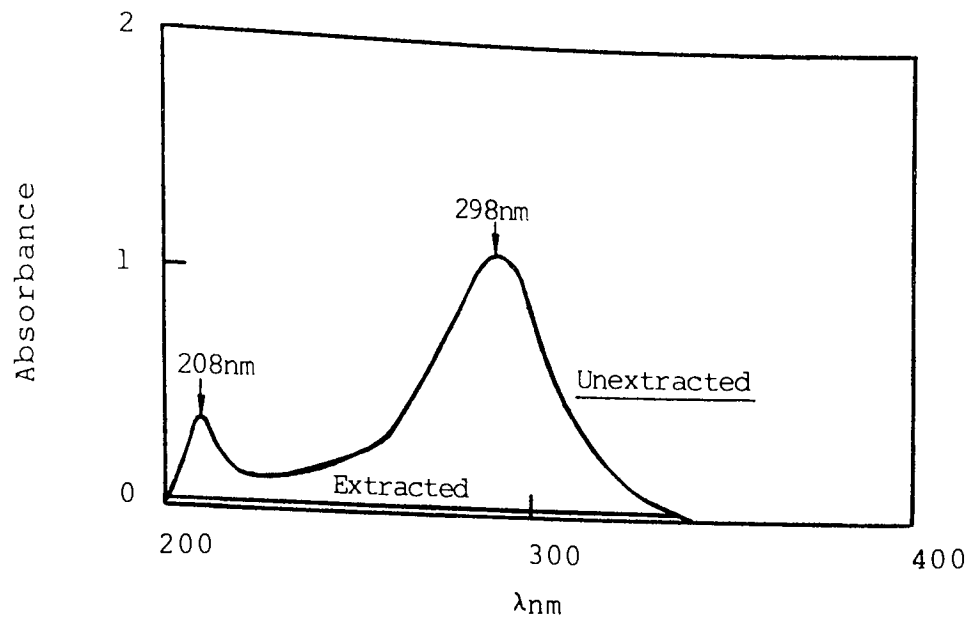


Figure 6.11A Ultraviolet spectrum before and after extraction of a 200 $\mu$ m PP(HF22) film containing 1%APSA and 0.2%di-cumyl peroxide (DCP) processed in the RAPRA torque rheometer(180 $^{\circ}$ C,60rpm,8mins,CM).See Table 6.6.

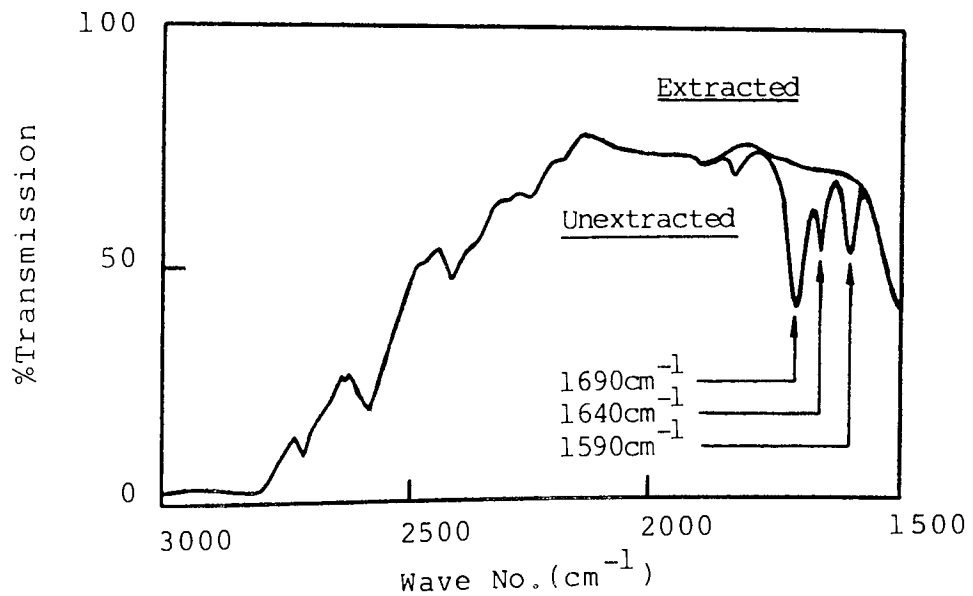


Figure 6.11B Infra-red spectrum before and after extraction of a 200 $\mu$ m PP(HF22) film containing 1%APSA and 0.2%DCP processed in the RAPRA torque rheometer(180 $^{\circ}$ C,60rpm,8mins,CM).See Table 6.6.

Sample No.	APM (%)	Di-cumyl peroxide (%)	Concentration of APM $10^{-3}$ /100gPP)	MFI (g/10min)	%Binding of APM in PP	Carbonyl Index Induction Period of 200 $\mu$ m PP films(hours)	
						Unextracted	Extracted
1	0.25	0	0.95	3.00	57	25	5
2	0.25	0.125	0.95	3.28	90	80	50
3	0.25	0.25	0.95	3.68	95	80	100
4	0.375	0	1.42	2.44	68	25	5
5	0.375	0.187	1.42	3.27	90	80	50
6	0.375	0.375	1.42	3.59	95	100	350
7	0.50	0	1.89	2.12	75	25	5
8	0.50	0.25	1.89	2.59	90	300	500
9	0.50	0.50	1.89	3.10	95	600	850
10	1.0	0	3.79	1.96	70	50	5
11	1.0	0.50	3.79	2.14	91	1300	1500
12	1.0	1.0	3.79	2.76	97	2100	2500
13	HWM 25 control			4.46	-	1350	5

Table 6.7 Melt flow index(MFI),%Binding of stabiliser(APM) and carbonyl index induction periods(Wallace air oven 140°C,before and after extraction of 200 $\mu$ mPP films) of APM modified PP(HF22) with and without DCP processed in the RAPRA torque rheometer (180°C,60rpm,8mins,CM).

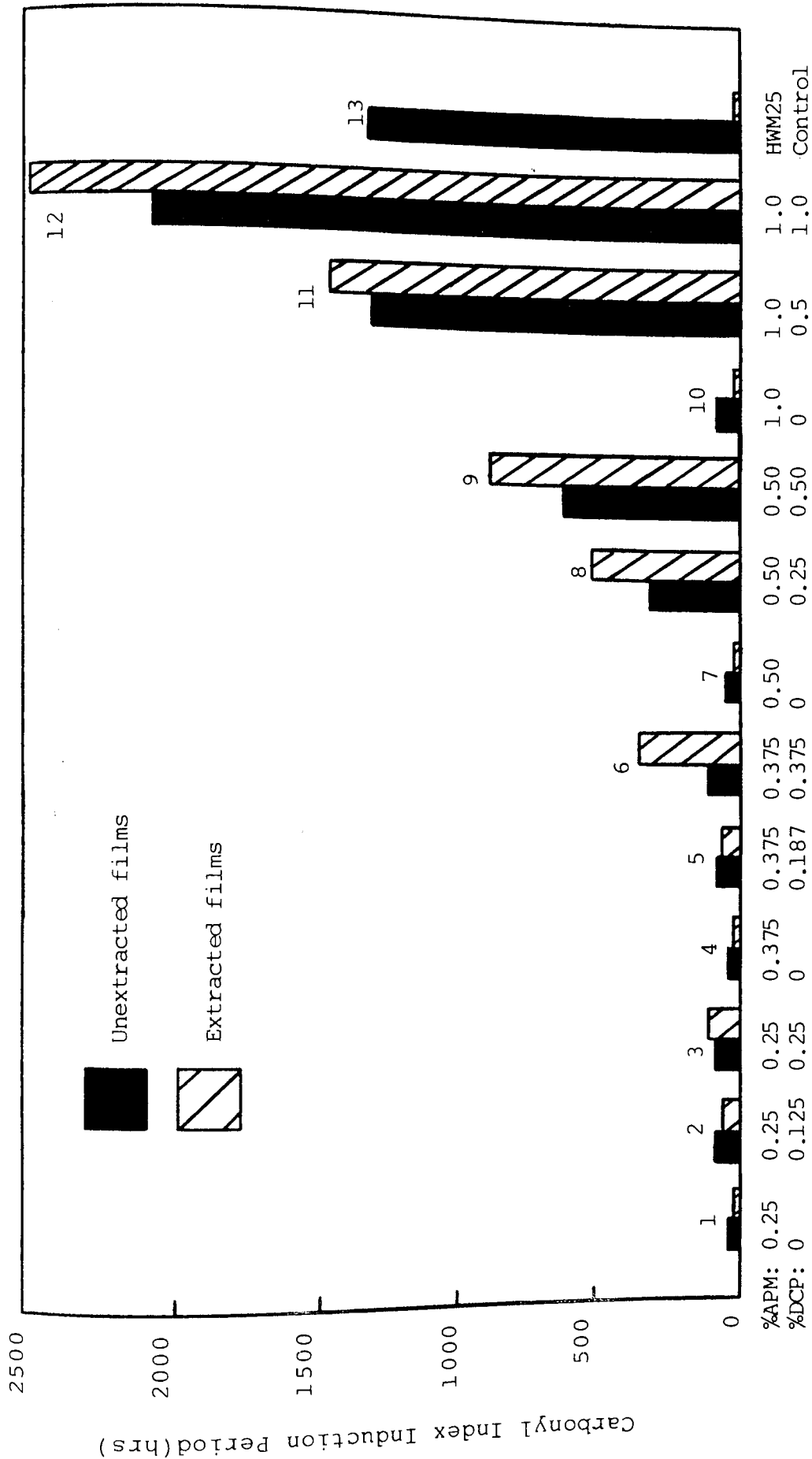


Figure 6.12 Carbonyl index induction periods(Wallace air oven,140°C before and after extraction of 200µm PP films) of APM modified PP(HF22) with and without di-cumyl peroxide(DCP) processed in the RAPRA torque rheometer(180°C, 60rpm, 8mins,CM).See Table 6.7.

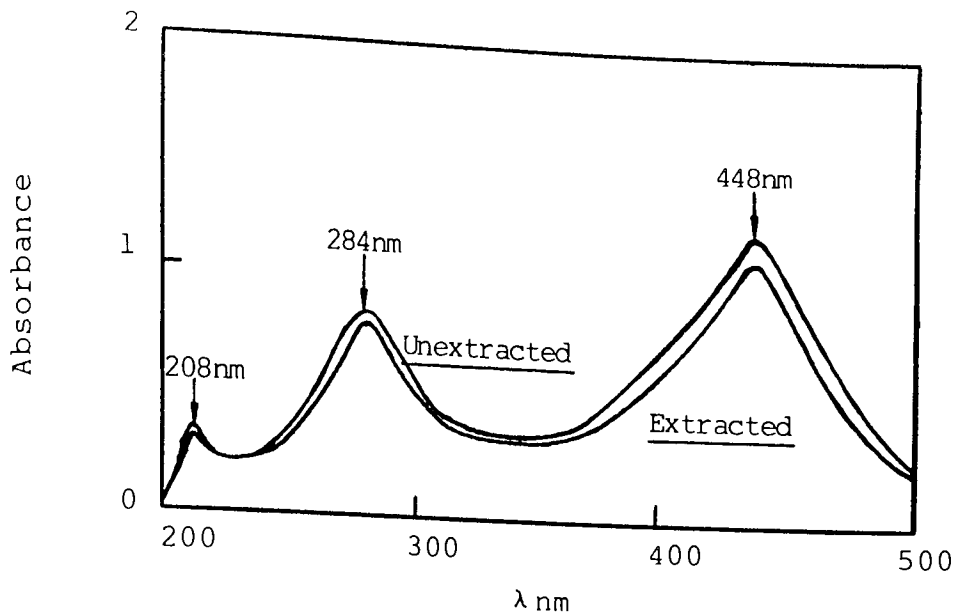


Figure 6.13A Ultraviolet spectrum before and after extraction of a 200 $\mu$ m PP(HF22) film containing 1%APM and 1%di-cumyl peroxide(DCP) processed in the RAPRA torque rheometer(180 $^{\circ}$ C,60rpm, 8mins,CM).See Table 6.7.

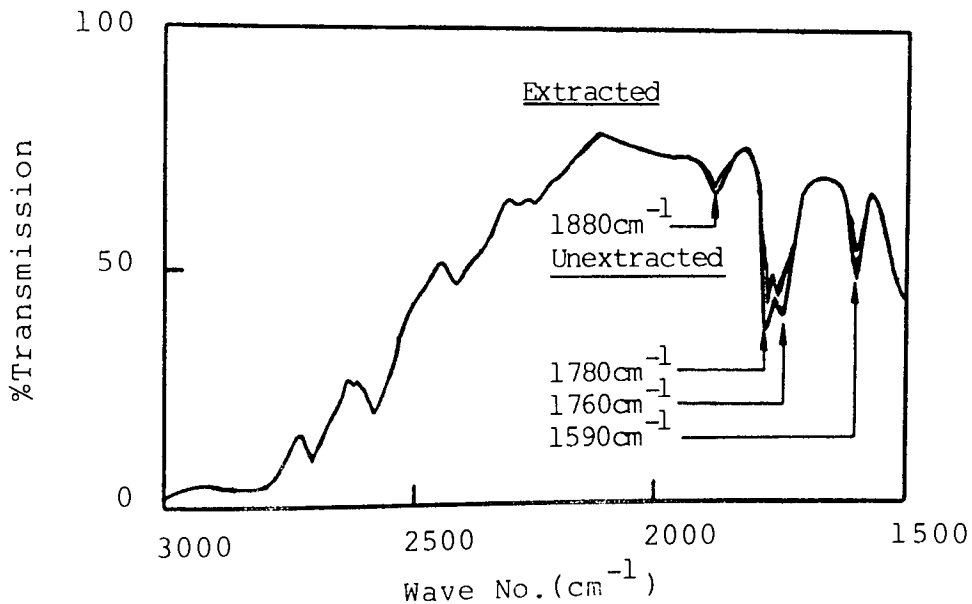


Figure 6.13B Infra-red spectrum before and after extraction of a 200 $\mu$ m PP(HF22) film containing 1%APM and 1%DCP processed in the RAPRA torque rheometer (180 $^{\circ}$ C,60rpm,8mins,CM).See Table 6.7.

Sample No.	AACT (%)	Di-cumyl peroxide (%)	Concentration of AACT (molx10 <sup>-3</sup> /100gPP)	MFI (g/10min)	%Binding of AACT in PP	Carbonyl Index Induction Period of 200µm PP films (hours)	
						Unextracted	Extracted
1	0.25	0	0.71	3.95	4	5	5
2	0.25	0.05	0.71	6.98	13	10	5
3	0.25	0.10	0.71	9.76	21	10	5
4	0.375	0	1.06	3.98	5	5	5
5	0.375	0.07	1.06	8.32	15	15	5
6	0.375	0.14	1.06	13.41	19	15	5
7	0.50	0	1.42	3.93	5	5	5
8	0.50	0.10	1.42	9.20	12	30	10
9	0.50	0.20	1.42	16.00	17	30	10
10	1.0	0	2.83	3.91	6	30	10
11	1.0	0.10	2.83	21.90	15	30	10
12	1.0	0.20	2.83	30.90	25	30	10
13	1.0	0.30	2.83	41.00	27	30	10

Table 6.8 Melt flow index(MFI), %Binding of stabiliser(AACT) and carbonyl index induction periods(Wallace air oven, 140°C before and after extraction of 200µm PP films) of AACT modified PP(HF22) with and without di-cumyl peroxide(DCP) processed in the RAPRA torque rheometer(180°C, 60rpm, 8mins, CM).

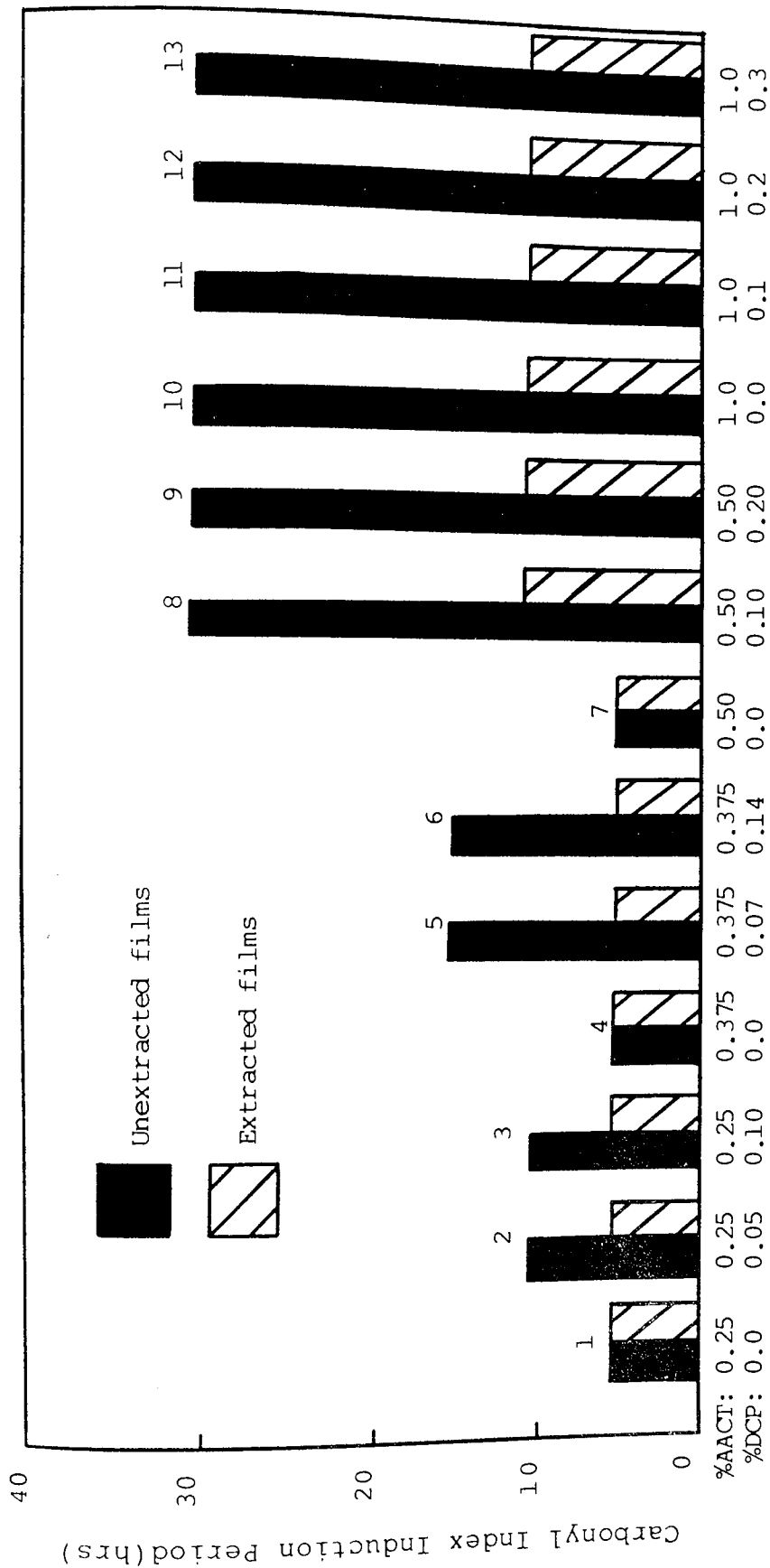


Figure 6.14 Carbonyl index induction periods (Wallace air oven, 140°C before and after extraction of 200µm PP films) of AACT modified PP (HF22) with and without di-cumyl peroxide (DCP) processed in the RAPRA torque rheometer (180°C, 60rpm, 8mins, CM). See Table 6.8.



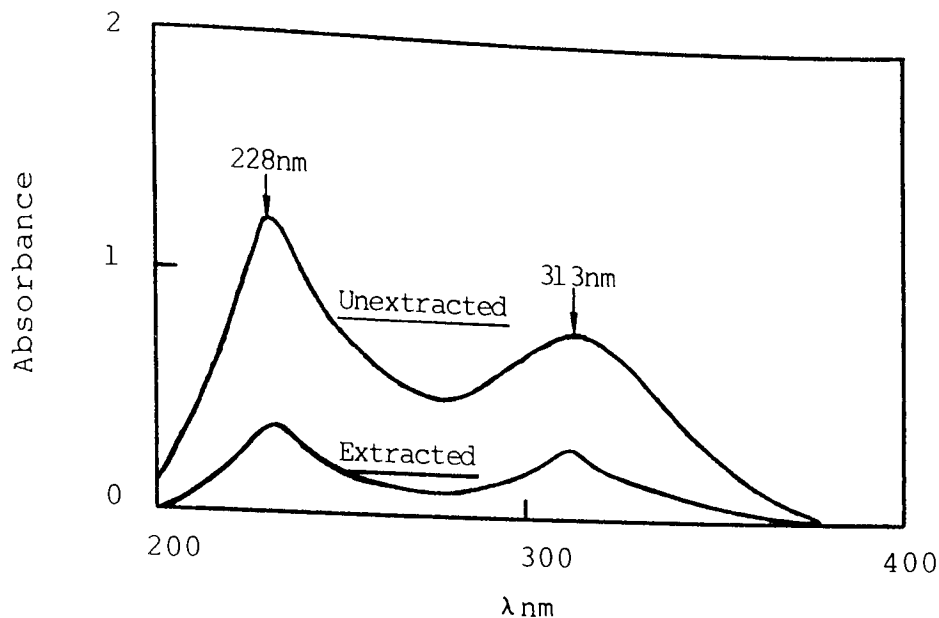


Figure 6.15A Ultraviolet spectrum before and after extraction of a 200 $\mu$ m PP(HF22) film containing 1% AACT and 0.2% di-cumyl peroxide (DCP) processed in the RAPRA torque rheometer (180 $^{\circ}$ C, 60rpm, 8mins, CM). See Table 6.8.

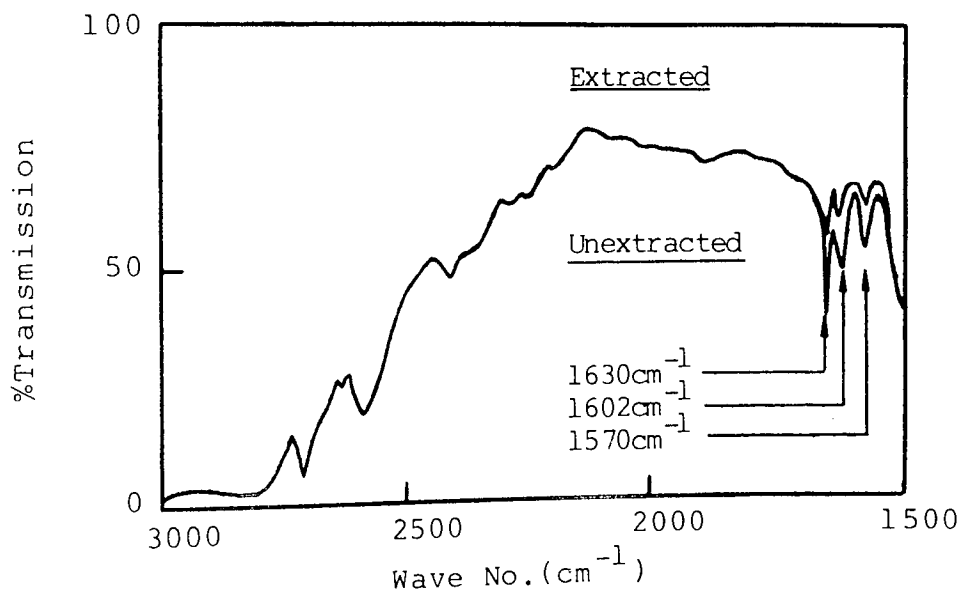


Figure 6.15B Infra-red spectrum before and after extraction of a 200 $\mu$ m PP(HF22) film containing 1% AACT and 0.2% di-cumyl peroxide (DCP) processed in the RAPRA torque rheometer (180 $^{\circ}$ C, 60rpm, 8mins, CM). See Table 6.8.

Sample No.	ADDT (%)	Di-cumyl peroxide (%)	Concentration of ADDT (molx10 <sup>-3</sup> /100gPP)	MFI (g/10min)	%Binding of ADDT in PP	Carbonyl Index Induction Period of 200µm PP films(hours)	
						Unextracted	Extracted
1	1.0	0	3.01	3.0	0	25	5
2	1.0	0.05	3.01	12.4	0	25	5
3	1.0	0.10	3.01	18.1	0	25	5
4	1.0	0.20	3.01	*	0	25	5
5	1.0	0.30	3.01	*	0	25	5

\* Too high to be measured

Table 6.9 Melt flow index(MFI), %Binding of stabiliser(ADDT) and carbonyl index induction

periods(Wallace air oven,140°C before and after extraction of 200µm PP films) of

ADDT modified PP(HF22) with and without di-cumyl peroxide(DCP) processed in the

RAPRA torque rheometer(180°C,60rpm,8mins,CM).

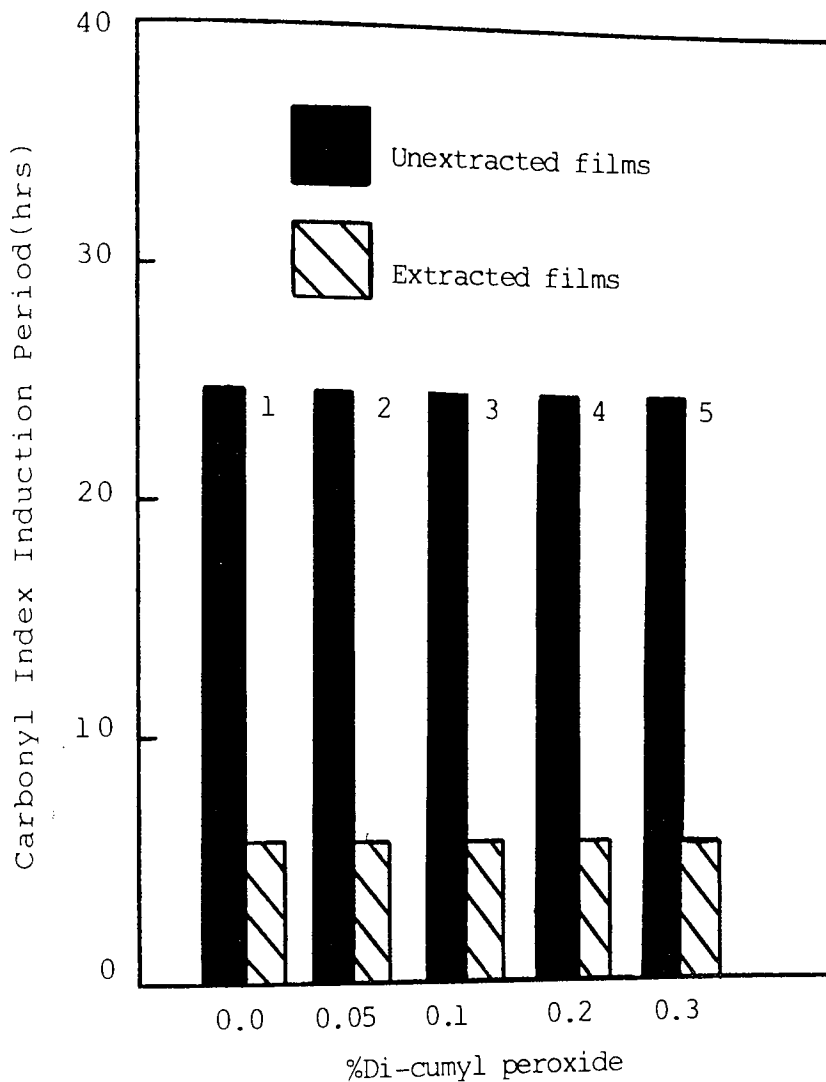


Figure 6.16 Carbonyl index induction periods(Wallace air oven,140°C before and after extraction of 200µm PP films) of 1%ADDT modified PP(HF22) with and without di-cumyl peroxide(DCP) processed in the RAPRA torque rheometer(180°C,60rpm,8mins,CM). See Table 6.9.

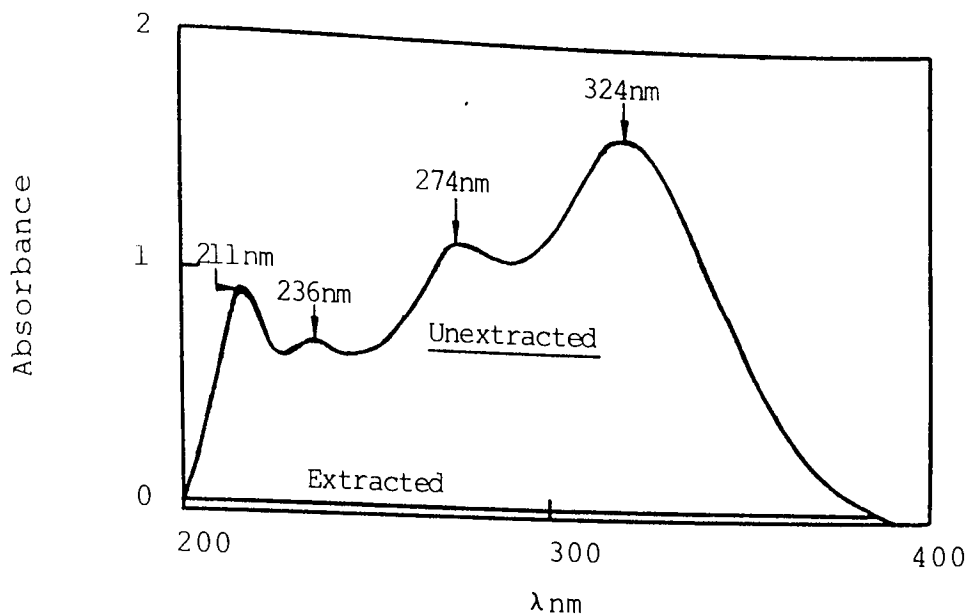


Figure 6.17A Ultraviolet spectrum before and after extraction of a 200 $\mu$ m PP(HF22) film containing 1%ADDT and 0.2%di-cumyl peroxide(DCP) processed in the RAPRA torque rheometer(180 $^{\circ}$ C, 60rpm,8mins,CM).See Table 6.9.

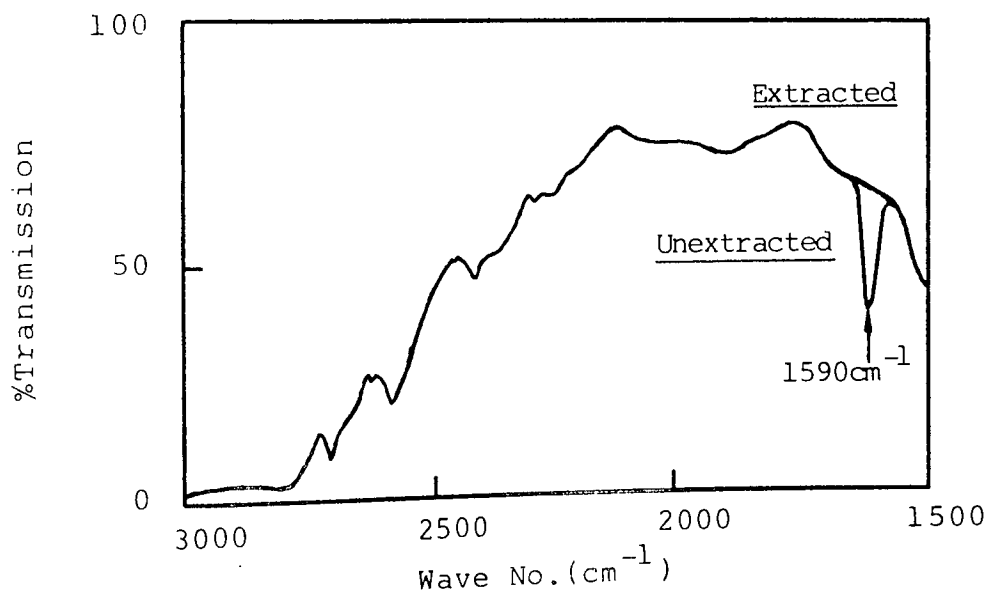


Figure 6.17B Infra-red spectrum before and after extraction of a 200 $\mu$ m PP(HF22) film containing 1%ADDT and 0.2%DCP processed in the RAPRA torque rheometer (180 $^{\circ}$ C,60rpm,8mins,CM).See Table 6.9.

Sample No.	Polymer (PP)	Polymer modification	Added Stabiliser (%)	DCP (%)	Added stabiliser concentration (molx10 <sup>-3</sup> /100gPP)	%Binding of stabiliser in PP	Carbonyl Index	
							Unextracted	Extracted
1	HF22	-	-	-	-	-	5	5
2	GWM22	-	-	-	-	0	1100	5
3	HWM25	-	-	-	-	0	1350	5
4	HF22	-	Irg1076(0.25%)	-	0.47	0	1100	5
5	HF22	-	Irg1010(0.25%)	-	0.21	0	1200	5
6	HF22	-	ADPA(1%)	-	5.45	0	25	5
7	HF22	1%MA/0.2%DCP:Ex	ADPA(1%)	-	5.45	10	45	15
8	HF22	5%MA/2.5%DCP:Ex	ADPA(1%)	-	5.45	70	300	150
9	HF22	-	APMA(1%)	0.2	3.55	50	370	100
10	HF22	-	APSA(1%)	0.05	3.52	0	30	5
11	HF22	-	APM(1%)	1	3.79	97	2100	2500
12	HF22	-	AACT(1%)	0.3	3.91	27	30	10
13	HF22	-	ADDT(1%)	0	3.01	0	25	5

Table 6.10 %Binding of stabilisers and carbonyl index induction periods(Wallace air oven,140°C before and after extraction of 200µm PP films) of optimised PP(HF22) stabilised systems containing DCP processed in the RAPRA torque rheometer(180°C,60rpm,8mins, CM).Commercially stabilised PP(HWM25 and GWM22) controls are included.

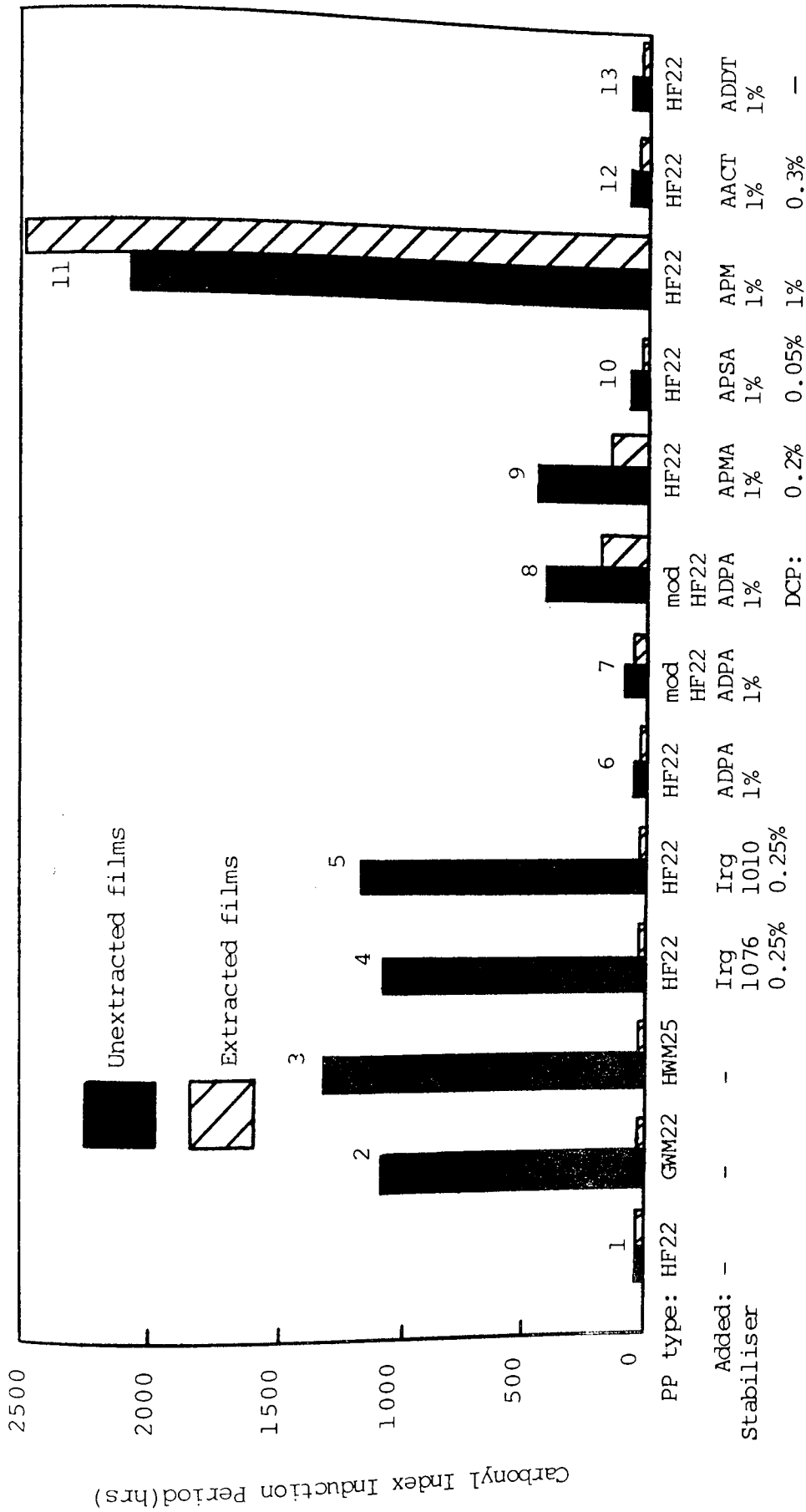


Figure 6.18 Carbonyl index induction periods (Wallace air oven, 140°C before and after extraction of 200µm PP films) of optimised PP(HF22) stabilised systems containing DCP and processed in RAPRA torque rheometer (180°C, 60rpm, 8mins, CM). Commercially stabilised PP (HWM25 and GWM22) controls are included. See Table 6.10.

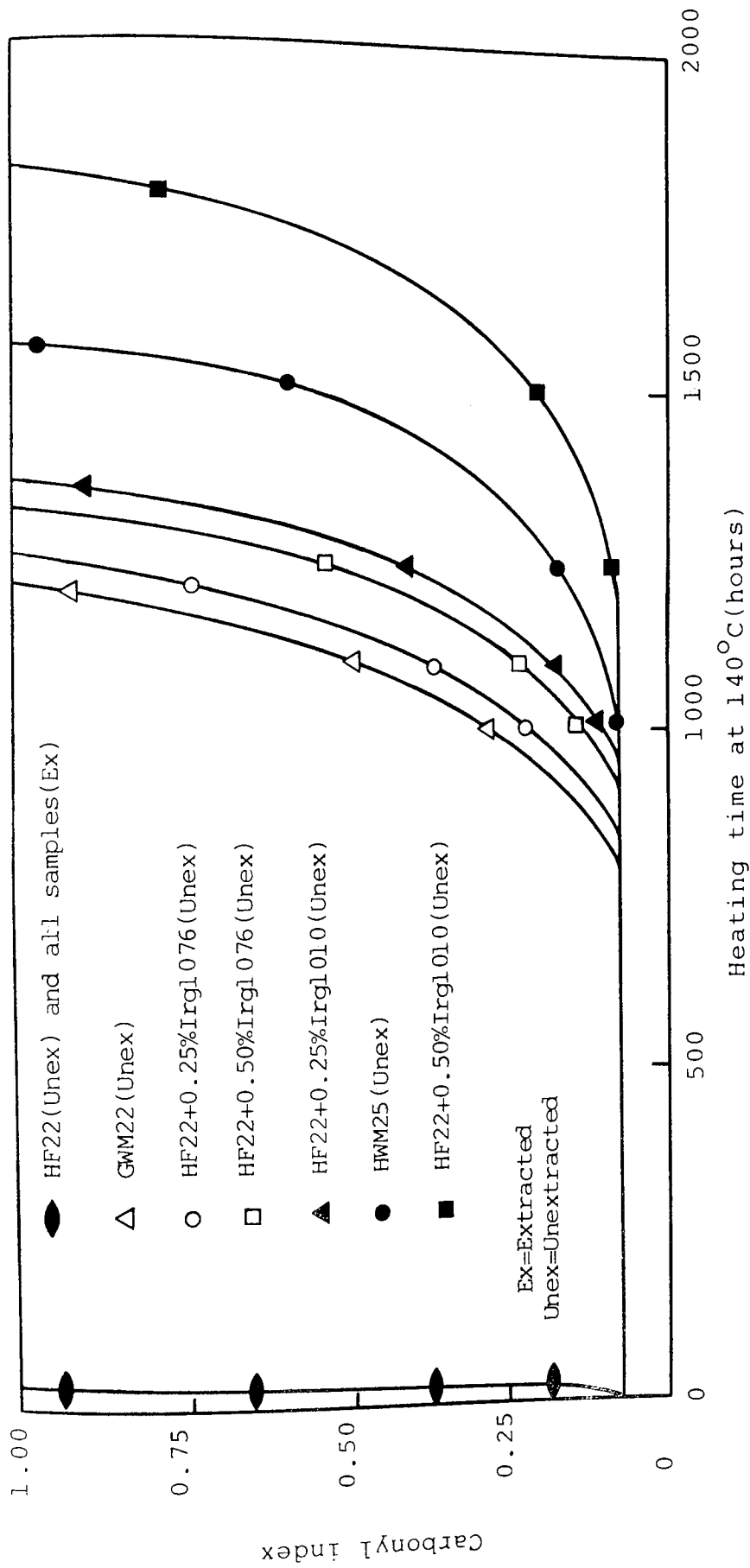


Figure 6.19 Carbonyl index(Wallace air oven,140°C before and after extraction of 200µm PP films) of commercially stabilised PP(HWM25 and GWM22) and unstabilised PP(HF22) with and without Irganox stabilisers(processed in the RAPRA torque rheometer, 180°C,60rpm,8mins,CM). See Table 6.1.

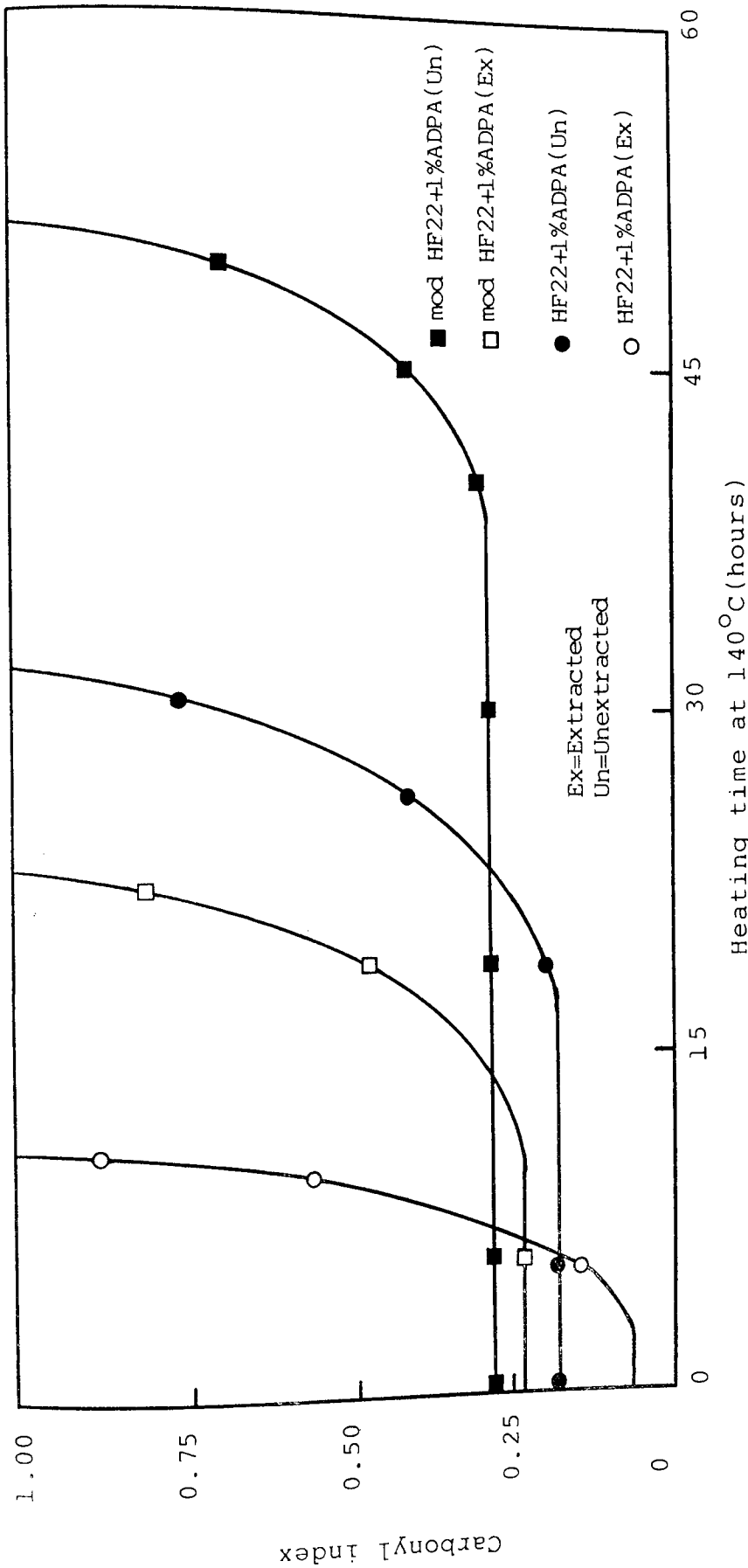


Figure 6.20 Carbonyl index(Wallace air oven,140°C before and after extraction of 200µm PP films) of unmodified and 1%maleic anhydride(MA)/0.2%di-cumyl peroxide(DCP) modified PP(HF22) containing 1%ADPA(processed in the RAPRA torque rheometer, 180°C,60rpm,8mins,CM). See Table 6.2.



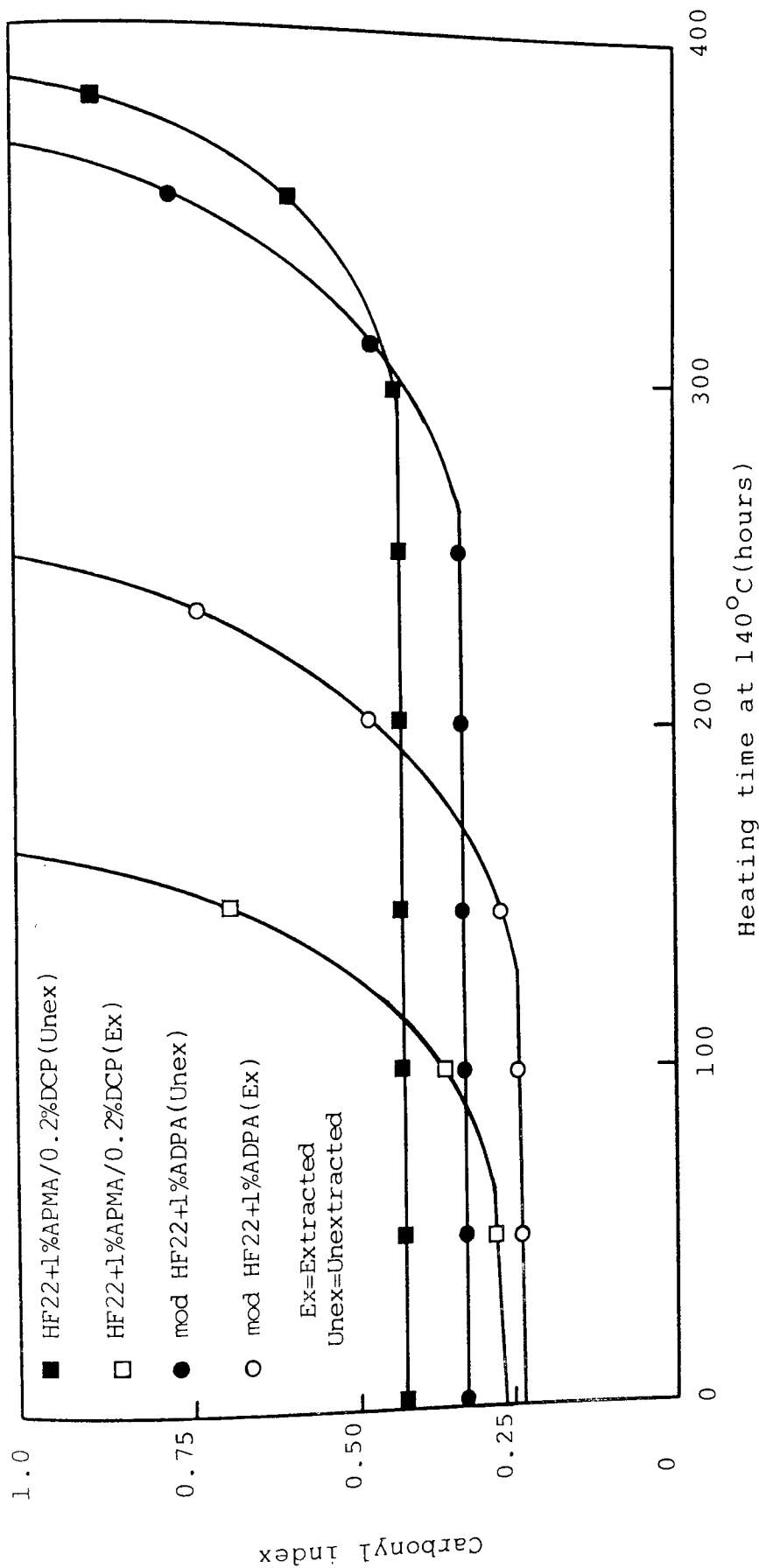


Figure 6.21 Carbonyl index (Wallace air oven, 140°C before and after extraction of 200µm PP films) of 5%maleic anhydride(MA)/2.5%di-cumyl peroxide(DCP) modified PP(HF22) containing 1%ADPA and PP(HF22) containing 1%APMA/0.2%DCP(both processed in the RAPRA torque rheometer, 180°C, 60rpm, 8mins, CM). See Tables 6.4 and 6.5.

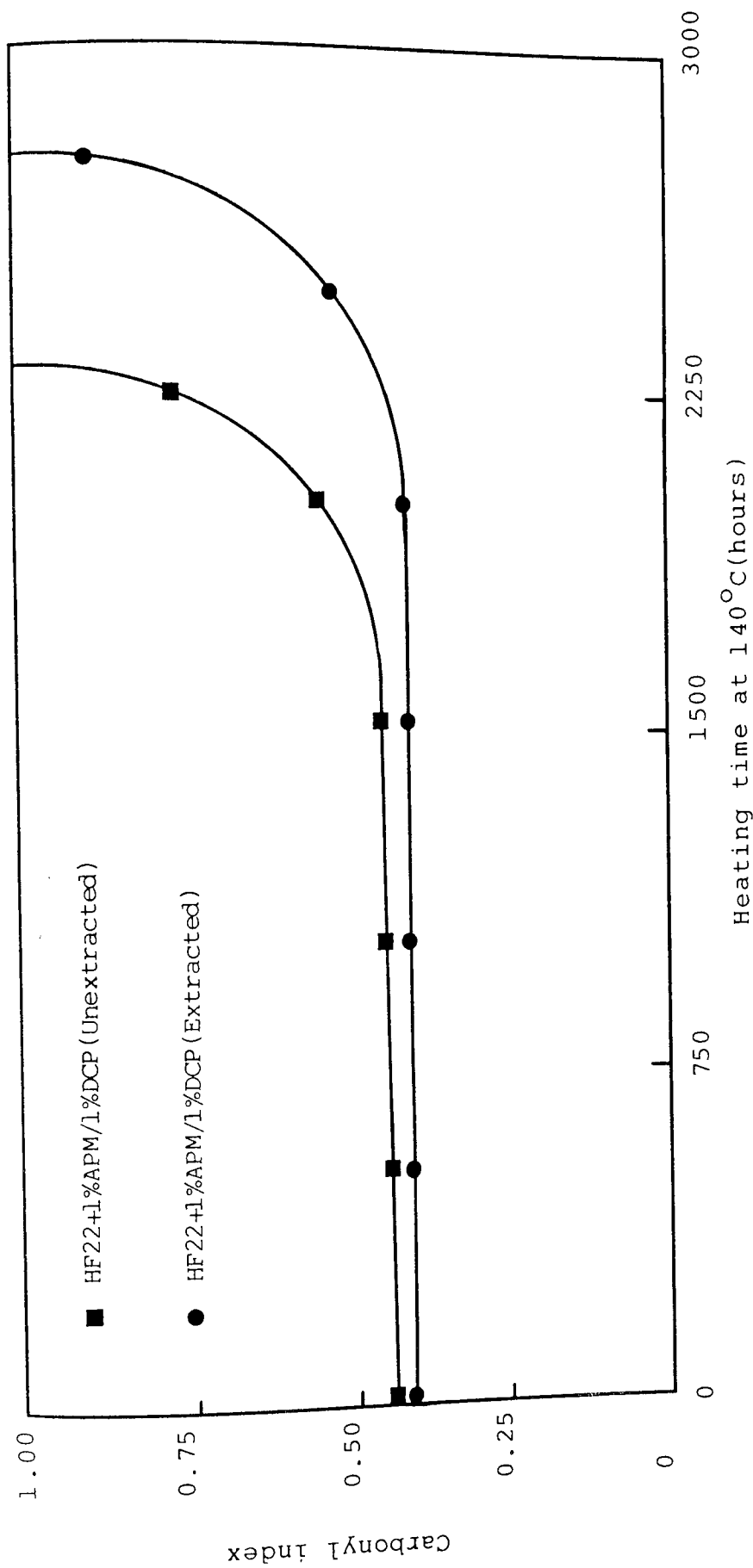


Figure 6.22 Carbonyl index (Wallace air oven, 140°C before and after extraction of 200µm PP films) of PP (HF22) containing APM and di-cumyl peroxide (DCP) processed in the RAPRA torque rheometer (180°C, 60rpm, 8mins, CM). See Table 6.7.

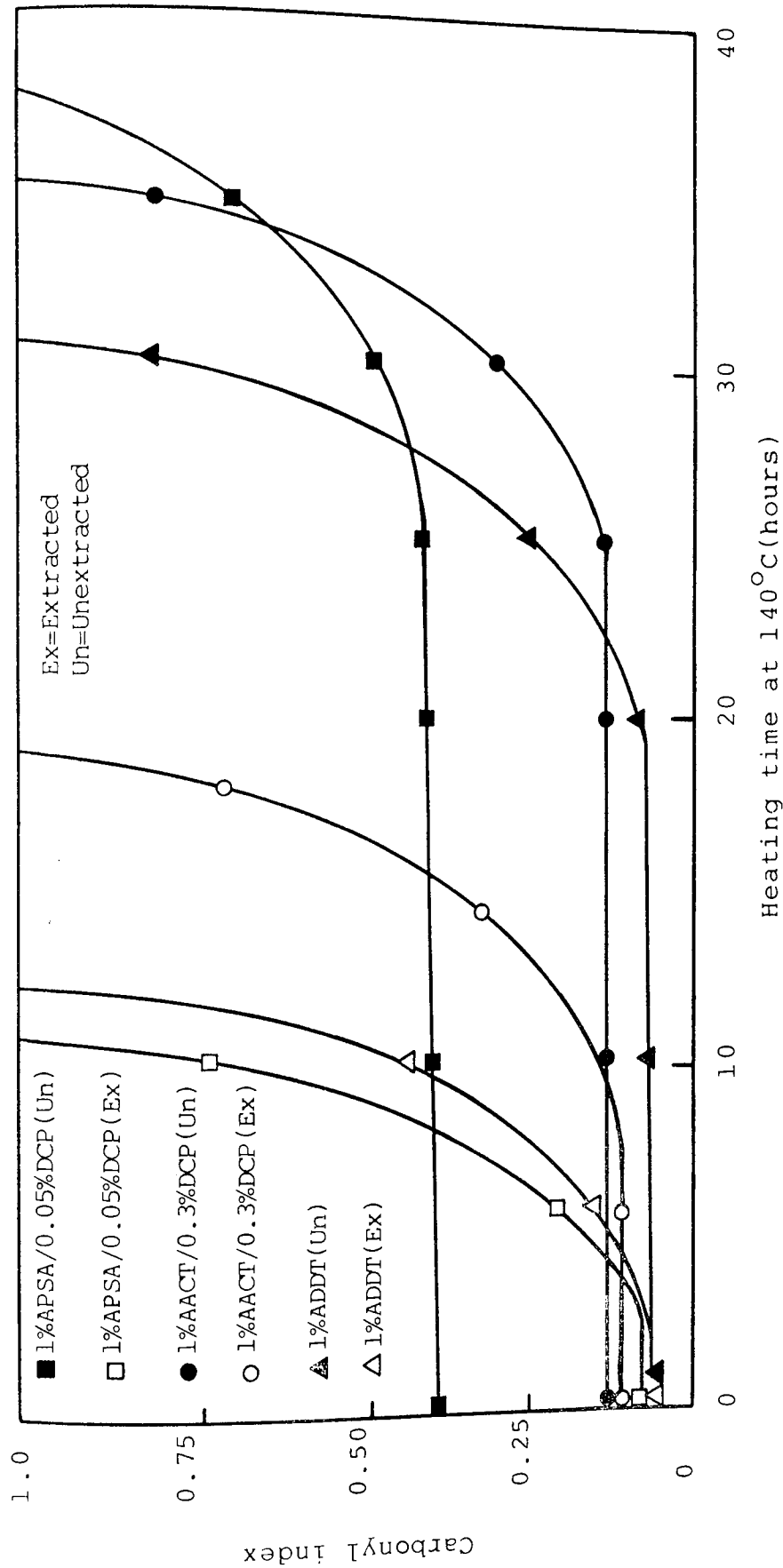


Figure 6.23 Carbonyl index (Wallace air oven, 140°C before and after extraction of 200µm PP films) of PP (HF22) containing APSA, AACT and ADDT all with di-cumyl peroxide (DCP) processed in the RAPRA torque rheometer (180°C, 60rpm, 8mins, CM). See Tables 6.6, 6.8 and 6.9.

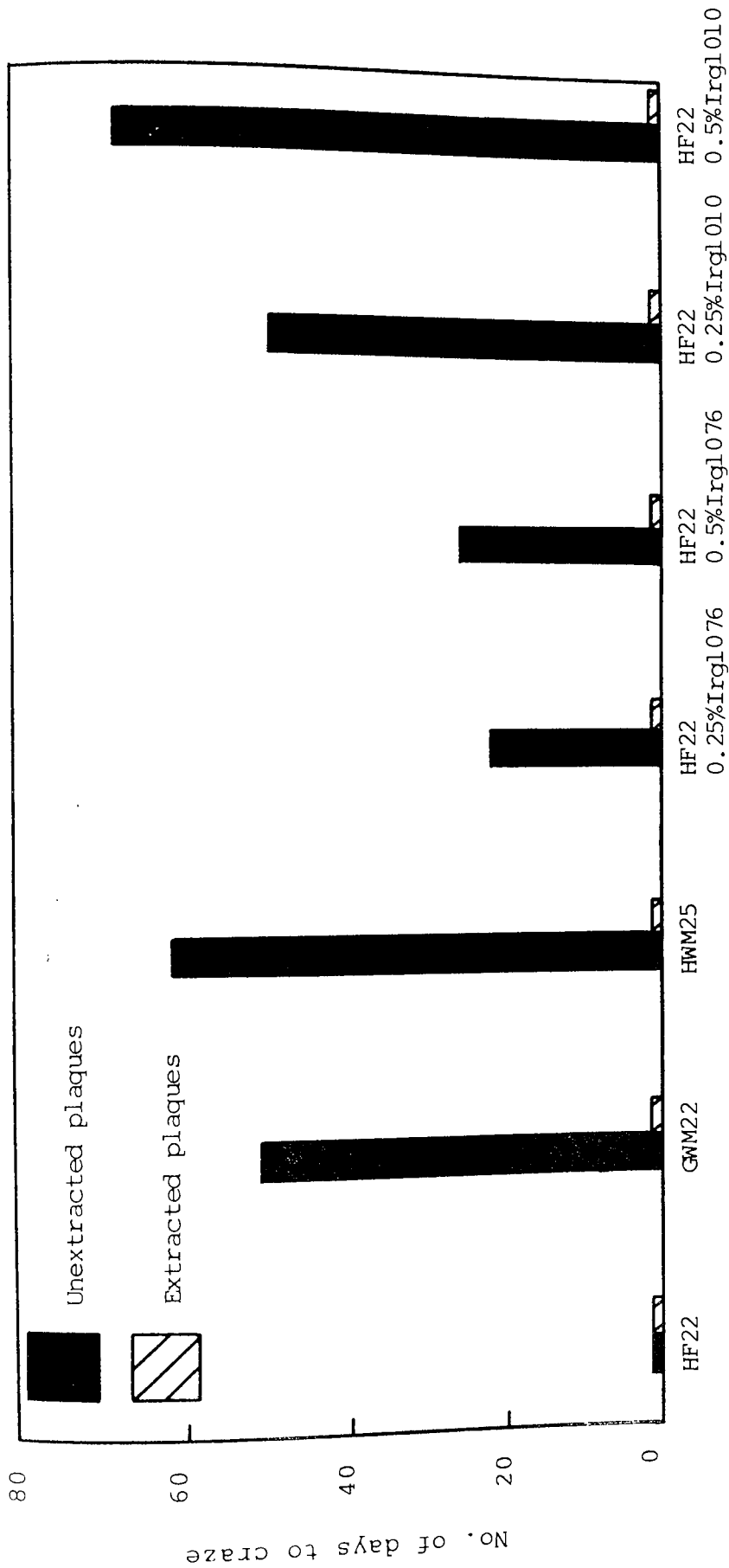


Figure 6.24 No. of days to craze (Wallace air oven, 150°C before and after extraction of 1mm PP plaques) of commercially stabilised PP (HWM25 and GWM22) and unstabilised PP (HF22) with and without Irganox stabilisers, homogenised (Buss Ko-Kneader) and injection moulded (Edgwick). See Scheme 6.6.

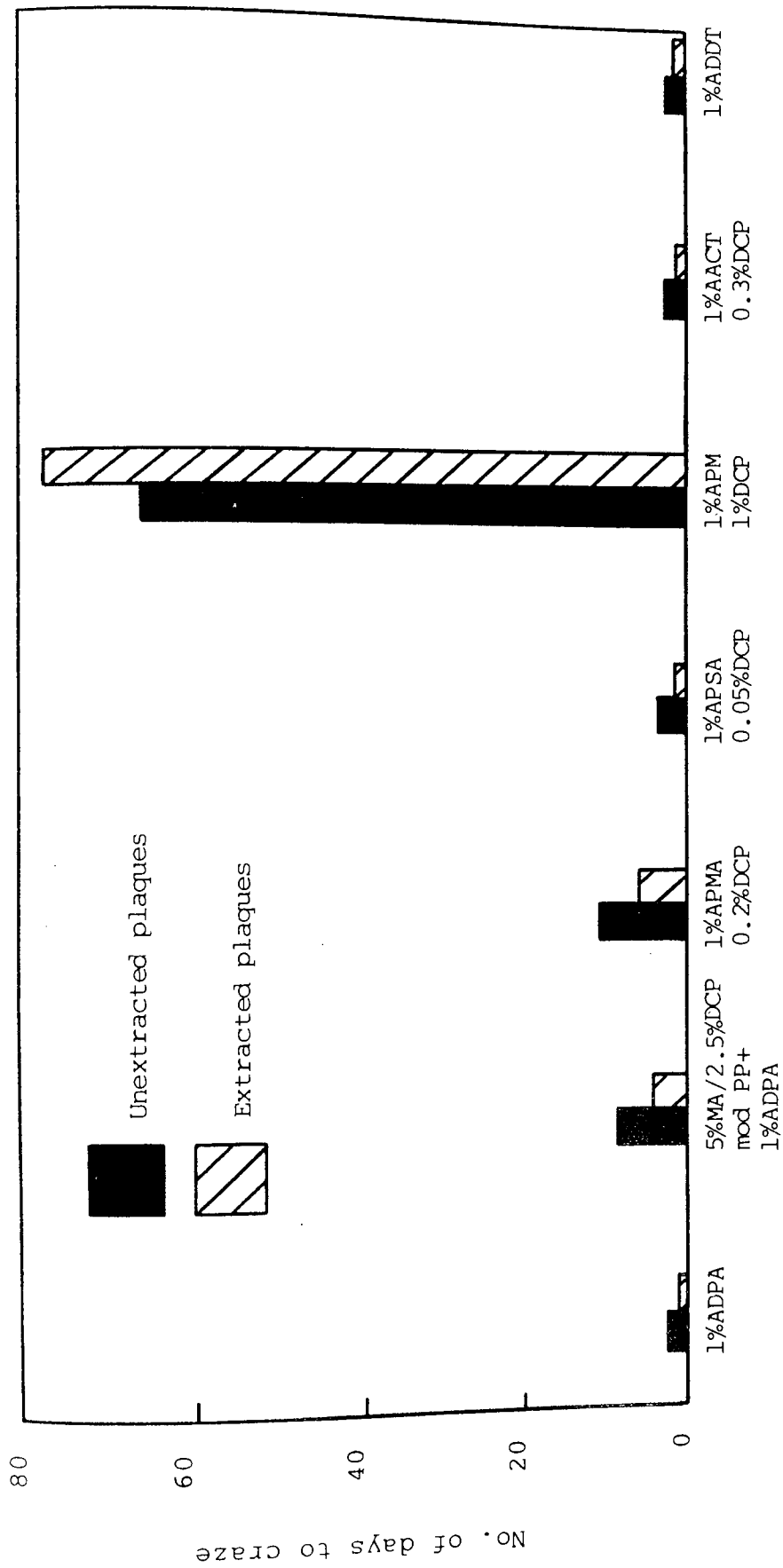


Figure 6.25 No. of days to craze (Wallace air oven, 150°C before and after extraction of 1mm PP plaques) of PP (HF22) containing previously optimised stabiliser systems (on 200µm PP films, Table 6.10), homogenised (Buss Ko-Kneader) and injection moulded (Edgwick). See Scheme 6.6.





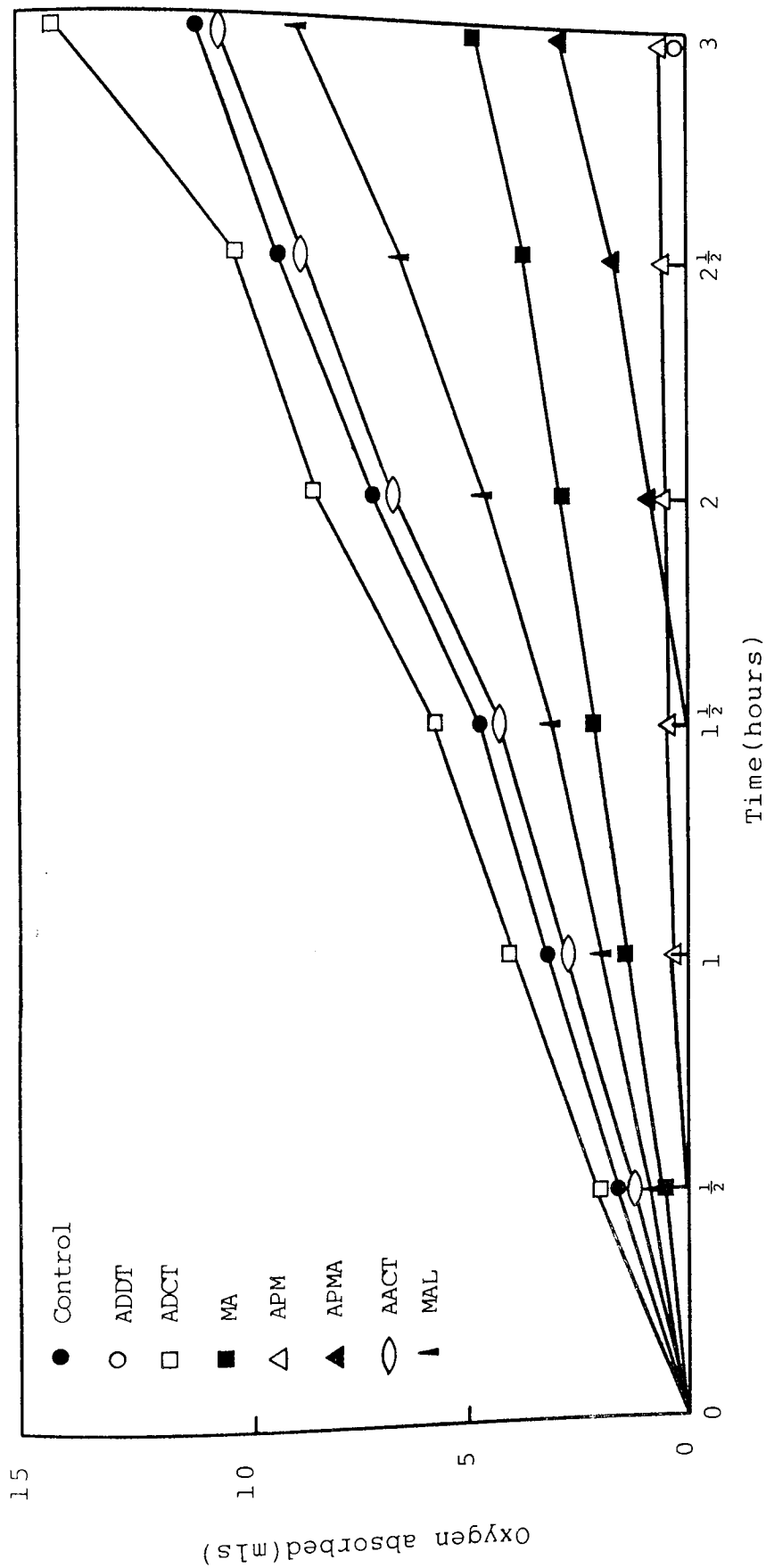


Figure 6.28 Oxygen absorption characteristics of cumene containing AZBN( $1 \times 10^{-2} \text{ moldm}^{-3}$ ) free radical initiator and PP modifiers/stabilisers( $5 \times 10^{-4} \text{ moldm}^{-3}$ ) in a molar ratio of 20:1.



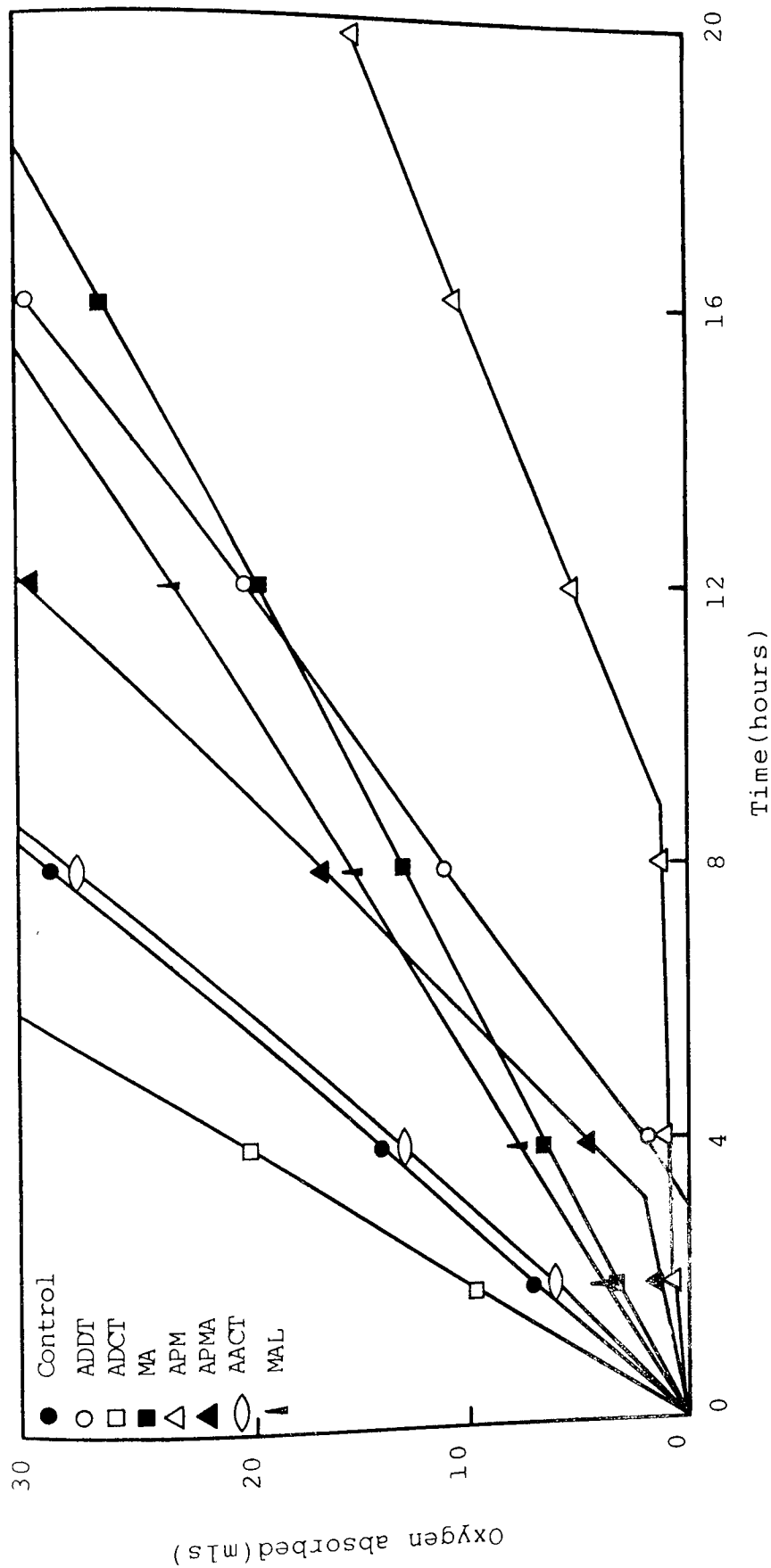


Figure 6.29 Oxygen absorption characteristics of cumene containing AZBN( $1 \times 10^{-2} \text{ mol dm}^{-3}$ ) free radical initiator and PP modifiers/stabilisers( $5 \times 10^{-4} \text{ mol dm}^{-3}$ ) in a molar ratio of 20:1.

CHAPTER SEVEN

CONCLUSIONS AND SUGGESTIONS  
FOR FURTHER WORK

## 7.1 Conclusions

1. Using a low cost commodity thermoplastic (polypropylene) modified with mechano-chemically bound additives and reinforced with Rockwool (mineral) and glass fibres (both A-1100 silane coupled), the following characteristics, essential for under-bonnet thermoplastic components have been successfully achieved:-
  - A) Superior mechanical performance to the 30% glass fibre reinforced commercial polypropylene grade (HW60/GR30) including excellent high temperature (to 150°C) dimensional stability and high impact strength at low temperatures (to -40°C).
  - B) High retention of mechanical performance after immersion in a range of fluids typically found in an under-bonnet environment.
  - C) Excellent thermal-oxidative stability in highly volatilising and extracting environments in which currently used commercial stabilisers are lost.
2. Melt viscosity (a function of processing temperature) during PP composite homogenisation and injection moulding was the major influence on fibre length degradation. The fact that the aspect ratio of LRWF was degraded much more than GF contributed to the mineral fibre's

Additive	Mechano-chemical binding to PP(HF22)	Melt stability of PP(HF22)	Thermal-oxidative stability of PP(HF22)	Mechanical performance of 30%GF reinforced PP(HF22)
MA	Good	Good	Poor	Excellent
SA	None	Poor	Poor	Poor
MAL	Good	Good	Poor	Good
APMA	Good	Fair	Good	Good
APSA	None	Poor	Poor	Poor
APM	Excellent	Excellent	Excellent	Good
ADCT	Good	Good	Poor	Excellent
AACT	Poor	Poor	Poor	Poor
ADDT	None	Poor	Poor	Poor

Table 7.1 Summary highlighting the influence of chemically bound modifiers on the melt and thermal-oxidative stability of PP(HF22) and their effectiveness in enhancing the mechanical performance of 30% glass fibre (GF, A-1100 silane coupled) reinforced PP(HF22)

inferior reinforcing behaviour. However, both LRWF and GF (30% loading, A-1100 silane coupled) reinforced unmodified PP(HWM25) showed greatly inferior mechanical performance compared with the commercial composite (HW60/GR30); this was due to poor interfacial fibre-matrix adhesion, clearly demonstrated by the very long fibre pull-out lengths from composite fracture surfaces.

3. Incorporation of EPDM to PP(HWM25) homopolymer and composites decreased mechanical properties (especially yield and flexural strengths) with the exception of Charpy impact strength which increased due to increased deformational ability and stress delocalisation.

Decreases in flexural and tensile moduli were modest because these were found to be influenced more by the loading of high modulus fibres than minor reductions in matrix modulus as a result of EPDM addition.

4. Mechano-chemical binding of maleic anhydride to polypropylene during melt processing occurred by a free radical mechanism, dependent upon the addition of dicumyl peroxide free radical initiator. The use of the saturated analogue, succinic anhydride, proved that carbon-carbon unsaturation was necessary for binding to the polymer. Melt processing of polypropylene in the presence of maleic anhydride resulted in good melt stability as a result of preferential macro-alkyl free radical binding rather than disproportionate as they do

in its absence to give reduced molecular weight. Cross-linking of polypropylene was attributed to macro-alkyl free radical termination by a grafted MA radical. The presence of hindered phenol antioxidants (Irganox-type) in commercially stabilised PP(HWM25) inhibited free radical grafting of MA. The highest mechanical performance therefore, was obtained using unstabilised PP(HF22).

5. The improved mechanical performance of polypropylene reinforced with 30% glass fibre (A-1100 silane coupled) was in direct proportion to the concentration of bound MA; unstabilised PP(HF22) gave the best results. Scanning electron micrographs of these samples show very short fibre pull-out lengths at the fracture surface which was attributed to improved interfacial adhesion.
6. The mechanical performance of A-1100 silane coupled LRWF reinforced PP(HF22) was best improved by melt processing with di-cumyl peroxide alone, probably because the mineral fibre was coated with a "tenside" layer which possibly contained chemically unsaturated groups allowing macro-alkyl free radical addition during melt processing.
7. The use of other unsaturated chemical modifiers, MAL, APM and ADCT, were also found to chemically bind to PP(HF22) during melt processing in the presence of DCP and increased (in proportion to their degree of binding)

the mechanical performance of A-1100 silane coupled GF composites through enhanced interfacial fibre-matrix adhesion.

8. Another consequence of such PP/GF composite modification increasing the interfacial adhesion to allow higher transfer of stress from the ductile matrix to high modulus reinforcing fibre, was the excellent high temperature dimensional stability, good low temperature impact strength and high retention of mechanical properties after immersion in a variety of hot fluids.
9. The increase in interfacial fibre-matrix adhesion due to MA modification was shown to be a consequence firstly of free radical binding to the polymer via its carbon-carbon unsaturation, and secondly, by further melt processing with A-1100 silane coupled GF resulting in condensation between the bound anhydride and the coupling agent's primary amino group to give a stable amide bond and hence a continuous chemical link between the modified polymer and the reinforcing fibre.
10. Commercial Irganox (1076 and 1010) stabilisers were very effective antioxidants in a highly volatilising environment because of their inherently high stabilising activity (a characteristic of hindered phenols) and high molecular weight, but were inappropriate for use in under-bonnet components because they were easily extracted from the polymer by solvents.

11. The free radical binding of MA to PP(HF22) was exploited to obtain grafted unextractable antioxidant by subsequent melt processing with ADPA. The grafting reaction caused ring opening of the bound anhydride with amide formation with the primary amine of ADPA. However, adequate thermal-oxidative stability of such modified PP(HF22) was not attained because binding of MA in sufficient quantities proved elusive.
  
12. Outstanding thermal-oxidative stability of PP(HF22) containing APM (melt processed in the presence of DCP) was obtained; very high free radical binding, a result of high electron density in the maleimide ring (due to the presence of the aromatic amine) rendered the stabiliser unextractable. APM's diaryl-amino group's stabilising ability was thought to be supplemented by its oxidation (a result of the high DCP concentration used for melt processing) to nitroxyl which catalytically scavenges alkyl and alkylperoxyl radicals.
  
13. The cyanuric chloride derivative stabilisers, AACT and ADDT, were poor thermal-oxidative PP(HF22) stabilisers due to low chemical binding (allowing antioxidant loss in volatilising and solvent extracting environments), the possibility of an addition reaction between chlorine (from the cyanuric ring) and the diaryl-amino group during melt processing, and isomerism of these additives



to species unable to donate diaryl amino hydrogen to a degradative radical.

14. APM, APMA and ADDT stabilisers were shown to act in a free radical chain-breaking mode and exhibited no peroxide decomposing activity at all. Free radical consumption was by two sources: the diaryl-amino stabilising group responsible for induction periods during oxygen absorption solution studies, and unsaturated modifying groups (used for the free radical binding to PP) which reduced the rate of oxygen absorption after the induction period. Additives used solely as modifiers for enhancing the mechanical performance of PP(HF22) composites (such as MA and MAL) showed no induction period, being devoid of diaryl — amino stabilising groups, but did give a reduced rate of oxygen absorption.

## 7.2 Suggestions For Further Work

In view of the observations and conclusions made in this work, the following suggestions are recommended for further work:-

1. Because the maintenance of fibre length during homogenisation and injection moulding of composites is essential to enhance the level of stress transfer from the matrix to the reinforcing fibre, other compounding

techniques such as twin screw extrusion and dry-blending should be evaluated.

2. A more detailed understanding of the chemistry at the modified (MA, APM and ADCT) PP-fibre (silane coupled) interface is essential if further improvements in interfacial adhesion are to be made.
3. It is thought that there is scope for further development of RWF reinforcement of PP, but this will only be made possible when the constitution of the protective surface "tenside" layer is established. Its removal and subsequent silane coupling should also be attempted.
4. Synthesis of chemical modifiers containing a silane coupling agent function for melt processing with unstabilised PP in the presence of DCP and non-coupled fibres should be tried to see if this provides a better way of enhancing composite interfacial fibre-matrix adhesion.
5. Synthesis of cyanuric chloride derivatives with all three chlorines substituted would eliminate the potentially unfavourable reaction in the PP melt of chlorine with amino stabiliser liberating HCl.
6. The beneficial effect of DCP on APM as a thermal-oxidative stabiliser of PP(HF22) must be thoroughly

investigated to confirm the suspected oxidation of diarylamine to nitroxyl, thought to be responsible for cyclical scavenging of alkyl and alkylperoxyl radicals.

7. These modified composites should be moulded into the appropriate under-bonnet components in order that their suitability may be comprehensively evaluated in-service.

## REFERENCES

1. Mandy, F., *Plastics and Rubber International*, 119-125, June (1976).
2. Milewski, J.V., *Plastics Engineering*, No. 11, 23-28, Nov (1978).
3. Stedfeld, R., *Materials Engineering*, No. 1, 42, Jan (1981).
4. Miller, W.G., *British Plastics*, 43, No. 8, 59-63, Aug (1970).
5. Banks, M.T., *Machine Design*, 51, 88-90, Sept (1979).
6. *The Engineer*, 61-63, May (1982),
7. Wehrenberg, R.H., *Materials Engineering*, No. 5, 47-52, May (1981).
8. *British Plastics*, 43, No. 12, 83-86, Dec (1970).
9. Abrahams, M., Dimmock, J., *Plastics and Polymers*, 187-193, June (1971).
10. Davis, J.H., *Plastics and Polymers*, 137-143, April (1971).
11. Bader, M.G., Bowyer, W.H., *Composites*, 4, 150-156, July (1973).
12. Freed, W.T., McNally, D., Sell, J.W., Shaner, J.R., *Polym. Eng. Sci.*, 18, 396-403, (1978).
13. Folkes, M.J., "Short Fibre Reinforced Thermoplastics" (pub. John Wiley and Sons Ltd), Chapt. 4, 60-61, (1982).
14. Stade, K., *Polym. Eng. Sci.*, 18, 107-113, (1978).
15. Stade, K., *Polym. Eng. Sci.*, 17, 50-57, (1977).
16. Rains, R.K., Shen, K.S., *SPE-ANTEC*, 270-273, (1978).
17. Freed, W.T., McNally, D., *SPE-ANTEC*, 79-87, (1974).
18. Best, J.R., *SPE-ANTEC*, 150-153, (1972).
19. Darlington, M.W., Gladwell, B.K., Smith, G.R., *Polymer*, 18, No. 12, 1269-1274, (1977).

20. Folkes, M.J., "Short Fibre Reinforced Thermoplastics" (pub. John Wiley and Sons Ltd), Chapt. 2, 5-29, (1982).
21. Filbert, W.C., SPE-Journal, 25, No. 1, 65-69, (1969).
22. Folkes, M.J., "Short Fibre Reinforced Thermoplastics" (pub. John Wiley and Sons Ltd.), Chapt. 5, 94-100, (1982).
23. Taylor, R.B., Plastics Technology, 16, 48-50, July (1970).
24. Folkes, M.J., "Short Fibre Reinforced Thermoplastics" (pub. John Wiley and Sons Ltd.), Chapt. 5, 83-85, (1982).
25. Ghosh, S.K., Johnson, W., J. Mat. Sci., 16, No. 2, 285-301, (1981).
26. Bright, P.F., Crowson, R.J., Folkes, M.J., J. Mat. Sci., 13, No. 11, 2497-2506, (1978).
27. Darlington, M.W., McGinley, P.L., Smith, G.R., J. Mat. Sci., 11, 877-886, (1976).
28. Bader, M.G., Bailey, J.E., Curtis, P.T., J. Mat. Sci., 13, 377-390, (1978).
29. McNally, D., Polymer Plastics Technology and Engineering, 8, 101-154, (1977).
30. Avery, J.A., Kramer, M., SPE-ANTEC, 356-357, (1974).
31. Motoyshui, M., Japanese Plastics Age, 13, No. 145, 33-41, Sept/Oct (1975).
32. Akiyuma, T., Sone, T., Japanese Plastics Age, 10, No. 11, 21-26, Nov (1972).
33. Du Pont, Plastics Technology, 24, No. 12, 11-13, Nov (1978).
34. Wehrenberg, R.H., Materials Engineering, No. 4, 38-43, April (1980).
35. Crowson, R.J., Folkes, M.J., Polym. Eng. Sci., 20, 934-940, (1980).

36. Ramsteiner, F., Theysohn, R., *Composites*, 10, 111-119, April (1979).
37. Richards, R.W., Sims, D., *Composites*, 2, 214-219, Dec (1971).
38. Bright, P.F., Darlington, M.W., *Plastics and Rubber Processing and Applications*, 1, No. 2, 139-147, June (1981).
39. Folkes, M.J., "Short Fibre Reinforced Thermoplastics", (pub. John Wiley and Sons Ltd.), Chapt. 4, 59, (1982).
40. Stephenson, R.C., Turner, S., Whale, M., *SPE-ANTEC*, 347-351, (1977).
41. Darlington, M.W., McGinley, P.L., Smith, G.R., *Plastics and Rubber Processing and Applications*, 2, No. 1, 51-58, Feb (1977).
42. Lavengood, R.E., *Polym. Eng. Sci.*, 12, 49-52, (1972).
43. Wenger, R.M., *SPI 36th ANTEC, Reinf. Plast.*, 9-D, (1981).
44. Culbertson, B.M., Trivedi, B.C., "Maleic Anhydride", (pub. Plenum Publishing Corporation, New York), Chapt. 11, 459, (1982):
45. Krul, L.P., Osipenko, I.F., Polikarpov, A.P., Prokopchuk, N.R., *J. Polym. Sci. Polym. Lett.*, 22, (3), 153, (1984).
46. Minoura, Y., Mizunuma, S., Neda, M., Oba, M., *Kogyo Kagaku Zasshi*, 71, (3), 432, (1968); *Chem. Abstr.*, 69, 28223y, (1968).
47. Hasegawa, A., Ide, F., Kamada, K., *Kobunshi Kagaku*, 25, (275), 167, (1968); *Chem. Abstr.*, 69, 59758f, (1968).
48. Minoura, Y., Mizunuma, S., Oba, M., Ueda, M., *J. Appl. Polym. Sci.*, 13, (8), 1625, (1969).
49. Nippon Oil, Japanese Patent, 27, 336, (1980).
50. Baramboim, N.K., Protasov, V.G., *Plast. Massy.*, 2, 8, (1969); *Chem. Abstr.*, 70, 107029p, (1969).

51. Barab'ol't, N.K., Protasov, V.G., Plast. Massy., 3, 22, 1970 (Chem. Abstr., 77, 153349k, 1972).
52. Barab'ol't, N.K., Protasov, V.G., Chem. Abstr., 79, 6057b, 1973.
53. Barab'ol't, N.K., Protasov, V.G., Plaste. Kaut., 12, 12, 89, 1972 (Chem. Abstr., 76, 141634z, 1972).
54. Barab'ol't, N.K., Protasov, V.G., Plaste. Kaut., 23, 3, 185, 1976 (Chem. Abstr., 84, 181024g, 1976).
55. Gabara, W., Onzagna, J.D., Chem. Abstr., 66, 116107g, 1967.
56. Barab'ol't, N.K., Baranova, L.P., Protasov, V.G., Sterlingov, I.D., Chem. Abstr., 64, 17797f, 1966.
57. Baschkin, A., Saraga, L.T.M., J. Colloid and Interface Sci., 43, 3, 473, 1973.
58. Union Carbide U.S. Patent, 3,216,885, 1965.
59. Ciba Geigy, Swiss Patent, 571,033, 1975.
60. Dow Chemical, British Patent, 844,231, (1960).
61. Gul, V.E., Glukhova, E.M., Ishevskii, G.M., Itskova, T.G., Tolmacheva, M.N., Vasileva, O.V., USSR Patent, 732,306, (1980).
62. Gaylord, N.G., Am. Chem. Soc. Div. Org. Coat. Plast. Prepr., 40, 456, (1979).
63. Rhone-Poulenc Ind., French Patent, 2,429,804, (1980).
64. Motoyshi, M., Japanese Plastics Age, 13, No.145, 41, Sept/Oct (1975).
65. Monte, S.J., Sugerman, G., SPE-ANTEC, 228-236, (1977).
66. Cessna, L.C., Hanna, R.D., Thompson, J.B., SPE-Journal, 25, No.10, 35-39, Oct (1969).



67. Vaughan, D.J., SPE-ANTEC, 330-331, (1977).
68. McFarren, G.A., Sanderson, T.F., Schappell, F.G.S., Polym. Eng. Sci., 17, 46-49, (1977).
69. Newbould, J., J. Appl. Polym. Sci., 19, 907-908, (1975).
70. Morrell, S.H., Plastics and Rubber Processing and Applications, 1, No. 2, 179-186, (1981).
71. Monte, S.J., Sugerman, G., SPE-ANTEC, 27, (1976).
72. Conroy, A.P., Skinner, D.L., Plastics Engineering, No. 8, 28-30, (1977).
73. Inoue, H., Kohama, S., J. Appl. Polym. Sci., 19, 1939-1954, (1975).
74. Rastogi, A.K., Chemical Technology, 5, No. 6, 349-355, (1975).
75. Koenig, J.L., Shih, P.T.K., Materials Science and Engineering, 20, No. 2, 137-143, Aug(1975).
76. Koenig, J.L., Shih, P.T.K., Materials Science and Engineering, 20, No. 2, 145-154, Aug(1975).
77. Koenig, J.L., Shih, P.T.K., Materials Science and Engineering, 20, No. 2, 127-136, Aug(1975).
78. Ishida, H., Koenig, J.L., J. Polym. Sci., 17, 615, (1979).
79. Plueddemann, E.P., "Silane Coupling Agents", (pub. Plenum Press, New York), Chapt. 5, 131, (1982).
80. Gaehde, J., Plaste Kaut., 22, (8), 626, (1975).
81. Zisman, W.A., Ind. Eng. Chem., 35, (10), 19, (1963).
82. Cerlin, E.H., Dynes, P.J., Kaeble, D.H., Journal of Adhesion, 6, 23, (1974).
83. Bascom, W.D., J. Colloid and Interface Sci., 27, 789, (1968).

84. Lee, L.Hn., *J. Colloid and Interface Sci.*, 27, 751, (1968).
85. Plueddemann, E.P., *Modern Plastics*, 54, 102, (1966).
86. Plueddemann, E.P., "Silane Coupling Agents", (pub. Plenum Press, New York), Chapt. 5, 134, (1982).
87. Kahn, F.J., *Appl. Phys. Lett.*, 22, (8), 386, (1973).
88. Cooper, E.R., Erickson, P.W., Volpe, A.A., *SPI 19th ANTEC, Reinf. Plast.*, 21-A, (1964).
89. Kumins, C.A., Roteman, J., *J. Polym. Sci., Part A*, 1, 527, (1963).
90. Plueddemann, E.P., Stark, G.L., *SPI 35th ANTEC, Reinf. Plast.*, 20-C, (1980).
91. Plueddemann, E.P., *SPI 29th ANTEC, Reinf. Plast.*, 24-A, (1974).
92. Plueddemann, E.P., "Silane Coupling Agents", (pub. Plenum Press, New York), Chapt. 5, 136, (1982).
93. Binder, K., Sobell, R., Vickovich, St., *Chem. Kunst-Aktuell*, 29, (4), 168, (1975).
94. Bolland, J.L., *J. Chem. Soc.*, 492, (1949).
95. Former, E.H., *Trans. Faraday Soc.*, 38, 348, (1942).
96. Bolland, J.L., *Trans. Faraday Soc.*, 44, 669, (1948).
97. Bolland, J.L., *Quarterly Review*, 3, 1, (1949).
98. Blumberg, M., McTigue, F.H., *Appl. Polym. Symp.*, 4, 175, (1967).
99. Oswald, H.J., Roldan, L.G., Turi, E., *ACS Preprints*, 5, (2), 538, (1964).
100. Cutzer, M.J., Gottfried, G., *J. Appl. Polym. Sci.*, 5, 612, (1961).

101. Chakraborty, K.B., Scott, G., *Polymer*, 18, 98, (1977).
102. Dhanly, J., Guillet, J.E., Hartley, G.H., *Advances in Chemistry*, 70, (1969).
103. Carlsson, D.J., Wiles, D.M., *Rev. Macromol. Chem.*, (I), 14B, 65, (1976).
104. Holsworth, J.D., Scott, G., Williams, D., *J. Chem. Soc.*, 4692, (1964).
105. Scott, G., *J. Polym. Sci. Symp.*, 57, 357, (1978).
106. Scott, G., *Chemistry in Britain*, 9, 269, (1973).
107. Carlsson, D.J., Suprunchuck, T., Wiles, D.M., *J. Appl. Polym. Sci.*, 16, 615, (1972).
108. Shelton, J.R., "Polymer Stabilisation", (Ed. Hawkins, W.L., pub. Wiley Interscience, New York), Chapt. 2, 31, (1972).
109. Grassie, N., "The Chemistry of High Polymer Degradation Process", (pub. Interscience, New York), Chapt. 2, 56, (1956).
110. Mercurio, A., Tobolsky, V.A., *J. Am. Chem. Soc.*, 81, 5535; (1959).
111. Bevilacqua, P., English, E., *J. Polym. Sci.*, 49, 495, (1961).
112. Decker, C., Mayo, F.R., *J. Polym. Sci. Polym. Chem. Ed.*, 11, 2847, (1973).
113. Scott, G., "Developments in Polymer Stabilisation-4", (Ed. Scott, G., Pub. Applied Science Publishers Ltd), Chapt. 1, 1, (1981).
114. Scott, G., "Developments in Polymer Stabilisation-7", (Ed. Scott, G., pub. Elsevier Applied Science Publishers Ltd.), Chapt. 2, 67, (1984).

115. Henman, T.J., "Developments in Polymer Stabilisation -1", (Ed. Scott, G., pub. Applied Science Publishers Ltd.), Chapt. 2, 59, (1979).
116. Scott, G., Rubber. Chem. Tech., 44, 1421, (1971).
117. Scott, G., "Atmospheric Oxidation and Antioxidants", (pub. Elsevier), Chapt. 4, 115-169, (1965).
118. Scott, G., "Atmospheric Oxidation and Antioxidants", (pub. Elsevier), Chapt. 3, 99, (1965).
119. Scott, G., "Developments in Polymer Stabilisation-7", (Ed. Scott, G., pub. Elsevier Applied Science Publishers Ltd.), Chapt. 2, 68, (1984).
120. Scott, G., Chemical Communications, 24, 1572, (1968).
121. Cowell, G.K., Plastics Engineering, 32, 51, (1976).
122. Henman, T.J., "Developments in Polymer Stabilisation -1", (Ed. Scott, G., pub. Applied Science Publishers Ltd), Chapt. 2, 39, (1979).
123. Edemskaya, V., Miller, V.B., Shlyapnikov, Y.A., Vys. Soed., 16B, 489, (1974).
124. Pospisil, J., "Developments in Polymer Stabilisation -1", (Ed. Scott, G., pub. Applied Science Publishers Ltd), Chapt. 1, 1, (1979).
125. Scott, G., "Developments in Polymer Stabilisation-7", (Ed. Scott, G., pub. Elsevier Applied Science Publishers Ltd.), Chapt. 2, 77, (1984).
126. Lorenz, O., Rubb. Chem. Tech., 34, 816, (1961).
127. Henman, T.J., "Developments in Polymer Stabilisation -1", (Ed. Scott, G., pub. Applied Science Publishers Ltd), Chapt. 2, 95, (1979).

128. Scott, G., *Pure Appl. Chem.*, 30, 267, (1972).
129. Scott, G., *Eur. Polym. J. Suppl.*, 189, (1969).
130. Lappin, G.R., "Encyclopedia of Polymer Science and Technology", (Eds. Bikales, N.M., Gaylord, N.G., Mark, H.F., pub. Wiley), 14, (1971).
131. Luston, J., "Developments in Polymer Stabilisation-2", (Ed. Scott, G., pub. Applied Science Publishers Ltd.), Chapt. 5, 185, (1980).
132. Cain, M.E., Gazely, K.F., Gelling, I.R., *Rubb. Chem. Tech.*, 45, 204, (1972).
133. Bua, E., Cicchetti, O., Dubini, M., Parrini, P., *Eur. Polym. J.*, 4, 419, (1968).
134. Burmistrov, E.F., Guschina, M.A., Kiseleva, M.A., Kochanov, Y.V., Temchin, Y.I., *Vysokomol. Soedin.*, A12, 1901, (1970).
135. Frank, H.P., Lehner, H., *J. Polym. Sci. Pt. C.*, Symp. No. 31, 193, (1970).
136. Ambrovic, P., Mikovic, J., *Eur. Polym. J. Suppl.*, 371, (1969).
137. Billingham, N.C., Prentice, P., Walker, T.J., *J. Polym. Sci. Pt. C.*, Symp. No. 57, 287, (1976).
138. Billingham, N.C., Calvert, P.D., Prentice, P., Ryan, T.G., *Polymer Preprints*, 18, 476, (1977).
139. Calvert, P.D., Ryan, T.G., *Polymer*, 19, 611, (1978).
140. Caucik, P., Durmis, J., Holcik, J., Karvac, M., *Eur. Polym. J.*, 11, 219, (1975).
141. Shlyapnikov, Y.A., Yushkhevichute, S.S., *Plast. Massy.*, 12, 62, (1966).

142. Angert, L.G., Kuzminskii, A.S., Zenchenko, A.I., Kolloid, Zh., 22, 2, (1960).
143. Burmistrov, E.F., Temchin, Y.I., Plast. Massy., 4, 41 (1967).
144. Bullard, H.L., Hollingshead, W.S., Spacht, R.B., Wills, D.C., Rubb. Chem. Tech., 38, 134, (1965).
145. Bullard, H.L., Hollingshead, W.S., Spacht, R.B., Wills, D.C., Rubb. Chem. Tech., 37, 210, (1964).
146. Plant, M.A., Scott, G., Eur. Polym. J., 7, 1173, (1971).
147. Durmis, J., Holcik, J., Karvas, M., Kassovicova, D., Eur. Polym. J., 12, 173, (1976).
148. Conner, W.P., Weimer, R.P., Text. Res. J., 39, 1150, (1969).
149. Scott, G., "Developments in Polymer Stabilisation-4", (Ed. Scott, G., pub. Applied Science Publishers Ltd.), Chapt. 6, 181, (1981).
150. Scott, G., J. Rubb. Res. Inst., Sri Lanka, 54, 106, (1977).
151. Thomas, D.K., "Developments in Polymer Stabilisation -1", (Ed. Scott, G., pub. Applied Science Publishers Ltd), Chapt. 4, 137, (1979).
152. Phillips, L.N., Thomas, D.K., Wright, W.W., British Patent App. No. 900, (1965).
153. Evans, B.W., Scott, G., Eur. Polym. J., 10, 453, (1974).
154. Ladd, F.C., Canadian Patent, 808, 737, (1969).
155. Kleiner, E.K., German Patent, 1, 931, 452, (1970).
156. Kavchok, R.W., Meyer, G.E., Naples, J.F., Rubb. Chem. Tech., 46, 106, (1973).
157. Grimm, D.C., Horvarth, J.W., Stevick, J.A., Rubb. Chem. Tech., 48, 337, (1975).

158. Burdon, J.R., Horvarth, J.W., Meyer, G.E., Naples, F.J.,  
Paper presented at ACS Meeting, Chicago, Aug(1973).
159. Oo, K.M., Tahan, M., Eur. Polym. J., 13, 915, (1977).
160. Cain, M.E., Knight, G.T., Lewis, P.M., Saville, B.,  
Rubber Journal, 150(2), 204, (1968).
161. Cain, M.E., Gazely, K.F., Gelling, I.R., Lewis, P.M.,  
Rubb. Chem. Tech., 45, 204, (1972).
162. Fryns, J.H.G., Blok, A.P., Bolsmann, T.A.B.M., Rec.  
Trav. Chim. Pays-Bas, 27, 310, (1978).
163. Katbah, A., Scott, G., Chem. Ind., 573, (1980).
164. Scott, G., Setoudeh, E., Polym. Deg. Stab., 5, 1, (1983).
165. Scott, G., Setoudeh, E., Polym. Deg. Stab., 5, 11, (1983).
166. Scott, G., Ajiboye, O., Polym. Deg. Stab., 4, 415, (1982).
167. Scott, G., Tavakoli, S.M., Polym. Deg. Stab., 4, 343, (1982).
168. "Inorphil mineral fibre", Technical data sheet, Laxa  
Bruk, Sweden.
169. Chem. Abstr., 60, 14430a, (1964).
170. Bryan, C.E., Conger, R.P., Dovell, F.S., Snyder, R.H., Stiteler,  
C.H., Tawney, P.O., J. Org. Chem., 25, No. 1, 56-60, (1960).
171. Banks, C.K., Pearlman, W.M., J. Am. Chem. Soc., 70, 3726-3728,  
(1948).
172. "Buss Ko-Kneader PR46" Operators Manual, Buss Ltd, Basle,  
Switzerland.
173. "Edgwick 1214-HY Type S(MkII) screw injection moulding  
machine", Operators manual, Alfred Herbert Ltd.
174. Annual Book of ASTM Standards, Vol. 8.01, ASTM D538M,  
248-259, (1984).

175. Annual Book of ASTM Standards, Vol. 8.01, ASTM D790M, Method I, 414-425, (1984).
176. Vincent, P., Impact Tests And Service Performance Of Plastics, Plastics Institute, London (1971).
177. Young, W.J., "Introduction To Polymers", (pub. Chapman and Hall, London), Chapt. 5, 232-236, (1981).
178. Annual Book Of ASTM Standards, Vol. 8.02, ASTM D2236-81, 310, (1984).
179. Annual Book Of ASTM Standards, Vol. 8.02, ASTM D2990-77, 707-717, (1984).
180. Annual Book Of ASTM Standards, Vol. 8.01, ASTM D543-67, 195-199, (1984).
181. Paul, K.T., RAPRA Bulletin, 26, 29, (1972).
182. British Standard, 2782, 105C, Pt. I, (1965).
183. "Wallace Multi-cell Ageing Oven, Mk. III", Operating instructions, H.M. Wallace Ltd., Croydon, Surrey.
184. British Standard, 903, Pt. A19, (1975).
185. "Ewing Instrumental Methods Of Chemical Analysis", (pub. McGraw Hill), 82, (1960).
186. Kriz, G., Lampman, G., Pavia, D., "Introduction To Spectroscopy", (pub. Saunders Company, New York), Chapt. 5, 186, (1979).
187. Erwin, L., Turkovich, R.V., Polym. Eng. Sci., 23, 743-749, (1983).
188. Richards, R.W., Sims, D., Composites, 2, 214-220, Dec. (1971).
189. Murphy, T.P., Modern Plastics, 42, 127-134, June (1965).
190. Darlington, M.W., Smith, G.R., Polymer, 16, No. 6, 459-462, (1975).



191. Blumentritt, B.F., Cooper, S.L., Vu, B.T., *Polym. Eng. Sci.*, 15, 428-436, (1975).
192. Hsu, E.C., Temple, C.S., SPI 36th ANTEC, *Reinf. Plast.*, 9-F, (1981).
193. Folkes, M.J., "Short Fibre Reinforced Thermoplastics", (pub. John Wiley and Sons Ltd.), Chapt. 2, 25, (1982).
194. Folkes, M.J., "Short Fibre Reinforced Thermoplastics", (pub. John Wiley and Sons Ltd.), Chapt. 5, 92, (1982).
195. Dao, K.C., *Polymer*, 25, No. 10, 1527-1533, (1984).
196. Folkes, M.J., "Short Fibre Reinforced Thermoplastics", (pub. John Wiley and Sons Ltd.), Chapt. 3, 48, (1982).
197. Peiffer, D.G., *J. Appl. Polym. Sci.*, 24, 1451-1455, (1979).
198. Aglietto, M., Ciardelli, F., Petraghani, A., Ruggeri, G., *Eur. Polym. J.*, 19, 863-866, (1983).
199. Gaylord, N.G., Mishra, M.K., *J. Polym. Sci. Polym. Lett.*, 21, (1), 23-30, (1983).
200. Chodak, I., Zimanyova, E., *Eur. Polym. J.*, 20, 81-84, (1984).
201. Denisov, E.T., Griva, A.P., *J. Polym. Sci. Polym. Chem.*, 14, (5), 1051-1064, (1976).
202. Elayaperumal, P., Gaylord, N.G., *J. Polym. Sci. Polym. Lett.*, 21, (10), 781-784, (1983).
203. Gaylord, N.G., Mehta, M., *J. Polym. Sci. Polym. Lett.*, 20, (9), 481-486, (1982).
204. Gabara, W., Porejko, S., *J. Polym. Sci., Pt. A-1*, 5, 1539-1545, (1967).
205. Ogorkiewicz, R.M., "Engineering Properties of Thermoplastics", (pub. Wiley Interscience), Chapt. 3, 68, (1970).
206. Bergen, R.L., *SPE Journal*, 24, 77-80, Aug (1968).

207. Oliver, P.C., "Glass Reinforced Plastics", (Ed. Parkyn, B., pub. Butterworth and Co.), Chapt. 17, 237, (1970).
208. McCammond, D., Wark, C.A., Polym. Eng. Sci., 14, No. 12, 831-839, Dec (1974).
209. Ogorkiewicz, R.M., "Engineering Properties of Thermoplastics", (pub. Wiley Interscience), Chapt. 2, 43-48, (1970).
210. Plueddemann, E.P., "Silane Coupling Agents", (pub. Plenum Press, New York), Chapt. 1, 13, (1982).
211. Boenig, H.V., "Polyolefins", (pub. Elsevier Publishing Co.), Chapt. 4, 153, (1966).
212. Schweiger, F., Kunststoffe, 51, 256, (1961).
213. Horsley, R.A., "Thermoplastics", (Ed. Ogorkiewicz, R.M., pub. Iliffe Books Ltd.), Chapt. 2, 37, (1969).
214. Whelan, A., "Injection Moulding Materials", (pub. Applied Science), Chapt. 6, 221, (1982).
215. Ogorkiewicz, R.M., "Engineering Properties of Thermoplastics", (pub. Wiley Interscience), Chapt. 2, 28, (1970).
216. Plueddemann, E.P., "Silane Coupling Agents", (pub. Plenum Press, New York), Chapt. 7, 193, (1982).
217. Plueddemann, E.P., "Silane Coupling Agents", (pub. Plenum Press, New York), Chapt. 5, 115, (1982).
218. Bascom, W.D., Macromolecules, 5, 792, (1972).
219. Plueddemann, E.P., "Silane Coupling Agents", (pub. Plenum Press, New York), Chapt. 4, 99, (1982).
220. Billingham, N.C., "Developments in Polymer Stabilisation-3", (Ed. Scott, G., pub. Applied Science Publishers Ltd.), Chapt. 5, 139-191, (1980).

221. Wolkeba, Z., *Int. Polym. Sci. Tech.*, 2, (12), T/34, (1975).
222. Gilroy, H.M., Howard, J.B., *Polym. Eng. Sci.*, 15, 268-71, (1975).
223. Albarino, R.V., Schonhorn, H., *J. Appl. Polym. Sci.*, 17, 3323-3335, (1973).
224. Gillick, J.G., Kuczkowski, J.A., *Rubb. Chem. Tech.*, 57, 621-650, (1984).
225. Coomarasamy, A., Silva, L.B.K., Suranimala, R.C., *J. Rubb. Res. Inst. Sri Lanka*, 59, 31-45, (1981).
226. Kirpichev, V.P., Maglysh, G.N., Yakubchik, A.I., *Rubb. Chem. Tech.*, 43, 1225-1229, (1970).
227. Van der Burg, S., Relyea, D.I., Tawney, P.O., Wensch, W.J., *Rubb. Chem. Tech.*, 38, 352-366, (1965).
228. Berger, H., Bolsman, T.A.B.M., Brouwer, D.M., "Developments in Polymer Stabilisation-6", (Ed. Scott, G., pub. Applied Science Publishers Ltd), Chapt. 1, 1-29, (1983).
229. Denisov, E.T., "Developments in Polymer Stabilisation-3", (Ed. Scott, G., pub. Applied Science Publishers Ltd), Chapt. 1, 1, (1980).
230. Denisov, E.T., Kharitonov, V.V., Varlamov, V.T., *Dokl. Akad. Nauk. SSSR*, 220, 620, (1975).
231. Bolsman, T.A.B.M., Brouwer, D.M., *Rev. Trav. Chim. Pay-Bas*, 97, 320, (1978).
232. Mori, K., Nakamura, Y., Saitch, Y., Tamura, K., *Int. Polym. Sci. Tech.*, 12, (2), T/56, (1985).
233. Ladd, E.C., (U.S. Rubber Co.), *U.S. Pat.*, 3,148,196, (1968).
234. Bateman, L., *Quart. Rev.*, 8, 147, (1954).
235. Scott, G., *Chem. and Ind.*, 7, 271, (1963).